

UNCLASSIFIED

AD NUMBER

AD869035

LIMITATION CHANGES

TO:

Approved for public release; distribution is unlimited.

FROM:

Distribution authorized to U.S. Gov't. agencies and their contractors;
Administrative/Operational Use; FEB 1970. Other requests shall be referred to Army Aviation Materiel Labs., Fort Eustis, VA.

AUTHORITY

USAAMRDL ltr, 18 Jun 1971

THIS PAGE IS UNCLASSIFIED

AD

USAAVLABS TECHNICAL REPORT 69-88

ROTOR AEROELASTIC INSTABILITY AND TRANSIENT CHARACTERISTICS

By

Charles F. Niebanck

Lawrence J. Bain

February 1970

**U. S. ARMY AVIATION MATERIEL LABORATORIES
FORT EUSTIS, VIRGINIA**

CONTRACT DA 44-177-AMC-203(T)

UNITED AIRCRAFT CORPORATION

SIKORSKY AIRCRAFT DIVISION

STRATFORD, CONNECTICUT

This document is subject to special
request controls, and each transmittal
to foreign governments or foreign
nationals may be made only with
prior approval of U.S. Army Aviation
Materiel Laboratories, Fort Eustis,
Virginia 23054



RECEIVED
FEB 1970
448

DISCLAIMERS

The findings in this report are not to be construed as an official Department of the Army position unless so designated by other authorized documents.

When Government drawings, specifications, or other data are used for any purpose other than in connection with a definitely related Government procurement operation, the United States Government thereby incurs no responsibility nor any obligation whatsoever; and the fact that the Government may have formulated, furnished, or in any way supplied the said drawings, specifications, or other data is not to be regarded by implication or otherwise as in any manner licensing the holder or any other person or corporation, or conveying any rights or permission, to manufacture, use, or sell any patented invention that may in any way be related thereto.

DISPOSITION INSTRUCTIONS

Destroy this report when no longer needed. Do not return it to the originator.

[illegible]



DEPARTMENT OF THE ARMY
HEADQUARTERS US ARMY AVIATION MATERIEL LABORATORIES
FORT EUSTIS, VIRGINIA 23604

This report has been reviewed by the U. S. Army Aviation Materiel Laboratories and is considered to be technically sound.

The report is published for the exchange of information and the stimulation of ideas.

Task 1F162204A13903
Contract DA 44-177-AMC-203(T)
USAAVLABS Technical Report 69-88
February 1970

ROTOR AEROELASTIC INSTABILITY AND TRANSIENT CHARACTERISTICS

SER-50597

by

Charles F. Nicbanck

Lawrence J. Bain

Prepared by

United Aircraft Corporation
Sikorsky Aircraft Division
Stratford, Connecticut

for

U. S. ARMY AVIATION MATERIEL LABORATORIES
FORT EUSTIS, VIRGINIA

This document is subject to special export controls, and each transmittal to foreign governments or foreign nationals may be made only with prior approval of US Army Aviation Materiel Laboratories, Fort Eustis, Virginia 23604.

FOREWORD

This report describes the results of a test program which was performed by Sikorsky Aircraft under Contract DA 44-177-AMC-203(T), Task 1F162204A13903, with the U. S. Army Aviation Materiel Laboratories. The test program in this report was performed in conjunction with a separate investigation of rotor wake characteristics and yaw effects on rotor performance, which was carried out under the same contract. The work of this contract was monitored for USAAVLABS by Mr. Patrick Cancro.

The test planning, analysis, and discussion pertaining to the rotor transient investigation presented in this report were the work of Mr. Lawrence J. Bain. The similar tasks which pertained to the aerelastic instability portion of the test program were carried out by Mr. Charles F. Niebanck.

TABLE OF CONTENTS

	<u>Page</u>
SUMMARY	111
FOREWORD	v
LIST OF ILLUSTRATIONS	viii
LIST OF TABLES	xiv
LIST OF SYMBOLS	xx
INTRODUCTION	1
DESCRIPTION OF MODEL	3
TEST PROCEDURE AND INITIAL OBSERVATIONS	9
DESCRIPTION OF DATA AND DATA REDUCTION	15
DESCRIPTION OF THEORETICAL CALCULATIONS	22
ANALYSIS OF TRANSIENT DATA	28
ANALYSIS OF INSTABILITY DATA	40
PRACTICAL OPERATING LIMITS	66
CONCLUSIONS	68
LITERATURE CITED.	72
APPENDIXES	
I. Description of Facilities and Equipment	258
II. Tables of Maximum and Minimum Blade Response	260
III. Tables of Blade Response Harmonics	273
DISTRIBUTION	426

LIST OF ILLUSTRATIONS

<u>Figure</u>		<u>Page</u>
1	Sikorsky Compound Helicopter Model in United Aircraft Corporation 18-Foot Wind Tunnel	96
2	Three-View Drawing of Sikorsky Compound Helicopter Model . .	97
3	Dynamically Scaled Model Blade Construction	98
4	Blade Mass Properties	99
5	Blade Stiffness Properties.	100
6	Blade Flapwise Natural Frequency Versus Rotor Speed	101
7	Blade Chordwise Natural Frequency Versus Rotor Speed	102
8	Blade Torsional Natural Frequency Versus Rotor Speed	103
9	Blade First Flapwise Bending Mode Shape; $\Omega_s R = 700$ ft/sec. .	104
10	Blade First Chordwise Bending Mode Shape; $\Omega_s R = 700$ ft/sec	105
11	Blade First Torsional Mode Shape; $\Omega_s R = 700$ ft/sec	106
12	Model Blade Bearing Friction Test Results	107
13	Rotor Operating Conditions for Transient Testing	108
14	Theoretical Fixed-Azimuth Stability Boundaries and Selected Data Points	109
15	Sample Control Position Transient Input; $V_s = 300$ kn, $\mu = 1.026$, $TAN \delta_3 = 1.0$, $\alpha_r = 0.0^\circ$, $\theta_{cs} = 0.0^\circ$, $\Delta\theta_c = 4.0^\circ$, $a_{1ss} = 0.0^\circ$, $\Delta a_{1s} = 2.4^\circ$, $b_{1ss} = 0.0^\circ$, $\Delta b_{1s} = -1.4^\circ$, Run 60, Point 28	110
16	Frequency and Damping of Calculated Fixed-Azimuth Flutter Mode	113
17	Torsional Damping From Stall Flutter Calculations; $\alpha_s = 0.0^\circ$, $a_{1s} = 0.0^\circ$, $b_{1s} = 0.0^\circ$	117
18	Experimental and Theoretical Blade Lag Angle During Transient Conditions; $V_s = 120$ kn, $\mu = 0.29$, $Y_{CG}/c = 0.25$	120

<u>Figure</u>		<u>Page</u>
19	Experimental and Theoretical Blade Flapwise Bending Moments During Transient Conditions; $V_s = 120$ kn, $\mu = 0.29$, $Y_{CG}/c = 0.25$	121
20	Experimental and Theoretical Blade Flap Angle During Transient Conditions; $V_s = 120$ kn, $\mu = 0.29$, $Y_{CG}/c = 0.25$	124
21	Experimental and Theoretical Blade Torsional Moment During Transient Conditions; $V_s = 120$ kn, $\mu = 0.29$, $Y_{CG}/c = 0.25$	126
22	Experimental and Theoretical Blade Lag Angle During Transient Conditions; $V_s = 200$ kn, $\mu = 0.50$, $Y_{CG}/c = 0.25$	127
23	Experimental and Theoretical Blade Flapwise Bending Moments During Transient Conditions; $V_s = 200$ kn, $\mu = 0.50$, $Y_{CG}/c = 0.25$	129
24	Experimental and Theoretical Blade Flap Angle During Transient Conditions; $V_s = 200$ kn, $\mu = 0.50$, $Y_{CG}/c = 0.25$	135
25	Experimental and Theoretical Blade Torsional Moment During Transient Conditions; $V_s = 200$ kn, $\mu = 0.50$, $Y_{CG}/c = 0.25$	137
26	Experimental and Theoretical Blade Lag Angle During Transient Conditions; $V_s = 300$ kn, $\mu = 1.03$, $Y_{CG}/c = 0.25$	139
27	Experimental and Theoretical Blade Flapwise Bending Moments During Transient Conditions; $V_s = 300$ kn, $\mu = 1.03$, $Y_{CG}/c = 0.25$	141
28	Experimental and Theoretical Blade Flap Angle During Transient Conditions; $V_s = 300$ kn, $\mu = 1.03$, $Y_{CG}/c = 0.25$	148
29	Experimental and Theoretical Blade Torsional Moment During Transient Conditions; $V_s = 300$ kn, $\mu = 1.03$, $Y_{CG}/c = 0.25$	150
30	Theoretical Blade Lag Angle During Transient Conditions; $V_s = 300$ kn, $\mu = 1.03$, $Y_{CG}/c = 0.25$, Control Input Applied 3/4 Revolution After Experimental Input	152

Figure**Page**

31	Theoretical Blade Flapwise Bending Moment During Transient Conditions; $V_s = 300$ kn, $\mu = 1.03$, $Y_{CG}/c = 1.25$, Control Input Applied $3/4$ Revolution After Experimental Input	153
32	Theoretical Blade Flap Angle During Transient Conditions; $V_s = 300$ kn, $\mu = 1.03$, $Y_{CG}/c = 0.25$, Control Input Applied $3/4$ Revolution After Experimental Input	157
33	Theoretical Blade Torsional Moment During Transient Conditions; $V_s = 300$ kn, $\mu = 1.03$, $Y_{CG}/c = 0.25$, Control Input Applied $3/4$ Revolution After Experimental Input	158
34	Blade Response Versus Azimuth During Retreating Blade Aeroelastic Limits Testing; $Y_{CG}/c = 0.25$, $\alpha_s = 0.0^\circ$, $a_{1s} = b_{1s} = 0.0^\circ$, $V_s = 332$ kn, $\theta_c = 2.0^\circ$	159
35	Blade Response Versus Azimuth During Advancing Blade Aeroelastic Limits Testing; $Y_{CG}/c = 0.25$, $\alpha_s = 0.0^\circ$, $a_{1s} = b_{1s} = 0.0^\circ$, $\theta_c = 2.0^\circ$	163
36	Blade Response Versus Azimuth During Advancing Blade Aeroelastic Limits Testing; $Y_{CG}/c = 0.25$, $\alpha_s = 0.0^\circ$, $a_{1s} = b_{1s} = 0.0^\circ$, $\Omega_s R = 700$ ft/sec, $\theta_c = 4.0^\circ$	167
37	Blade Response Versus Azimuth During Advancing Blade Aeroelastic Limits Testing; $Y_{CG}/c = 0.25$, $\alpha_s = 0.0^\circ$, $a_{1s} = b_{1s} = 0.0^\circ$, $\Omega_s R = 500$ ft/sec, $\theta_c = 4.0^\circ$	172
38	Blade Response Versus Azimuth During Combined Advancing and Retreating Blade Aeroelastic Limits Testing; $Y_{CG}/c = 0.30$, $\alpha_s = 0.0^\circ$, $a_{1s} = b_{1s} = 0.0^\circ$, $V_s = 332$ kn, $\Omega_s R = 404$ ft/sec, $\mu = 1.39$, $\theta_c = 4.0^\circ$	177
39	Blade Response Versus Azimuth During Advancing Blade Aeroelastic Limits Testing; $Y_{CG}/c = 0.35$, $\alpha_s = 0.0^\circ$, $a_{1s} = b_{1s} = 0.0^\circ$, $\Omega_s R = 700$ ft/sec, $\theta_c = 4.0^\circ$	182
40	Blade Response Versus Azimuth During Advancing Blade Aeroelastic Limits Testing; $Y_{CG}/c = 0.35$, $\alpha_s = 0.0^\circ$, $a_{1s} = b_{1s} = 0.0^\circ$, $\Omega_s R = 500$ ft/sec, $\theta_c = 4.0^\circ$	188

41	Blade Response Versus Azimuth During Advancing and Combined Advancing and Retreating Blade Aeroelastic Limits Testing; $Y_{CG}/c = 0.35$, $\alpha_s = 0.0^\circ$, $a_{1s} = b_{1s} = 0.0^\circ$	194
42	Blade Response Versus Azimuth During Stall Flutter Testing; $Y_{CG}/c = 0.25$, $\alpha_s = 0.0^\circ$, $a_{1s} = b_{1s} = 0.0^\circ$, $V_s = 121$ kn, $\Omega_s R = 700$ ft/sec, $\nu = 0.29$	199
43	Blade Response Versus Azimuth During Stall Flutter Testing; $Y_{CG}/c = 0.25$, $\alpha_s = 0.0^\circ$, $a_{1s} = b_{1s} = 0.0^\circ$, $V_s = 145$ kn, $\Omega_s R = 700$ ft/sec, $\nu = 0.35$	204
44	Blade Response Versus Azimuth During Stall Flutter Testing; $Y_{CG}/c = 0.25$, $\alpha_s = 0.0^\circ$, $a_{1s} = b_{1s} = 0.0^\circ$	209
45	Blade Response Versus Azimuth During Combined Advancing Blade Aeroelastic Limits and Stall Flutter Testing; $Y_{CG}/c = 0.30$, $\alpha_s = 0.0^\circ$, $a_{1s} = b_{1s} = 0.0^\circ$, $\theta_c = 11.0^\circ$	214
46	Blade Response Versus Azimuth During Recovery From Violent Instability; $Y_{CG}/c = 0.35$, $\alpha_s = 0.0^\circ$, $V_s = 260$ kn, $\Omega_s R = 500$ ft/sec, $\nu = 0.88$, $\theta_c = 4.0^\circ$, $A_{1s} = -1.3^\circ$, $B_{1s} = 4.6^\circ$	221
47	Blade Response Versus Azimuth During Violent Instability; $Y_{CG}/c = 0.35$, $\alpha_s = 0.0^\circ$, $V_s = 120$ kn, $\Omega_s R = 700$ ft/sec, $\nu = 0.29$, $\theta_c = 6.8^\circ$, $A_{1s} = -2.7^\circ$, $B_{1s} = 6.1^\circ$	225
48	Blade Response Versus Frequency During Violent Instability; $Y_{CG}/c = 0.35$, $\alpha_s = 0.0^\circ$, $V_s = 120$ kn, $\Omega_s R = 700$ ft/sec, $\nu = 0.29$, $\theta_c = 6.8^\circ$, $A_{1s} = -2.7^\circ$, $B_{1s} = 6.1^\circ$	229
49	Blade Lag and Flap Response Versus Frequency During Retreating Blade Limits Testing; $Y_{CG}/c = 0.25$, $\alpha_s = 0.0^\circ$, $a_{1s} = b_{1s} = 0.0^\circ$, $V_s = 332$ kn, $\theta_c = 2.0^\circ$	233
50	Range of Blade Lag Response During Retreating Blade Aeroelastic Limits Testing; $\alpha_s = 0.0^\circ$, $a_{1s} = b_{1s} = 0.0^\circ$, $V_s = 332$ kn	234
51	Range of Blade Flapwise Bending Response During Retreating Blade Aeroelastic Limits Testing; $\alpha_s = 0.0^\circ$, $a_{1s} = b_{1s} = 0.0^\circ$, $V_s = 332$ kn	235

<u>Figure</u>		<u>Page</u>
52	Range of Blade Torsional Response During Retreating Blade Aeroelastic Limits Testing; $\alpha_s = 0.0^\circ$, $a_{1s} = b_{1s} = 0.0^\circ$, $V_s = 332$ kn	236
53	Range of Blade Flapping Response During Retreating Blade Aeroelastic Limits Testing; $\alpha_s = 0.0^\circ$, $a_{1s} = b_{1s} = 0.0^\circ$, $V_s = 332$ kn	237
54	Range of Blade Chordwise Bending Response During Retreating Blade Aeroelastic Limits Testing; $\alpha_s = 0.0^\circ$, $a_{1s} = b_{1s} = 0.0^\circ$, $V_s = 332$ kn	238
55	Range of Blade Lag Response During Advancing Blade Aeroelastic Limits Testing; $\alpha_s = 0.0^\circ$, $a_{1s} = b_{1s} = 0.0^\circ$, $\Omega_s R = 700$ ft/sec	239
56	Range of Blade Flapwise Bending Response During Advancing Blade Aeroelastic Limits Testing; $\alpha_s = 0.0^\circ$, $a_{1s} = b_{1s} = 0.0^\circ$, $\Omega_s R = 700$ ft/sec	240
57	Range of Blade Torsional Response During Advancing Blade Aeroelastic Limits Testing; $\alpha_s = 0.0^\circ$, $a_{1s} = b_{1s} = 0.0^\circ$, $\Omega_s R = 700$ ft/sec	241
58	Range of Blade Flapping Response During Advancing Blade Aeroelastic Limits Testing; $\alpha_s = 0.0^\circ$, $a_{1s} = b_{1s} = 0.0^\circ$, $\Omega_s R = 700$ ft/sec	242
59	Range of Blade Chordwise Bending Response During Advancing Blade Aeroelastic Limits Testing; $\alpha_s = 0.0^\circ$, $a_{1s} = b_{1s} = 0.0^\circ$, $\Omega_s R = 700$ ft/sec	243
60	Range of Blade Lag Response During Stall Flutter Testing; $Y_{CG}/c = 0.25$, $\alpha_s = 0.0^\circ$, $a_{1s} = b_{1s} = 0.0^\circ$	244
61	Range of Blade Flapwise Bending Response During Stall Flutter Testing; $Y_{CG}/c = 0.25$, $\alpha_s = 0.0^\circ$, $a_{1s} = b_{1s} = 0.0^\circ$	245
62	Range of Blade Torsional Response During Stall Flutter Testing; $Y_{CG}/c = 0.25$, $\alpha_s = 0.0^\circ$, $a_{1s} = b_{1s} = 0.0^\circ$	246
63	Range of Blade Flapping Response During Stall Flutter Testing; $Y_{CG}/c = 0.25$, $\alpha_s = 0.0^\circ$, $a_{1s} = b_{1s} = 0.0^\circ$	247

<u>Figure</u>		<u>Page</u>
64	Range of Blade Lag Response During Combined Advancing Blade Aeroelastic Limits and Stall Flutter Testing; $\alpha_s = 0.0^\circ$, $a_{1s} = b_{1s} = 0.0^\circ$, $\Omega_s R = 700$ ft/sec, $\theta_c = 10.0^\circ$	248
65	Range of Blade Flapwise Bending Response During Combined Advancing Blade Aeroelastic Limits and Stall Flutter Testing; $\alpha_s = 0.0^\circ$, $a_{1s} = b_{1s} = 0.0^\circ$, $\Omega_s R = 700$ ft/sec, $\theta_c = 10.0^\circ$	249
66	Range of Blade Torsional Response During Combined Advancing Blade Aeroelastic Limits and Stall Flutter Testing; $\alpha_s = 0.0^\circ$, $a_{1s} = b_{1s} = 0.0^\circ$, $\Omega_s R = 700$ ft/sec, $\theta_c = 10.0^\circ$	250
67	Range of Blade Flapping Response During Combined Advancing Blade Aeroelastic Limits and Stall Flutter Testing; $\alpha_s = 0.0^\circ$, $a_{1s} = b_{1s} = 0.0^\circ$, $\Omega_s R = 700$ ft/sec, $\theta_c = 10.0^\circ$	251
68	Range of Blade Lag Response During Advancing Blade Aeroelastic Limits Testing at Reduced Simulated Rotational Tip Speed; $\alpha_s = 0.0^\circ$, $a_{1s} = b_{1s} = 0.0^\circ$, $\Omega_s R = 500$ ft/sec	252
69	Range of Blade Flapwise Bending Response During Advancing Blade Aeroelastic Limits Testing at Reduced Simulated Rotational Tip Speed; $\alpha_s = 0.0^\circ$, $a_{1s} = b_{1s} = 0.0^\circ$, $\Omega_s R = 500$ ft/sec	253
70	Range of Blade Torsional Response During Advancing Blade Aeroelastic Limits Testing at Reduced Simulated Rotational Tip Speed; $\alpha_s = 0.0^\circ$, $a_{1s} = b_{1s} = 0.0^\circ$, $\Omega_s R = 500$ ft/sec	254
71	Range of Blade Flapping Response During Advancing Blade Aeroelastic Limits Testing at Reduced Simulated Rotational Tip Speed; $\alpha_s = 0.0^\circ$, $a_{1s} = b_{1s} = 0.0^\circ$, $\Omega_s R = 500$ ft/sec	255
72	Range of Blade Chordwise Bending Response During Advancing Blade Aeroelastic Limits Testing at Reduced Simulated Rotational Tip Speed, $\alpha_s = 0.0^\circ$, $a_{1s} = b_{1s} = 0.0^\circ$, $\Omega_s R = 500$ ft/sec	256
73	United Aircraft Research Laboratories 18-Foot Main Wind Tunnel	257

LIST OF TABLES

<u>Table</u>		<u>Page</u>
I	Ratios of Model Parameters to Full Scale	74
II	Calculated Effect of Inertial Coupling on Flapwise and Torsional Natural Frequencies	75
III	Calculated Natural Modes With Inertial Coupling (Blade C.G. at .30 Chord)	76
IV	Calculated Natural Modes With Inertial Coupling (Blade C.G. at .35 Chord)	77
V	Model Blade Structural Damping Test Results - Bending and Torsional Static Modes	78
VI	Rotor Parameters for Transient Test Conditions (Blade Center of Gravity at .25 Chord)	79
VII	Rotor Parameters for Instability Test Conditions (Blade Center of Gravity at .25 Chord)	85
VIII	Rotor Parameters for Instability Test Conditions (Blade Center of Gravity at .30 Chord)	87
IX	Rotor Parameters for Instability Test Conditions (Blade Center of Gravity at .35 Chord)	88
X	Structural Damping Coefficients for the Rotating Blade (Blade Center of Gravity at .25 Chord)	89
XI	Calculated Flutter Modes	90
XII	Calculated Stall Flutter Conditions	91
XIII	Blade Response During Instability	92
XIV	Blade Nonharmonic Response	93
XV	Maximum and Minimum Blade Motions and Loads (Blade Center of Gravity at .25 Chord, Tangent $\delta_3 = 1.0$)	260
XVI	Maximum and Minimum Blade Motions and Loads (Blade Center of Gravity at .25 Chord, Tangent $\delta_3 = 0.0$)	264
XVII	Maximum and Minimum Blade Motions and Loads (Blade Center of Gravity at .25 Chord, Tangent $\delta_3 = 0.0$)	268

<u>Table</u>	<u>Page</u>
XVIII Maximum and Minimum Blade Motions and Loads (Blade Center of Gravity at .30 Chord, Tangent $\delta_3 = 0.0$)	270
XIX Maximum and Minimum Blade Motions and Loads (Blade Center of Gravity at .35 Chord, Tangent $\delta_3 = 0.0$)	272
XX Blade Lag Motion Harmonics - Run 50 (Blade Center of Gravity at .25 Chord)	273
XXI Blade .30R Flapwise Bending Moment Harmonics - Run 50 (Blade Center of Gravity at .25 Chord)	275
XXII Blade .60R Flapwise Bending Moment Harmonics - Run 50 (Blade Center of Gravity at .25 Chord)	277
XXIII Blade Flap Motion Harmonics - Run 50 (Blade Center of Gravity at .25 Chord)	279
XXIV Blade .35R Torsional Moment Harmonics - Run 50 (Blade Center of Gravity at .25 Chord)	281
XXV Blade Lag Motion Harmonics - Run 51 (Blade Center of Gravity at .25 Chord)	283
XXVI Blade .30R Flapwise Bending Moment Harmonics - Run 51 (Blade Center of Gravity at .25 Chord)	285
XXVII Blade .60R Flapwise Bending Moment Harmonics - Run 51 (Blade Center of Gravity at .25 Chord)	287
XXVIII Blade Flap Motion Harmonics - Run 51 (Blade Center of Gravity at .25 Chord)	289
XXIX Blade .35R Torsional Moment Harmonics - Run 51 (Blade Center of Gravity at .25 Chord)	291
XXX Blade Lag Motion Harmonics - Runs 64-67 (Blade Center of Gravity at .25 Chord)	293
XXXI Blade .30R Flapwise Bending Moment Harmonics - Runs 64-67 (Blade Center of Gravity at .25 Chord)	295
XXXII Blade .18R Torsional Moment Harmonics - Runs 64-67 (Blade Center of Gravity at .25 Chord)	297
XXXIII Blade Flap Motion Harmonics - Runs 64-67 (Blade Center of Gravity at .25 Chord)	299

<u>Table</u>		<u>Page</u>
XXXIV	Blade .35R Torsional Moment Harmonics - Run 64 (Blade Center of Gravity at .25 Chord)	301
XXXV	Blade Lag Motion Harmonics - Run 68 (Blade Center of Gravity at .25 Chord)	302
XXXVI	Blade .30R Flapwise Bending Moment Harmonics - Run 68 (Blade Center of Gravity at .25 Chord)	304
XXXVII	Blade .60R Flapwise Bending Moment Harmonics - Run 68 (Blade Center of Gravity at .25 Chord)	306
XXXVIII	Blade .18R Torsional Moment Harmonics - Run 68 (Blade Center of Gravity at .25 Chord)	308
XXXIX	Blade Flap Motion Harmonics - Run 68 (Blade Center of Gravity at .25 Chord)	310
XL	Blade Lag Motion Harmonics - Runs 69-70 (Blade Center of Gravity at .25 Chord)	312
XLI	Blade .30R Flapwise Bending Moment Harmonics - Runs 69-70 (Blade Center of Gravity at .25 Chord) . .	314
XLII	Blade .60R Flapwise Bending Moment Harmonics - Run 69 (Blade Center of Gravity at .25 Chord)	316
XLIII	Blade .18R Torsional Moment Harmonics - Runs 69-70 (Blade Center of Gravity at .25 Chord)	317
XLIV	Blade Flap Motion Harmonics - Runs 69-70 (Blade Center of Gravity at .25 Chord)	319
XLV	Blade Lag Motion Harmonics - Run 71 (Blade Center of Gravity at .25 Chord)	321
XLVI	Blade .30R Flapwise Bending Moment Harmonics - Run 71 (Blade Center of Gravity at .25 Chord)	323
XLVII	Blade .18R Torsional Moment Harmonics - Run 71 (Blade Center of Gravity at .25 Chord)	325
XLVIII	Blade Flap Motion Harmonics - Run 71 (Blade Center of Gravity at .25 Chord)	327
XLIX	Blade Lag Motion Harmonics - Run 72 (Blade Center of Gravity at .25 Chord)	329
L	Blade .30R Flapwise Bending Moment Harmonics - Run 72 (Blade Center of Gravity at .25 Chord)	331

<u>Table</u>		<u>Page</u>
LI	Blade .18R Torsional Moment Harmonics - Run 72 (Blade Center of Gravity at .25 Chord)	333
LII	Blade Flap Motion Harmonics - Run 72 (Blade Center of Gravity at .25 Chord)	335
LIII	Blade Lag Motion Harmonics - Run 74 (Blade Center of Gravity at .30 Chord)	337
LIV	Blade .30R Flapwise Bending Moment Harmonics - Run 74 (Blade Center of Gravity at .30 Chord)	339
LV	Blade .18R Torsional Moment Harmonics - Run 74 (Blade Center of Gravity at .30 Chord)	341
LVI	Blade Flap Motion Harmonics - Run 74 (Blade Center of Gravity at .30 Chord)	343
LVII	Blade .30R Chordwise Bending Moment Harmonics - Run 74 (Blade Center of Gravity at .30 Chord)	345
LVIII	Blade .35R Torsional Moment Harmonics - Run 74 (Blade Center of Gravity at .30 Chord)	347
LIX	Blade Lag Motion Harmonics - Runs 75-76 (Blade Center of Gravity at .30 Chord)	349
LX	Blade .30R Flapwise Bending Moment Harmonics - Runs 75-76 (Blade Center of Gravity at .30 Chord)	351
LXI	Blade .18R Torsional Moment Harmonics - Runs 75-76 (Blade Center of Gravity at .30 Chord)	353
LXII	Blade Flap Motion Harmonics - Runs 75-76 (Blade Center of Gravity at .30 Chord)	355
LXIII	Blade .30R Chordwise Bending Moment Harmonics - Runs 75-76 (Blade Center of Gravity at .30 Chord)	357
LXIV	Blade .35R Torsional Moment Harmonics - Runs 75-76 (Blade Center of Gravity at .30 Chord)	359
LXV	Blade Lag Motion Harmonics - Runs 77-78 (Blade Center of Gravity at .30 Chord)	361
LXVI	Blade .30R Flapwise Bending Moment Harmonics - Runs 77-78 (Blade Center of Gravity at .30 Chord)	363
LXVII	Blade .18R Torsional Moment Harmonics - Runs 77-78 (Blade Center of Gravity at .30 Chord)	365

<u>Table</u>	<u>Page</u>
LXVIII Blade Flap Motion Harmonics - Runs 77-78 (Blade Center of Gravity at .30 Chord)	367
LXIX Blade .30R Chordwise Bending Moment Harmonics - Runs 77-78 (Blade Center of Gravity at .30 Chord) . .	369
LXX Blade Lag Motion Harmonics - Run 79 (Blade Center of Gravity at .30 Chord)	371
LXXI Blade .30R Flapwise Bending Moment Harmonics - Run 79 (Blade Center of Gravity at .30 Chord)	373
LXXII Blade .18R Torsional Moment Harmonics - Run 79 (Blade Center of Gravity at .30 Chord)	375
LXXIII Blade Flap Motion Harmonics - Run 79 (Blade Center of Gravity at .30 Chord)	376
LXXIV Blade .30R Chordwise Bending Moment Harmonics - Run 79 (Blade Center of Gravity at .30 Chord)	378
LXXV Blade .35R Torsional Moment Harmonics - Run 79 (Blade Center of Gravity at .30 Chord)	380
LXXVI Blade Lag Motion Harmonics - Run 80 (Blade Center of Gravity at .30 Chord)	381
LXXVII Blade .30R Flapwise Bending Moment Harmonics - Run 80 (Blade Center of Gravity at .30 Chord)	383
LXXVIII Blade .18R Torsional Moment Harmonics - Run 80 (Blade Center of Gravity at .30 Chord)	385
LXXIX Blade Flap Motion Harmonics - Run 80 (Blade Center of Gravity at .30 Chord)	387
LXXX Blade .30R Chordwise Bending Moment Harmonics - Run 80 (Blade Center of Gravity at .30 Chord)	389
LXXXI Blade Lag Motion Harmonics - Run 81 (Blade Center of Gravity at .30 Chord)	391
LXXXII Blade .30R Flapwise Bending Moment Harmonics - Run 81 (Blade Center of Gravity at .30 Chord)	393
LXXXIII Blade .18R Torsional Moment Harmonics - Run 81 (Blade Center of Gravity at .30 Chord)	394
LXXXIV Blade Flap Motion Harmonics - Run 81 (Blade Center of Gravity at .30 Chord)	396

<u>Table</u>		<u>Page</u>
LXXXV	Blade .30R Chordwise Bending Moment Harmonics - Run 81 (Blade Center of Gravity at .30 Chord)	398
LXXXVI	Blade Lag Motion Harmonics - Runs 83-84 (Blade Center of Gravity at .35 Chord)	400
LXXXVII	Blade .30R Flapwise Bending Moment Harmonics - Runs 83-84 (Blade Center of Gravity at .35 Chord)	402
LXXXVIII	Blade .60R Flapwise Bending Moment Harmonics - Runs 83-84 (Blade Center of Gravity at .35 Chord)	404
LXXXIX	Blade .18R Torsional Moment Harmonics - Runs 83-84 (Blade Center of Gravity at .35 Chord)	406
XC	Blade Flap Motion Harmonics - Runs 83-84 (Blade Center of Gravity at .35 Chord)	408
XCI	Blade .30R Chordwise Bending Moment Harmonics - Runs 83-84 (Blade Center of Gravity at .35 Chord)	410
XCII	Blade .35R Torsional Moment Harmonics - Run 84 (Blade Center of Gravity at .35 Chord)	412
XCIII	Blade Lag Motion Harmonics - Runs 85-86 (Blade Center of Gravity at .35 Chord)	414
XCIV	Blade .30R Flapwise Bending Moment Harmonics - Runs 85-86 (Blade Center of Gravity at .35 Chord)	416
XCV	Blade .60R Flapwise Bending Moment Harmonics - Runs 85-86 (Blade Center of Gravity at .35 Chord)	418
XCVI	Blade Flap Motion Harmonics - Runs 85-86 (Blade Center of Gravity at .35 Chord)	420
XCVII	Blade .30R Chordwise Bending Moment Harmonics - Runs 85-86 (Blade Center of Gravity at .35 Chord)	422
XCVIII	Blade .35R Torsional Moment Harmonics, Runs 85-86 (Blade Center of Gravity at .35 Chord)	424

LIST OF SYMBOLS

AP	computer symbol for positive cosine component of Pth rotor harmonic in dynamic data (where P is an integer), in.-lb or deg (as stated)
A_{1s}	lateral cyclic pitch with respect to the shaft, deg
a_m	cosine part of a discrete frequency component in the dynamic data
a_{1s}	longitudinal component of blade first harmonic flapping motion at hinge with respect to the shaft, deg (positive for blade low at $\psi = 0^\circ$)
a_{1ss}	flapping component a_{1s} for the initial steady part of a transient data point, deg
BETA	computer symbol for blade flapping at hinge, deg
BP	computer symbol for positive sine component of Pth rotor harmonic in dynamic data (where P is an integer), in.-lb or deg (as stated)
B_{1s}	longitudinal cyclic pitch with respect to the shaft, deg
b	number of blades
b_m	sine part of a discrete frequency component in the dynamic data
b_{1s}	lateral component of blade first harmonic flapping motion at hinge with respect to the shaft, deg (positive for blade low at $\psi = 90^\circ$)
b_{1ss}	flapping component b_{1s} for the initial steady part of a transient data point, deg
C_o	blade reference chord, ft
C_L/σ	rotor lift coefficient-solidity ratio, $C_L/\sigma = L/\pi R^2 \rho (\Omega R)^2 \sigma$
C_D/σ	rotor drag coefficient-solidity ratio, $C_D/\sigma = D/\pi R^2 \rho (\Omega R)^2 \sigma$
C_Y/σ	rotor side force coefficient-solidity ratio, $C_Y/\sigma = Y/\pi R^2 \rho (\Omega R)^2 \sigma$
C_Q/σ	rotor torque coefficient-solidity ratio, $C_Q/\sigma = Q/\pi R^3 \rho (\Omega R)^2 \sigma$
C_{PM}/σ	rotor pitching moment-solidity ratio, $C_{PM}/\sigma = PM/\pi R^3 \rho (\Omega R)^2 \sigma$

C_{RM}/σ	rotor rolling moment coefficient-solidity ratio, $C_{RM}/\sigma = RM/\pi R^3 \rho (\Omega R)^2 \sigma$
c	blade chord, ft (unless otherwise stated)
D	rotor drag force, lb, positive rearward
DELTA 3	computer symbol for pitch flap coupling angle, deg, $\text{DELTA}3 = \delta_3 = \arctan (-\partial\theta_0/\partial\beta)$
E	Young's modulus, lb/in. ² (for the fiber glass blade bending, $E = 2.25 \times 10^6$ lb/in. ²)
E_1	"A" actuator extension (degrees A_{1s} when B_{1s} and θ_c are zero)
E_2	"B" actuator extension (degrees B_{1s} when A_{1s} and θ_c are zero)
E_3	collective follower position (degrees of collective pitch)
e	base of the system of natural logarithms
F_c	optional constant correction value, in.-lb or deg, (as stated)
f_{SN}	blade static natural frequency
GJ	blade torsional stiffness, lb-in. ²
g	structural damping coefficient
I_c	blade cross-section area chordwise moment of inertia, in. ⁴
I_F	blade cross-section area flapwise moment of inertia, in. ⁴
I_θ	blade torsional mass moment of inertia per unit span, lb-sec ²
L	rotor lift force, lb, positive up
M_m	blade mass per unit span, lb/in.
$M_{1.90}$	actual blade tip Mach number at $\psi = 90^\circ$
M_T	generalized mass of the blade first torsional natural mode, ft-lb-sec ² , $M_T = \int_0^R I_\theta [W_{T1}(x)]^2 dr$
MU	computer symbol for advance ratio ($\mu = V_S/\Omega_S R$)
$M_{F.30R}$	blade flapwise bending moment at 0.30R, in.-lb, positive for upward bending
$M_{F.60R}$	blade flapwise bending moment at 0.60R, in.-lb, positive for upward bending

$M_{C.30R}$	blade chordwise bending moment at 0.30R, in.-lb, positive for rearward bending
$M_{T.18R}$	blade torsional moment at 0.18R, in.-lb, positive for nose-up twisting
$M_{T.35R}$	blade torsional moment at 0.35R, in.-lb, positive for nose-up twisting
m	an integer
N	actual rotor rotational speed, rpm
n	an integer
ΩS^*R	computer symbol for simulated rotational tip speed, ($\Omega_s R$), ft/sec
P	an integer
PM	rotor pitching moment, positive nose up, ft-lb
Q	rotor torque, positive for motor driving rotor, ft-lb
Q_{ij}	conversion coefficient for the transformation of actuator positions E_1, E_2, E_3 into control inputs A_{1s}, B_{1s} , and θ_c
q_{FPn}	amplitude of the Pth flapwise natural mode contribution to the nth flutter mode
$q_{\theta Pn}$	amplitude of the Pth torsional natural mode contribution to the nth flutter mode
R	rotor radius, ft (unless otherwise stated)
R_A	amplitude ratio of successive cycles of a damped vibration
R_c	physical equivalent of calibration signal, in.-lb or deg (as stated)
RM	rotor rolling moment, positive for starboard side down, ft-lb
RP	amplitude of Pth rotor harmonic in dynamic data (where P is an integer), in.-lb or deg (as stated)
RS	average value of dynamic data, in.-lb or deg (as stated)
r	distance along a rotor radius, in. (unless otherwise stated)
r_m	resultant amplitude of a discrete frequency component in the dynamic data, in.-lb or deg (as stated)

S	ratio of full-scale to model size
T	a time interval of arbitrary length, sec
THEC	computer symbol for collective pitch (θ_c), deg
t	time, sec
V	actual forward speed, kn
V _s	simulated forward speed, kn
W _D	instantaneous value of dynamic data, in.-lb or deg (as stated)
W _{FP} (x)	flapwise blade deflection as a function of fractional radius for the Pth flapwise natural mode, normalized to unit tip deflection, in.
W _n (x,t)	flapwise blade deflection for the nth linear combination (nth flutter mode) of flapwise natural modes, in.
W _n (1.)	amplitude of W _n (x,t) at the blade tip, in.
W _O	average of digital tape values from a dynamic zero point
W _R	average of digital tape values from a "RCAL" calibration record
W _T	individual data value on the digital tape
W _{TP} (x)	torsional blade deflection as a function of fractional radius for the Pth torsional natural mode, normalized to unit tip deflection, rad
W _Z	average of digital tape values from a "ZCAL" calibration record
x	rotor fractional radius, $x = r/R$
Y	rotor sideforce, positive to starboard, lb
Y _{CG/c}	blade center-of-gravity position aft of blade leading edge, divided by blade chord
ZETA	computer symbol for blade lag at hinge, deg
α_c	rotor control axis angle of attack, deg, $\alpha_c = \alpha_s - \beta_{1s}$
α_f	fuselage angle of attack, deg
α_s	shaft angle of attack, deg (for this test, $\alpha_f = \alpha_s$)

β	blade flapping at hinge, deg (unless otherwise stated)
Δa_{1s}	increment in a_{1s} applied during a transient condition, deg
Δb_{1s}	increment in b_{1s} applied during a transient condition, deg
$\Delta \theta_c$	increment in θ_c applied during a transient condition, deg
$\Delta \psi$	increment of ψ between digital values of dynamic data, deg
δ_3	pitch-flap coupling angle, deg, $\delta_3 = \arctan(-\partial \theta_o / \partial \beta)$
ζ	blade lag angle at hinge, deg
ζ_{AD}	critical damping ratio of blade torsional mode from stall flutter calculations
ζ_{CF}	critical damping ratio of an aeroelastic mode from classical flutter calculations
θ_o	blade pitch angle with respect to the plane of rotation at the control horn, deg, $\theta_o = \theta_c - A_{1s} \cos \psi - B_{1s} \sin \psi - \beta \tan \zeta_3$
θ_c	collective pitch, deg
θ_{cs}	collective pitch for the initial steady part of a transient data point, deg
$\theta_{en}(x,t)$	torsional blade deflection for the nth linear combination (nth flutter mode) of torsional natural modes, rad
$\bar{\theta}_n(1.)$	amplitude of $\theta_{en}(x,t)$ at the blade tip, rad
λ	uniform inflow velocity divided by rotational tip speed
λ_n	real part (decay) of the eigenvalue for the nth aeroelastic mode from the classical flutter calculations
μ	advance ratio $\mu = V_B / \Omega_B R = V / \Omega R$
$\Xi_{\alpha 3}$	integrated stall flutter torsional damping parameter
ρ	air density, slugs/ft ³
σ	rotor solidity $\sigma = bc / \pi R$
ϕ_m	phase angle of a discrete frequency component in the dynamic data, rad
$\phi_{nw}(1.)$	phase of flapwise motion at the blade tip for the nth aeroelastic mode, deg

$\phi_{n\theta}^{(1.)}$	phase of torsional motion at the tip for the nth aeroelastic mode, deg
ψ	azimuth position of rotor blade, zero over the tail, and increasing in a counterclockwise sense as seen from above, deg
Ω	actual rotor rotational speed, rad/sec
Ω_s	simulated rotor rotational speed, rad/sec
$\Omega_s R$	simulated tip speed, ft/sec
ω	frequency, rad/sec
ω_m	discrete frequency of an amplitude component present in the dynamic data, rad/sec
ω_n	frequency of the nth aeroelastic mode from classical flutter calculations, rad/sec
ω_T	stall flutter frequency (assumed equal to the blade first torsional natural frequency), cps

SUBSCRIPTS

i	imaginary part of a complex quantity
r	real part of a complex quantity
v	vibratory amplitude of dynamic data

INTRODUCTION

ROTOR TRANSIENT CHARACTERISTICS

Helicopter response to control inputs depends on the rotor blade behavior during and following the input. If the control input is rapid, blade response may become greater than that experienced during the steady-state conditions before and after the transient. In addition, the sudden application of a control change may trigger a rotor instability if that tendency exists because of rotor operating condition or blade configuration. The time required to reach a steady-state condition following a control change is some indication of the time required to reach a steady-state condition following a sharp gust disturbance. Experimental information on transient behavior of a rotor demonstrates the suitability of that aspect of rotor operation for a particular configuration, and aids in the development of theories for the calculation of rotor transient response.

The method reported in Reference 1 can, in principle, provide a theoretical prediction of rotor response to a transient, and this capability was utilized in Reference 2. Rotor transient airloads were also investigated as reported in Reference 3. One of the basic obstacles to obtaining transient control input rotor data in the wind tunnel has been the lack of a sufficiently fast-acting control system. The control transients applied during this test program were essentially complete after approximately one-fourth of a revolution.

Samples of the transient data obtained during this test program were compared with theoretical data which was calculated by the method of Reference 1. The transient behavior of the dynamically scaled model was measured at simulated forward speeds up to 300 knots with and without pitch-flap coupling. A variety of control inputs were investigated, including pure collective inputs, pure cyclic inputs for various amounts of longitudinal and lateral flapping, and various combined cyclic and collective inputs.

AEROELASTIC INSTABILITY

The operation of new rotor designs and the penetration of unfamiliar rotor operating regimes require that careful attention be given to rotor blade aeroelastic behavior in general, and especially to the possibility of catastrophic instabilities.

In order to predict rotor blade aeroelastic behavior, various theoretical methods have evolved. Confident use of these theories requires that suitable test results be obtained to verify the calculated behavior. Sufficiently detailed test results also provide invaluable guidance for the improvement of the theories.

The aeroelastic theories of rotor blade instability vary widely in complexity. Reference 4 describes a simple torsion-flapping static

stability analysis. Reference 5 contains the far more elaborate development of a fixed-azimuth flutter analysis which is mathematically similar to a fixed-wing analysis. The method of Reference 6 considers the time-varying coefficients in the blade differential equations of flutter motion. Finally, the method of Reference 1 is a timewise, step-by-step integration of the complete blade equations of motion.

A comparison of the fixed-azimuth flutter theory calculation with earlier test data and with some calculations by the method of Reference 6 appears in Reference 5.

The use of a dynamically scaled model appears to offer the best set of compromises for the experimental study of rotor instability, since the destruction of the model will not result in a loss of personnel or aircraft.

The test program and resulting data that are described in this report demonstrate the operation of the fully articulated rotor for extreme conditions. Previously developed discrete-azimuth blade aeroelastic stability theories for torsional divergence, classical flutter, and stall flutter are described. The results of applying these theories to the dynamically scaled model are presented and compared to the behavior of the model during the test.

During the testing, a number of violent instabilities were encountered, which may not be suitable for analysis with discrete-azimuth theories. These instabilities arose suddenly, with no perceptible warning from blade stress or motion measurements that an unstable condition was about to be encountered.

DESCRIPTION OF MODEL

GENERAL

The Sikorsky Aircraft Compound Helicopter Model is a generalized configuration suitable for a transport compound helicopter. The model scale is considered to be one-eighth of full size, representing an aircraft of approximately 40,000 pounds gross weight. Figure 1 depicts the model mounted in the 18-foot UARL Wind Tunnel for previous tests. In the test program described in this report, the model configuration consisted of the rotor and the fuselage only. Figure 2 is a dimensioned three-view drawing of the model. It is important to note that the rotor, rotor drive system, and rotor control system were all mounted on a six-component strain gage balance, which was itself mounted on the basic keel structure of the model. The entire model was rigidly supported through the keel structure on a single main support strut and a pitch strut.

ROTOR SYSTEM

The dynamically scaled 9-foot-diameter model rotor that was tested to provide the data described in this report was of a conventional articulated type, with both flapping and lag hinges. The four untwisted blades had a 0.353-foot chord, which resulted in a solidity (σ) of 0.100. The coincident flapping and lagging hinge was located at a fractional radius of 0.0555. The lag hinge was restrained by a viscous damper, which was set at a damping constant of 1.39 foot-pound-seconds. The blade airfoil section was NACA 0012. Provision was made for the adjustment of blade pitch-flap coupling angle (δ_3). This parameter was set at 45 and 0 degrees for the transient testing, and at 0 degrees for the instability testing.

FUSELAGE

The fuselage was a streamlined fiber glass shell which was mounted independently to the basic keel structure of the model. A separate fuselage strain gage balance was available for measuring fuselage aerodynamic loads, although this capability was not needed for this test program. The fuselage frontal area was 1.25 square feet, and the total fuselage length was 9 feet.

DRIVE SYSTEM

The rotor was powered by a variable-speed 19-horsepower electric motor, through a transmission which provided a speed reduction of approximately 13.5 to 1. The rotor speed could be set at any desired value within the motor power limitations.

CONTROL SYSTEM

Rotor cyclic and collective pitch angles were remotely controlled by the model operator through an electrically controlled hydraulic servo system. The cyclic and collective pitch were applied to the blades through a conventional swash plate mechanism, which was controlled by three actuators. The motions of the three actuators were automatically coordinated so that the motion of the corresponding dial on the model control console applied lateral cyclic pitch (A_{1s}), longitudinal cyclic pitch (B_{1s}), or collective pitch (θ_c). The control console was furnished with two sets of the above three control knobs, which can be termed the basic and transient increment controls. The basic controls were applied to the model immediately as the dials were moved. The settings of the transient increment knobs were automatically added to those on the basic controls by turning on a control switch. This made it possible to suddenly apply a control increment by setting the transient increment knobs, and then turning the control switch on. The transient control switch was duplicated as part of an automatic system to be discussed under the heading "Test Procedure and Initial Observations". This automatic system was necessary to coordinate tape recorder operation and transient application at a constant blade azimuth angle.

BLADES

General Description

The dynamically scaled blades were fiber glass replicas of typical full-scale construction, similar to those described in Reference 8. Figure 3 is an exploded view showing the blade construction and external dimensions.

For the purposes of this test program, the chordwise center of gravity of the blades was changed from the normal 25 percent chord to the 30 percent and the 35 percent chord position. The blade leading edge counterweights could not be removed from the existing blades, so an alternate method had to be used to alter the center-of-gravity position.

The most practical method for accomplishing the center-of-gravity position change was found to be the cementing of individual steel weights along the trailing edge of each "pocket". The weights measured 2.22 inches in the spanwise direction, 0.46 inch in the chordwise direction, and were 0.02 inch thick. The weights were cemented to the lower surface of the trailing edge to move the center of gravity to the 30 percent chord position, and to both the upper and the lower surface to move the center of gravity to the 35 percent chord position.

The blade Lock number was 5.84 for the blade with the center of gravity at the 25 percent chord position. For the blades with the 30 percent and 35 percent chord center-of-gravity positions, the Lock numbers were 5.43 and 5.03 respectively.

The blade-distributed mass and stiffness properties are shown in Figures 4 and 5. The addition of the trailing edge weights resulted in only a small change in blade mass per inch of span. The torsional mass moment of inertia was changed significantly, with a corresponding decrease in torsional frequency. Since the weights were attached individually to the nonstructural pockets making up the aft portion of the blade, they had a negligible effect on blade stiffness.

Discussion of Blade Dynamic Scaling

The blade flapwise, chordwise, and torsional stiffnesses were scaled so that they were one-fourth as stiff as geometrically similar blades built of aluminum. The blades were weighted so that their mass was equal to the mass of the aluminum blades. This resulted in blade natural frequencies which were one-half those of the aluminum blades. Operation of the fiber glass dynamically scaled rotor at an arbitrary condition simulated the operation of the aluminum bladed model rotor at rotational and forward speeds twice as high. This simulation included most of the rotor parameters which have a strong effect on aeroelastic behavior. The forces and accelerations were approximately one-fourth those of the aluminum model at the simulated condition. Velocities and frequencies were approximately one-half those of the simulated condition, and displacements were approximately the same. Reynolds and Mach number effects were not included in the simulation. The use of the reduced-stiffness model greatly expanded the regime of possible rotor operating conditions which could be reached within the wind tunnel limitations. The model power required was also approximately one-eighth that required for full-scale operating speeds.

The effect of dynamic scaling on various rotor parameters is summarized in Table I. The dynamically similar blades whose properties are listed in Table I are the fiber glass blades used for this test, and an aluminum blade of equal size and mass properties but with four times the elastic stiffness. They are related to a hypothetical full-scale aluminum prototype, geometrically similar to the models, with a size scaling factor S with respect to the models. These results have been obtained by using recognized dynamic scaling theory, as discussed in Reference 8.

Natural Frequencies and Mode Shapes

The uncoupled flapwise bending, chordwise bending, and torsional natural frequencies and modes were calculated. The calculated uncoupled natural frequencies are presented as a function of rotor rpm in Figures 6, 7, and 8. The results are shown for the three blade center-of-gravity configurations. The addition of the trailing edge weights had a very small effect on the bending natural frequencies and an appreciable effect on the torsional frequencies. The calculated flapping and lagging natural frequencies about the blade hinges were 1.044 and 0.309 cycles per revolution respectively. The addition of the trailing edge weights had a negligible effect on the flapping and lagging natural frequencies. The first uncoupled flapwise bending, chordwise bending, and torsional mode shapes are plotted in Figures 9, 10, and 11. The trailing edge weights had, as

expected, a very small effect on the uncoupled bending mode shapes and a negligible effect on the torsional mode shape.

The effect of flapwise-torsion coupling on the natural vibration of the blade was studied by using the uncoupled natural modes in the blade classical flutter program. In order to study the natural vibration of the blade with the flutter program, the air density was set at an infinitesimally small value. The output of the flutter program was a new set of natural frequencies, with inertial coupling considered. The modes corresponding to these frequencies were calculated as linear combinations of the input uncoupled mode shapes. Expressing this concept mathematically, a coupled modal flapwise deflection at an arbitrary fractional radius is given by

$$w_n(x,t) = [q_{F1n} w_{F1}(x) + q_{F2n} w_{F2}(x) + q_{F3n} w_{F3}(x) + q_{F4n} w_{F4}(x)] \cos \omega_n t \quad (1)$$

In a similar fashion, the torsional deflection at an arbitrary fractional radius is given by

$$\theta_{en}(x,t) = [q_{\theta 1n} w_{T1}(x) + q_{\theta 2n} w_{T2}(x)] \cos \omega_n t \quad (2)$$

Note that all the natural modes have at least a small amount of both flapwise and torsional motion when coupling is present. The subscript n in the above equations refers to a particular coupled mode.

The frequencies of the coupled modes are given in Table II; note that the coupled modal frequencies are quite close to the uncoupled modal frequencies.

The contributions of each uncoupled mode to the coupled natural modes are given in Table III for the blade with the center of gravity at the 30 percent chord. Also shown in Table III are the corresponding resultant blade tip motions. Similar results are given in Table IV for the blade with the center of gravity at the 35 percent chord. The last two columns in these tables are the blade tip motion amplitudes during natural vibrations. Note that the modes are normalized to a flapwise tip vibration of approximately 1 inch or a torsional tip vibration of 1 radian.

The flapwise and chordwise natural frequencies increase markedly with rotor RPM, while the torsional natural frequencies are affected very slightly. This familiar result causes torsional and certain flapwise modal frequencies to be equal at certain rotor rotational speeds. When coupling is present, as in the blades used for this test, the relative amounts of flapwise and torsional motion in a given mode will change markedly as the rotor speed for equal flapwise and torsional frequency is approached. This is evident in the results presented in Tables III and IV. Operating the rotor at a speed for a flapwise and torsional mode of equal frequency could conceivably result in unfavorable coupling and a tendency to flutter. It is also possible that favorable coupling may exist, with a reduction in blade vibration.

Static Testing

Static Load Calibration

Each of the instrumented blades used in this test was supported as a cantilever, known static loads were applied in the flapwise and chordwise directions, and the tip deflection was noted. The blades were then loaded with known torsional couples, and the blade twisting deflection was observed. This procedure related known loads to cantilever tip deflections. The calibration with respect to the strain gage bending and torsional bridges was conveniently carried out by applying known cantilever deflections and by observing the output of the instrumentation. By using the load-deflection relationship, the output of the strain gage instrumentation was related to local blade bending and twisting moments.

Structural Damping and Natural Frequency

The structural damping, static natural frequencies, and hinge bearing friction of the model blades were determined by test on the nonrotating blades. The information was obtained by hanging the blade vertically on its bearings in the rotor head, with the lag damper disconnected. A vibratory force was applied with a variable frequency pulsating air jet. Frequency was varied and the blade response noted by monitoring strain gage output on an oscillograph. When a resonant peak was encountered, the air jet was instantaneously interrupted, and the decay of vibrations was recorded on the oscillograph. Frequency and structural damping values were obtained from the decay records. As indicated on the results tabulated in Table V, data was not obtained for all the listed modes of each blade tested. Enough data was obtained to permit evaluation of the effects of structural damping on the wind tunnel test results. Comparison of the test frequencies with the calculated static frequencies in Table II shows that satisfactory agreement exists. The blade hinge bearing friction under light load was obtained by recording the decay of blade motion as it was allowed to swing on its bearings in the rotor head, while suspended vertically. Examination of the decay records showed that blade pendulum motion suddenly ceased when the amplitude decayed to a certain level, indicating that damping was of a Coulomb rather than a viscous type. Following the blade swing tests, similar tests were performed with the blade replaced by a pendulum loaded with various weights. The radius of gyration of the loaded pendulum was approximately equal to that of the blade, so that all pendulum tests were carried out at the same frequency. Practical considerations did not permit loading the pendulum to the equivalent of centrifugal force at full RPM, but the loadings used were sufficient to establish the bearing friction coefficient. Following the pendulum tests, the blade flapping bearings were removed from the rotor head and mounted in a special fixture, which permitted blade swing tests in the same set of bearings in the flapwise and chordwise direction. This final test was performed to demonstrate whether or not aerodynamic damping had any

appreciable effect on the static blade damping tests. The results of the blade swing and pendulum tests are presented in Figure 12. The effective Coulomb friction torque was calculated from the decay records by using the known blade mass properties and by assuming that all changes in amplitude were caused by classical Coulomb friction.

The blade damping data obtained for the nonrotating case must be considered in terms of its effect on the rotating blade. The primary effect of blade rotation is to greatly reduce the significance of structural damping on blade flapping and bending modes. For this reason, the scatter evident in the blade static damping measurements can be considered unimportant. This subject will be discussed in greater detail under the report subheading on classical flutter.

Relationship of Fiber Glass Blade Loadings to Aluminum Blade Stresses

The extreme fiber stresses were measured for known bending moments on a geometrically similar aluminum model blade, and the torsional stresses were measured at spar mid-chord for known twisting couples. These stresses would be the same on a geometrically similar full-scale prototype 8 times larger than the model, under bending moments and twisting couples 8^3 times as large. The similar loads applied to the fiber glass model to produce the same bending and twisting deflections are one-fourth those applied to the aluminum model. This provides an equivalence relationship between fiber glass model bending and twisting moments and model and full-scale aluminum blade stresses under dynamically similar operating conditions. Thus, 60 inch-pounds of flapwise moment on the fiber glass model corresponds to 10,000 psi stress on the aluminum blades. Similarly, 125 inch-pounds of chordwise moment and 85 inch-pounds of torsional moment correspond to 10,000 psi stress.

TEST PROCEDURE AND INITIAL OBSERVATIONS

In addition to actual data points, each wind tunnel run consisted of calibration records, static zero points, and dynamic zero points.

Prior to the start of each wind tunnel run, a series of calibration records was automatically placed on each magnetic tape data channel. The series consisted of a record of zero electrical input, a record of known electrical input which corresponded to a transducer output for a known physical quantity, and a record of transducer output from the model with the rotor stationary and the wind tunnel off. In later discussions of data reduction, these calibration records will be referred to as "ZCAL", "RCAL", and "XCAL" records respectively.

When the calibration records were complete, the static zero points were obtained. These were data records taken with the model rotor stationary and the wind tunnel off. For cases where model angle of attack was to be varied during the run, static zeros were taken at positive, zero, and negative angles of attack. These data were used primarily to provide weight tare corrections for rotor balance data reduction.

Following the static zero points, the rotor was brought up to speed and the dynamic zero points were taken. These data were taken with the wind tunnel off and the rotor at zero cyclic and collective pitch. Under these conditions, blade flapping, bending, and torsional loadings were considered zero. The dynamic zero data provided a physical zero reference for most of the data channels.

After the dynamic zero was obtained, the wind tunnel was turned on and the actual data points were taken. At the conclusion of the run, a final dynamic zero, a second set of static zeros, and a second set of calibration records were taken.

During the test, selected dynamic data channels were monitored on an oscilloscope to determine that blade moment limits were not exceeded. All dynamic channels could also be displayed on an oscillograph for on-line operational checking. Provision was also made for on-line frequency analysis of dynamic data. It was expected that inspection of successive on-line spectra would reveal incipient instability before dangerous conditions were reached. In practice, it was found that dangerous instabilities could be encountered very suddenly. In most cases, no appreciable excitation of the incipient unstable mode was present before the dangerous condition was entered. The on-line frequency analysis equipment did indicate that certain expected frequency responses were actually occurring.

TRANSIENT TESTING

The phase of the wind tunnel tests during which the rotor blade transient response data were obtained involved variations of the following operational parameters:

<u>Parameter</u>	<u>Range of Variation</u>
Pitch-Flap Coupling	$\tan \delta_3 = 1.0, 0.0$
Forward Speed	$V_s = 120, 200, 300$ knots
Shaft Angle of Attack	$\alpha_f = -8, -4, 0, 4, 8$ degrees
Collective Pitch	$\theta_c = 0$ to 12 degrees
First Harmonic Flapping	$a_{1s} = -8$ to +4 degrees $b_{1s} = -4$ to +2 degrees

Seventy-nine separate conditions were used as initial operating points. The parameter settings for these points and the corresponding final operating points are listed in Table VI. The rotor speed-forward speed combinations tested are shown in Figure 13.

During this phase of the tests, two different data acquisition procedures were followed. At normal steady-state conditions, rotor and tunnel parameters were set, and the magnetic tape system was manually activated and automatically shut down after a prespecified recording time determined from the rotor speed. The record lengths were normally 5 to 10 seconds. Following the magnetic tape shutdown, the rotor balance data were manually recorded from Baldwin SR-4 strain indicators. A specially designed automatic system was used to actuate the magnetic tape system during the transient conditions. The functions of this system are described in step 9 below. The experimental procedure followed for each of the 79 sets of test points was as follows.

1. The initial steady-state operating condition was established, and dynamic and rotor balance data were taken in the normal way.
2. The transient increment controls for $\Delta\theta_c$, Δa_{1s} , and Δb_{1s} were set for zero increment.
3. The transient control switch was turned on.
4. The test final operating condition was established by slowly dialing the transient increment controls.
5. Dynamic and rotor balance data were taken in the normal way, and the settings of the transient increment controls were recorded.

6. The transient increment controls were returned to zero increment, reestablishing the initial steady-state condition.
7. The transient control switch was turned off.
8. With the transient increment controls deactivated, the settings recorded in step 5 were redialed. The rotor operating condition remained at the initial steady-state condition.
9. Control was transferred to the automatic system that:
 - (a) activated the magnetic tape system
 - (b) paused 3 seconds while the initial steady-state dynamic data were recorded
 - (c) turned on the transient increment controls which were activated by the next zero rotor azimuth signal
 - (d) shut down the magnetic tape system after a pre-specified recording time
10. Rotor balance data for the post transient steady-state condition were recorded from the strain indicators.

For each of the transient conditions, the rotor was observed to reach its final state rapidly and smoothly.

INSTABILITY TESTING

Advancing Blade Aeroelastic Limit

Each of the blade configurations was operated at a simulated rotational tip speed ($\Omega_s R$) of 700 ft/sec. The collective pitch was left at a constant setting, while rotor first harmonic flapping was kept at zero by using cyclic pitch. Data were taken at successively higher tunnel speeds, as shown by the upper rows of points in Figure 14. In the case of the 25 percent chord and 30 percent chord center-of-gravity configurations, the tunnel speed was limited by excessive model vibration. (Figure 35 shows sample data from this part of the test. The superimposed time history of torsional response for two successive revolutions is shown.) In the case of the 35 percent chord center-of-gravity configuration, the tunnel speed was limited by a violent rotor instability, which appeared suddenly as speed was being increased without any discernible warning from on-line monitoring equipment.

The tunnel speed limits for the 30 percent chord center-of-gravity blade and the 35 percent chord center-of-gravity blade were also found in a similar manner at a simulated rotational tip speed ($\Omega_s R$) of 500 ft/sec. With the 30 percent chord center-of-gravity blade, the tunnel speed was again limited by model vibration. Another violent instability was encountered with the 35 percent chord center of gravity. In this case, seemingly stable operation was obtained at the actual condition of

instability, and data were taken before the sudden onset of violent nonharmonic blade motions and high stresses. Time history data of blade loadings and motions were obtained with the on-line oscillograph just after tunnel power was terminated. (These data appear in Figure 46.) Post-test analysis of the data taken immediately before this incident showed a relatively small amount of random nonharmonic blade motion and stress.

Retreating Blade Aeroelastic Limit

The three different blade center-of-gravity configurations were operated at high tunnel speed, and data was taken at constant collective pitch and zero first harmonic flapping for successively lower rotational speeds, as shown by the right-hand vertical rows of points in Figure 14. Advance ratios ($V_s/\Omega_g R$) of approximately 1.4 were reached at a simulated forward speed of 328 knots with the 25 percent chord and 30 percent chord center-of-gravity configurations. The limitation to further reductions in rotational speed was due to increasing torsional stress. (Figure 34 shows sample data from this part of the test. The superimposed time history of torsional response for two successive revolutions is shown.) Coupled flapping and lagging motions at a frequency of 0.25 cycle per revolution were noted during post-test data reduction for the highest advance ratios reached. These motions were small but growing rapidly with increasing advance ratio when the blade torsional stress limit was reached. The cyclic pitch requirements for the removal of blade flapping at the higher advance ratio conditions were large enough to cause the rotor to operate in a negative lift condition.

The 35 percent chord center-of-gravity configuration blade was operated at a simulated forward speed of 232 knots during this phase of the testing, and an advance ratio limit of approximately 1.6 was reached, with further decreases in rotational speed limited by impending loss of control.

It should be noted that the retreating blade aeroelastic limits for all three blade configurations were encountered in a gradual or "soft" manner, and no dangerous blade motions or stresses were experienced in this phase of the testing.

Stall Flutter

The 25 percent chord and 30 percent chord center-of-gravity blades were operated at simulated speeds of 120 knots, 144 knots, 168 knots, and 200 knots. The simulated rotational tip speed ($\Omega_g R$) was kept at 700 ft/sec, and blade first harmonic flapping was kept at zero by using cyclic pitch. At each speed, data were obtained at successively higher collective pitch settings. Moderately high torsional stresses were encountered, but no dangerous or stress-limited conditions were encountered. The maximum collective pitch of approximately 12 degrees was defined by control system limitations. (Figure 43 shows sample data from this part of the test. The superimposed time history for two successive revolutions is also shown.)

The behavior of the 35 percent chord center-of-gravity blade was again dramatically different from the other two configurations. Attempts to raise the collective pitch past 7 degrees at a simulated forward speed of only 120 knots and a simulated rotational speed of 700 ft/sec resulted in still another violent instability. Time history data of blade loadings and motions were obtained with the tape recorder as the wind tunnel was shut down. (These data appear in Figure 47.) Data taken at the same condition with a collective pitch of 5 degrees showed no evidence of impending instability, either from the standpoint of stress or motion amplitude or from the results of frequency analysis.

Combined Stall Flutter and Advancing Blade Aeroelastic Limits

The 25 percent chord and 30 percent chord center-of-gravity blade configurations were operated at forward speed and rotational speed combinations encountered during the Advancing Blade Aeroelastic Limits testing previously described. Blade first harmonic flapping was again kept at zero. The collective pitch was raised as far as possible at each speed, and data were taken.

This phase of the testing was generally limited by the cyclic pitch available from the rotor control system. It was possible to operate the rotor with zero blade first harmonic flapping at a collective pitch as high as 10 degrees at a simulated forward speed of 330 knots. The 30 percent chord center-of-gravity blade did encounter stress limitations at simulated speeds higher than 290 knots. The testing of the 35 percent chord center-of-gravity blade was very restricted for this phase, with collective pitch limited to 5 degrees for the prevention of instability.

Flapping Limits

Each of the blade center-of-gravity configurations was operated at a simulated forward speed of 180 knots, constant collective pitch, and zero first harmonic flapping. Data were taken at successively lower rotational speeds, as shown by the left-hand vertical rows of points in Figure 14, until rotor response to control changes became excessively sluggish. All blade configurations behaved similarly for this part of the test. No discrete frequency subharmonic motions were discernible, although random variations in blade flapping motion were present. Advance ratios of approximately 1.6 were reached during this part of the test.

Combined Flapping and Retreating Blade Aeroelastic Limit

The 25 percent chord and 30 percent chord center-of-gravity blade configurations were operated at gradually increasing simulated forward speeds between 180 and 328 knots, as shown by the lower rows of points on Figure 14. At each tunnel speed, the rotational speed was reduced until control response was excessively sluggish or blade stress was becoming too high. Collective pitch was kept constant, and blade first harmonic flapping was kept at zero. The two blade configurations behaved in similar fashion during this phase of the testing. The highest advance ratio reached with the rotor controllable was approximately 1.91, at a

simulated forward speed of 258 knots. At a simulated forward speed of 280 knots and an advance ratio of 1.94, control of the rotor was actually lost, and a retreating blade nearly struck the fuselage. Control was immediately regained by bringing up rotational speed.

DESCRIPTION OF DATA AND DATA REDUCTION

MEASURED QUANTITIES

Tunnel Parameters

The barometric pressure, tunnel test section to settling chamber differential pressure, and tunnel settling chamber temperature were recorded manually.

Model Parameters

The rotor rotational speed, shaft angle of attack, control console dial settings, first harmonic flapping resolver output, and rotor balance output were recorded manually.

Dynamic Data

The positions of two of the three swash plate actuators and the collective follower positions were measured to define swash plate motion. Blade flapping and lagging motions were measured at the respective blade hinges. Blade flapwise and chordwise bending moments were measured at 30 percent and 60 percent of the rotor radius, and blade torsional moment was measured at 18 percent and 35 percent of the rotor radius. These data were recorded on the F.M. magnetic tape recorder. Additional data supplied to the magnetic tape were a zero azimuth signal, which occurred when the instrumented blade passed over the tail of the model, and a 60-per-revolution sample command signal, which was electronically doubled for off-line analogue to digital conversion.

ROTOR PERFORMANCE DATA

Signals from the six-element rotor balance were manually recorded from Baldwin SR-4 Precision Indicators (Type L-50). Wind tunnel parameters were also manually recorded. These data were transferred to punched cards and reduced and tabulated by a UNIVAC 1108 digital computer. The data reduction program, using appropriate wind tunnel operating parameters, resolved the balance data into six wind-axis forces and moments. Force data were corrected for the effects of gravity, and wind tunnel corrections based on the methods described in References 9 and 10 were applied. The blockage correction to velocity was less than 2 percent of the wind tunnel velocity, and the wall correction to angle of attack was no greater than 0.5 degree. Rotor head aerodynamic lift and drag tares were removed from the reduced data, and all forces and moments were converted to coefficient form and tabulated.

Rotor operating conditions and performance for each data point of the program appear in Tables VI through IX. Each transient case gave rise to three rotor performance readings as discussed in the Test Procedure. The first of these was a reading taken for the initial steady state. The second was a reading of the final steady-state condition entered with the

controls moved slowly. The third reading was taken after the transient input had taken place and the rotor had reached its final steady state. In the tables, these points are called "initial", "test final", and "post transient" respectively.

DYNAMIC DATA

The dynamic data included rotor control motions, blade motions, and blade moments. For the purposes of this test program, it was necessary to observe and evaluate a very wide range of possible rotor frequencies. Rotor lag motions at a frequency as low as 0.20 cycle per revolution were of interest, and theoretical calculations in Reference 4 indicated that torsional frequencies as high as 14 cycles per revolution might occur. In order to evaluate the lower frequency motions, approximately 50 rotor revolutions of data were recorded for steady-state data points. Transient data points included an initial steady state as well as a transient, and approximately 100 rotor revolutions of data were recorded for each transient point.

The dynamic data were recorded on F.M. magnetic tape and were converted off-line to digital form. The analogue to digital converter sampled each of the channels at the rate of 120 samples per revolution, in order to make certain that high-frequency motions were properly defined. The digital data for each test point started at a zero azimuth signal. The 120-per-revolution sampling rate was higher than necessary for some data channels. Using a lower rate for certain channels would have required an additional setup and additional processing time for the analogue to digital conversion.

During the progress of the test program, on-line monitoring revealed failure of various data channels. Repairs were made and data points were repeated when possible. The data obtained were sufficient to fulfill the objectives of the program.

Time History

Blade Load and Motion Data

Each time history value (W_D) at the various azimuth angles was expressed in terms of physical units by using the following expression:

$$W_D = \frac{R_C}{W_R - W_Z} (W_T - W_0) + F_C \quad (3)$$

where

R_C = A constant of proportionality, expressed in engineering units

W_R = Average of digital tape values from the "RCAL" calibration record for the wind tunnel run

W_Z = Average of digital tape values from the "ZCAL" calibration record for the wind tunnel run
 W_0 = Average of digital tape values from the dynamic zero record for the wind tunnel run
 F_C = Optional correction value in physical units
 W_T = An individual data value on the digital tape

The above calculation was performed by the digital computer for each individual data value of a time history for each data channel in each wind tunnel data point. Program options included selectable data points and channels. The time history samples extended from a selected starting zero azimuth signal to a selected ending zero azimuth signal. All time history samples for a given wind tunnel data point were selected with the same starting zero azimuth signal. The azimuth spacing of data values in the time history listing was selectable for multiples of 3 degrees. Extreme maximum and minimum values were read from the time history samples for each data channel available for each wind tunnel point. These values appear in tabular form in Appendix II. Detailed computer listings of time history samples for each transient and each instability data point are available at USAAVLABS.

Machine plotting of the time history data was utilized to permit the examination and evaluation of the large amount of data generated by this program. The transient data were plotted starting at the second zero azimuth signal before the onset of the transient and continuing until 5 complete revolutions were included. The 5-revolution sample length was chosen to present the most interesting portion of the entire transient time history record. In all cases, the rotor reached a representative steady-state condition in this interval. Some of the data channels did exhibit random variations between successive rotor revolutions even after a steady state condition had been reached. This was especially true for the blade torsional response data. Since the transient time history sample used to prepare the tables in Appendix II was longer than 5 revolutions, and because of occasionally appreciable random variations in the steady-state data, the maximum and minimum values listed there do not always appear on the plotted samples.

When the time history samples were plotted and analyzed, the time scale was expressed in a manner that would aid in the interpretation of the results. In the case of the transient data, the time scale was selected in terms of rotor revolutions. The last pre-transient steady-state rotor revolution was represented by the -1 to 0 revolution interval. The command signal to the rotor control system for a sudden input took place at 0 revolution. At this time the instrumented rotor blade was passing over the tail of the model. Measurable response of the control system began at an azimuth angle

of approximately 60 degrees and was essentially complete at approximately 150 degrees of the 0 to 1 rotor revolution. The remainder of the transient response was expressed in terms of succeeding rotor revolutions. (Samples of the transient response plots appear as Figures 18 through 33.) The instability test data were generally presented as a two-revolution sample, plotted against azimuth angle, except for a few cases where it was desirable to show a longer sample. The plots of the two-revolution samples were superimposed, so that the possible presence of nonharmonic frequency components would be more apparent. (Samples of these plots appear as Figures 34 through 45.) Note that the usual symbols making up each individual observation in the time histories have been deleted for the sake of clarity. The observations were taken at an azimuth angle of 0 degrees and continued at a spacing given by the parameter $\Delta\psi$ supplied for each plot.

Control Position

The reduction of control position data required special provisions, since the desired swash plate position could not be measured directly. As mentioned under the MEASURED QUANTITIES subheading, the extension of two of the three swash plate actuators (E_1 and E_2) and the collective follower position (E_3) were measured. The desired A_{1s} and B_{1s} cyclic pitch inputs were determined from the measured quantities by using the following expression:

$$\begin{Bmatrix} A_{1s} \\ B_{1s} \\ \theta_c \end{Bmatrix} = \begin{bmatrix} Q_{11} & Q_{12} & Q_{13} \\ Q_{21} & Q_{22} & Q_{23} \\ 0 & 0 & Q_{33} \end{bmatrix} \begin{Bmatrix} E_1 \\ E_2 \\ E_3 \end{Bmatrix} \quad (4)$$

The values of the Q_{ij} above were determined experimentally. Time history values of E_1 , E_2 , and E_3 were calculated by the program using Equation (3). The above calculation was carried out by the program for each azimuth angle of the control system transients to convert E_1 , E_2 , and E_3 into the desired A_{1s} , B_{1s} , and θ_c control positions.

Frequency Analysis

The frequency analysis used to study the data of this program is essentially the same as the familiar Fourier analysis. Usually, dynamic data are assumed to be periodic with respect to a rotor revolution. In this case, however, the presence of much lower frequencies is admitted. It can be shown that the Fourier type analysis can supply sufficiently accurate results for arbitrary frequencies of interest, provided these frequencies are high enough compared to the assumed fundamental.

As a starting point for the discussion, let it be assumed that a time history segment of data extending from time $t = 0$ to an arbitrary time $2T$ exists, and that it can be represented in that interval with practical accuracy by a series of the type

$$W_D(t) = \sum r_m \cos(\omega_m t + \phi_m) = \sum [a_m \cos \omega_m t + b_m \sin \omega_m t] \quad (5)$$

where m takes the values of the integers.

Letting $W_D(t)$ be represented in the form of Equation (5), the following integrals may be evaluated as in the formation of the usual Fourier coefficients:

$$\begin{aligned} \frac{1}{T} \int_0^{2T} W_D(t) \cos \omega t dt &= \sum \left[a_m \left(\frac{\sin 2(\omega_m - \omega)T}{2(\omega_m - \omega)T} + \frac{\sin 2(\omega_m + \omega)T}{2(\omega_m + \omega)T} \right) \right. \\ &\quad \left. - b_m \left(\frac{\cos 2(\omega_m - \omega)T}{2(\omega_m - \omega)T} + \frac{\cos 2(\omega_m + \omega)T}{2(\omega_m + \omega)T} - \frac{1}{2(\omega_m - \omega)T} - \frac{1}{2(\omega_m + \omega)T} \right) \right] \quad (6) \end{aligned}$$

$$\begin{aligned} \frac{1}{T} \int_0^{2T} W_D(t) \sin \omega t dt &= \sum \left[-a_m \left(\frac{\cos 2(\omega - \omega_m)T}{2(\omega - \omega_m)T} + \frac{\cos 2(\omega + \omega_m)T}{2(\omega + \omega_m)T} - \frac{1}{2(\omega - \omega_m)T} \right) \right. \\ &\quad \left. - \frac{1}{2(\omega + \omega_m)T} \right) + b_m \left(\frac{\sin 2(\omega_m - \omega)T}{2(\omega_m - \omega)T} - \frac{\sin 2(\omega_m + \omega)T}{2(\omega_m + \omega)T} \right) \right] \quad (7) \end{aligned}$$

When $\omega \rightarrow \omega_m$, certain terms in the above series have the following limits:

$$\lim_{\omega \rightarrow \omega_m} \left[\frac{\sin 2(\omega_m - \omega)T}{2(\omega_m - \omega)T} \right] = 1 \quad (8)$$

$$\lim_{\omega \rightarrow \omega_m} \left[\frac{\cos 2(\omega - \omega_m)T}{2(\omega - \omega_m)T} - \frac{1}{2(\omega - \omega_m)T} \right] = 0 \quad (9)$$

When the Fourier analysis is carried out in the usual way, $W_D(t)$ contains only a fundamental frequency ω_1 . Then the interval $2T$ is chosen as the period of the fundamental frequency. In this case,

$$T = \frac{\pi}{\omega_1} \quad \text{and} \quad \omega_m = m\omega_1 \quad (10)$$

and the expressions Equation (6) and Equation (7) become the following with ω chosen as an integral multiple n of ω_1 :

$$\begin{aligned} \frac{1}{T} \int_0^{2T} W_D(t) \cos n\omega_1 t dt &= \sum \left[a_m \left(\frac{\sin 2(m-n)\pi}{2(m-n)\pi} + \frac{\sin 2(m+n)\pi}{2(m+n)\pi} \right) \right. \\ &\quad \left. - b_m \left(\frac{\cos 2(m-n)\pi}{2(m-n)\pi} + \frac{\cos 2(m+n)\pi}{2(m+n)\pi} - \frac{1}{2(m-n)\pi} - \frac{1}{2(m+n)\pi} \right) \right] \quad (11) \end{aligned}$$

$$\frac{1}{T} \int_0^{2T} W_D(t) \sin n\omega_1 t dt = \sum \left[-a_m \left(\frac{\cos 2(n-m)\pi}{2(n-m)\pi} + \frac{\cos 2(n+m)\pi}{2(n+m)\pi} \right) - \frac{1}{2(n-m)\pi} - \frac{1}{2(n+m)\pi} \right] + b_m \left(\frac{\sin 2(m-n)\pi}{2(m-n)\pi} - \frac{\sin 2(m+n)\pi}{2(m+n)\pi} \right) \quad (12)$$

It can be seen that all the terms of the series (11) and (12) vanish except for the terms where $n = m$.

This gives the familiar definition of the Fourier coefficients:

$$a_m = \frac{1}{T} \int_0^{2T} W_D(t) \cos \left(\frac{m\pi t}{T} \right) dt \quad (13)$$

$$b_m = \frac{1}{T} \int_0^{2T} W_D(t) \sin \left(\frac{m\pi t}{T} \right) dt \quad (14)$$

$$a_0 = \frac{1}{2T} \int_0^{2T} W_D(t) dt \quad (15)$$

It should be noted that for application to rotor frequency analysis, the above results will still be rigorously correct for the determination of components at rotor harmonic frequencies, if the interval $2T$ is chosen as an integral number of rotor revolutions.

Results similar to Equations (13), (14), and (15) can be obtained for arbitrary frequencies as well as for the integer multiples of the fundamental, if the interval length $2T$ is sufficiently long. This can be seen from inspection of Equations (6) and (7). The denominators of all terms grow with $2T$, while the numerators are of order unity, unless for some term $\omega \rightarrow \omega_m$. For these terms, as $(\omega - \omega_m)T$ approaches zero, the results shown in Equations (8) and (9) will be obtained. It is therefore desired that the other terms should be small compared with unity.

If the lowest frequencies of interest are approximately 1.26 radians per revolution (0.20 cycle per revolution), terms like $1/2(\omega_m + \omega)T$ are approximately equal to 0.01 for T of 25 revolutions.

The way in which terms such as Equations (8) and (9) approach their limits affects the accuracy of the frequency analysis in a manner which is more difficult to assess. As $\omega \rightarrow \omega_m$, Equation (8) approaches its limit in an oscillatory manner and is non-zero when $(\omega_m - \omega)T$ is not an odd multiple of $\pi/2$. Therefore, the analysis will not be accurate for arbitrary frequency components which are sufficiently close together. This limitation is also controlled by the size of the interval T . With $T = 25$, the amplitude of the oscillation of the term on the left side of Equation (8) is 0.02 when $(\omega_m - \omega)$ is 0.97 radian per revolution (0.16 cycle per revolution).

For the application of the above considerations to this program, the digital computer program calculated time history values W_D as in Equation (3) for a selected channel. The interval over which the values were calculated was selectable between any two zero azimuth signals. The azimuth spacing of the values was also selectable as a multiple of 3 degrees. The integrals on the left-hand side of Equations (6) and (7) were computed numerically for a specified list of frequencies. Then the resultant amplitude was calculated as the square root of the sum of the squares of the two integrals. The expenditure of computer time for frequency analysis was minimized by choosing shorter analysis intervals for higher frequencies and larger azimuth increment spacing for the lower frequencies. The analysis for rotor frequencies of less than one per cycle utilized an azimuth spacing of 12 degrees and an interval of 50 revolutions. The analysis for rotor harmonics used an azimuth spacing for W_D of 3 degrees and an interval of 10 revolutions. The operation of the frequency analysis program was checked by analyzing a record containing a signal of arbitrary frequency. The numerical procedure was also checked by determining the known frequency components of a square wave. Additional checks were made by comparing the results of the on-line frequency analysis made during the wind tunnel test.

The frequency analysis was used to provide harmonic components of all available dynamic data from the instability portion of the test. These results are presented in tabular form in Appendix III.

DESCRIPTION OF THEORETICAL CALCULATIONS

NORMAL MODE TRANSIENT ANALYSIS

The Normal Mode Transient Analysis is a step-by-step timewise integration of the elastic rotor blade equations of motion. The analysis uses rotating blade natural vibration modes as elastic degrees of freedom. The use of these orthogonal or "normal" modes gives rise to the designation "Normal Mode Transient Analysis". As used in this investigation, the aerodynamic loadings were determined by quasi-steady strip theory, with the effects of aerodynamic stalling, drag, and torsional moment included.

When a steady-state rotor condition is being analyzed, the integration proceeds in small but finite timewise steps from an arbitrary starting value. After a number of rotor revolutions, the predicted motions will become cyclic within a desired tolerance. This is the usual solution desired, and performance, load, and stress calculations are usually based on these cyclic motions. On the other hand, the prediction of rotor behavior following a disturbance is a basic capability which was utilized for the purposes of this investigation.

The basic differential equations used in the Normal Mode Transient Analysis are presented in Reference 1.

The calculations for the rotor transient conditions were carried out by first establishing the theoretical counterpart of the experimental initial condition. It was found possible to obtain satisfactory correlation with respect to blade shaft angle and first harmonic flapping by accepting small deviations between measured and calculated C_L/σ and control position. These deviations were less than 0.005 for C_L/σ and 1 degree for B_{1s} and θ_c . Deviations of 3 degrees in A_{1s} were experienced at the 120- and 250-knot simulated speed conditions without pitch-flap coupling. Otherwise, the A_{1s} discrepancy was also less than 1 degree.

When the calculated initial condition was established, the measured control position time history was introduced into the calculations. A sample time history of a typical control change is shown in Figure 15. Rotor behavior was calculated for at least 3 full revolutions after the control input. Additional revolutions were calculated if there was any doubt that the rotor had reached a steady-state condition.

FIXED-AZIMUTH AEROELASTIC INSTABILITY THEORIES

In recent years, the availability of more advanced computing equipment has facilitated progress in methods for predicting rotor blade behavior. The more sophisticated methods, such as the previously described Normal Mode Transient Analysis, provide information of useful accuracy for conventional rotors operating under ordinary conditions. It is advantageous, however, to develop simpler and more rapid methods to investigate specific idealized types of aeroelastic instability. These simpler methods are intended for the rapid definition of problem areas

during the preliminary design stages for new aircraft. The three fixed-azimuth aeroelastic theories described in the following subsections were developed with this objective in mind, and were used to calculate theoretical data for comparison with the test results generated by this program.

Fixed-Azimuth Torsional Divergence

One of the basic aeroelastic investigations applying to fixed wings is the torsional divergence analysis, as explained in Reference 11.

Consideration of the torsional divergence phenomenon for a fixed wing leads to an examination of similar situations existing for helicopter rotors. Obviously, unlike a flight condition for a fixed wing, the relative velocity on a rotor blade varies along the span. In forward flight, the velocity distribution is rapidly and continuously changing. Therefore, the static stability analysis for torsional divergence applies only to an instantaneous condition for a helicopter blade in forward flight.

The torsional divergence situation for a helicopter blade usually develops on the retreating blade for advance ratios greater than unity. The blade is then traveling backwards (sharp edge first) through the air for part of each revolution, and the aerodynamic center of pressure moves close to what is normally the 75 percent chord position. This produces a large torsional moment arm about the blade elastic axis and center-of-gravity position at or near the normal 25 percent chord position. Hence, torsional divergence can be encountered for the retreating blade even though the relative velocity is comparatively low. If the blade center of gravity is aft of the aerodynamic center of pressure on an advancing blade, torsional divergence can, of course, occur there as well.

The torsional divergence analysis used to generate the stability boundaries shown in Figure 14 is essentially a two-degree-of-freedom static stability analysis, which is fully described in Reference 4. The first torsional natural vibration mode and the rigid blade flapping mode were used as these two degrees of freedom. Aerodynamic lift was assumed to be proportional to blade twisting deflection and dynamic pressure calculated from the local relative tangential velocity. Aerodynamic lift was assumed to be the only aerodynamic effect present. The distributed lift force was assumed to act at the 25 percent chord for forward flow and at the 75 percent chord for retreating blade reverse flow. The virtual work done by the aerodynamic force was calculated for the flapping and torsional modes. The aerodynamic virtual work was set equal to the virtual work done against centrifugal effects and the change in torsional strain energy. The result was two coupled linear homogeneous equations in the flapping and torsional degrees of freedom, whose determinant was evaluated. Combinations of forward speed and rotational speed were found for which this determinant was zero. The loci of these points are the torsional divergence boundaries appearing in Figure 14. Boundaries were established at the 270 degree azimuth position and, in the case of the aft center-of-gravity blades, at the 90 degree azimuth position. Note that the boundaries sloping down to the right are for the advancing blade,

while those sloping up to the right are for the retreating blade.

Fixed-Azimuth Classical Flutter Analysis

The classical flutter phenomenon for fixed wings has been studied for many years, and is discussed in detail in Reference 11.

As with the torsional divergence analysis, it is natural to attempt to apply the fixed-wing classical flutter analysis to the helicopter rotor blade. In forward flight, however, the relative velocity at the blade is constantly changing, instead of remaining constant with time. In addition, the velocity varies along the span, and there are multiple nonplanar blade wakes.

In order to convert the rotor blade classical flutter problem to a form basically similar to the fixed-wing flutter problem, a number of simplifying assumptions are required. The most important of these is the assumption that aerodynamic forces appropriate to a discrete azimuth can be used in the equations of motion to determine the blade flutter characteristics in that azimuth region. The other simplifying assumptions include consideration of small displacements, consideration of the blade as a series of two-dimensional strips, and zero steady-state blade twist, collective and cyclic pitch, and lag angle. The important centrifugal effects present on a helicopter blade were carefully considered in the development of the equations of motion. The aerodynamic effects were calculated by using fixed-wing, two-dimensional, compressible-flow flutter coefficients obtained from the previously existing literature. As usual in flutter analyses, natural vibration modes were used as degrees of freedom. Further details and development of this flutter analysis are contained in Reference 5.

The classical flutter analysis predicts the frequency and damping of blade aeroelastic vibrations for a series of desired rotor operating conditions. When a flight condition is found for which the damping of any aeroelastic mode is negative, a flutter condition has been predicted. The locus of flight conditions for which the damping of a particular mode is zero lies between regions of positive and negative damping, and is termed a flutter boundary.

The flutter analysis was applied to the model blade, with rigid blade flapping, the first three flapwise bending modes, and the first two torsional modes considered as degrees of freedom. Structural damping was shown by test to be small, and was neglected. The 90 degree and 270 degree azimuth locations were used to determine advancing and retreating blade boundaries. As with the torsional divergence boundaries, the advancing blade boundaries slope down to the right and the retreating blade boundaries slope up to the right.

The results of the calculations fulfilled qualitative expectations. The 25 percent chord center-of-gravity blade displayed no advancing blade flutter boundary, even at advancing blade velocities well above those to be tested. The similar calculations for the aft center-of-gravity blades

predicted advancing blade instability at speeds well below the advancing blade torsional divergence speeds. The flutter mode was principally composed of rigid blade flapping and blade twisting, at a frequency somewhat below the torsional natural frequency.

The calculated flutter behavior at the 270 degree azimuth position was similar for all three configurations. The predicted retreating blade flutter boundary was at speeds just below the predicted retreating blade static torsional divergence boundary. Furthermore, the flutter mode consisted almost entirely of torsional motion and was of a low frequency. Thus, the flutter and static torsional divergence solutions tended to be equivalent at the 270 degree azimuth position.

The frequency and damping of the calculated fixed-azimuth flutter modes are plotted in Figure 16 as a function of simulated forward speed at a number of constant rotational tip speeds. The rate of decrease of damping with forward speed is rapid as the line of zero damping is reached, so that structural damping can have little effect. This can be appreciated by using the classical simplified relationship $g=2\zeta_{CF}$ between structural damping coefficient and critical damping ratio. If structural damping is $g = 0.02$, for example, a viscous damping of $\zeta_{CF} = -0.01$ is required to establish neutral damping. This would shift the calculated flutter boundary by 2 simulated knots or less.

It should be pointed out that the rotating blade flapwise and chordwise structural damping ratio is even smaller than the measured static values. This is a result of centrifugal effects, which greatly increase blade effective stiffness without introducing any additional damping. The structural damping of the rotating blade natural modes was estimated by using the results of the previously described static damping tests in the flutter program with zero air density. The effects of Coulomb hinge damping on the apparent structural damping coefficient depend on the flapping amplitude. The Coulomb damping effects are large for very small motions but decrease sharply for motions observed in practice. The effects of Coulomb damping were included in the rotating blade damping calculations by assuming a representative amplitude for the flapping mode. This amplitude was 0.1 degree at the flapping hinge. The Coulomb damping coefficient was added to the structural damping obtained by using the static modes with the measured frequency and damping in the flutter program with zero air density. The total estimated structural damping for the flapwise and torsional modes of the 25 percent chord center-of-gravity blade is given in Table X for three rotational speeds. The structural damping of the other two blade configurations is of a similar magnitude. The structural damping is, as mentioned previously, too small to have any appreciable effect on the fixed-azimuth flutter calculations.

The classical flutter calculation also provides information as to the participation of the input modes in each of the modes of aeroelastic vibration. The motion of any point on the blade elastic axis is given in real form by the expressions

$$\begin{aligned}
w_n(x,t) = & \sum_p \left[(q_{FPnr} + iq_{FPni}) w_{FP}(x) \right] e^{(\lambda_n + i\omega_n)t} \\
& + \sum_p \left[(q_{FPnr} - iq_{FPni}) w_{FP}(x) \right] e^{(\lambda_n - i\omega_n)t} \quad (16)
\end{aligned}$$

$$\begin{aligned}
\theta_n(x,t) = & \sum_p \left[(q_{\theta Pnr} + iq_{\theta Pni}) w_{TP}(x) \right] e^{(\lambda_n + i\omega_n)t} \\
& + \sum_p \left[(q_{\theta Pnr} - iq_{\theta Pni}) w_{TP}(x) \right] e^{(\lambda_n - i\omega_n)t} \quad (17)
\end{aligned}$$

If $\omega \neq 0$, the above represent damped oscillations, which have a critical damping ratio given by

$$\zeta_{CF} = -\frac{\lambda_n}{\omega_n} \quad (18)$$

The calculated flutter modes for some selected operating conditions are detailed in Table XI. The last four columns are the resultant motions at the blade tip, normalized with respect to the largest flapwise modal amplitude and phase. In terms of the nomenclature of Table XI, the tip motions during the various conditions are

$$w_n(1., t) = \bar{w}_n(1.) e^{-\omega_n \zeta_{CF}} \cos(\omega_n t - \phi_{nw}(1.)) \quad (19)$$

$$\theta_n(1., t) = \bar{\theta}_n(1.) e^{-\omega_n \zeta_{CF}} \cos(\omega_n t - \phi_{n\theta}(1.)) \quad (20)$$

The damping (ζ_{CF}) and frequency ($\omega/2\pi$) of the flutter modes are given in Figure 16.

Fixed-Azimuth Stall Flutter Analysis

The aerodynamic hysteresis effects resulting from the vibration of an airfoil through the stall angle can give rise to the single-degree-of-freedom instability known as stall flutter. The mechanism of this instability results from the tendency of the airfoil to remain unstalled while it is pitching up, and its tendency to remain stalled while it is pitching down. The stalled airfoil pitching moment is negative about the blade torsional axis and is almost zero when it is unstalled. Thus the air-stream will do work on the blade torsional vibration mode, and small amplitudes will tend to grow larger. A more detailed discussion of stall flutter is given in Reference 12.

The aerodynamic aspects of stall flutter have not been suitable for a strictly analytical study, since unsteady, viscous, and sometimes compressible flow effects are involved. Experimental studies reported in Reference 12 have, however, provided two-dimensional data on unsteady, stalled flow which are the basis of a useful blade stall flutter analysis. Pressure measurements on a vibrating airfoil were converted to aerodynamic damping coefficients dependent on mean angle of attack and reduced frequency. These coefficients were negative for mean angles of attack near the stall. The stall flutter analysis assumes a hypothetical torsional vibration in the first natural mode and frequency. Then, the aerodynamic torsional damping is calculated for a series of two-dimensional chordwise strips at a selected azimuth angle, using the damping coefficients derived from the experimental data. The damping of the strips is integrated to give an aerodynamic damping coefficient for the whole blade. The process is repeated for azimuth angles at selected intervals. The mean angle of attack for each chordwise strip and azimuth angle was obtained from calculations using the method of Reference 1 applied to the model blade. The quasi-steady effects of blade stall and blade twisting were considered in these preliminary calculations, which were carried out with the assumption of a uniform inflow. The rotor parameters and calculated performance for the stall flutter analysis conditions are given in Table XII. The calculations for the rotor conditions of Table XII provided distributions of angle of attack and Mach number with respect to blade radial station and azimuth. These results were used in the stall flutter analysis of Reference 12, and the variation of blade damping with azimuth was calculated. The blade damping parameter Ξ_{α_3} resulting from the Reference 12 calculations was converted into blade critical damping ratio in torsion by using the following relationship:

$$\zeta_{AD} = \frac{\rho C_D^2 R^3}{4 M_T} \frac{\Omega^2}{\omega_T^2} (1 + \mu \sin \psi)^2 \Xi_{\alpha_3} \quad (21)$$

The generalized mass (M_T) of the torsional mode was 1.185×10^{-4} slug-ft². The results of the blade damping calculations, converted into critical damping ratio, are shown in Figure 17.

ANALYSIS OF TRANSIENT DATA

The transient response of the rotor system to sudden control changes was measured at 79 rotor operating conditions. As described in the Experimental Procedures section of this report, each transient condition includes data at three test points: the initial steady state, the test final steady state, and the actual transient condition. The rotor performance data for each of the test points are listed in Table VI, and the measured maximum and minimum values of blade motion and bending moments are listed in Tables XV and XVI.

In general, the rotor system was well behaved during the transient conditions. The rotor blades usually attained the final steady-state condition within three or four revolutions, without excessive overshoot of flapping or blade bending moments. Time histories of rotor blade flapping and lag motions and flapwise bending and torsional moments are presented in Figures 18 through 29 for twelve representative conditions.

EVALUATION OF ROTOR BLADE TRANSIENT RESPONSE AT 120 KNOTS

The blade lag motion at a forward speed of 120 knots, shown in Figure 18, exhibits three distinctive characteristics: a high harmonic frequency component, a first harmonic frequency component, and a highly damped subharmonic motion. The high-frequency response persists at all the 120-knot conditions, but always at an amplitude of one-half degree or less. This response is unaffected by rapid changes in the rotor control settings. The first harmonic lag motion evident in the measured data varies with the rotor operating condition in a manner similar to the variation in rotor blade flapping, with larger first harmonic flapping corresponding to larger first harmonic lag motion. The third characteristic is the appearance of a damped subharmonic response, at approximately one-third cycle per revolution, on the introduction of the rapid control change. The magnitude of this response is related to the rate of change in first harmonic flapping response resulting from the control change. The subharmonic response is a reaction of the natural rigid body mode of the blade to a disturbance and, as such, exhibits a larger amplitude with a larger disturbance. The size of the disturbance is reflected in the resulting change in rate of change of flapping.

The rotor blade flapwise bending moments at the 120-knot initial steady-state conditions are primarily governed by the first elastic modal response of the blade occurring at a frequency of 3 cycles per revolution, as seen in the experimental data presented in Figure 19. The calculated natural frequency of the first elastic flapwise mode is 2.75 cycles per revolution. In the case of the lateral flapping transient, Figures 19(d) and 19(e), no significant change in flapwise bending moments occurs with or without pitch-flap coupling. Figures 19(b) and 19(c), however, present data from two transient conditions, one with and one without pitch-flap coupling. In each of these cases a collective pitch change of $\Delta\theta_c = 4.0$ degrees takes place, and a change in harmonic content as well as an increase in amplitude occurs. The moment increase occurs during the first

and second rotor revolutions following the pitch change, and then a final steady-state condition is reached in which the peak-to-peak moment has returned to a value near that of the initial condition. During the transient, the second elastic mode of the blade comes into play at a frequency of 5 cycles per revolution. The calculated natural frequency of the mode is 5.23 cycles per revolution. The first mode becomes dominant again when the final steady-state condition is reached. The appearance of the higher elastic mode is, similar to the subharmonic lag motion response, a rapidly damped natural mode response to the disturbance. As expected, the presence of the pitch-flap coupling moderates the flapwise bending moment response during and following the transient.

The flapping response during the transient conditions at 120 knots exhibits no unusual behavior. As expected, the presence of the pitch-flap coupling results in a smaller flapping response to the collective pitch change, and the final state is reached more rapidly. It is notable that this state is reached within one revolution with the pitch-flap coupling and in only two revolutions without it, even though the flapping amplitude is twice as large. As mentioned before, this rapid attainment of the final steady condition was characteristic of the entire spectrum of test conditions. Representative flapping transients at 120 knots are shown in Figure 20.

The rotor blade torsional moments, presented in Figure 21, exhibit the most significant response to the sudden control inputs. With the pitch-flap coupling absent, a large-amplitude oscillation with a high 5-cycle-per-revolution content occurs immediately following the control change. This oscillation damps out somewhat as the final steady-state condition is reached, so the peak moments occur within one revolution after the control change. Comparison of the signature of this response with that of the corresponding flapwise bending moment time histories indicates a similarity in harmonic content. With a calculated torsional natural frequency of 6.2 cycles per revolution at this operating condition, flapwise-torsional coupling with a frequency in the 5-to 6-cycle per revolution range would be expected with the introduction of pitch-flap coupling. It might also be expected that the torsional oscillation induced by the rapid control change would be damped through the absorption of energy in the flapwise mode. Such a damping effect is observable in Figure 21(b).

The transient torsional moments shown in Figures 21(a) and 21(c) have a signature which characterizes stall flutter. The two conditions considered represent heavily loaded states, $C_L/\sigma = 0.1$, where such a response would be expected. In the case involving a change in first harmonic lateral flapping, it can be found by comparing points in Table XV and XVI that the introduction of negative b_{1s} flapping, as shown in Figure 20(b), induces a more severe torsional oscillation than does the introduction of positive b_{1s} flapping. It is not obvious, without a much more extensive analysis, why this is the nature of the phenomenon, but throughout the 120-knot test conditions, the same trend is evident both in the presence and absence of pitch-flap coupling.

CORRELATION OF ROTOR BLADE TRANSIENT RESPONSE AT 120 KNOTS

On comparing the experimental data with theoretical transient blade responses, several noteworthy items are observed which would not appear in a comparison of purely steady-state results. First, the appearance of the subharmonic lag motion is predicted. The precise degree of correlation is dependent on the accuracy of the calculated flapping motion, which is a measure of the relative severity of the theoretical disturbance. The same is true of the first harmonic lag motion correlation. The theoretical results are compared to the experimental data in Figure 18. The degree of flapping correlation is related to the change in rotor lift resulting from the rapid control change. Figure 20 shows that the calculated flapping amplitude following the lateral cyclic pitch change compares well with the experimental data, although in the case without pitch-flap coupling, an error of approximately 1 degree in the coning angle and a phase error of about 30 degrees are present. In these cases, the rotor lift does not significantly change during the transient. At the other two conditions shown, the rotor lift is increased by 46 percent as a result of the control change, and the calculated flapping response, which does not reflect the change in inflow associated with the lift change, overshoots the experimental values by as much as 100 percent. In addition, it is seen that the theoretical case with pitch-flap coupling attains steady state as rapidly as the corresponding experimental response, while the theoretical case without pitch-flap coupling does not attain the final state until 5 or 6 revolutions following the transient. It is also seen in both cases that the calculated coning angle is too low, reflecting the pre-transient inflow value. In line with the analysis of these data and in agreement with the investigation reported in Reference 3, it would be expected that updating the rotor inflow during the transient computations would substantially increase the degree of correlation of the flapping responses and consequently that of the lag motion responses.

The torsional response calculations show the remaining item peculiar to the transient responses. Figure 21 reveals that the calculated response does not exhibit any of the retreating blade oscillation experienced by the tested blade. In the case of the lateral flapping change, the calculated torsional moment does not respond to the control input. Following the collective pitch change, the calculated torsional moment reaches a more negative peak on the retreating azimuth angles, but lacks the proper response frequency. Two characteristics can be identified from the comparison of the calculated torsional moment with the experimental data. It is first seen that the calculated torsional moment breaks downward at a lower azimuth angle than the experimental moment, implying a breakaway in the blade pitching moment at a lower angle of attack. This is in agreement with the difference in the characteristics of the two-dimensional, quasi-steady airfoil characteristics used in the theory and oscillating airfoil characteristics as described in Reference 12. The second characteristic is indicated by the large damping of the calculated response relative to that of the measured results. This effect is also in accord with the difference between steady and unsteady airfoil performance. The incorporation of unsteady aerodynamic effects in the theory could be expected to improve the degree of correlation of torsional moments.

The further comparison of the theoretical and experimental transient blade responses at 120 knots reveals some items worthy of mention but not peculiar to the existence of the transient condition. First, the high harmonic content of the lag motion does not appear in the theoretical results. In the absence of chordwise bending moment data for these operating conditions, the source of the high-frequency lag response cannot be specifically determined, and consequently no explanation as to why this response is not predicted can be offered. The steady lag angle predicted by the theory is seen to be low by an amount related to the magnitude of the angle or, correspondingly, the rotor torque. Such a discrepancy was not unexpected, since the initial rotor operating conditions were theoretically determined by specifying lift, control angles, and first harmonic flapping rather than by rotor performance alone. Consequently, theoretical values of rotor drag and torque deviated somewhat from the measured values.

The second aspect of the general comparison of the 120-knot responses is the lack of consistent correlation of the flapwise bending moments. The calculated moments generally lack the correct harmonic content. At the operating conditions under consideration, it would be expected that the inclusion of wake-induced velocity effects would improve the flapwise bending correlation. However, without an improved prediction of the torsional response as discussed above, complete agreement between measured and calculated flapwise moments, at the operating conditions considered here, is unlikely.

Finally, the qualitative effect of the pitch-flap coupling is adequately handled by the theory, although at the 120-knot conditions this is not as critical to the overall degree of correlation as the effects of inflow and unsteady aerodynamics.

EVALUATION OF ROTOR BLADE TRANSIENT RESPONSE AT 200 KNOTS

The blade lag motion responses at the 200-knot conditions exhibit essentially the same characteristics as those at 120 knots. The 200-knot responses are presented in Figure 22. The subharmonic and first harmonic components induced by the rapid control change and the higher harmonic, small-amplitude oscillations are all present. The higher harmonic components now exhibit a lower frequency, primarily 4 cycles per revolution, than was seen at the 120-knot conditions; but as before, they are not noticeably affected by the control changes. The observed 4-cycle-per-revolution frequency would imply that this motion is a response to first mode chordwise bending of the rotor blade. The calculated natural frequency of this mode is 3.75 cycles per revolution. The first and subharmonic lag components are seen to vary in relation to the change in first harmonic flapping following the control change and are thus affected by the presence or absence of pitch-flap coupling.

The rotor blade flapwise moment responses, shown in Figure 23, consist primarily of a third harmonic component through the entire transient sequence. This is evidence of the first elastic flapwise mode response. Although the harmonic content does not change as much at these

conditions as at the 120-knot conditions, the peak-to-peak moments during the revolutions immediately following the control change show the increase over the steady-state values that was seen at 120 knots. This is also evident from maximum-minimum flapwise moment data presented in Tables XV and XVI. As expected, the ultimate flapwise moment response is more severe in the absence of pitch-flap coupling, although the maximum values are attained more slowly. Comparison of the flapwise moment transients between the two operating conditions considered at 200 knots indicates the effect of pitch-flap coupling to be greater for the combined collective and cyclic pitch change than for the pure collective pitch change. Comparison of the transient flapping motions from Figure 24 shows the pitch-flap coupling effect to be greater for the collective pitch change than for the combined pitch change. This would indicate that the energy entering the flapping mode because of the pure collective pitch change is transmitted to the elastic modes when the flapping response is controlled with cyclic pitch. Comparison of rotor performance changes resulting from the control inputs in question offers some clarification of the flapwise bending response. Table VI gives the rotor lift and drag coefficients of the 200-knot conditions without pitch-flap coupling. For the combined pitch change, the rotor lift is increased by 50 percent to yield a final C_L/σ of 0.075 while the rotor drag remains small, C_D/σ less than 0.001. In the pure collective pitch change case, C_L/σ doubles, reaching a value of 0.105; while the drag, significant to begin with, also doubles, C_D/σ reaching a value of 0.0126. Full-scale wind tunnel data reported in Reference 13 indicate that increasing lift at constant, low drag will result in a significant increase in flapwise stress, while a similar lift increase accompanied by a large drag increase will not result in a particularly large stress increase.

As previously mentioned, the flapping response at the 200-knot conditions presented in Figure 24 exhibits two characteristics. In the combined pitch change case, the amounts of first harmonic flapping prior to and following the control change were prespecified, so the differences between the steady states of the cases with and without pitch-flap coupling are the result of different higher harmonic compositions. In the motions shown, the amplitude difference amounts to approximately 0.5 degree. The effect of the pitch-flap coupling is to cause the flapping to undershoot slightly before reaching the final steady state. In response to the collective pitch change at 200 knots, the expected flapping motions occur. The first harmonic flapping amplitude increases from 0.0 to 1.5 degrees with the pitch-flap coupling and to 4.7 degrees without pitch-flap coupling. As with the similar transients at 120 knots, the final steady state is reached sooner with the pitch-flap coupling present. In both of the conditions shown in Figure 24, the higher harmonic flapping seen in the initial state is not significantly affected by the control change, although it necessarily is a smaller percentage of the total flapping in the final state.

The torsional moment transient responses at 200 knots, presented in Figure 25, are somewhat similar in character to those examined at 120 knots, although certain differences do exist. In general, the maximum torsional moment amplitude persists into the final steady-state condition

rather than being confined to the transient revolutions as before. An exception to this can be seen at points 16 and 19 of run 53 presented in Table XVI. In these two cases, the transient torsional moment does exceed the steady-state values. However, it is seen that both the initial and final steady-state conditions represent relatively severe conditions in terms of torsional moment amplitude. Table VI shows that these are low-drag, high-power conditions. Full-scale wind tunnel data presented in Reference 13 show that the torsional moment sensitivity does increase with decreasing drag at the levels of rotor lift considered here. It is also evident from the torsional moment data presented in Table XVI that the moment amplitudes are increased with the increase in forward speed from 120 to 200 knots. At both speeds, nevertheless, the harmonic content of the torsional moment is similar, and the effect of the pitch-flap coupling is also similar. It is worth noting from Figure 25 that the two responses without pitch-flap coupling as well as the two with it are very similar in spite of the difference in rotor operating conditions and control changes. This effect is consistent with the nature of the stall-induced torsional oscillation. The onset and quenching of the oscillation occur in the same general azimuth region for a wide range of conditions. The oscillation itself is governed by the dynamic characteristics of the rotor blade. The reduction of the torsional moment response by the pitch-flap coupling is again evident, but the mechanism through which this is accomplished is not immediately obvious. The coupling of flapwise and torsional modes may play a role in this effect. Harmonic analysis of the final steady-state data from point 22 of run 60 and point 11 of run 54 show, however, that no marked difference in the harmonic content of the flapwise moment is present, even though there is a 50 percent reduction in the amplitude of the fifth and sixth torsional moment harmonic components for the case with pitch-flap coupling.

CORRELATION OF ROTOR BLADE TRANSIENT RESPONSE AT 200 KNOTS

Only one basic difference exists between the degree of lag motion correlation at 200 knots and that at 120 knots. In the 200-knot case, the 4-cycles-per-revolution higher-harmonic response does appear in the theoretical results, although at a small amplitude. The theoretical chordwise bending moment response at the conditions considered contains a dominating fourth harmonic component, giving support to the suggestion that the measured higher harmonic lag motion is a response to the chordwise elastic deflection of the blade. Other than this, the theoretical and experimental motions display the first harmonic and subharmonic components that would be expected from the analysis of the 120-knot results. The effect of the pitch-flap coupling is also qualitatively similar.

The most significant difference in the correlation of the 200-knot conditions relative to that at 120 knots is the improvement in the theoretical flapwise bending moments. This is not surprising when it is considered that the flapwise response at the conditions in question is primarily first elastic mode bending. In all cases shown in Figure 23, the calculated initial steady-state flapwise moments agree much better with the measured values than was the case at 120 knots. The consistent discrepancy between the calculated and measured transient results is seen to

be too little theoretical outboard moment and too much theoretical inboard moment. This is most evident in the cases without pitch-flap coupling. The implication of this discrepancy is that the second elastic flapwise mode is overexcited in the theoretical analysis. The final steady-state moments in point 14 of run 54 further confirm this, as the theoretical results obviously contain a larger 5-cycle-per-revolution component than the measured response. It is not clear that improving the treatment of the transient inflow with azimuthal variations induced by wake effects, as discussed with regard to the 120-knot correlation, would result in a higher degree of flapwise moment correlation. It is more likely, since the experimental response consists primarily of the natural response of one blade mode, that consideration of the time variation of uniform inflow would yield an improved flapwise moment correlation.

As in the 120-knot cases, the qualitative effect of the pitch-flap coupling is adequately predicted by the theory. At 200 knots, this effect is more significant in terms of reducing peak-to-peak blade bending moments than was true at the lower speed; however, as will be seen below, it still maintains an important role with respect to reductions in the torsional moments.

Considering the rotor blade flapping response to the combined collective and cyclic pitch change, comparison of the motion shown in Figures 24(a) and (b) reveals that the calculated transient flapping contains an excess of second harmonic flapping and a deficiency of first harmonic flapping. Because second harmonic flapping is a function of rotor inflow (for example, see Reference 14), it can be expected that incorporation of a transient uniform inflow in the analysis will improve the flapping correlation in this case as well as in the case with only a collective pitch change. This case, shown in Figures 24(c) and (d), exhibits an excessive theoretical first harmonic flapping similar to the results discussed at 120 knots.

As in the case of the 120-knot torsional responses, the comparison of calculated and measured torsional moments at 200 knots, presented in Figure 25, shows a low degree of correlation. The nature of the disagreement at this forward speed is essentially the same as that discussed for the 120-knot cases. The early downward break of the calculated moment and the excessive damping of the calculated response both result from the use of quasi-steady aerodynamic theory in the theoretical analysis.

EVALUATION OF ROTOR BLADE TRANSIENT RESPONSE AT 300 KNOTS

The lag motion data presented in Tables XV and XVI show that the control changes introduced at 300 knots result in only small lag motion changes. The time histories presented in Figure 26 indicate the nature of the transient lag response. The reason for the general lack of response stems from the fact that the control changes were generally smaller at this forward speed and were introduced at unloaded rotor conditions, $C_L/\sigma = 0.01$. These limitations were imposed by the sensitivity of the flapping and the flapwise and chordwise bending moment at this forward speed.

Flapwise moment responses are presented in Figure 27. In each case considered, the flapwise moments increase with the control change. As with the transients at the lower forward speeds, the pitch-flap coupling causes a more rapid convergence to the final state. In the cases having only collective pitch change, it should be noted that although the final flapwise moments are nearly equal, the control change was 4 degrees with the pitch-flap coupling and 1 degree without it. No other effects peculiar to the flapwise transient responses are evident from the data in Figure 27.

The transient flapping response shown in Figure 28 is similarly well behaved. The last revolution in each time history sample is typical of the time histories of all succeeding revolutions. As before, the pitch-flap coupling results in a more rapid convergence to the final steady-state condition. In addition, the third harmonic flapping, associated with the first mode elastic bending, is seen to persist throughout the transient in the presence of the pitch-flap coupling, while without it the third harmonic flapping is noticeably suppressed. The longitudinal flapping transients show no unusual characteristics.

The torsional responses at 300 knots appear in two characteristic forms. At some operating conditions, the torsional moment response is not unlike that presented in Figure 25 for the 200-knot operating conditions. Figures 29(a) and 29(b) show two such cases. Although there are similarities between the signatures of these time histories and those examined at 200 knots, the 300-knot amplitudes are much smaller. In addition, the retreating blade oscillations are more rapidly damped than in the 200-knot cases. The other characteristic torsional response is seen in Figures 29(c) and 29(d). In these cases, a single large peak moment occurs on the retreating side of the rotor disk. This behavior is characteristic of impending torsional divergence.

Significantly different torsional moment transient behavior is observable following each of the two types of control changes considered in Figures 29(c) and 29(d). In the case of the forward longitudinal flapping increment, the transient response is not substantially different from the initial steady-state condition either in signature or in amplitude. On the other hand, the aft longitudinal flapping increment noticeably changes the character of the torsional moment. Not only is the amplitude reduced, but the overall response tends to become similar to that seen in Figure 29(b) for point 11 of run 55. This is reasonable in that the rotor lift and flapping in the final steady states are nearly identical between point 7 of run 56 and point 11 of run 55.

Contrary to the effect of pitch-flap coupling seen at the lower forward speeds, comparison of data from Table XV for point 29 of run 47 with the response of point 29 of run 55, Figure 29(c), shows that the pitch-flap coupling increases the maximum torsional moment by a factor of about 2. This is in agreement with results published in References 15 and 4, which show the detrimental effect of pitch-flap coupling on torsional moments as the torsional divergence boundary is approached.

CORRELATION OF ROTOR BLADE TRANSIENT RESPONSE AT 300 KNOTS

The degree of correlation of blade lag motion at 300 knots is essentially the same as that obtained at the lower forward speeds. Figure 26 shows the comparison of the measured and calculated results. The relative absence of the higher harmonic content is again evident in the theory, and in point 29 of run 55, the subharmonic component is predicted by the theory but not seen in the experimental data. Nothing unique to this forward speed is revealed through comparison of experimental and theoretical lag motions.

The comparison of flapwise bending moments at 300 knots does reveal certain items not encountered at the lower forward speeds. Figure 27 shows a generally poor correlation of pre-transient conditions with a subsequent improvement in correlation as the transient response progresses. These results can be attributed to the fact that, in general, it was difficult to generate a completely satisfactory theoretical, pre-transient condition at this forward speed. Since the experimental parameters were zeroed for these conditions ($\theta_c = a_{1s} = b_{1s} = a_s = 0$ degrees), the measured response is a result of unsteady effects and interference from the model fuselage. Consequently, the compromises involved in attempting to theoretically achieve the measured values of lift, flapping, control settings, and shaft angle did not result in a uniform degree of correlation in the pre-transient conditions. In the case that includes pitch-flap coupling, the calculated flapwise moment is extremely small. In the other cases, the response has the correct order of magnitude but not the correct harmonic content. The introduction of the control changes results in an increase in rotor loading and a consequent reduction in the influence of the extraneous disturbances. Thus, the nature of the correlation following the control change is essentially as expected from consideration of the lower speed correlation. In the case of the collective pitch change without pitch-flap coupling, the calculated response is slower in attaining the final steady-state condition than the experimental response and slightly overshoots the measured final values. Correspondingly, the response with pitch-flap coupling reaches the final value rapidly with no overshoot. During the longitudinal flapping changes, the calculated response builds up more slowly than during the collective pitch change case and does not overshoot the measured final values. The high third harmonic content observable in the experimental flapwise bending moments is also evident in the theoretical results and indicates a significant participation of the first flapwise elastic mode at its natural frequency.

The comments made above concerning the generation of the theoretical pre-transient cases also apply to the flapping motions. Figure 28 shows a general lack of agreement between the initial steady-state motions from theory and experiment. However, as with the flapwise moments, the correlation during the transient response is much improved. The higher harmonic response in the theoretical results does not build up sufficiently, particularly in the case which includes pitch-flap coupling, but the first harmonic response correlation is much improved over that obtained at the lower speeds. This can be attributed to the diminishing effect of lift-induced inflow on rotor blade response as advance ratio increases. In

the two cases where longitudinal flapping increments are considered, the theoretical response during the rotor revolution that includes the control change and the following revolution correlates poorly with the experimental data. This is due in part to the problem of generating the correct pre-transient flapping, but this is evidently not the sole reason because Figure 28(d) shows that even with an apparently reasonable entry into the first transient revolution, the theoretical flapping fails to respond rapidly enough. This effect is consistent with the slow response of the no-pitch-flap-coupling cases examined at the lower speeds. Figure 28(a) shows that the 300-knot case with pitch-flap coupling does respond as rapidly to the control change as does the measured flapping motion.

The correlation of the measured and calculated torsional moments presents a new situation at the 300-knot conditions. In the absence of the large-amplitude, stall-induced oscillations, the measured torsional response is more accurately predicted than was the case at the lower forward speeds. Except where pitch-flap coupling is included, the calculated peak torsional moments, shown in Figure 29, are consistently low, although the qualitative responses to the control changes are good. The most reasonable explanation for the low moment peaks is that the reverse flow aerodynamic characteristics of the model blades are not exact enough in the theory. In this situation, where the blade is in an unstable attitude, a small error in lift curve slope, for example, will result in a significant error in the retreating blade torsional response. Since the case with pitch-flap coupling, Figure 29(a), does not exhibit the retreating blade moment peak, the correlation between theory and experiment is generally good in terms of total amplitude. Figure 29(a) shows, however, that the harmonic content of the measured response is not attained by the theory. The use of quasi-steady aerodynamics in the theory could be expected to produce such a result through excessive damping. This effect was seen at the lower forward speeds.

Some general summary comments are appropriate at this point concerning the evaluation of the experimental transient data and the correlation of theory and experiment. Of course, the complete analysis of transient rotor blade response must eventually include the consideration of chordwise elastic blade response and disturbances other than control changes. However, the present data show several significant effects and indicate the proper direction in which to seek improvements in analytical methods.

No noticeably unusual rotor behavior was observed during the actual wind tunnel testing of rotor blade response to rapid control inputs. At a few conditions, however, the rotor blade response immediately following the control change included flapwise and torsional moment amplitudes larger than the amplitudes in the initial or final steady-state conditions. The data show that these increased moments persist for only one or two rotor revolutions. The rapid control changes sometimes excited a sub-harmonic lag motion which decayed within one or two cycles.

The correlation of the transient responses measured in the wind tunnel with those calculated using the Normal Mode Transient Analysis is not consistent throughout the range of operating conditions considered. At the lower forward speeds, the results indicate that the inclusion of a transient rotor inflow, possibly including nonsteady, wake induced effects, is necessary to cause the theory to yield a realistic response, particularly rotor blade flapping. At the more extreme low-speed conditions, the addition of unsteady effects associated with blade stall appears to be a requirement to attain a reasonable degree of torsional response correlation. At the higher forward speeds, the most significant aspect of the correlation analysis is the basic problem of theoretically generating a prespecified operating condition in terms of rotor performance, control settings, and angle of attack. The high sensitivity of the rotor system at advance ratios of 1.0 and above forces the analyst to make judgment on parametric values that could be ignored at lower advance ratios.

EFFECT OF AZIMUTH ANGLE OF CONTROL INPUT

Changes in rotor blade transient response, resulting from a variation in the rotor azimuth angles over which the rotor control change takes place, were investigated by using the Normal Mode Transient Analysis. Initial steady-state conditions corresponding to point 28 of run 60 and point 11 of run 55 were used. The rotor control changes for the same test points were modified to take place at azimuth angles 270 degrees larger and were used in the theoretical analysis. The resulting transient responses are presented in Figures 30 through 33.

The revised control inputs begin at the 270-degree azimuth of the first revolution appearing in Figures 30 through 33. This revolution starts at zero and extends to 1 on the azimuth scale of Figures 30 through 33. Because of the lag which appears in the sample data of Figure 15, however, most of the actual change starts at the numeral 1 on the azimuth scale of Figures 30 through 33 and is essentially complete at the 90-degree azimuth of that revolution.

Comparison of these results with the theoretical transients presented in Figures 26 through 29 indicates that the revised control change causes a larger blade response than the original control change.

No significant change in the lag motion without pitch-flap coupling is observable. With the pitch-flap coupling, a much larger control increment is used, and an increase in the subharmonic amplitude occurs.

The flapwise bending moments, flapping motions, and torsional moments show a definite increase in response with the pitch-flap coupling when subjected to the revised control change. The blade response during the actual control change is, of course, quite different between the two sets of cases, but in the second revolution following the control change, the flapwise moment amplitudes are 30 percent larger with the 0- to 90-degree azimuth control change than with the 90- to 180-degree azimuth control change. The overall harmonic content of the response is

essentially the same in both cases by the end of the second transient revolution. The increases in flapping and torsional moment responses are on the order of 10 percent in the third and fourth transient revolutions. During the actual control change, these responses also differ significantly from those following the original control change. As with the flapwise moments, the flapping and torsional moment signatures are unaffected three or four revolutions after the control change.

Without the pitch-flap coupling, the third and fourth revolution flapwise moment, flapping, and torsional moment responses are not significantly different following either the earlier or the later control change. As expected, the responses during the first transient revolution are quite different, and the 0- to 90-degree azimuth control change case is seen to converge to the final values more rapidly than the 90- to 180-degree case.

The physical significance of the differences in transient responses following control changes at different azimuth angles is that, in general, a rapid change in rotor controls will result in a different response by each individual blade of the rotor system. This will exhibit itself in multiple tip path planes and blade root shear forces that are not integrated out before reaching the nonrotating system. The wind tunnel tests showed that these effects are only short term in duration since no unusual behavior was observed in the experiments. The analytical results imply, however, that the erratic rotor behavior may last for 5 rotor revolutions following the control change. Effects of this duration could not be visually observed in the wind tunnel due to the frequency scaling involved, nominally 0.1 second per rotor revolution.

The theoretical effect of transient control input azimuth phasing on the blade response persists for a longer period of time for the case considered here with pitch-flap coupling than for the case without pitch-flap coupling. This is probably related to the much larger control increment required to produce a given amount of flapping when pitch-flap coupling of the amount used here is present. It can be seen in Figure 30 that subharmonic motion is noticeably larger for the case with pitch-flap coupling. This motion requires several revolutions to damp out. While it is present, the various coupling mechanisms cause it to affect blade flapwise and torsional response.

ANALYSIS OF INSTABILITY DATA

GENERAL DISCUSSION

Each of the known types of rotor blade instability pertinent to this investigation is discussed separately in the following paragraphs. It is usual to treat these phenomena as separate entities, using certain appropriate simplifying assumptions or experimental conditions. This approach has led to basic understanding and simple, qualitatively useful methods. Real rotor systems, however, do not necessarily observe these assumptions or restrictions. For example, the violent instabilities experienced during the testing of the blades with aft center of gravity can not be clearly placed into any one of the categories of instability to be discussed below.

Torsional Divergence

The concept of rotor blade torsional divergence follows directly from the similar consideration for a fixed wing, as discussed in Reference 11. Torsional divergence results from a static aerodynamic torsional load which increases in linear fashion with the product of dynamic pressure and angle of attack. If the structural deflection due to the torsional load results in an increase in angle of attack, a so-called negative aerodynamic spring is present. Since the elastic restoring moment resisting the torsional load is proportional to the deflection only, a dynamic pressure which is sufficiently high will result in a rate of static torsional load increase with deflection which exceeds the rate of increase of the elastic restoring moment. This situation is referred to as torsional divergence.

The torsional divergence investigation is clearly applicable to a fixed wing in steady flight, or possibly to a rotor blade in hovering flight, where the relative velocity along the blade is constant in time.

Conventional helicopter blades are, however, mass balanced about the 25 percent chord position of the unstalled aerodynamic center of pressure. This practice causes the torsional couple to remain small when the blade is operating in hover or in the advancing azimuth regime of the rotor disc during forward flight.

When a helicopter rotor is operating at an advance ratio greater than unity, the entire blade is traveling backwards (sharp edge first) through the air for part of each revolution. Under these conditions, the aerodynamic center of pressure moves close to the normal 75 percent chord position. The static flapping restraint for the blade is furnished by a centrifugal force component acting through the blade center of gravity. Hence there is a static torsional couple caused by aerodynamic lift and centrifugal restraining forces whose arm is approximately one-half chord. This large couple causes the torsional divergence situation to be encountered, even though the relative velocities are low on the retreating side of the blade. The elastic axis position in the typical helicopter

blade has little influence on the static torsional moment, because most of the resistance to aerodynamic loadings is due to centrifugal stiffness, which acts at the local blade center of gravity.

If the rotor blade is not mass-balanced, the torsional divergence situation can be encountered on the advancing side of the rotor disc. Since dynamic pressure is much higher than on the retreating side of the rotor disc, a much smaller displacement of the blade center of gravity aft of the center of pressure is required to produce torsional divergence at a given forward speed. Reference 4 contains additional discussion on helicopter blade torsional divergence, with nondimensional charts of divergence boundaries for a wide range of parameters.

The limitations of the torsional divergence theory as applied to the helicopter blade are quite obvious. The blade loadings are applied at time rates which make torsional inertia effects important. Furthermore, the basic torsional forcing moments can be unacceptably large even though a condition for torsional divergence has not been encountered.

Classical Flutter

The classical flutter instability for rotor blades, like torsional divergence, also follows directly from the fixed-wing classical flutter problem, as discussed in Reference 11, for example.

The term "classical flutter" usually refers to the self-excited oscillation of an aerodynamic surface in unstalled flow. Usually classical flutter involves at least two modes of motion, such as airfoil pitching and airfoil plunging. In this case, the elastic, inertial, and aerodynamic properties of the airfoil result in out-of-phase pitching and plunging vibrations. When flutter occurs, the phasing between the motions results in a mechanism which extracts energy from the airstream and feeds it into the structural vibration. If the maximum pitch angle occurs when upward plunging velocity is at its maximum, it can readily be seen that the aerodynamic lift can be in a direction to add energy to the vibration. The pitch angle, velocity, and aerodynamic force will all be reversed when one-half cycle of vibration has passed, and energy input to the structure will continue. The flutter frequency is usually high enough so that the aerodynamic forces have a significant phase difference from the motions, and these phase differences are customarily accounted for in flutter analysis.

Classical flutter occurs in a flow regime where aerodynamic forces are linear with respect to the airfoil motions. Therefore, flutter amplitude will grow with time until nonlinear effects become important or the structure is destroyed.

The classical flutter problem for the helicopter blade in hover is similar mathematically to the fixed-wing classical flutter problem. The major differences are the presence of a helical wake, the variation in velocity along the blade, and the various stiffness and inertial effects caused by rotation.

The classical flutter problem for helicopter blades in forward flight presents a much more complicated problem than the fixed-wing flutter problem. The large, rapid, timewise variation in relative velocity at a blade section requires that the differential equations of motion have time-varying coefficients. The fixed-wing flutter problem is conveniently presented in terms of small motions about some steady equilibrium position. The helicopter blade in forward flight is subject to continuous vibratory loadings and cyclic changes in relative angle of attack which often extend into the stall or reverse flow regime. Because of these large vibratory loadings and resultant blade motions, a purely linear stability analysis for helicopter blade flutter in forward flight has much less practical significance than the typical fixed-wing flutter analysis. The cyclic vibratory loadings and deflections may strongly affect the parameters of the linear stability problem, making the consideration of nonlinear terms necessary for a comprehensive mathematical treatment.

The cyclic variation of flow conditions for the helicopter blade can result in an instability which is limited to certain azimuth regions. If these regions are not too large, the blade passes through them rapidly enough that amplitudes remain acceptable. Thus, the theoretically predicted instability boundary may be penetrated without producing any practically significant change in rotor blade response.

Stall Flutter

Stall flutter refers to the aerodynamically self-excited vibration of an airfoil in the stalled regime. The flow conditions for stall flutter are separated, unsteady, viscous, and compressible. A purely theoretical prediction of the airfoil loadings under these conditions has not as yet been obtained. The available methods of predicting stall flutter depend on the application of airloads data obtained from sinusoidally vibrating two-dimensional sections.

The mechanism of stall flutter results from the rapid motions of the airfoil as it vibrates in pitch. If the frequency of vibration is sufficiently high for a given chord and forward velocity, the steady-state flow conditions will not become established. The airfoil will tend to remain unstalled when pitching upward, and will tend to remain stalled when pitching down. If the stalled pitching moment is negative with respect to the unstalled pitching moment, work will be done on the airfoil as it vibrates. This work is reflected as a negative damping of torsional vibrations.

Stall flutter of helicopter blades occurs intermittently in forward flight as the blade passes through a region of high angle of attack on the retreating azimuth. With conventional blades, only one or two cycles of vibration can take place while the blade is in the unstable azimuth regime. However, the initial entry of the blade into stall will generally provide a large torsional impulse, which will excite torsional vibration. The vibration will tend to persist for one or two cycles until the blade passes into the region of high positive damping on the advancing side of the rotor.

The prediction of stall flutter currently depends on the application of data acquired for a steady-state vibration to a condition where a vibration is impulsively started and quenched. This is probably less of a shortcoming than the problem of accurately predicting the blade angle of attack variation with azimuth on the retreating side of the rotor disc for a given flight condition. Obviously, this angle of attack variation must be known accurately, since the blade aerodynamic pitching loads change radically as soon as stall is encountered.

Flapping Instability

The resistance of the conventional articulated or hingeless helicopter blade to flapping forces is basically the result of centrifugal force components normal to the blade. These components are approximately proportional to small blade flapping angles with respect to the plane of rotation through the rotor hub. The magnitude of these components obviously also depends on the square of the rotational speed. Flapping instability refers to a condition for which the centrifugal flapping resistance is overcome by aerodynamic flapping forces. The flapping instability of the rotor in forward flight was explored in this experimental investigation.

If the helicopter is in forward flight, the upward flapping or flapwise bending of a helicopter blade in the forward half of the azimuth results in an increase in blade angle of attack. This increase in angle of attack causes an increase in blade lift, which is basically resisted by a corresponding increase in the centrifugal force components normal to the blade. If the rotor rotation is slowed, the rate of increase of the centrifugal force component with rotor flapping will become smaller. As shown in Reference 16, a transient negative spring rate in flapping can develop for advance ratios less than $\mu = 0.8$. As advance ratio increases even further, the magnitude and azimuth range of the negative spring rate increases. According to the analogue computer study of Reference 16, this negative spring rate in flapping is responsible for the flapping instabilities that may occur.

Flapping instability has been studied theoretically, as in Reference 16, without considering the effects of coupling with in-plane motions of the blade, such as motion about the lag hinge. More elaborate investigations, one of which is cited in the next section, include consideration of in-plane motion.

Flap-Lag Instability

Helicopter blade flapping and in-plane motions, such as chordwise bending or motion about the lag hinge, have an influence on each other which is referred to as flap-lag coupling. This coupling is primarily due to Coriolis forces. These effective forces arise when the blades acquire a finite flapping angle. The Coriolis forces are of second order from a strict mathematical standpoint, but they are definitely not negligible for blade flapping angles obtained in practice, especially when the rotor is heavily loaded.

In Reference 17, the coupled flap-lag motion of a helicopter blade is studied theoretically. The coupled flap-lag motion was found to be unstable under some circumstances. The coning angle of the rotor determines the amount of unstable coupling. It was also found in Reference 15 that the lag hinge damping of the articulated rotor can be sufficient to suppress flap-lag instability. It does not appear that a simple explanation of flap-lag instability in physical terms is available.

References (16) and (17) do not comment specifically on the operating domains for which a pure flapping instability would be encountered and those for which flap-lag type of instability would appear. The flap-lag instability predicted in Reference (17) can appear at an advance ratio as low as 0.4, for a blade Lock number of 10. The pure flapping instability of Reference (16) is predicted to lie between advance ratios of 2.0 and 2.4 for blade Lock numbers between 12 and 4. Therefore, the more complicated flap-lag theory must be considered in a specific set of rotor stability calculations. In Reference 2, for example, a set of articulated blades was found to be free from flap-lag instability for a certain range of operating conditions. Response of the blades to a sharp-edged gust could then be realistically studied in terms of flapping motion only.

COMPARISON OF THEORY AND EXPERIMENT

Torsional Divergence

As shown by the right-hand vertical rows of points in Figure 14, the theoretical torsional divergence boundary was approached for the 25 percent chord and the 30 percent chord center-of-gravity blades by reducing rotational speed at a constant simulated forward speed of 332 knots. Figure 34 shows time history plots for data points 67-11 and 67-12. A four-revolution sample of blade lag time history is shown, so that the subharmonic motion can be seen. The other plots in Figure 34 are the superimposed time histories of two successive revolutions. The time histories for data points 72-8, 72-9, 75-10, 75-11, 81-8, and 81-9 are qualitatively similar, except for aft center-of-gravity effects and smaller amounts of the subharmonic motion. The conditions for these data points, which are similar to those for 67-11 and 67-12, are given in Tables VII and VIII.

The inboard end of the blade airfoil section is in reverse flow from $\psi = 190$ degrees to $\psi = 350$ degrees for the two data points shown in Figure 34. The entire blade is in reverse flow from $\psi = 225$ degrees to $\psi = 315$ degrees. The large pulse of torsional elastic response shown in Figures 34(e) and 34(f) begins as the blade tip passes into reverse flow. Reference to Table VII shows that $\theta_c = 2.0$ degrees and $B_{1s} = 4.8$ degrees for data point 67-12. The static blade calibration tests provided information about the blade torsional deflection for a given static load. If it is assumed that the blade dynamic torsional deflection mode is approximately the same as the first torsional natural mode, the blade tip torsional deflection with respect to the root may be estimated for the various dynamic loading conditions. The peak torsional deflection for the response shown in Figure 34(f) has been estimated as approximately 9 degrees in

this way.

In order to obtain qualitative information about what actually took place during the condition of Figure 34(f), an estimate of static aerodynamic torsional load at the start of the pulse was made. To facilitate this, induced inflow was neglected, and the relative tangential velocity at $\psi = 230$ degrees was assumed. The blade angle of attack was assumed to be -174.3 degrees as given by the combination of cyclic and collective pitch. Reference to Figures 34(d) and 34(h) shows that flapping and flapwise bending deflection and velocity are small at $\psi = 230$ degrees and therefore do not contribute to blade angle of attack. A lift curve slope of 2π and a center of pressure at the 75 percent chord position were also assumed. The result of this calculation was an estimated aerodynamic blade torsion at $\psi = 230$ degrees of 59.2 inch-pounds about the 25 percent chord. This large, suddenly applied load produced the large torsional acceleration around $\psi = 230$ degrees. The sudden loading was a result not of an instability, but of the passage of the blade into a reverse flow region with a moderately large reverse flow angle of attack. The torsion was the result of a couple between the aerodynamic downward lift at the 75 percent chord and the inertial force required at the 25 percent chord to accelerate the blade mass downward.

The blade elastic twist and cyclic pitch caused the blade reverse flow stalling angle to be encountered soon after $\psi = 230$ degrees. At $\psi = 270$ degrees, the blade angles of attack were estimated to range from -173 degrees at the inboard section to -164 degrees at the tip. Figure 5(c) of Reference 18 shows that reverse flow stalling began at an angle of attack of approximately -173 degrees. Reverse flow velocities continued to increase until the azimuth position reached $\psi = 270$ degrees, while the moment coefficient continued to decrease because of blade stalling. This apparently caused blade torsional aerodynamic loading to remain relatively constant at 60 inch-pounds between $\psi = 240$ degrees and $\psi = 280$ degrees. During this interval, the blade deflection and corresponding elastic moments built rapidly as shown in Figure 34(f). Once $\psi = 270$ degrees was passed, reverse flow velocities decreased and blade torsional load decreased rapidly. The decrease of load was even more rapid than the build-up. This was probably due to a delay in the establishment of unstalled flow.

The flapwise motion of the blade during the conditions of Figure 34 was predominately a three-per-revolution excitation of the first flapwise bending mode. The plunging velocities due to this motion caused comparatively small angle of attack changes.

The results shown in Figure 34 have been shown to be primarily the forced response in torsion and flapping due to the passage of the blade through the reverse flow region. The loadings due to the initial angle of attack were high and rapidly caused blade elastic twist into the stall regime. The reverse flow stall caused the peak loadings to be much smaller than a linear aerodynamic theory would have predicted.

It can be seen that other operating conditions would reduce the torsional loads obtained for the conditions of Figure 34. If the cyclic pitch were reduced from the values used in the conditions of Figure 34, the blade reverse flow angles of attack would approach 180 degrees, both as a direct effect and because of increased blade rearward flapping. This in turn would permit higher forward velocities or lower rotational velocities and a closer approach to the theoretical divergence or classical flutter boundaries. This would obviously not be a practical operating condition for the rotor, since the application of cyclic pitch control for the reduction of blade flapping would cause excessive blade stresses.

Retreating Blade Classical Flutter

The test conditions shown in Figure 34, which were discussed in terms of torsional divergence, also represent the closest approach to the theoretical retreating blade classical flutter boundary, which is practically coincident with the retreating blade torsional divergence boundary. As mentioned in the previous discussion, response to dynamic blade loadings became excessive before the theoretical stability boundary was encountered. The forced response experienced during the test approximated a half cycle at 13 cycles per second. The incipient flutter mode, from an interpolation in Figure 16, has a frequency of approximately 45 cycles per second for the condition of Figure 34. Reference to Table XI shows that the calculated incipient flutter mode has the first flapwise bending mode out of phase with torsion. The forced experimental response was found to have essentially in-phase first flapwise bending and torsion motions.

Figure 15 of Reference 4, which used the method of Reference 1, presents the torsional response of a helicopter blade in reverse flow at a small initial angle of attack. The response appears as an intermittent high-frequency flutter, rather than the single pulse per revolution experienced for similar conditions during the test. This is another indication that a flutter type response may be encountered on retreating blades if the angles of attack are kept close to 180 degrees.

Advancing Blade Classical Flutter

The comparison of theory and experiment for the fixed-azimuth flutter calculations must be rather limited from a quantitative sense. The fixed-azimuth calculation makes the basic assumption that conditions existing in a certain azimuth region exist for all time. Inspection of the test data to be presented in the following paragraphs shows that this simplification is a very drastic one for the rotor in forward flight. Even at advance ratios as low as $\mu = 0.3$, the flapwise bending, torsional, and rigid blade flapping time histories do not exhibit more than one cycle of motion which can even approximate the type of coupled near-sinusoidal motion which exists for a fixed wing. Even if this one cycle of vibration is quite unstable from a fixed-wing flutter standpoint, the buildup of successively larger vibrations which characterizes fixed-wing flutter cannot occur. This, of course, makes the fixed-azimuth flutter calculation, in itself, very conservative. This fact was confirmed by the test results. The $\psi = 90$ degrees advancing blade flutter boundaries were

penetrated with no noticeable change in blade response. The rotor was operated at conditions far in excess of these boundaries, with only moderate increases in blade loadings and motions, as expected.

The unexpected incidents of violent and sudden rotor instability which occurred during the experimental investigation for the blades with center of gravity at the 35 percent chord appear to be related to advancing blade excitation. While each of the incidents occurred beyond the fixed-azimuth flutter boundary, it cannot be concluded that this will always be the case. For example, the forward speed for violent instability at a rotational tip speed of $\Omega_s R = 700$ feet per second was lowered from $V_s = 208$ knots to $V_s = 120$ knots by raising collective pitch from 4.0 degrees to 6.8 degrees on the trimmed rotor. The predicted fixed-azimuth flutter forward speed was 20 knots for this rotational speed. It is at least plausible to expect that a slightly higher collective pitch would cause violent instability to occur in hover at $\Omega_s R = 700$ feet per second, although this would not be predicted by the fixed-azimuth flutter theory.

In spite of the above considerations, it is worthwhile to compare the experimentally determined blade response to the predicted fixed-azimuth flutter response. This comparison can lead to improved judgement and to the creation of a more realistic and possibly simpler analysis. The blade motions over limited azimuth regions of the blade will be treated in the comparison as if they were sinusoidal vibrations. Simultaneous motions occurring in torsion, flapwise bending, or flapping will also be considered as taking place at the same frequency, even if this is only approximately correct. Thus, the terms "frequency" and "phase" will be applied to a short time interval during which the fixed-azimuth flutter motions may approximate the experimental motions. These terms, which have a definite meaning within the fixed-azimuth flutter calculation, do not, in a strict sense, apply to the actual response of the blade.

In order to relate the blade response to the predicted fixed-azimuth flutter modes, the relationship between blade tip deflection and moments was determined from the natural mode calculations and checked with the aid of the static blade calibration results. One inch of tip motion in the blade first flapwise bending mode was found to be equivalent to 34.6 inch-pounds of flapwise bending at the 30 percent radius station, 51.0 inch-pounds of bending at the 60 percent radius station, and -2.4 degrees of blade flapping at the hinge. One inch of tip motion in the blade rigid flapping mode is equivalent to 1.1 degrees of blade flapping at the hinge. One degree of blade pitch at the tip in the first torsional mode produces a moment of 7.5 inch-pounds at the 18 percent radius station and 7.0 inch-pounds at the 35 percent radius station.

Sample time history data for the blades balanced about the 25 percent chord location are presented in Figure 35 for comparison with the behavior of the aft center-of-gravity blades. The data are presented as the superimposed time histories of two successive revolutions. The data of Figure 35 were taken during test points 65-3 and 67-7. The rotor conditions for these points are given in Table VII. The various time histories are similar for these two data points. Some reverse flow

excitation is evident in torsion and bending in both cases.

Figure 36 presents data at $\Omega_s R = 700$ feet per second and two simulated forward speeds for the blade with the center-of-gravity location at the 30 percent chord. The rotor operating conditions for these points, 74-5 and 74-9, are given in Table VIII. The calculated flutter onset for this blade at that rotational speed is $V_s = 150$ knots, as shown on Figure 16(c). The flutter onset is defined by the change from positive to negative damping of the critical aeroelastic mode. The damping versus forward speed at various constant rotational speeds is given in Figure 16(c). Both data points shown in Figure 36 are well into the theoretically unstable regime. Data point 74-9 was taken at the highest speed reached with the $\Omega_s R = 700$ -feet-per-second rotational tip speed and the 30 percent chord center-of-gravity blade. As shown in Figure 36, the blade response was still quite moderate at this speed. Further increases in speed were prevented by an observed increase in model vibration. This may have been related to the nonharmonic lag motion evident in Figure 36(b). Frequency analysis showed a discrete frequency lag motion component of 0.46 degree amplitude at 0.215 cycle per revolution.

In order to determine the more detailed effects of the aft center-of-gravity location, Figure 35(a) can be compared with Figure 36(b), 35(c) with 36(d), 35(e) with 36(f), and 35(g) with 36(h). The conditions for the two data points involved were practically identical. The only dramatic change occurred in the torsional time history. A torsional vibration appeared, grew in amplitude in the advancing azimuth regime, and decayed in the retreating azimuth regime. The instantaneous frequency of the torsional oscillations was lower on the advancing than on the retreating azimuth region. These amplitude and frequency variations fulfill qualitative expectations from the fixed-azimuth flutter considerations. From a more quantitative standpoint, the frequency of torsional oscillation in Figure 36(f) for the cycle between $\psi = 40$ degrees and $\psi = 140$ degrees is 3.6 cycles per revolution or 45 cycles per second. The frequency of the cycle between $\psi = 240$ degrees and $\psi = 320$ degrees is 4.5 cycles per revolution or 55 cycles per second. These frequencies may be compared to the torsional natural frequency of 55.6 cycles per second given in Table II and the predicted flutter frequency of 29 cycles per second, shown in Figure 16(c). It is evident that the large predicted drop in the frequency of the torsional mode did not occur.

Evidence of coupling between torsional and flapwise motion in the advancing azimuth region is present. The flapwise bending peak in Figure 36(d) at $\psi = 140$ degrees is out of phase with torsion. Comparison of Figures 35(g) and 36(h) shows that the aft center-of-gravity blade has an additional advancing azimuth flapping motion which is also out of phase with torsion. This phase relationship is not similar to that calculated for the flutter mode at $V_s = 220$ knots, as shown in Table XI. The relative order of magnitude of these motions is, however, roughly comparable to the calculated flutter mode for $V_s = 220$ knots. Comparison of the data of Figure 36(e) and 36(f) shows that the torsional magnitude increases with forward speed and that frequency is relatively unaffected. The flapwise bending response in Figure 36(c) is very small, but it appears that

flapwise bending response is approximately in phase with torsion at this lower speed. This phase relationship is similar to that shown in Table XI for forward speeds of $V_g = 160$ knots and $V_g = 220$ knots.

The data shown in Figure 37 are also for the 30 percent chord center-of-gravity blade, and are from points 75-4 and 75-7. The corresponding rotor operating conditions are given in Table VIII. Figures 37(b) and 35(b), 37(d) and 35(d), 37(f) and 35(f), and 37(h) and 35(h) can be directly compared to determine the effect of the 30 percent chord center of gravity. The most obvious effect is, as before, the torsional vibration buildup on the advancing azimuth region, as shown in Figure 37(f). The rotational tip speed ($\Omega_g R$) is 500 feet per second. Thus the relative velocities are smaller over most of the azimuth than in Figure 36, which presents data with $\Omega_g R = 700$ feet per second. This is probably the reason for the much more rapid quenching of the torsional vibrations in the retreating azimuth region. The torsional vibrations excited on the advancing azimuth are almost completely decayed when the reverse flow torsional impulse begins around $\psi = 260$ degrees.

By referring to Figure 16(c) and Figure 37, it can be seen that test point 75-4 lies on the calculated flutter boundary and that test point 75-7 lies well beyond it.

The frequency of the cycle of torsional vibration between $\psi = 60$ degrees and $\psi = 140$ degrees in Figure 37(f) is 4.5 cycles per revolution or 40 cycles per second. The cycle of vibration between 180 degrees and 240 degrees is 6.0 cycles per revolution or 53 cycles per second. As before, these frequencies may be compared with the torsional natural frequency of 55.7 cycles per second given in Table II and the predicted flutter frequency of 30 cycles per second, shown in Figure 16(c). As at $\Omega_g R = 700$ feet per second the experimental advancing blade response frequency at $\Omega_g R = 500$ feet per second is much higher than the predicted flutter frequency.

The coupling of torsion with flapwise bending and flapping is much more prominent for point 75-7 than for point 74-9. Flapping is out of phase with the torsional pulse at $\psi = 100$ degrees in Figure 37(f), while flapwise bending is in phase. Consideration of the relative amounts of flapwise bending and flapping indicate that the blade flapwise motion in this region is principally first-mode bending. These results do not agree qualitatively or quantitatively with the calculated flutter mode at $V_g = 320$ knots, as given by Table XI.

Figure 38 presents data from point 75-11, which is at the same forward speed as point 75-7 but at a lower rotational speed of $\Omega_g R = 404$ feet per second. The advancing azimuth torsional response is qualitatively the same in Figure 38(c) and Figure 37(f). The retreating azimuth response is much greater because of increased reverse flow. The flapwise response in Figure 38(b) is quite different from that in Figure 37(d). The flapping time histories shown in Figure 38(d) and Figure 37(h) are, on the other hand, quite similar on the advancing azimuth region. The nonharmonic lag motion appearing in Figure 38(a) has a significant discrete frequency

component at 0.29 cycle per revolution. The nonharmonic flapping motion has discrete frequency components at 0.29, 0.71, and 1.29 cycles per revolution. These nonharmonic motions will be discussed separately.

The forward flight advancing azimuth excitation of the blade with the 30 percent chord center-of-gravity location does not generally conform, even instantaneously, to the predicted fixed-azimuth flutter frequency or mode shape. It is probable that the very short time interval during which the blade is theoretically susceptible to fixed-wing type flutter prevents the noticeable self-excited buildup of a fixed-wing type flutter mode.

The sample data from the advancing blade aeroelastic limits testing of the blade with the center of gravity at 35 percent chord will be discussed next. Figure 39 shows data from test points 83-3 and 83-5. The operating conditions for these points are given in Table IX. Both points were taken at a rotational tip speed ($\Omega_s R$) of 700 feet per second. As for the blade with the 30 percent chord center of gravity, a torsional vibration arose which grew in amplitude on the advancing side and decayed on the retreating side. This vibration is evident in the time history results given in Figures 39(f) and (g). The increase in forward speed from $V_s = 138$ knots to $V_s = 187$ knots did not affect the frequency of vibration and caused only a moderate increase in amplitude.

The frequency of the torsional vibration cycle which extends from $\psi = 0$ degrees to $\psi = 150$ degrees in Figure 39(g) is 2.4 cycles per revolution or 30 cycles per second. The frequency of the cycle which extends from $\psi = 240$ degrees to $\psi = 360$ degrees is 3.0 cycles per revolution or 37 cycles per second. These frequencies may be compared with the natural torsional frequency of 48.8 cycles per second from Table II and the predicted flutter frequency of 27 cycles per second from Figure 16(d). Considering the fact that the flutter frequency is predicted only for an azimuth angle of $\psi = 90$ degrees, this is a satisfactory agreement.

The blade response for point 83-5 is moderate, and evidence of coupling between flapwise bending and torsion does not appear in Figure 39(d) for the inboard flapwise bending. Figure 39(e) does, however, show an outboard flapwise bending response which has a waveform similar to the torsional response. The relative amounts of flapwise bending and torsional response agree to within 20 percent with the calculated flutter mode for $V_s = 80$ knots, which is given in Table XI. The phase relationship between bending and torsion is not as predicted, but this may be a result of the substantially higher forward speed of test point 83-5. The predicted involvement of the rigid blade flapping mode also does not occur.

After point 83-5 was taken, the wind tunnel velocity was slowly increased, while the torsional stress amplitude was continuously monitored. The stress amplitudes remained close to the moderate values corresponding to Figure 39(g) until a simulated speed of 208 knots was reached. At this point, the blade stresses suddenly increased beyond the allowable limits, and violent nonharmonic blade flapping motions were observed. The wind tunnel was shut down and the model stabilized before a record of the blade

motions could be obtained.

The data shown in Figure 40 were taken at a rotational tip speed ($\Omega_s R$) of 500 feet per second. Data points 84-3 and 84-6 were taken at forward speeds (V_s) of 187 knots and 259 knots respectively. The rotor operating conditions for these two data points are given in Table IX. The type of advancing blade excitation noted for the test points of Figure 39 occurred again, as shown in Figure 40(f) and (g). A nonharmonic torsional vibration is evident in Figure 40(g). This particular data point is for an operating condition at which a violent instability later occurred spontaneously, and this nonharmonic is probably a manifestation of that incipient instability. The nonharmonic motion shown for the two revolutions in Figure 40(g) was not typical for the entire record of 50 revolutions, and only appeared occasionally at random intervals.

The cycle of torsional vibration in Figure 40(g) between $\psi = 40$ degrees and $\psi = 160$ degrees has a frequency of 3.0 cycles per revolution or 27 cycles per second. The cycle of torsional vibration between $\psi = 220$ degrees and $\psi = 290$ degrees has a frequency of 5.1 cycles per revolution or 45.6 cycles per second. These frequencies may be compared with the torsional natural frequency of 47.1 cycles per second from Table II and the calculated flutter frequency of 27 cycles per second from Figure 16(d). As with the results shown in Figure 39 for data points 83-3 and 83-5, these frequencies agree well with the fixed-azimuth considerations. The coupling of torsion with flapwise bending is not plainly apparent, as can be seen from Figures 40(d) and (e). The coupling that does exist appears to cause flapwise bending to be in phase with torsion. The flapping motion about the hinge is out of phase with torsion around the azimuth angle $\psi = 120$ degrees, as shown in Figure 40(i). A comparison with the predicted flutter mode for $V_s = 140$ knots from Table XI shows that the predicted relatively large amounts of flapwise bending do not appear. The relative amounts of rigid blade flapping and torsion and their phase are, however, correct within about 50 percent.

Even though the blade response was quite moderate while the data shown in Figure 40 (for data point 84-6) were taken, the rotor was in fact operating at a condition for which a violent instability was possible. After the data were taken for point 84-6, and before any of the controls were operated to obtain the next test point, rotor response changed suddenly. Blade stresses and motions became nonharmonic and greater than allowable, and the wind tunnel was shut down. During the recovery of the model from the instability, some time history data were obtained with the on-line oscillograph. These data will be presented and discussed later. Frequency analysis of the data of point 84-6 showed nonharmonic flapping motions of only 0.3 degree at a frequency of 0.5 cycle per revolution, and torsional nonharmonic moments of only 0.74 inch-pound at a frequency of 0.5 cycle per revolution and only 2.4 inch-pounds at 4.5 cycles per revolution. These frequency components are obviously present in the time history of the instability, which will be presented and discussed later.

Figure 41 presents time history data for two additional data points taken with the 35 percent chord center-of-gravity blade. Point number

85-3 is another point close to a violent instability, and 85-8 is the point of highest reverse flow velocity obtained with this blade.

The data for point 85-3 in Figure 41 was taken for a speed slightly lower and a collective pitch slightly higher than for point 83-3 shown in Figure 39. The corresponding data channels show good quantitative agreement. The relatively small changes reflect the differences in the operating condition. An attempt to raise collective pitch at the forward speed and rotational speed of point 85-3 resulted in another sudden violent instability when a collective pitch of 6.8 degrees was reached. The instability again was characterized by high nonharmonic blade loads and motions. Analysis of the data of point 85-3, which was taken at a collective pitch of 5.0 degrees, did not produce any indication whatever that a violently unstable condition would be entered by raising the collective pitch 1.8 degrees. In the case of this instability, data were obtained on the magnetic tape, and a full frequency analysis of the motions during the instability could be carried out. This will be discussed later.

The data from test point 85-8 also appear in Figure 41. These data repeat the patterns of previous data, which are a growth of torsional amplitude on the advancing azimuth and a decay on the retreating azimuth. As with previously discussed data, the frequency of the vibration is lower on the advancing azimuth. The coupling between flapwise bending and torsion again exists only on the advancing azimuth region, as can be seen from Figures 41(d) and 41(j).

Consideration of the time history data presented in Figures 35 through 41 shows that the aft center-of-gravity offset consistently caused an advancing blade torsional vibration. The coupling of the torsional motions with flapwise motions in the manner of a fixed-wing flutter was not, however, consistently observable. When it was observable, agreement with the fixed-azimuth flutter mode was sporadic.

Since, at most, one cycle of vibration is possible before the blade passes out of the theoretically unstable regime, the rapid increase in torsional vibration must be explained in terms of a forced phenomenon. This contention is strengthened by observing the torsional moment time history in Figure 37(e) for data point 75-4. This point is very close to the 90-degree fixed-azimuth stability boundary, yet the torsional amplitude more than doubles in one cycle. Since negative damping of the fixed-azimuth flutter mode is not sufficient to explain this rapid growth in blade torsional vibration, some other mechanism must be responsible.

In order to gain some preliminary insight into what actually occurred when the rotor blade with center of gravity at 35 percent chord was operated in forward flight, some simple calculations were based on the data for point 83-5, which are shown in Figures 39(b), 39(d), 39(e), 39(g), 39(i), and 39(k). Assuming zero rotor inflow velocity, a lift curve slope of 2π , and a center of pressure at 25 percent chord, a static aerodynamic blade torque of 25.2 inch-pounds was estimated at an azimuth angle of $\psi = 0$ degrees and 13.9 inch-pounds at $\psi = 90$ degrees. These calculations considered the elastic blade twist corresponding to the elastic moment

time history shown in Figure 39(g). Obviously, the elastic torsional response shown in that figure is readily explained on the basis of blade response to cyclic loadings. In addition to causing torsional load directly, the aft center of gravity causes a negative aerodynamic spring effect in torsion. This negative spring effect is considered in the fixed-azimuth torsional divergence and flutter analyses. Consideration of the blade dynamic deflections corresponding to the moment time history of Figure 39(g) indicates that they are the same order of magnitude as the cyclic pitch changes. For example, estimated blade root pitch is 5.5 degrees and tip pitch is 4.2 degrees at an azimuth angle $\psi = 0$ degrees. At $\psi = 90$ degrees, the blade root pitch is -1.2 degrees, but the blade tip pitch is 2.5 degrees. Thus, over this quadrant of the azimuth, only 1.7 degrees of pitch change appears at the blade tip, in contrast to 6.7 degrees at the blade root. At $\psi = 90$ degrees, however, the blade positive torsional deflection reaches its peak and begins to decrease. When the blade is at $\psi = 135$ degrees, the torsional deflection is negative, and estimated blade pitch is -0.8 degree at the root and -3.2 degrees at the tip. Over the azimuth sector $90 < \psi < 135$ degrees, +0.4 degree of pitch change appears at the root, in contrast to -5.7 degrees of pitch change at the blade tip. When the blade reaches $\psi = 180$ degrees, torsional deflection is almost zero, and the tip and root blade pitch practically coincide. It is probable that the magnification of cyclic pitch change in the second azimuth quadrant compensates for the loss of cyclic pitch change in the first quadrant.

The above considerations lead to a preliminary explanation of the violent instabilities observed during the course of the wind tunnel testing. In simple terms, dynamic blade twisting was caused by the response of the blade with aft center of gravity to the cyclic loads on the advancing side of the azimuth. These dynamic deflections were of relatively low frequency because of the negative aerodynamic torsional spring effect. For some flight conditions, these deflections overcame the cyclic pitch input required to control blade flapping, as well as the angle of attack changes due to flapping velocity which stabilize the blade tip path plane.

Instabilities of the above type depend on rotor loading and are not predictable by a fixed-azimuth consideration of the unloaded blade, although it may be found that such a fixed-azimuth calculation will always provide a conservative boundary.

The approach of Reference 6 should be suitable for studying the types of instabilities encountered. Reference 6 considers the cyclically varying parameters of the linear differential equations of motion. The method of Reference 1 also can be applied to the problem, if unsteady aerodynamic effects do not play an important part in the mechanism of the instability. The method of Reference 1 is a step-by-step timewise numerical integration of the equations of motion, with full consideration of quasi-steady nonlinear effects.

Stall Flutter

The agreement between theory and experiment for the fixed-azimuth stall flutter analysis is reasonably good from a qualitative standpoint, in that the predicted retreating blade vibrations materialized for rotor conditions found to be theoretically subject to stall flutter. Since stall flutter occurs at a relatively high frequency, the fixed-azimuth assumption has a relatively greater correspondence to physical reality. As will be shown in the discussions to follow, the blade torsional dynamic loadings, as well as the torsional instability, contribute to the levels of torsional response noted for retreating blade stall flutter.

The accuracy of the stall flutter prediction method used in this investigation, or any similar improved method, depends in turn on an accurate determination of retreating blade angle of attack for a given flight condition. This may sometimes prove difficult, since when stall flutter occurs the rotor is operating in a condition for which heavy blade stalling is present. Rotor performance and corresponding blade motion predictions tend to be less accurate under these conditions.

For the present investigation, the variation of angle of attack and relative velocity with azimuth and radius was determined by using the Normal Mode Transient Analysis described in Reference 1. In order to make the geometrical relationships in this calculation as much like the experimental relationships as possible, the collective pitch range to be used in the test was also used in the Normal Mode Transient Analysis. The cyclic pitch used in the analysis was that setting which resulted in a calculated zero first harmonic flapping response for a given flight condition. This procedure was also followed experimentally. The calculated rotor performance was not used as a basis for comparing stall flutter theory and experiment. The calculated rotor conditions which provided the angle of attack and relative velocity variation needed for the stall flutter analysis are summarized in Table XII. These may be compared with similar experimental conditions in Table VII, such as 68-3 through 68-7, 68-13 through 68-16, and 51-7 through 51-11. It can be noted that the calculated results overestimate longitudinal cyclic pitch requirements, underestimate rotor lift, and agree relatively well with experimental rotor torque. The experimental conditions for the theoretically predicted lift coefficients shown in Table XII would occur at collective pitch settings approximately 4 degrees lower, and it is virtually certain that stall flutter would not be experienced for these conditions. The consideration of variable rotor inflow may improve the agreement between calculated rotor performance and experimental performance for a given collective pitch.

The experimental stall flutter condition time histories are given in Figures 42 through 45. Figure 42 contains data from points 68-3, 68-6, and 68-7 which were taken at a rotational tip speed ($\Omega_s R$) of 700 feet per second and a simulated forward speed of $V_s = 121$ knots. Figure 17(a) shows the calculated variation of aerodynamic torsional damping ratio with azimuth for these rotor conditions. The calculated negative critical damping ratios are far too small to explain the sudden onset of torsional

vibration appearing in Figures 42(k) and 42(l). Using the simple expression for the amplitude ratio of oscillations

$$R_A = e^{-2\pi\zeta_{AD}} \quad (22)$$

and letting, for example, $\zeta_{AD} = -0.04$ (from Figure 17(a)), one obtains $R_A = 1.46$. This means that with no other effects present, the oscillation would gradually increase, with each successive cycle of oscillation 1.46 times the preceding one. The actual blade torsional time history in Figures 42(k) and 42(l) shows a rather abrupt nose-down response, which is due to blade stalling. The resulting torsional vibration is sustained for 1.5 cycles by negative and low damping in the retreating azimuth region. The frequency of the oscillation is approximately 6.3 cycles per revolution or 78 cycles per second. This agrees well with the torsional natural frequency of 75.3 cycles per second, which is given in Table II. The return of the blade to the unstalled, high positive damping region in the advancing azimuth part of the rotor disc results in a rapid quenching of the torsional vibration. Inspection of the data for lag, flapwise bending, and flapping in Figures 42(a) through 42(i) and Figures 42(m) through 42(o) shows that no discernible direct coupling exists between the torsional vibrations and lag and flapwise responses. Figure 43 shows data from points 68-8, 68-11, and 68-12. These are shown instead of data from points 68-13 through 68-16 because of an intermittent failure of the torsional strain gage. The stall flutter response at this higher speed ($V_s = 145$ knots) is slightly greater than the similar data for Figure 42, which were taken at $V_s = 122$ knots. The size of the unstable azimuth sector shown in Figure 17(b) for $V_s = 170$ knots is somewhat larger than the corresponding region in Figure 17(a) for 120 knots. The calculated negative damping is numerically smaller, however, primarily because of the lower relative velocities. The data in Figure 43 for $V_s = 145$ knots are qualitatively similar to those in Figure 42 for $V_s = 120$ knots.

Figures 44(a), 44(c), 44(e), 44(g), and 44(i) show data from point 51-11, which corresponds to the last of the calculated conditions in Table XII. These calculations provided the torsional damping data shown in Figure 17(c). The stall flutter response shown in Figure 44(i) at this forward speed ($V_s = 202$ knots) is slightly smaller than the corresponding data from Figure 43(i), which were taken for $V_s = 145$ knots. The torsional vibration has a less abrupt initiation, but its subsequent buildup is more rapid than at the lower speeds. The less abrupt initiation could be caused by lower relative velocities existing around $\psi = 270$ degrees for the condition of Figure 44(i) than for the condition of 43(i) or 42(i). It would appear, however, that the negative damping is somewhat greater than the predicted variation given in Figure 17(c). In the azimuth region $240 < \psi < 340$ degrees of Figure 44(i), for example, the second torsional cycle is approximately twice the amplitude of the first one. Using the inverse of Equation (22), one obtains $\zeta_{AD} = -0.110$.

The above comparison of theory and experiment shows that stall flutter will occur as predicted by the fixed-azimuth stall flutter analysis if the retreating blade angles of attack used in the analysis are

reasonably close to those existing experimentally. It appears that the magnitudes of the negative damping are of the correct order of magnitude. The torsional impulse which accompanies blade stalling appears to have a significant effect on the stall flutter amplitude. The information from the fixed-azimuth stall flutter analysis therefore provides only a very approximate indication of the severity of the stall flutter.

Figures 44(b), 44(d), 44(f), 44(h), and 44(j) show data from test point 51-16, which was taken at high collective pitch and high forward speed ($V_0 = 304$ knots). The advance ratio was 1.03 for this condition. The blade torsional response for this condition is shown in Figure 44(j). Stall flutter was not present, and the blade responded to reverse flow loadings, as shown in Figure 34 and discussed earlier in this section under the subheading Torsional Divergence. The torsional amplitude of the reverse flow response was approximately equal to the stall flutter response experienced at lower speeds.

Figure 45 presents data taken with the 30 percent chord center-of-gravity blades for data points 76-4, 78-4, and 79-10. The rotor operating conditions for these points are given in Table VIII. Point 76-4 is comparable to point 68-6 shown in Figure 42, point 78-4 is comparable to point 68-11 shown in Figure 43, and point 79-10 is comparable to point 51-16 shown in Figure 44.

Comparison of Figures 45(h) and 45(i) for the 30 percent chord center-of-gravity blades with Figures 42(k) and 43(k) respectively for the 25 percent chord center-of-gravity blades shows that the stall flutter portion of the blade response was not aggravated by the aft center-of-gravity offset. In fact, some alleviation of stall flutter appears in Figure 45(h). A larger excitation resulted on the advancing blade, however. The frequency of the advancing blade torsional motion was approximately equal to the frequency noted for the similar response in point 74-5, shown in Figure 36(e). The advancing blade response decays rapidly at high collective pitch angles, instead of persisting into the retreating azimuth region as in Figure 36(e). It is interesting to note that the coexisting retreating azimuth stall flutter and advancing azimuth excitation do not aggravate each other but, on the contrary, appear to interfere with each other. A rotor blade with aft center-of-gravity offset has a tendency to become unstable at lower forward speeds under higher loadings. This does not appear to be a result of any interaction between stall flutter and advancing blade excitation.

Advancing Azimuth Excitation at High Collective Pitch

Examination of the flapwise bending response for data points 76-4 and 78-4, which is shown in Figures 45(d), 45(e), and 45(g), and comparison of these with Figures 42(h), 43(e), and 45(h) show little if any direct coupling of the flapwise bending response to the advancing azimuth torsional excitation. The blade flapping data for point 78-4, shown in Figure 45(k), does show out-of-phase coupling with blade torsion on the advancing azimuth. The data in Figure 45(k) may be compared with Figure

43(n) for the blade with the center of gravity at the 25 percent chord operating at the same condition. This advancing azimuth coupling of flapping and torsion is approximately the same as in the predicted fixed-azimuth classical flutter mode at a forward speed (V_s) of 140 knots, which is given in Table XI.

Data for point 79-10, which corresponds to point 51-16, is also given in Figure 45. At this higher speed and high collective pitch condition, the changes caused by aft center of gravity are more dramatic. By comparing Figure 45(q) with 44(k), 45(l) with 44(h), and 45(f) with 44(d), it can be seen that a very obvious coupling effect exists between flapwise and torsional motions on the advancing azimuth region. The relative phasing of flapping and torsion is similar to that for the calculated fixed-azimuth flutter mode at 320 knots, as given in Table XI. The experimental motion has a much larger proportion of blade flapping and flapwise bending. The blade lag motion shown in Figure 45(c) contains a noticeable nonharmonic motion. Frequency analysis showed this motion to be 0.50 degree amplitude at 0.30 cycle per revolution.

The comparisons made in the above paragraphs are a further demonstration that the advancing azimuth aft center-of-gravity blade excitation is fundamentally a forced phenomenon. Figures 45(q) and 37(f), 45(l) and 45(h), and 45(f) and 37(d) may be compared to show that collective pitch, and therefore blade loading, has an important effect on the magnitudes and relative proportions of the various blade response measurements.

DISCUSSION OF VIOLENT INSTABILITIES

Flapping Instability

Each of the rotors was operated at various forward speeds with the rotor rotational speed reduced as far as possible. At all but the highest forward speeds, reduction in rotational speed was limited by a noticeable sluggishness in rotor control response. Rotational speed was reduced until it was felt that control of the rotor was about to be lost. The highest advance ratio reached with the rotor controllable was 1.91, at a simulated speed of 258 knots. At a simulated speed of 280 knots and an advance ratio of 1.94, control of the rotor was lost. Control was immediately regained by bringing up rotational speed.

During this part of the testing, the blade first harmonic flapping was kept as small as possible through the use of cyclic pitch, although random wandering of the blade tip paths was noted at the minimum rotational speeds. Post-test analysis of the data taken at the minimum rotational speeds showed, however, that blade motions and loads increased gradually with forward speed. Frequency analysis showed that rotor harmonics were the only significant discrete frequency components present at simulated forward speeds below 300 knots. The random wandering of the blade tip paths was recorded as randomly varying bursts of first harmonic flapping motions.

At simulated forward speeds of 300 knots and greater, the reduction in rotational speed was limited by rapidly increasing retreating blade torsional loadings, accompanied by peak torsional deflections as high as 11 degrees. Under these conditions, a coupled flap-lag motion developed at a discrete frequency. This incipient instability will be discussed later.

As mentioned previously, all instabilities resulting from the slowing of the rotor were encountered in a gradual manner, and it was clearly evident from either rotor response or blade stress amplitude monitoring that a dangerous condition was being approached.

Instability Due to Aft Center-of-Gravity Location

A number of violent instabilities were encountered with the blade center of gravity at the 35 percent chord position. These were encountered while increasing forward speed at constant rotational speed and by raising collective pitch at constant forward speed and rotational speed.

Rotor blade response for conditions close to instability has been discussed under the comparison of the experimental data and the advancing blade classical flutter theory. As mentioned under that discussion, the theoretical advancing blade classical flutter boundary was penetrated, and blade torsional response increased gradually with forward speed or collective pitch until a sudden violent instability occurred. Analysis of the data showed that the blade cyclic airloads caused blade torsional deflections in the advancing azimuth region, and that these were large enough to interfere with the cyclic blade angle of attack changes which normally control and stabilize the rotor. It did not appear that the fixed-wing type of flutter instability could produce the blade response noted, since it was present for too limited an azimuth sector.

The first of the instabilities referred to occurred as the forward speed was raised to $V_8 = 208$ knots, starting from data point 83-5. The rotor operating conditions for data point 83-5 are given in Table IX. No data were obtained while the rotor was in its unstable mode, although large blade stresses and flapping motions were observed. Detailed analysis of the data from point 83-5 showed that nonharmonic motions at discrete frequencies were very small.

Instability was encountered at the operating condition of data point 84-6, which was at a simulated speed of 256 knots. Instability was entered spontaneously after data had been taken for point 84-6. The data shown in Figure 46 were taken with the on-line oscillograph during wind tunnel shutdown. The unstable oscillations were decaying but were still very prominent. Inspection of Figures 46(a) and 46(d) shows that a one-half-per-revolution lag and flap motion was present. Inspection of the torsional time history in Figure 46(c) shows that a 4.5-cycle-per-revolution frequency component is also present. This is especially obvious during the second revolution shown on Figure 46(c). The 4.5-cycle-per-revolution frequency is equivalent to 39.8 cycles per second. The local variation of

frequency with azimuth appears similar to that recorded for point 84-6 and shown in Figure 40(g). The torsional amplitude shown is approximately equivalent to 5.5 degrees of elastic twist at the blade tip. The data of point 84-6 were carefully analyzed, and discrete frequency motions were found at 0.5 cycle per revolution in flapping and torsion and at 4.5 cycles per revolution in torsion. These were not present at point 84-5 which was taken at a speed of $V_g = 235$ knots, 24 knots lower than point 84-6. These motions were still extremely small at point 84-6. The 0.5-cycle-per-revolution components had an amplitude of only 0.3 degree in flapping and 0.7 inch-pound in torsion. The 4.5-cycle-per-revolution torsional response had an amplitude of only 2.4 inch-pounds. Even though the rotor was operating at a dangerous condition, the related nonharmonic response was not noticeable until the instability was triggered to a larger amplitude. Inspection of Figure 46(c) shows a torsional response at 4.5 cycles per revolution with an average amplitude of approximately 25 inch-pounds. By comparing with the 2.4-inch-pound amplitude at this frequency component that was present for data point 84-6, it can be seen that the nonharmonic motions grew spontaneously by a factor of at least 10 as the instability became established.

Instability was again encountered with the 35 percent chord center-of-gravity blade by raising collective pitch to approximately 7 degrees at a forward velocity (V_g) of 120 knots and a rotational tip speed ($\Omega_g R$) of 700 feet per second. Data point 85-3 was taken at the same conditions, except for a collective pitch of 5 degrees, as shown in Table IX. The instability again was entered suddenly; on this occasion, a record of the unstable motions was obtained on the F.M. tape recorder. An eight-revolution sample of this record is presented in Figure 47. The torsional time history of Figure 47(d) has a superficial resemblance to that of Figure 46, but the modulation of amplitude occurs at approximately 0.33 cycle per revolution instead of 0.5 cycle per revolution. The amounts of flapping and lag motion relative to torsion are also greater in the instability shown in Figure 47. In order to determine specific blade motions which play an important part in the instability, frequency analyses of the data were carried out. The plots of amplitude against frequency are shown in Figure 48. The components of the most important amplitudes are given in Table XIII. The a_m and b_m refer to the $\cos \omega_m t$ and $\sin \omega_m t$ components respectively at each frequency given. The time (t) is defined as zero at an arbitrary zero azimuth signal; therefore, the components given for the nonharmonic motions are only significant in relation to one another.

It is interesting to note that the important nonharmonic frequencies present do not reflect motion at a low integral subharmonic frequency such as 0.33 or 0.50 cycle per revolution. The frequencies present appear to be those of aeroelastic vibrations, which have become much greater than the normal harmonic forced vibration.

The blade flapping and lagging motion at 0.28 cycle per revolution is close to the calculated lag frequency of 0.309 cycle per revolution. The flapping components at 0.72 and 1.28 cycles per revolution are due to a lag frequency amplitude modulation of blade once-per-revolution flapping. The predominant torsional amplitude during the instability occurred at a

frequency of 3.40 cycles per revolution, which is equivalent to 42.1 cycles per second. This is slightly lower than the torsional natural frequency of 48.8 cycles per second from Table II, and much higher than the advancing blade classical flutter frequency of 27 cycles per second shown in Figure 16(d). It appears that the frequency of the torsional oscillations is locally lower in the advancing azimuth region, as for the stable rotor conditions previously discussed.

The peak torsional amplitudes appearing in Figure 47(d) represent a blade tip elastic deflection amplitude of approximately 13 degrees, and it is certain that blade stalling occurred at the tip. The large drag forces caused by this stalling may be responsible for the large lag motion shown in Figure 47(a). It can be seen that the blade velocity in the lag direction is greatest during the bursts of large torsional oscillation.

Each of the violent instabilities due to aft center-of-gravity location were encountered suddenly and reached a large though self-limited amplitude before any action could be taken. The amplitude-limiting mechanism was probably blade stalling. The fully articulated fiber glass blades were flexible enough to execute these large deflections without immediate failure.

DISCUSSION OF NONHARMONIC RESPONSE

As mentioned in previous discussions, rotor nonharmonic motion was observed at rotor conditions other than the violent instabilities. Discrete frequency subharmonic amplitudes during stable rotor operation were very small, with the exception of certain chordwise bending responses. At least a small amount of random variation in rotor blade response was always present in the recorded data. This was especially noticeable in the torsional response data from the retreating blade stress limit conditions and the stall flutter conditions. Examples of these conditions are points 67-12 and 68-7 respectively. Figure 42(1), for example, shows a typical variation in the amplitude of stall flutter response in the azimuth sector between $\psi = 240$ degrees and $\psi = 360$ degrees. A change in amplitude of approximately 20 percent takes place in this azimuth region between the two successive revolutions shown. The random response was very small during ordinary operating conditions, with some increase during conditions of incipient instability as noted above. The increase in random response was most noticeable for retreating blade incipient instabilities, where degradation in control response or high stress also demonstrated that an unstable condition was being approached. The increase in random response was also present as the violent advancing blade instabilities were approached, but remained generally very small compared to the harmonic response until the actual instability took place. Conceivably, these changes could provide a warning of an approach to an unstable condition, if they were not obscured by the harmonic response and random signal inputs from other sources.

The rotor nonharmonic response during stable rotor operation was of interest in some cases, in spite of the generally small amplitude. Some samples of nonharmonic response are given in Table XIV. The components a_m and b_m shown in the table are the coefficients of $\cos \omega_m t$ and $\sin \omega_m t$

respectively, and r_m is the resultant amplitude. The zero time reference is at an arbitrary zero azimuth signal; therefore, the components a_m and b_m have meaning only for the relative phasing of the various data channels at a particular data point. Thus, only the resultant amplitude r_m is given if only one data channel is involved in the nonharmonic at a given data point.

The first of the nonharmonic responses presented in Table XIV was present during points 67-9, 67-10, 67-11, and 67-12, which were taken with the blade center of gravity at 25 percent chord. The operating conditions for these points are given in Table VII. A similar response, also presented in Table XIV, was noted for the similar points 75-9, 75-10, 75-11, and 81-9, which were taken with the blade center of gravity at 30 percent chord. The operating conditions for these points are given in Table VIII. Blade lagging and flapping motion amplitude versus frequency plots between 0.02 and 1.0 cycle per revolution are given in Figure 49 for data points 67-9, 67-10, 67-11, and 67-12. The response can be described as a coupled lagging and flapping motion, which takes place at successively lower frequencies as rotor rotational speed drops. The frequency drops faster than the rotor rotational speed, and had reached approximately 0.25 cycle per revolution at an advance ratio (μ) of 1.47 and a simulated speed (V_s) of 332 knots. The pair of flapping amplitudes at frequencies of 1.0 plus lag frequency and 1.0 minus lag frequency can be shown to be a first harmonic flapping response modulated by the lag frequency. The blade elastic bending and twisting motions were found to include discrete amplitudes at the flap and lag motion frequencies. These were very small, as seen from Table XIV for data point 67-12 and point 75-11.

Coupled flap-lag motion similar to that described above also took place during data point 79-10, which was taken with the 30 percent chord center-of-gravity blade at an advance ratio (μ) of 1.0, a simulated forward speed (V_s) of 304 knots, and a collective pitch of 11 degrees.

The coupled flap-lag motion was observed only in the above instances of high speed over 300 knots. It was not observed at the higher advance ratios reached at somewhat lower forward and rotational speeds, nor at the high rotor lift conditions at lower advance ratios.

The coupled flap-lag response at lower rotor rotational speeds was probably inhibited by the viscous lag hinge damper. This damper furnished 9.4 percent of critical damping in uncoupled lag motion at a rotational tip speed ($\Omega_s R$) of 700 feet per second. At a rotational tip speed of 380 feet per second (point 67-12), the critical damping ratio was 17.7 percent. At a rotational tip speed of 184 feet per second (point 71-12), it rose to 35.8 percent.

A nonharmonic response of high frequency and small amplitude, which involved flapwise bending and torsion, took place during the stall flutter conditions. Both amplitude and frequency of the oscillation increased with cyclic pitch. Examples of this response are given in Table XIV for data points 68-3 through 68-7 and 68-9. The operating conditions for these data points are given in Table VII. The oscillation took place at approximately the fourth flapwise bending frequency of 167 cycles per

second, or 13.5 cycles per revolution, which is given in Table II. The recorded rotor azimuth signals were checked against an independent constant-frequency device, and it was found that rotor speed remained constant to within 1 revolution per minute (or 0.3 percent) during the recording of the data discussed above. Therefore, the observed frequency change does not represent a slowing of the rotor with a constant time frequency signal. The observed amplitudes are very small; however, they do exceed the harmonic excitations at comparable frequencies. The amplitudes continued to grow until the control limit collective pitch settings were reached.

The chordwise bending data obtained with the 30 percent chord center-of-gravity blade revealed some fairly strong nonharmonic response. Table XIV contains some samples of this response for data points 74-3 through 74-9, 75-6 through 75-8, 77-12, and 77-13. The operating conditions for these data points are given in Table VIII. The response at approximately 9.7 cycles per revolution is at a frequency close to the second chordwise natural mode, as shown in Figure 7. The larger response took place at a frequency of 10.52 cycles per revolution when rotational tip speed ($\Omega_g R$) was 700 feet per second, and at 5.26 to 5.28 cycles per revolution when rotational tip speed was 500 feet per second. These frequencies do not correspond to natural frequencies, and the response at the high rotational speed has almost exactly twice as many cycles per revolution as the response at the lower rotational speed. The in-plane hinge force corresponding to the 5.27 per revolution excitation may be estimated by assuming that the mode shape is the same as the first chordwise natural bending mode. On this basis, the 41.4-inch-pound moment for data point 75-8 produced an in-plane shear force of approximately 4.6 pounds. This is equivalent to 1200 pounds per blade on a hypothetical 72-foot full-scale rotor. Unfortunately, reliable chordwise bending data were not obtained for the 25 percent chord center-of-gravity blade, so it is not known if similar responses were taking place with the normal balanced blade configuration.

The remaining information in Table XIV is for data point 84-6, which became spontaneously unstable after data were taken. The nonharmonic motions, although small from a practical standpoint, suddenly became magnified by a factor of at least 10 when the instability became established. This data point was taken for the 35 percent chord center-of-gravity blade. The rotor operating conditions are given in Table IX.

EFFECTS OF OPERATING CONDITION ON INCIPIENT INSTABILITY

Torsional Divergence

Figures 50 through 54 show the effects on blade response of decreasing rotational speed at a constant simulated forward speed of 328 knots. The pairs of curves identified by the various symbols define the maximum and minimum blade excursions during a rotor revolution. The static fixed-azimuth torsional divergence boundary shown was calculated for an azimuth angle of 270 degrees. It can be seen that a practical limit for rotational speed is reached before the predicted stability limit, and that the

collective pitch is quite important. The effects of collective pitch shown in Figures 50 through 54 also include those of the corresponding amount of cyclic pitch required to remove first harmonic flapping motion, as shown in Tables VII and VIII.

The reduction of rotational tip speed at 332 knots beyond the minimum values shown in Figures 50 through 54 was prevented primarily by rapidly rising torsional response. Rapid changes in the other blade response channels were also taking place. The chordwise bending response contains a large 5-per-revolution component at a rotational tip speed ($\Omega_s R$) of 500 feet per second, due to resonance with the first chordwise bending mode, as can be seen from Table LXIII. Inspection of Tables XXXI and LX shows small peaks in harmonic components of flapwise bending response, which correspond to the flapwise bending natural frequencies. None of these flapwise resonances caused an important increase in flapwise blade stress for the lightly loaded rotor.

The effects of approaching the retreating blade aeroelastic limit or torsional divergence boundary by reducing rotational tip speed are gradual, except for chordwise bending resonances. The rate at which blade response changes with rotational tip speed also increases gradually.

Classical Flutter

Figures 55 through 59 show the effects on blade response of increasing forward speed at a constant rotational simulated tip speed ($\Omega_s R$) of 700 feet per second, with relatively low collective pitch settings. The pairs of curves identified by the various symbols define the maximum and minimum blade response during a typical rotor revolution. The changes in blade response with forward speed were very gradual with the 25 percent and 30 percent chord center-of-gravity blades, and no dramatic increase in response was noted with the 35 percent chord center-of-gravity blade until the sudden onset of violent instability. Note that the fixed-azimuth classical flutter boundary for this blade at a simulated tip speed ($\Omega_s R$) of 700 feet per second was at a simulated forward speed of only 20 knots.

The increase in torsional and chordwise bending response for the 30 percent chord center-of-gravity blade was mainly at a frequency of 4 cycles per revolution, as shown in Tables LV and LVII.

Stall Flutter

Figures 60 through 63 show the effect on blade response of increasing collective pitch at various constant forward speeds and rotational speeds. Without first harmonic flapping, the effect of collective pitch change predominates for the blade lag and torsional responses. By considering Figures 17 and 62, it can be seen that, as collective pitch is raised, considerable torsional blade response occurs even before a region of negative damping is encountered. This is a result of a torsional impulse due to retreating blade stalling. The torsional response tends to reach its maximum at a collective pitch of approximately 12 degrees for the rotor operating conditions tested. Examination of Table XXXVIII shows

that the blade torsional response increase occurs in the first, fourth, fifth, and sixth harmonics.

The effect of forward speed is felt indirectly as a gradual lowering of blade steady lag and cone positions. This is a result of increased cyclic pitch requirements to remove first harmonic flapping at higher forward speeds.

Figures 64 through 67 show the effect on blade response of an increase in forward speed at constant collective pitch. The collective pitch setting is high enough to result in retreating blade stall flutter at the lower forward speeds shown in Figures 64 through 67. Only a limited amount of torsional response data were obtained for Figure 66 because of instrumentation failure. The increase in torsional responses shown for the test points at forward speeds (V_g) over 320 knots was due to retreating blade excitation rather than stall flutter. The same observation is true for the gradually increasing response measured for the remainder of the blade data.

Figures 64 through 67 also show data, again limited by instrumentation difficulties, for the response of the 30 percent chord center-of-gravity blade to stall flutter. The increase in torsional response of this blade over the 25 percent chord center-of-gravity blade at the similar condition is due to advancing blade response rather than stall flutter.

Combined Advancing and Retreating Blade Aeroelastic Limit

Figures 68 through 72 show the effects on blade response of increasing forward speed at a constant rotational simulated tip speed ($\Omega_g R$) of 500 feet per second, with various collective pitch settings. At this rotational speed, the advancing blade classical flutter boundary was at 260 knots simulated speed for the 30 percent chord center-of-gravity blade and at 146 knots simulated speed for the 35 percent chord center-of-gravity blade. The retreating blade static torsional divergence and flutter boundaries were both at approximately 420 knots simulated speed.

The rise in blade torsional response with forward speed which appears in Figure 70 is predominately a retreating blade effect, except for the violent instability encountered with the 35 percent chord center-of-gravity blade. This retreating blade response is visible in Figure 37(f). The rise in blade flapping response is, however, due to an advancing blade excitation, as shown in Figure 37(h). The blade chordwise response is again due to excitation of the first chordwise bending mode. At a rotational tip speed ($\Omega_g R$) of 500 feet per second, this response is predominately at 5 cycles per revolution, as shown in Tables LXIII and LXXIV.

The effects of collective pitch and consequent blade loading are clearly present in the data of Figures 68 through 72. This is another demonstration of the necessity for considering the effects of blade loading as well as aeroelastic stability when rotor aeroelastic operating boundaries are determined.

PRACTICAL OPERATING LIMITS

The practical operating boundary for a full-scale prototype of the 25 percent chord center-of-gravity blade configuration tested may be estimated on the basis of the data obtained in this test program and on the basis of acceptable full-scale stresses.

The acceptable full-scale stress must, of course, be based on the blade material utilized, the configuration of the actual blade structure, and the desired fatigue life of the blade. For an aluminum structure, $\pm 4,000$ pounds per square inch vibratory shear stress and $\pm 8,000$ pounds per square inch bending stress may be tolerated for a finite time. These stresses correspond respectively to ± 34 inch-pounds in torsion, ± 48 inch-pounds in flapwise bending, and ± 100 inch-pounds in chordwise bending on the fiber glass model. Obviously, the full-scale rotor control system strength and stiffness must also be consistent with the loads encountered. Reference to Figures 50 through 54 indicates that the blade could be operated in smooth air at a forward speed of 330 knots at sea level and a rotational tip speed (ΩR) of 450 feet per second, without exceeding the approximate stress levels given above on a one-half peak-to-peak basis. This condition is at an advance ratio of 1.24, with an advancing blade tip Mach number of 0.89. The stress levels, however, change very rapidly with rotor control position and loading. Therefore, the operation of the rotor in turbulent air at the 330-knot condition is questionable for the stress limits given above.

The instability and transient test results do, however, demonstrate that the 300-knot forward speed, 500-foot-per-second rotational tip speed condition is practical for the operation of this particular rotor blade configuration. During the course of the transient response portion of this test, a variety of rotor loadings and control positions were tested. Examination of the data presented in Tables XV and XVI for runs 47, 55, and 56 shows that the levels of blade elastic moment given above were not exceeded on the basis of peak-to-peak response, either with or without the pitch-flap coupling. The 300-knot forward speed condition applies to sea level, and higher speeds would be possible by operating at a higher advance ratio at a higher altitude. It would also be possible to increase forward speed by using airfoil sections suitable for transonic operation in the blade tip region. This would allow higher advancing tip Mach numbers and lower advance ratios for a given speed.

Examination of the data for runs 47, 55, and 56 in Tables XV and XVI also discloses that blade stresses at 300 knots forward speed and 500 feet per second rotational speed are quite sensitive to variations in the other rotor parameters. Selection of the proper combination of parameters will result in blade loadings and stresses which are well under the limits given above. In general, it appears that application of forward cyclic pitch (positive BLS) will raise blade stresses. On a compound helicopter, where wings and additional propulsive devices are present, the rotor is not constrained to produce a unique value of lift and thrust for steady flight at a given aircraft weight and speed. Therefore, adjustment of

rotor operating parameters at a given aircraft flight condition may be made to produce the optimum combination of rotor performance and blade stress condition. The high stress conditions would then be encountered only when necessary for maneuvering or operating in turbulent air.

The effect of pitch-flap coupling on blade stress is not necessarily pronounced for rotor conditions of similar performance. As an example, points 47-34 and 56-8 may be compared, using Table VI, Table XV, and Table XVI. From Table VI, it can be seen that the rotor performance parameters for these conditions are approximately the same, with $C_L/\sigma = 0.03$, $C_D/\sigma = 0.01$, and $C_Q/\sigma = 0.002$. The 30 percent radius flapwise bending moment maximum and minimum values are 28 and -31 with pitch-flap coupling and 29 and -28 inch-pounds respectively without it. The torsional moment range at the 35 percent radius station is from 16 to -14 inch-pounds with pitch-flap coupling and from 15 to -12 inch-pounds without it. This is in contrast to the comparison previously made on page 34 between point 29 of run 47 and point 29 of run 55. These points have the same collective pitch, shaft angle, and first harmonic flapping. These two points have large angles of blade incidence in the reverse flow region, a condition which causes large positive (nose-up) torsional moments. These are aggravated by the statically unstable effect of the pitch-flap coupling in reverse flow.

The transient and stability testing of this program was carried out with the rotor shaft rigidly mounted. The operating limit of an actual aircraft will be affected to some extent by interactions among the rotor, the remainder of the aircraft, and control inputs. Therefore, the conclusions of this report will be most accurate for aircraft configurations and flight conditions with small perturbations in fuselage motion.

The high-speed, high-advance-ratio limits of operation for the 30 percent chord center-of-gravity blade configuration appear to be similar to those for the 25 percent chord center-of-gravity location. There is, however, a general increase in torsional blade load throughout most of the test conditions encountered. This increase in load is due to advancing blade excitation, which is relatively independent of the retreating blade effects which define the high-speed, high-advance-ratio limits. Thus, moderately high torsional loads exist for the 30 percent chord center-of-gravity blade at conditions for which the 25 percent chord center-of-gravity blade has low torsional loads. An example of this effect appears in Figure 57.

The 35 percent chord center-of-gravity blade was found to be unstable within the normal operating range of the rotor. Furthermore, the transition from stable to unstable operation was sudden, with no gradual increase in stress as the unstable condition was approached. This fact is significant with respect to the stability test results for the 30 percent chord center-of-gravity blade. Even though violent instability was not encountered, the test results provide no indication of the operating conditions for which this blade would become unstable. Thus, the margin of stability for the aft center-of-gravity blade cannot be demonstrated by test under steady flight conditions, unless instability is encountered.

CONCLUSIONS

TRANSIENT RESPONSE

Transient Response Characteristics

1. The measured rotor blade response in the steady-state condition following a rapid change in rotor control settings does not differ noticeably from the response in a steady-state condition which follows a slow control change.
2. Except for small subharmonic lag motions, the final steady-state blade response after a sudden control change is reached in less than 4 revolutions following a control change if a pitch-flap coupling ratio ($\partial\theta_0/\partial\beta$) of -1.0 is present. Without pitch-flap coupling, the final steady state is reached in less than 5 revolutions.
3. The rotor blade bending and twisting moments and torsional moments in the first and second revolutions following a rapid control change can achieve amplitudes which are greater than either pre-transient or post-transient steady-state amplitudes. This is particularly true at operating conditions where stall-induced torsional oscillations are experienced.
4. A pitch-flap coupling ratio ($\partial\theta_0/\partial\beta$) of -1.0 generally results in a reduction in the severity of blade response to rapid control changes. For some conditions, the final steady-state flapping response is reached in half the number of revolutions required for the rotor without pitch-flap coupling. At operating conditions near the torsional divergence boundary, the pitch-flap coupling may cause a moderate increase in the torsional moment amplitude.

Correlation of Transient Response With Theoretical Prediction

1. Normal mode transient analysis calculations of rotor blade flapping response following a rapid control change agree well in amplitude with experimental results when significant changes in rotor lift are not involved. When lift changes are involved, the agreement is poor.
2. The calculated first flapwise modal response agrees reasonably well with experiment. The steady lag angle and small-amplitude, high-harmonic components of lag motion are not accurately predicted by the theory.

3. The agreement of calculated blade torsional response with experiment is only qualitatively good when a substantial part of the blade is in reverse flow. The agreement of calculated blade torsional response with experiment is poor when blade stalling is present.
4. The qualitative effect of pitch-flap coupling is adequately handled by the theory at all forward speeds.
5. The theoretical effect of the azimuth position of a rapid control input is perceptible in blade lag motion for approximately 4 revolutions at a 300-knot condition when pitch-flap coupling is not present. A pitch-flap coupling ratio ($\partial\theta/\partial\beta$) of -1.0 results in a larger theoretical excitation of lag motion because of the rapid flapping response. The effect of control input azimuth change is similarly larger, and this effect is perceptible beyond 5 revolutions after the control change.
6. The calculated application of control input at a speed of 300 knots between azimuth angles of 0 and 90 degrees results in significantly larger amplitude blade response than the identical input between 90 and 180 degrees.

BLADE AEROELASTIC INSTABILITY

1. The fixed-azimuth torsional divergence, classical flutter, and stall flutter theories agreed with experiment only in a broad qualitative sense under selected operating conditions.
2. The torsional divergence stability boundary has the correct shape on a rotational speed versus forward speed plot. When significant blade loadings were present, the practical operating boundary for a given rotational speed was encountered at a considerably lower forward speed than the predicted fixed-azimuth torsional divergence stability boundary.
3. The classical flutter boundary for the lightly loaded rotor also has the correct geometric shape on a rotational speed versus forward speed plot. The incidents of violent instability which were encountered during this test occurred at a much higher forward speed than the predicted fixed-azimuth advancing blade flutter boundary for the same rotational speed. The existing fixed-azimuth flutter theory does not include the experimentally demonstrated effect of blade loading on the occurrence of violent instability. Therefore, it should not be concluded that an advancing blade classical flutter boundary will always be predicted at a higher speed than the speed for the occurrence of violent instability. The practical operating boundary was encountered at a considerably lower forward speed than the predicted fixed-azimuth retreating blade flutter boundary for the same rotational speed.

4. The fixed-azimuth stall flutter theory predicted the occurrence of stall flutter for the approximate rotor conditions at which it actually occurred. The predicted magnitude and extent of negative damping varied in the same qualitative manner with collective pitch as the torsional vibration components associated with stall flutter. The amplitude of stall flutter is strongly influenced by the strength of the torsional impulsive loading. This factor is not considered in the current theory, and therefore no quantitative prediction of the amplitude of stall-induced torsional vibrations is possible.
5. Operation of the model rotor with the blade center of gravity at the 35 percent chord position resulted in sudden violent instabilities. It appears that these instabilities are related to excessive torsional deflections induced by the aft center-of-gravity locations. These deflections interfere with the cyclic angle of attack changes which normally control and stabilize the rotor.
6. The presence of a safe margin between a stable operating condition and an impending aft center-of-gravity blade instability condition can not be reliably demonstrated from steady-state blade stress and motion measurements alone.

PRACTICAL OPERATING LIMITS

1. The rotor blade configuration tested with the center of gravity at the 25 percent chord remained within practical equivalent full-scale stress limits for a variety of fixed shaft angles and control positions at a sea level simulated forward speed (V_s) of 300 knots with an advance ratio of 1.0. This was true both with and without pitch-flap coupling. The provision of pitch-flap coupling decreased the flapping sensitivity of the rotor to loading. Pitch-flap coupling did, however, significantly aggravate the increase in blade torsional stress when high loadings in reverse flow were encountered.
2. The 25 percent center-of-gravity configuration tested can be operated in still air at a simulated forward speed as high as 332 knots with an advance ratio of 1.4, without pitch-flap coupling and without exceeding practical stress limits. The blade stress becomes very sensitive to loading and control position at this condition.
3. The limit of practical operation of the 30 percent chord center-of-gravity blade configuration was defined by the stress level due to retreating blade reverse flow response, and was similar to the limit for the 25 percent chord center-of-gravity blade. The 30 percent chord center-of-gravity blade configuration did, however, have a considerably higher vibratory stress level throughout the general range of test conditions. Also, the margin between the operating conditions at which data were taken

and those for which an aft-center-of-gravity instability might exist cannot be determined for the 30 percent chord center-of-gravity blade.

4. The 35 percent chord center-of-gravity blade was found to be violently unstable within the normal operating range of the rotor, and would therefore not be considered for practical use.

LITERATURE CITED

1. Arcidiacono, P. J., PREDICTION OF ROTOR INSTABILITY AT HIGH FORWARD SPEEDS, VOLUME I - STEADY FLIGHT DIFFERENTIAL EQUATIONS OF MOTION FOR A FLEXIBLE HELICOPTER BLADE WITH CHORDWISE MASS UNBALANCE, United Aircraft Corporation, Sikorsky Aircraft Division; USAAVLABS Technical Report 68-18A, U. S. Army Aviation Materiel Laboratories, Fort Eustis, Virginia, February 1969, AD685860.
2. Elman, H. L., Niebanck, C. F., and Bain, L. J., PREDICTION OF ROTOR INSTABILITY AT HIGH FORWARD SPEEDS, VOLUME V - FLAPPING AND FLAP-LAG INSTABILITY, United Aircraft Corporation, Sikorsky Aircraft Division; USAAVLABS Technical Report 68-18E, U. S. Army Aviation Materiel Laboratories, Fort Eustis, Virginia, February 1969, AD685862.
3. Segel, L., AIRLOADINGS ON A ROTOR BLADE AS CAUSED BY TRANSIENT INPUTS OF COLLECTIVE PITCH, Cornell Aeronautical Laboratory; USAAVLABS Technical Report 65-65, U. S. Army Aviation Materiel Laboratories, Fort Eustis, Virginia, October 1965, AD624860.
4. Niebanck, C. F., and Elman, H. L., PREDICTION OF ROTOR INSTABILITY AT HIGH FORWARD SPEEDS, VOLUME IV - TORSIONAL DIVERGENCE, United Aircraft Corporation, Sikorsky Aircraft Division; USAAVLABS Technical Report 68-18D, U. S. Army Aviation Materiel Laboratories, Fort Eustis, Virginia, February 1969, AD687323.
5. Astill, C. J., and Niebanck, C. F., PREDICTION OF ROTOR INSTABILITY AT HIGH FORWARD SPEEDS, VOLUME II - CLASSICAL FLUTTER, United Aircraft Corporation, Sikorsky Aircraft Division; USAAVLABS Technical Report 68-18B, U. S. Army Aviation Materiel Laboratories, Fort Eustis, Virginia, February 1969.
6. Crimi, P., A METHOD FOR ANALYZING THE AEROELASTIC STABILITY OF THE ROTOR IN FORWARD FLIGHT, Rochester Applied Science Associates, Report No. 68-10 (To be issued as a NASA Contractor Report), December 1968.
7. Bain, L. J., and Landgrebe, A. J., INVESTIGATION OF COMPOUND HELICOPTER AERODYNAMIC INTERFERENCE EFFECTS, United Aircraft Corporation, Sikorsky Aircraft Division; USAAVLABS Technical Report 67-44, U. S. Army Aviation Materiel Laboratories, Fort Eustis, Virginia, November 1967, AD665427.
8. Fradenburgh, E. A., and Kiely, E. F., DEVELOPMENT OF DYNAMIC MODEL ROTOR BLADES FOR HIGH SPEED HELICOPTER RESEARCH, United Aircraft Corporation, Sikorsky Aircraft Division; Proceedings of the Symposium on Aeroelastic and Dynamic Modeling Technology, Air Force Flight Dynamics Laboratory, Research and Technology Division, Air Force Systems Command, RTD-TDR-63-4197, Part I, Wright-Patterson Air Force Base, Dayton, Ohio, September 1963.
9. Pope, A., WIND TUNNEL TESTING, New York, John Wiley and Sons, 1954.

10. Heyson, H. H., LINEARIZED THEORY OF WIND TUNNEL JET BOUNDARY CORRECTION AND GROUND EFFECT FOR VTOL-STOL AIRCRAFT, NASA Technical Report R-124, National Aeronautics and Space Administration, Langley Field, Virginia, January 1962.
11. Scanlan, R. H., and Rosenbaum, R., INTRODUCTION TO THE STUDY OF AIRCRAFT VIBRATION AND FLUTTER, New York, The Macmillan Company, 1951.
12. Carta, F. O., and Niebanck, C. F., PREDICTION OF ROTOR INSTABILITY AT HIGH FORWARD SPEEDS, VOLUME III - STALL FLUTTER, United Aircraft Corporation, Sikorsky Aircraft Division; USAAVLABS Technical Report 68-18C, U. S. Army Aviation Materiel Laboratories, Fort Eustis, Virginia, February 1969, AD687322.
13. Paglino, V. M., and Logan, A. H., AN EXPERIMENTAL STUDY OF THE PERFORMANCE AND STRUCTURAL LOADS OF A FULL-SCALE ROTOR AT EXTREME OPERATING CONDITIONS, United Aircraft Corporation, Sikorsky Aircraft Division; USAAVLABS Technical Report 68-3, U. S. Army Aviation Materiel Laboratories, Fort Eustis, Virginia, March 1968, AD674187.
14. Bailey, F. J. Jr., A SIMPLIFIED THEORETICAL METHOD OF DETERMINING THE CHARACTERISTICS OF A LIFTING ROTOR IN FORWARD FLIGHT, NACA Report 716, The National Advisory Committee on Aeronautics, Langley Field, Virginia, 1941.
15. Fradenburgh, E. A., and Segel, R. M., MODEL AND FULL-SCALE COMPOUND HELICOPTER RESEARCH, United Aircraft Corporation, Sikorsky Aircraft Division; 21st Annual National Forum of the American Helicopter Society, Washington, D. C., May 12, 1965.
16. Sissingh, G. J., DYNAMICS OF ROTORS OPERATING AT HIGH ADVANCE RATIOS, Journal of the American Helicopter Society, Volume 13, No. 3, July 1968.
17. Hohenemser, K. H., and Heaton, P. W. Jr., AEROELASTIC INSTABILITY OF TORSIONALLY RIGID HELICOPTER BLADES, Journal of the American Helicopter Society, Volume 12, No. 2, April 1967.
18. Critzos, C. C., Heyson, H. H., and Boswinkle, R. W. Jr., AERODYNAMIC CHARACTERISTICS OF NACA 0012 AIRFOIL SECTION AT ANGLES OF ATTACK FROM 0° to 180° , NACA TN 3361, National Advisory Committee for Aeronautics, Langley Field, Virginia, January 1955.

TABLE 1. RATIOS OF MODEL PARAMETERS TO FULL SCALE		
Parameter	Fiber Glass Model	Aluminum Model
Linear Dimensions	$1/S$	$1/S$
Areas	$1/S^2$	$1/S^2$
Mass per Inch of Span	$1/S^2$	$1/S^2$
Total Mass	$1/S^3$	$1/S^3$
Elastic Stiffness	$1/4S^4$	$1/S^4$
Angular Velocity	$S/2$	S
Linear Velocity	$1/2$	1
Mach Number	$1/2$	1
Froude Number	$S/4$	S
Reynolds Number	$1/2S$	$1/S$
Forces	$1/4S^2$	$1/S^2$
Moments	$1/4S^3$	$1/S^3$
Power	$1/8S^2$	$1/S^2$
Elastic Strains	1	1
Natural Frequencies	$S/2$	S
Accelerations	$S/4$	S

TABLE II. CALCULATED EFFECT OF INERTIAL COUPLING ON FLAPWISE AND TORSIONAL NATURAL FREQUENCIES

Mode Description	Q, R	NEM	Modal Frequencies (cps)					
			25% Chord C.G.			35% Chord C.G.		
			Uncoupled	Coupled	Uncoupled	Coupled	Uncoupled	Coupled
Flapping	0	0	-	-	-	-	-	-
1st. Flapwise	0	0	11.6	11.2	11.3	11.2	11.3	11.9
2nd. Flapwise	0	0	35.1	35.0	36.0	37.0	35.9	35.9
3rd. Flapwise	0	0	50.4	50.0	79.0	79.0	76.0	75.9
4th. Flapwise	0	0	137.1	137.0	133.0	133.0	129.0	129.0
1st. Torsion	0	0	75.1	75.0	52.6	52.6	42.4	44.9
2nd. Torsion	0	0	221.0	221.0	159.0	159.0	129.0	131.0
Flapping	300	319	5.9	5.9	5.5	5.5	5.5	5.5
1st. Flapwise	300	319	15.0	15.0	17.7	17.7	17.4	17.5
2nd. Flapwise	300	319	44.3	44.3	43.4	43.4	42.6	42.9
3rd. Flapwise	300	319	54.5	54.5	51.3	51.3	51.4	51.7
4th. Flapwise	300	319	144.0	144.0	139.0	139.0	138.0	138.0
1st. Torsion	300	319	75.1	75.1	53.2	53.2	43.2	47.5
2nd. Torsion	300	319	221.0	221.0	159.0	159.0	129.0	137.0
Flapping	500	531	9.4	9.4	9.2	9.2	9.2	9.2
1st. Flapwise	500	531	15.7	15.7	15.5	15.5	15.4	15.2
2nd. Flapwise	500	531	47.7	47.7	46.8	46.8	46.9	47.1
3rd. Flapwise	500	531	59.0	59.0	56.2	56.2	57.0	57.1
4th. Flapwise	500	531	137.0	137.0	130.0	130.0	128.4	128.0
1st. Torsion	500	531	76.1	76.1	53.7	53.7	43.2	47.4
2nd. Torsion	500	531	221.0	221.0	160.0	160.0	130.0	137.0
Flapping	700	743	13.1	13.1	13.0	13.0	12.9	12.9
1st. Flapwise	700	743	16.0	16.0	15.9	15.9	15.8	15.8
2nd. Flapwise	700	743	48.9	48.9	48.3	48.3	48.0	48.3
3rd. Flapwise	700	743	59.0	59.0	57.9	57.9	58.0	58.0
4th. Flapwise	700	743	137.0	137.0	130.0	130.0	128.0	128.0
1st. Torsion	700	743	76.1	76.1	54.8	54.8	44.9	48.9
2nd. Torsion	700	743	221.0	221.0	161.0	161.0	131.0	139.0

TABLE III. CALCULATED SPIN-ORBIT SPLITTING WITH SPIN-ORBIT COUPLING (BLANK C.O. AT 30 CMOS)

Mode Description	n	Ω_R (rpm)	η_{PL} (in.)	η_{TL} (in.)	η_{TH} (in.)	η_{PH} (in.)	η_{TH} (rad.)	η_{PH} (rad.)	$\frac{\eta_{TH}}{\eta_{PH}}$	$\frac{P_{(L)}}{P_{(H)}}$
Flapping	1	0	1.000	.600	.000	.000	.000	.000	1.000	.000
1st. Flapwise	2	0	0.005	1.000	- .001	- .001	.000	.001	1.001	.001
2nd. Flapwise	3	0	0.020	.607	1.000	- .002	.000	.000	1.000	.000
3rd. Flapwise	4	0	0.016	.593	.001	1.000	- .004	.004	1.004	.012
4th. Flapwise	5	0	0.021	.621	.644	.011	1.000	- .021	1.000	.011
1st. Torsion	6	0	0.258	- .017	- .111	.004	1.000	.007	1.000	.007
2nd. Torsion	7	0	0.003	.269	- .009	.144	.017	.004	1.004	.004
Flapping	1	300	1.000	.004	- .001	.000	.000	.000	1.000	.000
1st. Flapwise	2	300	1.004	1.000	.007	.001	.001	.007	1.001	.006
2nd. Flapwise	3	300	0.009	- .021	1.000	.019	- .005	.014	1.004	.015
3rd. Flapwise	4	300	0.015	.011	- .012	1.000	.009	- .005	1.004	.014
4th. Flapwise	5	300	0.021	.020	0.06	.000	1.000	- .021	1.000	.021
1st. Torsion	6	300	.257	- .049	- .183	.004	.007	1.000	1.004	.004
2nd. Torsion	7	300	0.003	.272	- .011	.152	.046	.004	1.004	.004
Flapping	1	500	1.000	.006	- .001	.000	.000	.000	1.000	.000
1st. Flapwise	2	500	1.007	1.000	.058	.010	- .002	.040	1.010	.018
2nd. Flapwise	3	500	0.008	- .078	1.000	.051	.019	.114	1.000	.118
3rd. Flapwise	4	500	0.015	.030	- .044	1.000	.048	- .046	1.000	.021
4th. Flapwise	5	500	0.021	.017	.025	.018	1.000	- .021	1.004	.025
1st. Torsion	6	500	.254	- .047	- .076	.003	.004	1.000	1.004	.004
2nd. Torsion	7	500	0.003	.275	- .013	.171	.080	.005	1.000	.005
Flapping	1	700	1.000	.006	- .002	.000	.000	.000	1.000	.000
1st. Flapwise	2	700	0.014	1.000	.004	.017	- .001	.049	1.014	.046
2nd. Flapwise	3	700	0.023	- .055	1.000	.080	.049	- .135	1.000	.148
3rd. Flapwise	4	700	0.015	.011	- .081	1.000	.051	- .007	1.004	.015
4th. Flapwise	5	700	0.020	- .048	.016	.006	1.000	- .040	1.004	.040
1st. Torsion	6	700	.265	- .176	.204	.034	.019	1.000	1.004	.034
2nd. Torsion	7	700	0.012	.292	- .013	.229	.365	.016	1.000	.016

TABLE IV. CALCULATED NATURAL FREQUENCIES (Hz) AT 1000 GPa

Mode Description	ω_p (Hz)	ω_{ph} (Hz)	ω_{ph} (Hz)	ω_{ph} (Hz)	ω_{ph} (Hz)	ω_{ph} (Hz)	ω_{ph} (Hz)	ω_{ph} (Hz)	ω_{ph} (Hz)
Flapping	1	0	0	0	0	0	0	0	0
1st. Flapwise	2	0	0	0	0	0	0	0	0
2nd. Flapwise	3	0	0	0	0	0	0	0	0
3rd. Flapwise	4	0	0	0	0	0	0	0	0
4th. Flapwise	5	0	0	0	0	0	0	0	0
1st. Torsion	6	0	0	0	0	0	0	0	0
2nd. Torsion	7	0	0	0	0	0	0	0	0
Flapping	1	0	0	0	0	0	0	0	0
1st. Flapwise	2	0	0	0	0	0	0	0	0
2nd. Flapwise	3	0	0	0	0	0	0	0	0
3rd. Flapwise	4	0	0	0	0	0	0	0	0
4th. Flapwise	5	0	0	0	0	0	0	0	0
1st. Torsion	6	0	0	0	0	0	0	0	0
2nd. Torsion	7	0	0	0	0	0	0	0	0
Flapping	1	0	0	0	0	0	0	0	0
1st. Flapwise	2	0	0	0	0	0	0	0	0
2nd. Flapwise	3	0	0	0	0	0	0	0	0
3rd. Flapwise	4	0	0	0	0	0	0	0	0
4th. Flapwise	5	0	0	0	0	0	0	0	0
1st. Torsion	6	0	0	0	0	0	0	0	0
2nd. Torsion	7	0	0	0	0	0	0	0	0
Flapping	1	0	0	0	0	0	0	0	0
1st. Flapwise	2	0	0	0	0	0	0	0	0
2nd. Flapwise	3	0	0	0	0	0	0	0	0
3rd. Flapwise	4	0	0	0	0	0	0	0	0
4th. Flapwise	5	0	0	0	0	0	0	0	0
1st. Torsion	6	0	0	0	0	0	0	0	0
2nd. Torsion	7	0	0	0	0	0	0	0	0
Flapping	1	0	0	0	0	0	0	0	0
1st. Flapwise	2	0	0	0	0	0	0	0	0
2nd. Flapwise	3	0	0	0	0	0	0	0	0
3rd. Flapwise	4	0	0	0	0	0	0	0	0
4th. Flapwise	5	0	0	0	0	0	0	0	0
1st. Torsion	6	0	0	0	0	0	0	0	0
2nd. Torsion	7	0	0	0	0	0	0	0	0
Flapping	1	0	0	0	0	0	0	0	0
1st. Flapwise	2	0	0	0	0	0	0	0	0
2nd. Flapwise	3	0	0	0	0	0	0	0	0
3rd. Flapwise	4	0	0	0	0	0	0	0	0
4th. Flapwise	5	0	0	0	0	0	0	0	0
1st. Torsion	6	0	0	0	0	0	0	0	0
2nd. Torsion	7	0	0	0	0	0	0	0	0

2. MODES OF VIBRATION - FREQUENCY, CHORD C.G., AND CHORD C.G.				
MODE DESCRIPTION	BLADE NO. 23 25 CHORD C.G.	BLADE NO. 24 25 CHORD C.G.	BLADE NO. 25 30 CHORD C.G.	BLADE NO. 35 35 CHORD C.G.
	f _{SN} (CPS)	f _{SN} (CPS)	f _{SN} (CPS)	f _{SN} (CPS)
FIRST FLAPWISE BENDING	12.0 .13	11.1 .046	11.3 .061	10.7 .0446
SECOND FLAPWISE BENDING		36.5 .036		35.4 .025
FIRST CHORDWISE BENDING	40.0 .044		34.3 .034	36.5 .035
FIRST TORSION	70.3 .015	64.6 .021	56.0 .016	
* Mode could not be excited. ** Instrumentation failure.				

TABLE VI. ROTOR PARAMETERS FOR TRANSIENT TEST CONDITIONS
(BLADE CENTER OF GRAVITY AT .25 CHORD)

DATE	TIME	TEST	SCORE	REMARKS
10-1-54	5	TEST 1	100	
10-1-54	6	TEST 2	100	
10-1-54	7	TEST 3	100	
10-1-54	8	TEST 4	100	
10-1-54	9	TEST 5	100	
10-1-54	10	TEST 6	100	
10-1-54	11	TEST 7	100	
10-1-54	12	TEST 8	100	
10-1-54	13	TEST 9	100	
10-1-54	14	TEST 10	100	
10-1-54	15	TEST 11	100	
10-1-54	16	TEST 12	100	
10-1-54	17	TEST 13	100	
10-1-54	18	TEST 14	100	
10-1-54	19	TEST 15	100	
10-1-54	20	TEST 16	100	
10-1-54	21	TEST 17	100	
10-1-54	22	TEST 18	100	
10-1-54	23	TEST 19	100	
10-1-54	24	TEST 20	100	
10-1-54	25	TEST 21	100	
10-1-54	26	TEST 22	100	
10-1-54	27	TEST 23	100	
10-1-54	28	TEST 24	100	
10-1-54	29	TEST 25	100	
10-1-54	30	TEST 26	100	
10-1-54	31	TEST 27	100	
10-1-54	32	TEST 28	100	
10-1-54	33	TEST 29	100	
10-1-54	34	TEST 30	100	
10-1-54	35	TEST 31	100	
10-1-54	36	TEST 32	100	
10-1-54	37	TEST 33	100	
10-1-54	38	TEST 34	100	
10-1-54	39	TEST 35	100	
10-1-54	40	TEST 36	100	
10-1-54	41	TEST 37	100	
10-1-54	42	TEST 38	100	
10-1-54	43	TEST 39	100	
10-1-54	44	TEST 40	100	
10-1-54	45	TEST 41	100	
10-1-54	46	TEST 42	100	
10-1-54	47	TEST 43	100	
10-1-54	48	TEST 44	100	
10-1-54	49	TEST 45	100	
10-1-54	50	TEST 46	100	
10-1-54	51	TEST 47	100	
10-1-54	52	TEST 48	100	
10-1-54	53	TEST 49	100	
10-1-54	54	TEST 50	100	
10-1-54	55	TEST 51	100	
10-1-54	56	TEST 52	100	
10-1-54	57	TEST 53	100	
10-1-54	58	TEST 54	100	
10-1-54	59	TEST 55	100	
10-1-54	60	TEST 56	100	
10-1-54	61	TEST 57	100	
10-1-54	62	TEST 58	100	
10-1-54	63	TEST 59	100	
10-1-54	64	TEST 60	100	
10-1-54	65	TEST 61	100	
10-1-54	66	TEST 62	100	
10-1-54	67	TEST 63	100	
10-1-54	68	TEST 64	100	
10-1-54	69	TEST 65	100	
10-1-54	70	TEST 66	100	
10-1-54	71	TEST 67	100	
10-1-54	72	TEST 68	100	
10-1-54	73	TEST 69	100	
10-1-54	74	TEST 70	100	
10-1-54	75	TEST 71	100	
10-1-54	76	TEST 72	100	
10-1-54	77	TEST 73	100	
10-1-54	78	TEST 74	100	
10-1-54	79	TEST 75	100	
10-1-54	80	TEST 76	100	
10-1-54	81	TEST 77	100	
10-1-54	82	TEST 78	100	
10-1-54	83	TEST 79	100	
10-1-54	84	TEST 80	100	
10-1-54	85	TEST 81	100	
10-1-54	86	TEST 82	100	
10-1-54	87	TEST 83	100	
10-1-54	88	TEST 84	100	
10-1-54	89	TEST 85	100	
10-1-54	90	TEST 86	100	
10-1-54	91	TEST 87	100	
10-1-54	92	TEST 88	100	
10-1-54	93	TEST 89	100	
10-1-54	94	TEST 90	100	

TABLE VI - Continued

[illegible]

TABLE VI - Continued

RUN-PT NO	TYPE	TAB ₃ Ω ₃ PI/SEC	q ₁	M _{1,00}	μ	ε ₁	ε ₂ DEG	ε ₃ DEG	δ ₁ DEG	δ ₂ DEG	δ ₃ DEG	δ ₄ DEG	δ ₅ DEG	C _L /σ	C _D /σ	C _V /σ	C _Q /σ	C _{MA} /σ	C _{MA} /σ
49-5	INITIAL	0	700	-4.0	.367	.294	-8.6	8.0	0	0	0	-3.2	4.9	.0728	-.00405	-.00181	.00174	-.00004	.00175
49-5	TEST FINAL	0	700	-4.0	.367	.294	-8.7	8.0	0	0	0	-2.7	1.1	.0912	-.00112	-.00271	.00455	-.00417	.00254
49-7	POST TRANSIENT	0	700	-4.0	.367	.294	-8.7	8.0	0	0	0	-2.7	1.1	.0912	-.00112	-.00271	.00455	-.00417	.00254
49-8	INITIAL	0	700	-4.0	.367	.294	-8.6	8.0	0	0	0	-3.2	4.9	.0718	-.00394	-.00194	.00470	-.00413	.00104
49-9	TEST FINAL	0	700	-4.0	.367	.294	-13.4	10.0	1.5	4	4	-6.4	9.8	.0902	-.00391	-.00212	.00459	-.00159	.00175
49-10	POST TRANSIENT	0	700	-4.0	.367	.294	-13.4	10.0	1.5	4	4	-6.4	9.8	.0901	-.00384	-.00218	.00463	-.00159	.00175
49-11	INITIAL	0	700	-4.0	.367	.294	-13.3	10.0	1.5	4	4	-6.3	5.4	.0886	-.00364	-.00185	.00453	-.00159	.00175
49-12	TEST FINAL	0	700	-4.0	.369	.292	-11.4	10.0	2.0	0	0	-2.9	3.8	.0773	-.00721	-.00183	.00421	-.00183	.00164
49-13	POST TRANSIENT	0	700	-4.0	.369	.292	-11.4	10.0	2.0	0	0	-2.9	3.8	.0772	-.00720	-.00183	.00421	-.00183	.00164
49-14	INITIAL	0	700	-4.0	.369	.292	-13.3	10.0	0	0	0	-3.3	5.4	.0809	-.00887	-.00199	.00422	-.00183	.00164
49-15	TEST FINAL	0	700	-4.0	.369	.292	-12.6	10.0	0	0	0	-3.3	5.4	.0710	-.00916	-.00483	.00431	-.00000	.00167
49-16	POST TRANSIENT	0	700	-4.0	.369	.292	-12.6	10.0	0	0	0	-3.3	5.4	.0705	-.00904	-.00480	.00431	-.00000	.00167
49-17	INITIAL	0	700	-4.0	.369	.292	-13.1	10.0	0	0	0	-3.3	5.4	.0698	-.00887	-.00165	.00431	-.00005	.00167
49-18	TEST FINAL	0	700	-4.0	.369	.292	-13.6	10.0	0	0	0	-3.3	5.4	.0677	-.00844	-.00173	.00434	-.00005	.00167
49-19	POST TRANSIENT	0	700	-4.0	.369	.292	-13.6	10.0	0	0	0	-3.3	5.4	.0677	-.00844	-.00173	.00434	-.00005	.00167
49-20	INITIAL	0	700	-4.0	.369	.292	-13.1	10.0	0	0	0	-3.3	5.4	.0699	-.00890	-.00166	.00431	-.00004	.00163
49-21	TEST FINAL	0	700	-4.0	.369	.292	-10.6	10.0	2.0	0	0	-5.1	3.8	.0808	-.00715	-.00578	.00433	-.00213	.00679
49-22	POST TRANSIENT	0	700	-4.0	.369	.292	-10.6	10.0	2.0	0	0	-5.1	3.8	.0806	-.00728	-.00575	.00433	-.00213	.00679
49-23	INITIAL	0	700	-4.0	.369	.292	-13.1	10.0	0	0	0	-3.3	5.4	.0763	-.00896	-.00151	.00434	-.00005	.00170
49-24	TEST FINAL	0	700	-4.0	.369	.292	-11.9	10.0	2.0	0	0	-6.4	4.3	.0754	-.00764	-.00185	.00439	-.00192	.00285
49-25	POST TRANSIENT	0	700	-4.0	.369	.292	-11.9	10.0	2.0	0	0	-6.4	4.3	.0754	-.00764	-.00185	.00439	-.00192	.00285
49-26	INITIAL	0	700	-4.0	.366	.294	-9.0	8.0	0	0	0	-6.4	4.3	.0692	-.00644	-.00194	.00433	-.00191	.00283
49-27	TEST FINAL	0	700	-4.0	.366	.294	-12.8	8.0	0	0	0	-6.4	4.3	.0676	-.00712	-.00156	.00435	-.00494	.00175
49-28	POST TRANSIENT	0	700	-4.0	.366	.294	-12.8	8.0	0	0	0	-6.4	4.3	.0667	-.00709	-.00149	.00435	-.00494	.00175
49-30	INITIAL	0	700	-4.0	.369	.292	-10.8	12.0	4.0	0	0	-3.8	3.3	.0961	-.00715	-.00358	.00497	-.00397	.00319
49-31	TEST FINAL	0	700	-4.0	.369	.292	-11.3	12.0	4.0	0	0	-1.5	3.8	.0925	-.00700	-.00013	.00493	-.00379	.00122
49-32	POST TRANSIENT	0	700	-4.0	.369	.292	-10.9	12.0	4.0	0	0	-3.8	3.3	.0961	-.00732	-.00359	.00499	-.00395	.00216
49-33	INITIAL	0	700	-4.0	.369	.292	-10.2	12.0	4.0	0	0	-5.9	2.7	.0975	-.00737	-.00796	.00497	-.00364	.00444
49-34	TEST FINAL	0	700	-4.0	.369	.292	-10.2	12.0	4.0	0	0	-5.9	2.7	.0975	-.00737	-.00796	.00497	-.00364	.00444
49-35	POST TRANSIENT	0	700	-4.0	.369	.292	-10.2	12.0	4.0	0	0	-5.9	2.7	.0975	-.00737	-.00796	.00497	-.00364	.00444
49-36	INITIAL	0	700	-4.0	.390	.291	-4.0	4.0	0	0	0	-3.4	4.5	.0893	-.01235	-.00305	.00194	-.00494	.00259
49-37	TEST FINAL	0	700	-4.0	.390	.291	-3.3	8.0	1.0	2.7	2.7	-4.7	8.9	.1213	.01940	-.00341	.00576	-.00867	.00104
49-38	POST TRANSIENT	0	700	-4.0	.390	.291	-3.3	8.0	1.0	2.7	2.7	-4.7	8.9	.1213	.01940	-.00341	.00576	-.00867	.00104
49-39	INITIAL	0	700	-4.0	.367	.294	-1.9	8.0	0	0	0	-4.5	6.4	.1020	.00548	-.00354	.00577	-.00870	.00201
49-40	TEST FINAL	0	700	-4.0	.367	.294	-5.7	8.0	0	0	0	-4.5	6.4	.1020	.00548	-.00354	.00577	-.00870	.00201
49-41	POST TRANSIENT	0	700	-4.0	.367	.294	-5.7	8.0	0	0	0	-4.5	6.4	.1020	.00548	-.00354	.00577	-.00870	.00201
52-5	INITIAL	0	675	-4.0	.435	.503	-8.6	8.0	0	0	0	-4.5	12.7	.0548	.01160	-.00287	.00497	-.00702	.00228
52-5	TEST FINAL	0	675	-4.0	.435	.503	-8.5	10.0	-2.0	0	0	-4.5	12.7	.0782	.01164	-.00291	.00706	-.00674	.00195
52-5	POST TRANSIENT	0	675	-4.0	.435	.503	-8.5	10.0	-1.7	0	0	-4.5	12.7	.0782	.01164	-.00291	.00706	-.00674	.00195
52-6	INITIAL	0	675	-4.0	.435	.503	-8.6	8.0	0	0	0	-4.5	12.7	.0548	.01160	-.00287	.00497	-.00702	.00228
52-6	TEST FINAL	0	675	-4.0	.435	.503	-7.2	8.0	-2.0	0	0	-4.1	11.3	.0645	.01231	-.00258	.00498	-.00699	.00174
52-6	POST TRANSIENT	0	675	-4.0	.435	.503	-7.2	8.0	-2.0	0	0	-4.1	11.3	.0645	.01231	-.00258	.00498	-.00699	.00174
52-10	INITIAL	0	675	-4.0	.435	.503	-8.6	8.0	0	0	0	-4.5	12.7	.0548	.01160	-.00287	.00497	-.00702	.00228
52-11	TEST FINAL	0	675	-4.0	.435	.503	-8.6	10.0	-2.0	0	0	-4.5	12.7	.0778	.01164	-.00287	.00497	-.00699	.00174
52-12	POST TRANSIENT	0	675	-4.0	.435	.503	-8.6	10.0	-2.0	0	0	-4.5	12.7	.0778	.01164	-.00287	.00497	-.00699	.00174
52-13	INITIAL	0	675	-4.0	.435	.503	-2.2	4.0	0	0	0	-3.1	6.3	.0593	.01355	-.00202	.00703	-.00497	.00276
52-14	TEST FINAL	0	675	-4.0	.435	.503	-2.2	4.0	0	0	0	-3.1	6.3	.0593	.01355	-.00202	.00703	-.00497	.00276
52-15	POST TRANSIENT	0	675	-4.0	.435	.503	-2.2	4.0	0	0	0	-3.1	6.3	.0593	.01355	-.00202	.00703	-.00497	.00276
52-16	INITIAL	0	675	-4.0	.435	.503	-8.5	8.0	4.7	0	0	-4.1	12.7	.1072	.02489	-.00328	.00412	-.00271	.00190
52-17	TEST FINAL	0	675	-4.0	.435	.503	-8.5	8.0	4.7	0	0	-4.1	12.7	.1072	.02489	-.00328	.00412	-.00271	.00190
52-18	POST TRANSIENT	0	675	-4.0	.435	.503	-8.5	8.0	4.7	0	0	-4.1	12.7	.1072	.02489	-.00328	.00412	-.00271	.00190
52-19	INITIAL	0	675	-4.0	.434	.504	-2.0	4.0	0	0	0	-2.2	7.1	.0355	.02301	-.00323	.00535	-.00201	.00197
52-20	TEST FINAL	0	675	-4.0	.434	.504	-2.0	4.0	0	0	0	-2.2	7.1	.0355	.02301	-.00323	.00535	-.00201	.00197
52-21	POST TRANSIENT	0	675	-4.0	.434	.504	-2.0	4.0	0	0	0	-2.2	7.1	.0355	.02301	-.00323	.00535	-.00201	.00197
52-22	INITIAL	0	675	-4.0	.434	.504	-7.3	4.0	0	0	0	-2.2	7.1	.0367	.00612	-.00228	.00186	-.00398	.00207
52-23	TEST FINAL	0	675	-4.0	.434	.504	-7.3	4.0	0	0	0	-2.2	7.1	.0367	.00612	-.00228	.00186	-.00398	.00207
52-24	POST TRANSIENT	0	675	-4.0	.434	.504	-7.3	4.0	0	0	0	-2.2	7.1	.0367	.00612	-.00228	.00186	-.00398	.00207
52-25	INITIAL	0	675	-4.0	.434	.504	-7.3	4.0	0	0	0	-2.2	7.1	.0367	.00612	-.00228	.00186	-.00398	.00207
52-26	TEST FINAL	0	675	-4.0	.434	.504	-7.3	4.0	0	0	0	-2.2	7.1	.0367	.00612	-.00228	.00186	-.00398	.00207
52-27	POST TRANSIENT	0	675	-4.0	.434	.504	-7.3	4.0	0	0	0	-2.2	7.1	.0367	.00612	-.00228	.00186	-.00398	.00207
52-28	INITIAL	0	675	-4.0	.434	.504	-7.3	4.0	0	0	0	-2.2	7.1	.0367	.00612	-.00228	.00186	-.00398	.00207
52-29	TEST FINAL	0	675	-4.0	.434	.504	-7.3	4.0	0	0	0	-2.2	7.1	.0367	.00612	-.00228	.00186	-.00398	.00207
52-30	POST TRANSIENT	0	675	-4.0	.434	.504	-7.3	4.0	0	0	0	-2.2	7.1	.0367	.00612	-.00228	.00186	-.00398	.00207

TABLE VI - Continued

NO.	TYPE	γ_{AB}	Ω_{SM}	α	M_{100}	μ	α_{deg}	δ_{deg}	δ_{deg}	δ_{deg}	C_1/a	C_2/a	C_3/a	C_4/a	C_{50}/a	C_{90}/a
53-5	INITIAL	0	675	-4.0	435	503	-10.6	8.0	0	0	-3.1	6.7	0.360	0.0024	-0.0098	-0.0391
53-6	TEST FINAL	0	675	-4.0	435	503	-10.6	10.0	2.5	0	-3.1	6.7	0.364	0.0082	-0.0170	-0.0366
53-7	POST TRANSIENT	0	675	-4.0	435	503	-10.6	10.0	2.6	0	-3.1	6.7	0.367	0.0059	-0.0201	-0.0366
53-8	INITIAL	0	675	-4.0	435	503	-10.6	8.0	0	0	-3.1	6.7	0.364	0.0059	-0.0201	-0.0366
53-9	TEST FINAL	0	675	-4.0	435	503	-10.6	8.0	0	0	-3.1	6.7	0.367	0.0059	-0.0201	-0.0366
53-10	POST TRANSIENT	0	675	-4.0	435	503	-10.6	8.0	2.0	0	-3.1	6.7	0.367	0.0059	-0.0201	-0.0366
53-11	INITIAL	0	675	-4.0	435	503	-10.6	8.0	0	0	-3.1	6.7	0.364	0.0059	-0.0201	-0.0366
53-12	TEST FINAL	0	675	-4.0	435	503	-10.6	8.0	0	0	-3.1	6.7	0.364	0.0059	-0.0201	-0.0366
53-13	POST TRANSIENT	0	675	-4.0	435	503	-10.6	8.0	0	0	-3.1	6.7	0.364	0.0059	-0.0201	-0.0366
53-14	INITIAL	0	675	-4.0	435	503	-10.6	10.0	2.0	0	-3.1	6.7	0.367	0.0059	-0.0201	-0.0366
53-15	TEST FINAL	0	675	-4.0	435	503	-10.6	10.0	2.0	0	-3.1	6.7	0.367	0.0059	-0.0201	-0.0366
53-16	POST TRANSIENT	0	675	-4.0	435	503	-10.6	10.0	4.0	0	-3.1	6.7	0.367	0.0059	-0.0201	-0.0366
53-17	INITIAL	0	675	-4.0	435	503	-10.6	10.0	4.0	0	-3.1	6.7	0.367	0.0059	-0.0201	-0.0366
53-18	TEST FINAL	0	675	-4.0	435	503	-10.6	10.0	4.0	0	-3.1	6.7	0.367	0.0059	-0.0201	-0.0366
53-19	POST TRANSIENT	0	675	-4.0	435	503	-10.6	10.0	0	2.0	-2.1	10.4	0.661	0.0024	-0.0338	0.0699
53-20	INITIAL	0	675	-4.0	435	504	-10.3	10.0	0	1.9	-2.1	10.4	0.661	0.0011	-0.0015	0.0654
53-21	TEST FINAL	0	675	-4.0	435	504	-10.3	10.0	0	1.9	-2.1	10.4	0.661	0.0011	-0.0015	0.0654
53-22	POST TRANSIENT	0	675	-4.0	435	504	-10.3	10.0	0	1.9	-2.1	10.4	0.661	0.0011	-0.0015	0.0654
53-23	INITIAL	0	675	-4.0	435	504	-9.4	10.0	0	-2.0	-6.5	9.5	0.691	0.0005	-0.0321	0.0647
53-24	TEST FINAL	0	675	-4.0	435	504	-9.4	10.0	0	-2.0	-6.5	9.5	0.691	0.0005	-0.0321	0.0647
53-25	POST TRANSIENT	0	675	-4.0	435	504	-9.4	10.0	0	-2.0	-6.5	9.5	0.691	0.0005	-0.0321	0.0647
53-26	INITIAL	0	675	-4.0	435	504	-10.4	10.0	-2.0	-4.0	-8.9	10.5	0.582	0.0011	-0.0303	0.0642
53-27	TEST FINAL	0	675	-4.0	435	503	-10.1	10.0	-2.0	-4.0	-8.9	10.5	0.582	0.0011	-0.0303	0.0642
53-28	POST TRANSIENT	0	675	-4.0	435	503	-10.1	10.0	-2.0	-4.0	-8.9	10.5	0.582	0.0011	-0.0303	0.0642
53-29	INITIAL	0	675	-4.0	435	503	-10.1	10.0	-2.0	-4.0	-8.9	10.5	0.582	0.0011	-0.0303	0.0642
53-30	TEST FINAL	0	675	-4.0	435	503	-10.1	10.0	-2.0	-4.0	-8.9	10.5	0.582	0.0011	-0.0303	0.0642
53-31	POST TRANSIENT	0	675	-4.0	435	503	-10.1	10.0	-2.0	-4.0	-8.9	10.5	0.582	0.0011	-0.0303	0.0642
54-5	INITIAL	0	675	-4.0	435	503	-10.1	10.0	-2.0	-4.0	-8.9	10.5	0.582	0.0011	-0.0303	0.0642
54-6	TEST FINAL	0	675	-4.0	435	503	-10.1	10.0	-2.0	-4.0	-8.9	10.5	0.582	0.0011	-0.0303	0.0642
54-7	POST TRANSIENT	0	675	-4.0	435	503	-10.1	10.0	-2.0	-4.0	-8.9	10.5	0.582	0.0011	-0.0303	0.0642
54-8	INITIAL	0	675	-4.0	435	503	-10.1	10.0	-2.0	-4.0	-8.9	10.5	0.582	0.0011	-0.0303	0.0642
54-9	TEST FINAL	0	675	-4.0	435	503	-10.1	10.0	-2.0	-4.0	-8.9	10.5	0.582	0.0011	-0.0303	0.0642
54-10	POST TRANSIENT	0	675	-4.0	435	503	-10.1	10.0	-2.0	-4.0	-8.9	10.5	0.582	0.0011	-0.0303	0.0642
54-11	INITIAL	0	675	-4.0	435	503	-10.1	10.0	-2.0	-4.0	-8.9	10.5	0.582	0.0011	-0.0303	0.0642
54-12	TEST FINAL	0	675	-4.0	435	503	-10.1	10.0	-2.0	-4.0	-8.9	10.5	0.582	0.0011	-0.0303	0.0642
54-13	POST TRANSIENT	0	675	-4.0	435	503	-10.1	10.0	-2.0	-4.0	-8.9	10.5	0.582	0.0011	-0.0303	0.0642
54-14	INITIAL	0	675	-4.0	435	503	-10.1	10.0	-2.0	-4.0	-8.9	10.5	0.582	0.0011	-0.0303	0.0642
54-15	TEST FINAL	0	675	-4.0	435	503	-10.1	10.0	-2.0	-4.0	-8.9	10.5	0.582	0.0011	-0.0303	0.0642
54-16	POST TRANSIENT	0	675	-4.0	435	503	-10.1	10.0	-2.0	-4.0	-8.9	10.5	0.582	0.0011	-0.0303	0.0642
54-17	INITIAL	0	675	-4.0	435	503	-10.1	10.0	-2.0	-4.0	-8.9	10.5	0.582	0.0011	-0.0303	0.0642
54-18	TEST FINAL	0	675	-4.0	435	503	-10.1	10.0	-2.0	-4.0	-8.9	10.5	0.582	0.0011	-0.0303	0.0642
54-19	POST TRANSIENT	0	675	-4.0	435	503	-10.1	10.0	-2.0	-4.0	-8.9	10.5	0.582	0.0011	-0.0303	0.0642
54-20	INITIAL	0	700	-4.0	435	503	-10.6	10.0	2.2	0	-2.9	6.7	0.605	0.0031	-0.0050	0.0601
54-21	TEST FINAL	0	700	-4.0	435	503	-10.6	10.0	2.2	0	-2.9	6.7	0.605	0.0031	-0.0050	0.0601
54-22	POST TRANSIENT	0	700	-4.0	435	503	-10.6	10.0	2.2	0	-2.9	6.7	0.605	0.0031	-0.0050	0.0601
54-23	INITIAL	0	700	-4.0	435	503	-10.6	10.0	1.5	0	-2.9	6.7	0.605	0.0031	-0.0050	0.0601
54-24	TEST FINAL	0	700	-4.0	435	503	-10.6	10.0	1.5	0	-2.9	6.7	0.605	0.0031	-0.0050	0.0601
54-25	POST TRANSIENT	0	700	-4.0	435	503	-10.6	10.0	1.6	0	-2.9	6.7	0.605	0.0031	-0.0050	0.0601
54-26	INITIAL	0	700	-4.0	435	503	-10.6	10.0	0	0	-3.1	6.7	0.605	0.0031	-0.0050	0.0601
54-27	TEST FINAL	0	700	-4.0	435	503	-10.6	10.0	0	0	-3.1	6.7	0.605	0.0031	-0.0050	0.0601
54-28	POST TRANSIENT	0	700	-4.0	435	503	-10.6	10.0	3.0	0	-3.1	6.7	0.605	0.0031	-0.0050	0.0601

RUN-PT NO.	TYPE	TAN δ_3	Ω_R FYSEC	a_f	M ₁₉₀	μ	α_c DEG	α_{is} DEG	bis DEG	Abs DEG	Bis DEG	C _L /a	C _D /a	C _V /a	C _O /a	C _H /a	C _m /a
55-5	INITIAL	.0	500	.0	.433	1.026	-1.2	.0	-1.1	-1.4	1.2	-.0112	.00987	.00667	.00215	.00145	-.00018
55-6	TEST FINAL	.0	500	.0	.433	1.026	.4	.0	4.0	0	-2.2	-.0302	.01075	-.00088	.00168	-.00325	.00111
55-7	POST TRANSIENT	.0	500	.0	.433	1.026	-1.2	.0	4.1	0	-2.2	-.0307	.01093	-.00091	.00166	-.00330	.00113
55-8	INITIAL	.0	500	.0	.433	1.026	-1.2	.0	0	0	-1.4	-.0078	.00996	.00057	.00217	.00104	-.00012
55-9	TEST FINAL	.0	500	.0	.433	1.026	-1.2	.0	0	0	-1.4	-.0092	.00989	.00065	.00217	.00122	-.00017
55-10	POST TRANSIENT	.0	500	.0	.433	1.026	-1.1	1.0	4.0	0	-1.4	-.0302	.01079	.00063	.00185	-.00342	.00015
55-11	INITIAL	.0	500	.0	.433	1.026	-1.1	1.0	4.4	9	-1.4	-.0309	.01093	.00076	.00183	-.00340	.00016
55-12	TEST FINAL	.0	500	.0	.433	1.026	-1.2	.0	0	0	-1.4	-.0066	.01025	.00075	.00220	.00098	-.00023
55-13	POST TRANSIENT	.0	500	.0	.433	1.026	-1.2	.0	-2.0	-3.8	.8	-.0059	.00980	.00069	.00219	.00147	.00023
55-14	INITIAL	.0	500	.0	.433	1.026	-1.2	.0	-5.1	-3.8	.8	-.0079	.00987	.00077	.00222	.00166	.00025
55-15	TEST FINAL	.0	500	.0	.433	1.026	-1.2	.0	0	0	-1.4	-.0099	.00999	.00082	.00218	.00135	-.00017
55-16	POST TRANSIENT	.0	500	.0	.433	1.026	-1.6	.0	2.0	1.4	1.2	-.0125	.01007	.00032	.00217	.00110	-.00026
55-17	INITIAL	.0	500	.0	.433	1.026	-1.6	.0	2.0	1.4	1.6	-.0120	.01022	.00047	.00221	.00113	-.00235
55-18	TEST FINAL	.0	500	.0	.434	1.024	-6.1	4.0	0	0	-2.9	-.0100	.01203	.00037	.00173	.00683	.00015
55-19	POST TRANSIENT	.0	500	.0	.434	1.024	-4.6	4.0	0	0	-3.4	-.0253	.01146	.00188	.00221	.00088	.00186
55-20	INITIAL	.0	500	.0	.434	1.024	-4.6	4.0	0	0	-3.4	-.0234	.01133	.00201	.00225	.00089	.00189
55-21	TEST FINAL	.0	500	.0	.433	1.026	-6.0	4.0	0	0	-1.5	-.0118	.01210	.00031	.00174	.00134	-.00035
55-22	POST TRANSIENT	.0	500	.0	.433	1.026	-6.4	4.0	-2.0	0	-1.3	-.0313	.01325	.00066	.00115	.00400	-.00035
55-23	INITIAL	.0	500	.0	.433	1.026	-6.4	4.0	-2.1	0	-1.3	-.0311	.01346	.00047	.00107	.00401	-.00030
55-24	TEST FINAL	.0	500	.0	.433	1.026	-5.9	4.0	0	0	-1.7	-.0157	.01212	.00037	.00175	.00189	-.00000
55-25	POST TRANSIENT	.0	500	.0	.433	1.026	-5.2	4.0	2.0	0	-2.0	-.0039	.01147	-.00027	.00201	-.00051	.00084
55-26	INITIAL	.0	500	.0	.433	1.026	-5.2	4.0	2.1	0	-2.0	-.0039	.01137	.00002	.00205	-.00049	.00055
55-27	TEST FINAL	.0	500	.0	.433	1.026	-5.8	4.0	0	0	-1.7	-.0074	.01240	.00053	.00175	.00174	-.00003
55-28	POST TRANSIENT	.0	500	.0	.433	1.026	-7.1	4.0	-4.0	0	-1.0	-.0446	.01576	.00021	.00015	.00708	-.00051
56-5	INITIAL	.0	500	.0	.433	1.026	-5.8	4.0									

TABLE VI - Concluded

RUN-PT NO	TYPE	TAN δ	Ω_R FT/SEC	η	M_{LBO}	μ	α_C DEG	θ_C DEG	α_H DEG	β_H DEG	A_H DEG	B_H DEG	C_L/σ	C_0/σ	C_y/σ	C_θ/σ	C_{PM}/σ	C_{RM}/σ
60-5	INITIAL	1.0	700	-4.0	.367	.294	-7.7	8.0	.0	.0	-2.2	3.4	.0534	-.00213	-.00115	.00327	-.00028	.00116
60-6	TEST FINAL	1.0	700	-4.0	.367	.294	-7.1	10.0	.5	.5	-2.2	3.4	.0667	-.00262	-.00211	.00405	-.00070	.00223
60-7	POST TRANSIENT	1.0	700	-4.0	.367	.294	-5.9	4.0	.0	.0	-2.2	3.4	.0667	-.00267	-.00212	.00407	-.00073	.00225
60-8	INITIAL	1.0	700	8.0	.390	.291	5.9	4.0	.0	.0	-2.0	2.4	.0675	.01126	-.00152	-.00006	-.00000	.00138
60-9	TEST FINAL	1.0	700	8.0	.390	.291	6.1	8.0	1.0	1.0	-5.2	2.4	.0992	.01668	-.00442	.00094	-.00113	.00440
60-10	POST TRANSIENT	1.0	700	8.0	.390	.291	6.1	8.0	1.0	1.0	-5.2	2.4	.0982	.01666	-.00450	.00096	-.00113	.00442
60-11	INITIAL	1.0	675	-4.0	.435	.503	-9.3	8.0	.0	.0	-2.4	5.4	.0308	.00042	-.00055	.00325	-.00007	.00057
60-12	TEST FINAL	1.0	675	-4.0	.435	.503	-9.3	10.0	.6	.6	-2.4	5.4	.0461	-.00034	-.00178	.00407	-.00082	.00206
60-13	POST TRANSIENT	1.0	675	-4.0	.435	.503	-9.3	10.0	.6	.6	-2.4	5.4	.0465	-.00030	-.00175	.00408	-.00080	.00210
60-14	INITIAL	1.0	675	-4.0	.435	.503	-8.9	10.0	2.0	.0	-2.4	5.4	.0303	.00029	-.00044	.00323	-.00009	.00041
60-15	TEST FINAL	1.0	675	-4.0	.435	.503	-8.9	10.0	2.0	.0	-2.4	5.4	.0528	.00032	-.00166	.00411	-.00226	.00152
60-16	POST TRANSIENT	1.0	675	-4.0	.435	.503	-8.9	10.0	2.0	.0	-2.4	5.4	.0533	.00023	-.00179	.00412	-.00230	.00164
60-17	INITIAL	1.0	675	4.0	.435	.503	-6.3	8.0	-4.0	.0	-8.4	10.3	.0477	.00166	-.00170	.00321	-.00397	.00149
60-18	TEST FINAL	1.0	675	4.0	.435	.503	-6.2	10.0	-3.2	.0	-8.4	10.3	.0624	.00150	-.00362	.00442	-.00316	.00337
60-19	POST TRANSIENT	1.0	675	4.0	.435	.503	-6.2	10.0	-3.2	.0	-8.4	10.3	.0620	.00155	-.00340	.00440	-.00321	.00337
60-20	INITIAL	1.0	675	4.0	.435	.503	-6.3	8.0	-4.0	.0	-8.4	10.3	.0477	.00166	-.00176	.00322	-.00398	.00157
60-21	TEST FINAL	1.0	675	4.0	.435	.503	-6.0	10.0	-2.0	.0	-6.3	10.1	.0695	.00287	-.00324	.00435	-.00178	.00277
60-22	POST TRANSIENT	1.0	675	4.0	.435	.503	-6.0	10.0	-2.0	.0	-6.3	10.2	.0688	.00285	-.00312	.00435	-.00193	.00268
60-23	INITIAL	1.0	675	8.0	.437	.499	3.3	4.0	.0	.0	-2.6	4.9	.0701	.01117	-.00301	-.00015	-.00024	.00260
60-24	TEST FINAL	1.0	675	8.0	.437	.499	3.3	8.0	1.5	.0	-2.6	4.9	.0996	.01556	-.00721	.00139	-.00177	.00703
60-25	POST TRANSIENT	1.0	675	8.0	.437	.499	3.3	8.0	1.5	.0	-2.6	4.9	.1004	.01570	-.00732	.00139	-.00180	.00714
60-26	INITIAL	1.0	500	.0	.433	1.026	-2.2	.0	.0	.0	-1.4	.2	.0126	.00782	-.00043	.00230	-.00061	.00050
60-27	TEST FINAL	1.0	500	.0	.433	1.026	-1.1	4.0	2.4	2.4	-1.4	.2	.0362	.00918	-.00246	.00225	-.00304	.00402
60-28	POST TRANSIENT	1.0	500	.0	.433	1.024	-6.0	8.0	.0	.0	-5.1	10.0	.0437	.01331	-.00296	.00225	-.00302	.00404
60-29	INITIAL	1.0	500	4.0	.434	1.024	-6.0	4.0	-3.0	1.6	-5.1	10.0	.0136	.00988	-.00034	.00313	-.00027	.00257
60-30	TEST FINAL	1.0	500	4.0	.434	1.024	-6.0	4.0	-3.0	1.6	-5.1	10.0	.0128	.00976	.00016	.00253	-.00299	.00175
60-31	POST TRANSIENT	1.0	500	4.0	.434	1.024	-6.0	4.0	-3.0	1.6	-5.1	10.0	.0128	.00976	.00016	.00253	-.00299	.00175

TABLE VII. ROTOR PARAMETERS FOR INSTABILITY TEST CONDITIONS
(BLADE CENTER OF GRAVITY AT .25 CHORD)

RUN-PT NO.	TYPE	TAN δ	Ω_r FT/SEC	$M_{L_{10}}$	μ	α_c DEG	θ_c DEG	α_{10} DEG	β_{10} DEG	α_{10} DEG	θ_{10} DEG	C_L/σ	C_D/σ	C_V/σ	C_Q/σ	C_{M1}/σ	C_{M2}/σ
64-3	STEADY	.0	700	.416	.390	-1.9	2.0	.0	.0	-1.7	2.0	.0355	.00201	-.00058	.00173	-.00018	.00085
64-4	STEADY	.0	700	.432	.448	-2.4	2.0	.0	.0	-1.7	2.4	.0306	.00227	-.00052	.00171	-.00022	.00091
64-5	STEADY	.0	700	.449	.504	-2.6	2.0	.0	.0	-1.8	2.7	.0264	.00267	-.00016	.00165	-.00037	.00013
64-6	STEADY	.0	700	.468	.565	-2.8	2.0	.0	.0	-1.8	2.8	.0217	.00323	-.00041	.00174	-.00038	.00024
64-7	STEADY	.0	700	.488	.623	-3.0	2.0	.0	.0	-1.9	3.1	.0169	.00367	-.00042	.00163	-.00028	.00022
64-8	STEADY	.0	700	.504	.682	-3.1	2.0	.0	.0	-1.9	3.1	.0153	.00407	-.00029	.00162	-.00029	.00012
65-3	STEADY	.0	700	.504	.682	-3.2	2.0	.0	.0	-1.8	3.3	.0159	.00436	-.00041	.00191	-.00021	.00088
65-4	STEADY	.0	700	.524	.741	-3.4	2.0	.0	.0	-1.8	3.4	.0161	.00532	-.00050	.00185	-.00070	.00036
65-5	STEADY	.0	700	.539	.801	-3.6	2.0	.0	.0	-1.8	3.6	.0137	.00610	-.00037	.00188	-.00044	.00025
65-6	STEADY	.0	700	.560	.861	-3.6	2.0	.0	.0	-1.8	3.6	.0117	.00714	-.00031	.00196	-.00058	.00022
67-3	STEADY	.0	700	.539	.801	-3.7	2.0	.0	.0	-1.8	3.7	.0158	.00618	-.00036	.00192	-.00079	.00023
67-4	STEADY	.0	674	.530	.832	-3.7	2.0	.0	.0	-1.8	3.7	.0087	.00638	-.00004	.00207	-.00010	.00004
67-5	STEADY	.0	682	.521	.862	-3.7	2.0	.0	.0	-1.9	3.7	.0056	.00645	.00017	.00211	.00039	.00004
67-6	STEADY	.0	498	.437	1.000	-3.6	2.0	.0	.0	-1.8	3.6	.0063	.01059	.00050	.00218	-.00045	.00018
67-7	STEADY	.0	498	.455	1.126	-3.7	2.0	.0	.0	-1.8	3.7	.0026	.01181	.00048	.00212	-.00006	.00012
67-8	STEADY	.0	476	.445	1.181	-3.7	2.0	.0	.0	-1.8	3.7	.0014	.01300	.00049	.00200	-.00059	.00018
67-9	STEADY	.0	452	.436	1.243	-3.9	2.0	.0	.0	-1.8	3.9	.0016	.01479	.00078	.00174	-.00022	.00017
67-10	STEADY	.0	428	.424	1.312	-4.1	2.0	.0	.0	-1.7	4.1	.0016	.01692	.00079	.00139	-.00037	.00001
67-11	STEADY	.0	404	.414	1.388	-4.4	2.0	.0	.0	-1.3	4.4	.0022	.01971	.00098	.00083	-.00029	.00001
67-12	STEADY	.0	380	.407	1.474	-4.8	2.0	.0	.0	-.9	4.8	.0011	.02480	.00084	.00067	-.00057	.00036
68-3	STEADY	.0	700	.387	.204	-5.1	8.0	.0	.0	-3.7	5.5	.0920	.00053	-.00269	.00517	-.00002	.00220
68-4	STEADY	.0	700	.387	.214	-5.4	9.0	.0	.0	-4.2	6.3	.0960	.00039	-.00304	.00634	-.00016	.00252
68-5	STEADY	.0	700	.387	.244	-6.5	10.0	.0	.0	-4.5	7.0	.1014	.00110	-.00368	.00779	-.00015	.00293
68-6	STEADY	.0	700	.387	.244	-7.2	11.0	.0	.0	-4.9	7.7	.1056	.00208	-.00401	.00910	-.00020	.00314
68-7	STEADY	.0	700	.387	.244	-7.7	12.0	.0	.0	-5.4	8.3	.1100	.00269	-.00434	.01042	-.00017	.00336
68-8	STEADY	.0	700	.404	.311	-6.3	8.0	.0	.0	-3.7	6.6	.0824	.00021	-.00241	.00511	-.00029	.00204
68-9	STEADY	.0	700	.404	.311	-6.9	9.0	.0	.0	-4.3	7.2	.0888	.00071	-.00322	.00645	-.00020	.00270
68-10	STEADY	.0	700	.404	.311	-7.5	10.0	.0	.0	-4.4	7.9	.0938	.00172	-.00375	.00780	-.00015	.00311
68-11	STEADY	.0	700	.404	.311	-8.3	11.0	.0	.0	-5.1	8.6	.0986	.00246	-.00406	.00911	-.00015	.00316
68-12	STEADY	.0	700	.404	.311	-9.0	12.0	.0	.0	-5.6	9.4	.1029	.00347	-.00447	.01037	-.00014	.00355
68-13	STEADY	.0	700	.423	.410	-7.0	8.0	.0	.0	-3.8	7.2	.0751	.00030	-.00173	.00500	-.00001	.00184
68-14	STEADY	.0	700	.423	.410	-7.6	9.0	.0	.0	-4.4	8.0	.0799	.00057	-.00297	.00607	-.00013	.00242
68-15	STEADY	.0	700	.423	.410	-8.5	10.0	.0	.0	-4.9	8.7	.0856	.00126	-.00345	.00726	-.00005	.00281
68-16	STEADY	.0	700	.423	.410	-9.2	11.0	.0	.0	-5.2	9.5	.1131	.00183	-.00352	.00891	-.00222	.00275
68-17	STEADY	.0	700	.446	.476	-8.0	8.0	.0	.0	-3.8	8.1	.0826	.00098	-.00261	.00489	-.00009	.00209
68-18	STEADY	.0	700	.446	.476	-8.9	9.0	.0	.0	-4.3	9.0	.0860	.00039	-.00296	.00584	-.00008	.00248
68-19	STEADY	.0	700	.446	.476	-9.7	10.0	.0	.0	-4.4	9.9	.0737	.00031	-.00319	.00695	-.00006	.00252
68-20	STEADY	.0	700	.446	.476	-10.5	11.0	.0	.0	-4.9	10.7	.0786	.00084	-.00299	.00816	-.00007	.00254
69-3	STEADY	.0	700	.463	.546	-7.4	9.0	.0	.0	-4.4	7.5	.0859	.00404	-.00404	.00000	-.00000	.00000
69-4	STEADY	.0	700	.463	.546	-8.4	11.0	.0	.0	-5.2	9.0	.0974	.00633	-.00417	.00860	-.00040	.00008
69-5	STEADY	.0	700	.483	.610	-11.3	10.0	.0	.0	-4.5	11.3	.0560	.00231	-.00408	.00560	-.00008	.00163
69-6	STEADY	.0	700	.490	.634	-11.4	10.0	.0	.0	-4.4	11.4	.0526	.00239	-.01111	.00461	-.00027	.00295
69-7	STEADY	.0	700	.490	.659	-11.0	10.0	.0	.0	-4.2	11.7	.0483	.00394	-.01392	.00400	-.00004	.00406
70-3	STEADY	.0	700	.497	.689	-11.7	10.0	.0	.0	-4.4	11.8	.0486	.00374	-.00333	.00533	-.00002	.00249
70-4	STEADY	.0	700	.506	.682	-5.6	4.0	.0	.0	-2.5	5.6	.0229	.00447	-.00105	.00225	-.00015	.00101
70-5	STEADY	.0	700	.513	.706	-13.0	11.0	.0	.0	-4.4	13.0	.0454	.00546	-.00362	.00546	-.00004	.00249
70-6	STEADY	.0	700	.506	.682	-12.8	11.0	.0	.0	-4.4	12.8	.0501	.00467	-.00370	.00590	-.00014	.00291
70-7	STEADY	.0	700	.529	.731	-13.1	11.0	.0	.0	-4.4	13.1	.0444	.00464	-.00362	.00542	-.00031	.00283
70-8	STEADY	.0	700	.527	.756	-13.3	11.0	.0	.0	-4.2	13.4	.0407	.00768	-.00341	.00768	-.00022	.00261
70-9	STEADY	.0	700	.537	.784	-12.5	10.0	.0	.0	-3.9	12.5	.0330	.00816	-.00294	.00428	-.00006	.00223
70-10	STEADY	.0	700	.544	.808	-12.5	10.0	.0	.0	-3.8	12.5	.0325	.00942	-.00394	.00403	-.00015	.00248
71-3	STEADY	.0	366	.295	.795	-.9	.0	.0	.0	-1.4	.9	.0081	.00641	.00036	.00193	-.00029	.00019
71-4	STEADY	.0	362	.288	.847	-.8	.0	.0	.0	-1.4	.9	.0043	.00758	.00064	.00193	-.00038	.00032
71-5	STEADY	.0	340	.275	.906	-1.0	.0	.0	.0	-1.4	1.0	.0012	.00871	.00090	.00213	-.00014	.00038
71-6	STEADY	.0	316	.265	.974	-1.0	.0	.0	.0	-1.2	1.0	.0064	.00906	.00030	.00215	-.00046	.00015
71-7	STEADY	.0	292	.255	1.052	-1.0	.0	.0	.0	-1.2	1.0	.0062	.01120	.00042	.00228	-.00045	.00027
71-8	STEADY	.0	268	.245	1.144	-1.0	.0	.0	.0	-.9	1.0	.0054	.01321	.00078	.00246	-.00046	.00030
71-9	STEADY	.0	246	.235	1.254	-1.0	.0	.0	.0	-.8	1.0	.0055	.01555	-.00032	.00239	-.00060	.00010
71-10	STEADY	.0	222	.225	1.388	-1.1	.0	.0	.0	-.4	1.1	.0001	.01817	.00163	.00279	-.00050	.00004
71-11	STEADY	.0	198	.215	1.553	-1.3	.0	.0	.0	.2	1.3	.0037	.02205	.00084	.00272	-.00129	.00002
71-12	STEADY	.0	184	.209	1.664	-1.4	.0	.0	.0	.7	1.4	.0018	.02668	.00098	.00262	-.00071	.00000
72-3	STEADY	.0	236	.250	1.488	-1.1	.0	.0	.0	-.5	1.1	.0057	.01859	.00189	.00298	-.00093	.00078
72-4	STEADY	.0	202	.236	1.739	-1.4	.0	.0	.0	.6	1.4	.0039	.02688	.00189	.00276	-.00136	.00136
72-5	STEADY	.0	214	.259	1.842	-1.2	.0	.0	.0	.6	1.2	.0063	.02663	.00134	.00268	-.00166	.00188
72-6	STEADY	.0	220	.264	1.914	-1.8	.0	.0	.0	.5	1.5	.0088	.02932	.00175	.00294	-.00221	.00221
72-7	STEADY	.0	242	.313	1.891	-1.7	.0	.0	.0	.2	1.7	.0130	.03407	.00204	.00280	-.00128	.00189
72-8	STEADY	.0	296	.348	1.753	-2.0	.0	.0	.0	-.5	2.0	.0320	.02732	.00057	.00234	-.00037	.00063
72-9	STEADY	.0	366	.406	1.482	-1.4	.0	.0	.0	-2.0	1.4	.0008	.01043	.00110	.00282	-.00001	.00000

TABLE VII - Concluded

Run-PT NO	TYPE	TAN δ_3	Ω_R FT/SEC	$M_{1.90}$	μ	a_C DEG	θ_C DEG	q_S DEG	b_S DEG	A_S DEG	B_S DEG	C_L/σ	C_D/σ	C_Y/σ	C_Q/σ	C_{PH}/σ	C_{RM}/σ
50-5	STEADY	.0	700	.520	.731	-3.5	2.0	.0	.0	-1.8	3.5	.0066	.00341	-.00017	.00192	.00068	.00005
50-6	STEADY	.0	632	.491	.808	-3.5	2.0	.0	.0	-1.7	3.5	.0019	.00644	.00010	.00197	.00099	-.00007
50-7	STEADY	.0	500	.433	1.026	-3.6	2.0	.0	.0	-1.7	3.6	-.0106	.01033	.00037	.00198	.00131	-.00003
50-8	STEADY	.0	482	.426	1.042	-3.7	2.0	.0	.0	-1.7	3.7	-.0161	.01165	.00029	.00193	.00183	-.00000
50-9	STEADY	.0	457	.416	1.119	-3.8	2.0	.0	.0	-1.7	3.8	-.0229	.01290	.00052	.00175	.00226	-.00014
50-10	STEADY	.0	434	.406	1.180	-3.9	2.0	.0	.0	-1.5	3.9	-.0298	.01484	.00061	.00159	.00235	-.00016
50-11	STEADY	.0	410	.395	1.248	-4.1	2.0	.0	.0	-1.7	4.1	-.0367	.01695	.00076	.00126	.00223	-.00029
50-12	STEADY	.0	385	.385	1.327	-4.4	2.0	.0	.0	-1.4	4.4	-.0509	.01979	.00072	.00059	.00233	-.00033
51-3	STEADY	.0	700	.386	.294	-5.7	9.0	.0	.0	-4.3	6.2	.0955	-.00051	-.00325	.00612	.00016	.00282
51-4	STEADY	.0	700	.386	.294	-6.5	10.0	.0	.0	-4.6	7.0	.0996	-.00144	-.00367	.00724	.00035	.00306
51-5	STEADY	.0	700	.386	.294	-7.2	11.0	.0	.0	-5.0	7.7	.1036	-.00251	-.00405	.00860	.00135	.00317
51-6	STEADY	.0	700	.386	.294	-7.7	12.0	.0	.0	-5.4	8.2	.1084	-.00321	-.00431	.00987	.00225	.00341
51-7	STEADY	.0	675	.434	.504	-8.2	8.0	.0	.0	-4.0	8.3	.0597	.00097	-.00272	.00460	.00047	.00241
51-8	STEADY	.0	675	.434	.504	-9.1	9.0	.0	.0	-4.3	9.2	.0652	.00028	-.00303	.00556	.00049	.00251
51-9	STEADY	.0	675	.434	.504	-10.0	10.0	.0	.0	-4.6	10.1	.0696	.00028	-.00315	.00650	.00058	.00259
51-10	STEADY	.0	675	.434	.504	-10.7	11.0	.0	.0	-4.9	10.8	.0746	.00086	-.00369	.00752	.00053	.00293
51-11	STEADY	.0	675	.434	.504	-11.4	12.0	.0	.0	-5.3	11.5	.0801	.00138	-.00411	.00866	.00046	.00323
51-12	STEADY	.0	500	.433	1.026	-5.9	4.0	.0	.0	-2.0	5.9	-.0072	.01173	.00051	.00162	.00165	.00013
51-13	STEADY	.0	500	.433	1.026	-6.3	6.0	.0	.0	-2.4	6.3	-.0024	.01341	.00025	.00132	.00112	.00028
51-14	STEADY	.0	500	.433	1.026	-10.9	8.0	.0	.0	-2.9	10.9	-.0025	.01274	.00016	.00079	.00027	.00057
51-15	STEADY	.0	500	.433	1.026	-12.2	9.0	.0	.0	-3.2	12.2	-.0023	.01794	-.00008	.00039	.00151	.00075
51-16	STEADY	.0	500	.433	1.026	-13.5	10.0	.0	.0	-3.2	13.5	-.0006	.01982	-.00079	.00003	.00134	.00114

TABLE VIII. ROTOR PARAMETERS FOR INSTABILITY TEST CONDITIONS
(BLADE CENTER OF GRAVITY AT .30 CHORD)

RUN-PT NO.	TYPE	TAN δ FT/SEC	Ω_R	$M_{1,0}$	μ	θ_c DEG	θ_c DEG	θ_{10} DEG	θ_{10} DEG	θ_{10} DEG	θ_{10} DEG	C_L/e	C_D/e	C_Y/e	C_θ/e	$C_{\theta\theta}/e$	$C_{\theta\theta}/e$
74- 3	STEADY	.0	700	.398	.333	-3.0	4.0	.0	.0	-2.1	3.2	.0621	.00196	-.00067	.00272	-.00018	.00079
74- 4	STEADY	.0	700	.417	.390	-3.8	4.0	.0	.0	-2.2	3.9	.0581	.00222	-.00059	.00273	-.00031	.00075
74- 5	STEADY	.0	700	.433	.448	-4.5	4.0	.0	.0	-2.3	4.6	.0481	.00264	-.00014	.00252	-.00031	.00053
74- 6	STEADY	.0	700	.451	.504	-4.9	4.0	.0	.0	-2.3	5.0	.0420	.00317	.00019	.00245	-.00052	.00036
74- 7	STEADY	.0	700	.468	.545	-5.1	4.0	.0	.0	-2.3	5.2	.0371	.00372	.00040	.00244	-.00067	.00039
74- 8	STEADY	.0	700	.487	.623	-5.3	4.0	.0	.0	-2.2	5.4	.0327	.00434	.00094	.00238	-.00074	.00066
74- 9	STEADY	.0	700	.506	.682	-5.5	4.0	.0	.0	-2.2	5.5	.0297	.00522	.00131	.00231	-.00090	.00061
75- 3	STEADY	.0	500	.382	.793	-4.4	4.0	.0	.0	-2.5	4.9	.0227	.00652	-.00135	.00244	-.00104	.00111
75- 4	STEADY	.0	500	.400	.876	-4.9	4.0	.0	.0	-2.6	5.0	.0208	.00775	-.00134	.00248	-.00139	.00117
75- 5	STEADY	.0	500	.419	.958	-5.0	4.0	.0	.0	-2.6	5.0	.0187	.00925	-.00104	.00251	-.00162	.00096
75- 6	STEADY	.0	500	.435	1.040	-5.1	4.0	.0	.0	-2.7	5.1	.0145	.01135	-.00063	.00253	-.00155	.00063
75- 7	STEADY	.0	500	.455	1.126	-4.9	4.0	.0	.0	-2.6	4.9	.0110	.01393	.00063	.00255	-.00160	.00019
75- 8	STEADY	.0	475	.445	1.141	-5.1	4.0	.0	.0	-2.4	5.1	.0037	.01532	.00107	.00227	-.00130	.00053
75- 9	STEADY	.0	452	.435	1.243	-5.2	4.0	.0	.0	-2.2	5.2	-.0020	.01753	.00095	.00200	-.00120	.00049
75-10	STEADY	.0	427	.425	1.312	-5.0	4.0	.0	.0	-2.1	5.0	-.0043	.02067	.00175	.00171	-.00134	.00010
75-11	STEADY	.0	404	.415	1.388	-5.7	4.0	.0	.0	-2.0	5.7	-.0144	.02506	.00130	.00002	-.00150	-.00043
76- 3	STEADY	.0	700	.387	.294	-6.5	10.0	.0	.0	-4.7	7.0	.1055	-.00102	-.00468	.00039	-.00059	.00342
76- 4	STEADY	.0	700	.387	.294	-7.5	11.0	.0	.0	-5.2	8.0	.1081	-.00227	-.00484	.01084	-.00020	.00399
76- 5	STEADY	.0	700	.387	.294	-8.1	12.0	.0	.0	-5.6	8.7	.1124	-.00306	-.00506	.01236	-.00032	.00417
76- 6	STEADY	.0	700	.387	.294	-8.8	13.0	.0	.0	-6.1	9.3	.1157	-.00371	-.00543	.01380	-.00037	.00448
77- 3	STEADY	.0	700	.404	.351	-7.7	10.0	.0	.0	-2.5	8.0	.1000	-.00161	-.00418	.00037	-.00037	.00343
77- 4	STEADY	.0	700	.404	.351	-8.5	11.0	.0	.0	-5.2	8.9	.1033	-.00264	-.00444	.01075	-.00018	.00388
77- 5	STEADY	.0	700	.423	.410	-5.9	6.0	.0	.0	-2.8	6.0	.0686	.00155	-.00218	.00010	-.00044	.00179
77- 6	STEADY	.0	700	.446	.446	-5.0	4.0	.0	.0	-2.2	5.1	.0453	.00289	-.00109	.00244	-.00039	.00092
77- 7	STEADY	.0	700	.446	.446	-5.9	5.0	.0	.0	-2.7	6.0	.0514	.00256	-.00150	.00326	-.00027	.00131
77- 8	STEADY	.0	700	.464	.546	-5.3	4.0	.0	.0	-2.2	5.4	.0395	.00340	-.00112	.00263	-.00061	.00096
77- 9	STEADY	.0	700	.464	.546	-6.2	5.0	.0	.0	-2.6	6.3	.0461	.00315	-.00147	.00312	-.00064	.00128
77-10	STEADY	.0	700	.483	.610	-6.5	5.0	.0	.0	-2.4	6.5	.0415	.00400	-.00148	.00305	-.00068	.00117
77-11	STEADY	.0	700	.490	.634	-6.5	5.0	.0	.0	-2.3	6.5	.0395	.00431	-.00150	.00299	-.00093	.00119
77-12	STEADY	.0	500	.412	.926	-6.2	5.0	.0	.0	-2.8	6.2	.0233	.00919	-.00168	.00273	-.00177	.00142
77-13	STEADY	.0	500	.419	.958	-6.2	5.0	.0	.0	-2.8	6.2	.0216	.00992	-.00155	.00273	-.00172	.00128
78- 3	STEADY	.0	700	.404	.351	-8.1	10.0	.0	.0	-4.8	8.5	.0984	-.00159	-.00397	.00022	-.00026	.00313
78- 4	STEADY	.0	700	.404	.351	-8.9	11.0	.0	.0	-5.4	9.2	.1027	-.00240	-.00442	.01063	-.00025	.00384
78- 5	STEADY	.0	700	.404	.351	-9.7	12.0	.0	.0	-5.9	10.1	.1062	-.00336	-.00470	.01201	-.00028	.00377
78- 6	STEADY	.0	700	.423	.410	-9.2	10.0	.0	.0	-4.9	9.4	.0912	-.00123	-.00381	.00051	-.00035	.00308
79- 3	STEADY	.0	500	.353	.657	-13.0	13.0	.0	.0	-6.0	13.1	.0687	.00287	-.00061	.00028	-.00066	.00436
79- 4	STEADY	.0	500	.378	.766	-12.8	12.0	.0	.0	-5.4	12.8	.0493	.00868	-.00055	.00036	-.00111	.00436
79- 5	STEADY	.0	500	.397	.857	-13.2	12.0	.0	.0	-5.2	13.2	.0348	.01155	-.00066	.00058	-.00025	.00444
79- 6	STEADY	.0	500	.403	.890	-13.3	12.0	.0	.0	-5.0	13.3	.0372	.01352	-.00036	.00050	-.00142	.00436
79- 7	STEADY	.0	500	.412	.926	-13.4	12.0	.0	.0	-5.0	13.4	.0324	.01564	-.00036	.00049	-.00134	.00431
79- 8	STEADY	.0	500	.419	.958	-13.5	12.0	.0	.0	-5.0	13.4	.0307	.01767	-.00039	.00042	-.00151	.00429
79- 9	STEADY	.0	500	.426	.991	-13.5	12.0	.0	.0	-4.4	13.5	.0271	.02016	-.00060	.00022	-.00144	.00423
79-10	STEADY	.0	500	.449	1.026	-12.4	11.0	.0	.0	-4.5	12.4	.0228	.02145	-.00167	.00330	-.00157	.00419
79-11	STEADY	.0	500	.441	1.002	-9.1	8.0	.0	.0	-3.7	9.1	.0174	.01843	-.00064	.00276	-.00154	.00408
80- 3	STEADY	.0	387	.296	.795	-2.7	2.0	.0	.0	-1.8	2.7	.0153	.00739	-.00040	.00203	-.00175	.00036
80- 4	STEADY	.0	343	.286	.867	-2.6	2.0	.2	.0	-1.8	2.6	.0197	.00888	-.00054	.00190	-.00084	.00034
80- 5	STEADY	.0	339	.276	.906	-2.8	2.0	.0	.0	-1.8	2.8	.0117	.00941	-.00037	.00216	-.00162	.00042
80- 6	STEADY	.0	316	.265	.978	-2.9	2.0	.0	.0	-1.7	2.9	.0149	.01006	-.00046	.00217	-.00029	.00047
80- 7	STEADY	.0	292	.256	1.052	-3.0	2.0	-.2	.0	-1.5	3.0	.0035	.01221	-.00026	.00242	-.00090	.00013
80- 8	STEADY	.0	269	.246	1.104	-2.8	2.0	-.1	.0	-1.3	2.8	.0165	.01422	-.00066	.00239	-.00061	.00002
80- 9	STEADY	.0	245	.235	1.254	-2.9	2.0	.0	.0	-1.1	2.9	.0124	.01693	.00020	.00244	-.00020	-.00014
80-10	STEADY	.0	221	.225	1.308	-3.1	2.0	.0	.0	-1.6	3.1	.0181	.02090	.00021	.00249	-.00033	-.00008
80-11	STEADY	.0	211	.221	1.454	-3.3	2.0	.0	.0	-1.1	3.3	.0013	.02278	-.00045	.00235	-.00072	-.00000
81- 3	STEADY	.0	236	.251	1.478	-3.4	2.0	.0	.0	-1.6	3.4	-.0177	.02051	.00052	.00231	-.00122	-.00008
81- 4	STEADY	.0	218	.243	1.611	-3.5	2.0	.0	.0	-1.3	3.5	.0196	.02453	.00031	.00245	-.00020	-.00124
81- 5	STEADY	.0	232	.267	1.642	-3.5	2.0	.0	.0	-1.2	3.5	.0172	.03114	.00021	.00170	-.00060	-.00123
81- 6	STEADY	.0	260	.298	1.678	-3.9	2.0	.0	.0	-1.2	3.9	.0064	.02930	.00102	.00141	-.00082	-.00164
81- 7	STEADY	.0	288	.324	1.656	-4.2	2.0	-.5	-.5	-1.3	4.2	-.0083	.02915	-.00146	.00095	-.00131	-.00082
81- 8	STEADY	.0	314	.342	1.603	-4.1	2.0	.0	.0	-1.5	4.1	-.0035	.02833	.00049	.00100	-.00092	-.00031
81- 9	STEADY	.0	342	.409	1.431	-3.2	2.0	.0	.0	-2.4	3.3	.0215	.02249	.00001	.00210	-.00051	-.00004

TABLE IX. ROTOR PARAMETERS FOR INSTABILITY TEST CONDITIONS
(BLADE CENTER OF GRAVITY AT .35 CHORD)

Run-PT NO	TYPE	TAMB, °F/SEC	M _{1,20}	A	θ _C DEG	θ _E DEG	θ _M DEG	θ _W DEG	A _W DEG	B _W DEG	C ₁ /ε	C ₂ /ε	C ₃ /ε	C ₄ /ε	C ₅ /ε	C ₆ /ε
83-3	STEADY	0	700	390	3.3	-3.4	0	0	-1.0	3.6	0.632	0.0155	-0.0110	0.0308	0.0003	0.0107
83-4	STEADY	0	700	417	390	-4.7	0	0	-1.5	4.8	0.084	0.0219	-0.0031	0.0302	0.0035	0.0065
83-5	STEADY	0	700	435	450	-5.1	0	0	-1.5	5.2	0.09	0.0215	-0.0032	0.0279	0.0066	0.00003
84-3	STEADY	0	500	349	632	-4.2	0	0	-1.7	4.3	0.253	0.0447	-0.0052	0.0263	0.0052	0.0101
84-4	STEADY	0	500	364	708	4.5	0	0	-1.5	4.5	0.174	0.0354	0.01048	0.0190	0.0013	0.00351
84-5	STEADY	0	500	302	793	4.5	0	0	-1.3	4.5	0.134	0.0688	-0.0009	0.0278	0.0062	0.0066
84-6	STEADY	0	500	400	876	-4.6	0	0	-1.3	4.6	0.095	0.0830	0.0008	0.0288	-0.0009	0.0034
84-7	STEADY	0	475	372	832	-4.5	0	0	-1.6	4.5	0.114	0.0737	0.0004	0.0284	0.0021	0.0034
84-8	STEADY	0	451	361	876	-4.4	0	0	-2.0	4.4	0.119	0.0795	0.0004	0.0298	0.0000	0.0036
84-9	STEADY	0	428	352	924	-4.3	0	0	-2.0	4.3	0.096	0.0905	0.0002	0.0309	0.0014	0.0042
84-10	STEADY	0	381	332	1.048	-4.3	0	0	-2.3	4.3	0.017	0.1168	0.0085	0.0316	0.0015	0.0043
84-11	STEADY	0	357	322	1.107	-4.2	0	0	-2.2	4.2	0.002	0.1291	0.0040	0.0321	0.0003	0.0046
84-12	STEADY	0	334	312	1.185	-4.3	0	0	-2.1	4.3	0.040	0.1513	0.0040	0.0329	0.0009	0.0055
84-13	STEADY	0	310	302	1.275	-4.6	0	0	-1.6	4.6	0.156	0.1749	0.0005	0.0330	0.0018	0.0052
84-14	STEADY	0	287	291	1.380	-5.0	0	0	-1.1	5.0	0.296	0.2094	-0.0004	0.0238	0.0001	0.0048
84-15	STEADY	0	263	281	1.504	-5.2	0	0	-5	5.2	0.410	0.2480	0.0082	0.0193	0.0005	0.0042
84-16	STEADY	0	239	271	1.652	-5.6	0	5	0	5.6	0.657	0.3128	-0.0033	0.0099	0.0020	0.0052
85-3	STEADY	0	700	307	294	3.9	5.0	0	-2.2	4.3	0.752	0.0116	-0.0173	0.0368	0.0029	0.0141
85-4	STEADY	0	700	804	351	5.0	5.0	0	-2.1	5.3	0.488	0.0096	-0.0144	0.0381	0.0060	0.0126
85-5	STEADY	0	500	353	657	5.7	5.0	0	-2.0	5.6	0.258	0.0056	-0.0121	0.0395	0.0012	0.0086
85-6	STEADY	0	500	378	766	-5.7	5.0	0	-1.7	5.7	0.164	0.0757	-0.0042	0.0301	0.0051	0.0030
85-7	STEADY	0	400	354	1.067	-5.5	5.0	0	-2.7	5.5	0.015	0.1164	-0.0009	0.0321	0.0014	0.0030
85-8	STEADY	0	400	361	1.108	-2.1	2.0	0	-1.7	2.1	0.026	0.1164	-0.0009	0.0328	0.0051	0.0025
86-3	STEADY	0	307	296	795	-2.0	2.0	0	-1.7	2.0	0.084	0.0782	-0.0001	0.0250	-0.0039	0.0018
86-4	STEADY	0	363	386	847	-2.0	2.0	0	-1.7	2.0	0.062	0.0852	-0.0005	0.0259	-0.0023	0.0018
86-5	STEADY	0	339	376	906	-2.1	2.0	0	-1.6	2.1	0.043	0.0971	-0.0008	0.0286	-0.0008	0.0021
86-6	STEADY	0	316	365	974	-2.1	2.0	0	-1.6	2.1	0.042	0.1076	-0.0010	0.0286	-0.0052	0.0026
86-7	STEADY	0	292	256	1.052	-2.1	2.0	0	-1.4	2.1	0.019	0.1735	0.0165	0.0158	-0.0063	0.0043
86-8	STEADY	0	269	246	1.144	-2.0	2.0	0	-1.2	2.1	0.057	0.1419	0.0198	0.0314	-0.0099	0.0084
86-9	STEADY	0	245	235	1.254	-2.1	2.0	0	-9	2.1	0.036	0.1699	0.0298	0.0333	-0.0093	0.0135
86-10	STEADY	0	221	225	1.368	-2.1	2.0	0	-5	2.1	0.082	0.1968	0.0304	0.0347	-0.0185	0.0159
86-11	STEADY	0	211	221	1.456	-2.2	2.0	0	-4	2.2	0.012	0.2270	0.0269	0.0370	-0.0109	0.0131

TABLE X. STRUCTURAL DAMPING COEFFICIENTS FOR THE ROTATING BLADE (BLADE CENTER OF GRAVITY AT .25 CHORD)			
Mode Description	$\Omega_s R$ (ft/sec)	RPM	ξ
Flapping	300	319	.020
1st. Flapwise	300	319	.037
2nd. Flapwise	300	319	.034
3rd. Flapwise	300	319	.038
4th. Flapwise	300	319	.040
1st. Torsion	300	319	.019
2nd. Torsion	300	319	.019
Flapping	500	531	.012
1st. Flapwise	500	531	.020
2nd. Flapwise	500	531	.025
3rd. Flapwise	500	531	.032
4th. Flapwise	500	531	.035
1st. Torsion	500	531	.019
2nd. Torsion	500	531	.019
Flapping	700	743	.010
1st. Flapwise	700	743	.013
2nd. Flapwise	700	743	.019
3rd. Flapwise	700	743	.026
4th. Flapwise	700	743	.032
1st. Torsion	700	743	.018
2nd. Torsion	700	743	.018

TABLE XII. CALCULATED STALL FLUTTER CONDITIONS

Tan. δ_3	Ω_R (rps)	μ	α_c (deg)	α_{ls} (deg)	β_{ls} (deg)	α_{ls} (deg)	β_{ls} (deg)	λ	C_L/σ	C_D/σ	C_M/σ
.0	700	.29	9.0	-2.0	7.0	.0	.0	-.009	.0629	-.0001	.0067
.0	700	.29	10.5	-2.2	9.0	.0	.0	-.010	.0700	-.0030	.0083
.0	700	.29	12.0	-3.8	11.0	.0	.0	-.010	.0713	-.0047	.0100
.0	700	.41	9.0	-1.8	8.5	.0	.0	-.008	.0558	-.0012	.0060
.0	700	.41	10.5	-2.5	10.1	.0	.0	-.008	.0585	-.0017	.0074
.0	700	.41	12.0	-3.4	11.8	.0	.0	-.008	.0606	-.0026	.0091
.0	676	.50	9.0	-1.3	9.1	.0	.0	-.007	.0479	-.0002	.0056
.0	676	.50	10.5	-2.6	10.6	.0	.0	-.007	.0506	-.0006	.0068
.0	676	.50	12.0	-3.5	12.5	.0	.0	-.009	.0530	-.0013	.0082

TABLE XIII. BLADE RESPONSE DURING INSTABILITY												
ω_M/Ω	FREQUENCY (cps)	ζ		$M_{F.30R}$		β		$M_{.35P}$		b_m (deg)	a_m (in.-lb)	b_m (deg)
		θ_m (deg)	b_m (deg)	θ_m (in.-lb)	b_m (in.-lb)	θ_m (deg)	b_m (deg)	θ_m (in.-lb)	b_m (in.-lb)			
.0	.0	6.7	.0	3.4	.0	2.3	.0	6.7	.0			
.28	3.5	-3.4	3.6	.6	.5	1.1	-2	-3.6	-4.2			
.36	4.5	.4	1.2	.0	.0	.4	.0	.0	.0			
.40	5.0	-1.9	-.2	.0	.0	.6	.0	-.7	-5.6			
.72	8.9	.0	.0	-.9	-.2	-1.1	.5	-3.0	-.3			
1.00	12.4	-.1	.0	.4	-1.2	-.4	-.1	3.3	5.4			
1.28	15.9	.0	.0	.5	-.1	-.7	-.2	2.3	.2			
1.40	17.4	.0	.0	.2	1.6	-1.2	-.5	5.0	1.3			
1.72	21.3	.0	.0	-.5	.3	-.5	.0	1.1	-3.0			
2.00	24.8	.0	.0	.4	1.3	-.1	-.4	1.9	6.5			
2.28	28.2	.0	.0	-.5	1.4	.0	-.2	-.3	1.2			
2.40	29.7	.0	.0	-5.6	-2.7	.9	-.2	-14.4	2.0			
3.00	37.2	.0	.0	2.4	-1.7	.0	.2	-16.0	-5.1			
3.40	42.1	.0	.0	-1.0	5.2	.0	.0	-2.0	-44.2			
4.00	49.6	.0	.0	.2	-1.5	.0	.1	1.5	5.0			
4.40	54.5	.0	.0	2.0	-1.6	.0	.0	-8.5	1.1			
5.00	61.9	.0	.0	-.9	-3.3	.0	.1	1.8	-1.2			
5.40	66.9	.0	.0	-1.8	3.5	.0	.0	.4	1.0			
6.00	74.4	.0	.0	-.2	-.4	.0	.0	-.5	-.4			

TABLE XIV. BLADE NONHARMONIC RESPONSE					
RUN-PT NO.	$\frac{\omega}{\Omega}$	DATA CHANNEL	a_m	COMPONENTS b_m	r_m
67-9	.36	ζ	.1	.2	.2
	.36	β	.0	- .1	.1
67-10	.32	ζ	.1	.2	.3
	.32	β	.0	- .1	.1
	.68	β	.0	.0	.1
67-11	.28	ζ	.1	.6	.7
	.28	β	.1	- .3	.3
	.72	β	- .2	- .1	.2
	1.28	β	.0	.4	.4
67-12	.24	ζ	- .2	.9	.9
	.24	M _F .30R	.1	.5	.6
	.24	M _T .18R	- .2	.8	.8
	.24	β	- .3	- .4	.5
	.76	M _F .30R	- .2	.3	.4
	.76	M _T .18R	- .8	- .2	.8
	.76	β	- .2	.2	.3
	1.24	M _F .30R	- .4	- .1	.4
	1.24	M _T .18R	.8	.6	1.0
	1.24	β	- .2	.1	.2
68-3	13.58	M _F .30R	.4	- .4	.6
	13.58	M _F .60R	.6	.0	.6
	13.58	M _T .18R	.9	- .3	1.0
68-4	13.65	M _F .30R	- .2	.6	.7
	13.65	M _F .60R	- .1	.6	.6
	13.65	M _T .18P	- .5	1.1	1.2
68-5	13.74	M _F .30R	.8	- .1	.8
	13.74	M _F .60R	.7	- .2	.8
	13.74	M _T .18R	1.4	- .1	1.4
68-6	13.84	M _F .30R	.7	- .6	.8
	13.84	M _F .60R	.6	- .6	.8
	13.84	M _T .18R	1.3	- .9	1.6
68-7	13.96	M _F .30R	- .6	- .8	1.0
	13.96	M _F .60R	- .7	- .7	.9
	13.96	M _T .18R	- .9	-1.4	1.7
68-9	13.72	M _F .30R	.5	- .4	.7
	13.72	M _F .60R	.4	- .4	.6
	13.72	M _T .18R	1.0	- .7	1.2
74-3	9.70	M _C .30R	-5.2	-3.6	6.3
	10.52	M _C .30R	-19.8	-15.2	25.0

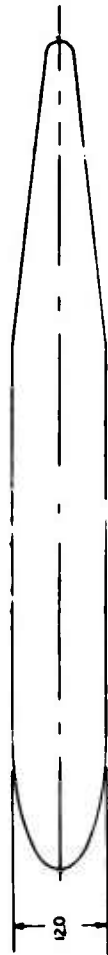
TABLE XIV - Continued

RUN-RT NO.	$\frac{\omega_m}{\Omega}$	DATA CHANNEL	COMPONENTS		
			a_m	b_m	r_m
74-4	9.71	M _{C.30R}	1.0	5.1	5.2
	10.52	M _{C.30R}	-16.2	-18.6	24.6
74-5	9.71	M _{C.30R}	2.3	- 4.7	5.2
	10.52	M _{C.30R}	-14.4	- 8.4	16.7
74-6	9.71	M _{C.30R}	3.6	- 3.4	5.0
	10.52	M _{C.30R}	10.8	12.0	16.0
74-7	9.71	M _{C.30R}	- .6	4.6	4.6
	10.52	M _{C.30R}	-12.2	- 8.3	15.6
74-8	9.70	M _{C.30R}	4.6	- 1.0	4.7
	10.52	M _{C.30R}	9.8	10.2	14.2
74-9	.22	ζ	- .5	.0	.5
	9.71	M _{C.30R}	2.7	- 3.3	4.3
	10.52	M _{C.30R}	10.1	- 8.6	12.3
75-6	5.26	M _{C.30R}	-	-	31.4
75-7	5.28	M _{C.30R}	-	-	34.0
75-8	5.27	M _{C.30R}	-	-	41.4
75-9	.35	ζ	.3	.0	.3
	.35	β	- .2	.0	.2
75-10	.33	ζ	.4	- .2	.5
	.33	β	- .3	- .1	.3
75-11	.29	ζ	.3	- .7	.8
	.29	M _{F.30R}	- .2	.0	.2
	.29	M _{T.18R}	- .1	.6	.7
	.29	β	- .4	.0	.4
	.71	M _{F.30R}	- .2	.3	.4
	.71	M _{T.18R}	- .3	- .3	.5
	.71	β	.3	.0	.3
	1.29	M _{F.30R}	.0	.5	.5
	1.29	M _{T.18R}	.5	- .2	.6
	1.29	β	.2	.0	.2
77-12	5.26	M _{C.30R}	-	-	8.8
77-13	5.26	M _{C.30R}	-	-	9.2
79-10	.29	ζ	- .4	- .3	.5
	.29	M _{F.30R}	- .1	.2	.3
	.29	β	.0	.3	.3
	.29	M _{C.30R}	- 2.3	1.4	2.6
	.71	M _{F.30R}	- .3	.1	.3
	.71	β	.1	.4	.4

TABLE XIV - Concluded					
RUN-PT NO.	$\frac{\omega_m}{\Omega}$	DATA CHANNEL	a_m	COMPONENTS b_m	r_m
81-9	.71	MC.30R	.4	.4	.5
	1.30	MC.30R	.2	.3	.4
	1.30	β	.2	- .2	.3
	1.30	MC.30R	.2	- .3	.4
	.27	ζ	.5	.4	.6
	.27	MT.18R	- .1	.7	.7
	.27	β	- .1	- .3	.3
	.73	MT.18R	- .6	.4	.7
	.73	β	.1	- .2	.3
	1.27	MT.18R	.7	.4	.8
	1.27	β	- .1	.0	.1
	.50	MT.18R	- .5	- .6	.7
	.50	β	- .1	- .3	.3
	4.52	MT.18R	.9	.5	1.0
84-6	4.53	MC.30R	.9	- 4.7	4.8



Figure 1. Sikorsky Compound Helicopter Model in United Aircraft Corporation 18-Foot Wind Tunnel.



ROTOR DATA

RADIUS 54 IN NO. OF BLADES 4
CHORD 42.4 IN $\sigma = 0.10$

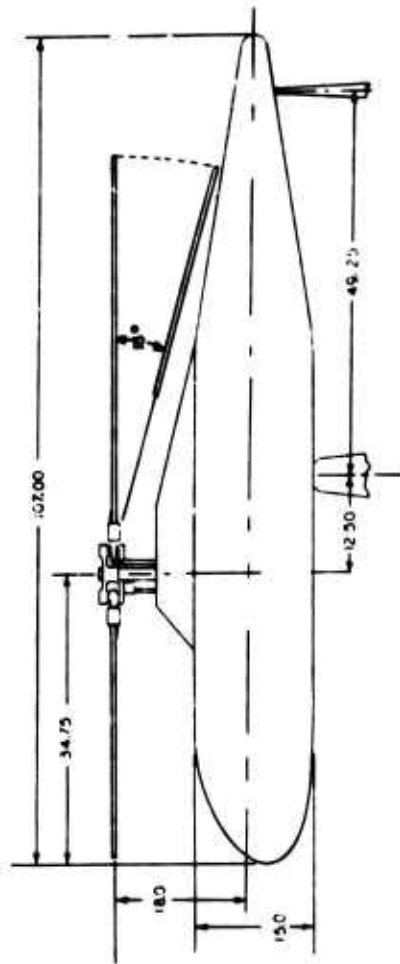
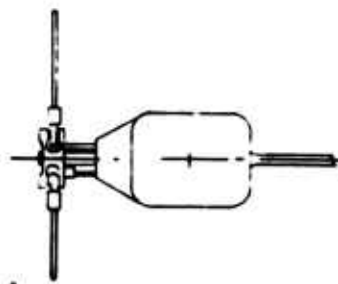


Figure 2. Three-View Drawing of Sikorsky Compound Helicopter Model.

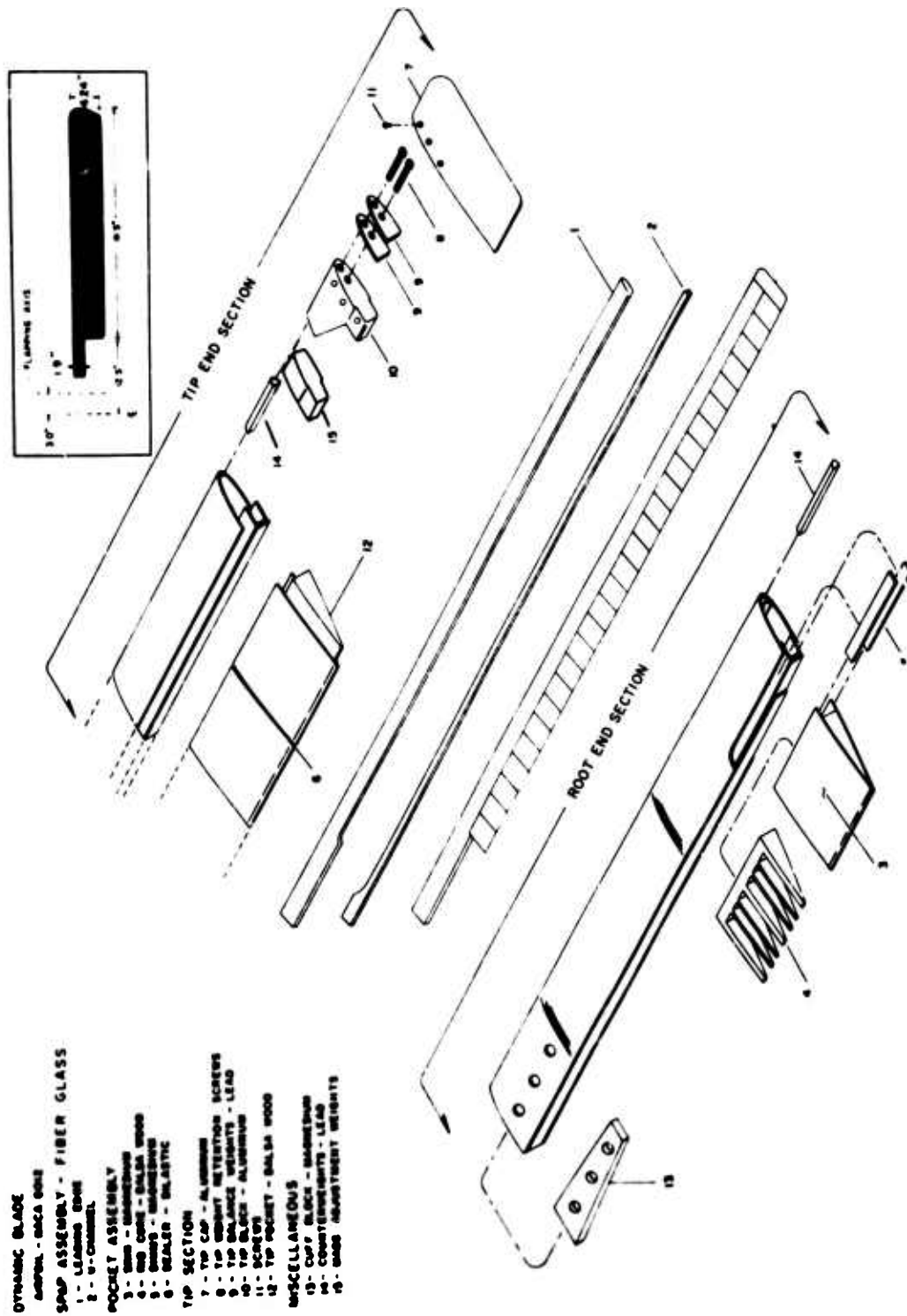


Figure 3. Dynamically Scaled Model Blade Construction.

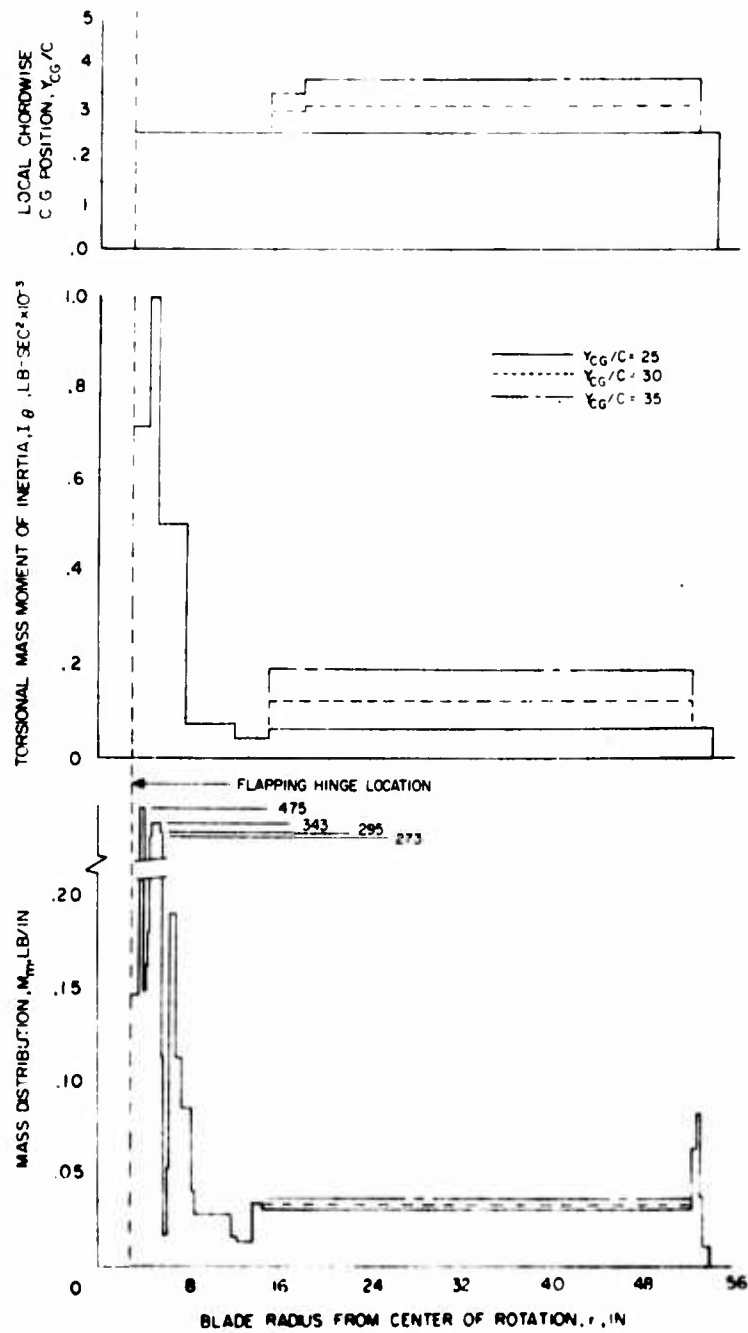


Figure 4. Blade Mass Properties.

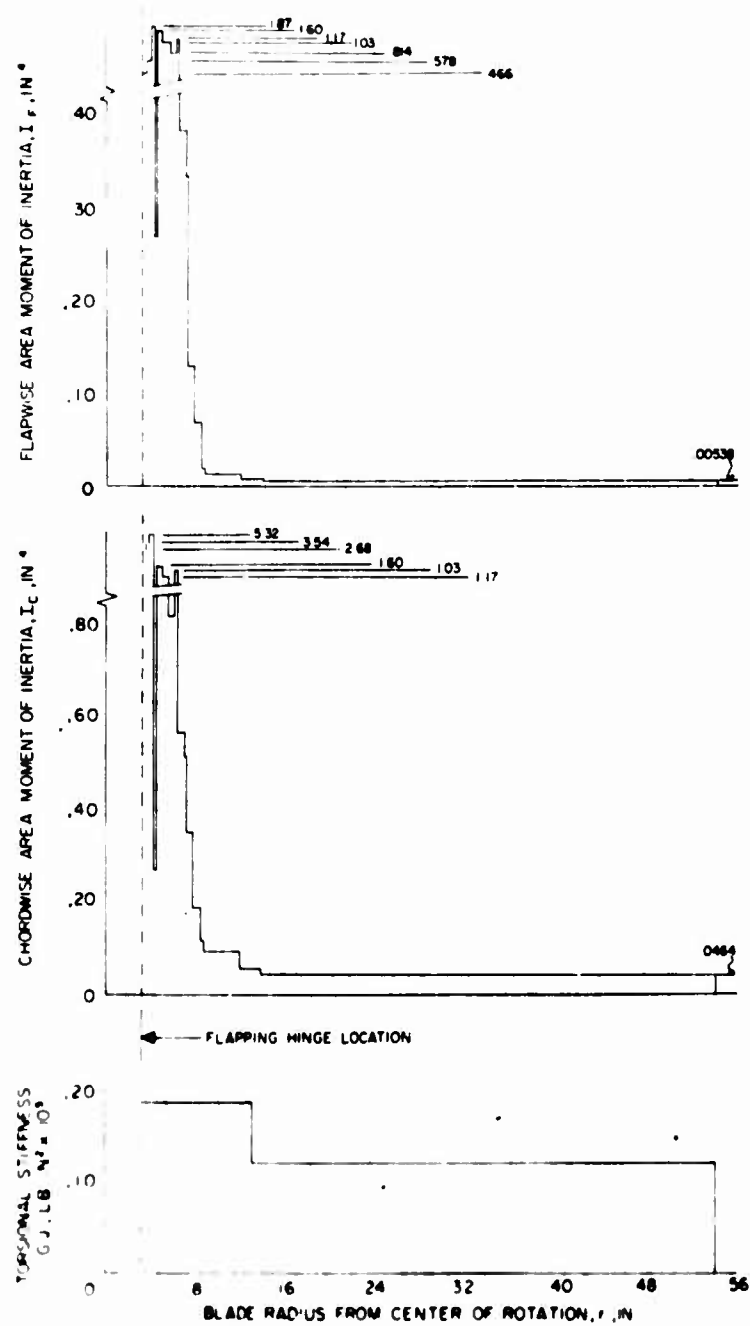


Figure 5. Blade Stiffness Properties.

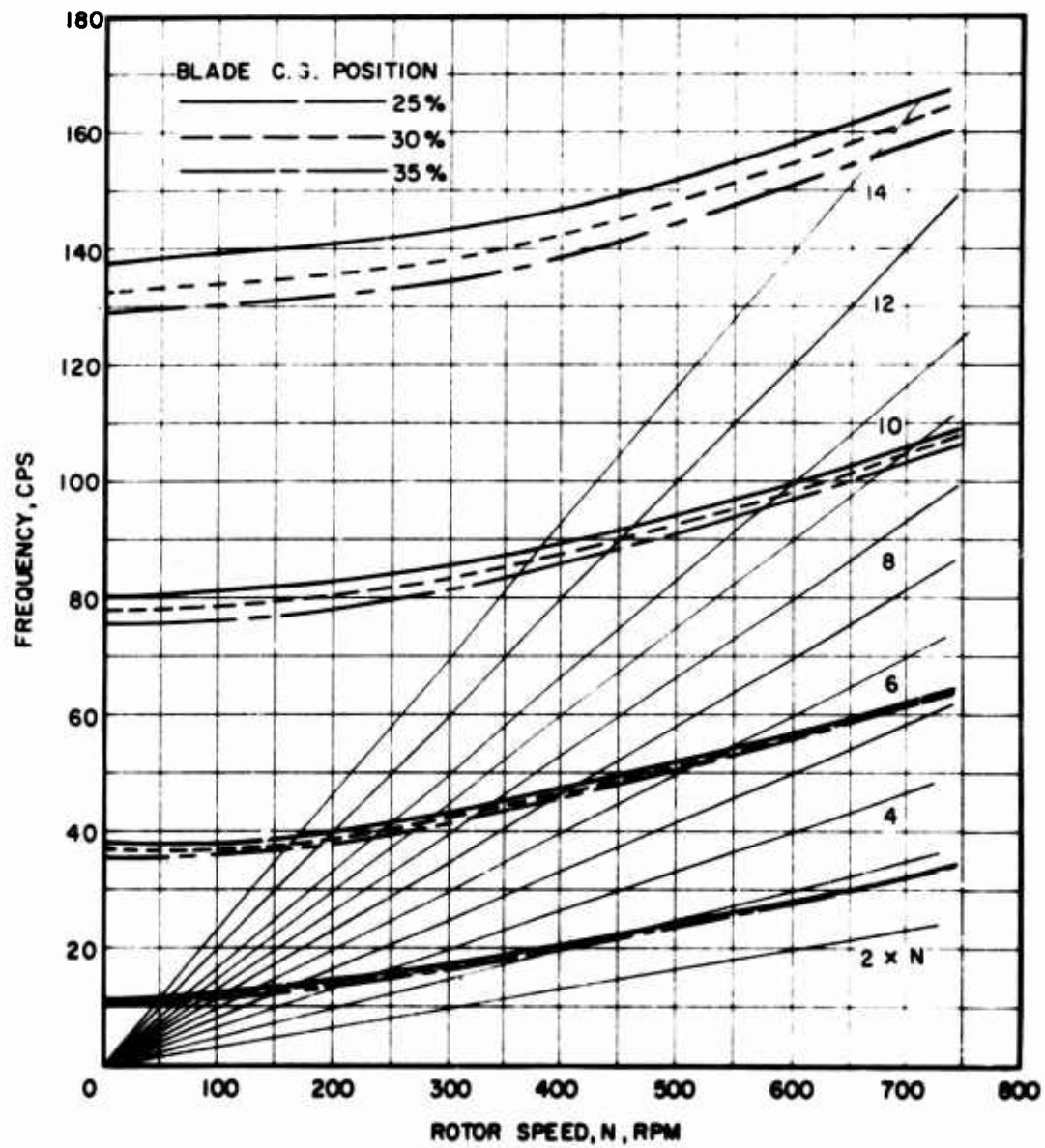


Figure 6. Blade Flapwise Natural Frequency Versus Rotor Speed.

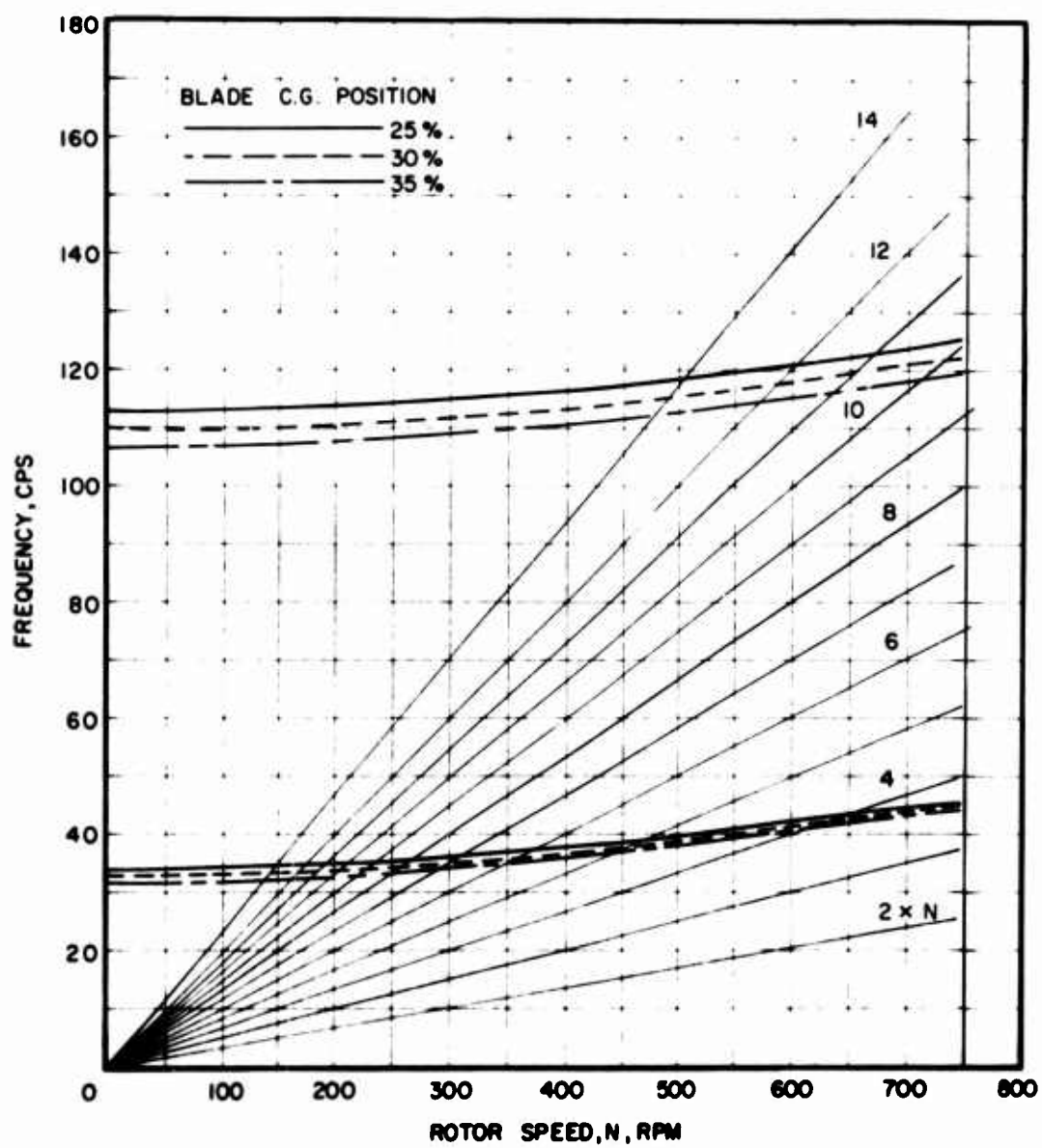


Figure 7. Blade Chordwise Natural Frequency Versus Rotor Speed.

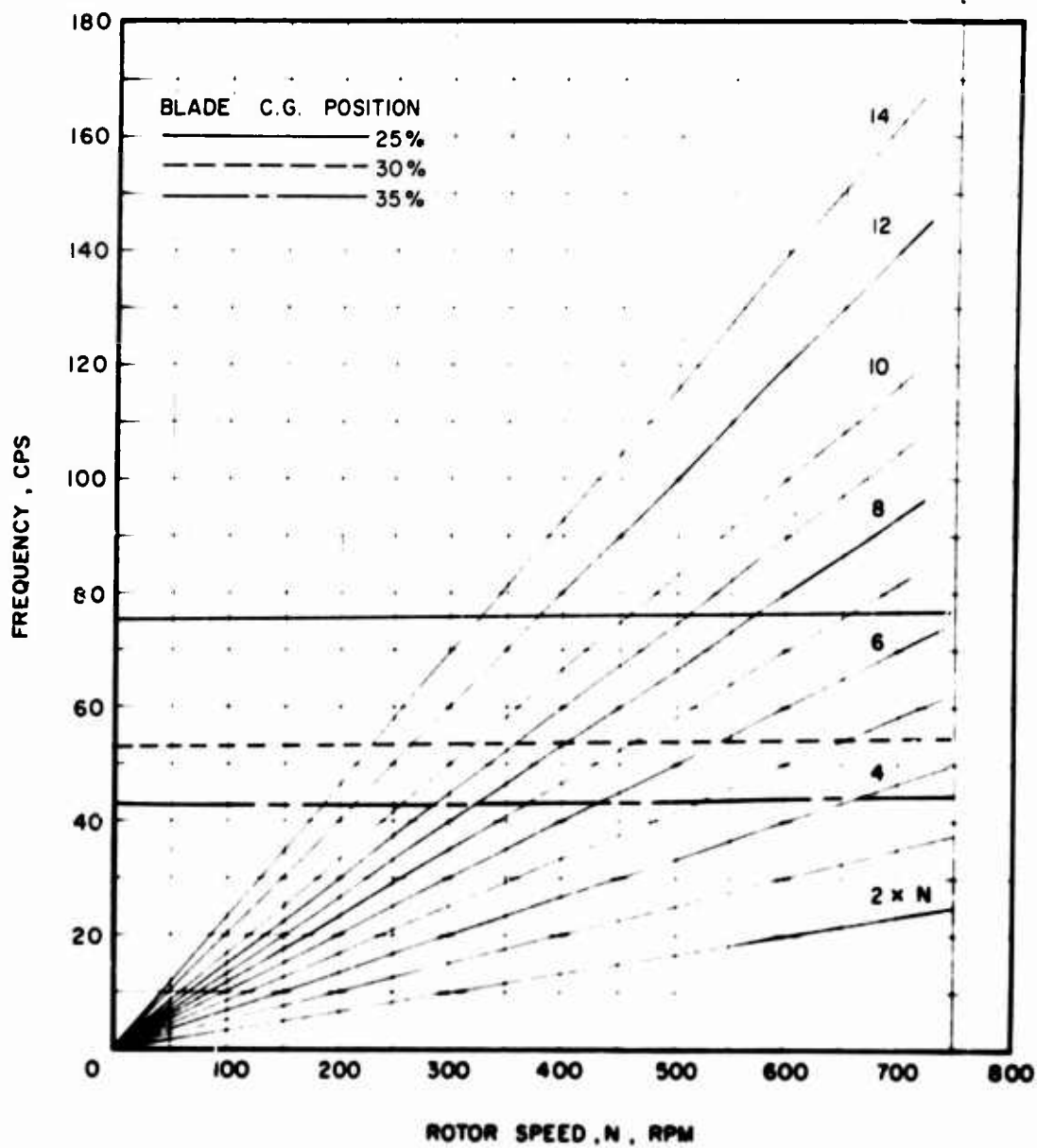


Figure 5. Blade Torsional Natural Frequency Versus Rotor Speed.

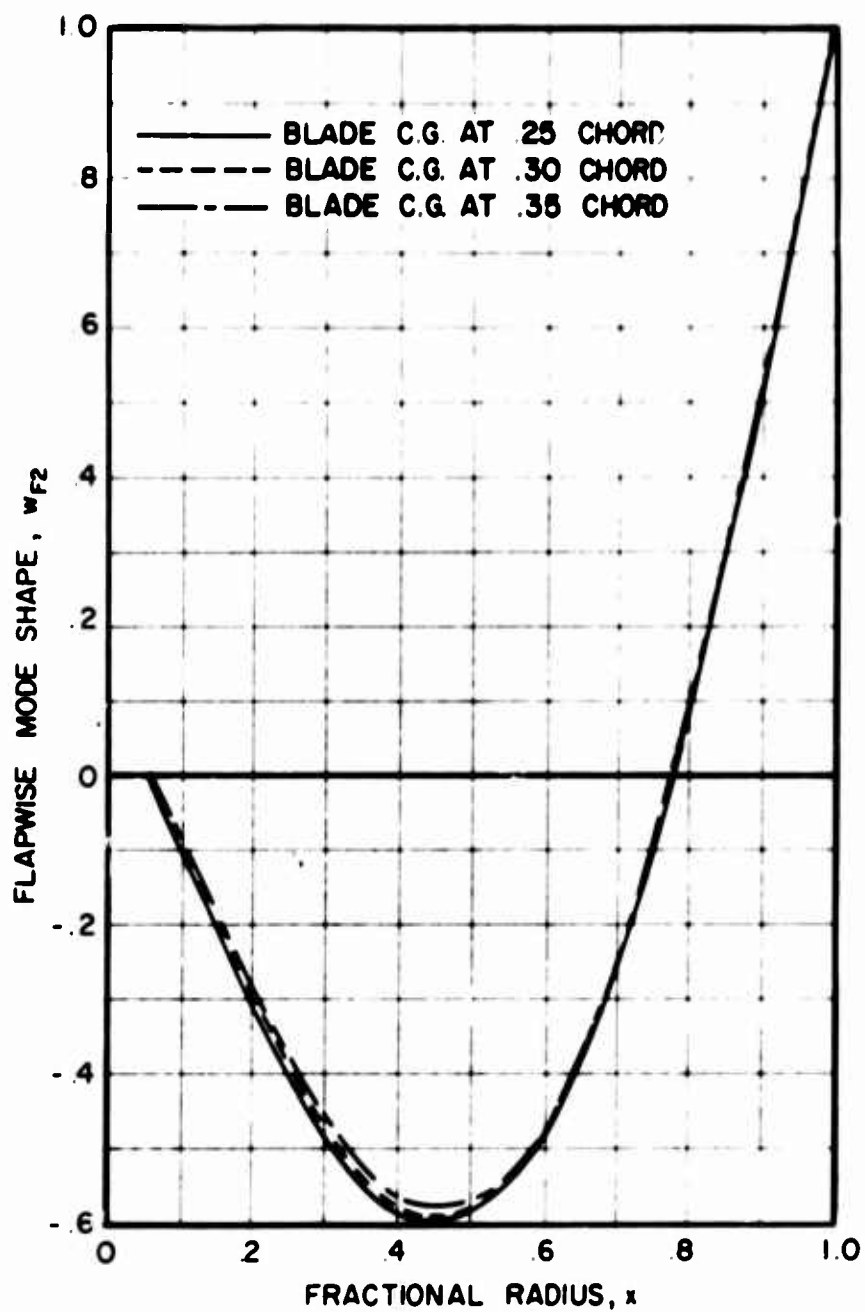


Figure 9. Blade First Flapwise Bending Mode Shape;
 $\Omega_s R = 700$ ft/sec.

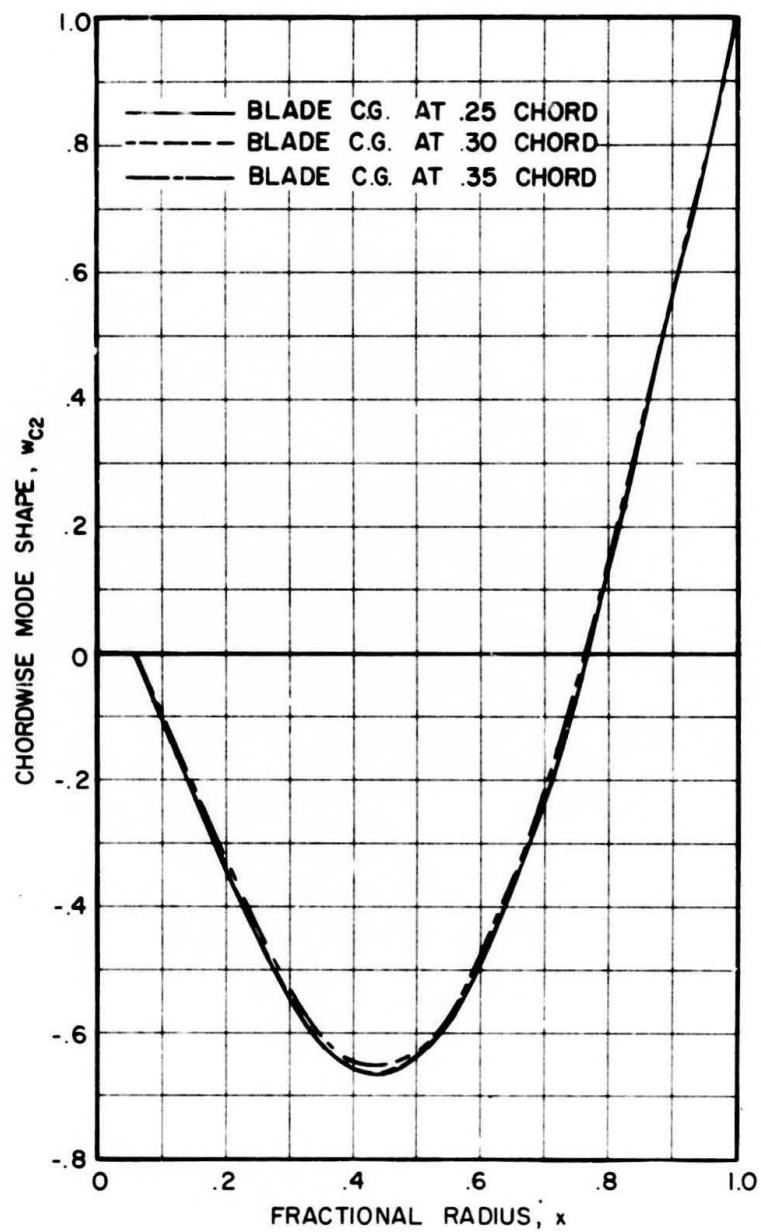


Figure 10. Blade First Chordwise Bending Mode Shape;
 $\Omega_s R = 700$ ft/sec.

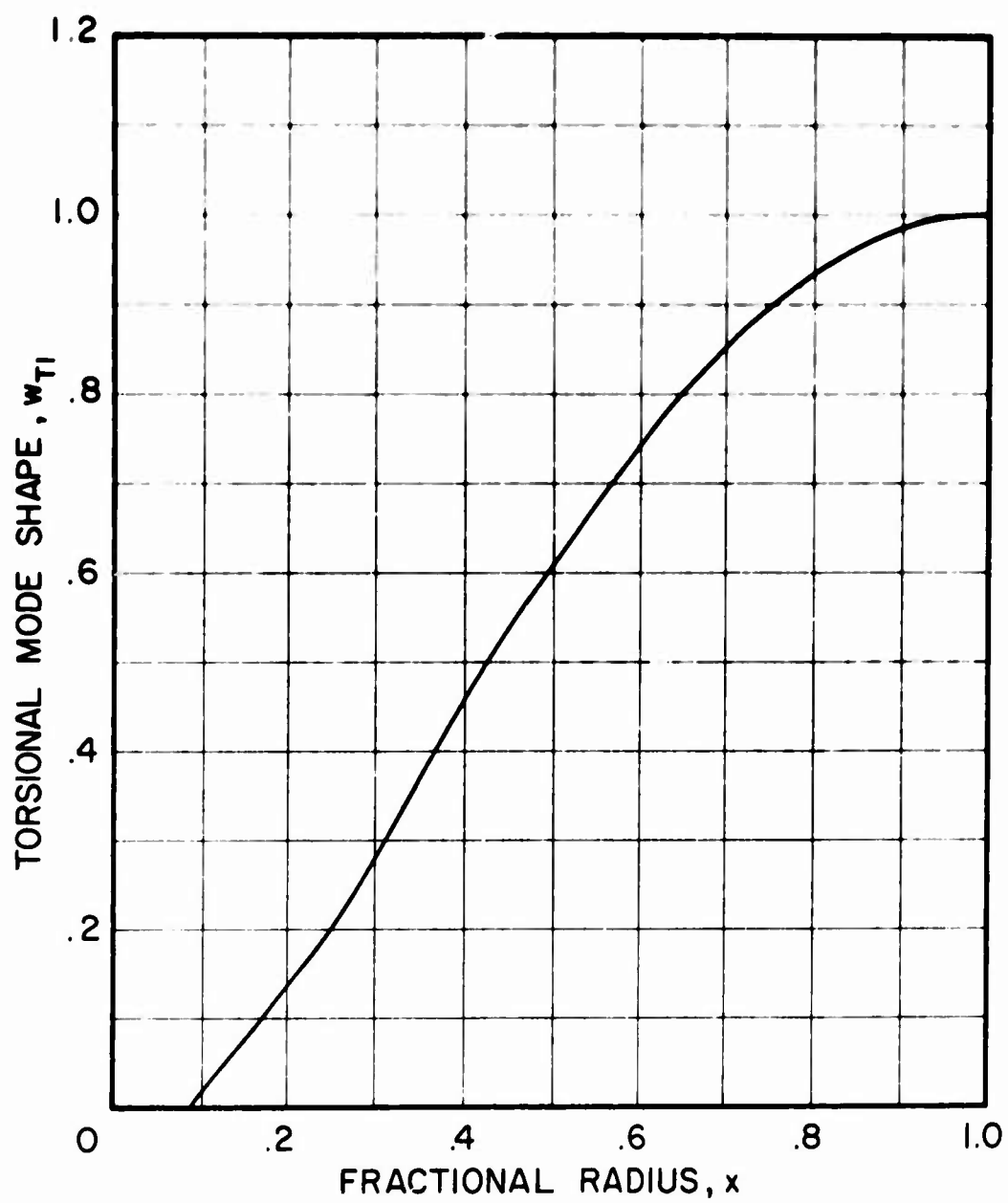


Figure 11. Blade First Torsional Mode Shape; $\Omega_s R = 700$ ft/sec.

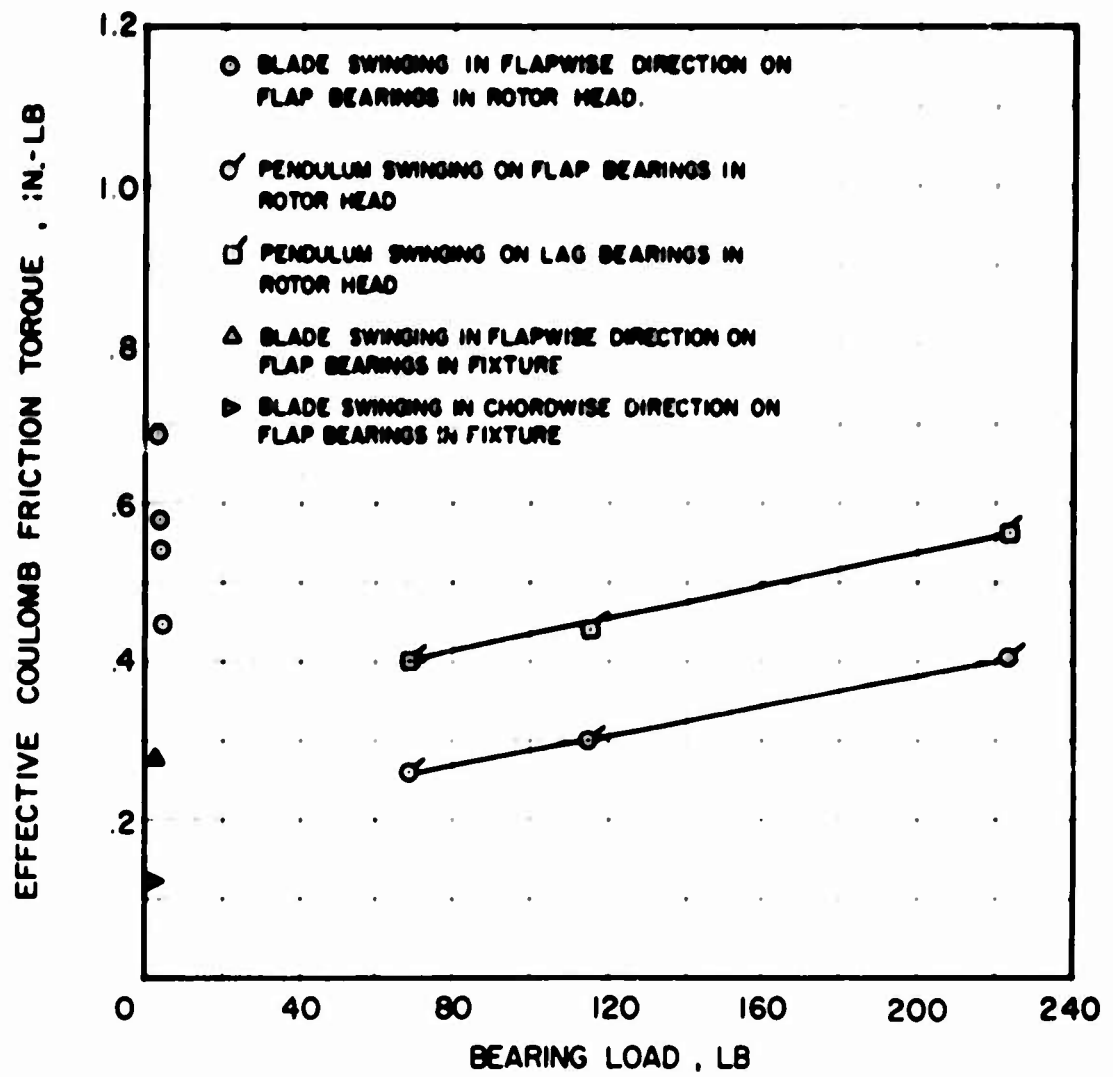


Figure 12. Model Blade Bearing Friction Test Results.

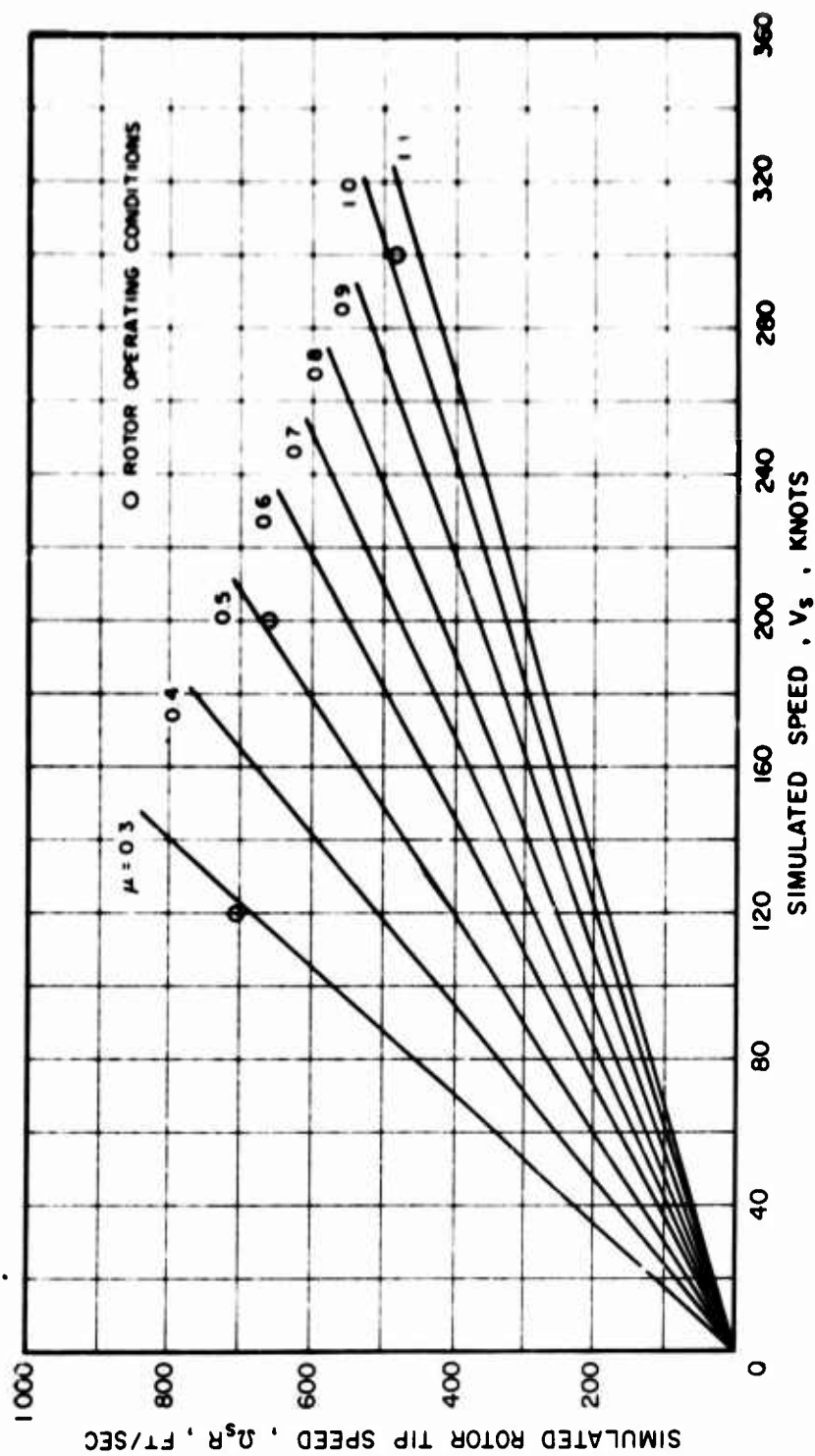


Figure 13. Rotor Operating Conditions for Transient Testing.

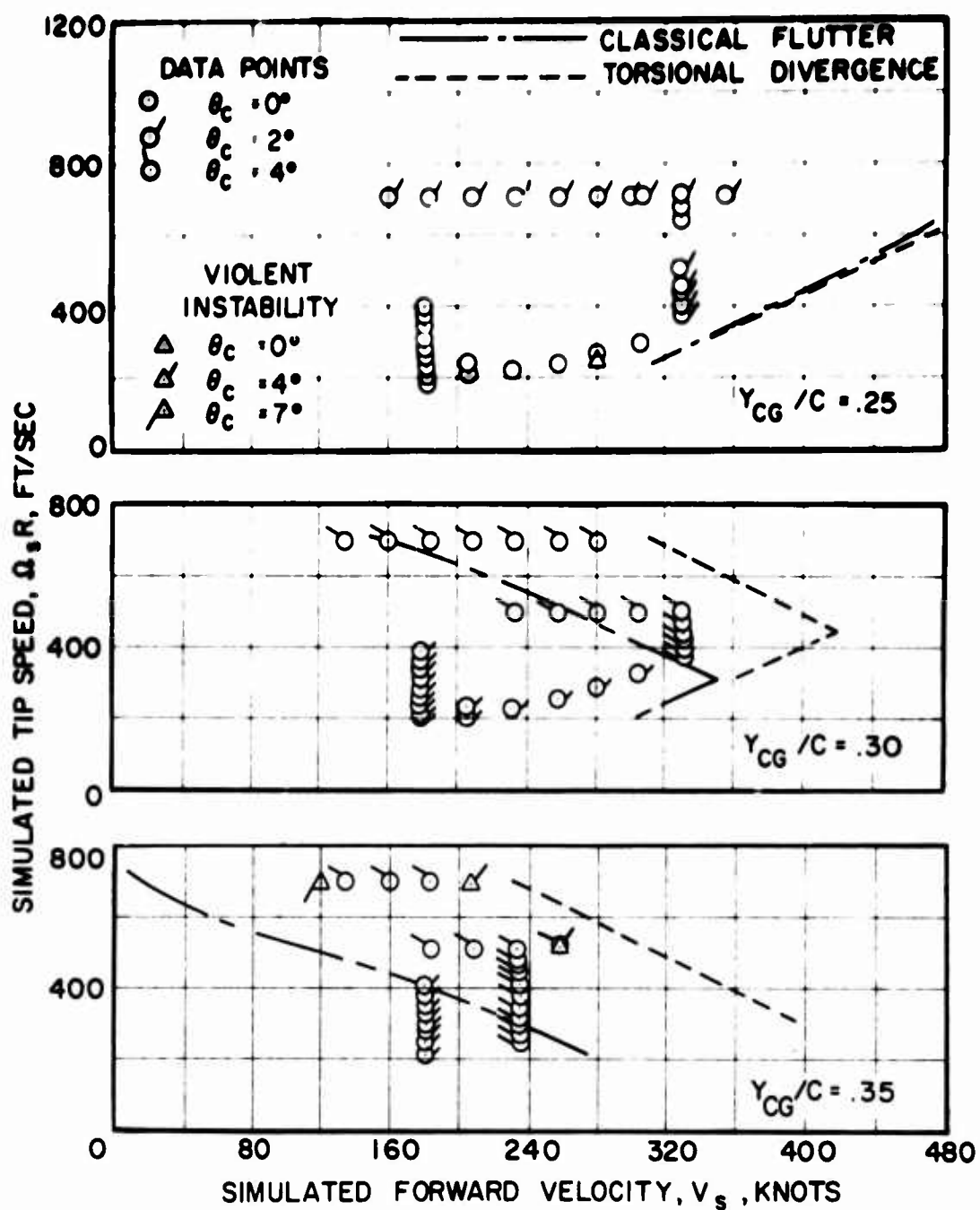
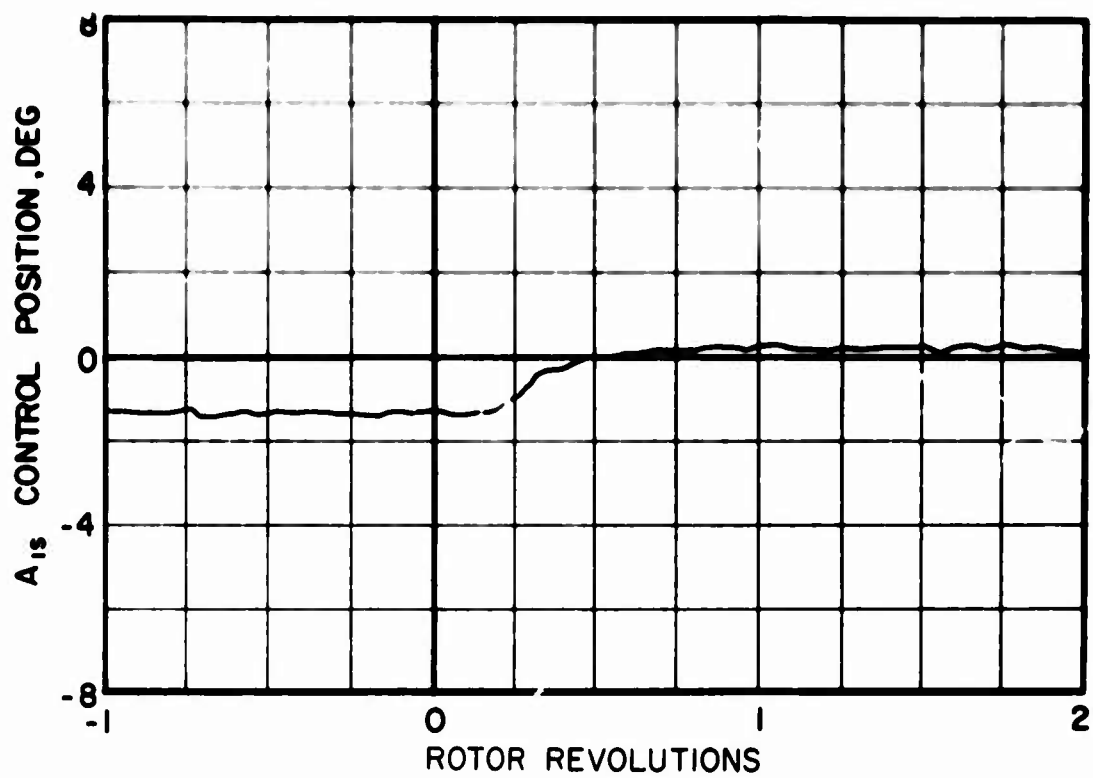


Figure 14. Theoretical Fixed-Azimuth Stability Boundaries and Selected Data Points.



(a)

Figure 15. Sample Control Position Transient Input; $V_s = 300$ kn,
 $\mu = 1.026$, $\text{TAN } \delta_3 = 1.0$, $\alpha_f = 0.0^\circ$, $\theta_{cs} = 0.0^\circ$,
 $\Delta\theta_c = 4.0^\circ$, $a_{1ss} = 0.0^\circ$, $\Delta a_{1s} = 2.4^\circ$, $b_{1ss} = 0.0^\circ$,
 $\Delta b_{1s} = -1.4^\circ$, Run 60, Point 28,

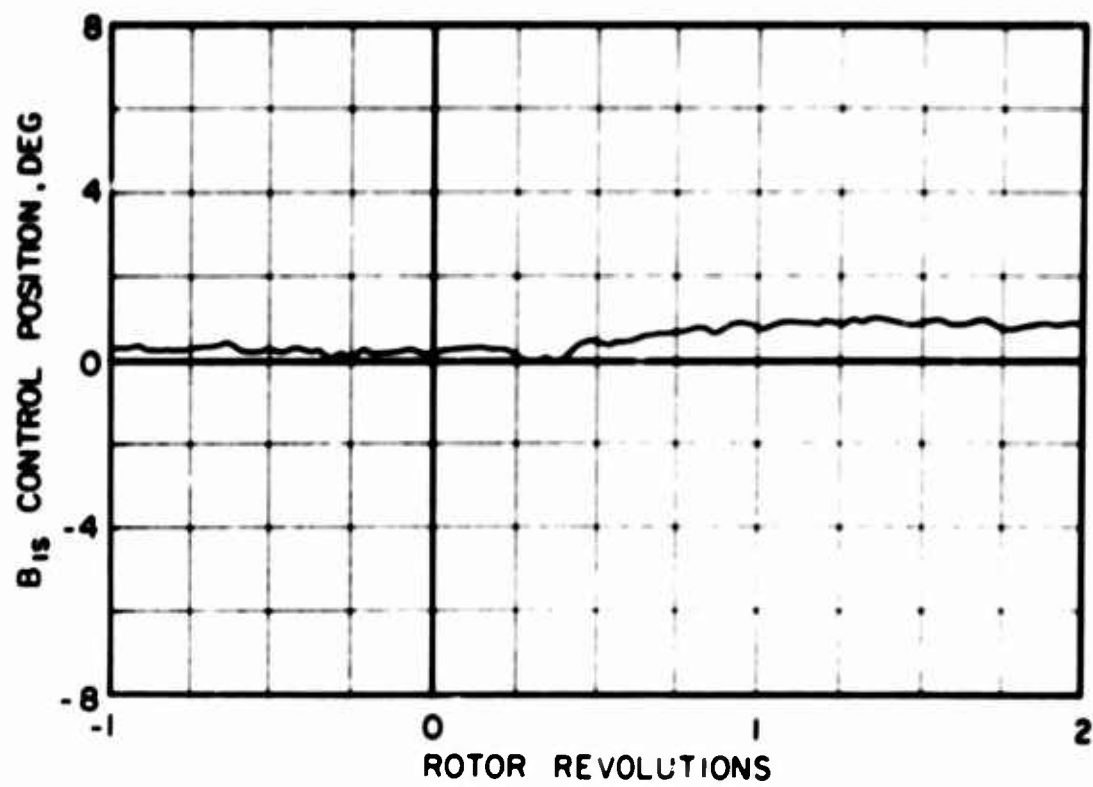
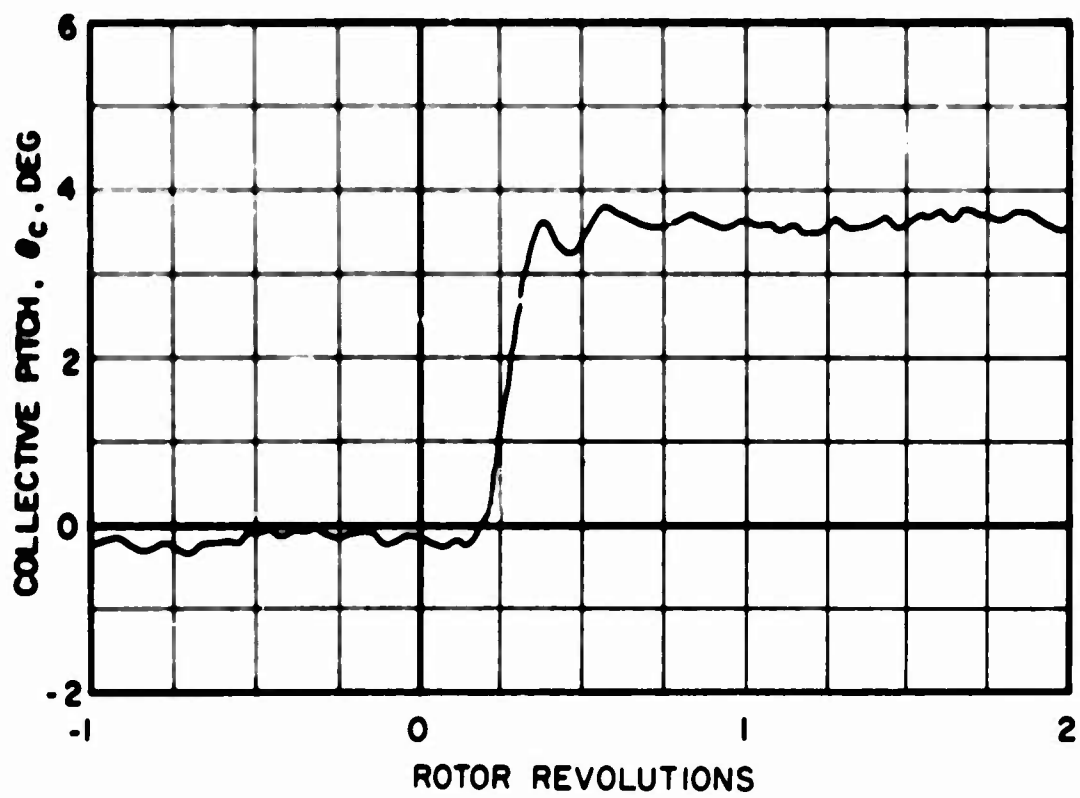
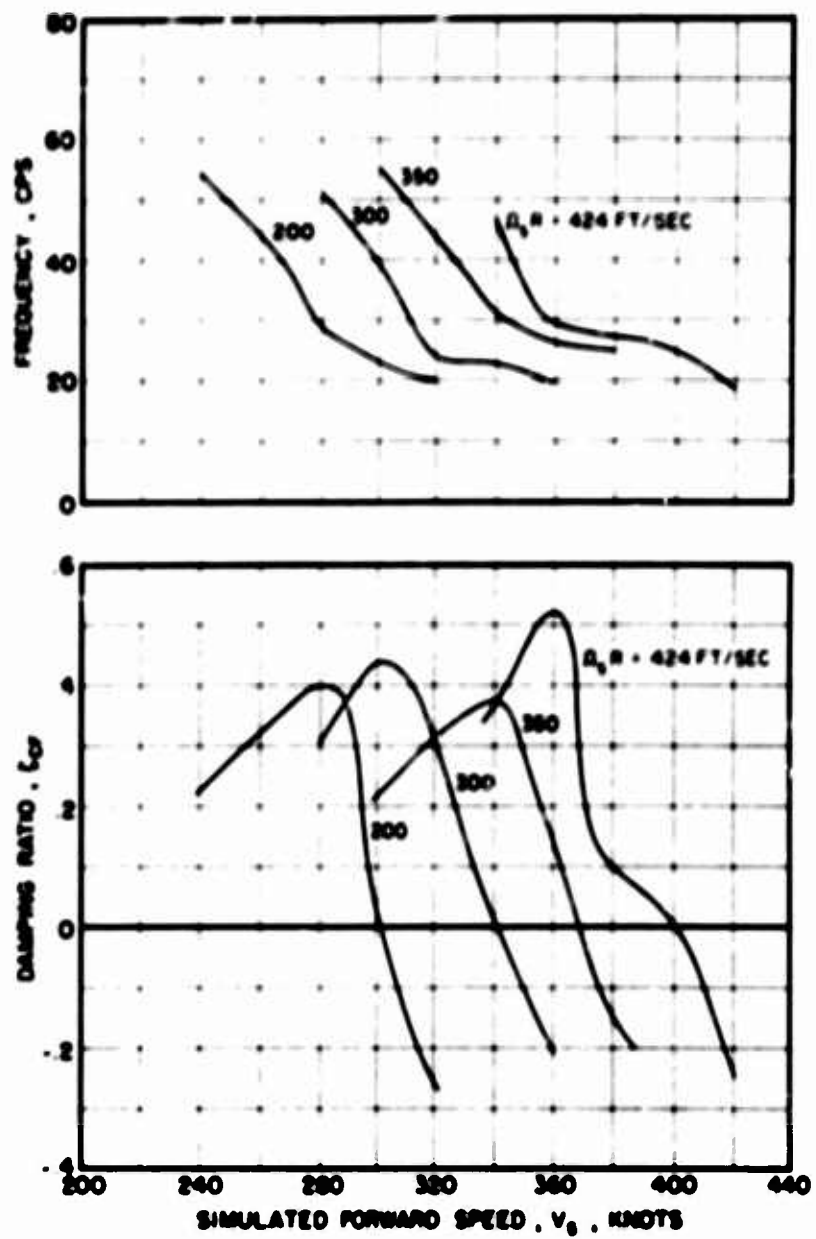


Figure 15. Continued.



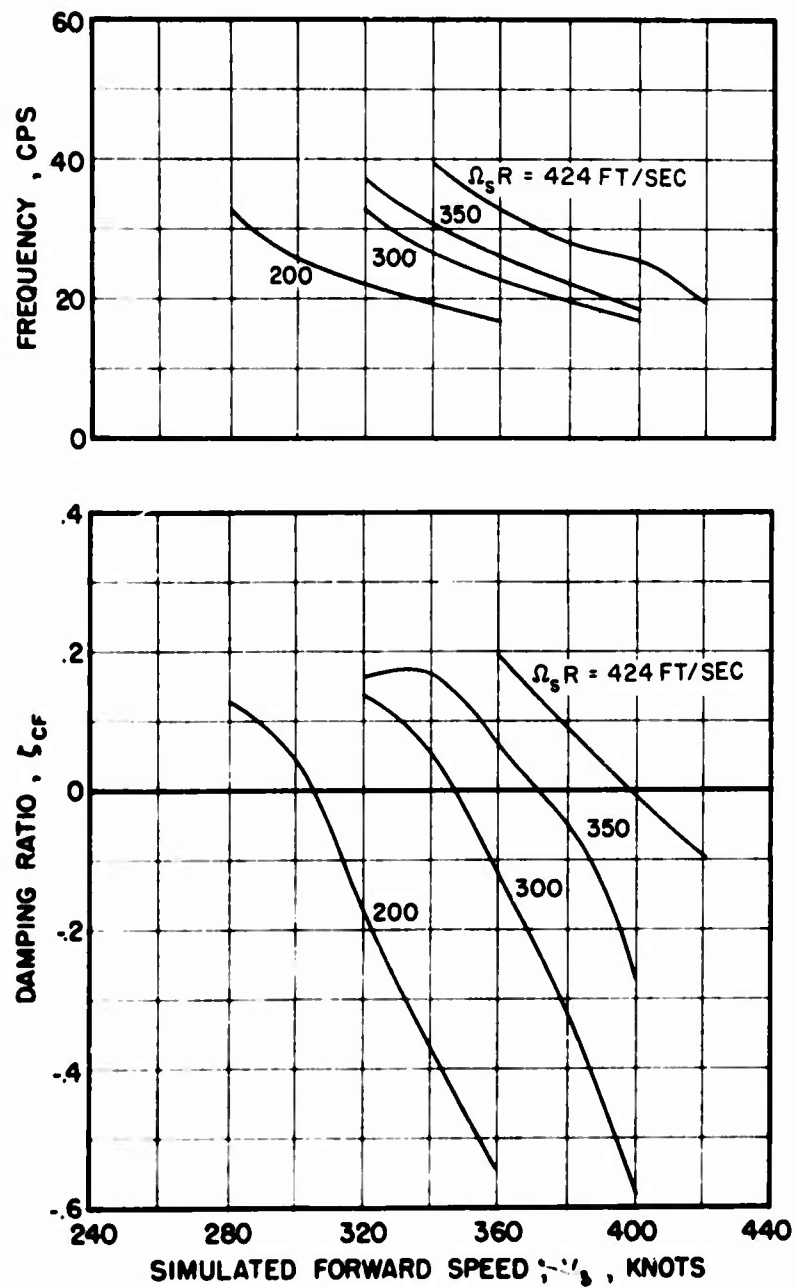
(c)

Figure 15. Concluded.



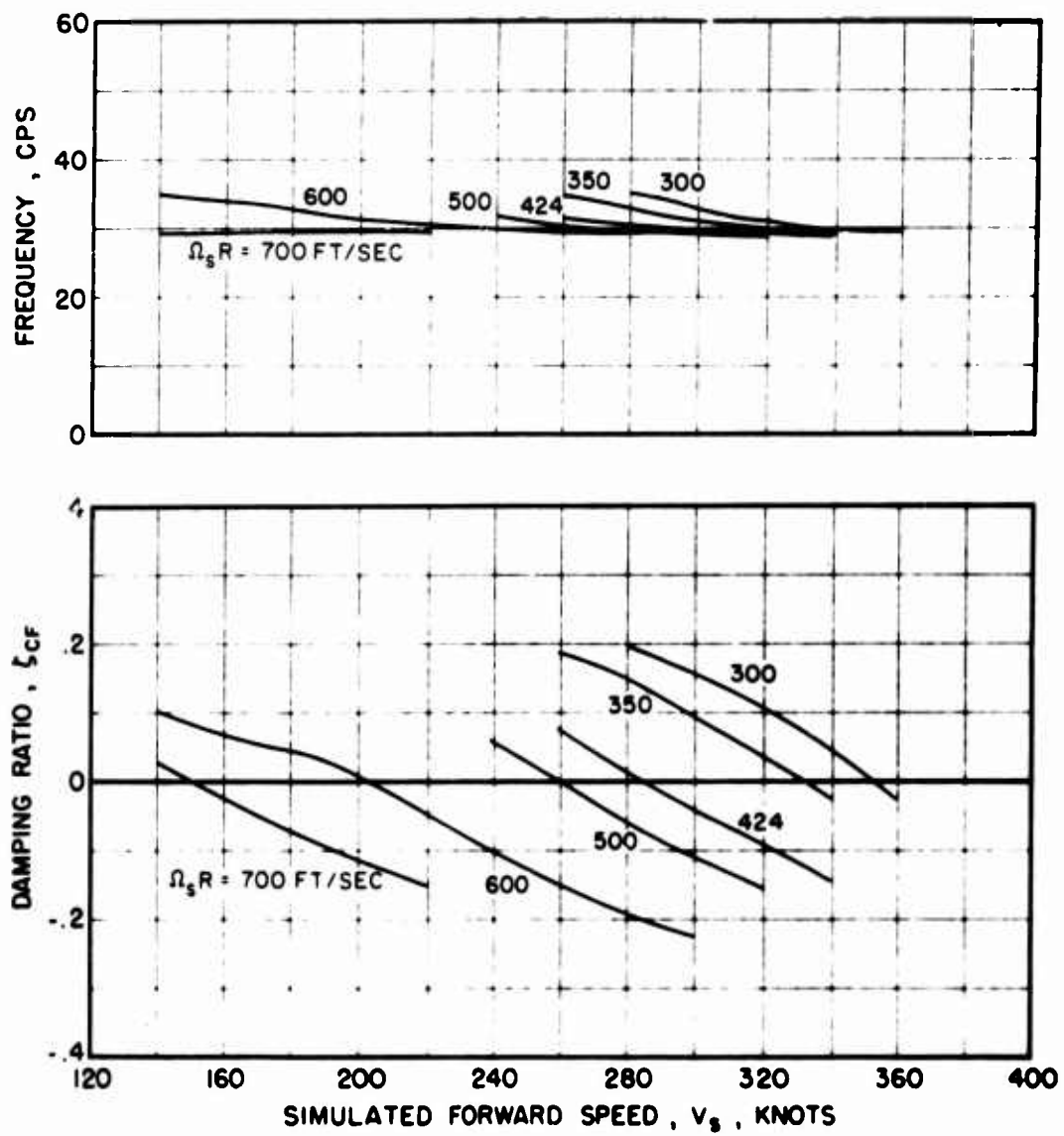
(c) $\psi = 270^\circ$, BLADE C.G. AT 25 CHORD

Figure 16. Frequency and Damping of Calculated Fixed-Azimuth Flutter Mode.



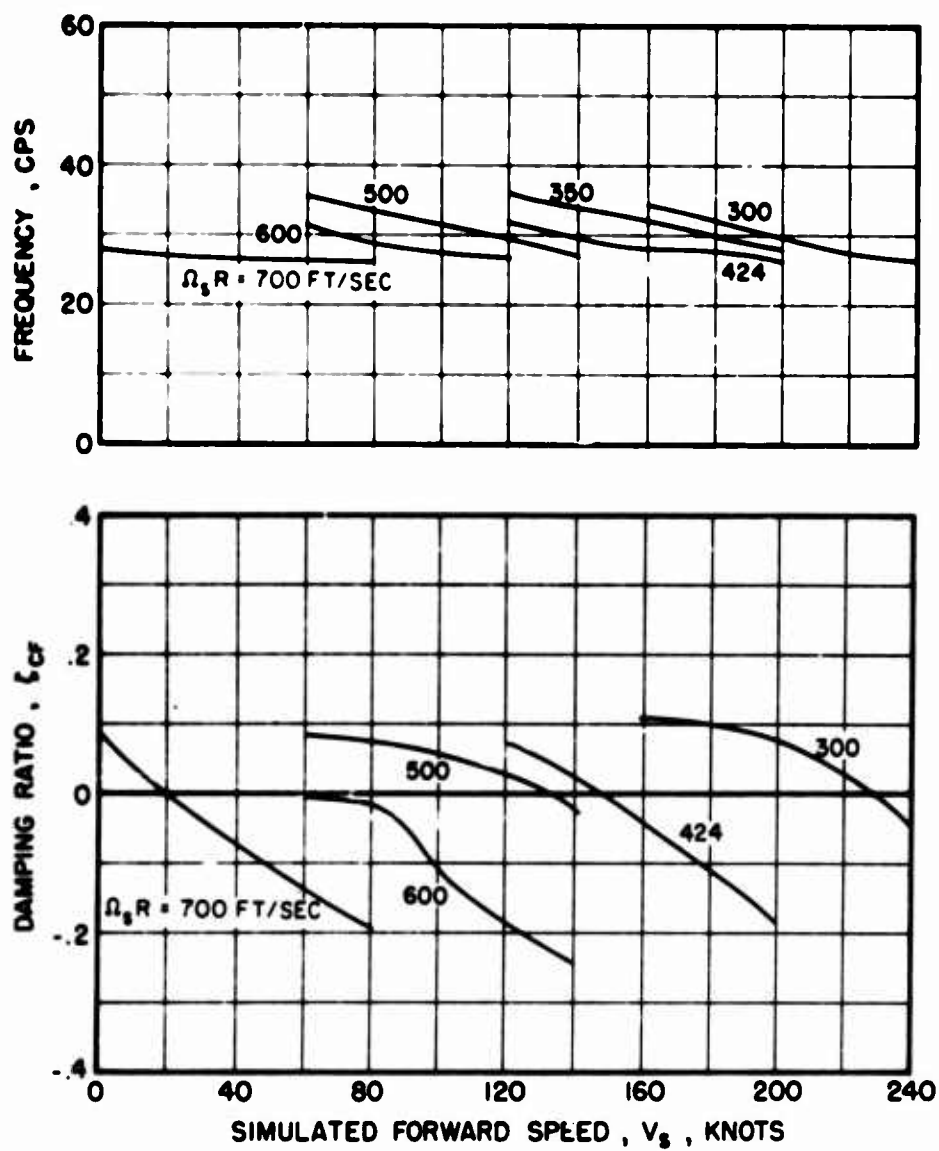
(b) $\psi = 270^\circ$, BLADE C.G. AT .30 CHORD

Figure 16. Continued



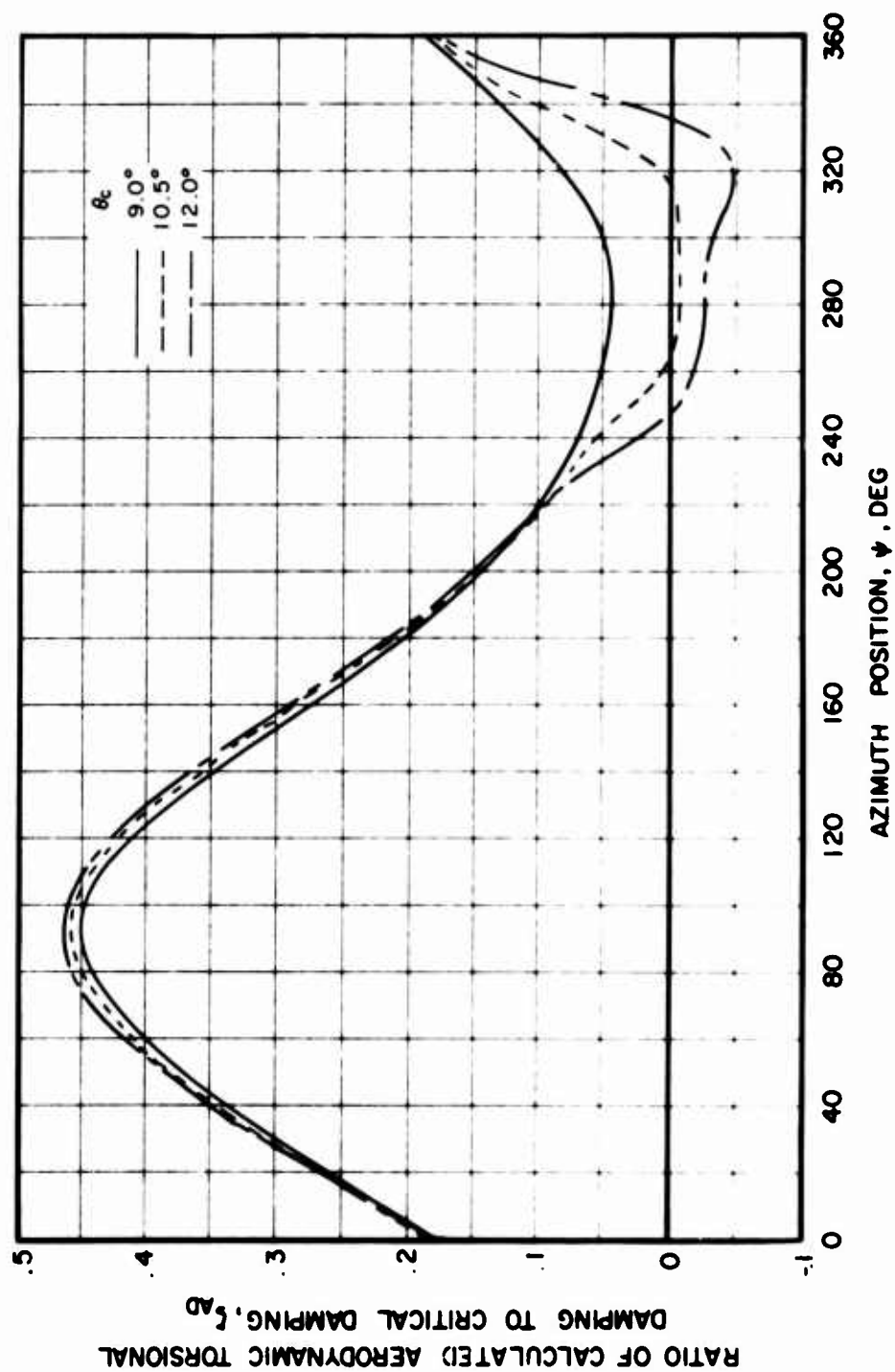
(c) $\psi = 90^\circ$, BLADE C G AT .30 CHORD

Figure 16. Continued.



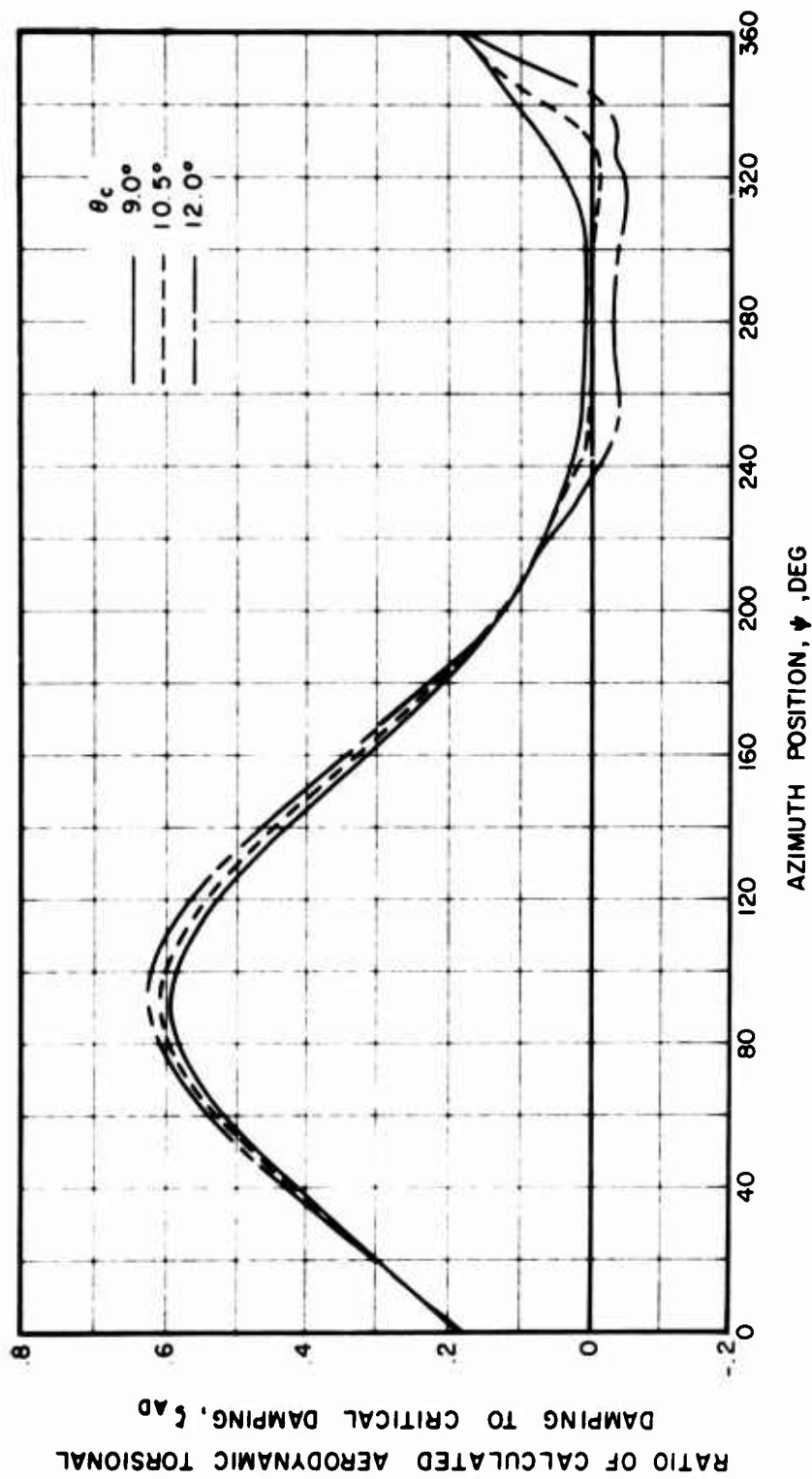
(d) $\psi = 90^\circ$, BLADE C.G. AT .35 CHORD

Figure 16. Concluded.



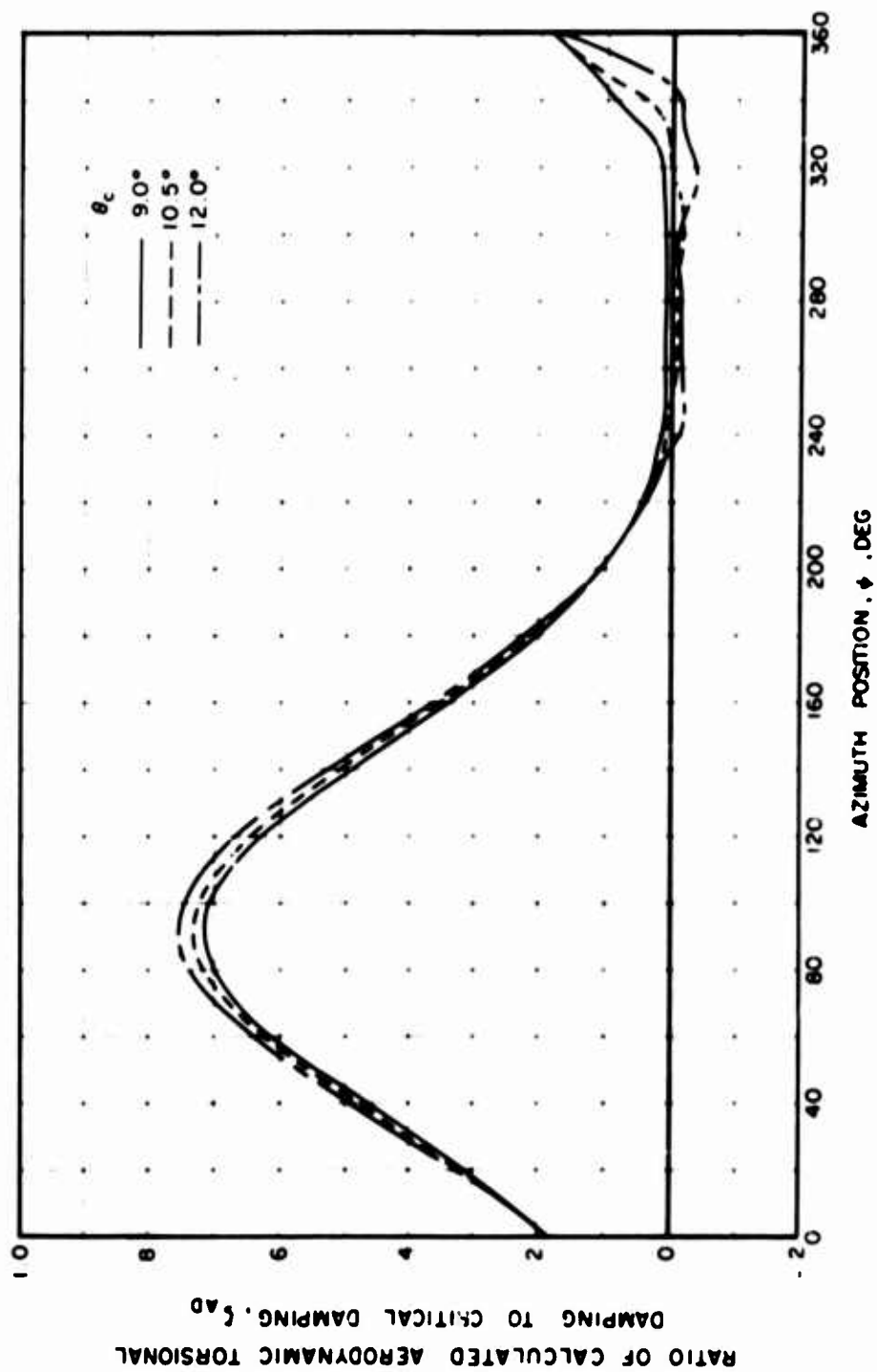
(a) $V_s = 120$ knots, $\mu = .29$

Figure 17. Torsional Damping From Stall Flutter Calculations;
 $\alpha_s = 0.0^\circ$, $\alpha_{ls} = 0.0^\circ$, $b_{ls} = 0.0^\circ$.



(b) $V_s = 170$ knots, $\mu = .41$

Figure 17. Continued.



(c) $V_g = .00$ knots, $\mu = .50$

Figure 17. Concluded.

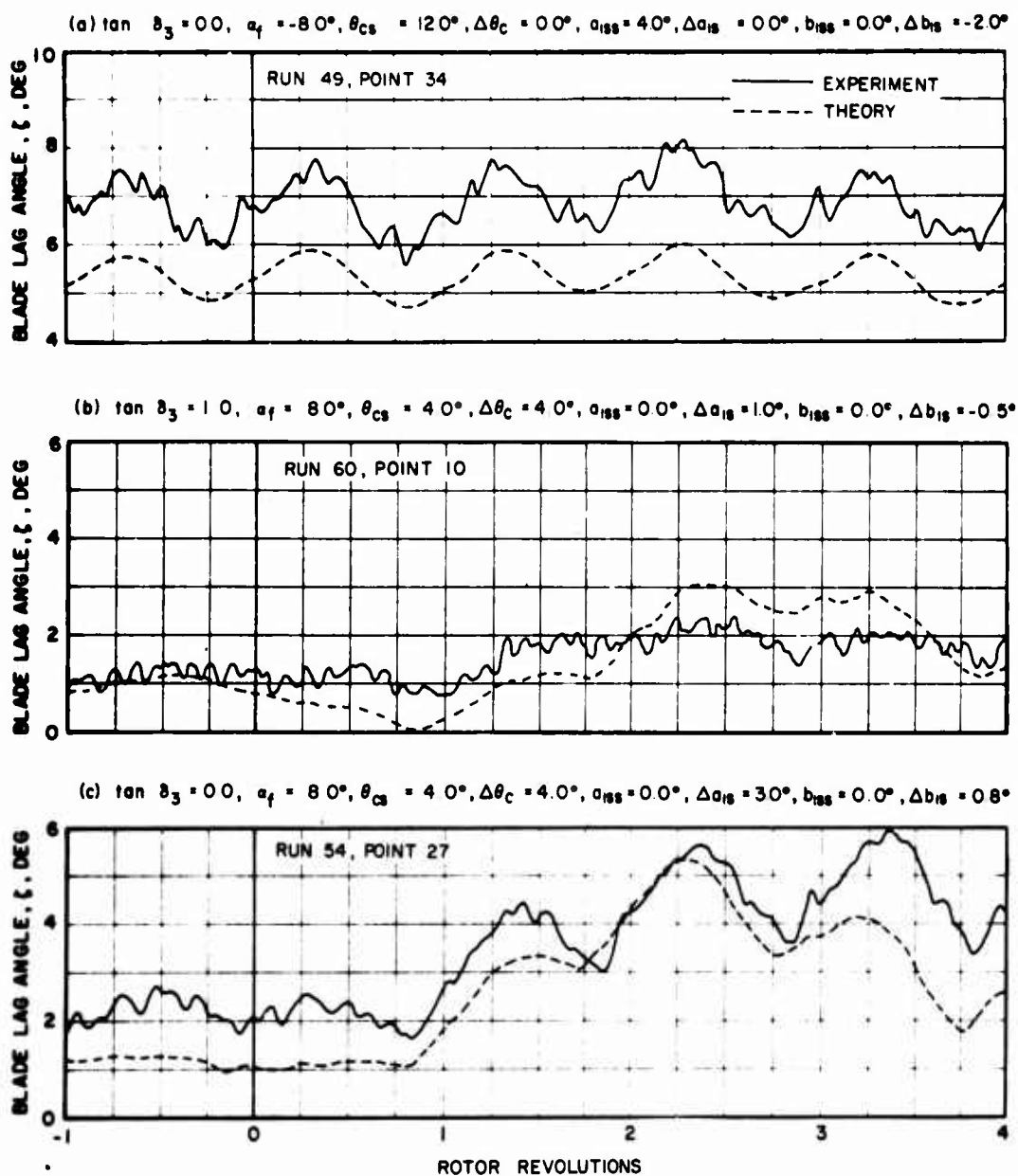


Figure 18. Experimental and Theoretical Blade Lag Angle During Transient Conditions; $V_s = 120$ kn, $\mu = 0.29$, $Y_{CG}/c = 0.25$.

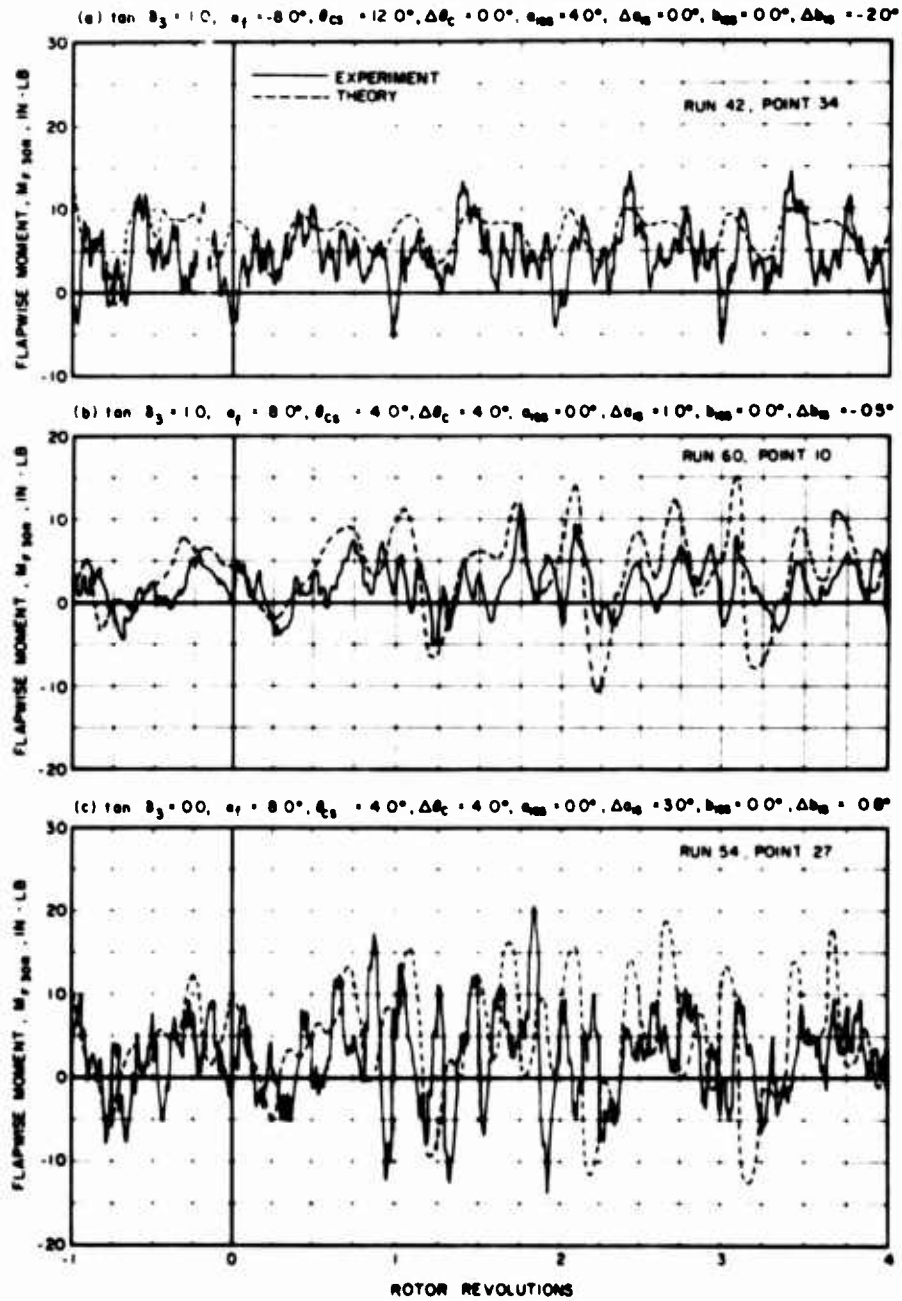


Figure 19. Experimental and Theoretical Blade Flapwise Bending Moments During Transient Conditions; $V_g = 120$ kn, $\mu = 0.29$, $Y_{CG}/c = 0.25$.

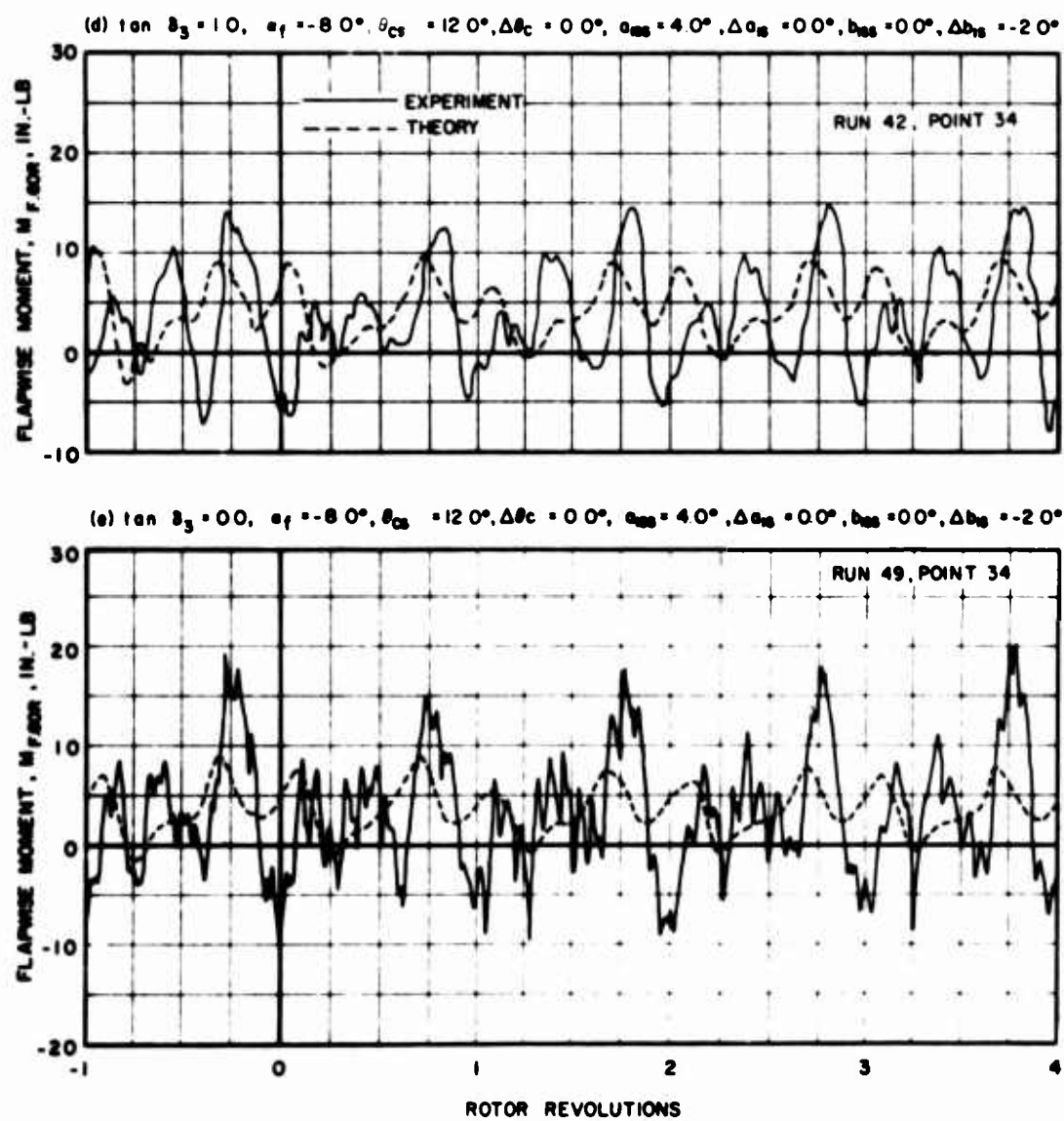
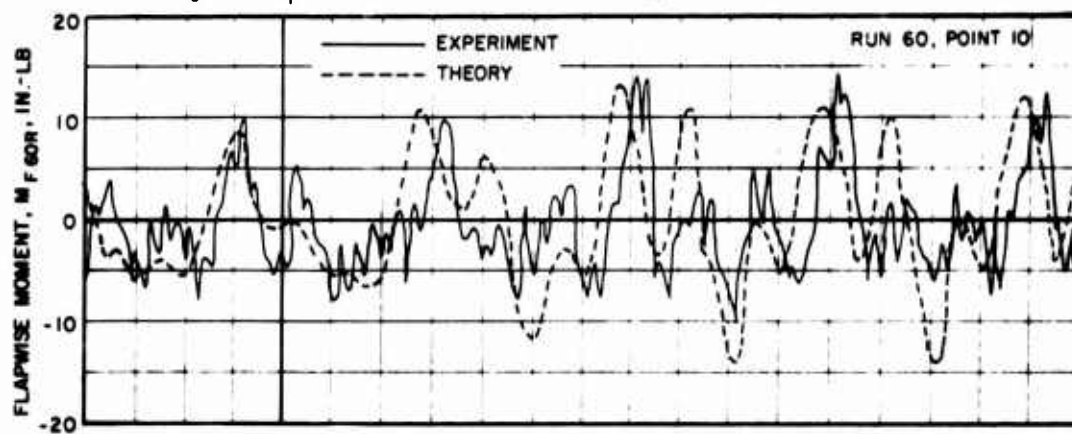


Figure 19. Continued.

(f) $\tan \delta_3 = 10$, $\alpha_f = 80^\circ$, $\theta_{cs} = 40^\circ$, $\Delta\theta_c = 40^\circ$, $\alpha_{iss} = 00^\circ$, $\Delta\alpha_{is} = 10^\circ$, $b_{iss} = 00^\circ$, $\Delta b_{is} = -05^\circ$



(g) $\tan \delta_3 = 00$, $\alpha_f = 80^\circ$, $\theta_{cs} = 40^\circ$, $\Delta\theta_c = 40^\circ$, $\alpha_{iss} = 00^\circ$, $\Delta\alpha_{is} = 30^\circ$, $b_{iss} = 00^\circ$, $\Delta b_{is} = 08^\circ$

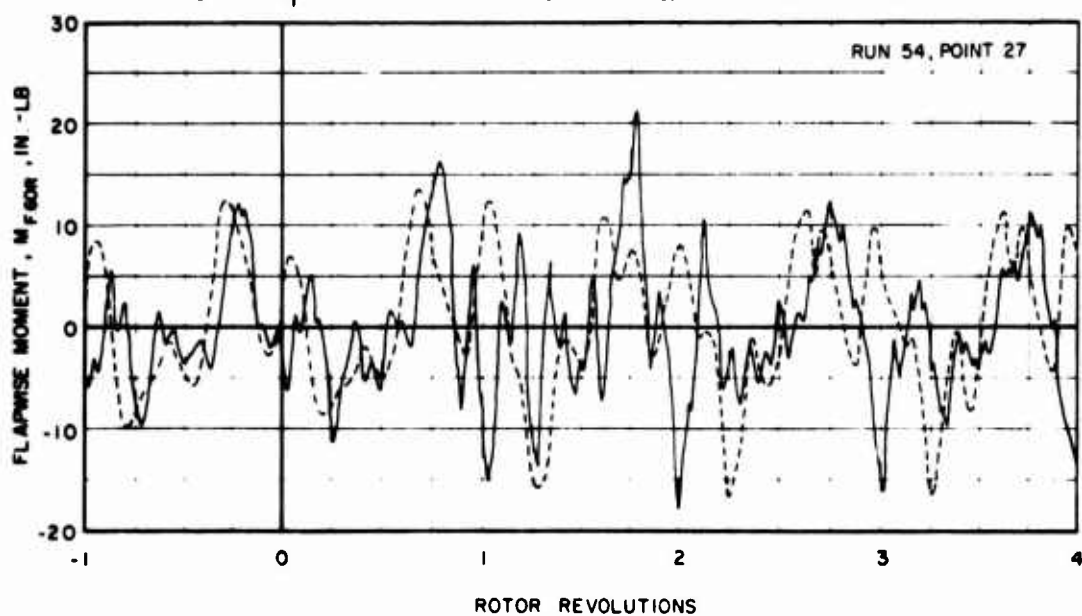


Figure 19. Concluded.

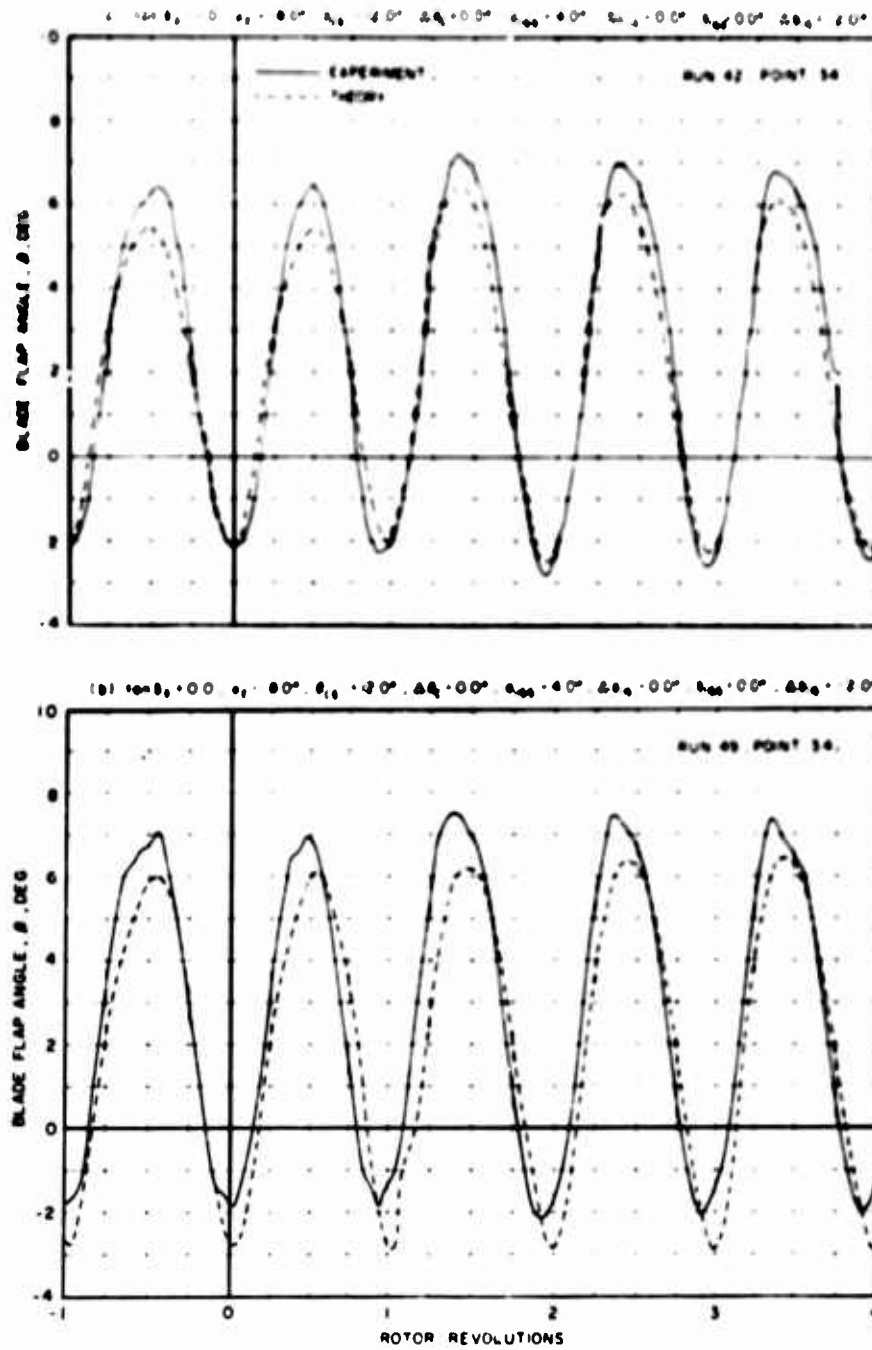


Figure 20. Experimental and Theoretical Blade Flap Angle During Transient Conditions; $V_s = 120$ kn, $\mu = 0.29$, $Y_{CG}/c = 0.25$.

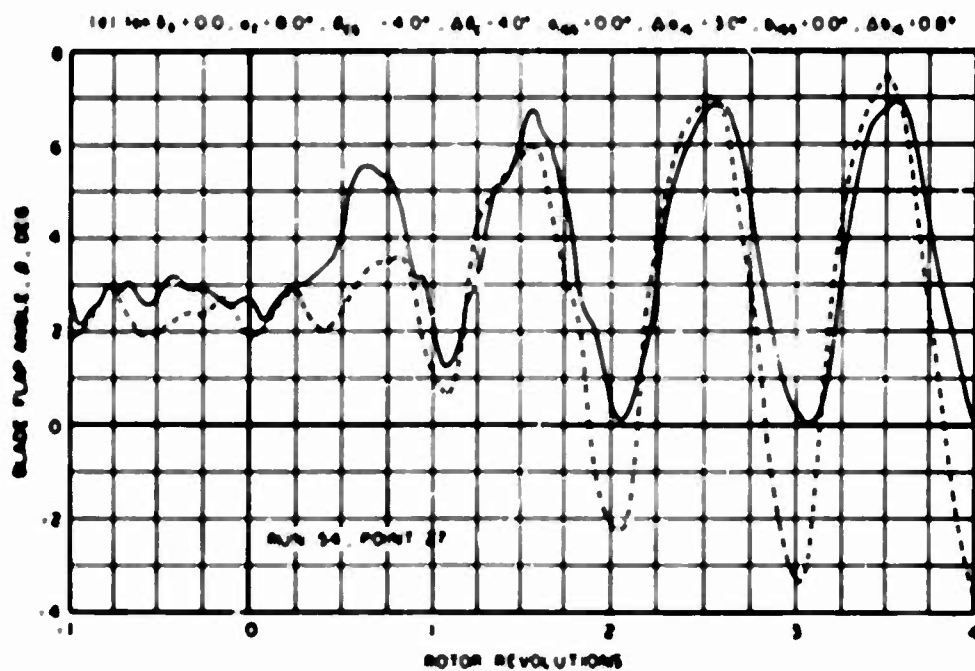
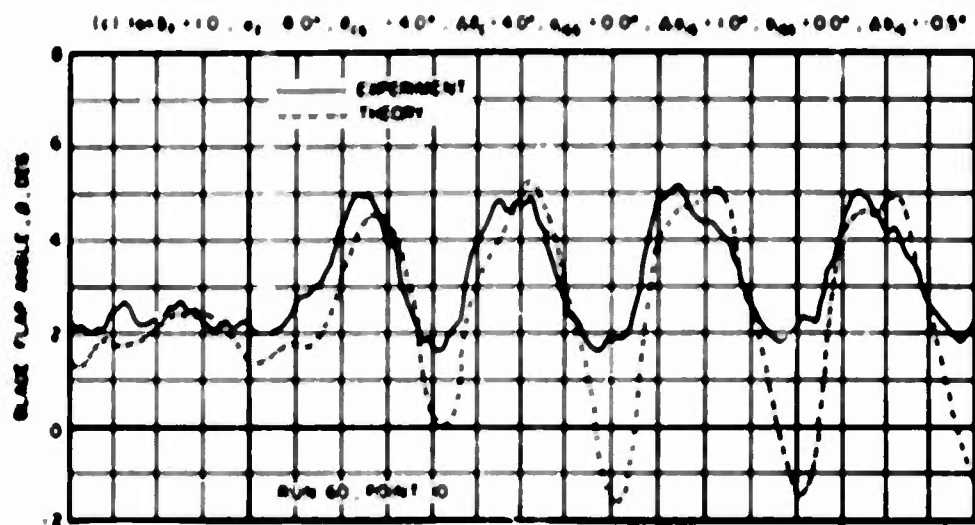


Figure 20. Concluded.

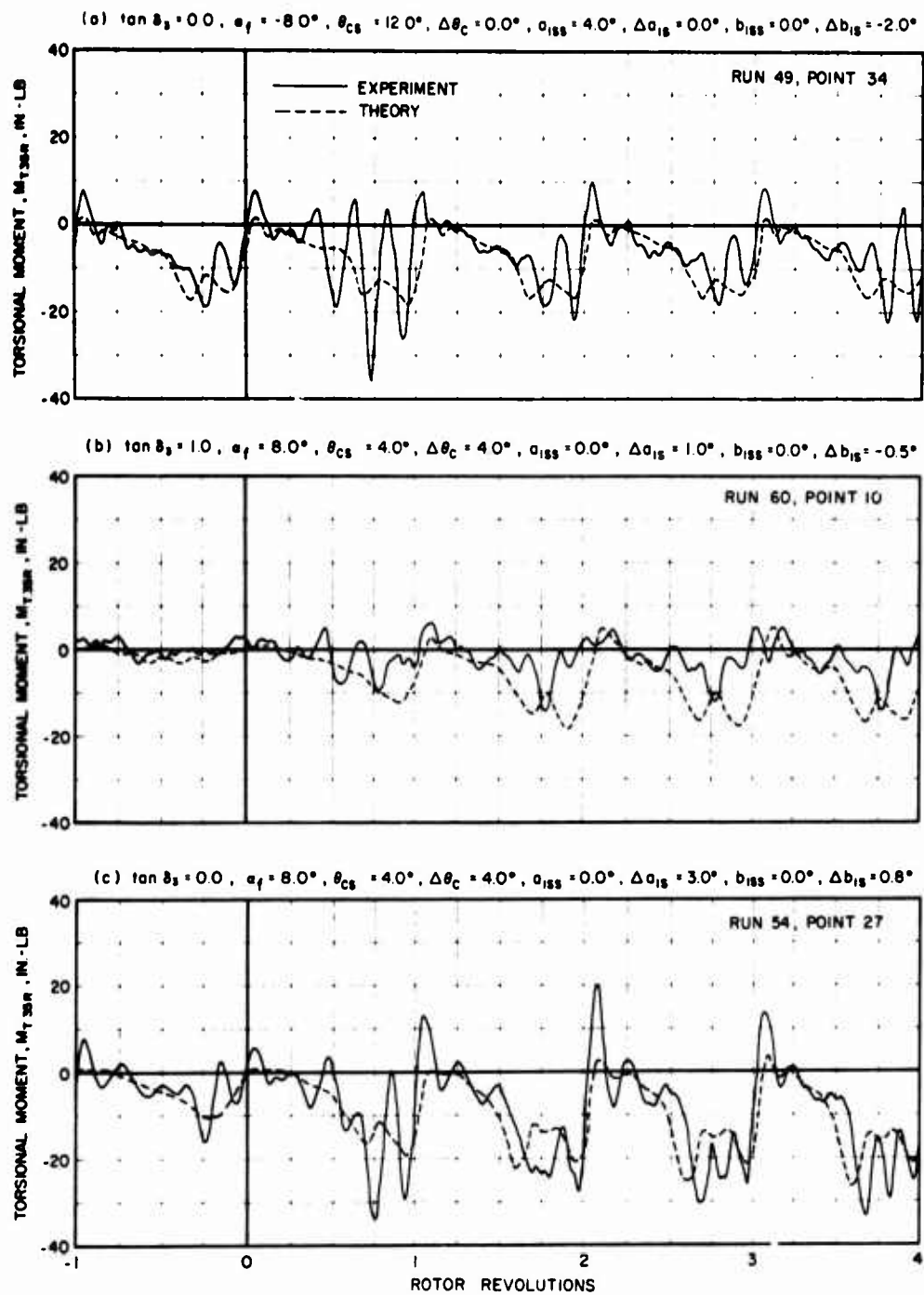


Figure 21. Experimental and Theoretical Blade Torsional Moment During Transient Conditions; $V_s = 120$ kn, $\mu = 0.29$, $Y_{CG}/c = 0.25$.

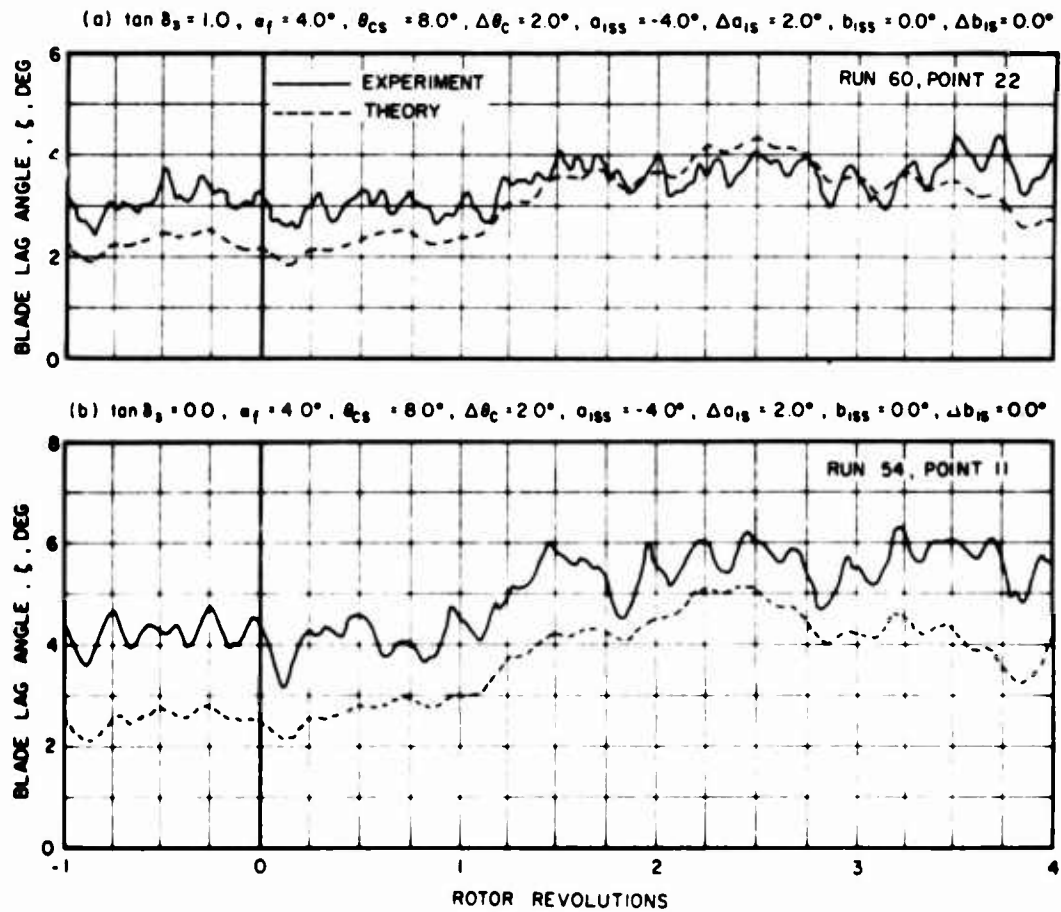


Figure 22. Experimental and Theoretical Blade Lag Angle During Transient Conditions; $V_s = 200$ kn, $\mu = 0.50$, $Y_{CG}/c = 0.25$.

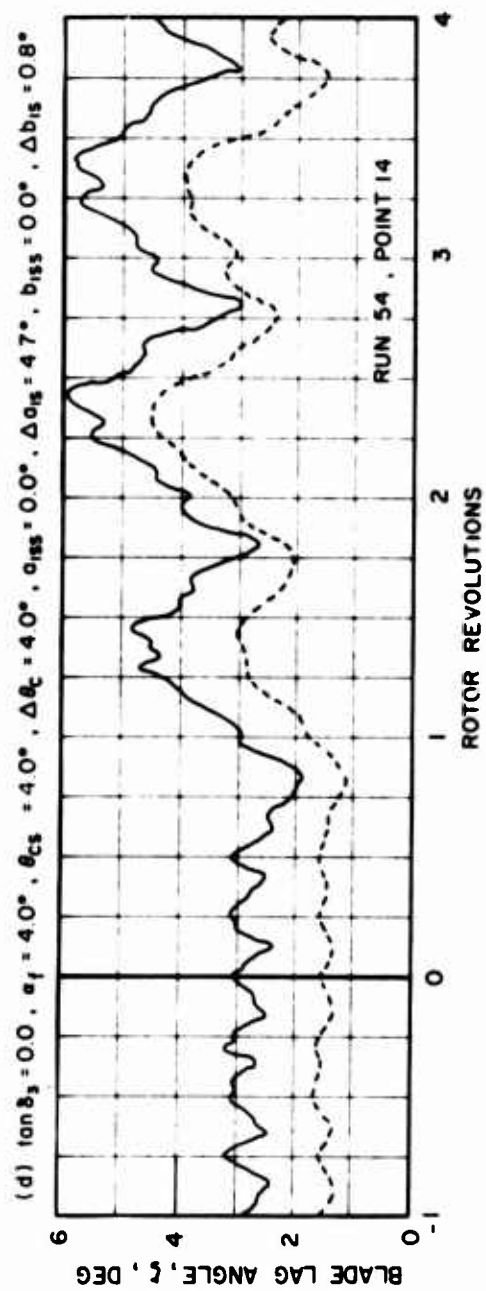
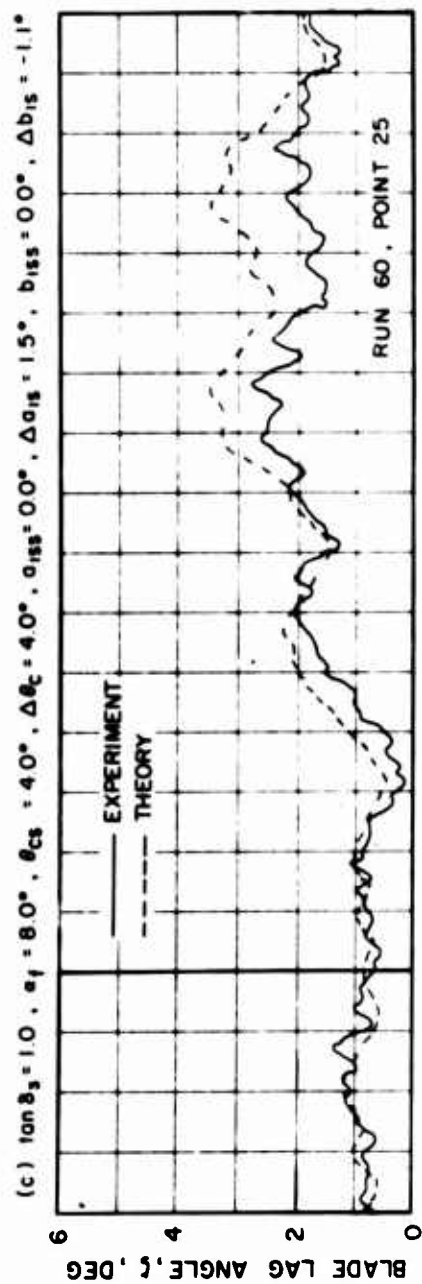


Figure 22. Concluded.

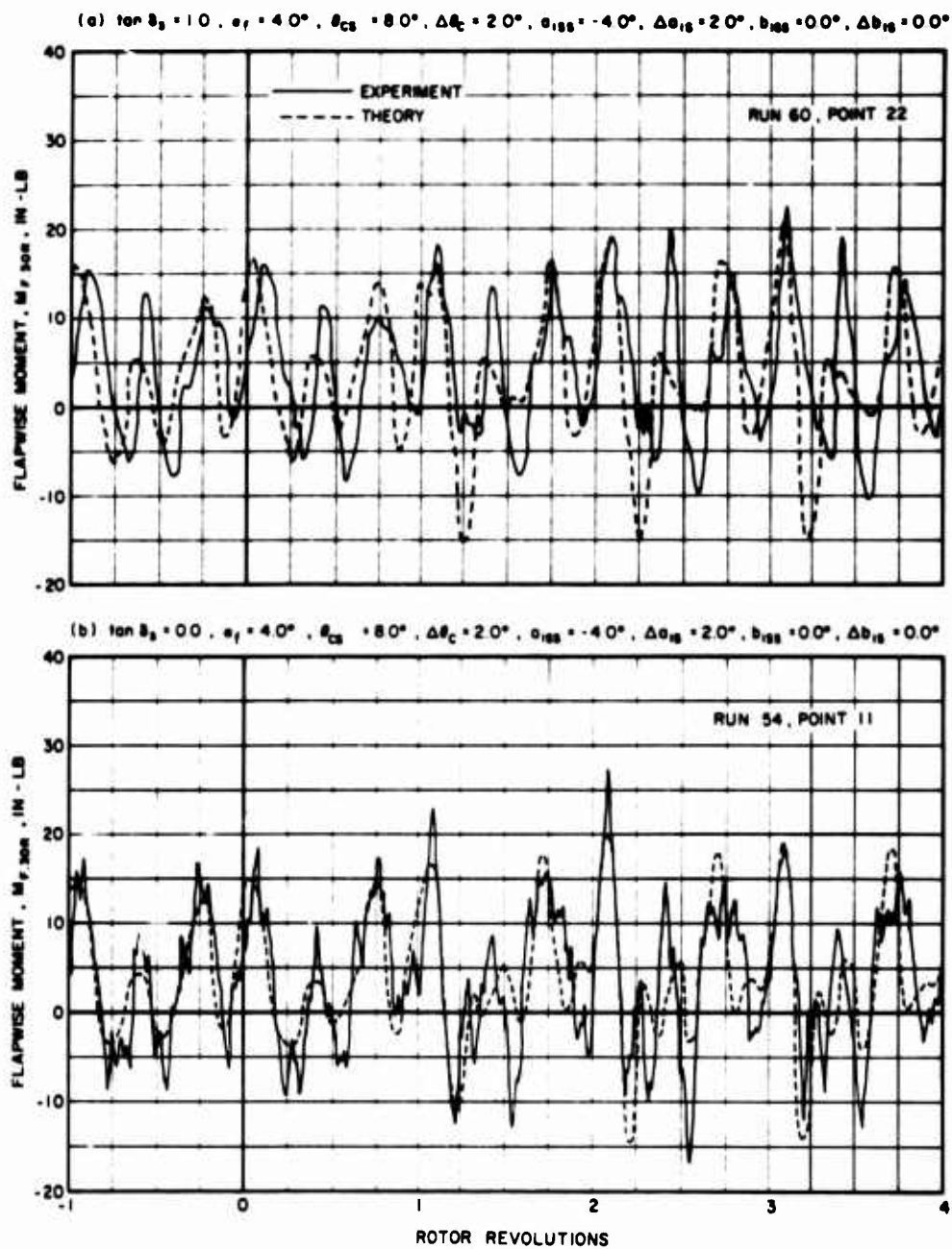


Figure 23. Experimental and Theoretical Blade Flapwise Bending Moments During Transient Conditions; $V_s = 200$ kn, $\mu = 0.50$, $Y_{CG}/c = 0.25$.

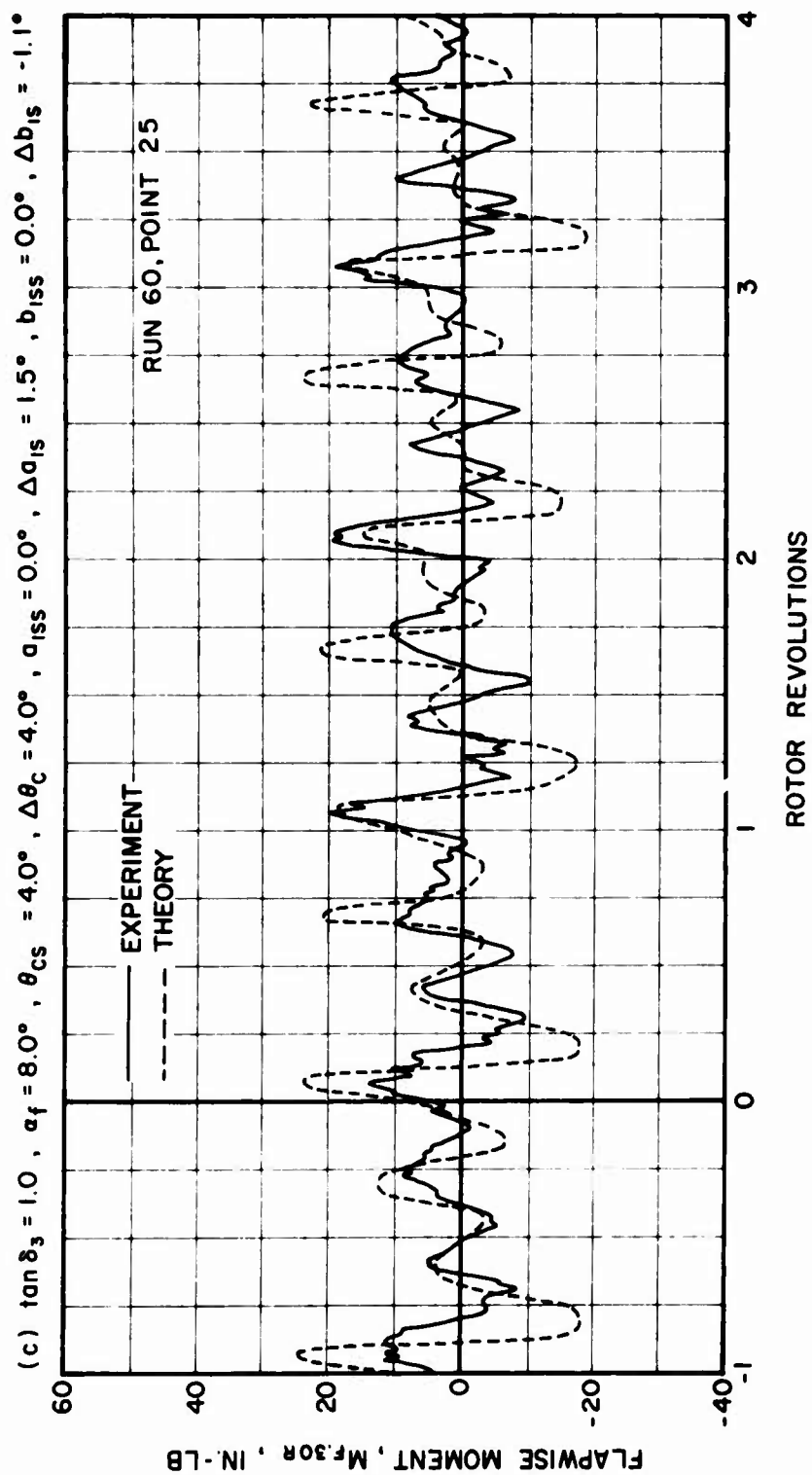


Figure 23. Continued.

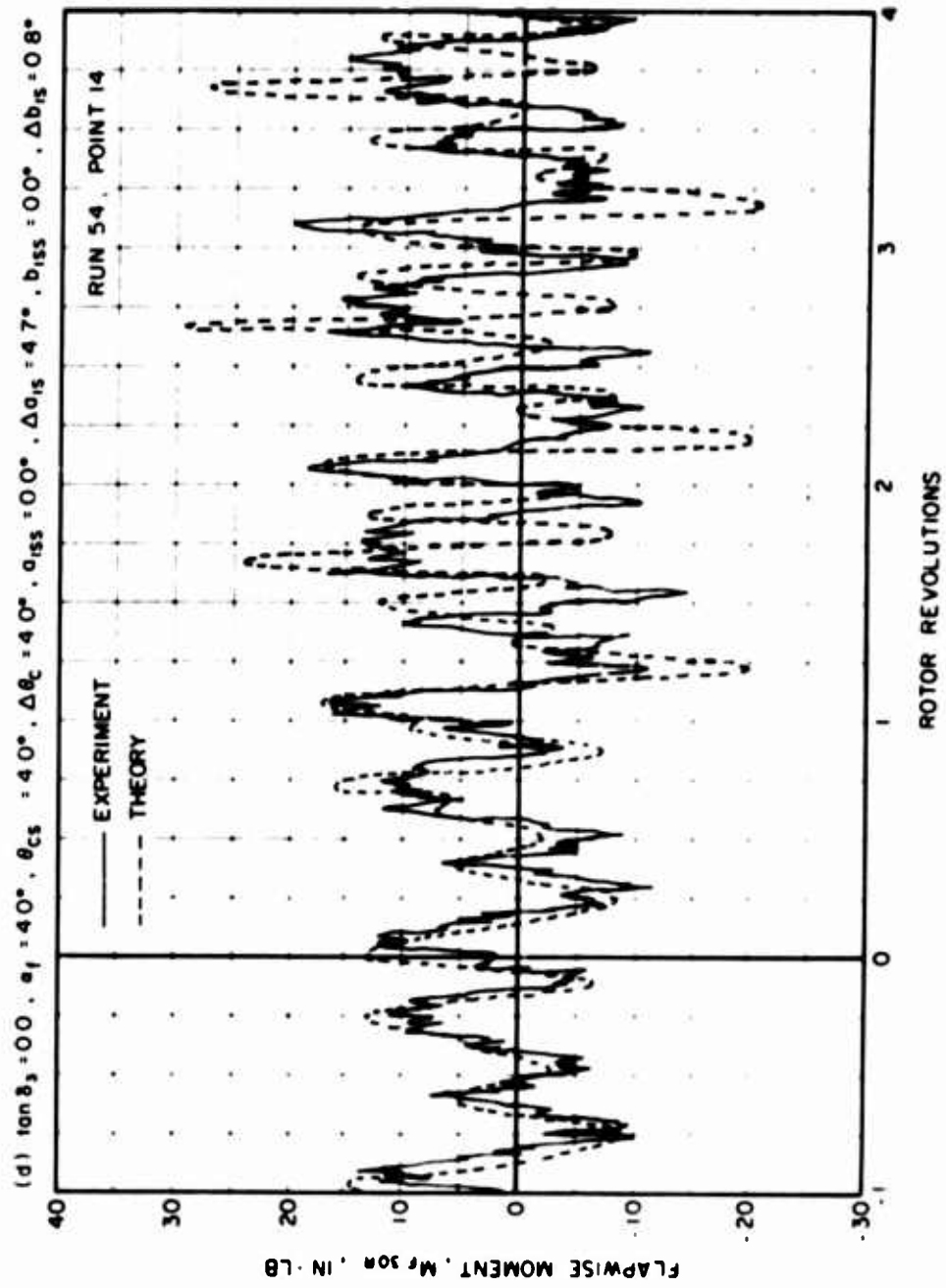


Figure 23. Continued.

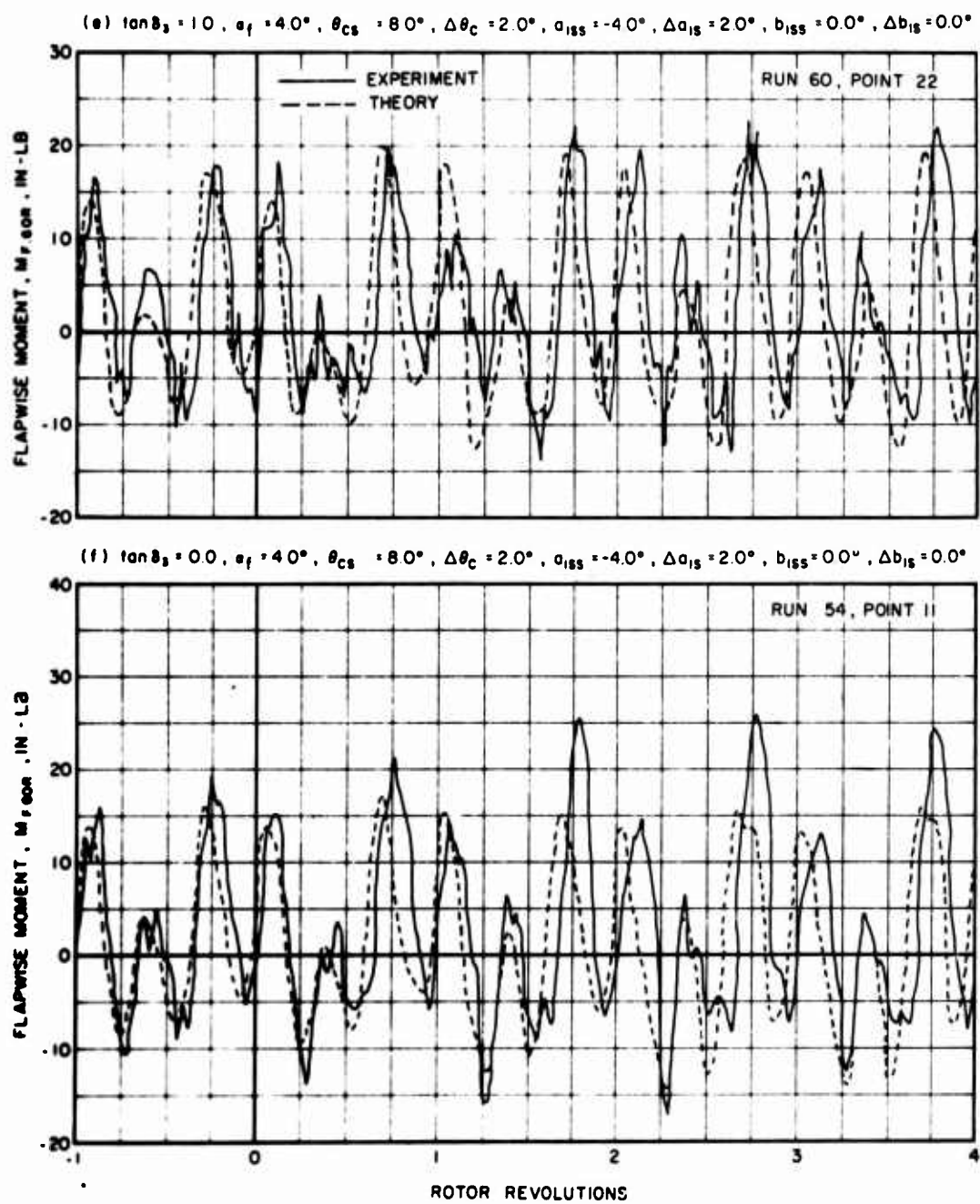


Figure 23. Continued.

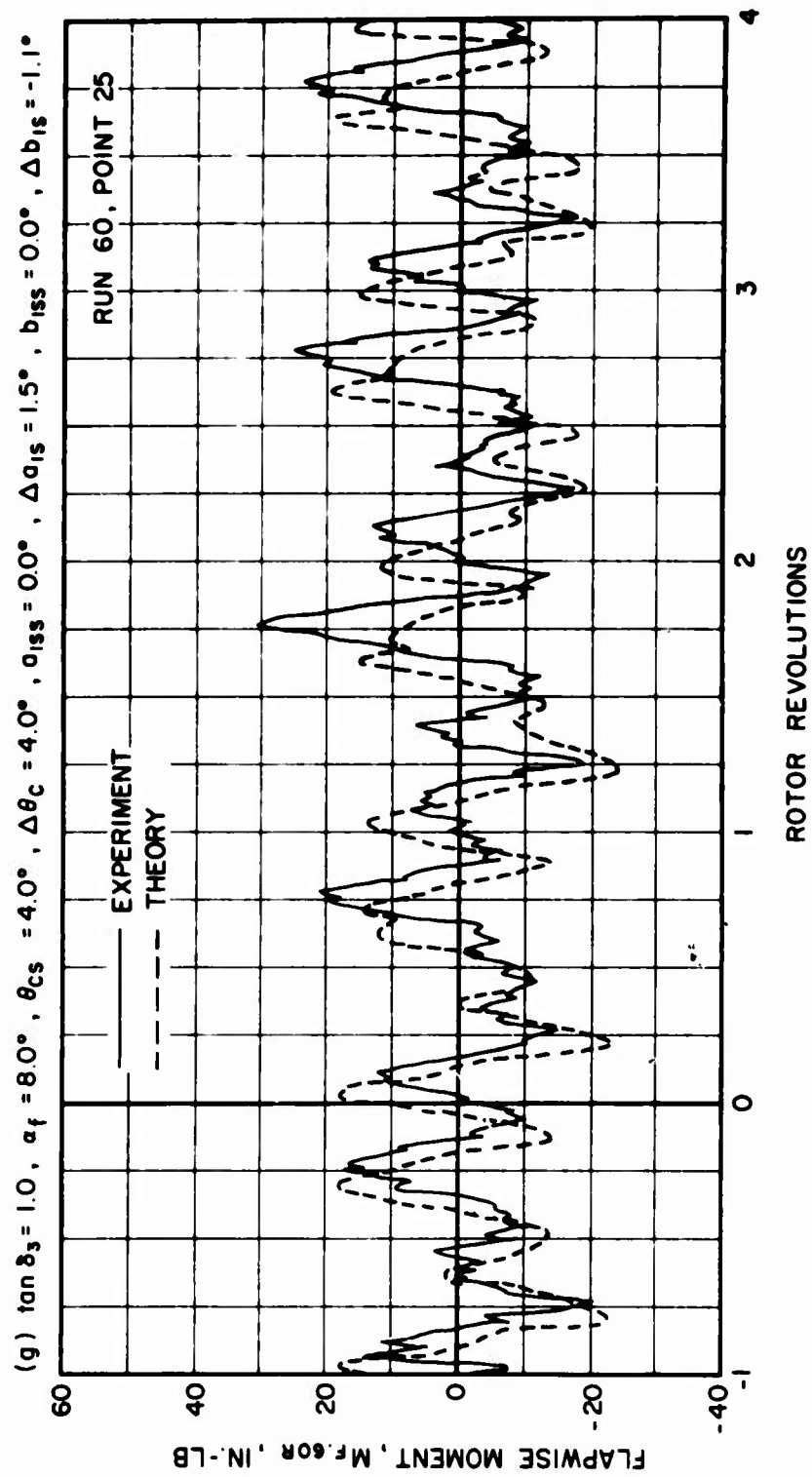


Figure 23. Continued.

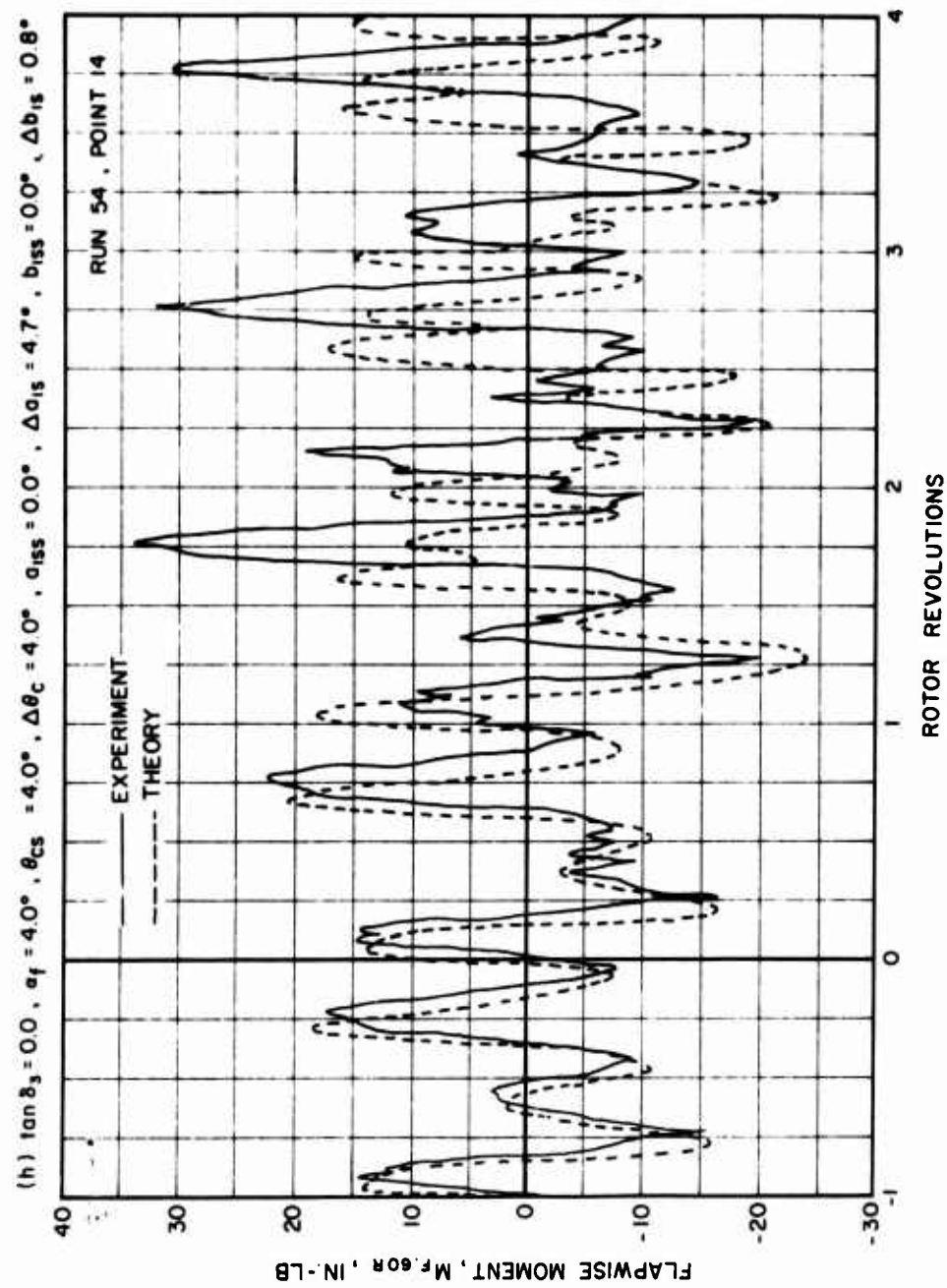


Figure 23. Concluded.

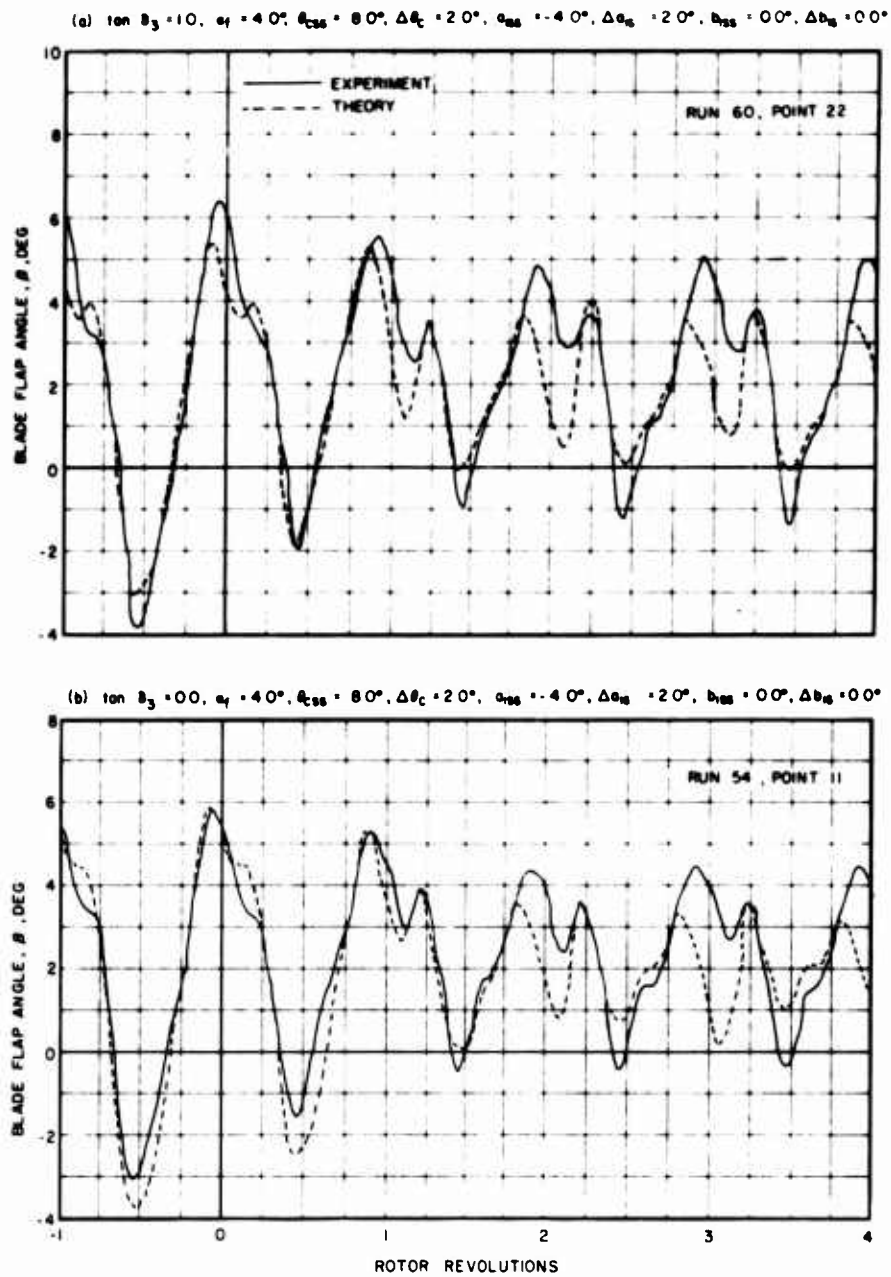


Figure 24. Experimental and Theoretical Blade Flap Angle During Transient Conditions; $V_s = 200$ kn, $\mu = 0.50$, $Y_{CG}/c = 0.25$.

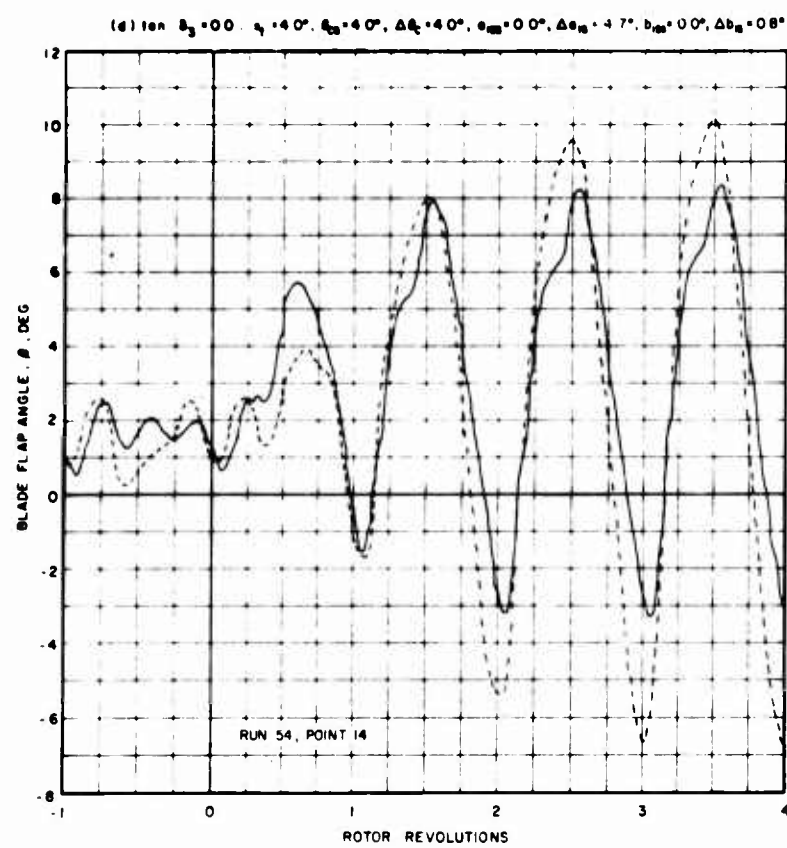
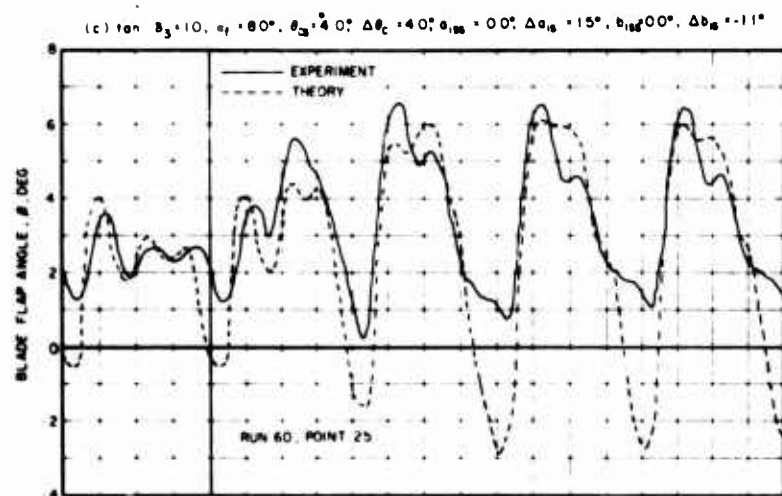


Figure 24. Concluded.

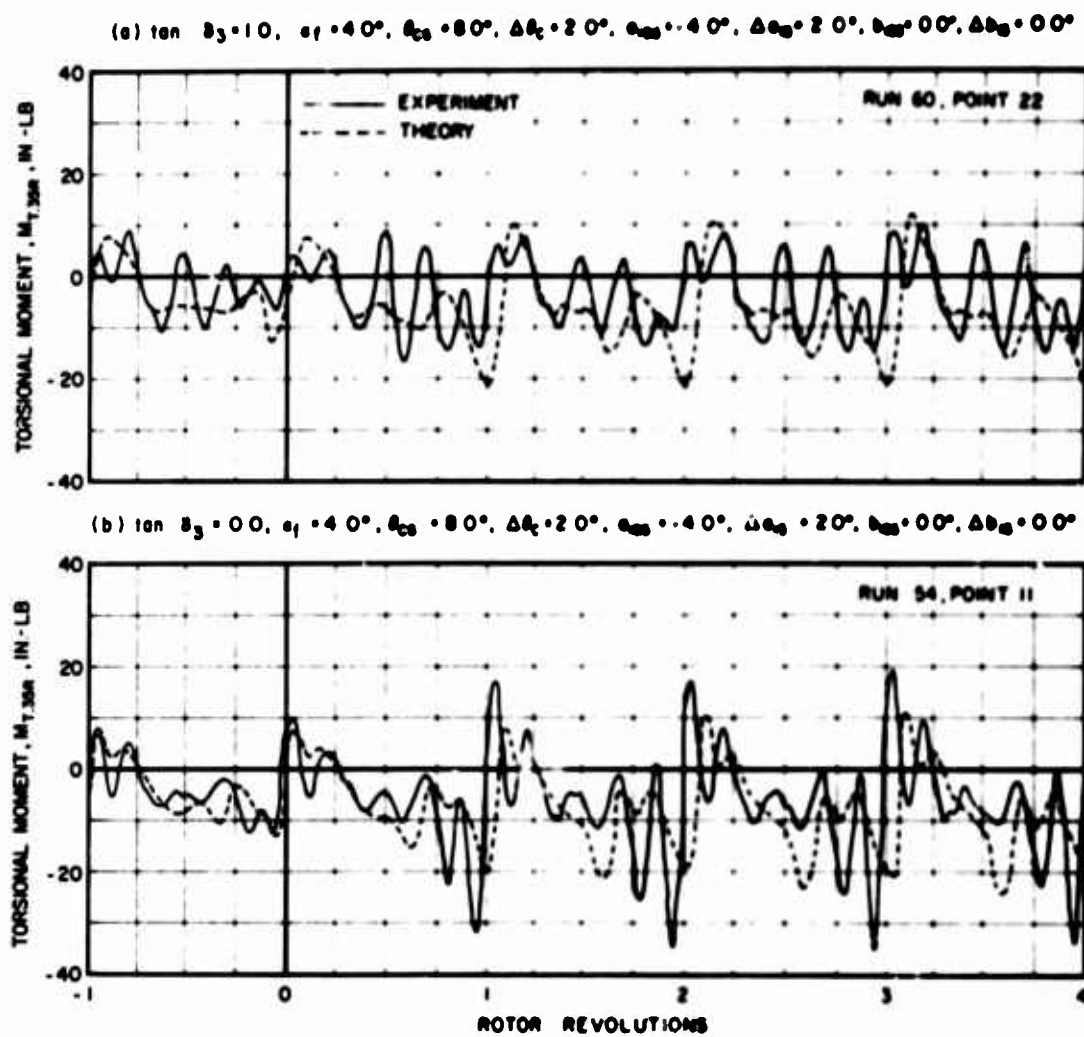


Figure 25. Experimental and Theoretical Blade Torsional Moment During Transient Conditions; $V_B = 200$ kn, $u = 0.50$, $Y_{CG}/c = 0.25$.

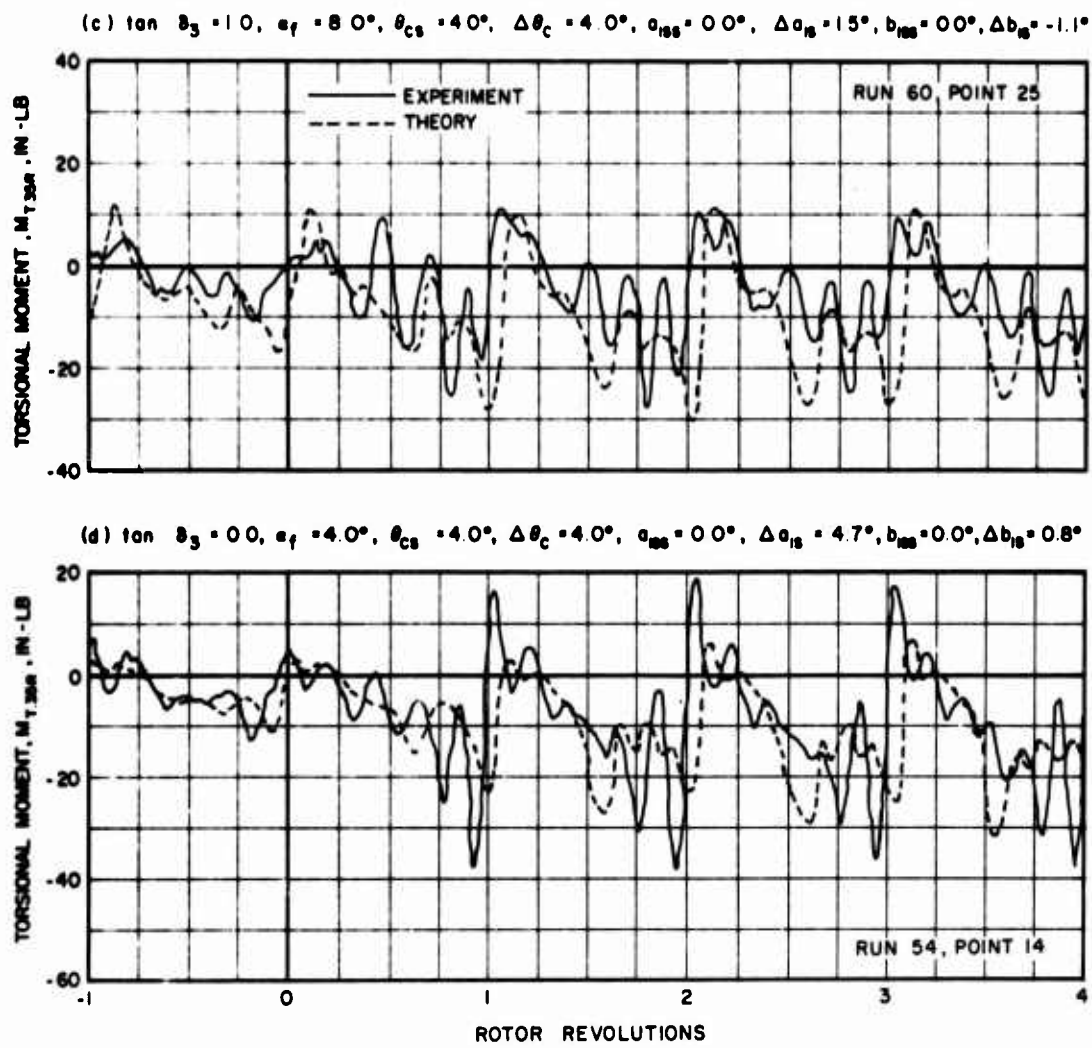


Figure 25. Concluded.

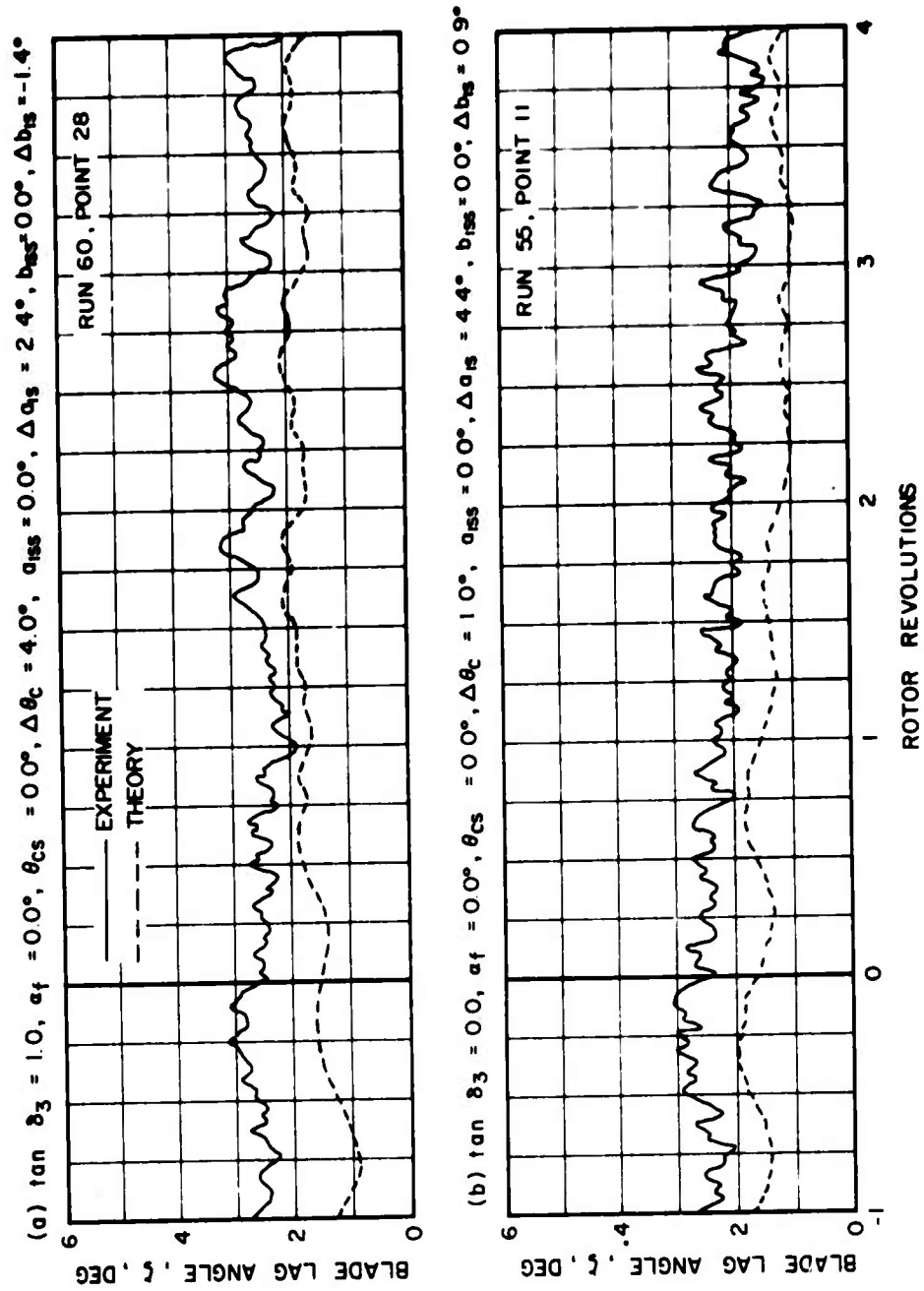


Figure 26. Experimental and Theoretical Blade Lag Angle During Transient Conditions; $V_s = 300$ kn, $\nu = 1.03$, $Y_{GG}/c = 0.25$.

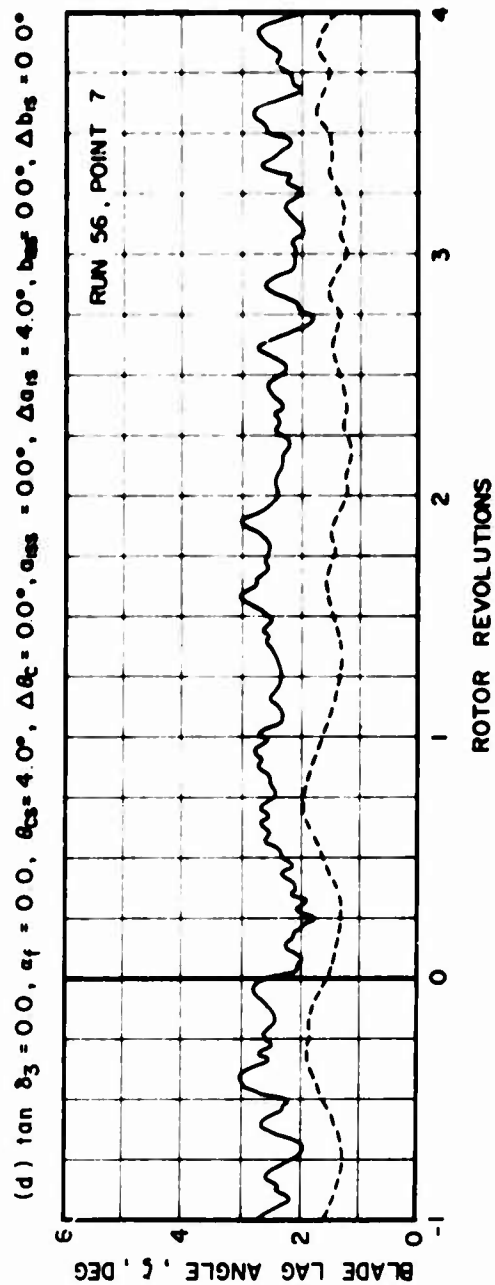
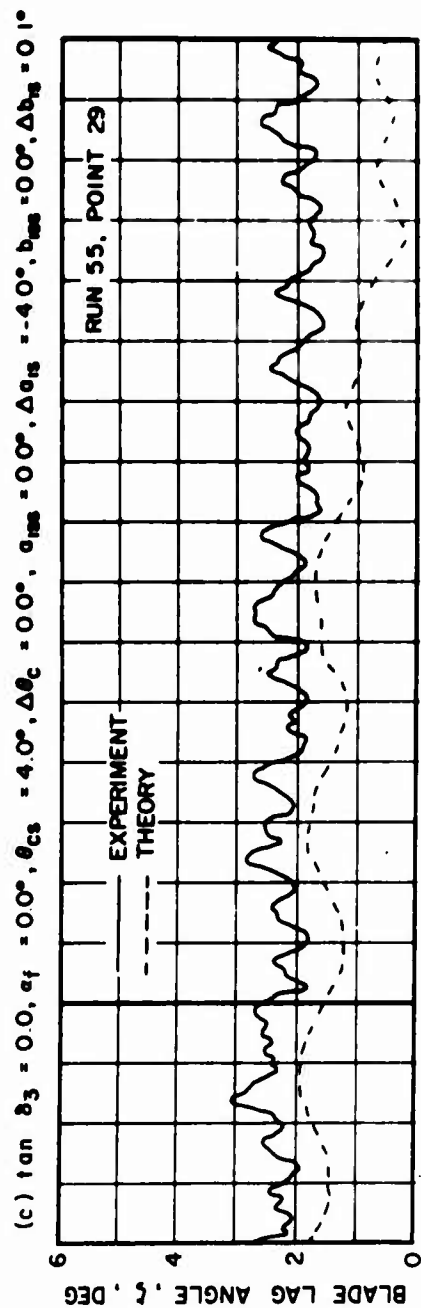


Figure 26. Concluded.

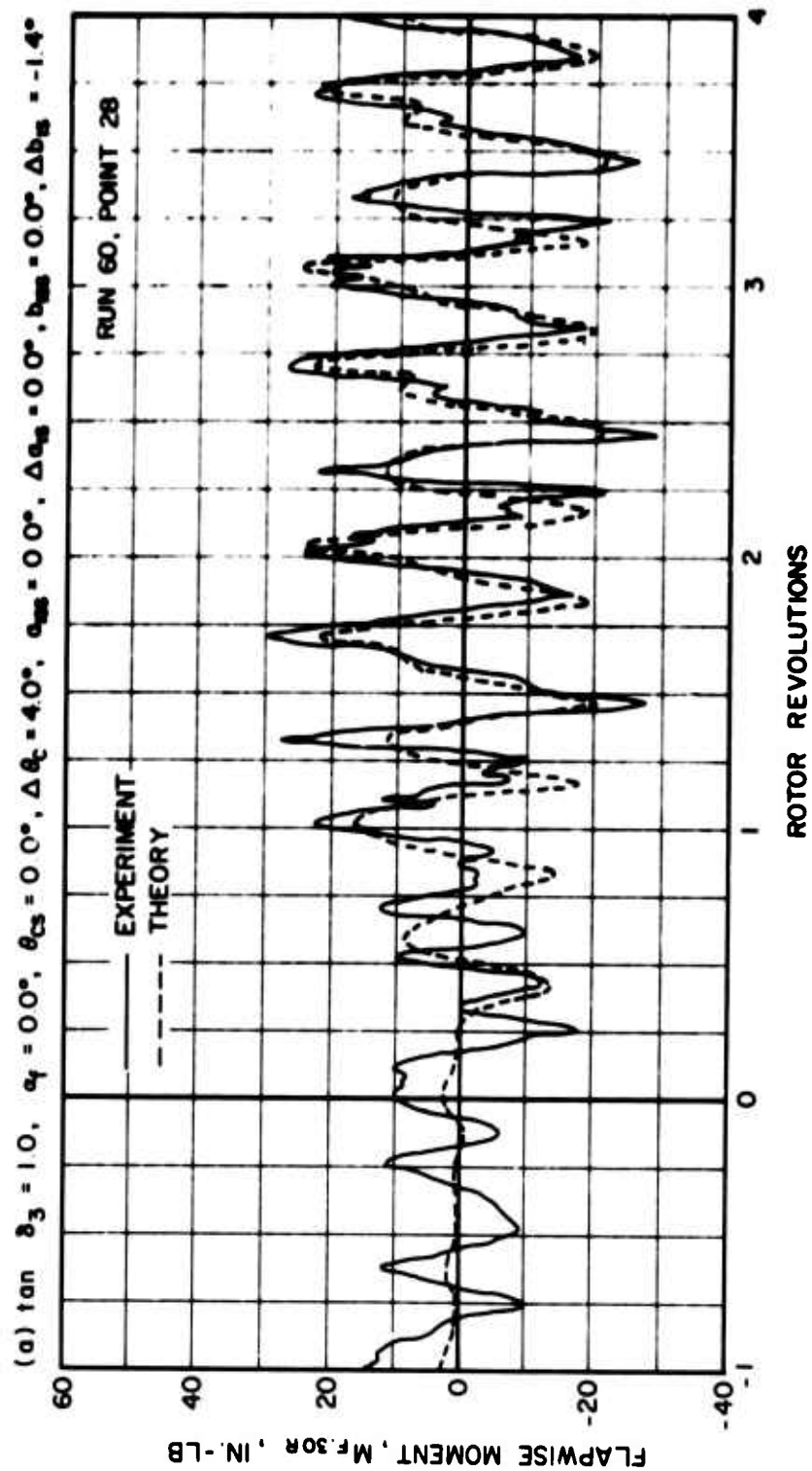


Figure 27. Experimental and Theoretical Blade Flapwise Bending Moments During Transient Conditions; $V_g = 300$ kn, $\mu = 1.03$, $Y_{CG}/c = 0.25$.

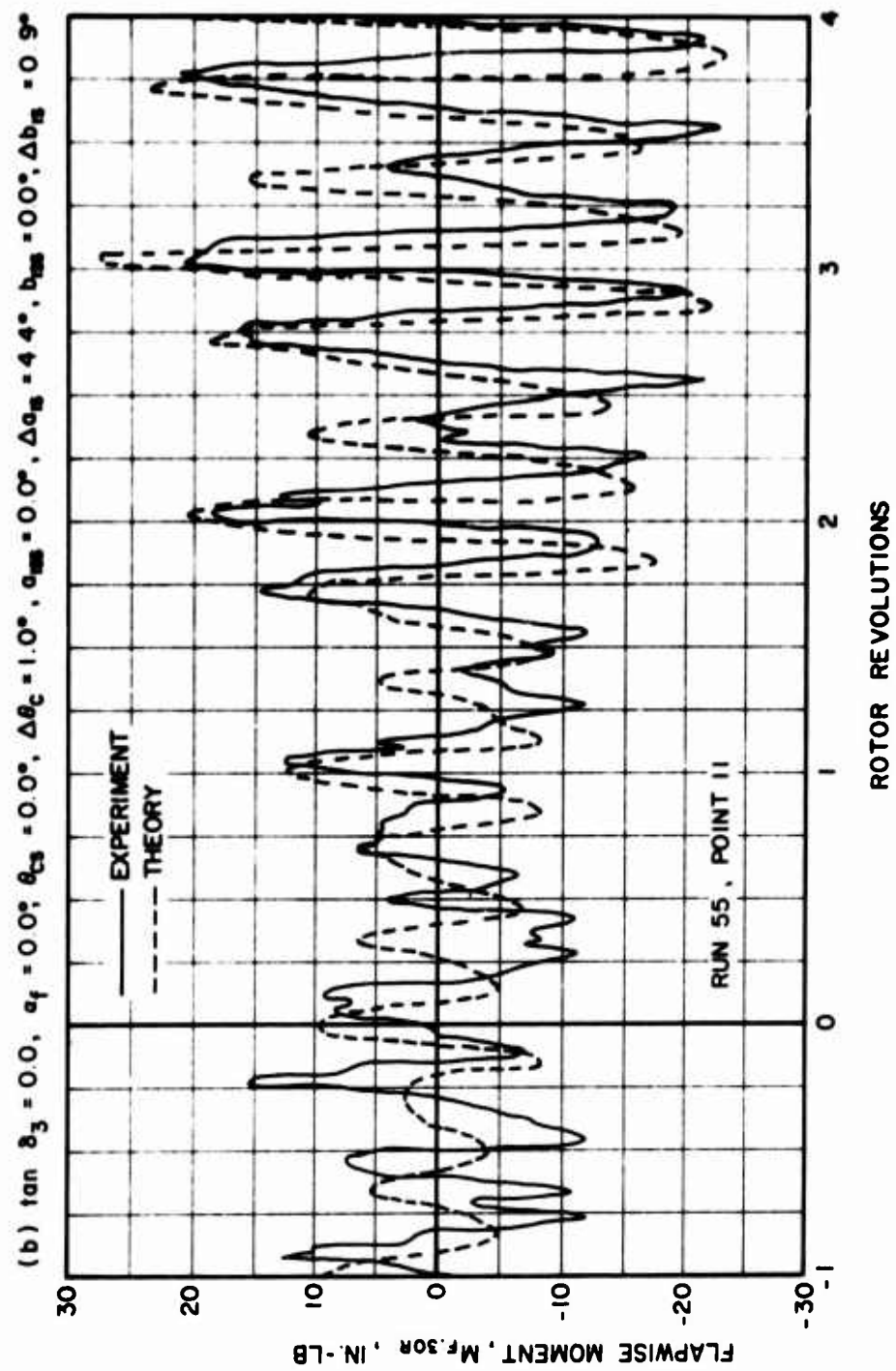


Figure 27. Continued.

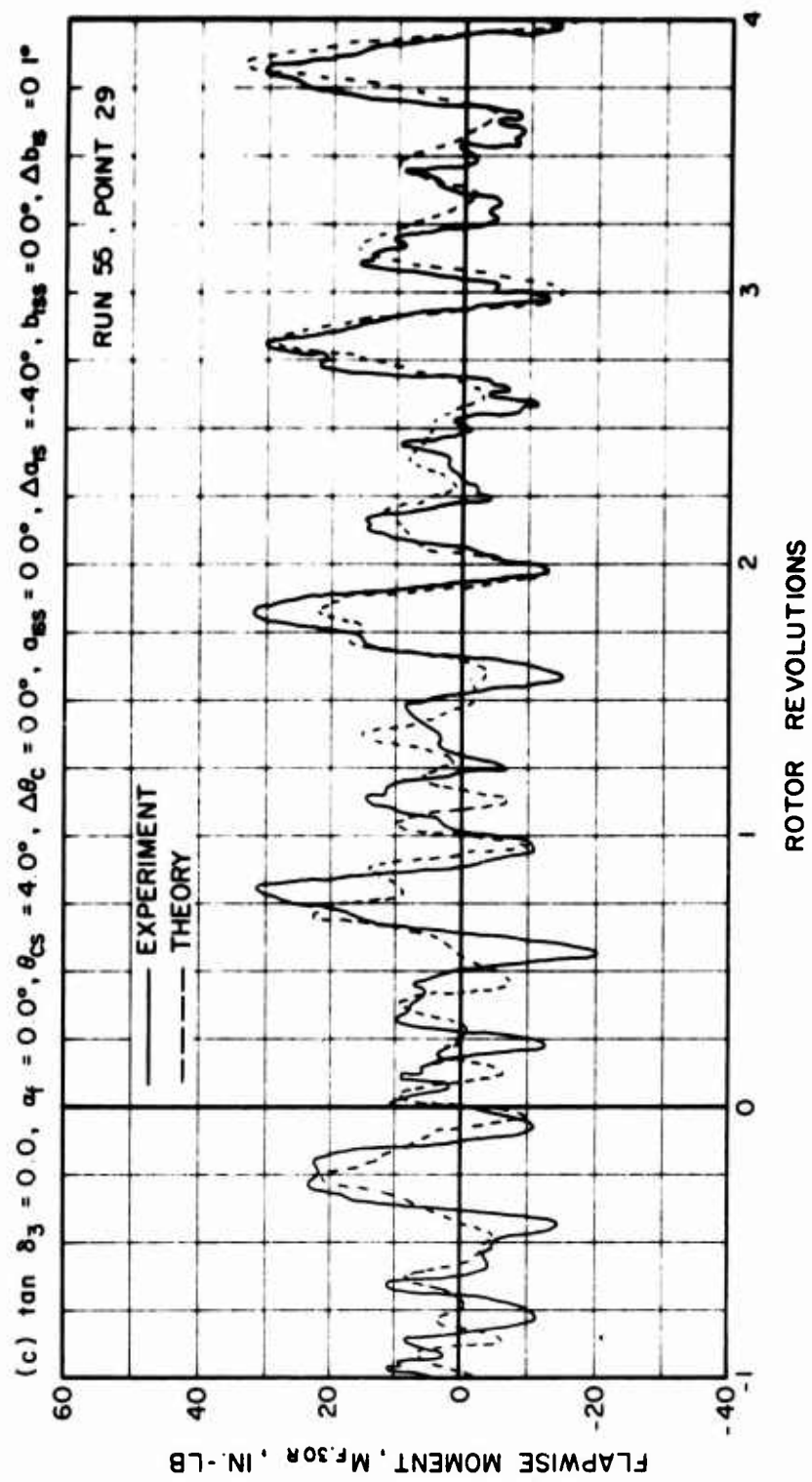


Figure 27. Continued.

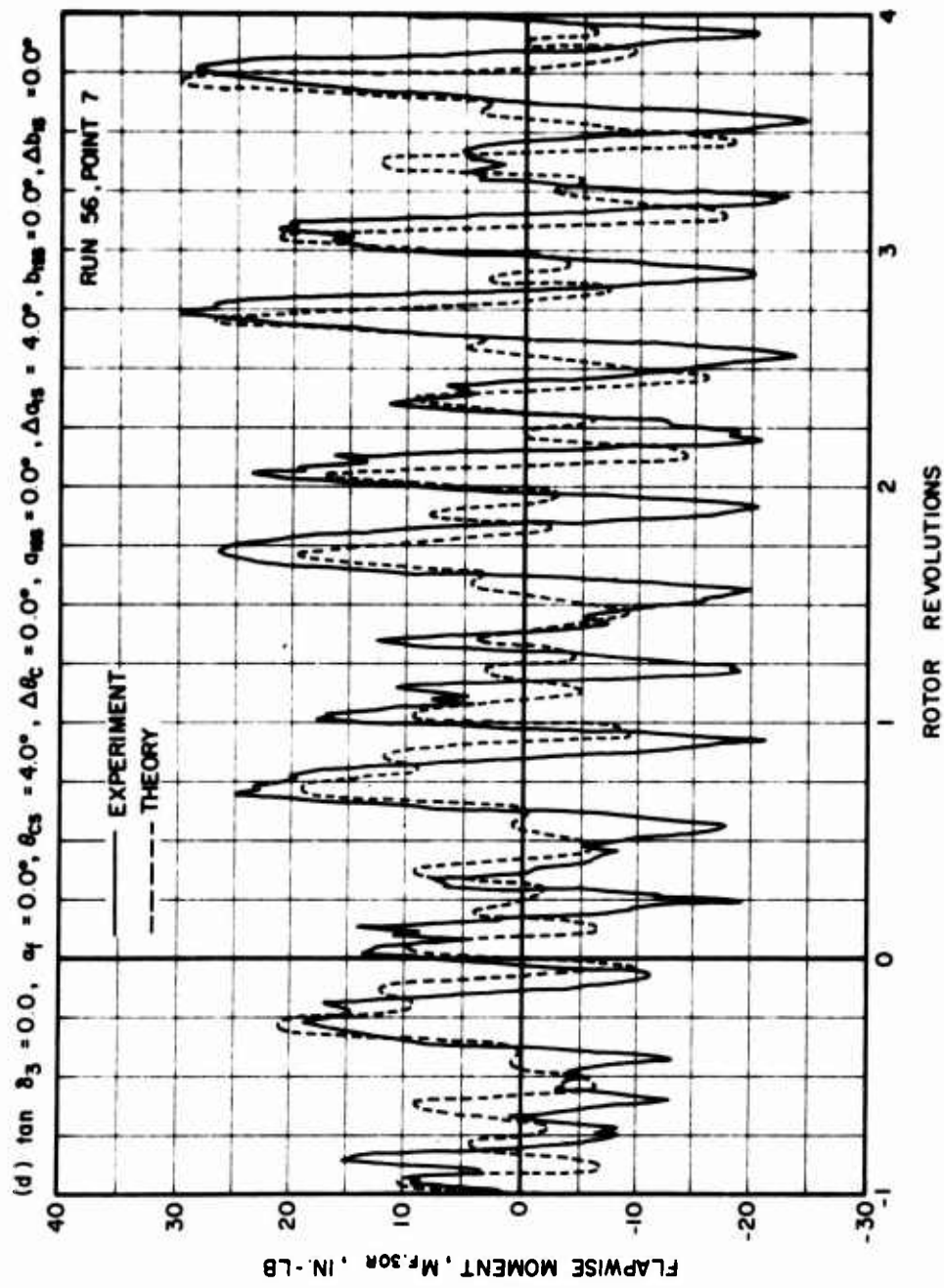


Figure 27. Continued.

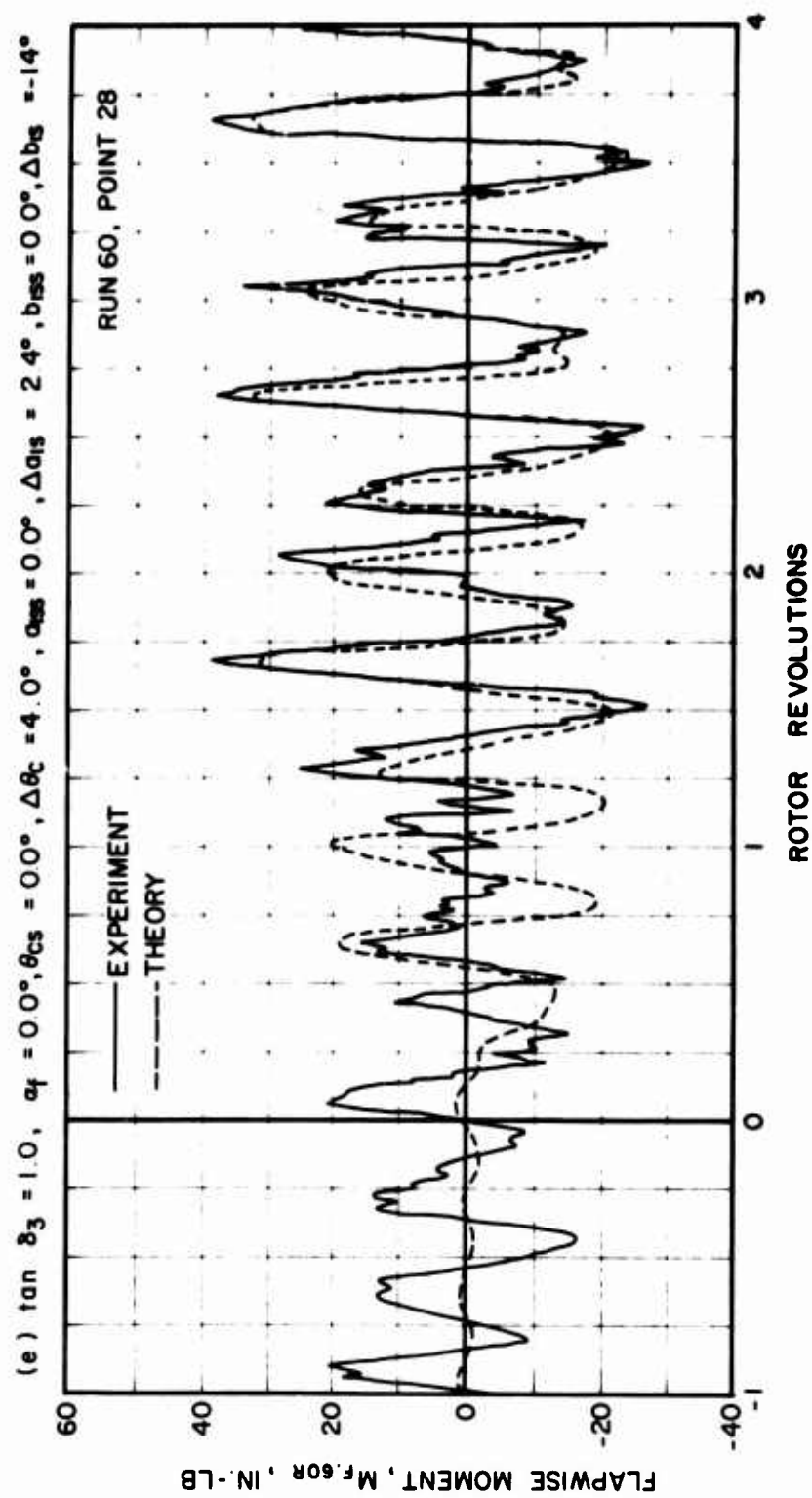


Figure 27. Continued.

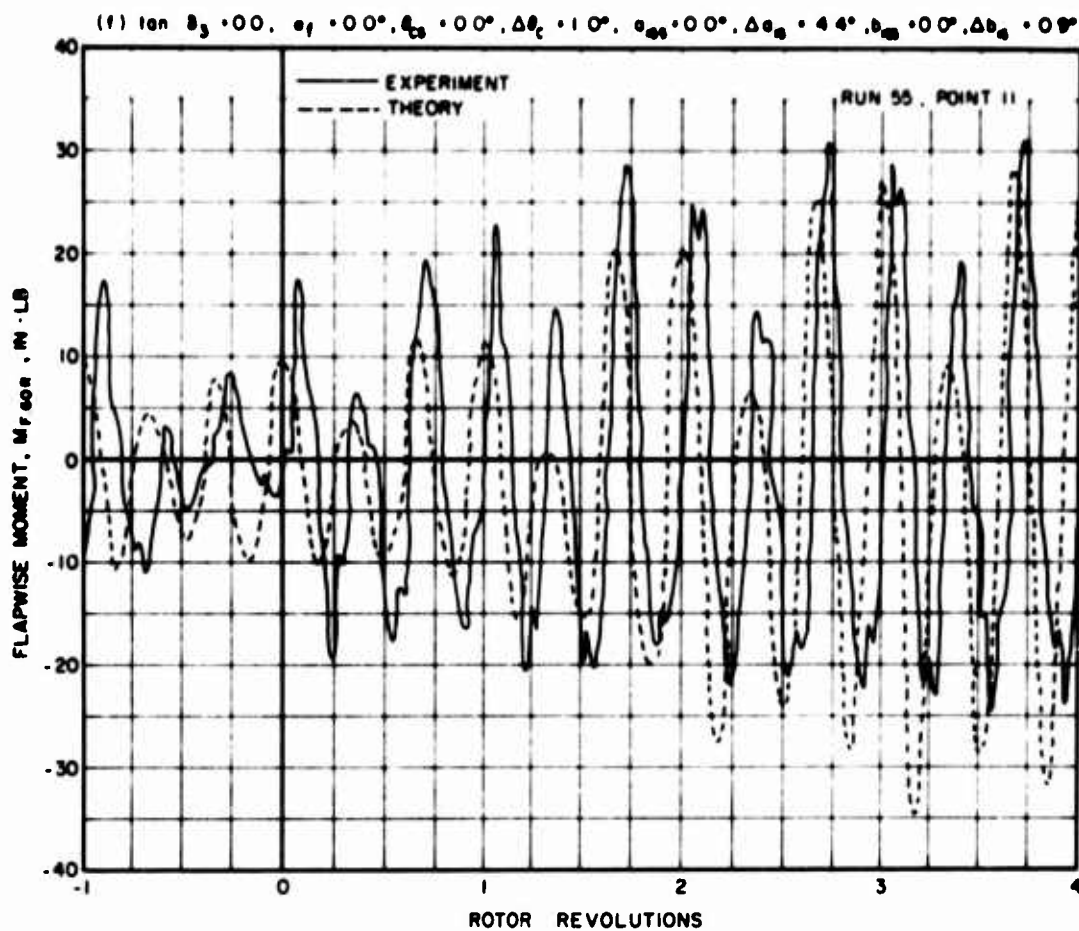


Figure 27. Continued.

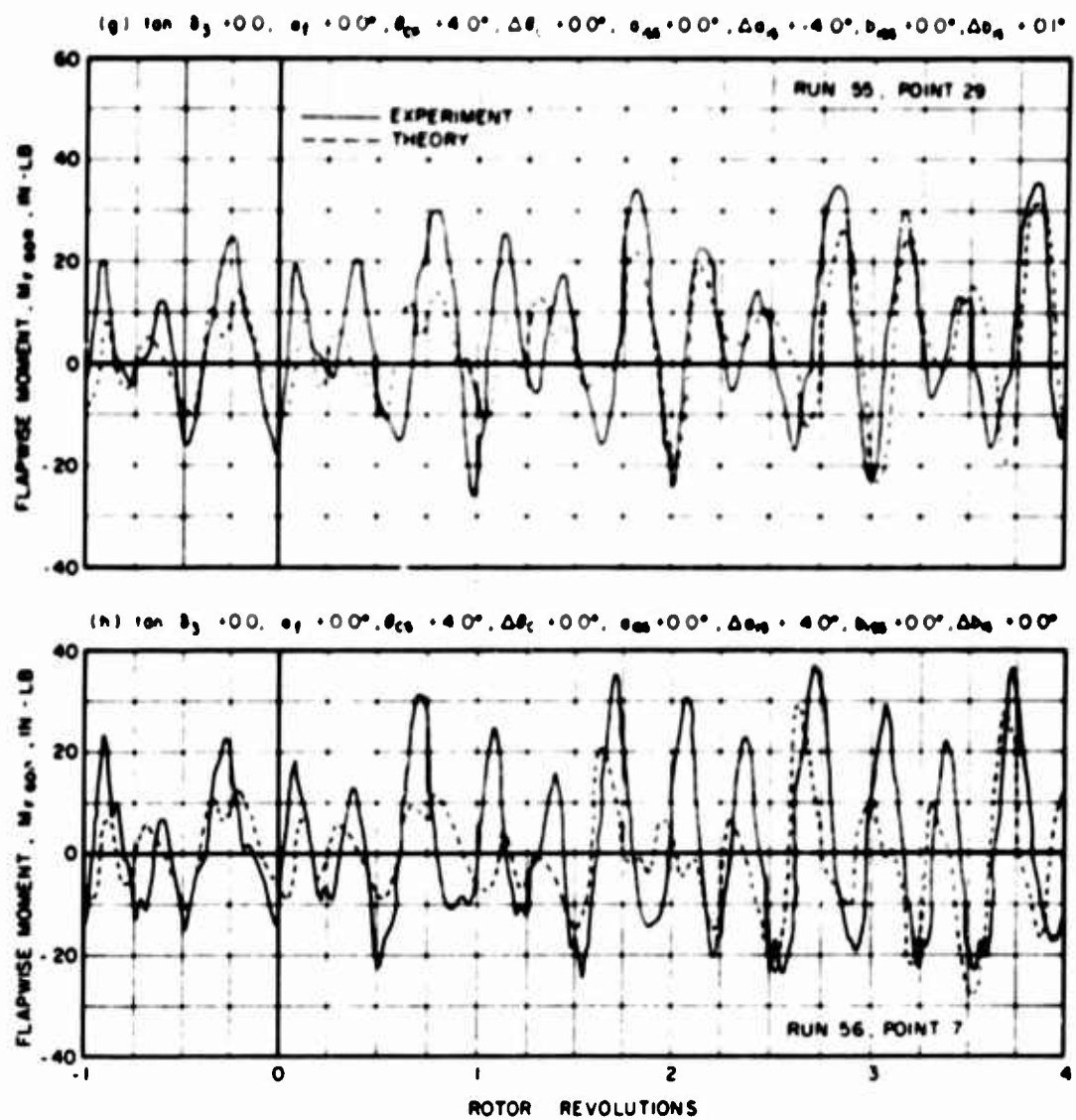


Figure 27. Concluded.

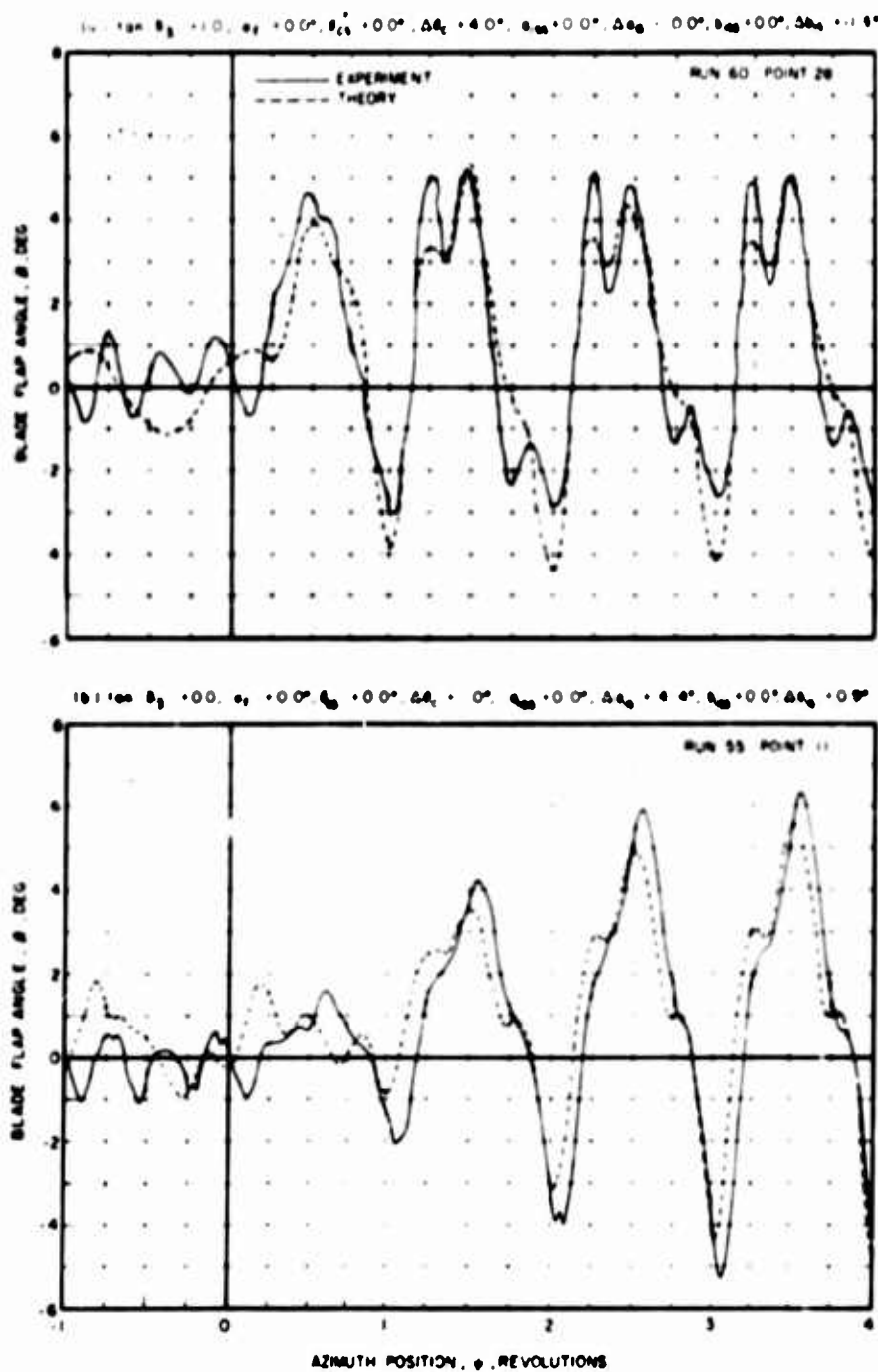


Figure 28. Experimental and Theoretical Blade Flap Angle During Transient Conditions; $V_S = 300$ kn, $\mu = 1.03$, $Y_{CG}/c = 0.25$.

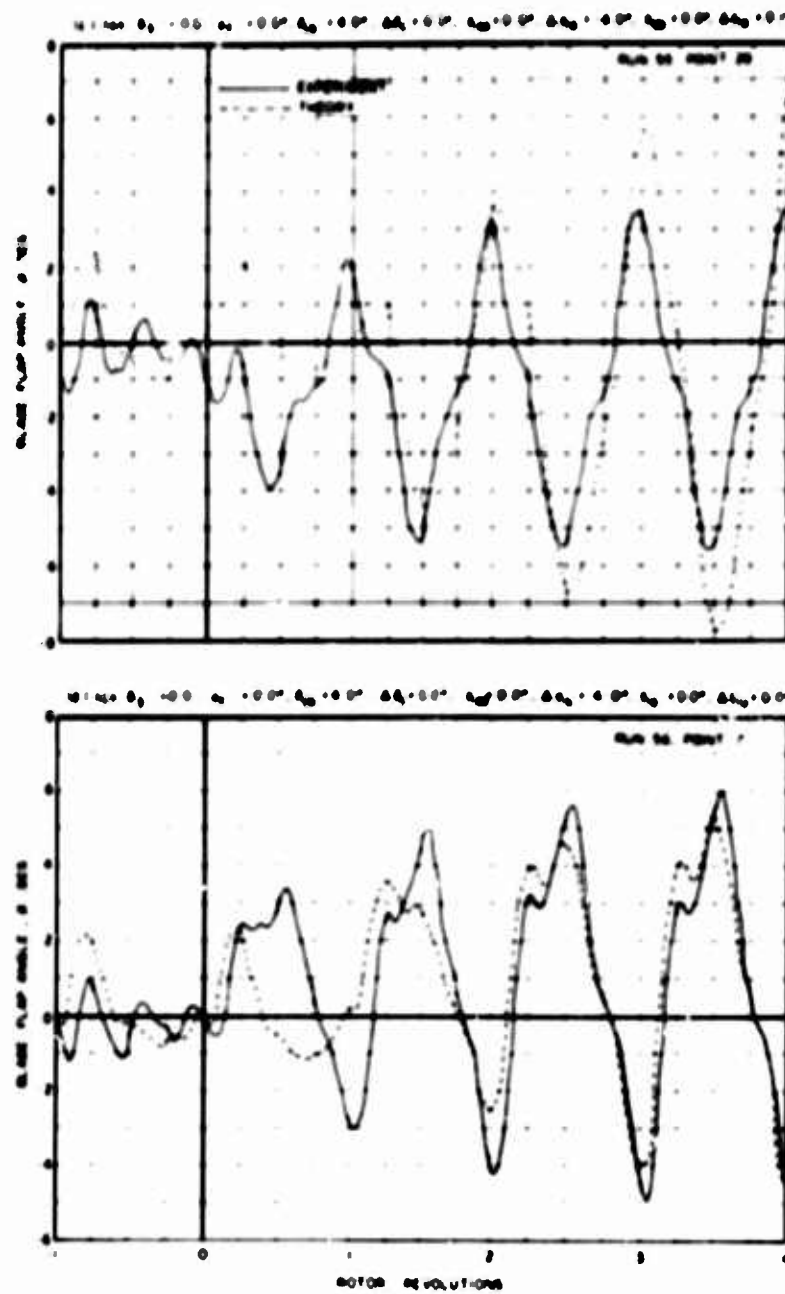


Figure 28. Concluded.

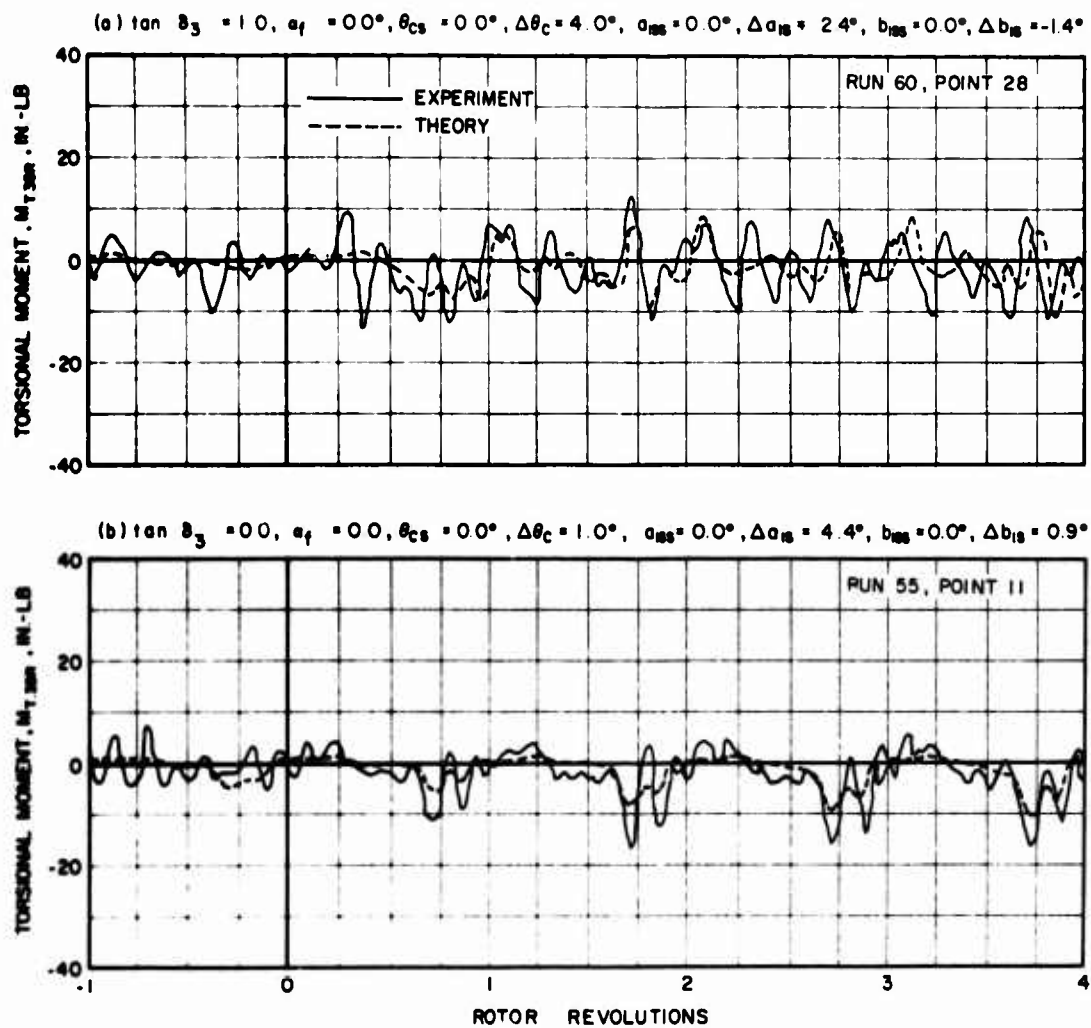


Figure 29. Experimental and Theoretical Blade Torsional Moment During Transient Conditions; $V_S = 300$ kn, $\mu = 1.03$, $Y_{CG}/c = 0.25$.

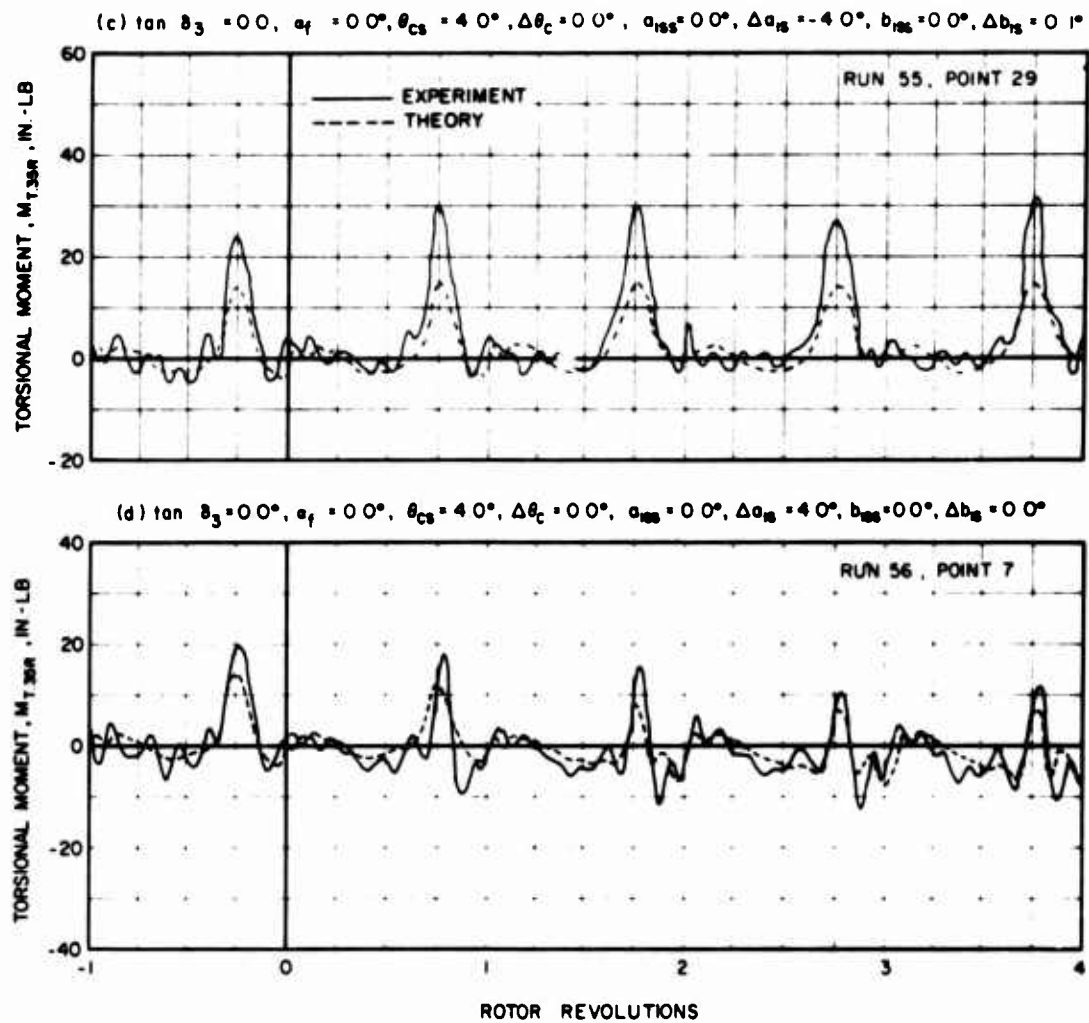


Figure 29. Concluded.

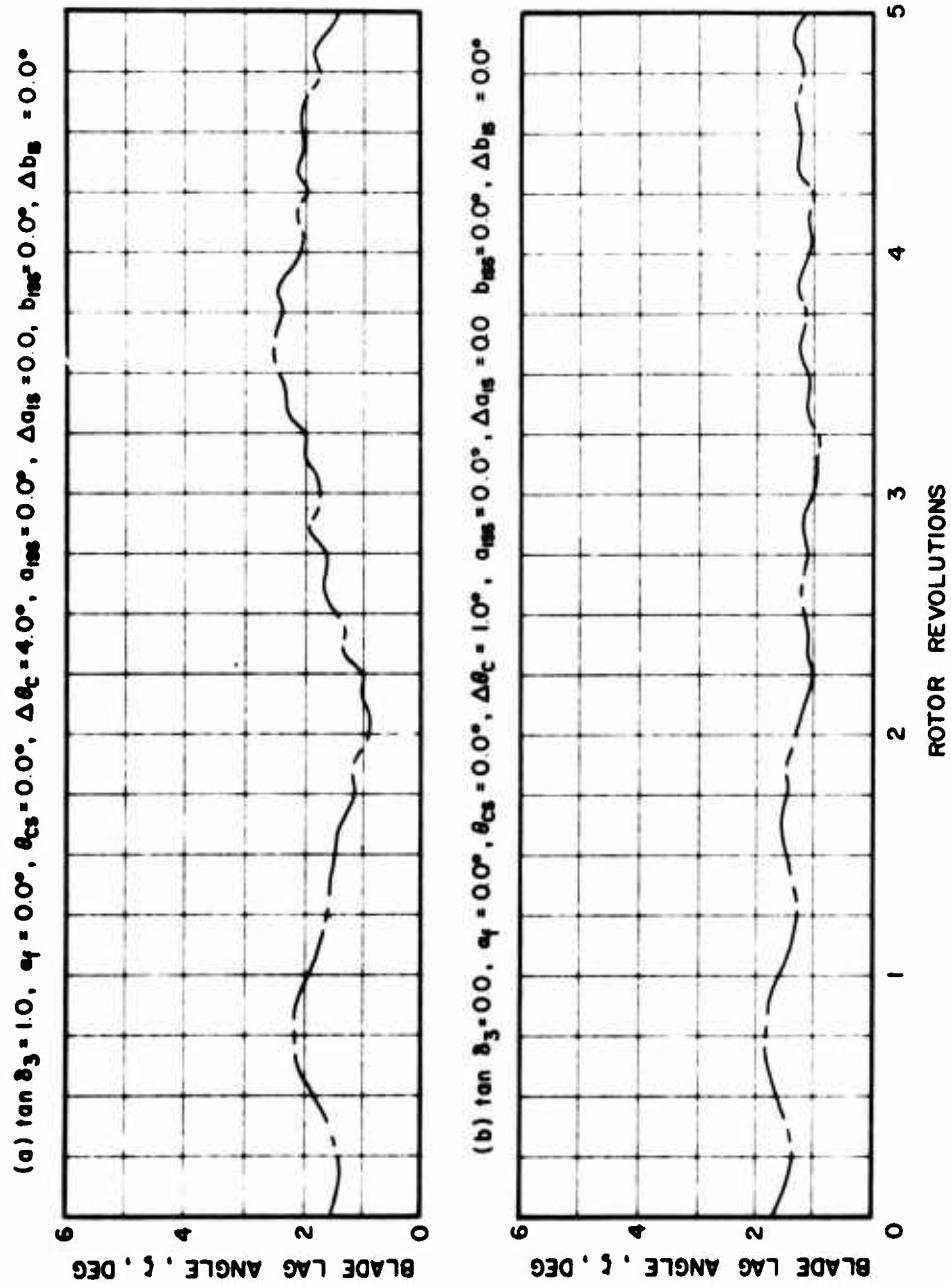


Figure 30. Theoretical Blade Lag Angle During Transient Conditions;
 $V_g = 300$ kn, $\mu = 1.03$, $Y_{CG}/c = 0.25$, Control Input
 Applied $3/4$ Revolution After Experimental Input.

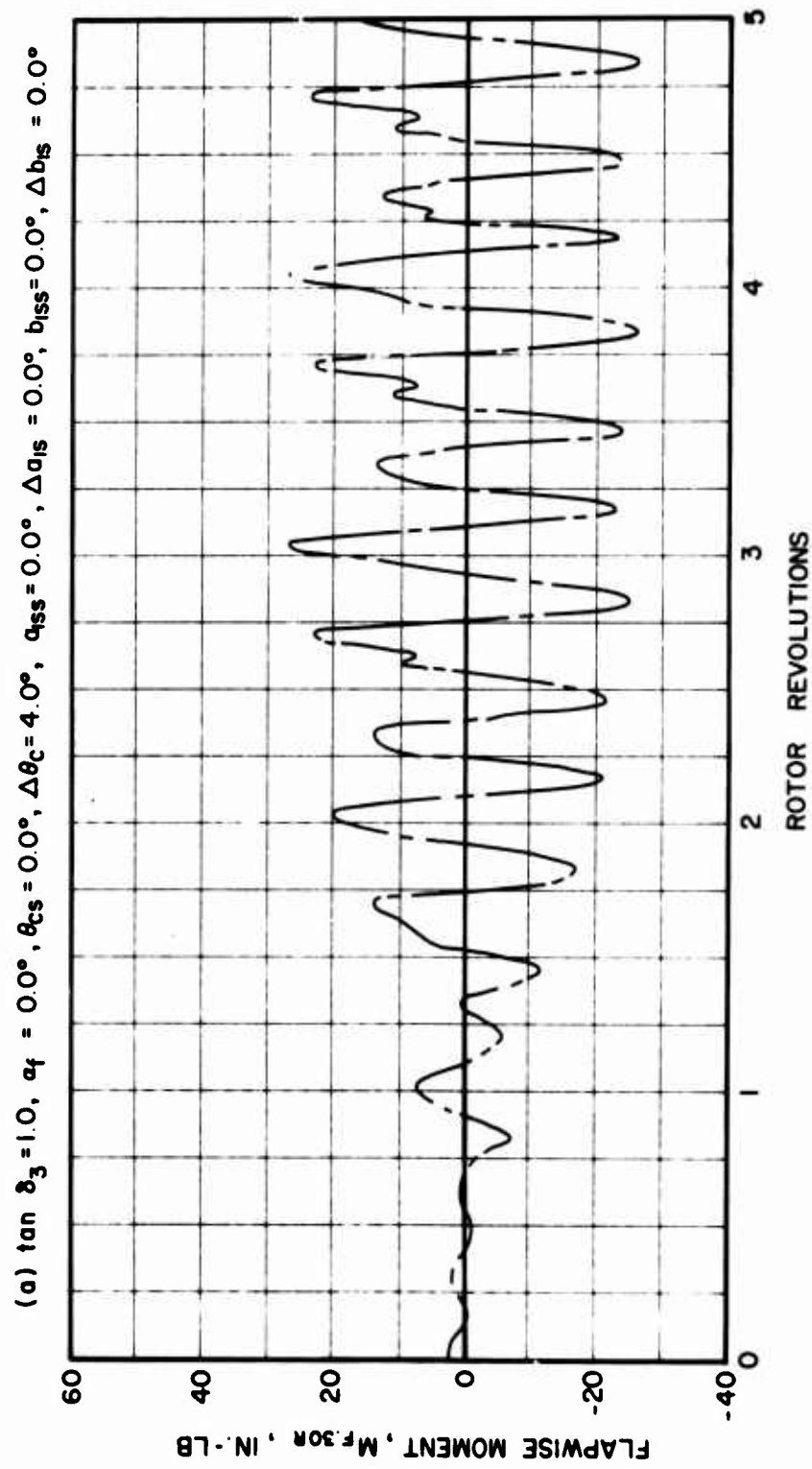


Figure 31. Theoretical Blade Flapwise Bending Moment During Transient Conditions; $V_s = 300$ kn, $\mu = 1.03$, $Y_{CG}/c = 0.25$, Control Input Applied 3/4 Revolution After Experimental Input.

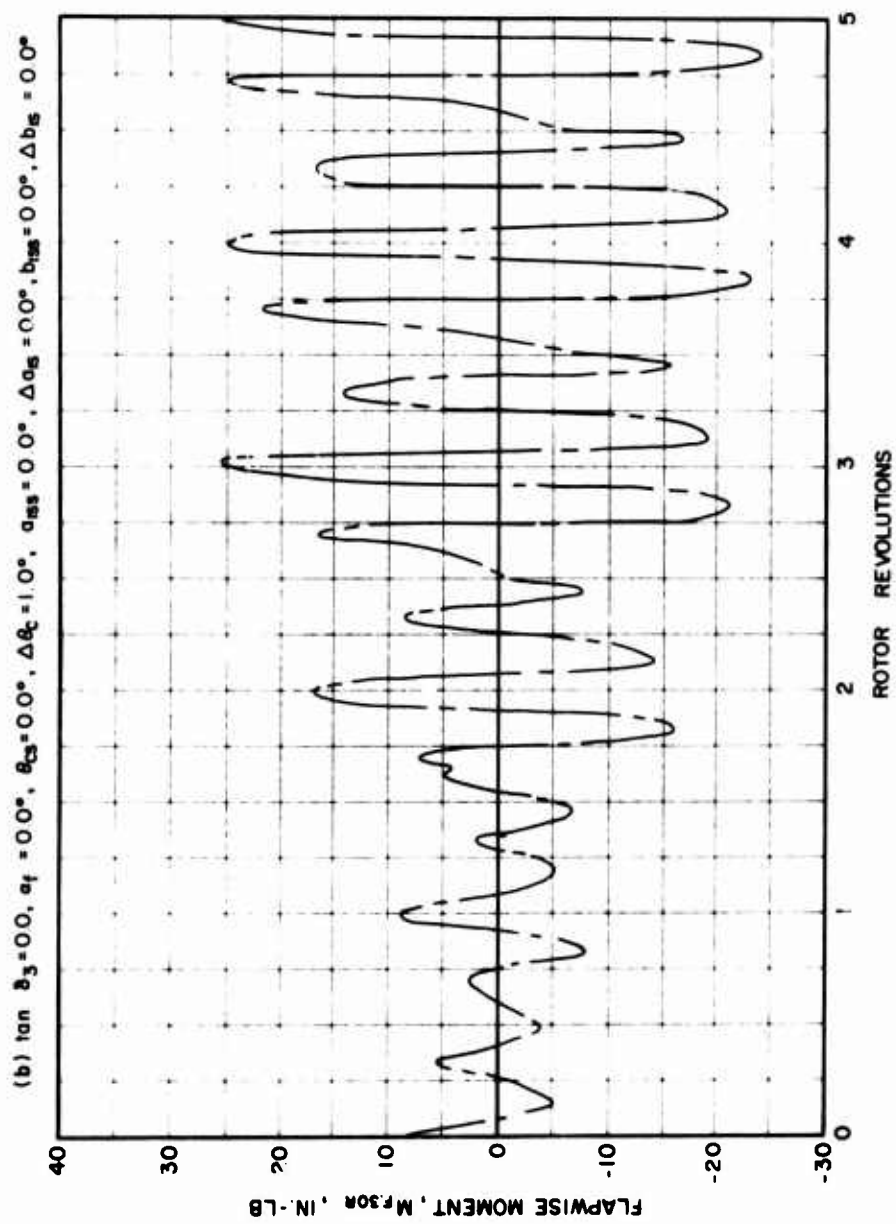


Figure 31. Continued.

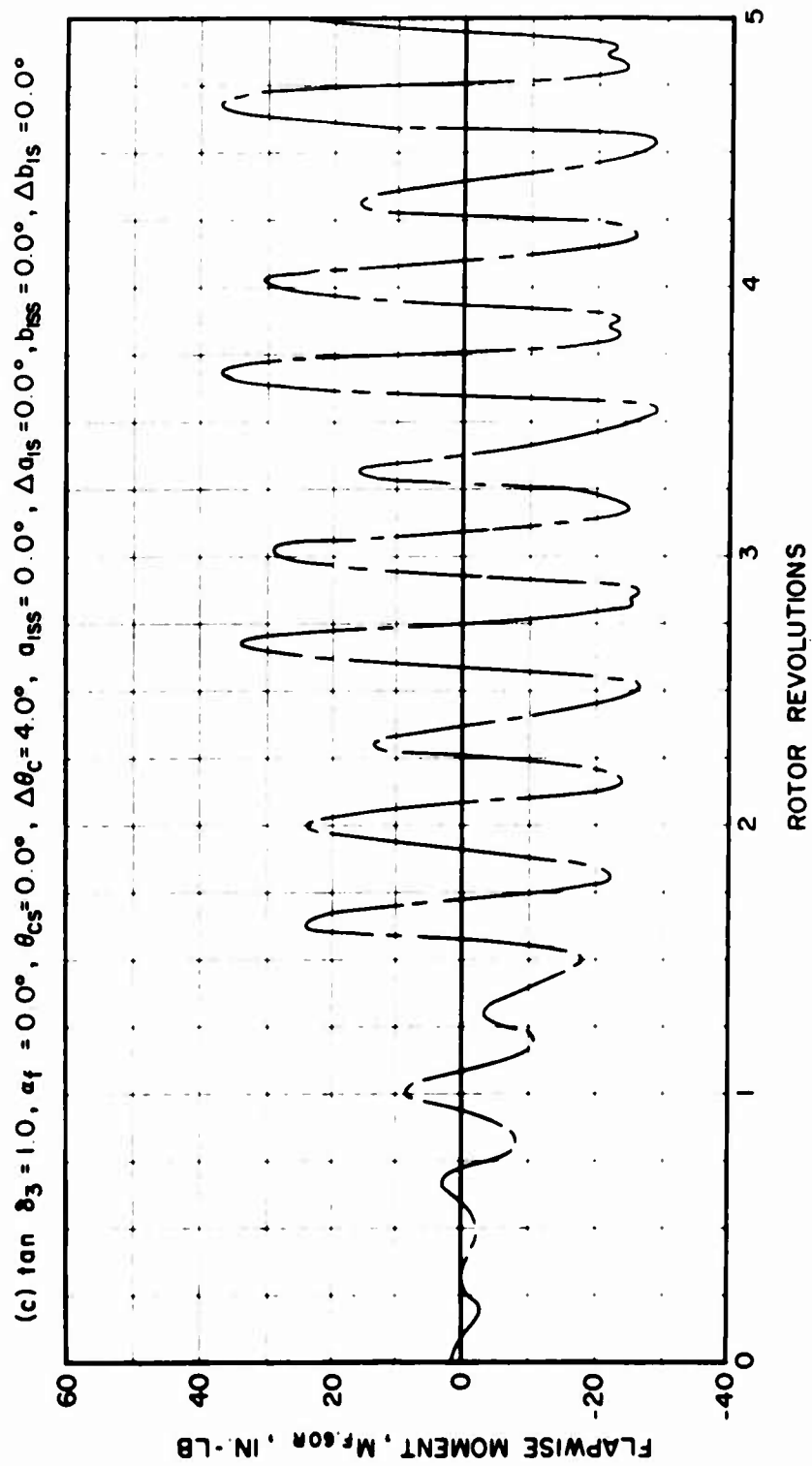


Figure 31. Continued.

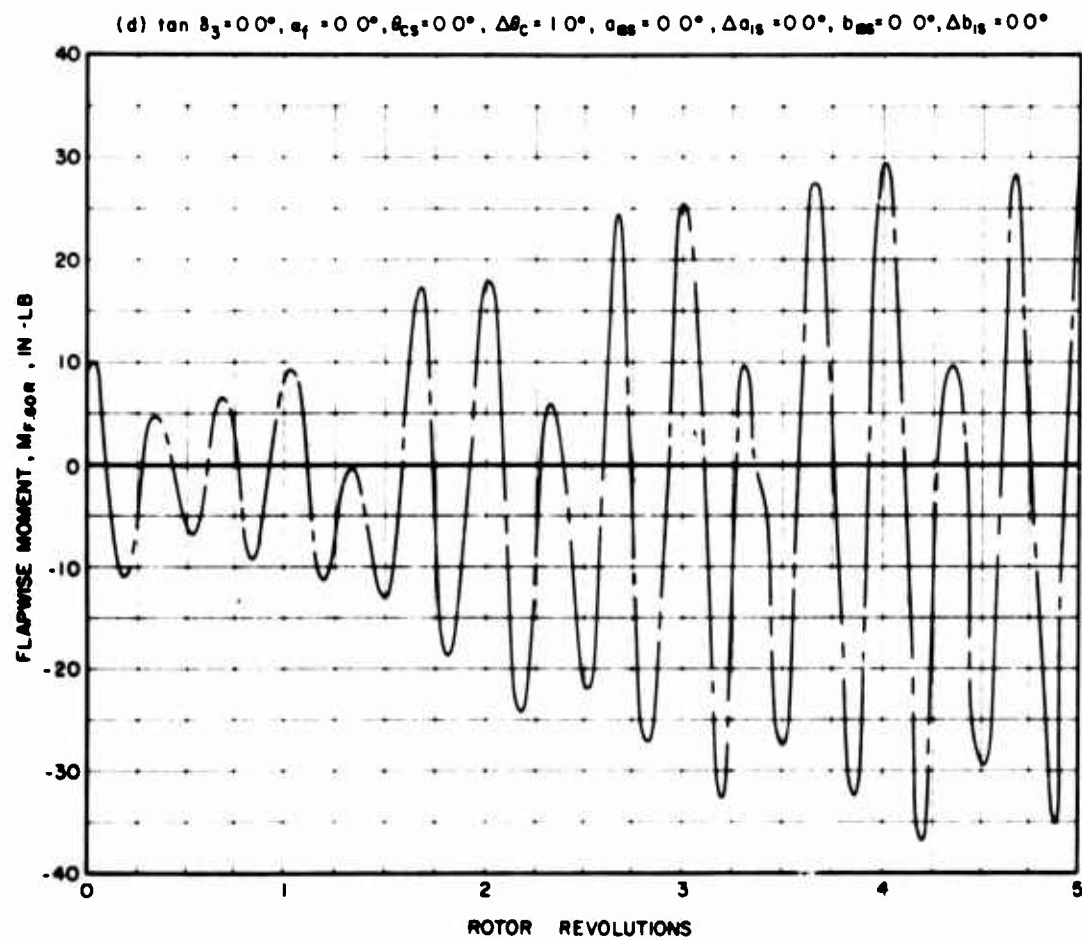


Figure 31. Concluded.

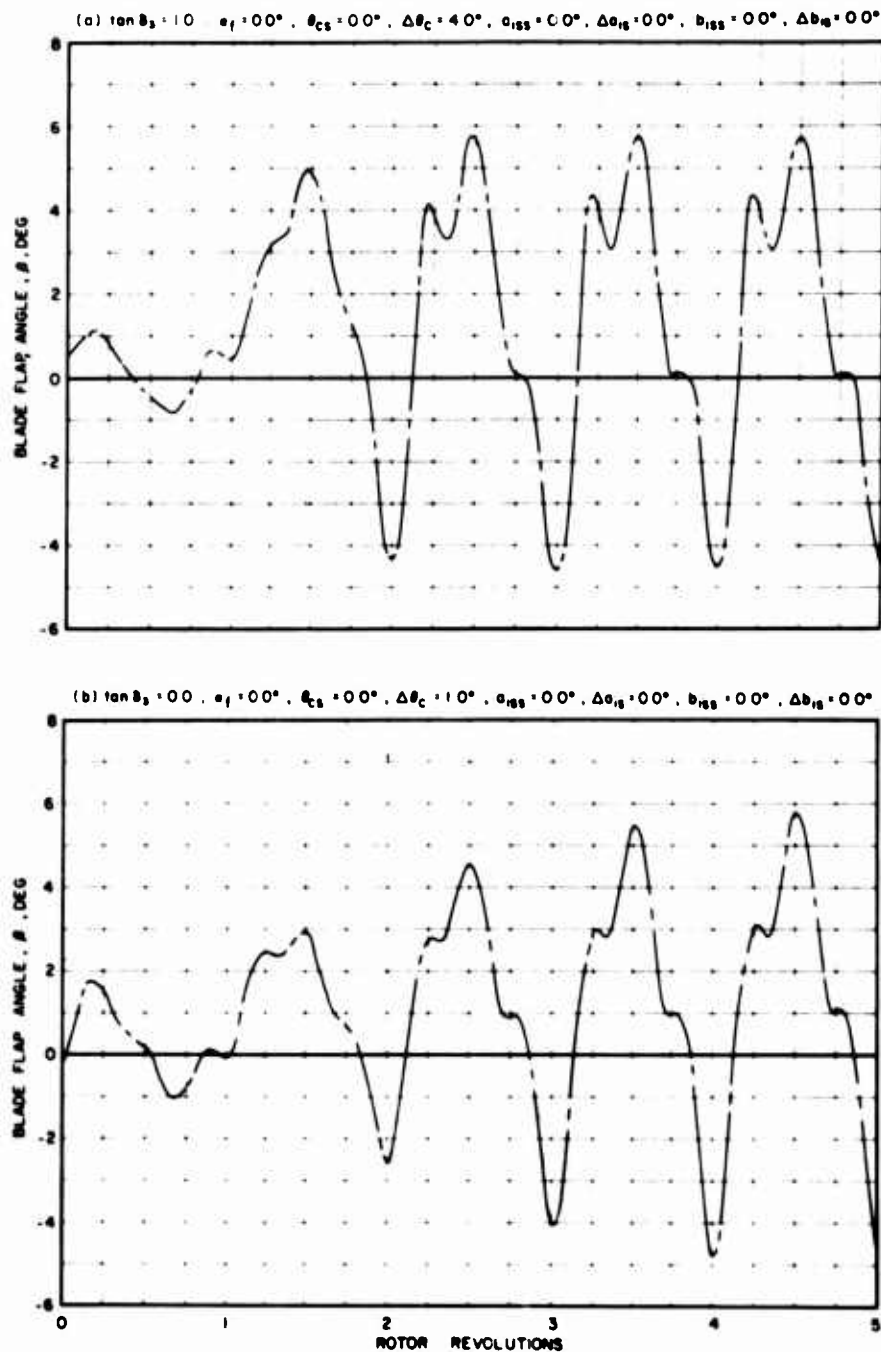


Figure 32. Theoretical Blade Flap Angle During Transient Conditions; $V_s = 300$ kn, $\mu = 1.03$, $Y_{CG}/c = 0.25$, Control Input Applied $3/4$ Revolution After Experimental Input.

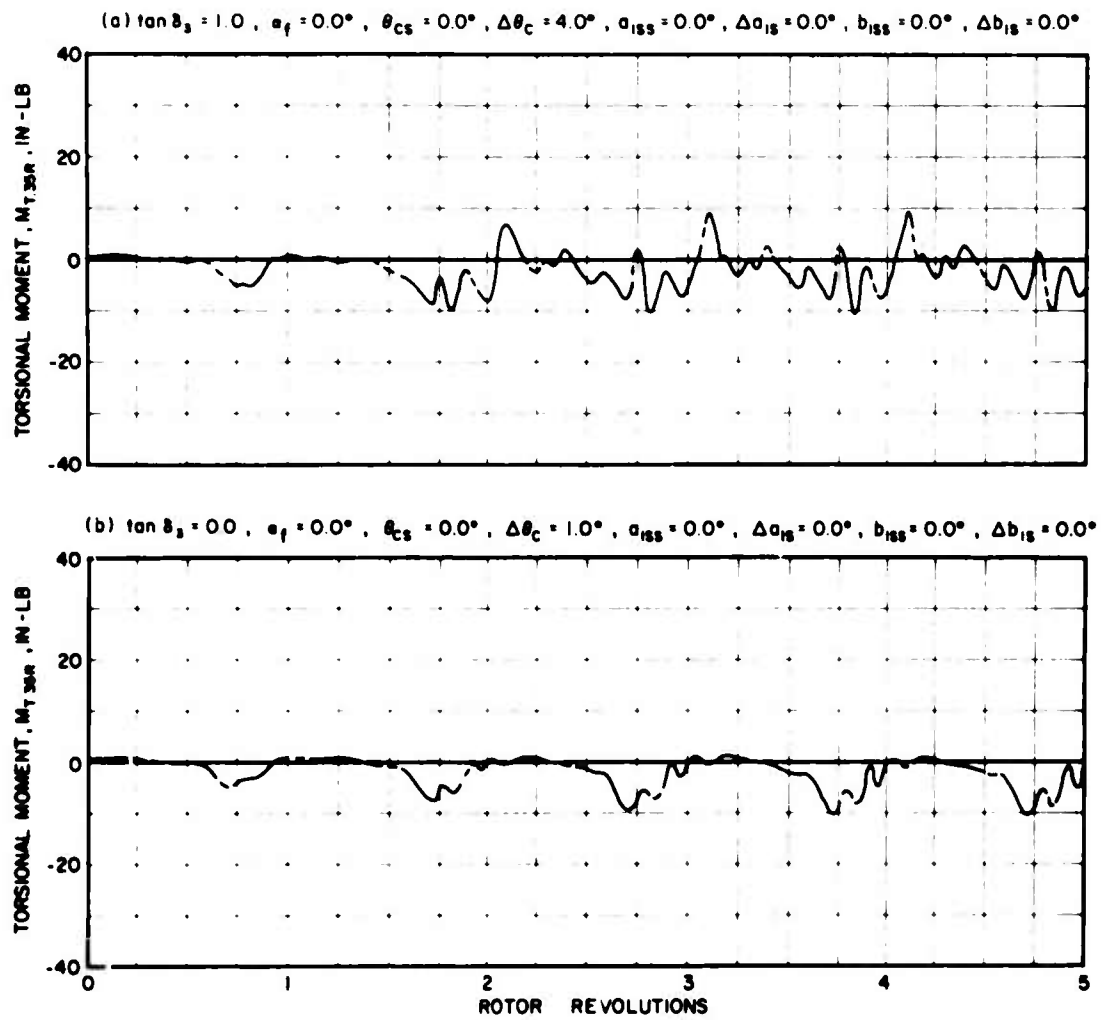


Figure 33. Theoretical Blade Torsional Moment During Transient Conditions; $V_s = 300$ kn, $\mu = 1.03$, $Y_{CG}/c = 0.25$, Control Input Applied 3/4 Revolution After Experimental Input.

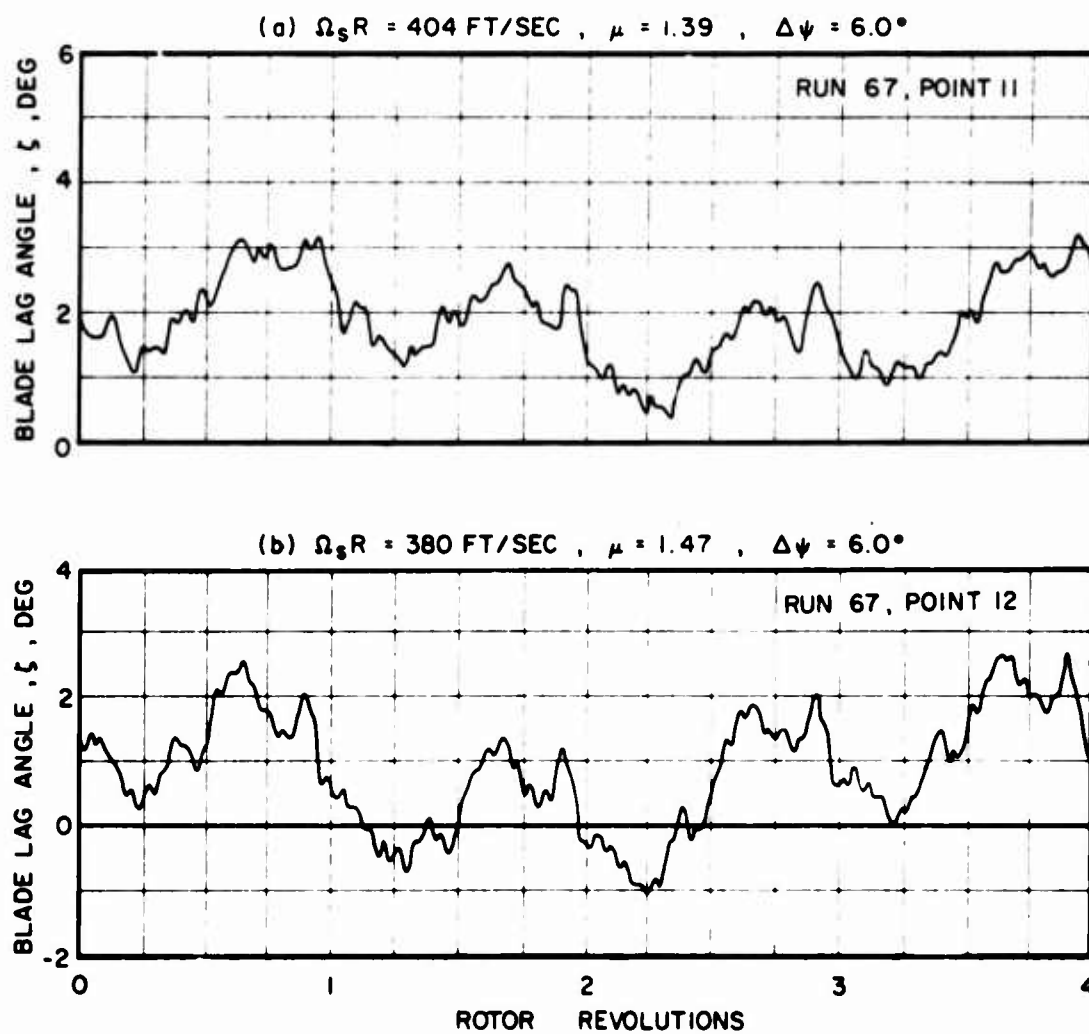


Figure 34. Blade Response Versus Azimuth During Retreating Blade Aeroelastic Limits Testing; $Y_{CG}/c = 0.25$, $\alpha_s = 0.0^\circ$, $a_{1s} = b_{1s} = 0.0^\circ$, $V_s = 332 \text{ kn}$, $\theta_c = 2.0^\circ$.

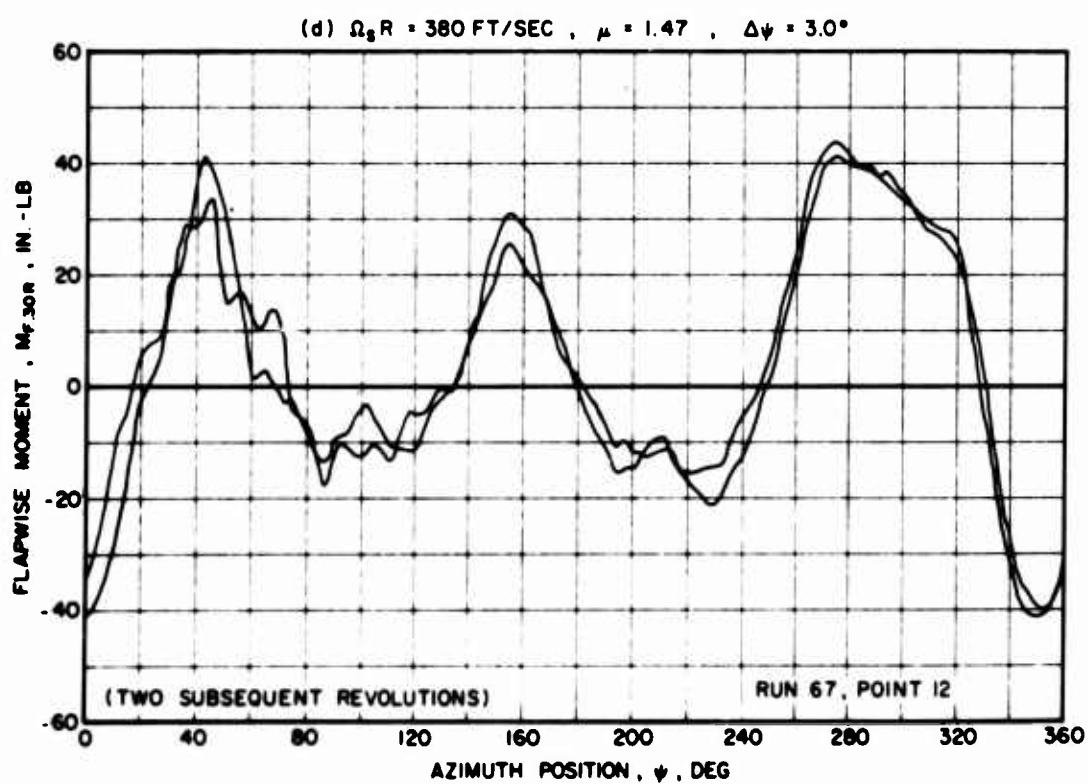
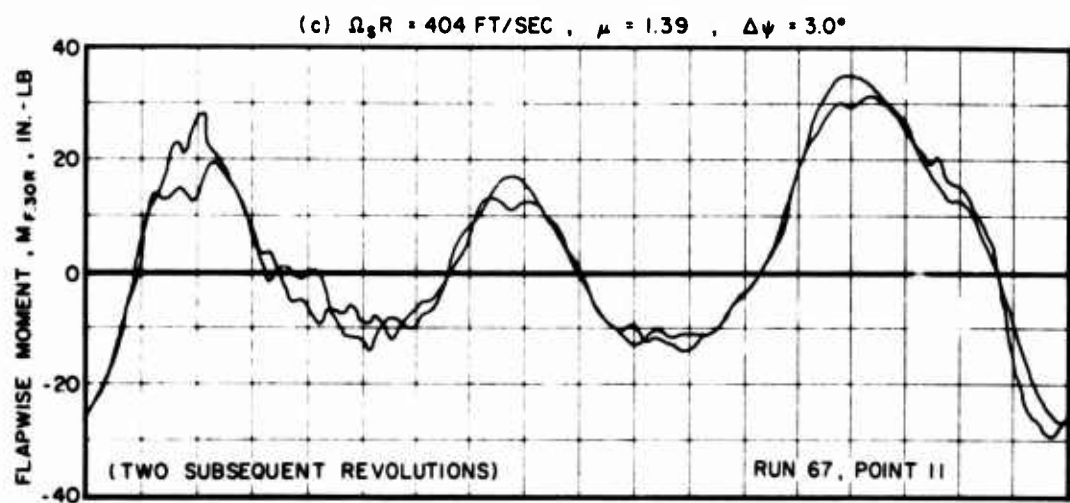


Figure 34. Continued.

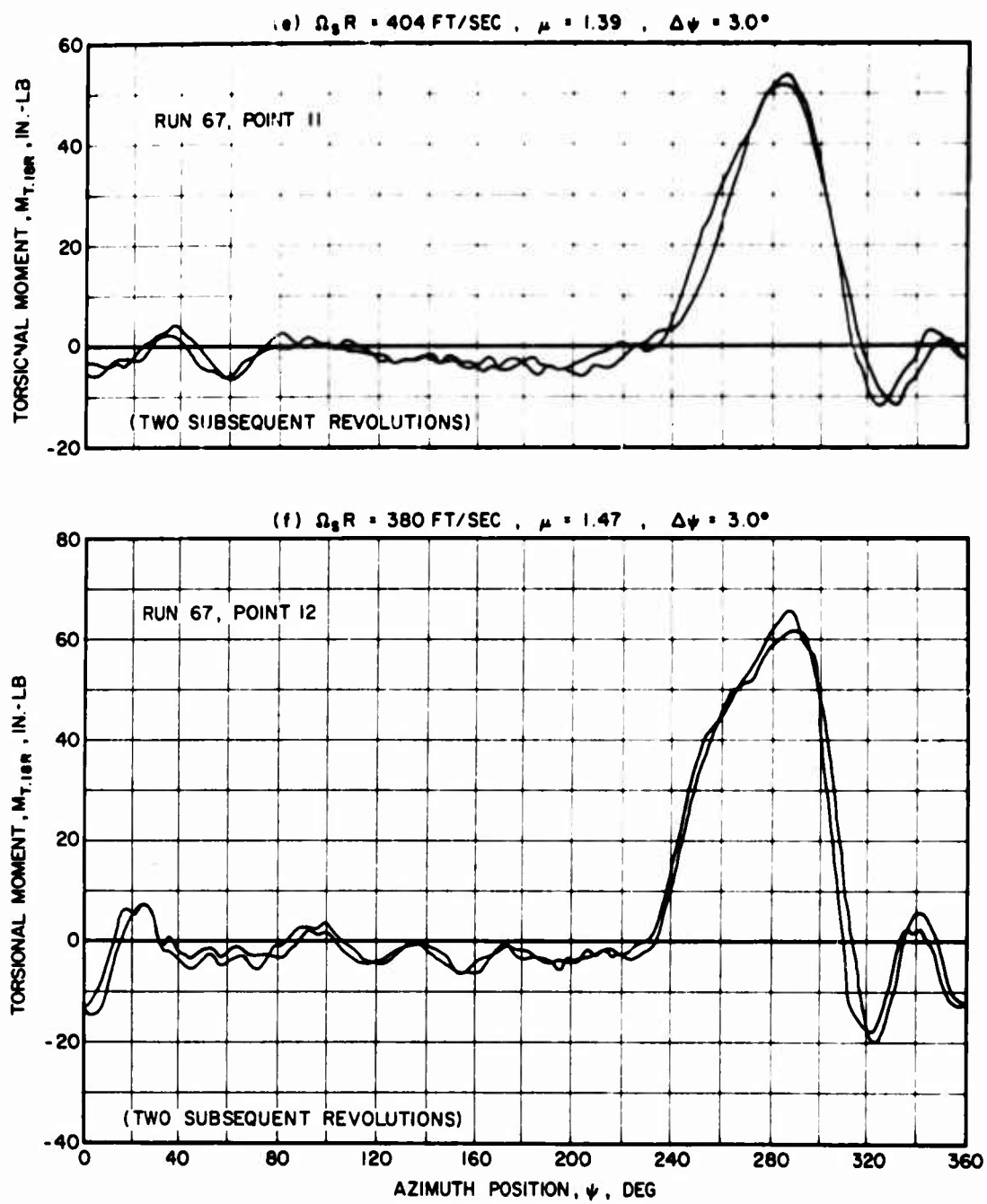


Figure 34. Continued.

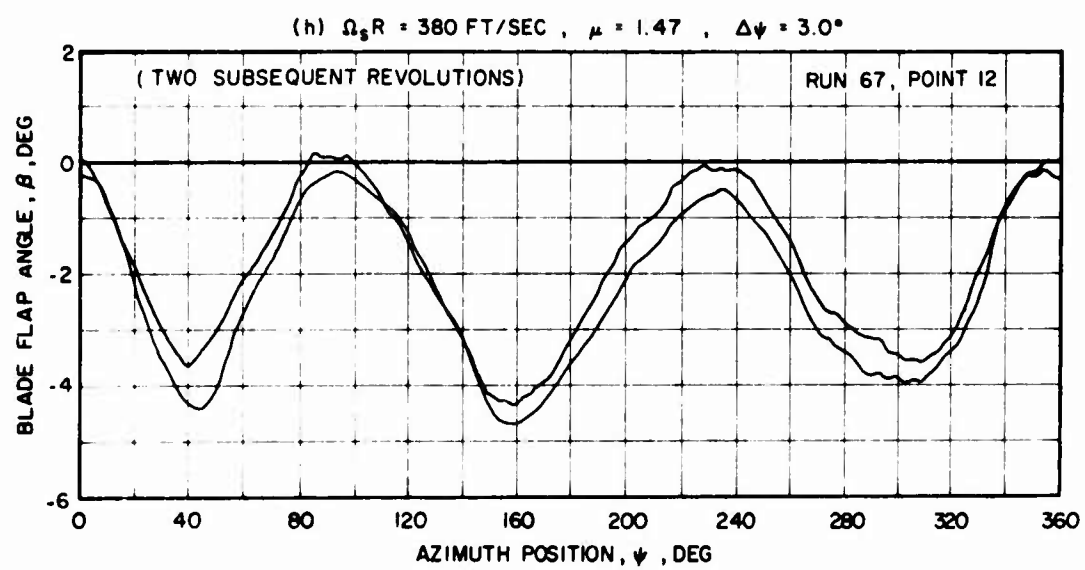
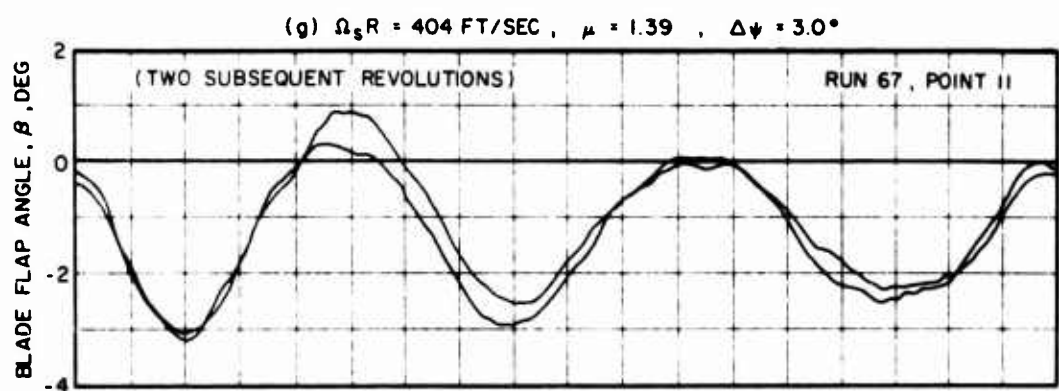


Figure 34. Concluded.

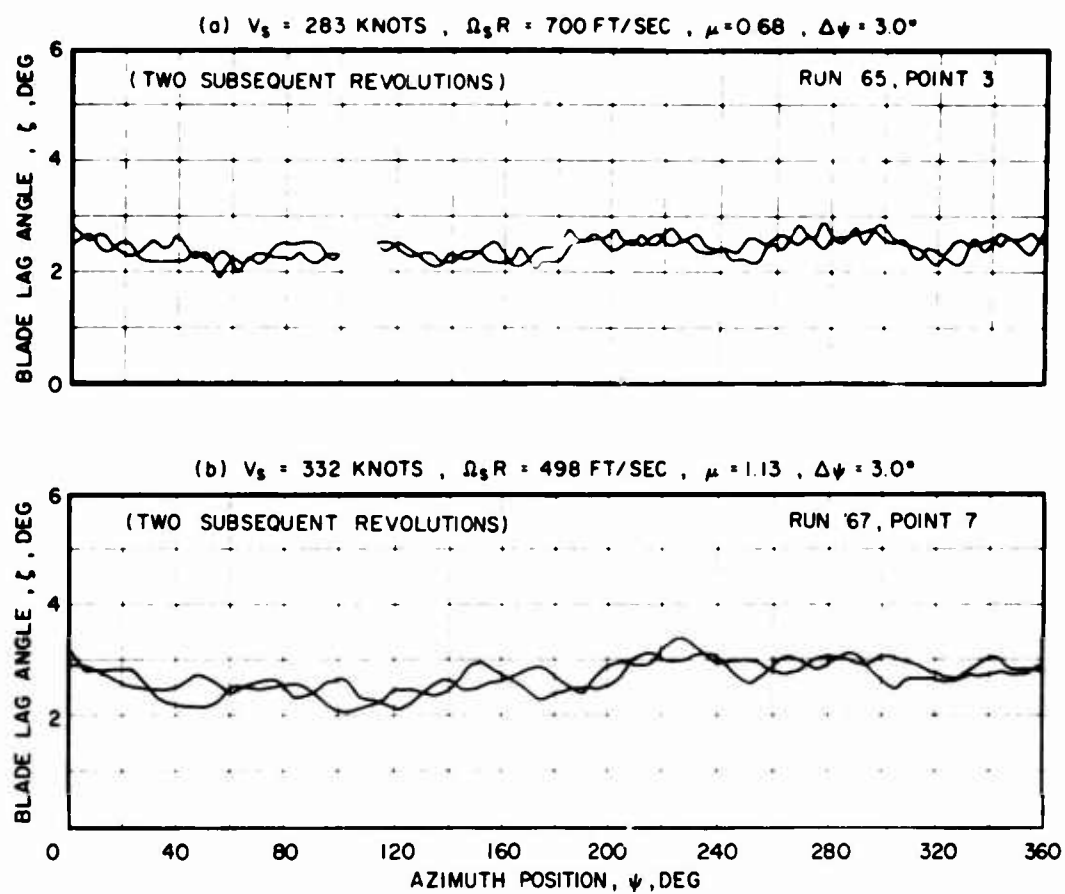


Figure 35. Blade Response Versus Azimuth During Advancing Blade Aeroelastic Limits Testing; $\gamma_{CG}/c = 0.25$, $\alpha_s = 0.0^\circ$, $a_{1s} = b_{1s} = 0.0^\circ$, $\theta_c = 2.0^\circ$.

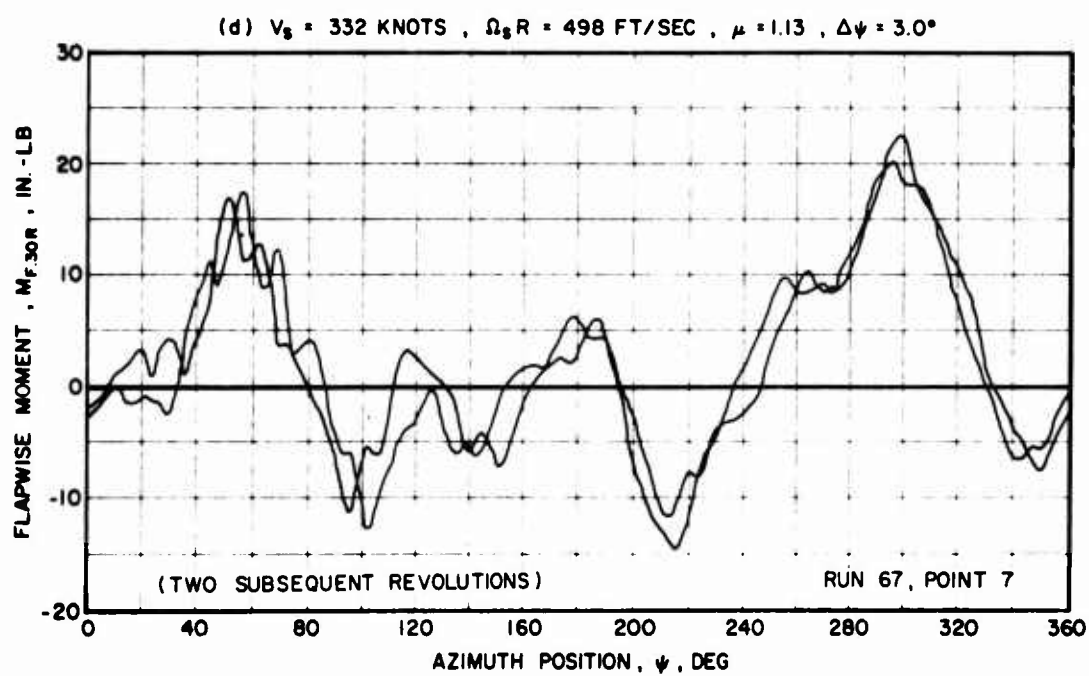
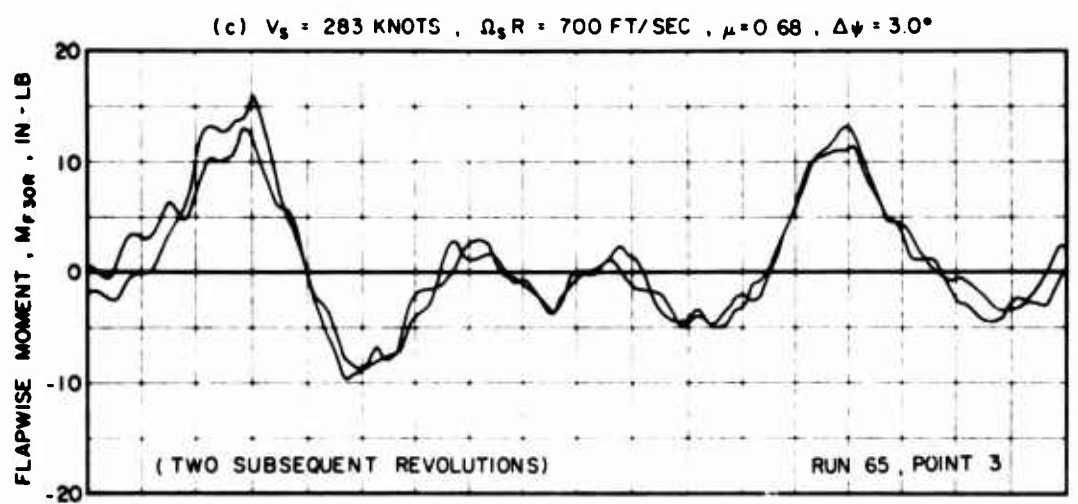


Figure 35. Continued.

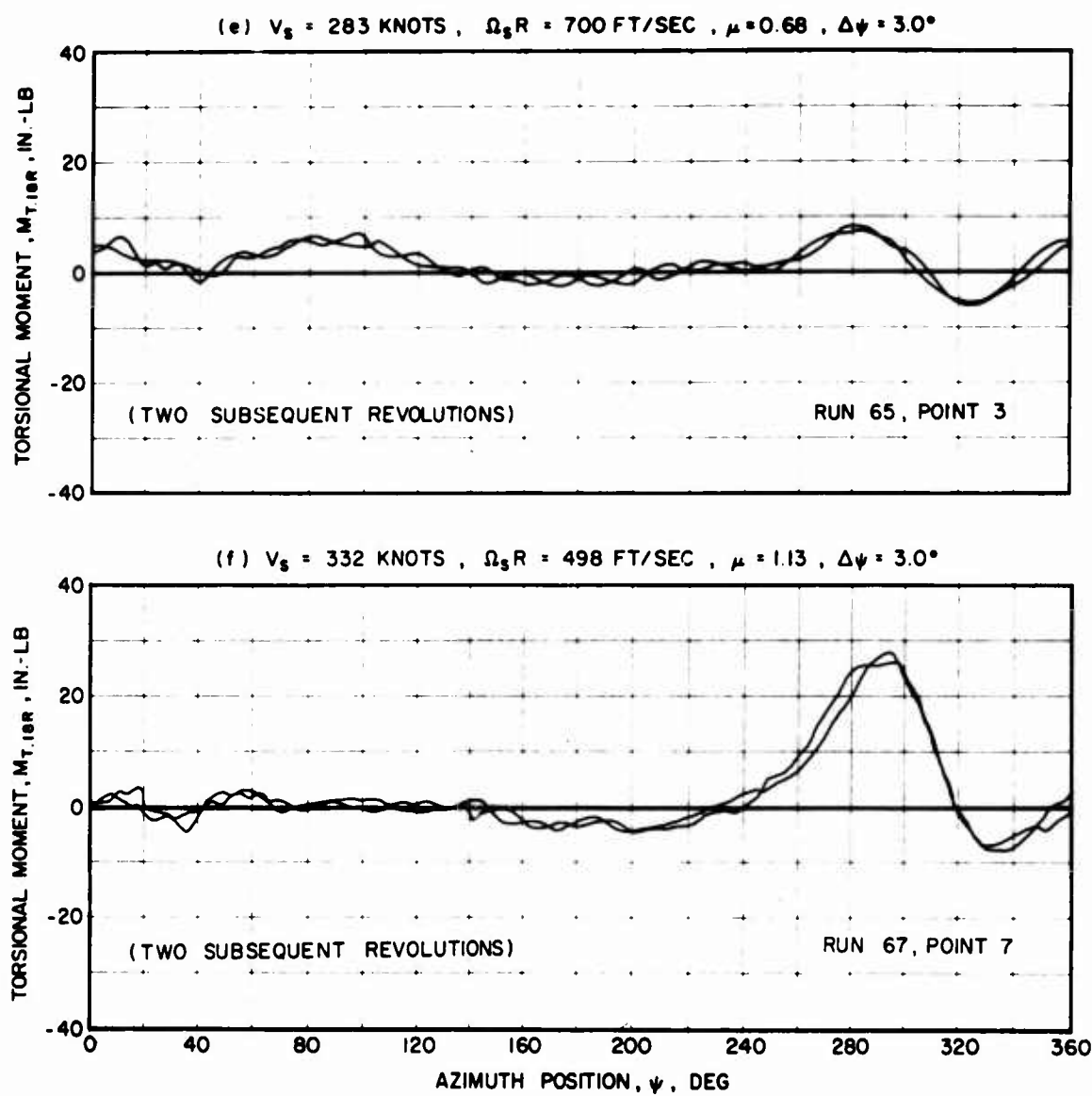


Figure 35. Continued.

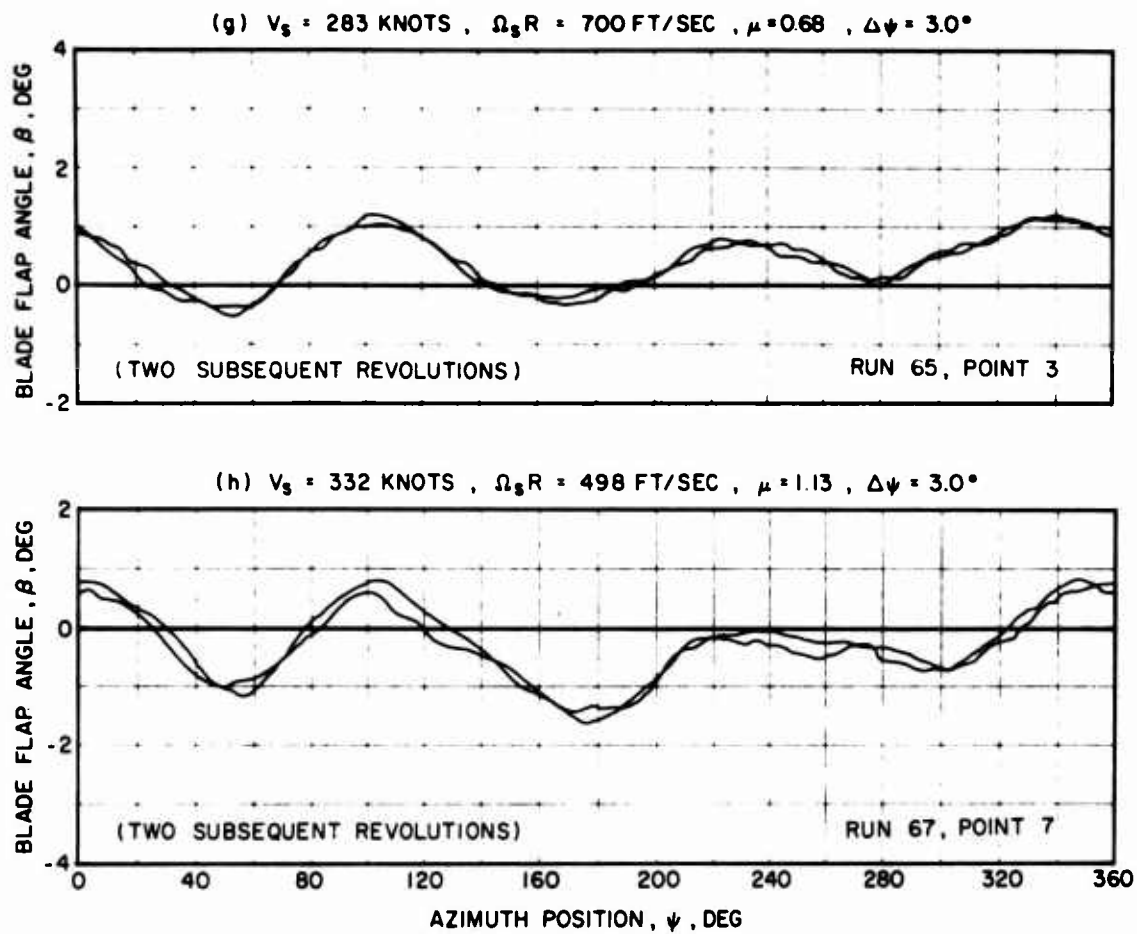


Figure 35. Concluded.

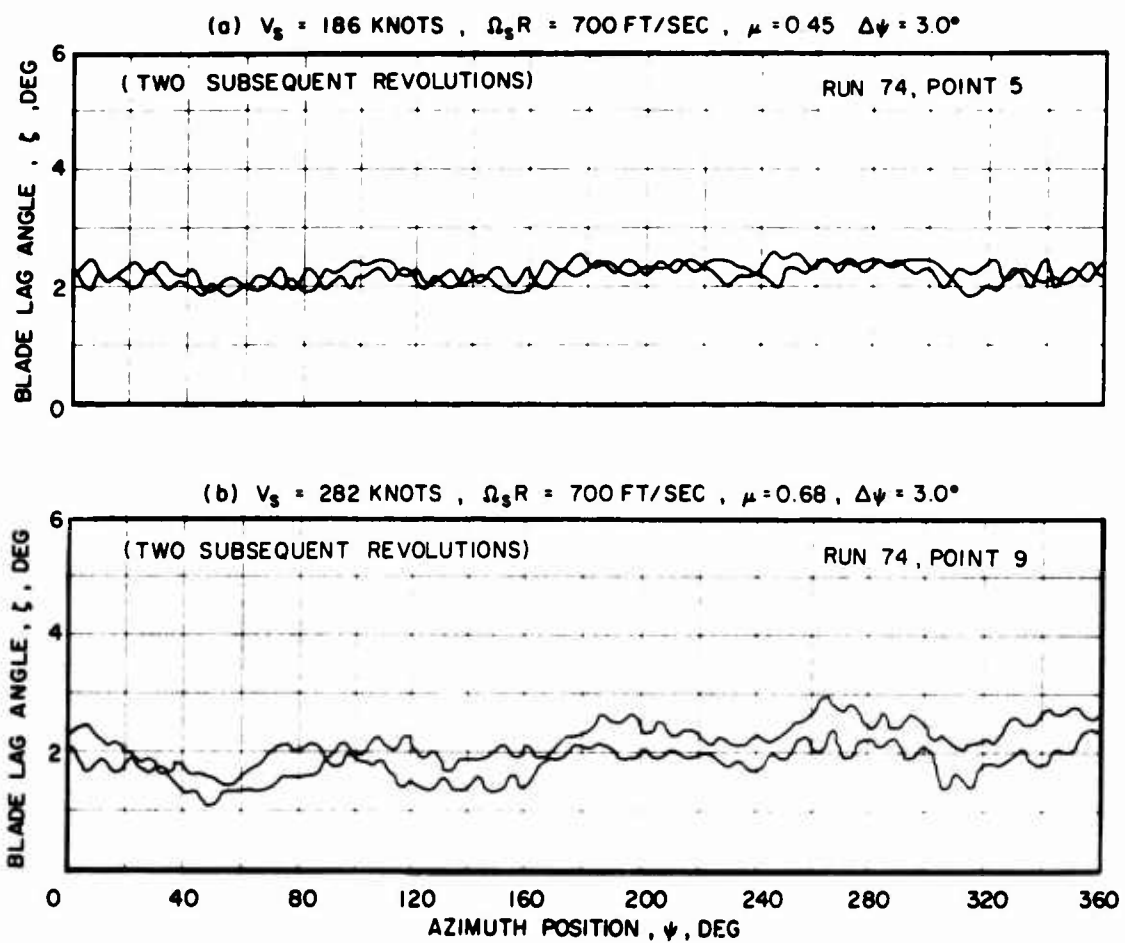


Figure 30. Blade Response Versus Azimuth During Advancing Blade Aerodynamic Model Testing;
 $c_{01}/c = 0.05$, $a_s = 1.0^\circ$, $a_{1s} = b_{1s} = 0.0^\circ$,
 $\Omega_s R = 700$ ft/sec, $\psi_0 = 4.0^\circ$.

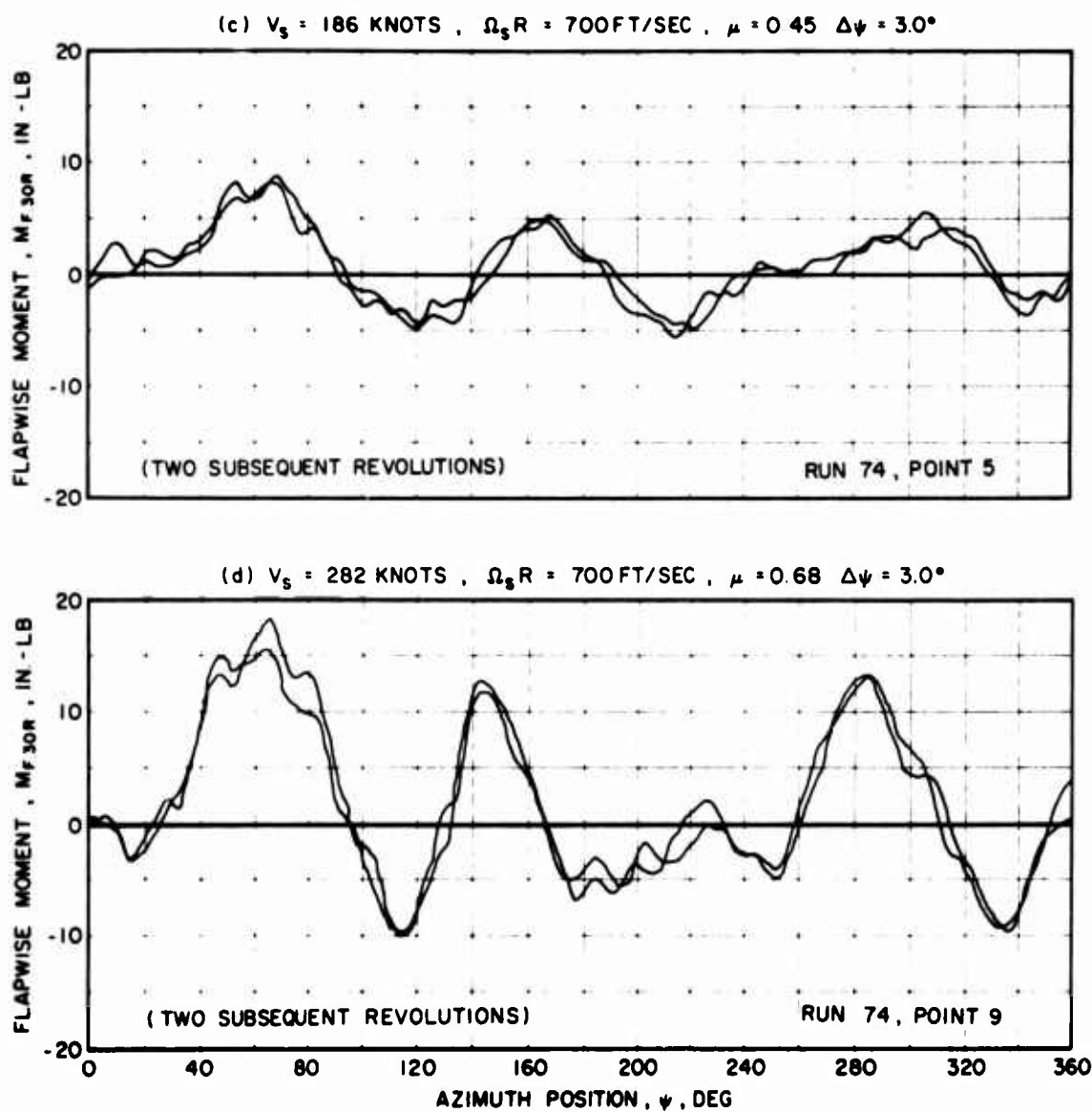


Figure 36. Continued.

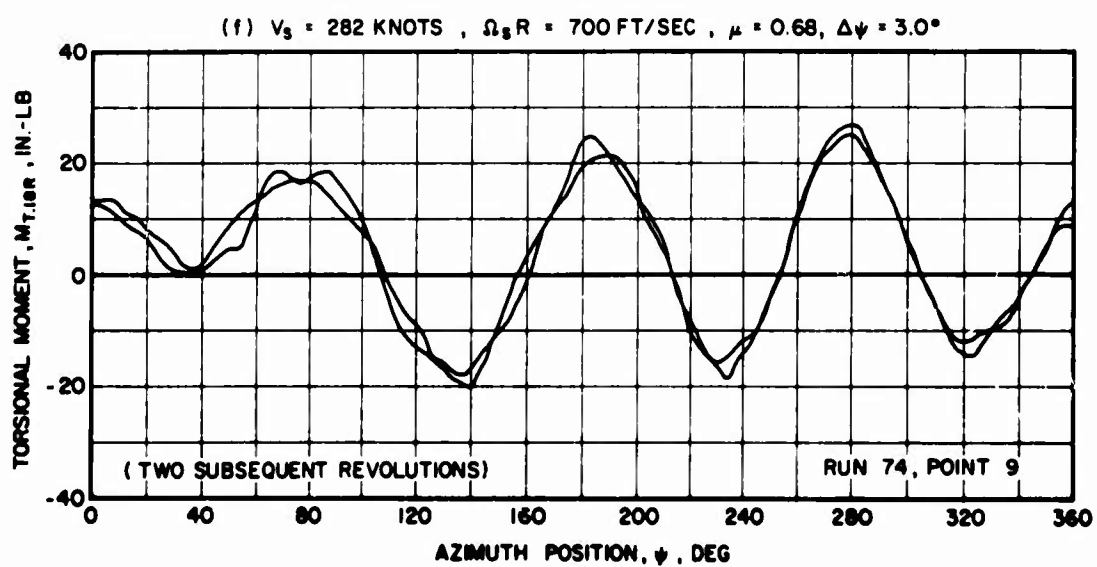
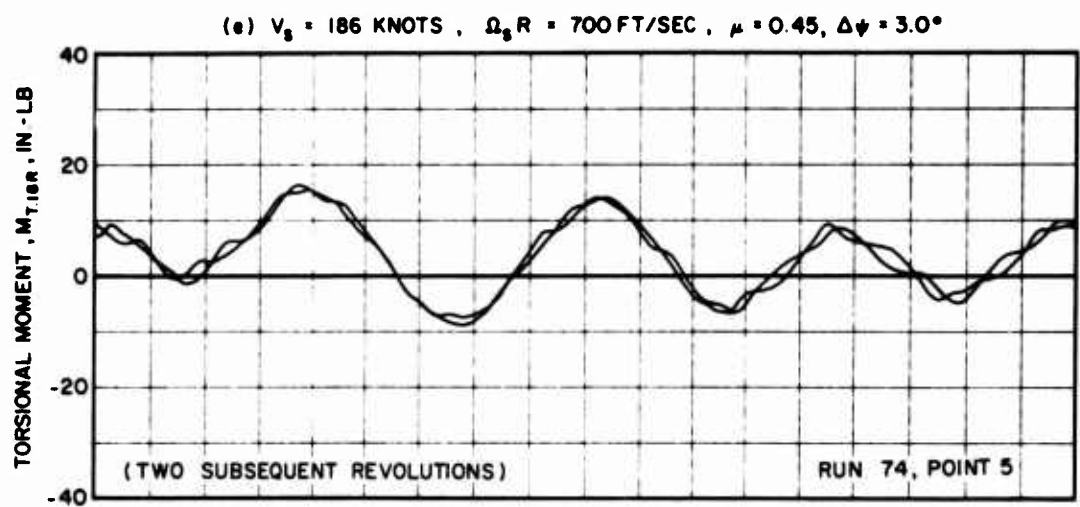


Figure 36. Continued.

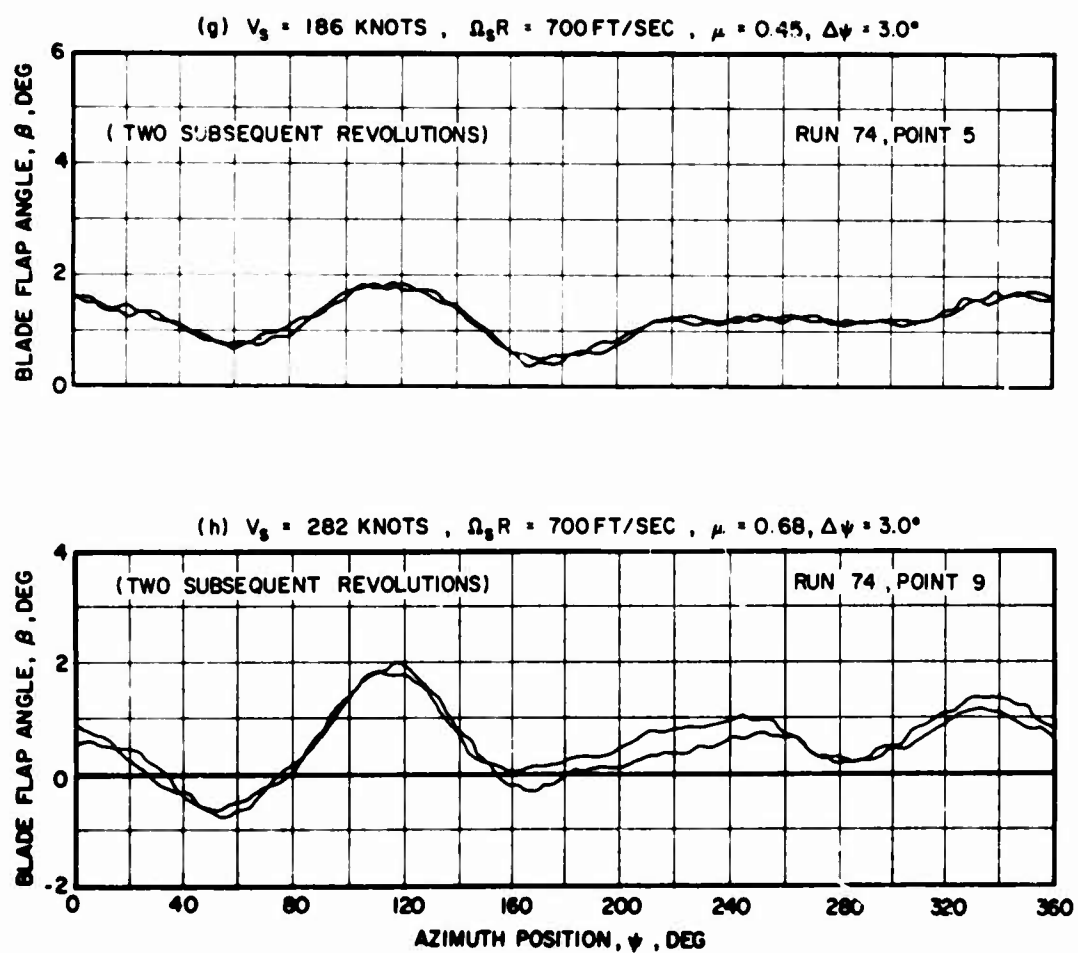


Figure 36. Continued.

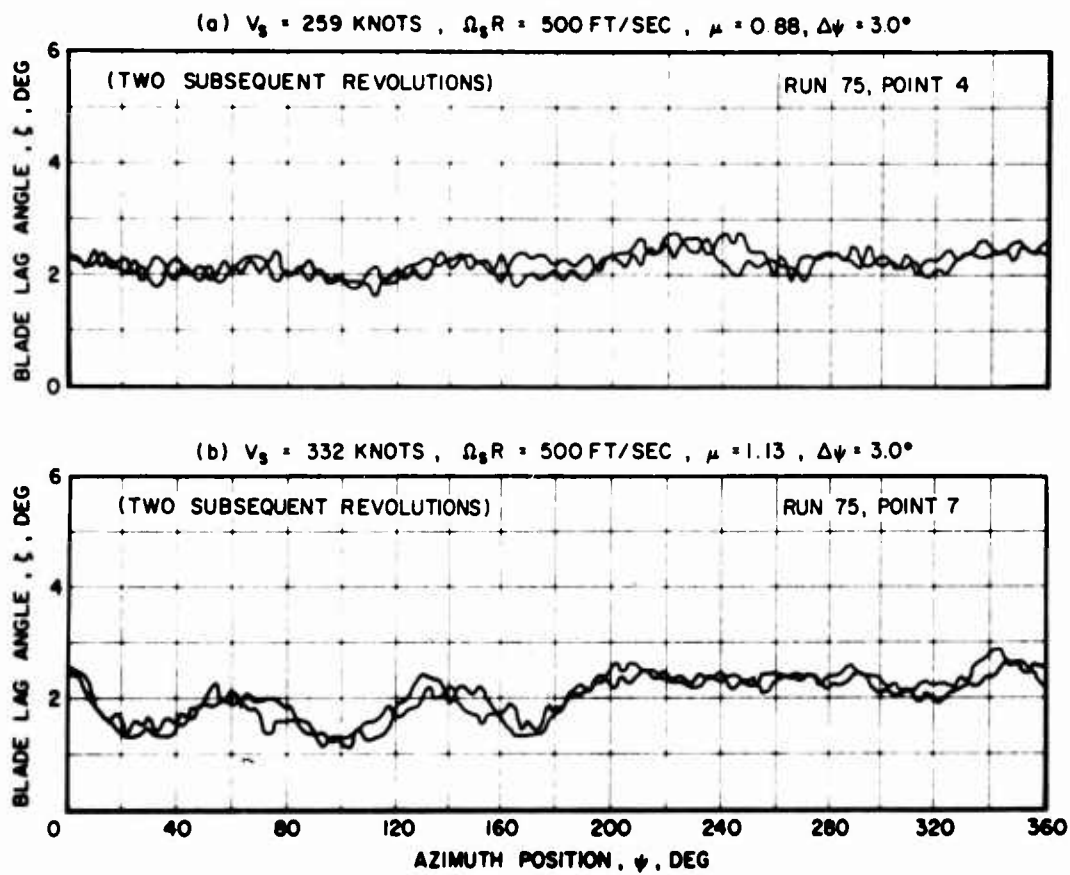


Figure 37. Blade Response Versus Azimuth During Advancing Blade Aeroelastic Limits Testing; $Y_{CC}/c = 0.25$, $\alpha_s = 0.0^\circ$, $a_{1s} = b_{1s} = 0.0^\circ$, $\Omega_s R = 500$ ft/sec, $\theta_c = 4.0^\circ$.

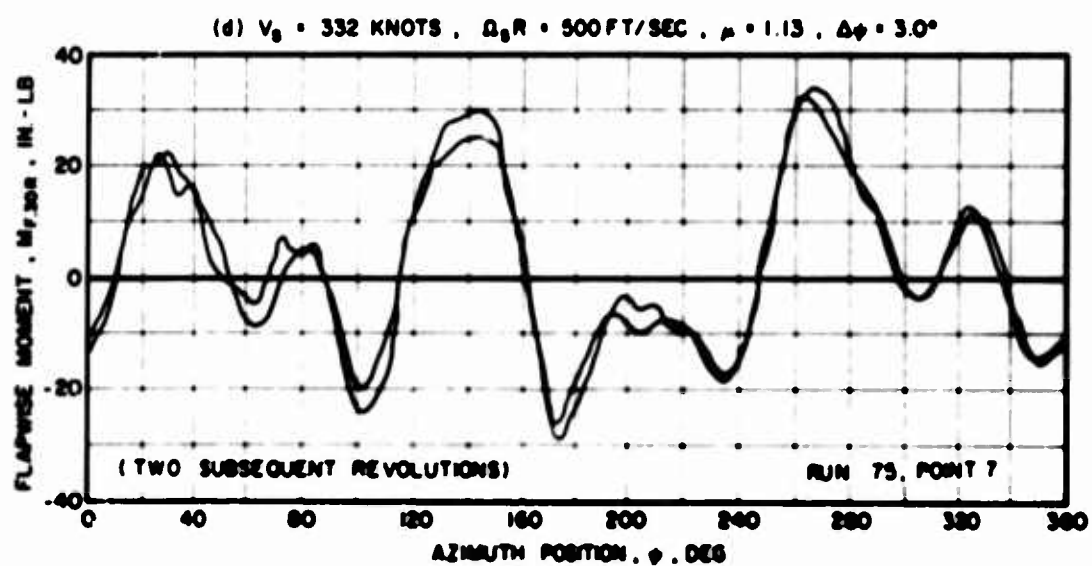
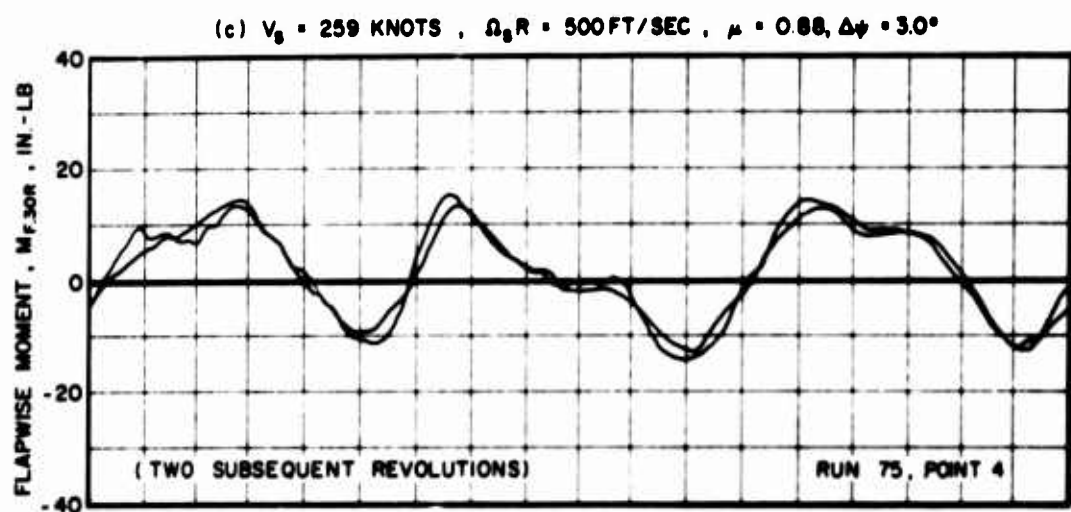


Figure 37. Continued.

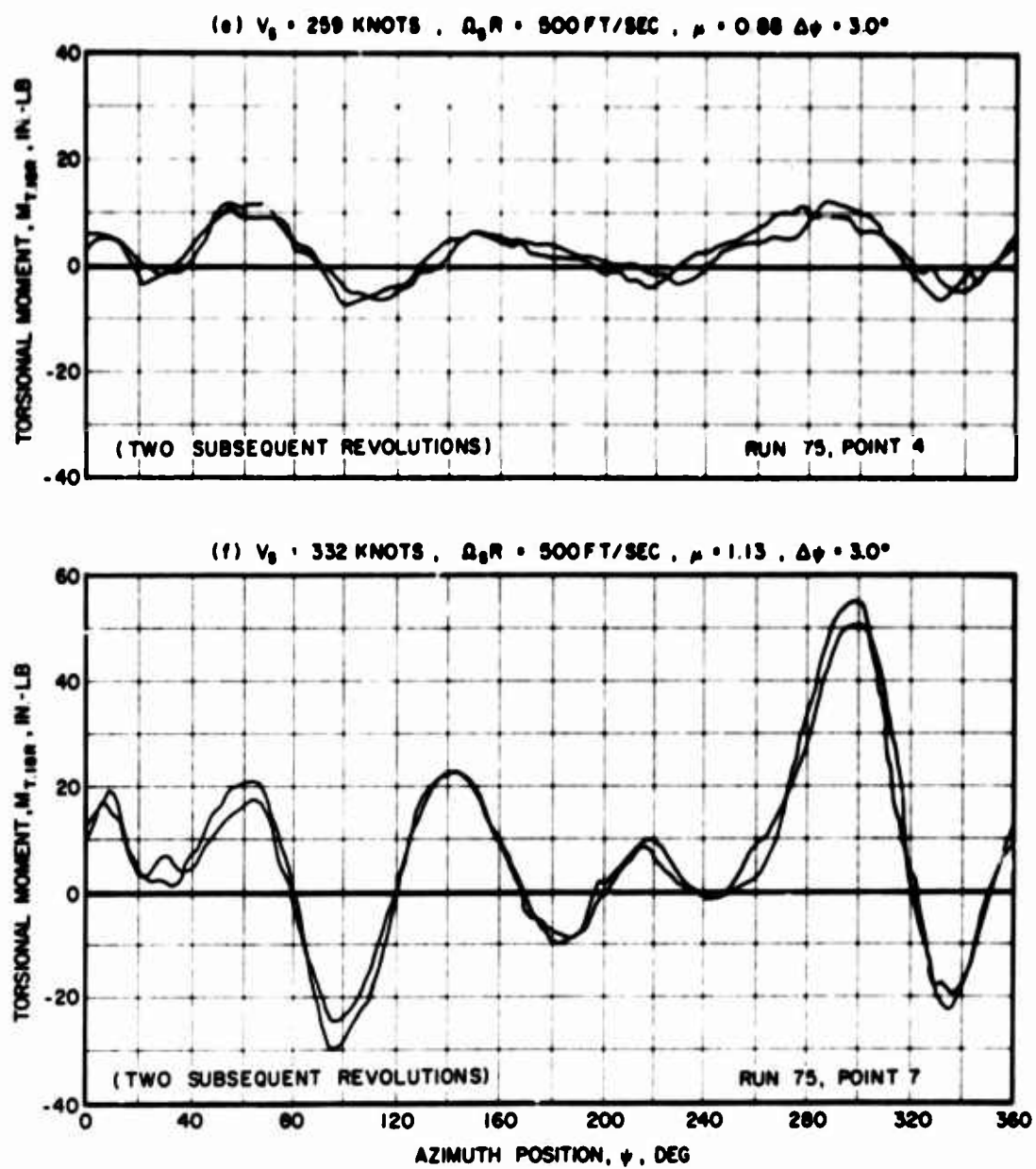


Figure 37. Continued.

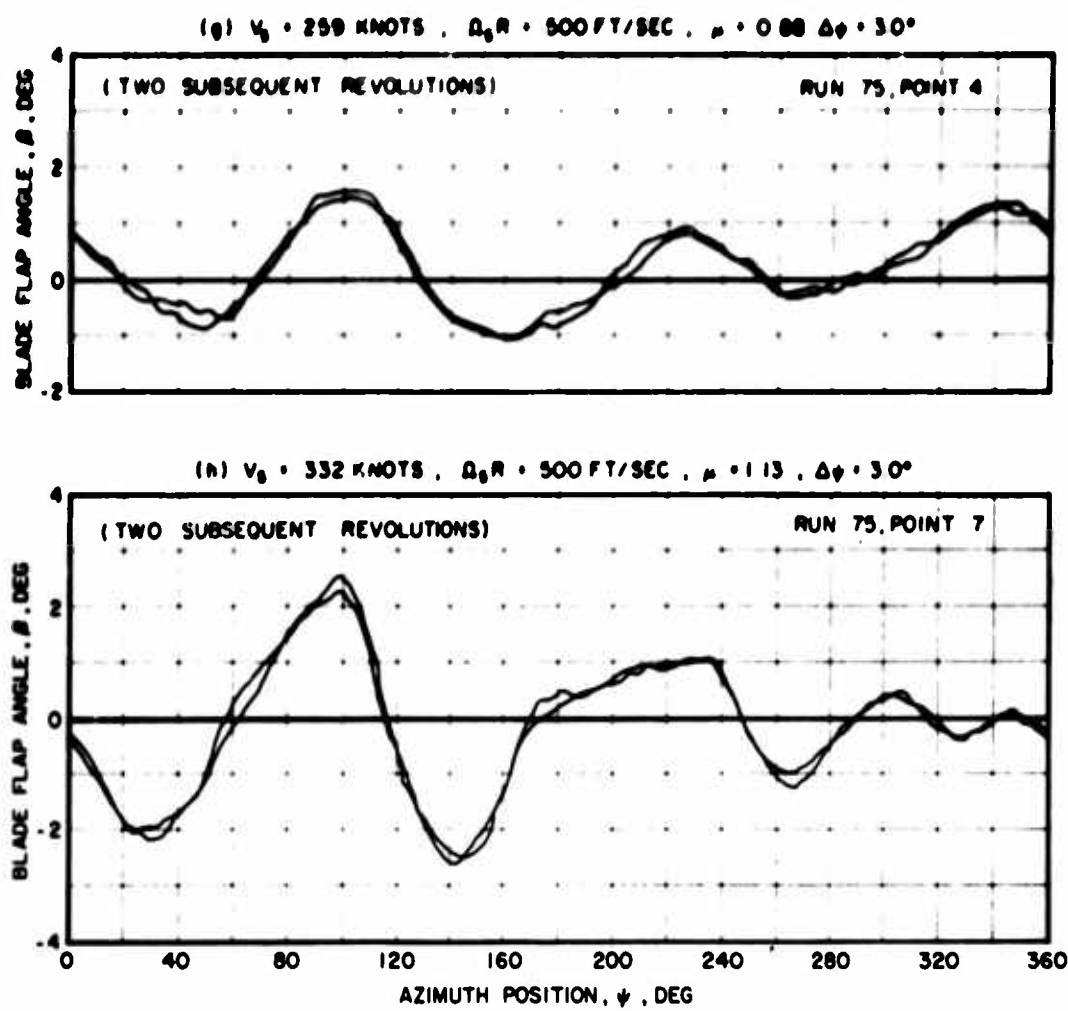


Figure 37. Continued.

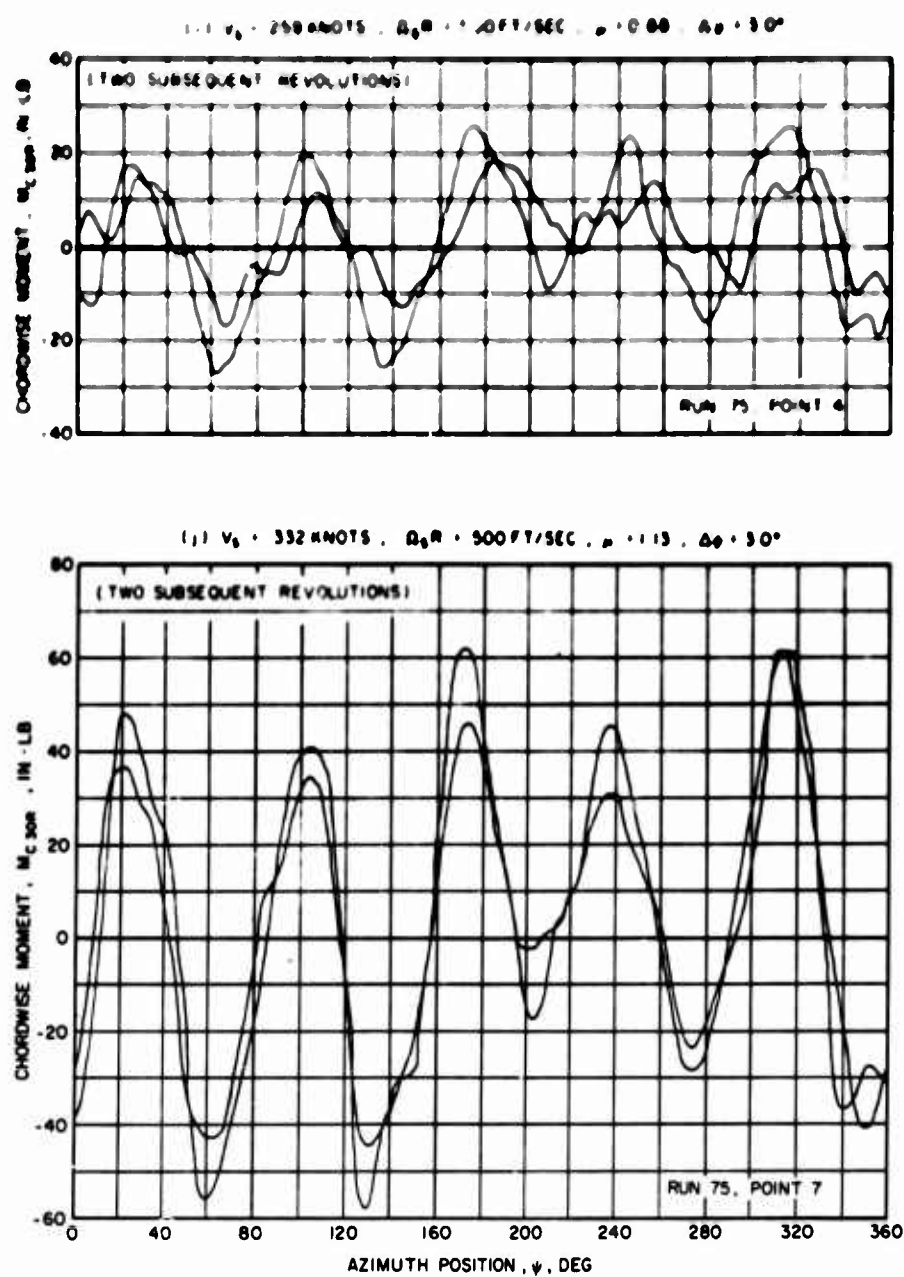


Figure 37. Concluded.

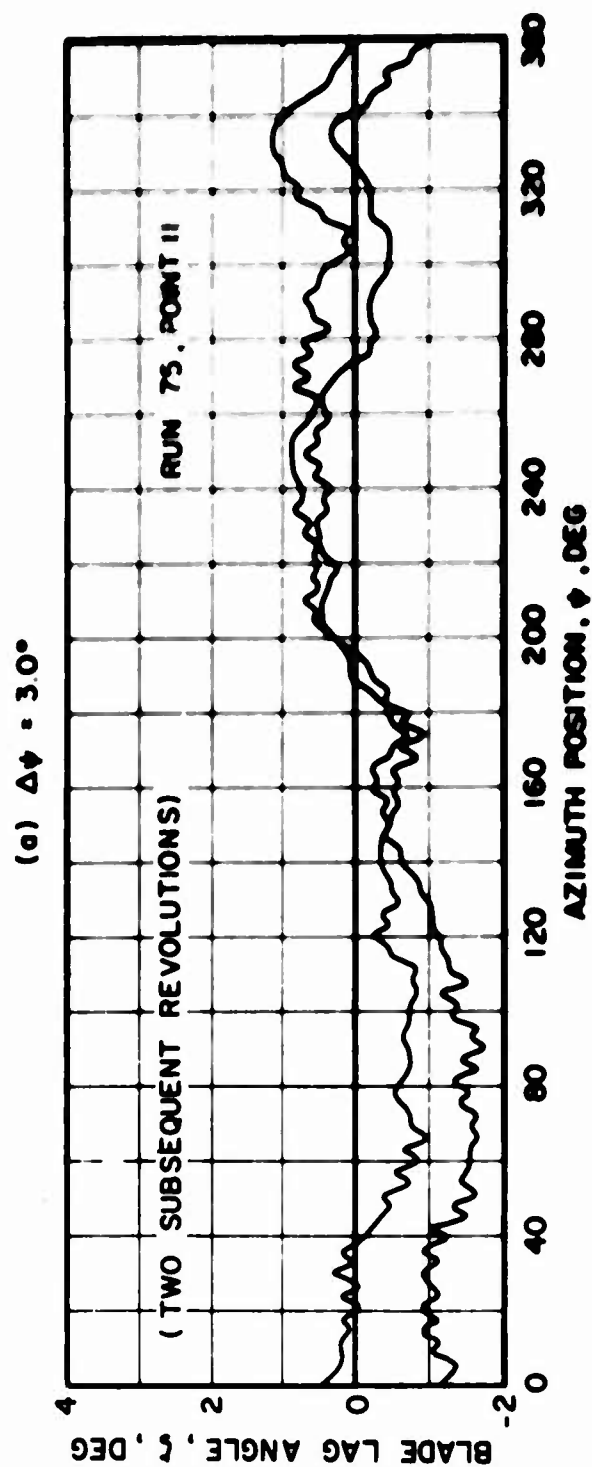


Figure 38. Blade Response Versus Azimuth During Combined Advancing and Retreating Blade Aeroelastic Limits
 Testing: $\gamma_{CG}/c = 0.30$, $\alpha_s = 0.0^\circ$, $\alpha_{ls} = b_{ls} = 0.0^\circ$,
 $V_s = 332$ km, $\Omega_{sR} = 404$ ft/sec, $\nu = 1.39$, $\theta_c = 4.0^\circ$.

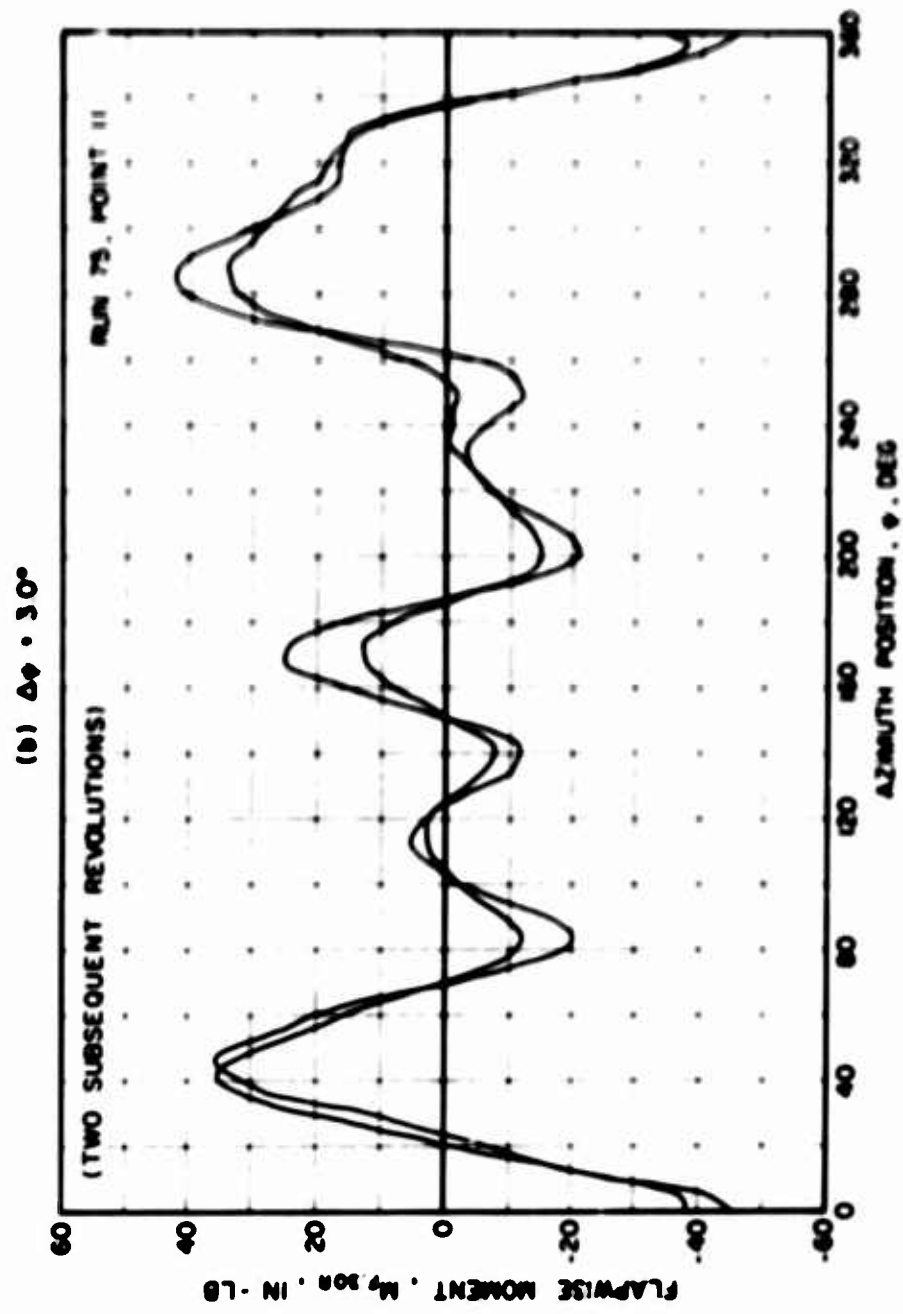


Figure 36. Continued.

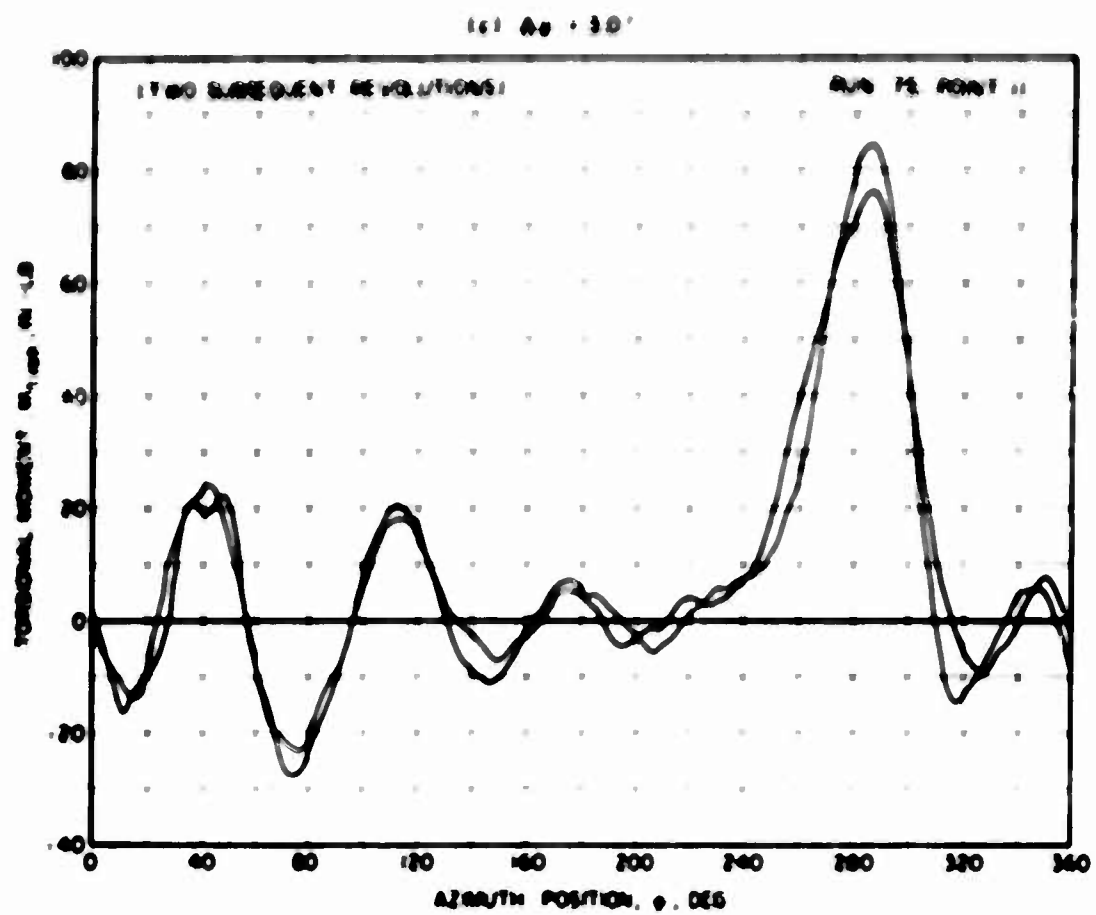


Figure 38. Continued.

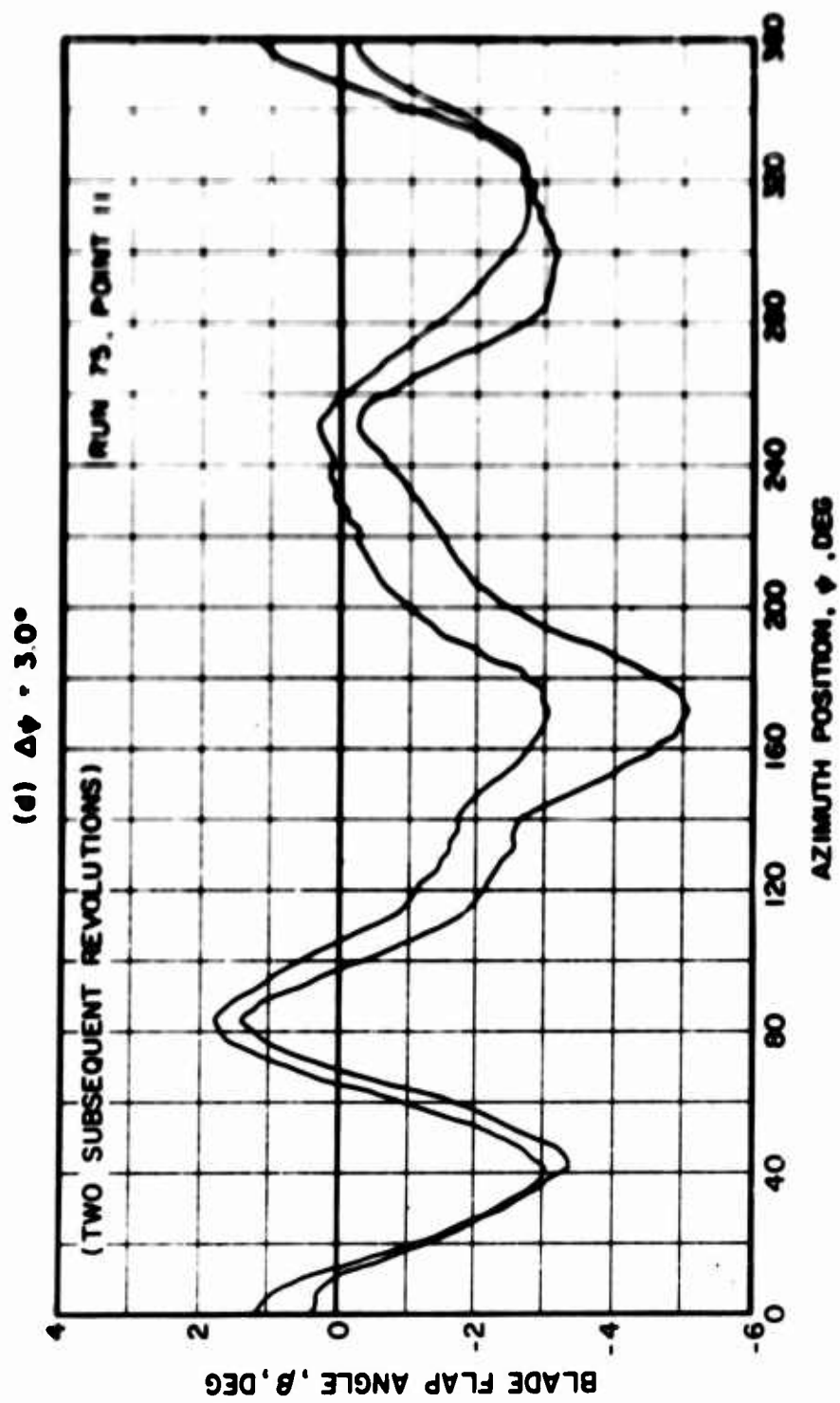


Figure 38. Continued.

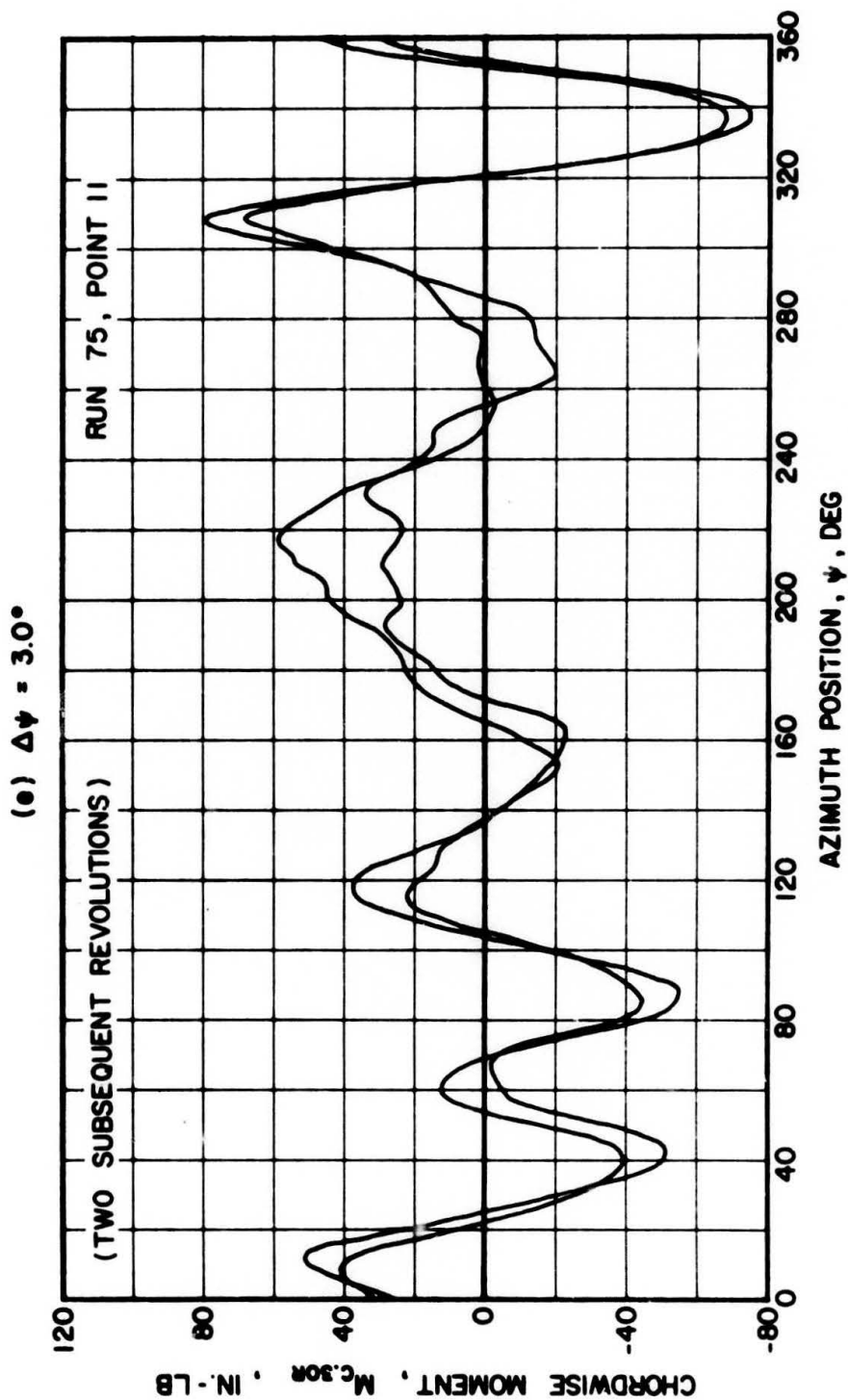


Figure 38. Concluded.

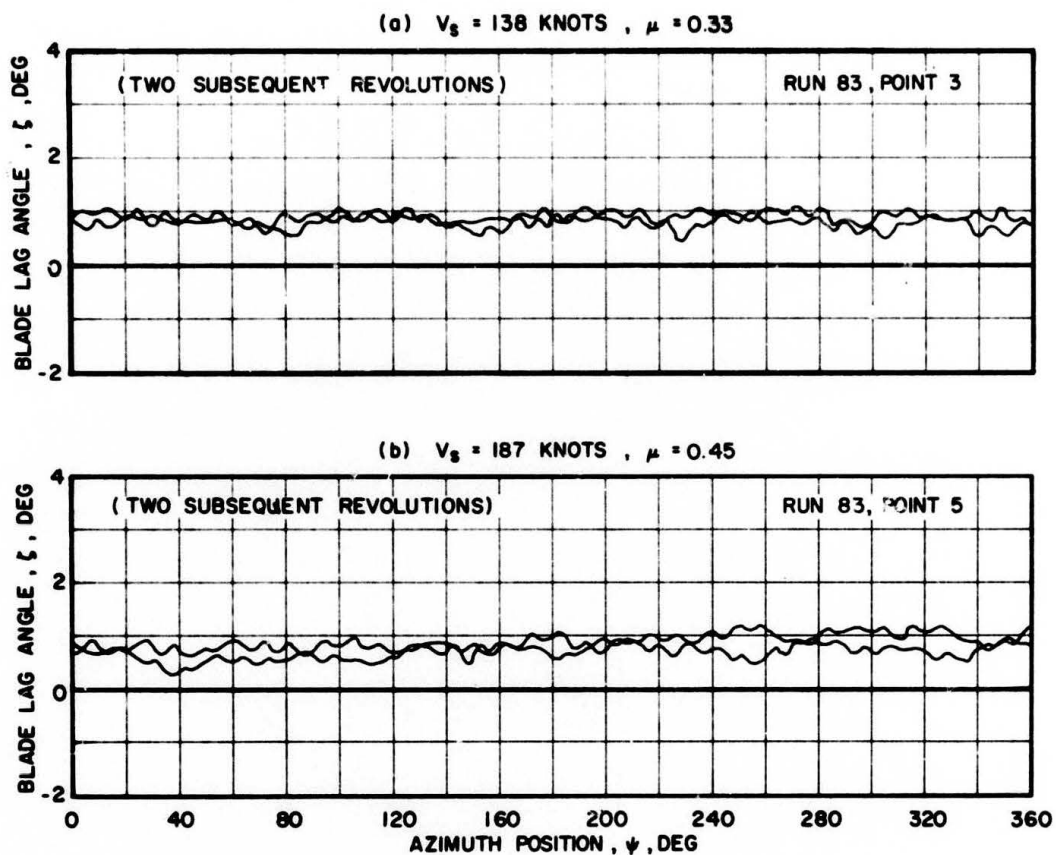


Figure 39. Blade Response Versus Azimuth During Advancing Blade Aeroelastic Limits Testing; $Y_{CG}/c = 0.35$, $\alpha_s = 0.0^\circ$, $a_{1s} = b_{1s} = 0.0^\circ$, $\Omega_s R = 700$ ft/sec, $\theta_c = 4.0^\circ$.

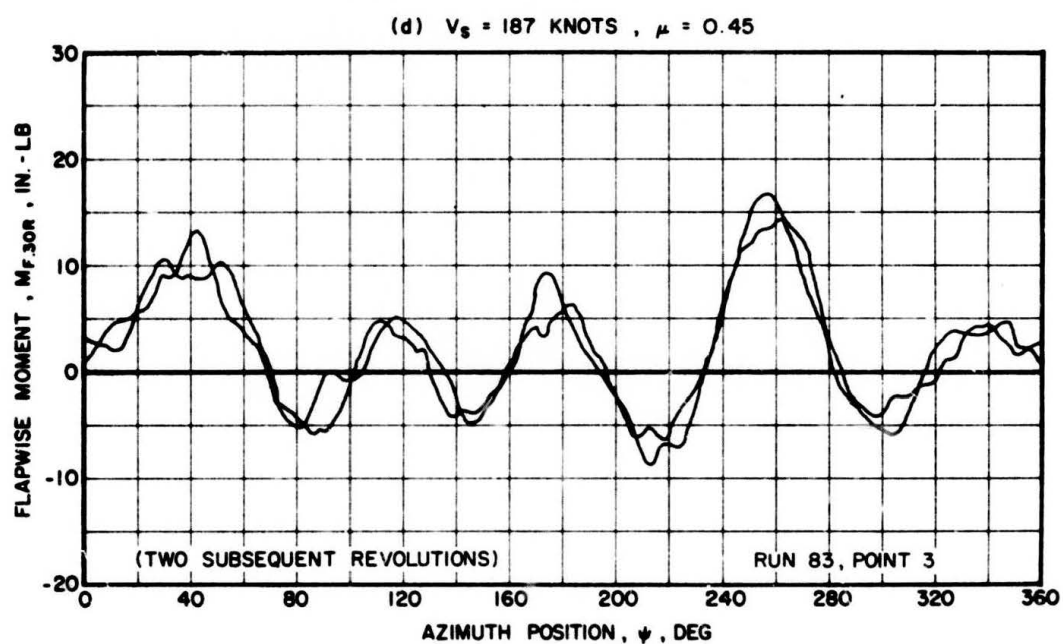
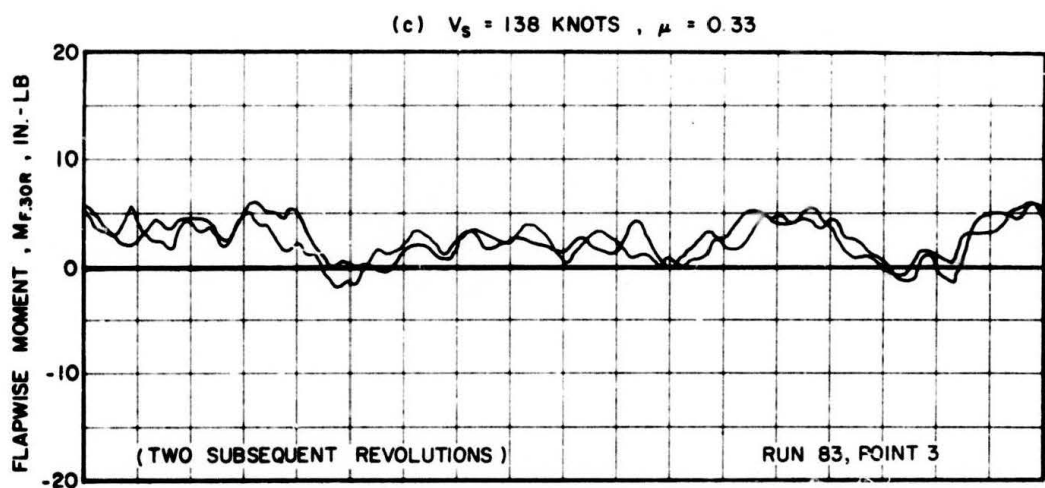


Figure 39. Continued.

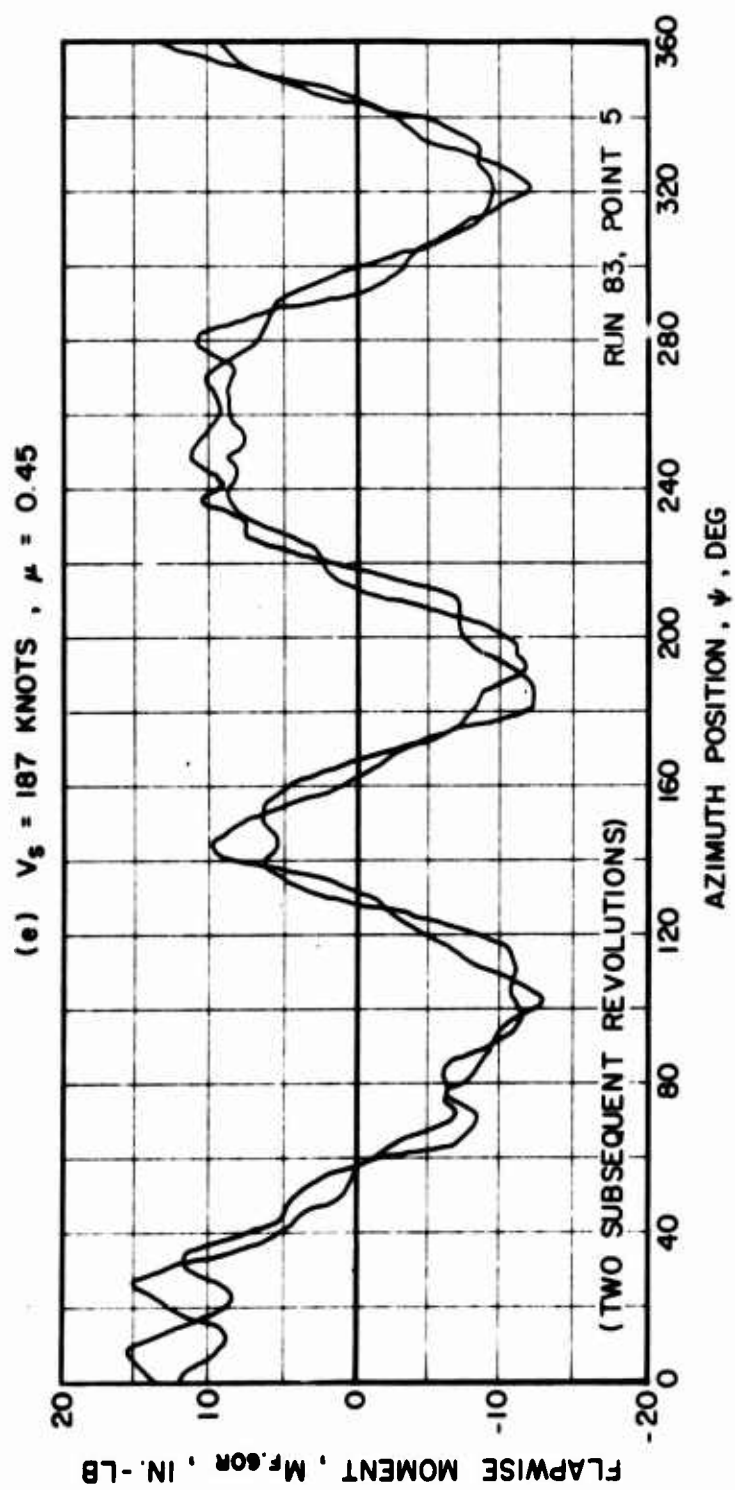


Figure 39. Continued.

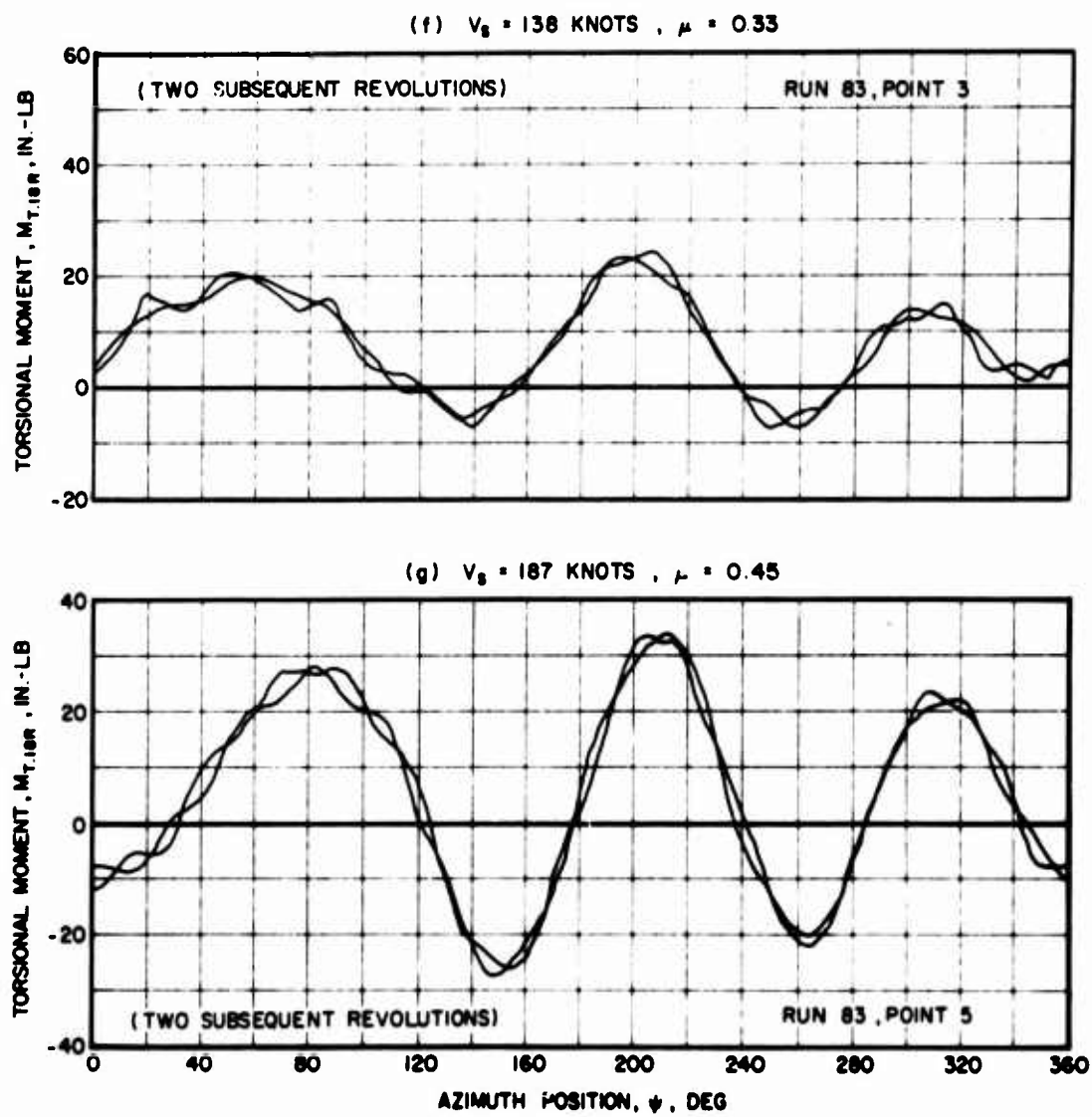


Figure 39. Continued.

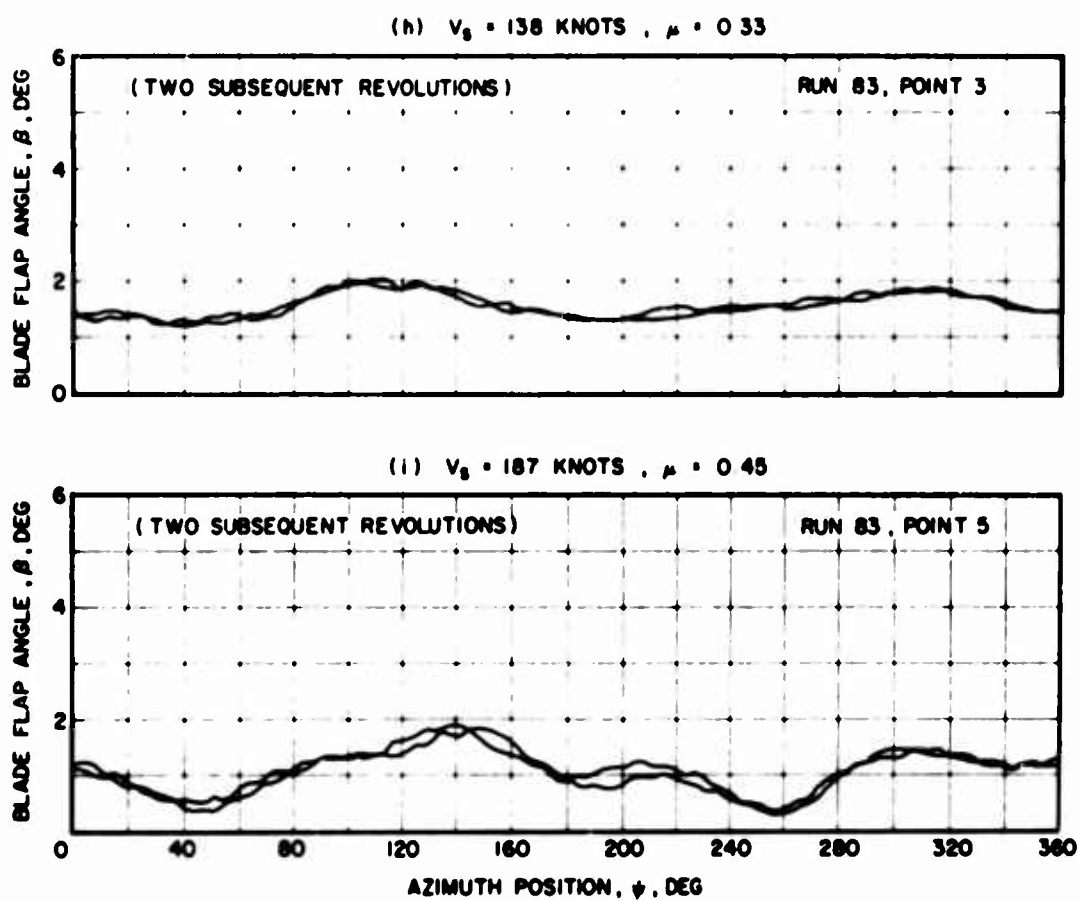


Figure 39. Continued.

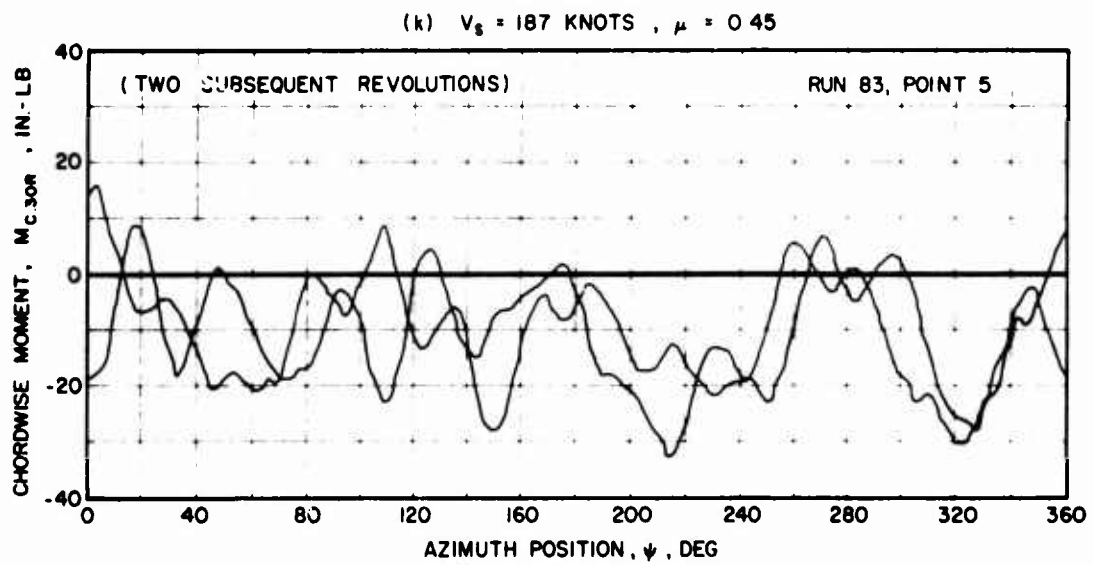
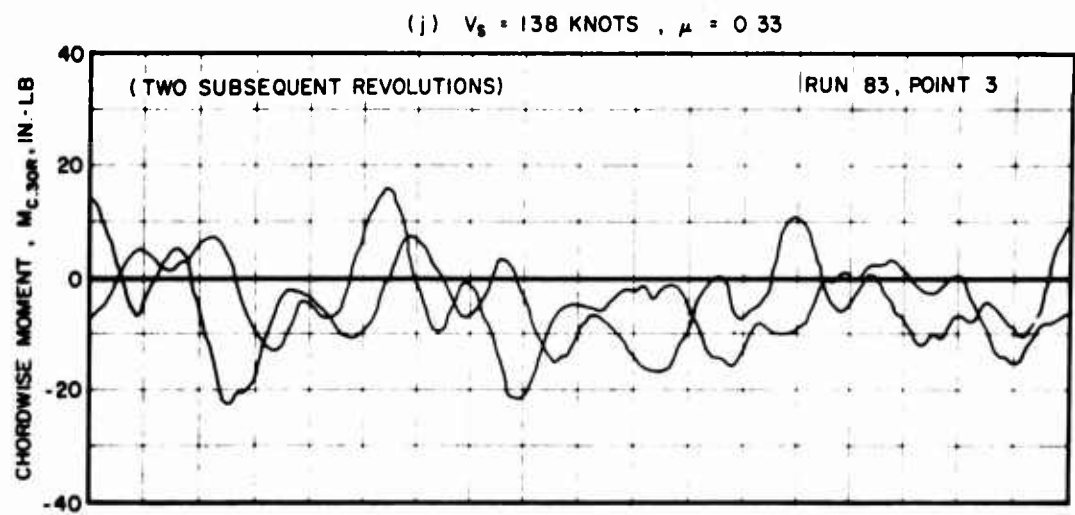


Figure 39. Concluded.

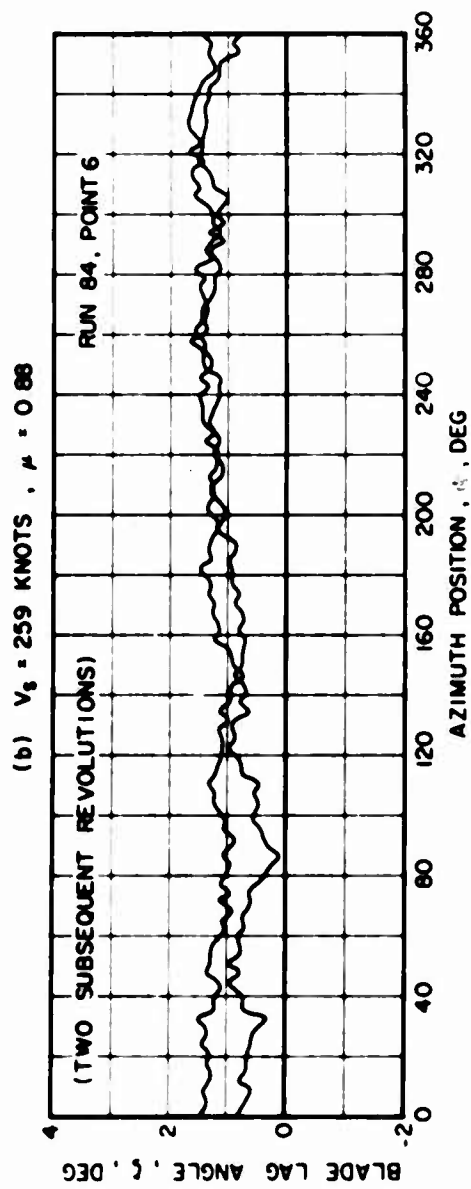
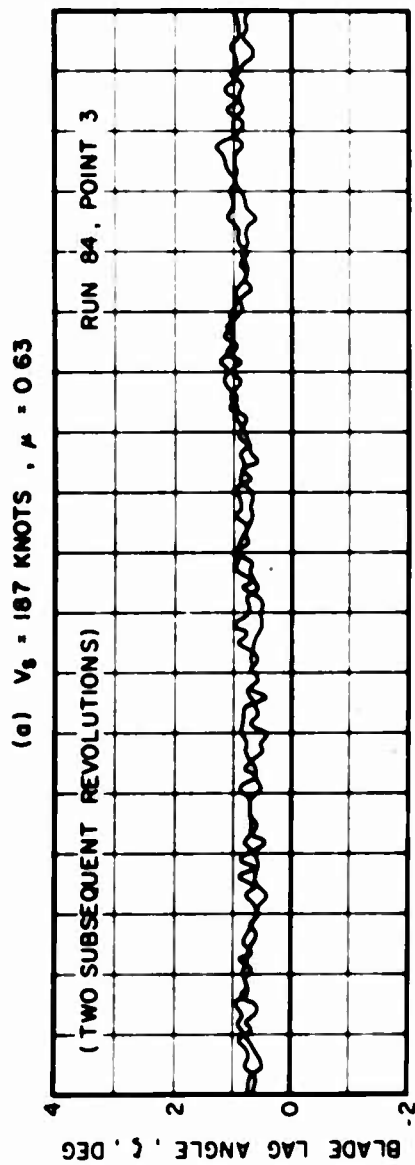


Figure 40. Blade Response Versus Azimuth During Advancing Blade Aeroelastic Limits Testing; $Y_{CG}/c = 0.35$, $\alpha_s = 0.0^\circ$, $a_{ls} = b_{ls} = 0.0^\circ$, $\Omega_s R = 500$ ft/sec, $\theta_c = 4.0^\circ$.

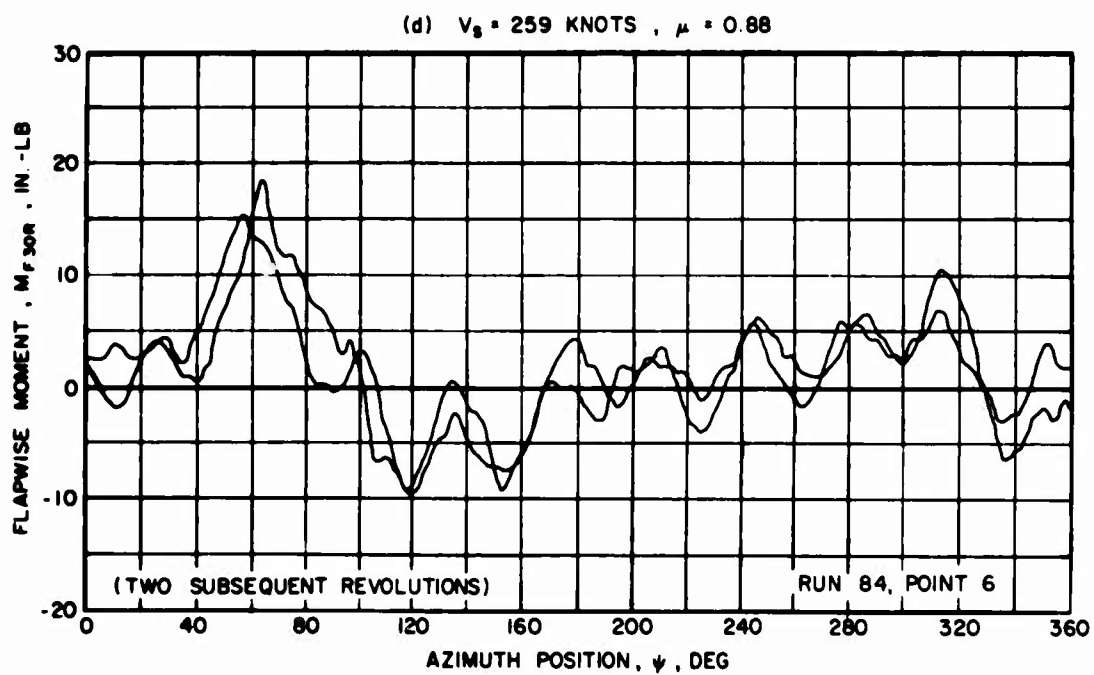
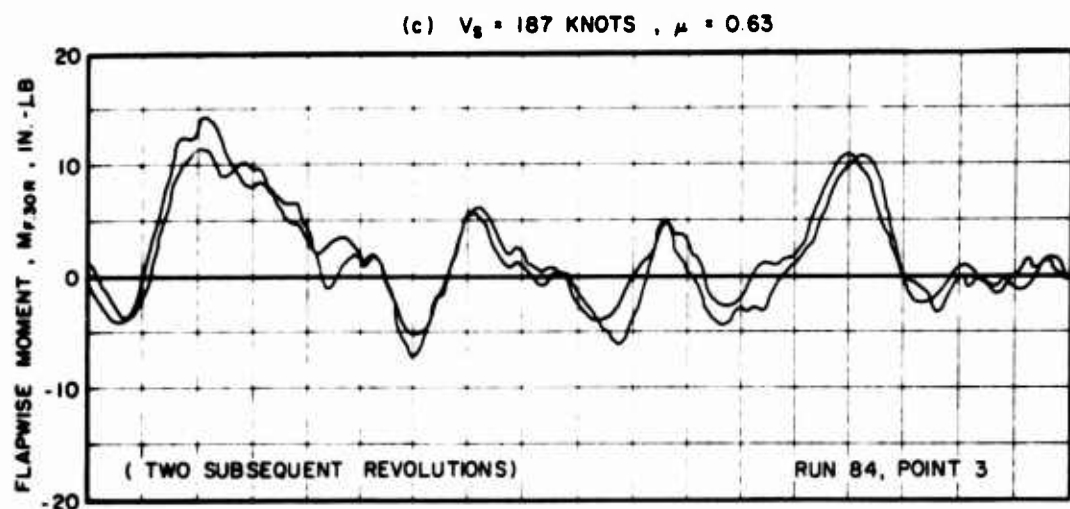


Figure 40. Continued.

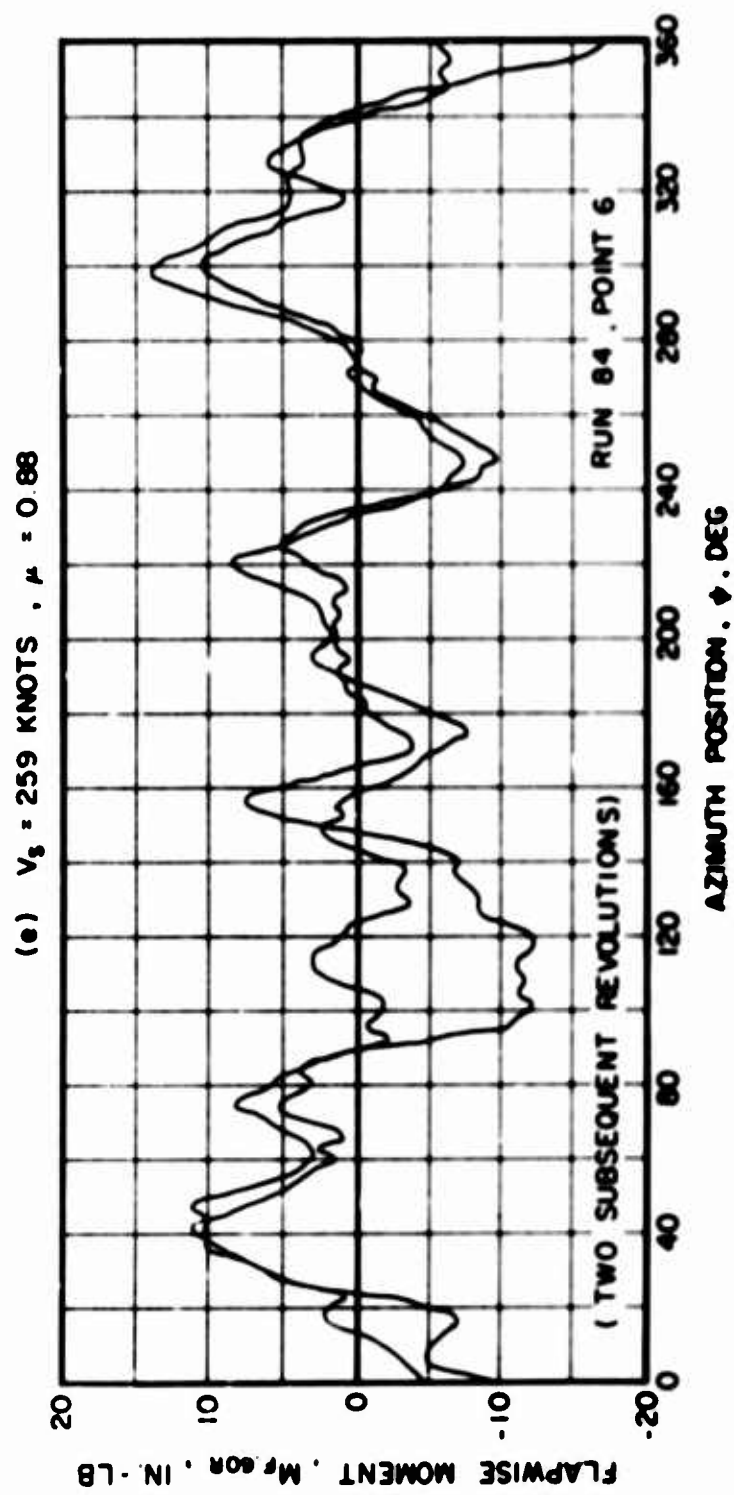


Figure 40. Continued.

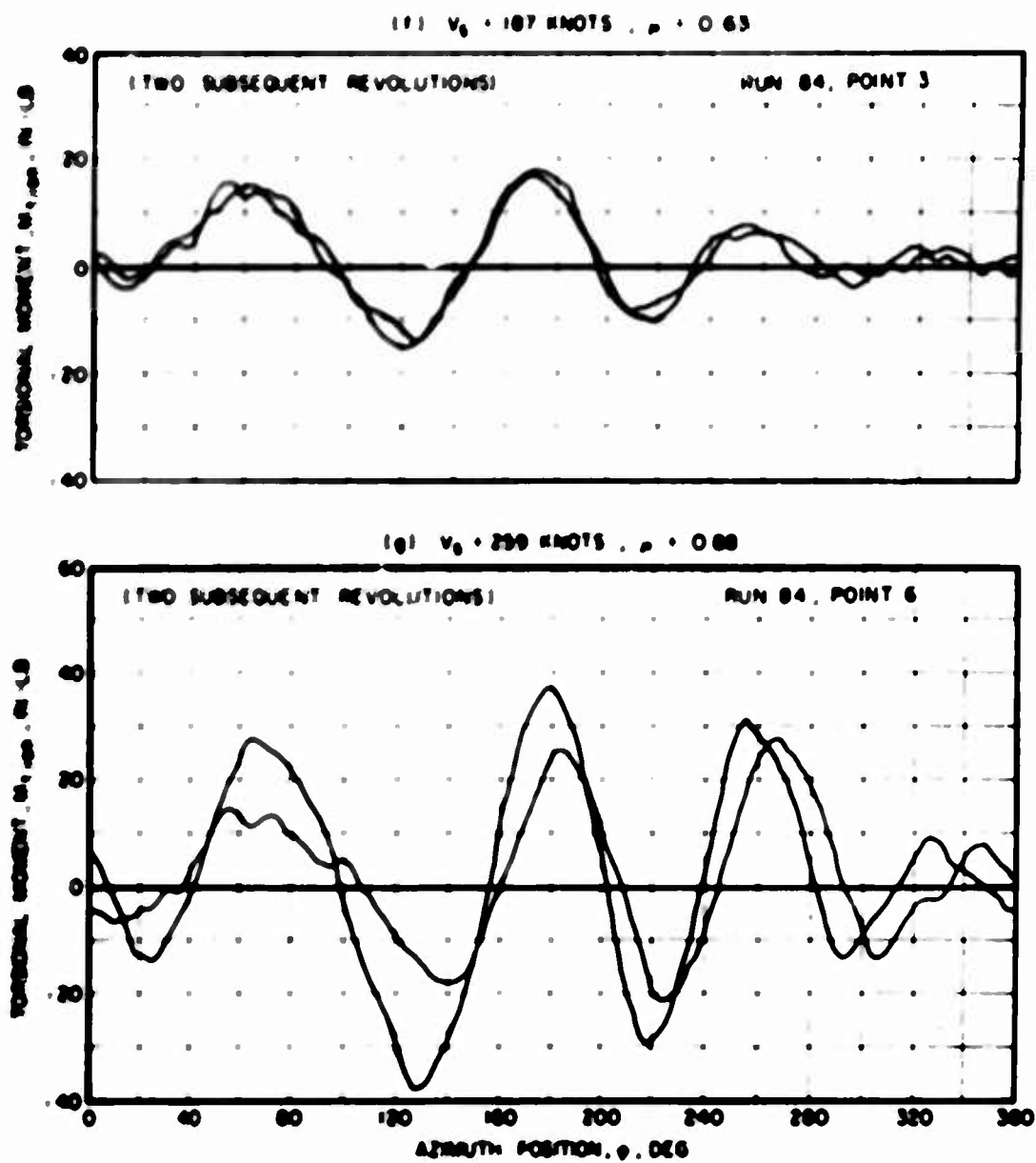


Figure 50. Continued.

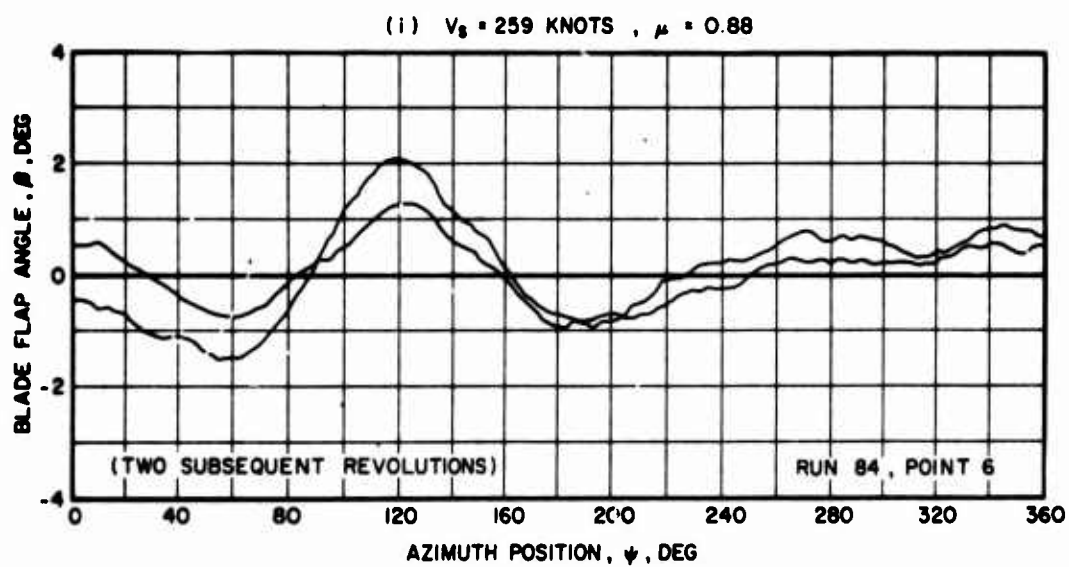
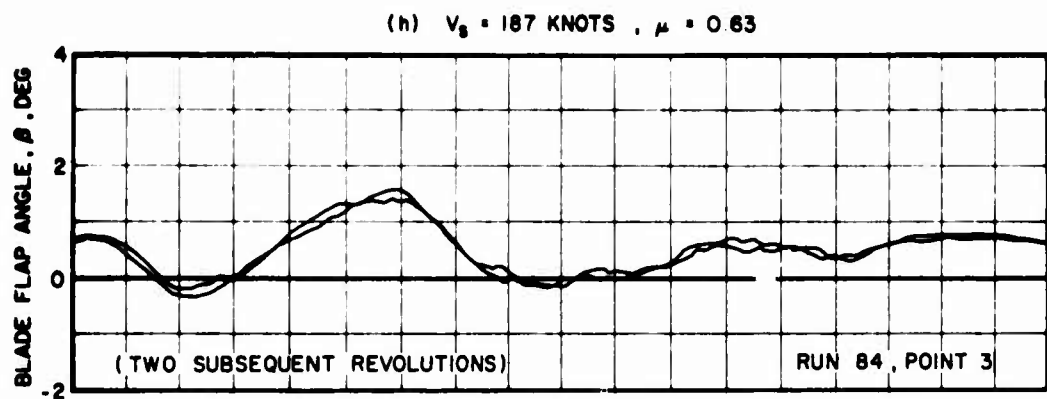


Figure 40. Continued.

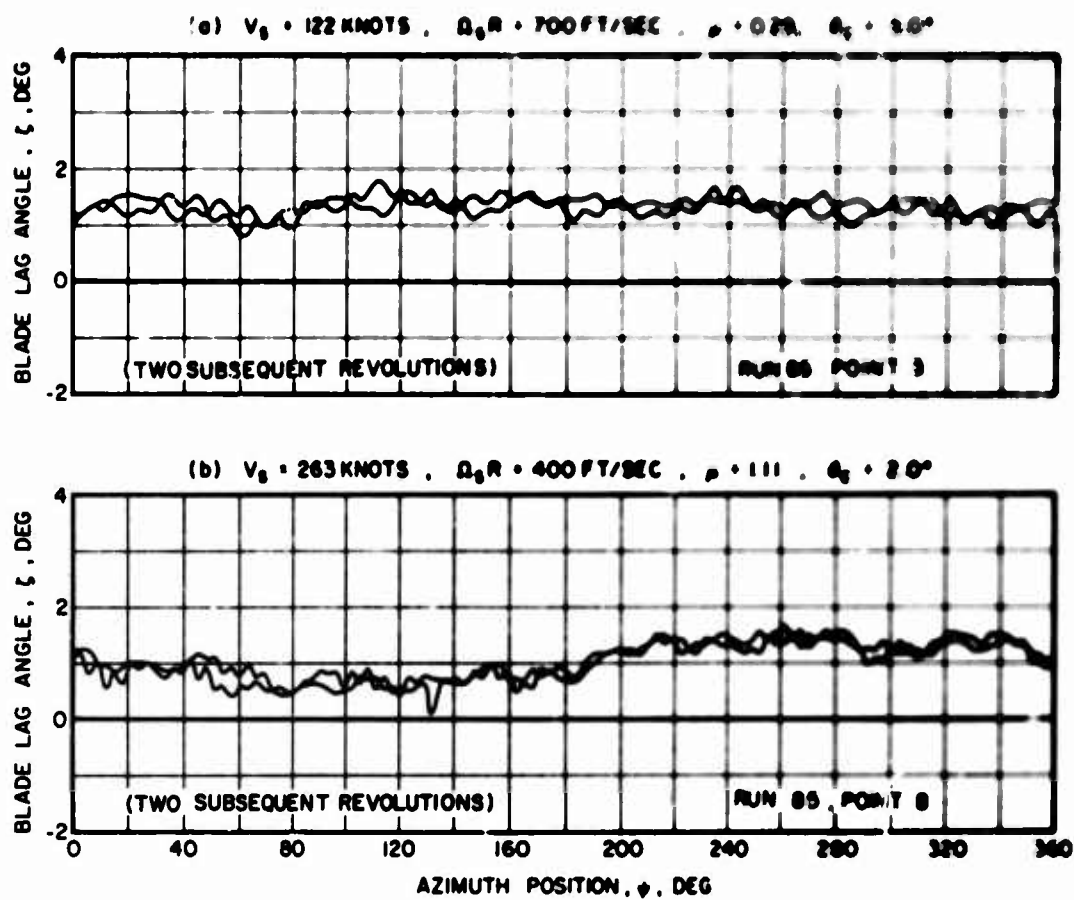


Figure 41. Blade Response Versus Azimuth During Advancing and Combined Advancing and Retreating Blade Aeroelastic Limits Testing; $Y_{CG}/c = 0.35$, $\alpha_s = 0.0^\circ$, $a_{1s} = b_{1s} = 0.0^\circ$.

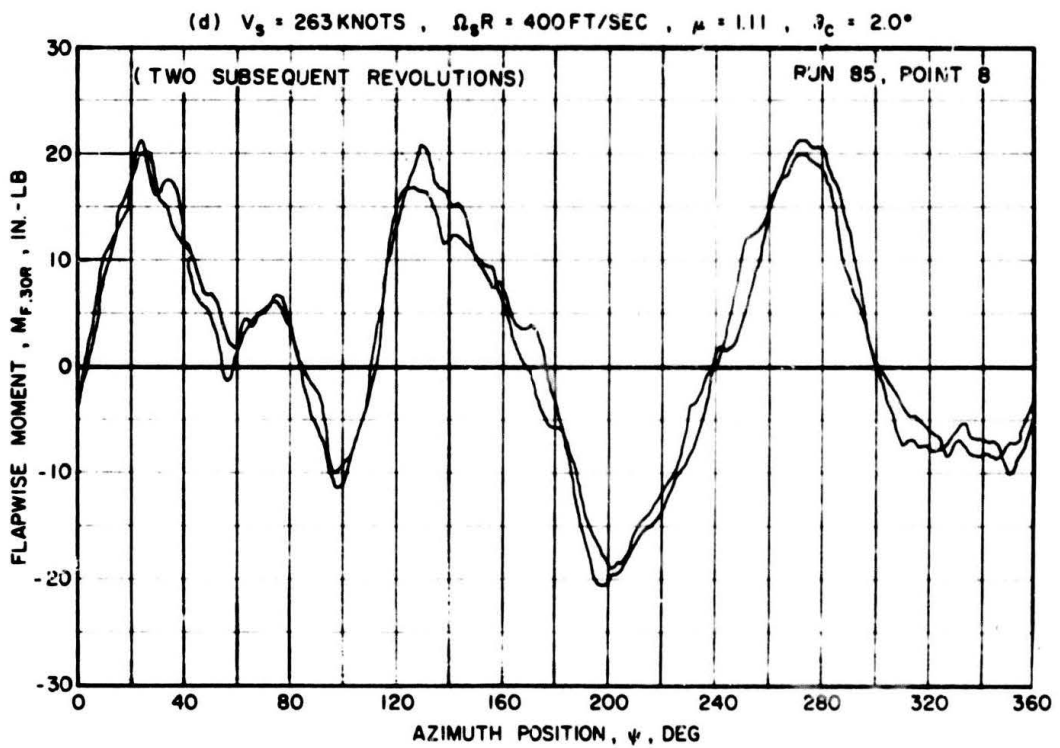
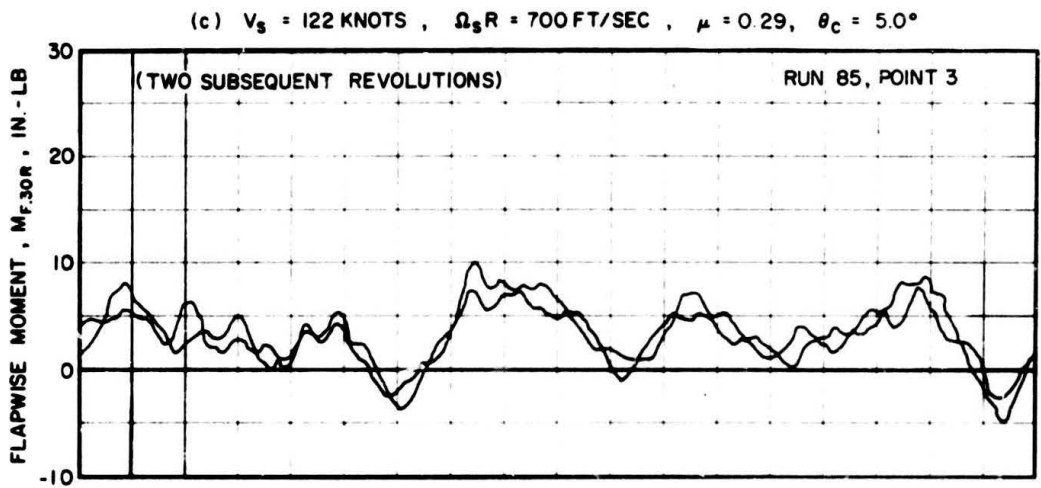


Figure 41. Continued.

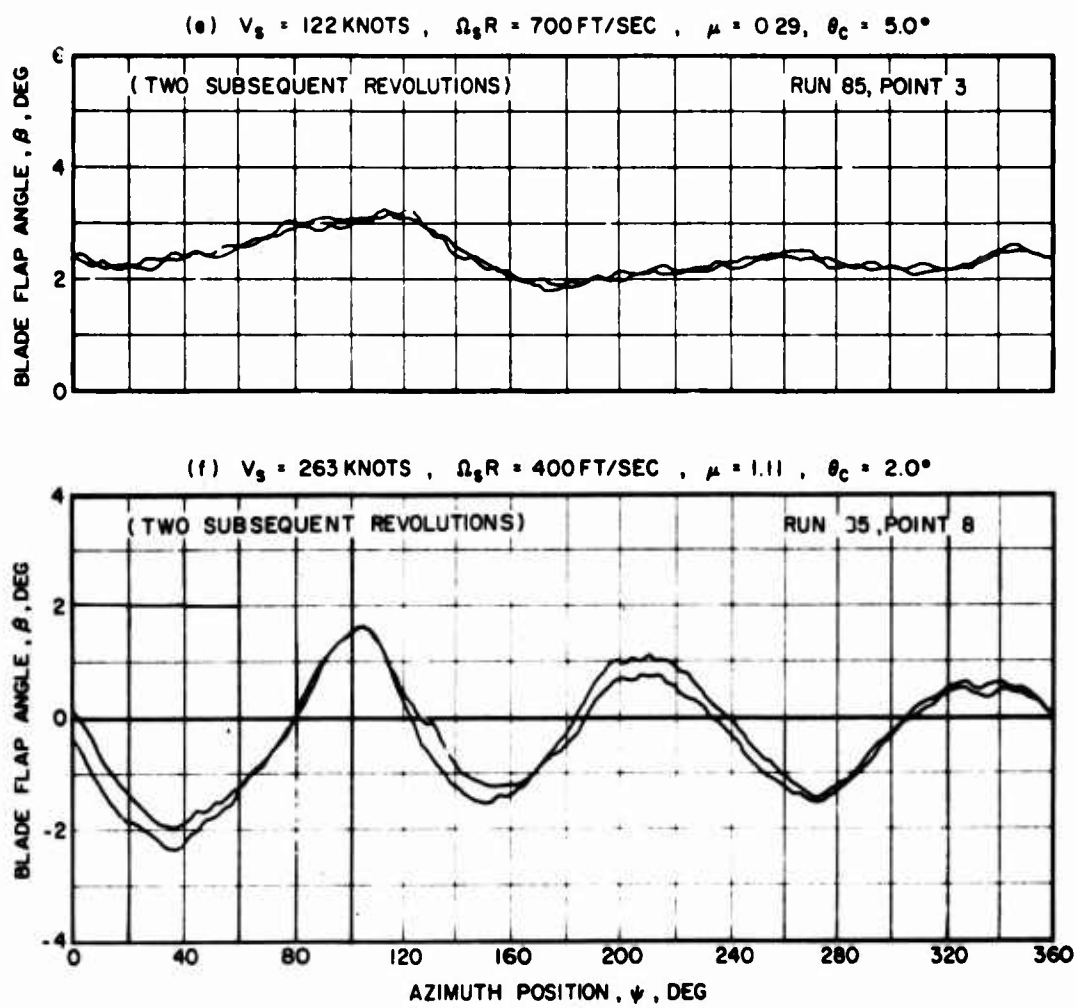


Figure 41. Continued.

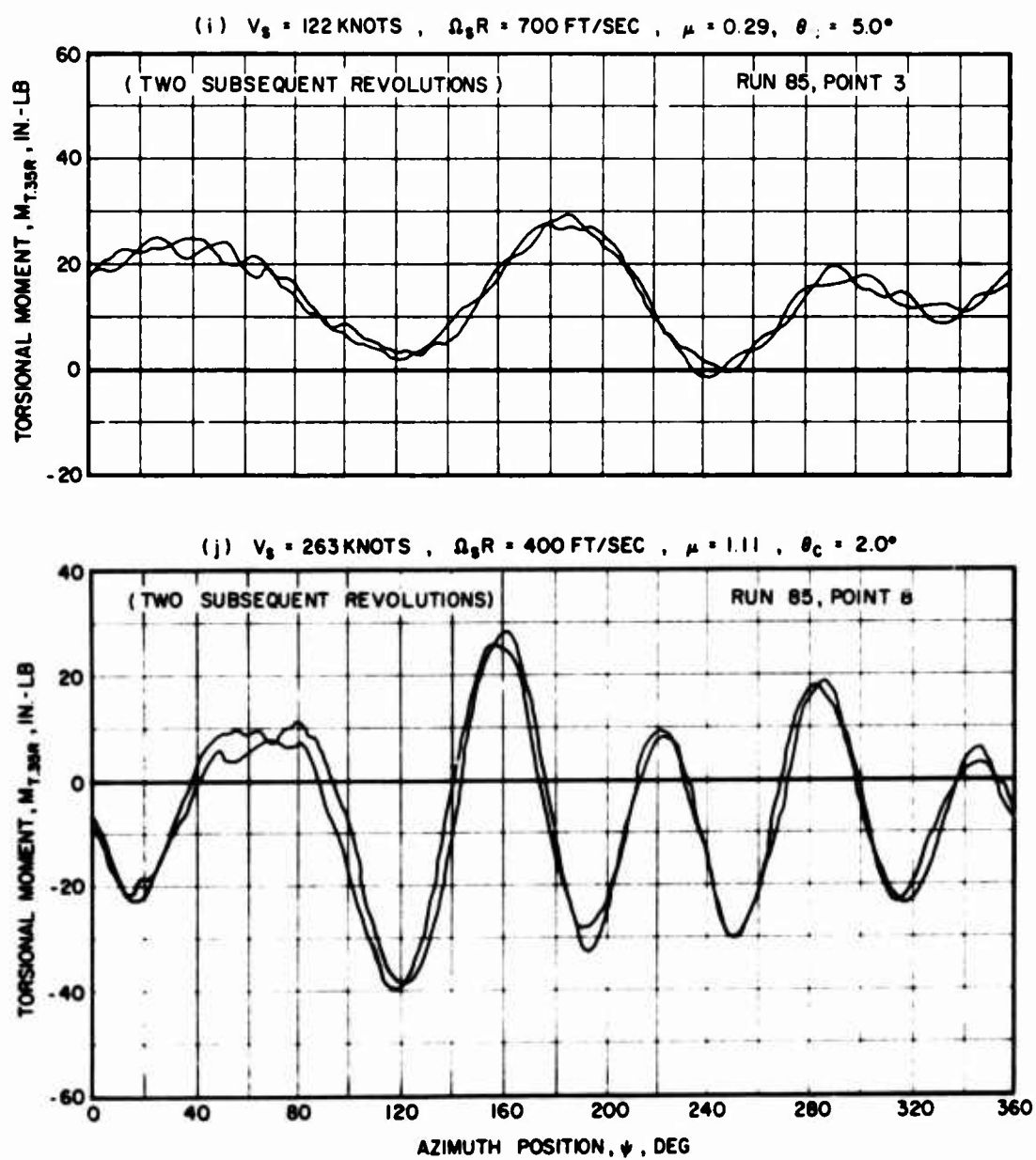


Figure 41. Concluded.

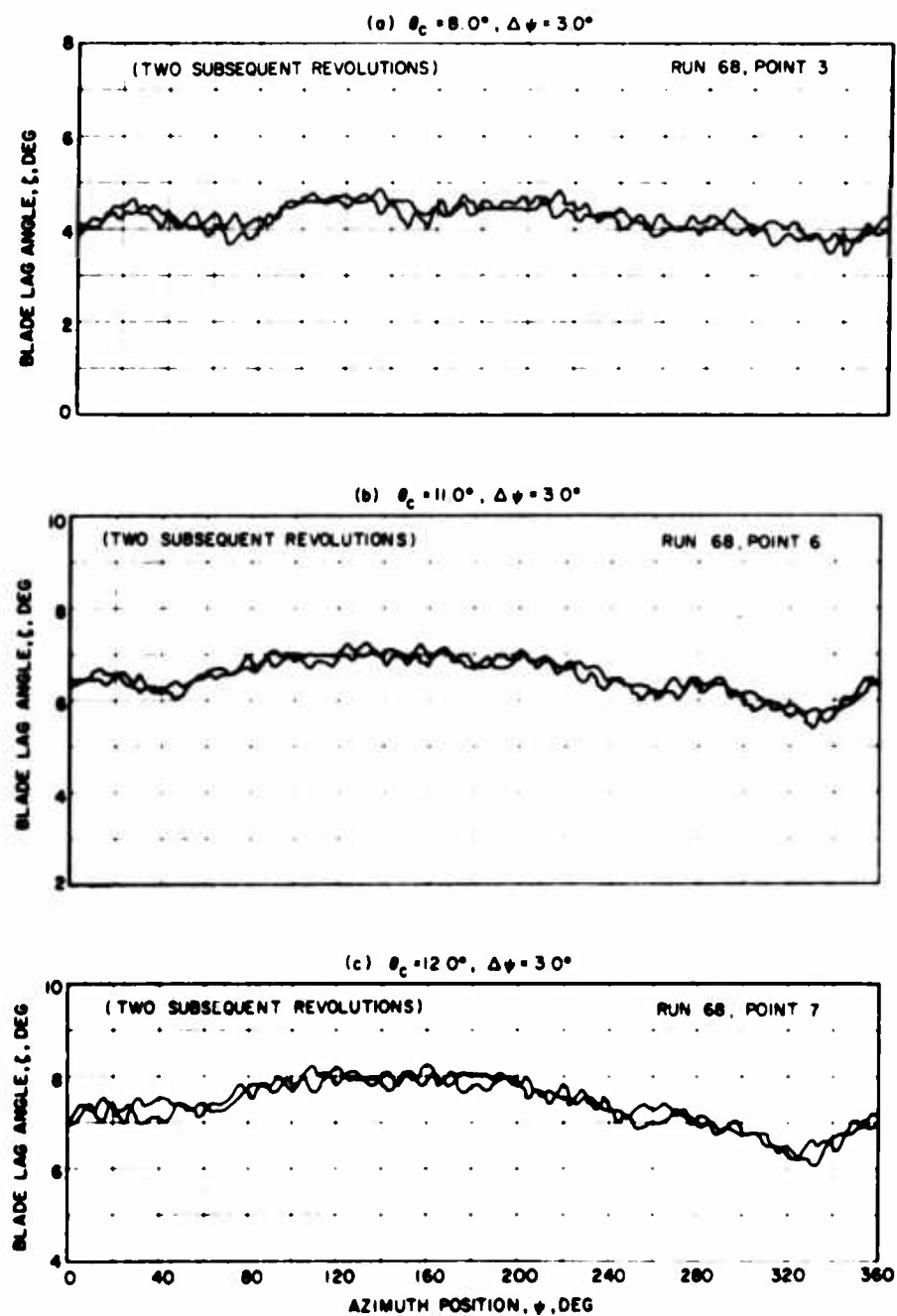


Figure 42. Blade Response Versus Azimuth During Stall Flutter Testing; $Y_{CG}/c = 0.25$, $\alpha_s = 0.0^\circ$, $a_{1s} = b_{1s} = 0.0^\circ$, $V_s = 121$ kn, $\Omega_s R = 700$ ft/sec, $\nu = 0.29$.

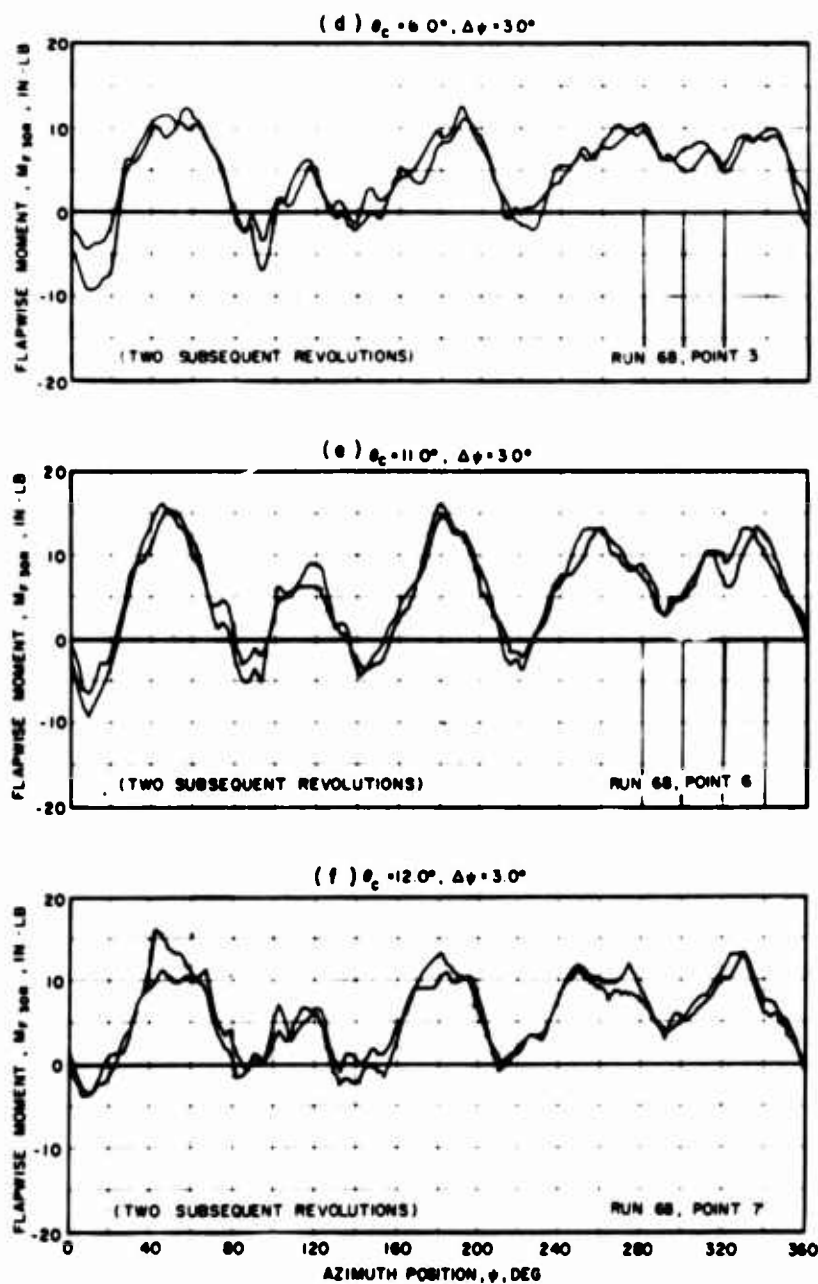


Figure 42. Continued.

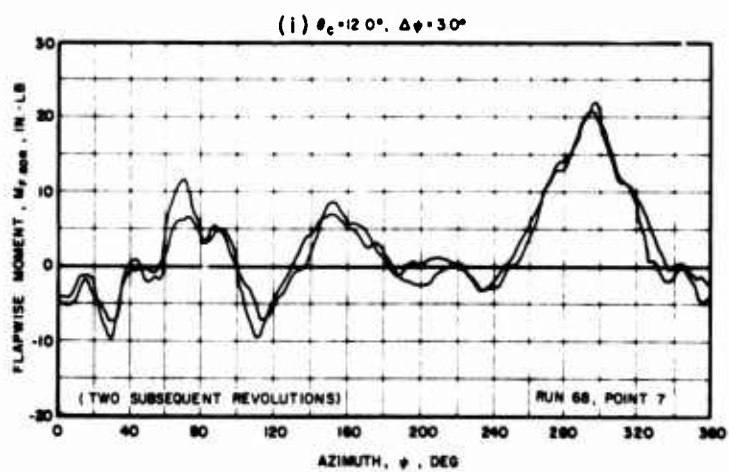
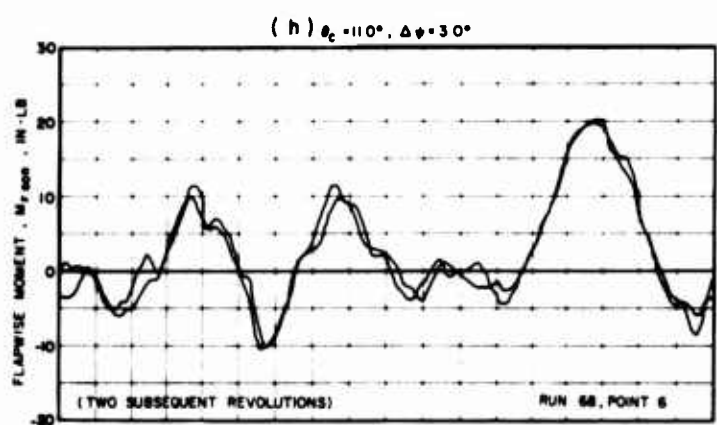
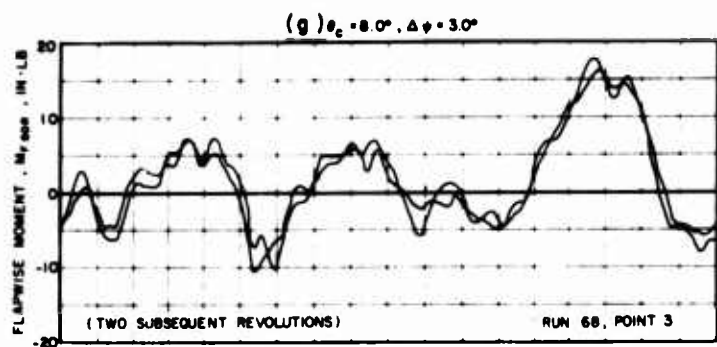


Figure 42. Continued.

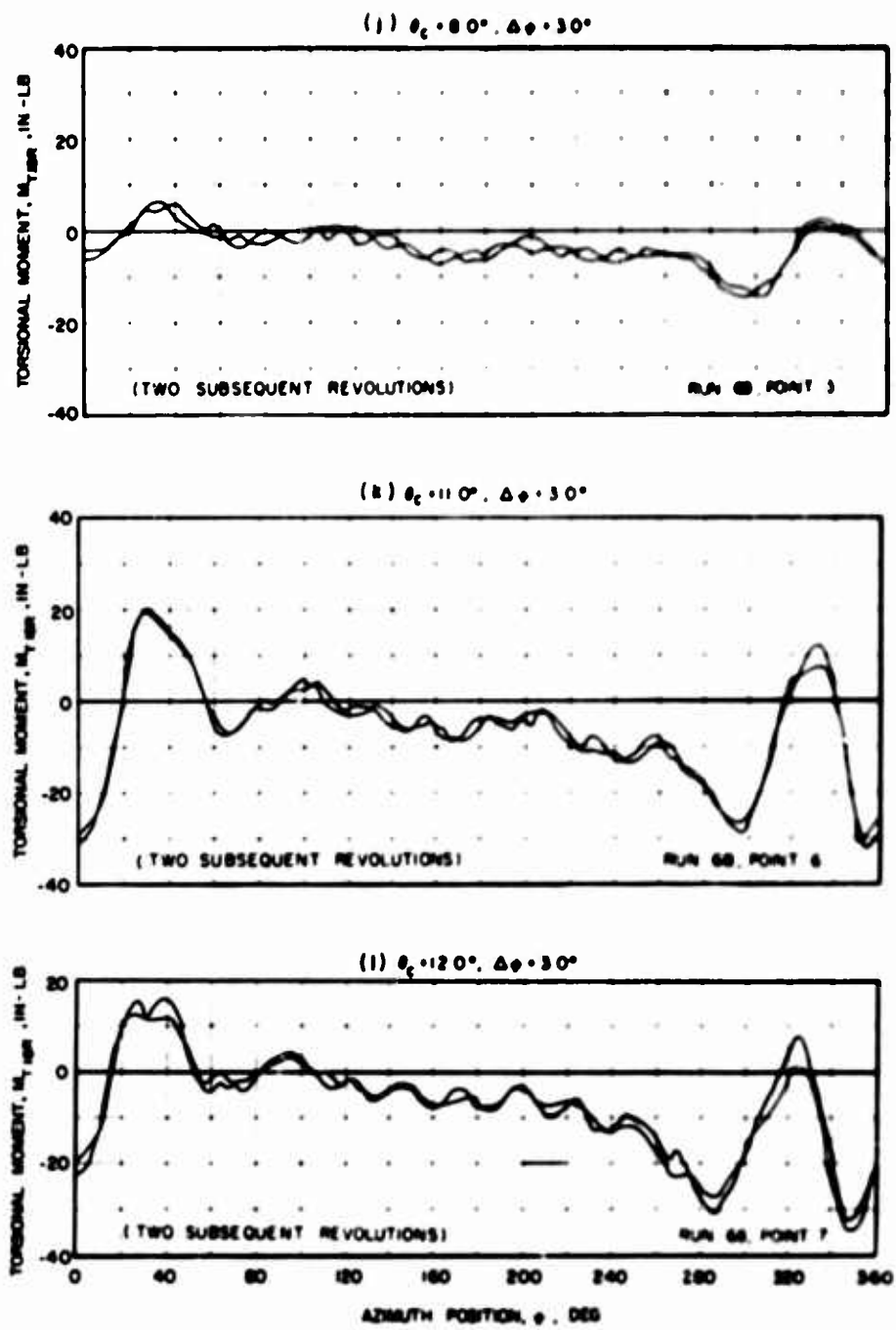


Figure 42. Continued.

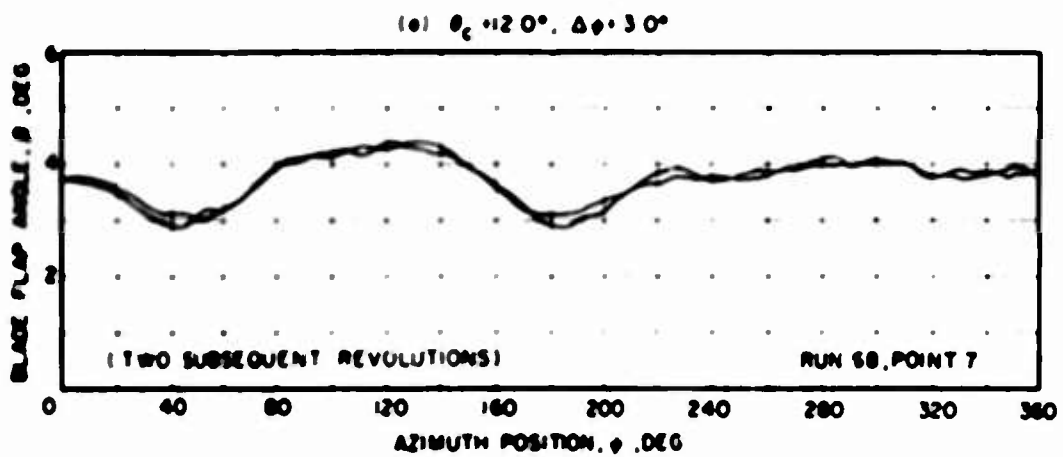
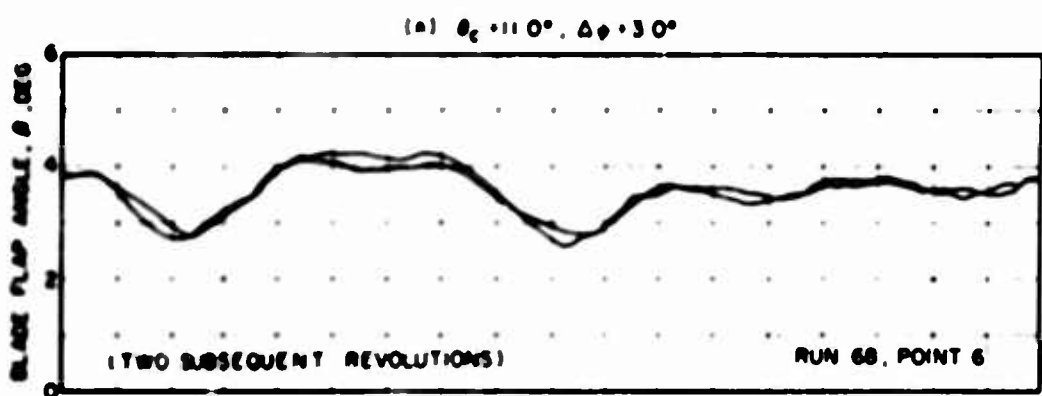
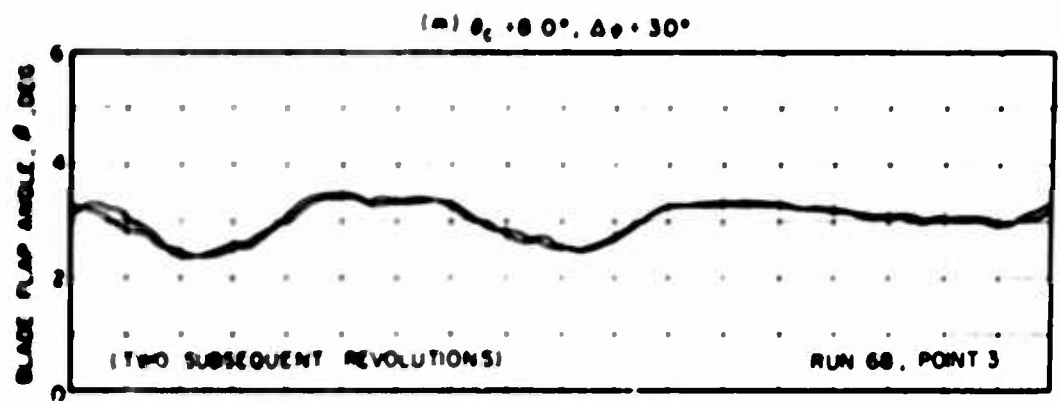


Figure 42. Concluded.

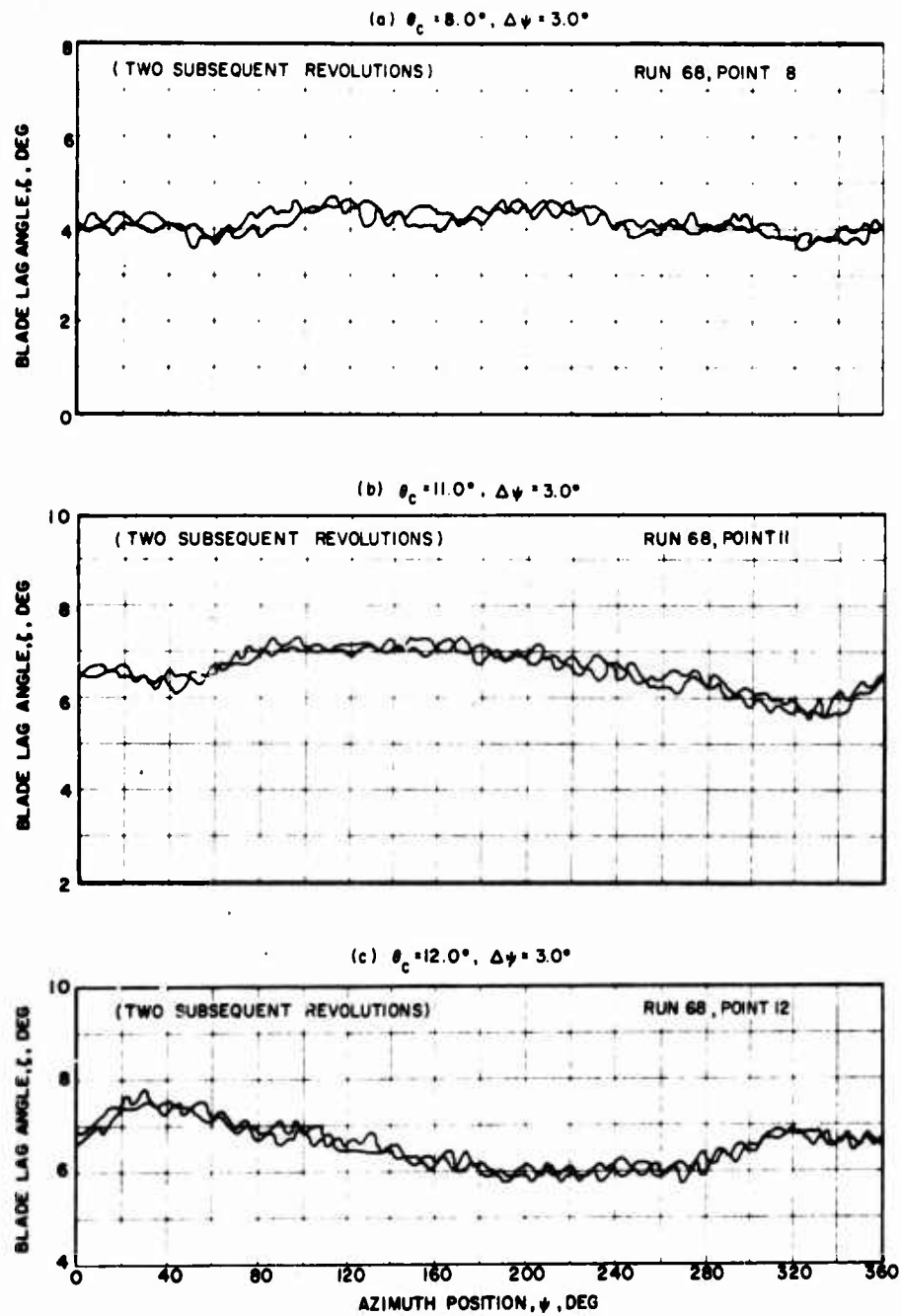


Figure 43. Blade Response Versus Azimuth During Stall Flutter Testing; $Y_{CG}/c = 0.25$, $\alpha_s = 0.0^\circ$, $a_{1s} = b_{1s} = 0.0^\circ$, $V_s = 145$ kn, $\Omega_s R = 700$ ft/sec, $\mu = 0.35$.

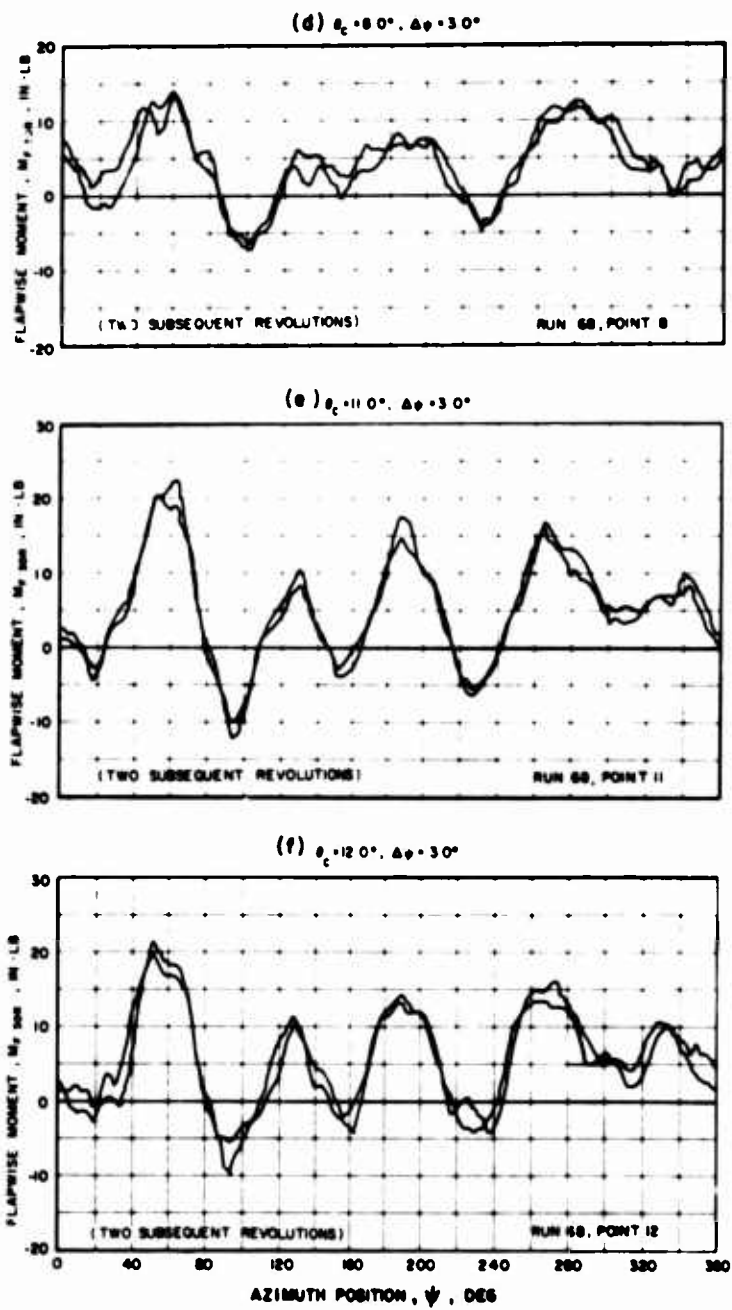


Figure 43. Continued.

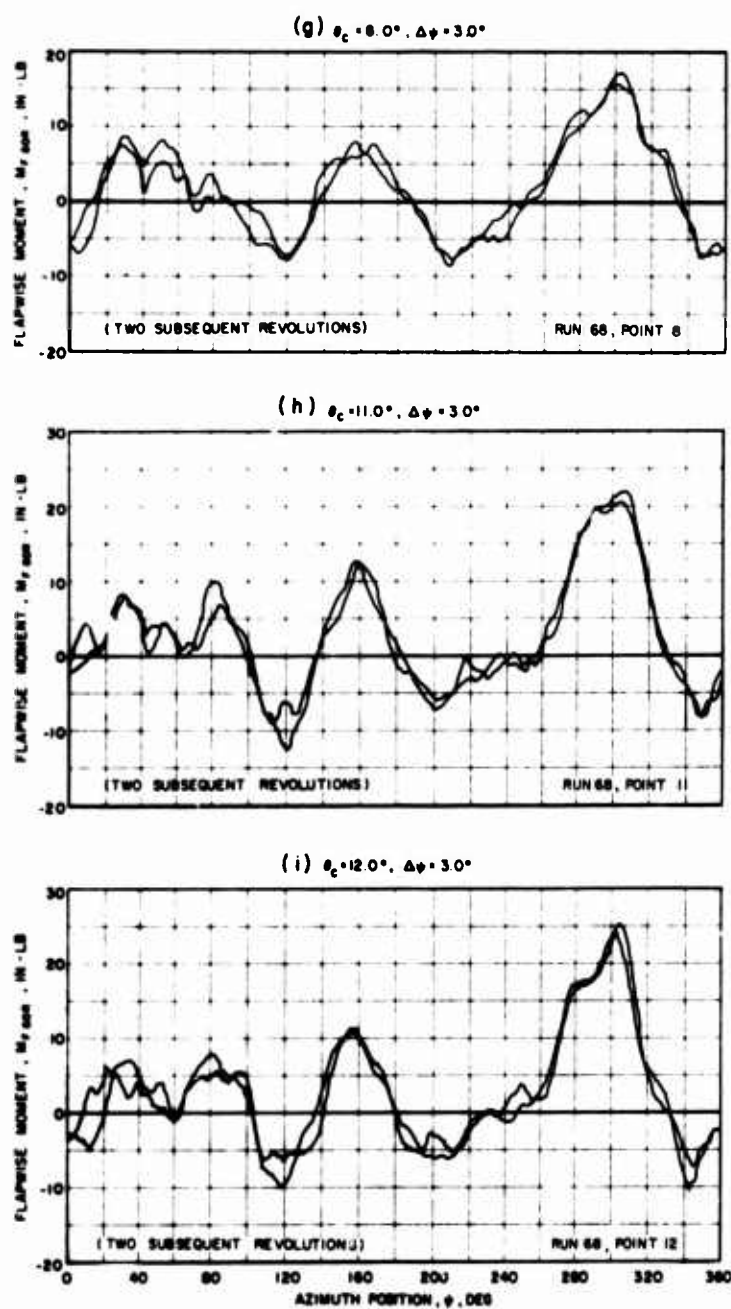


Figure 43. Continued.

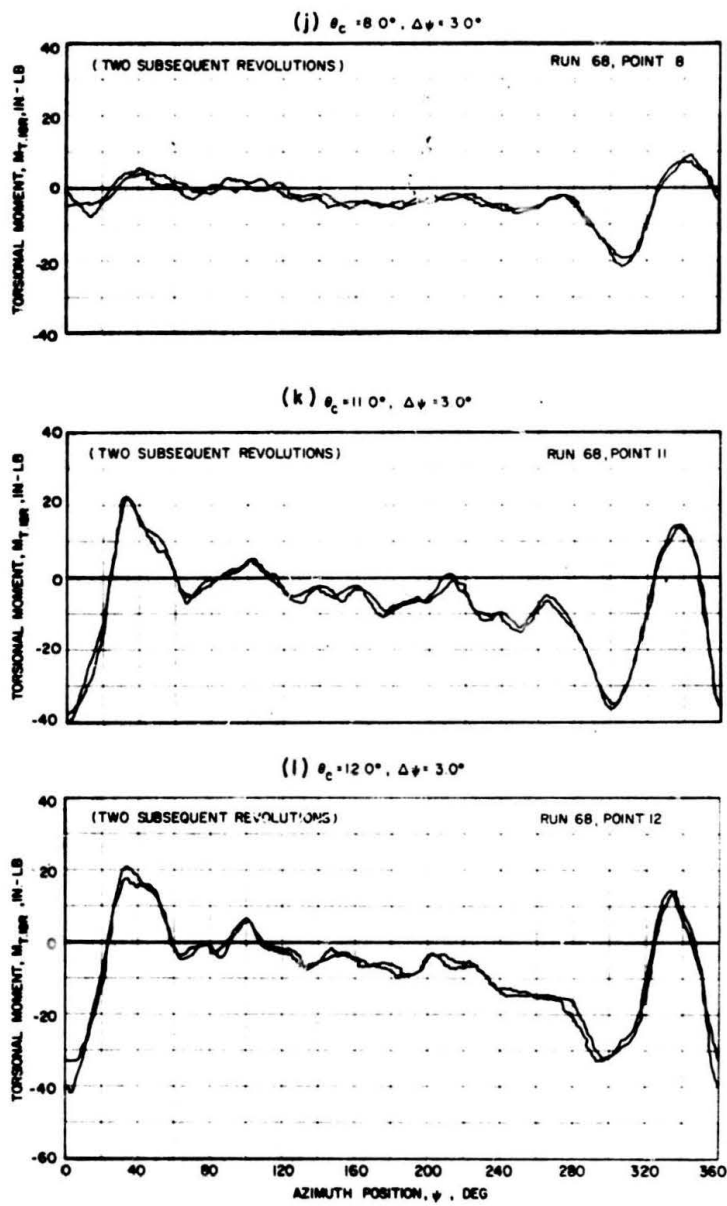


Figure 43. Continued.

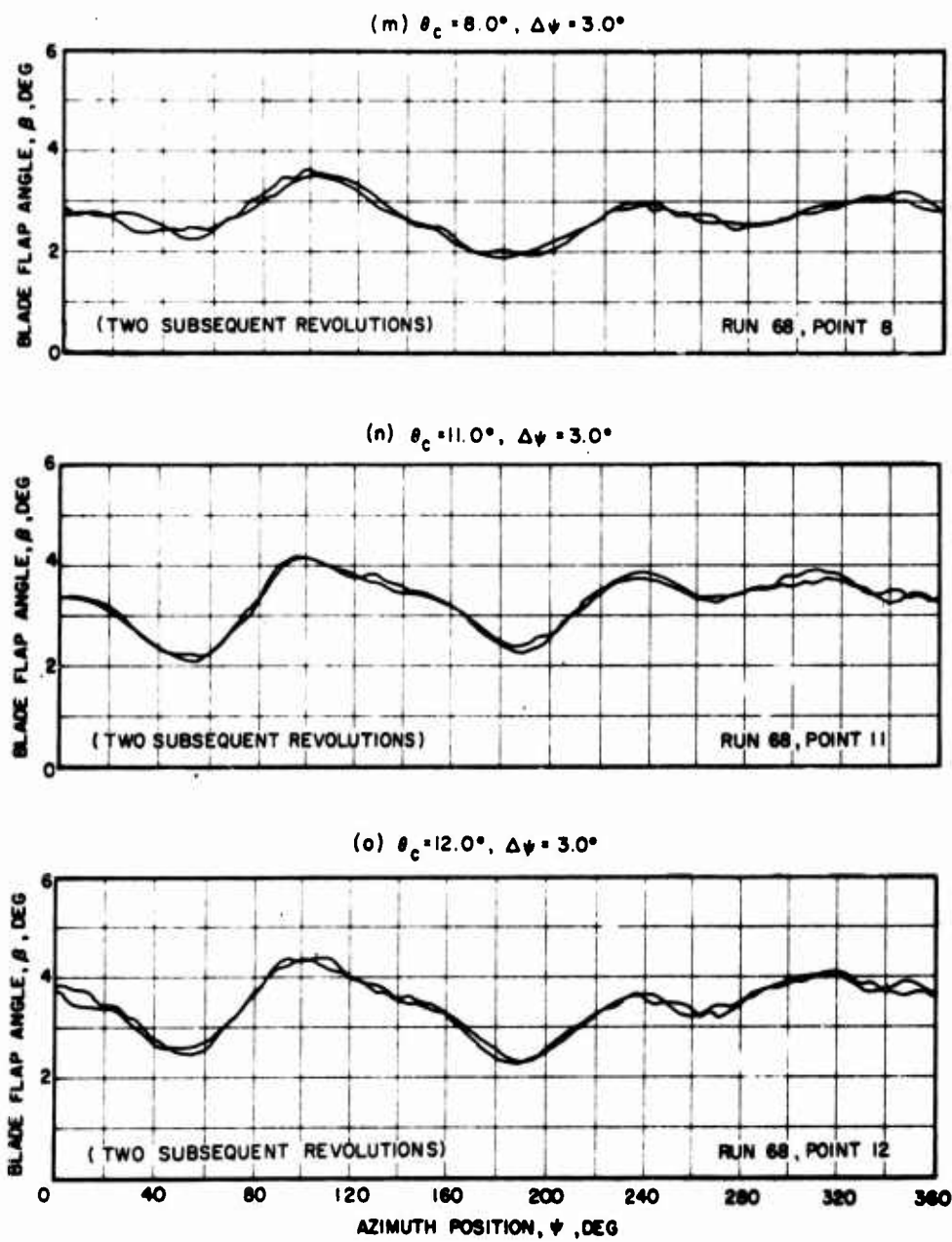


Figure 43. Concluded.

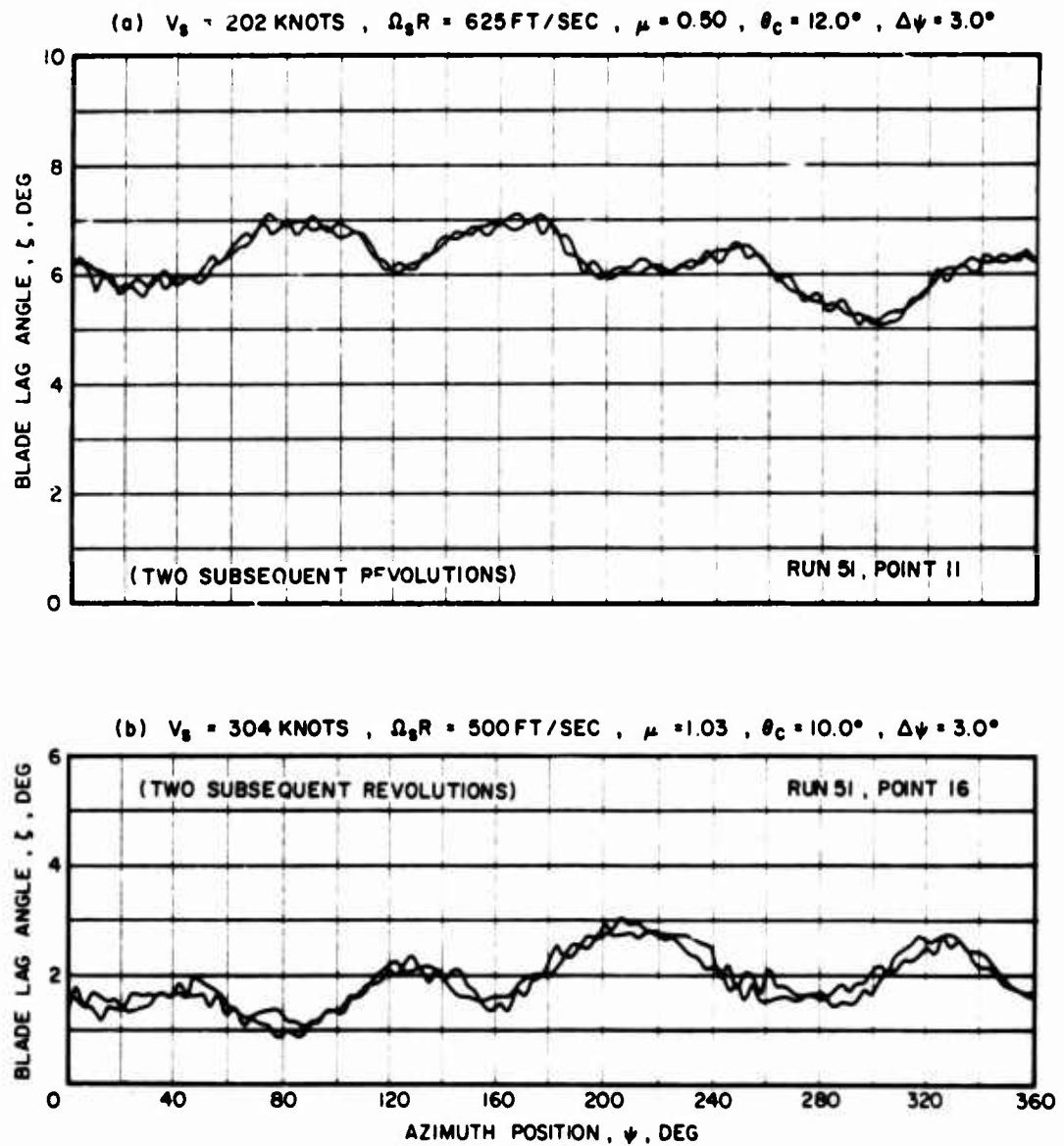


Figure 44. Blade Response Versus Azimuth During Stall Flutter Testing; $Y_{CG}/c = 0.25$, $\alpha_s = 0.0^\circ$, $a_{1s} = b_{1s} = 0.0^\circ$.

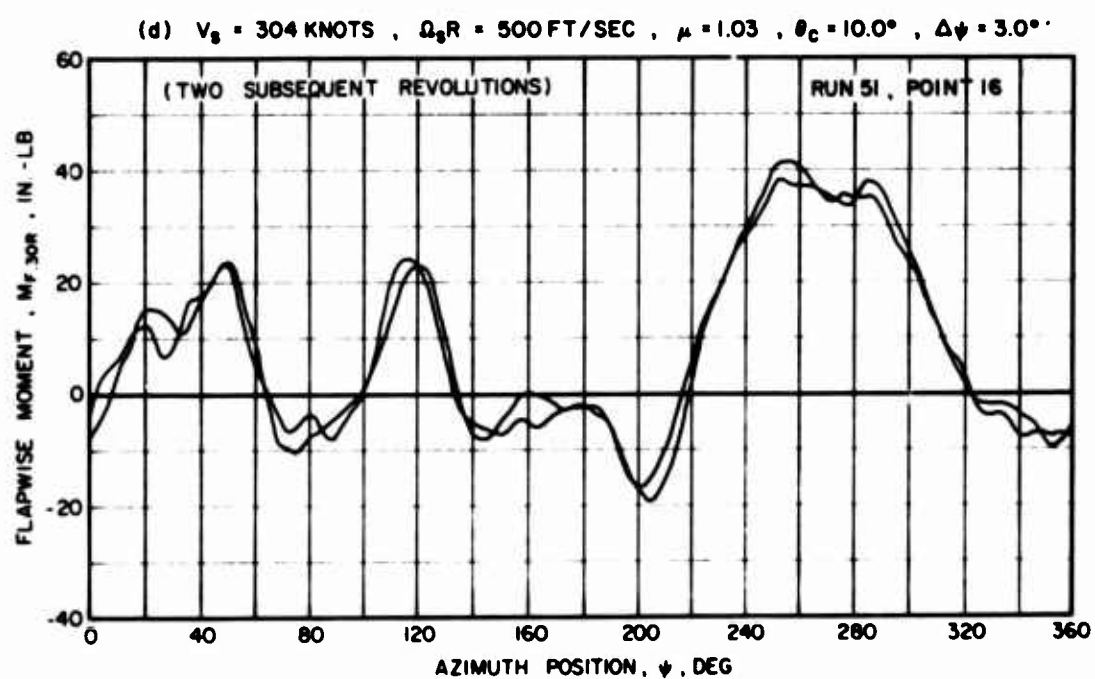
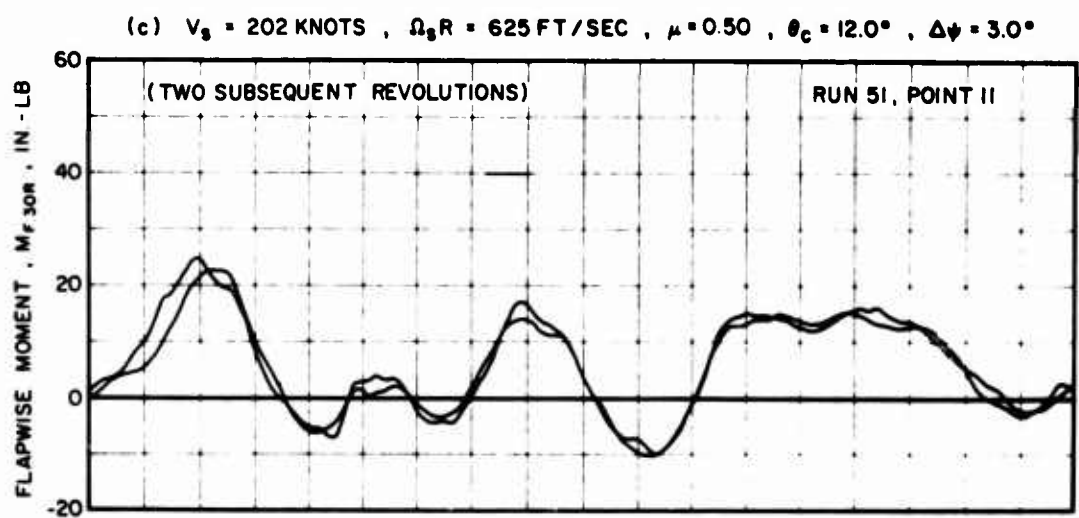


Figure 44. Continued.

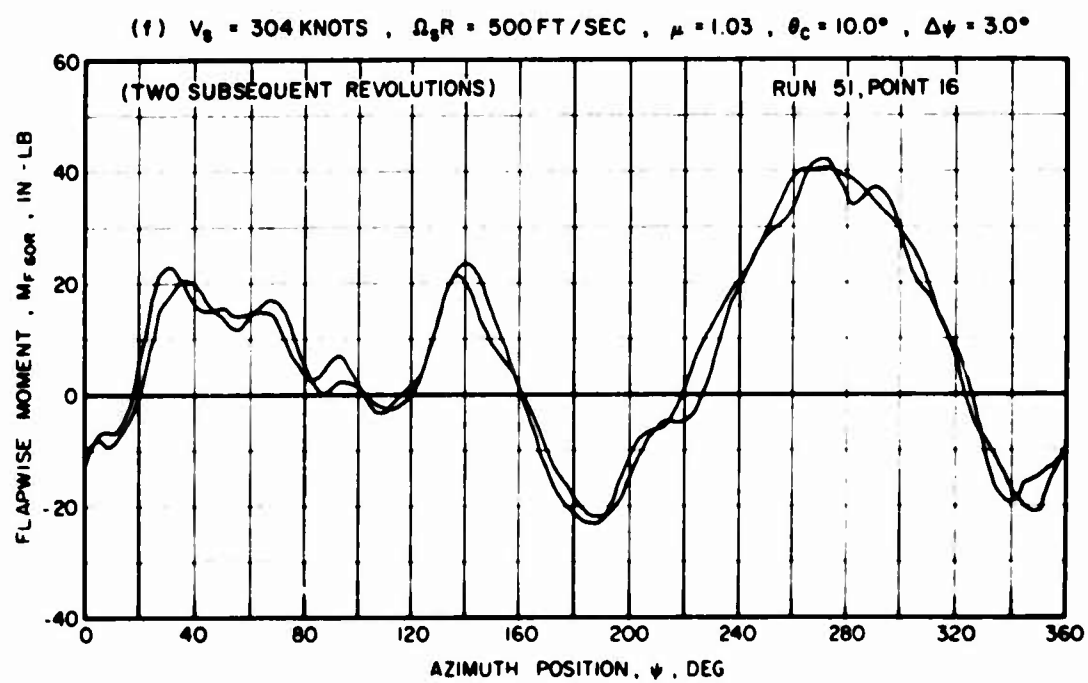
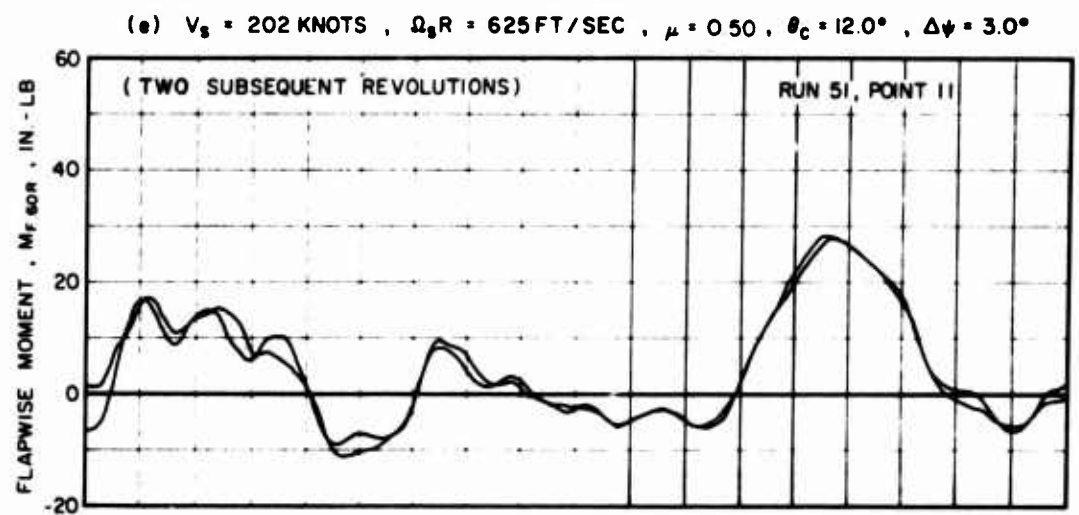


Figure 44. Continued.

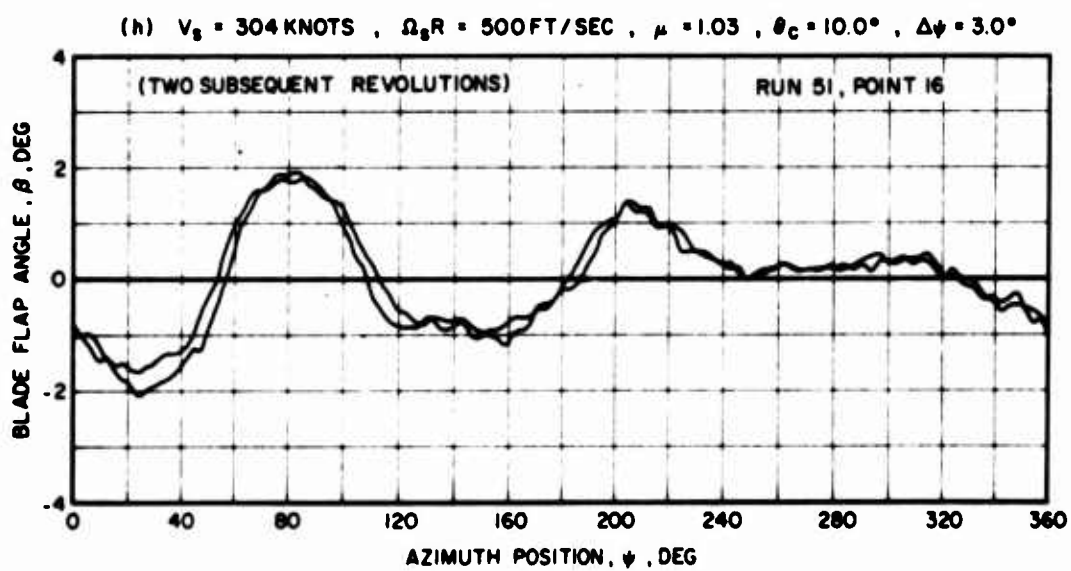
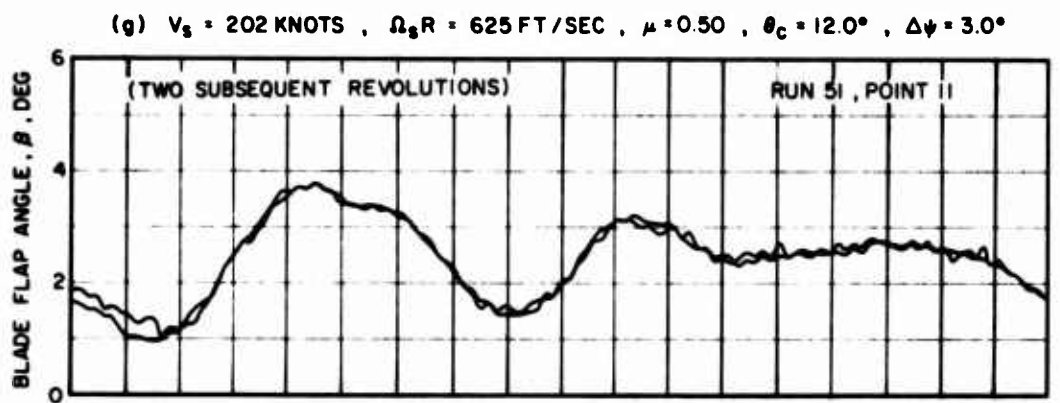


Figure 44. Continued.

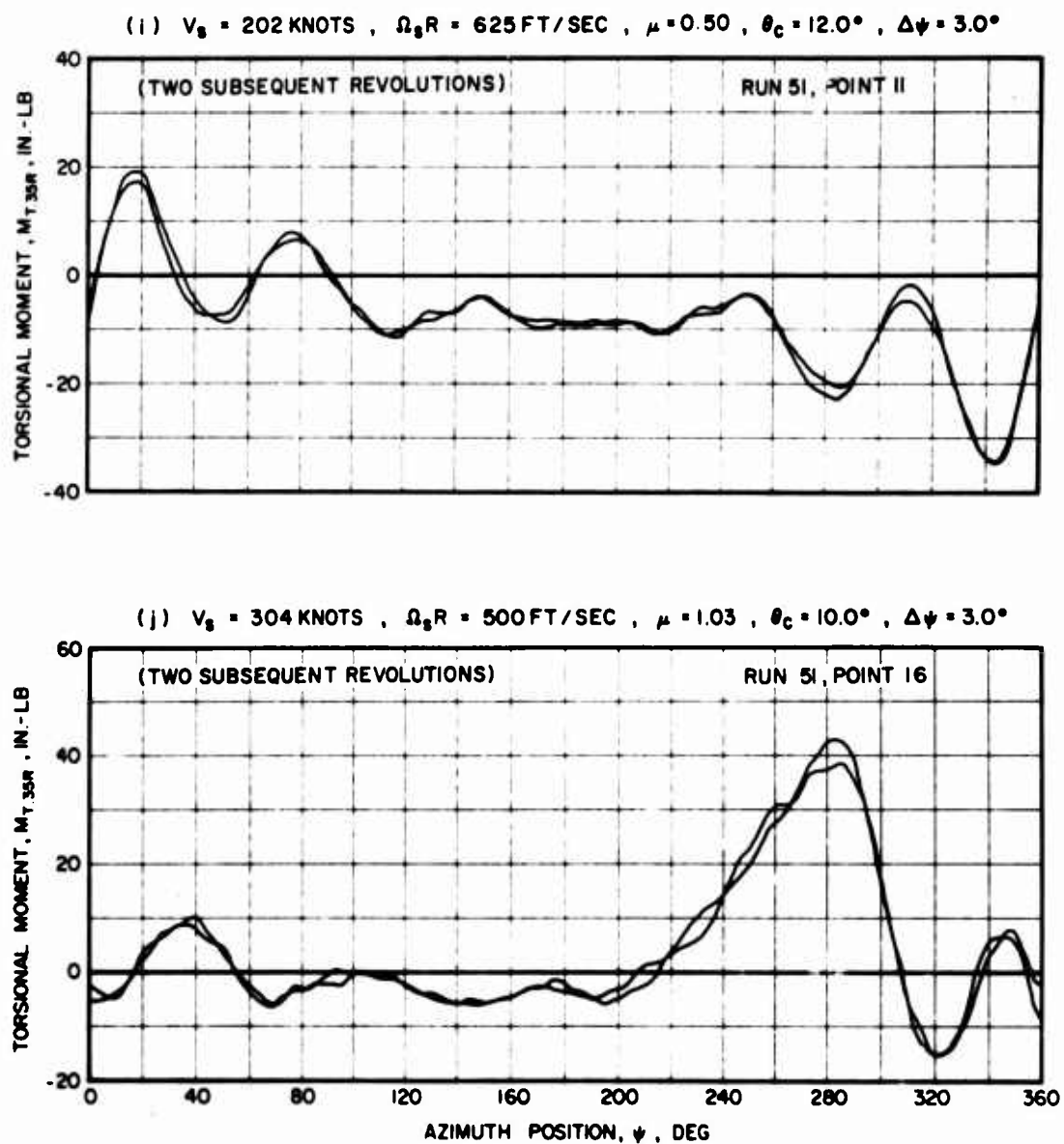


Figure 44. Concluded.

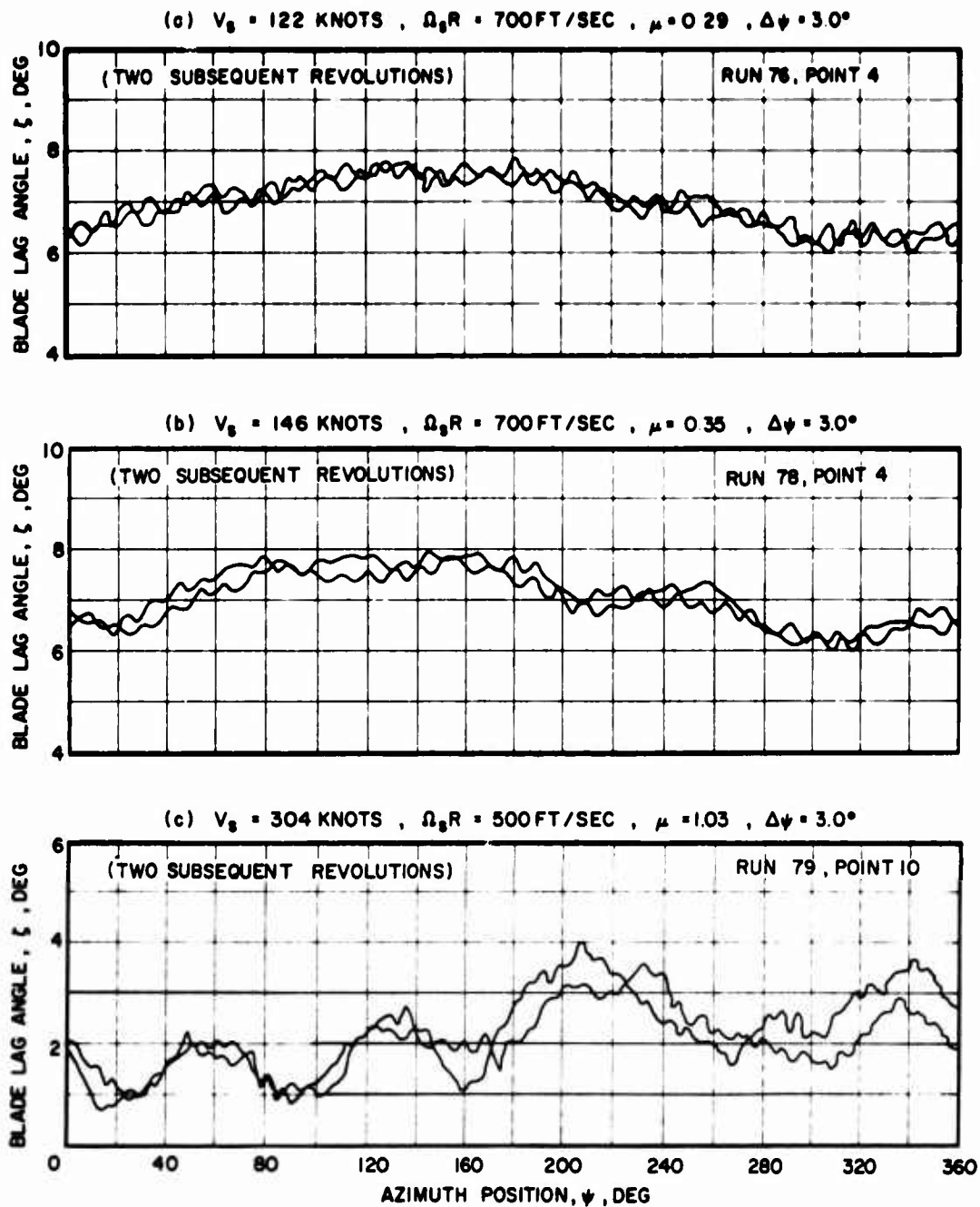


Figure 45. Blade Response Versus Azimuth During Combined Advancing Blade Aeroelastic Limits and Stall Flutter Testing; $Y_{CG}/c = 0.30$, $\alpha_s = 0.0^\circ$, $a_{1s} = b_{1s} = 0.0^\circ$, $\theta_c = 11.0^\circ$.

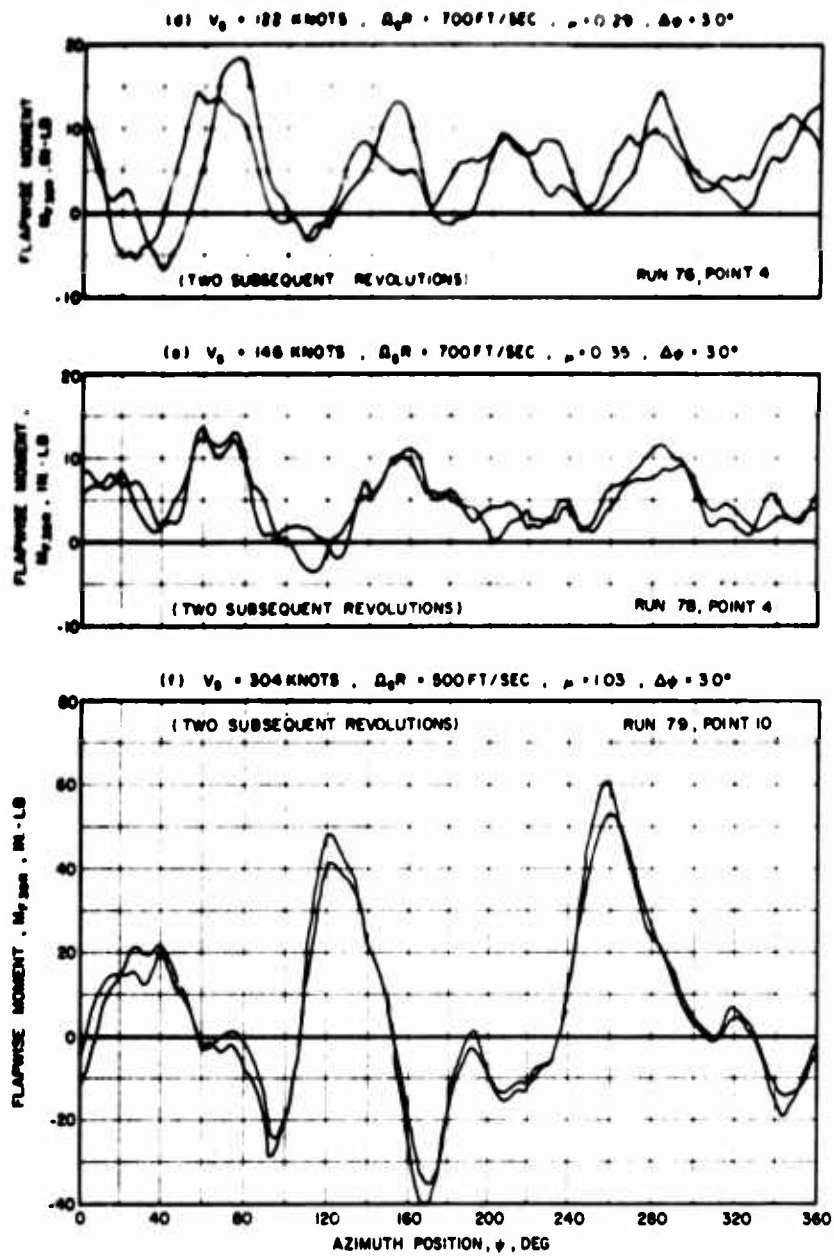


Figure 45. Continued.

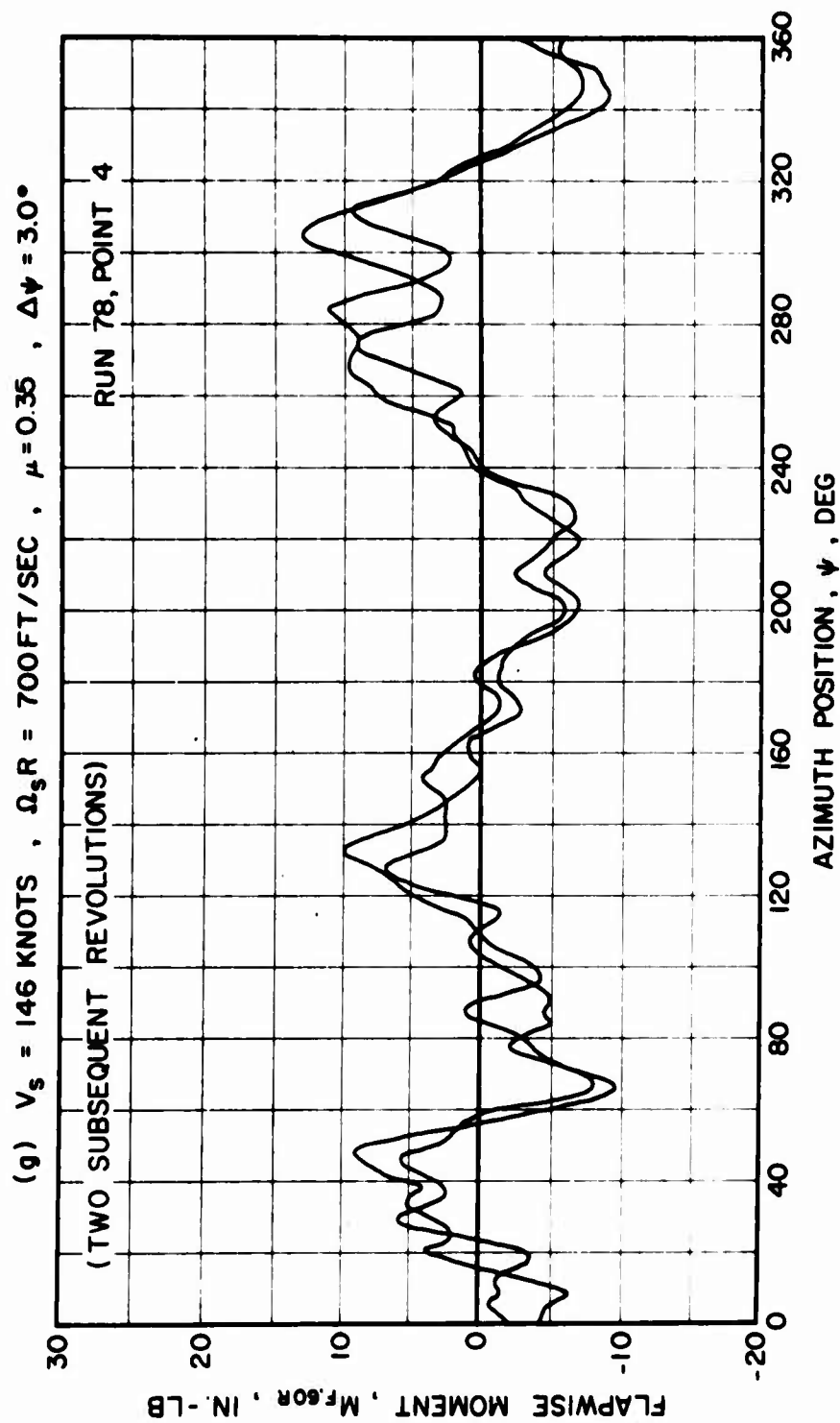


Figure 45. Continued.

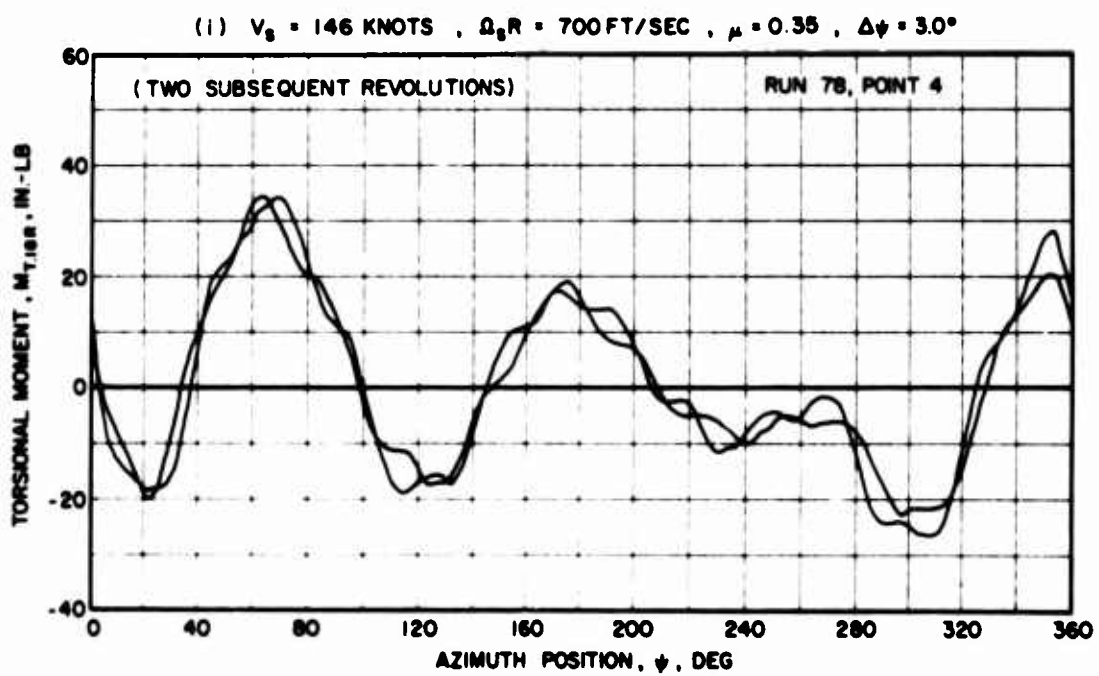
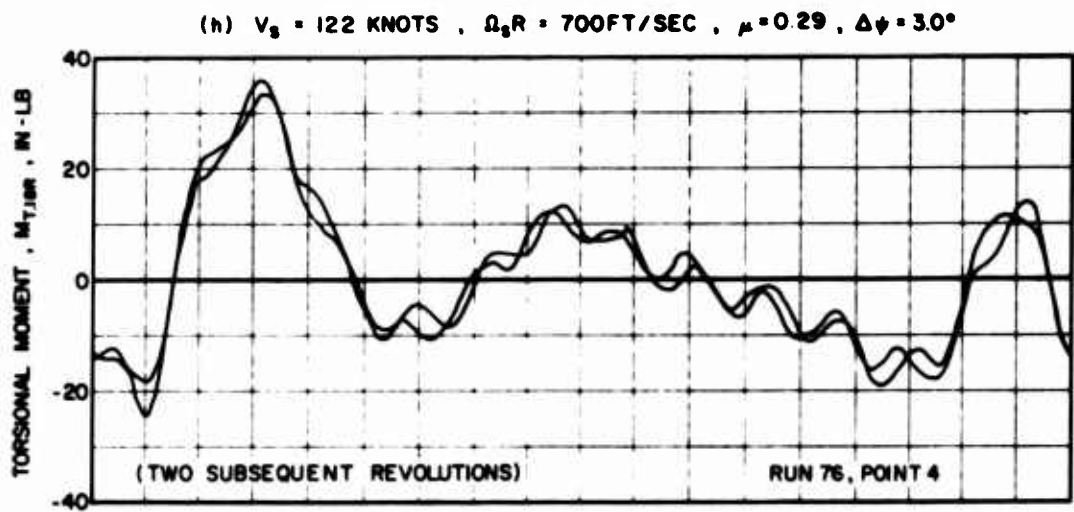


Figure 45. Continued.

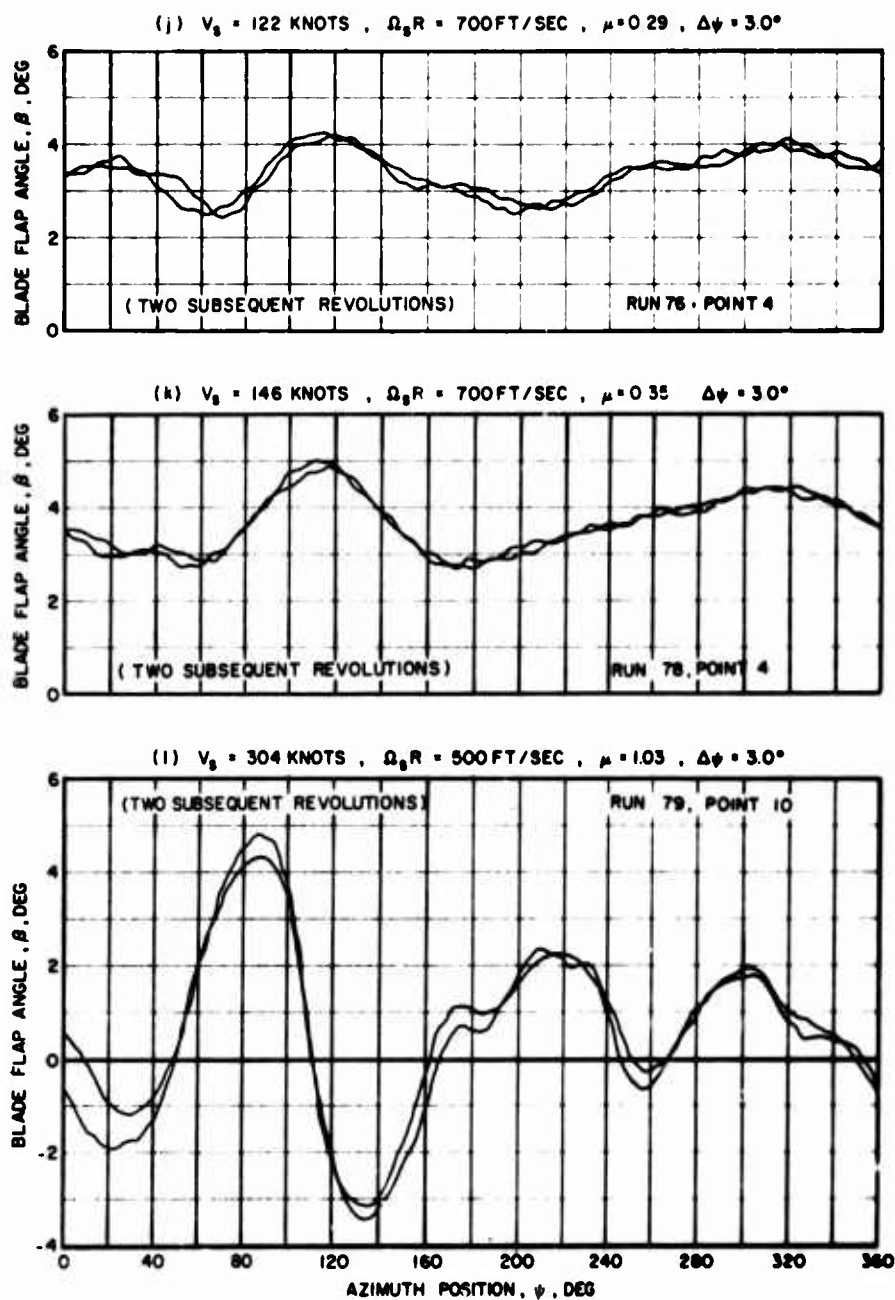


Figure 45. Continued.

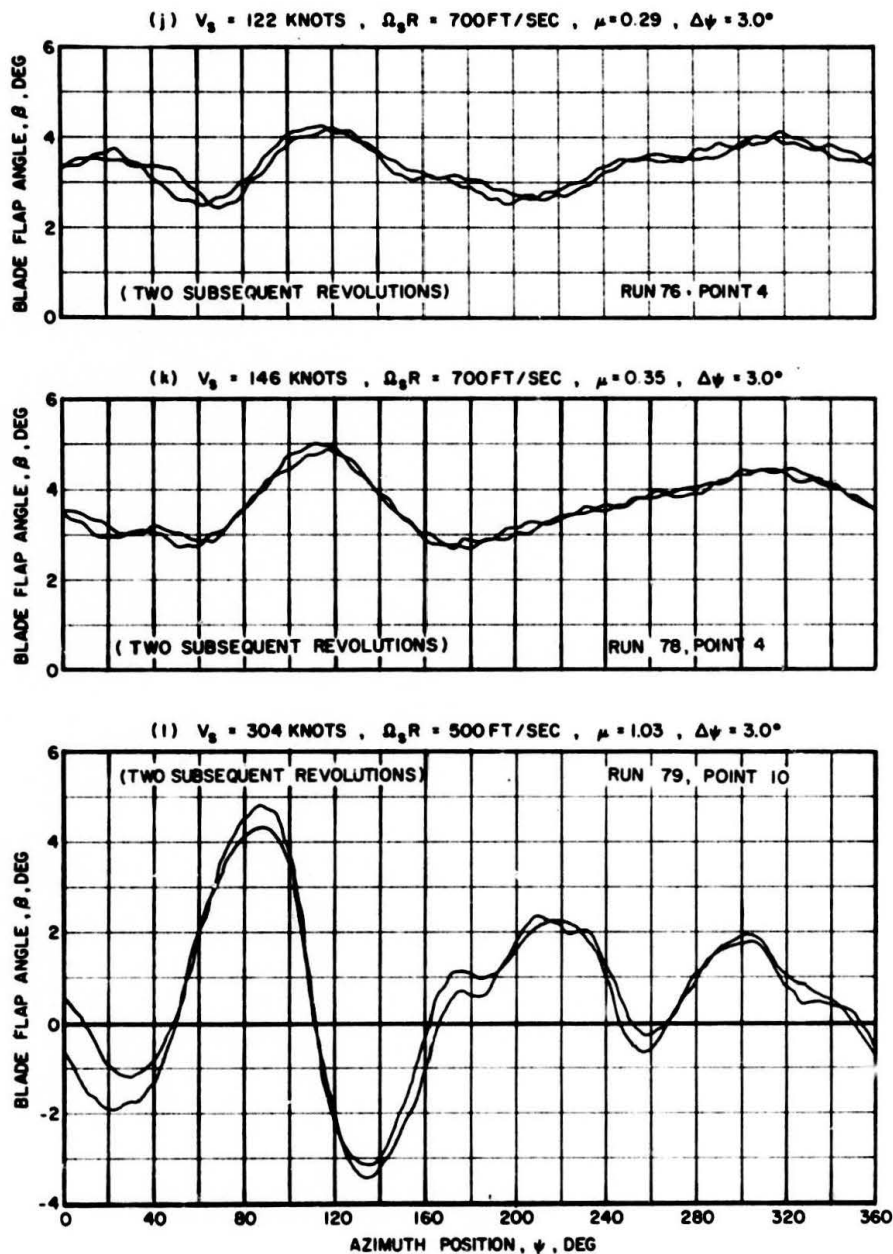


Figure 45. Continued.

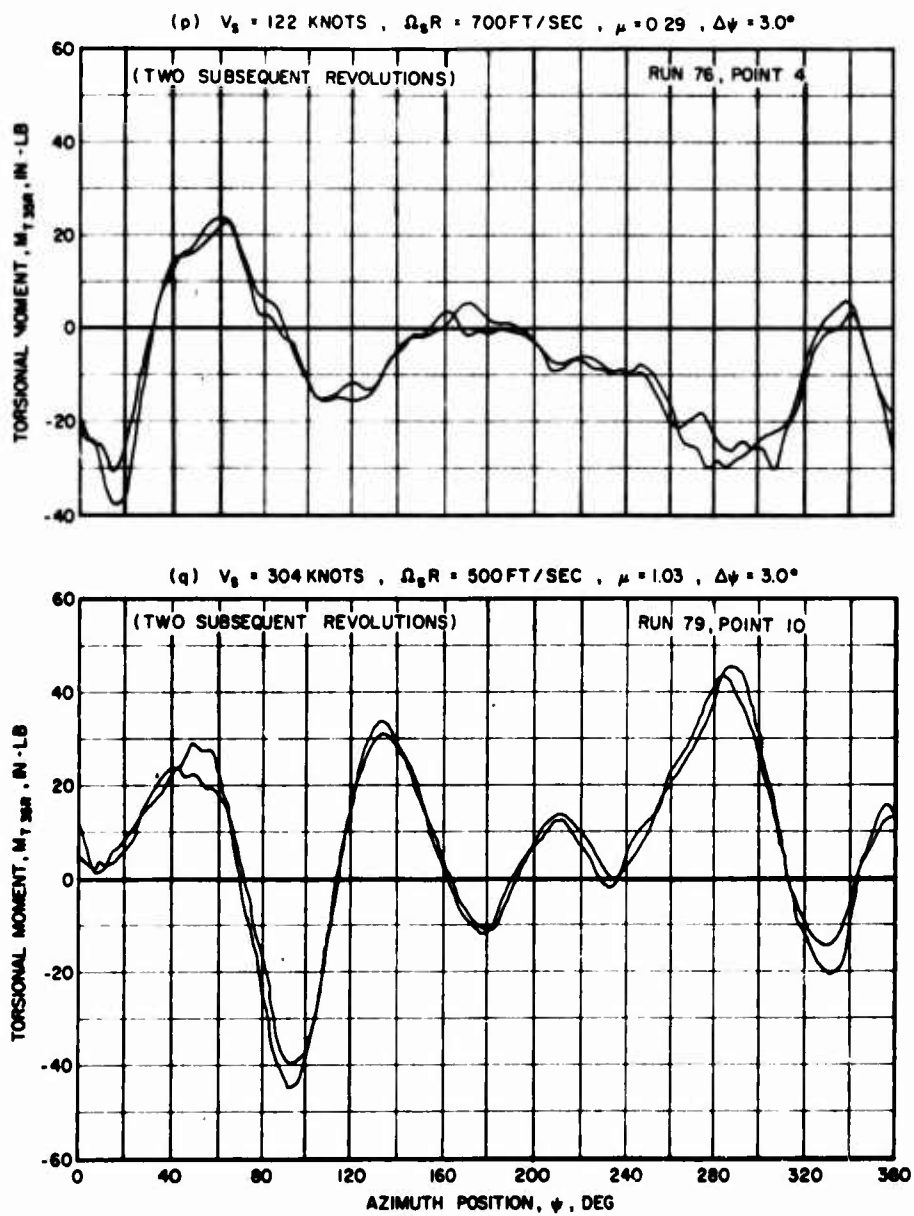
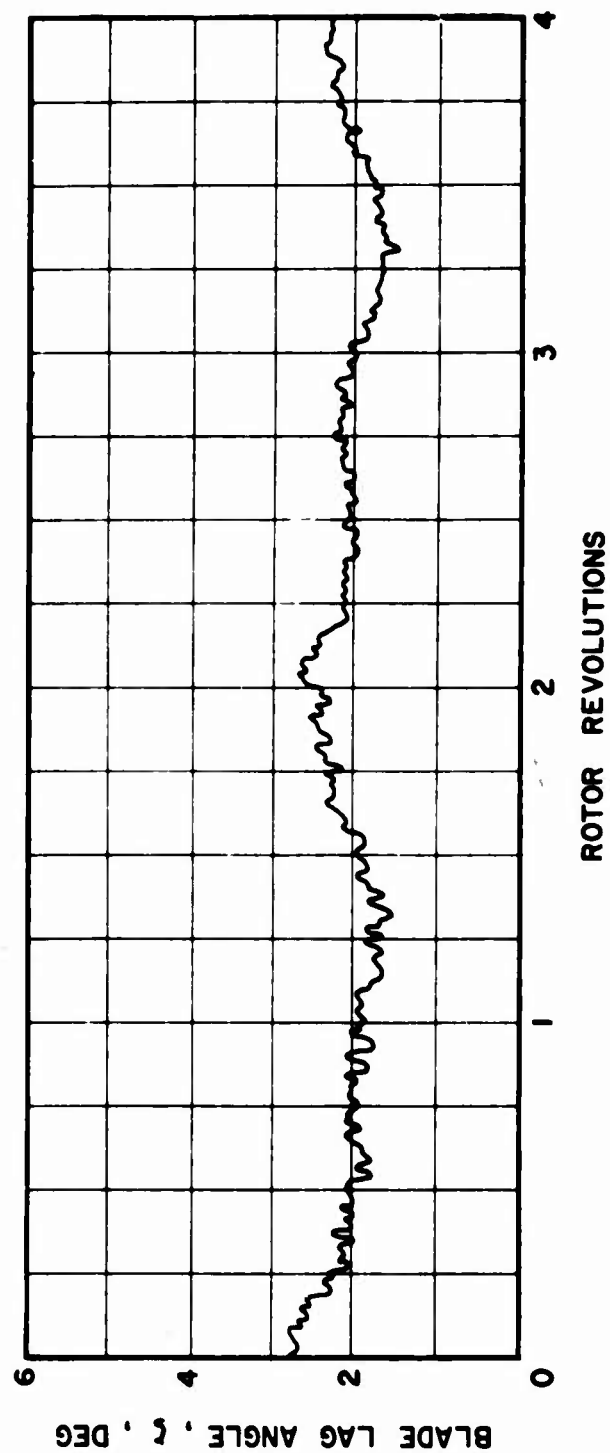
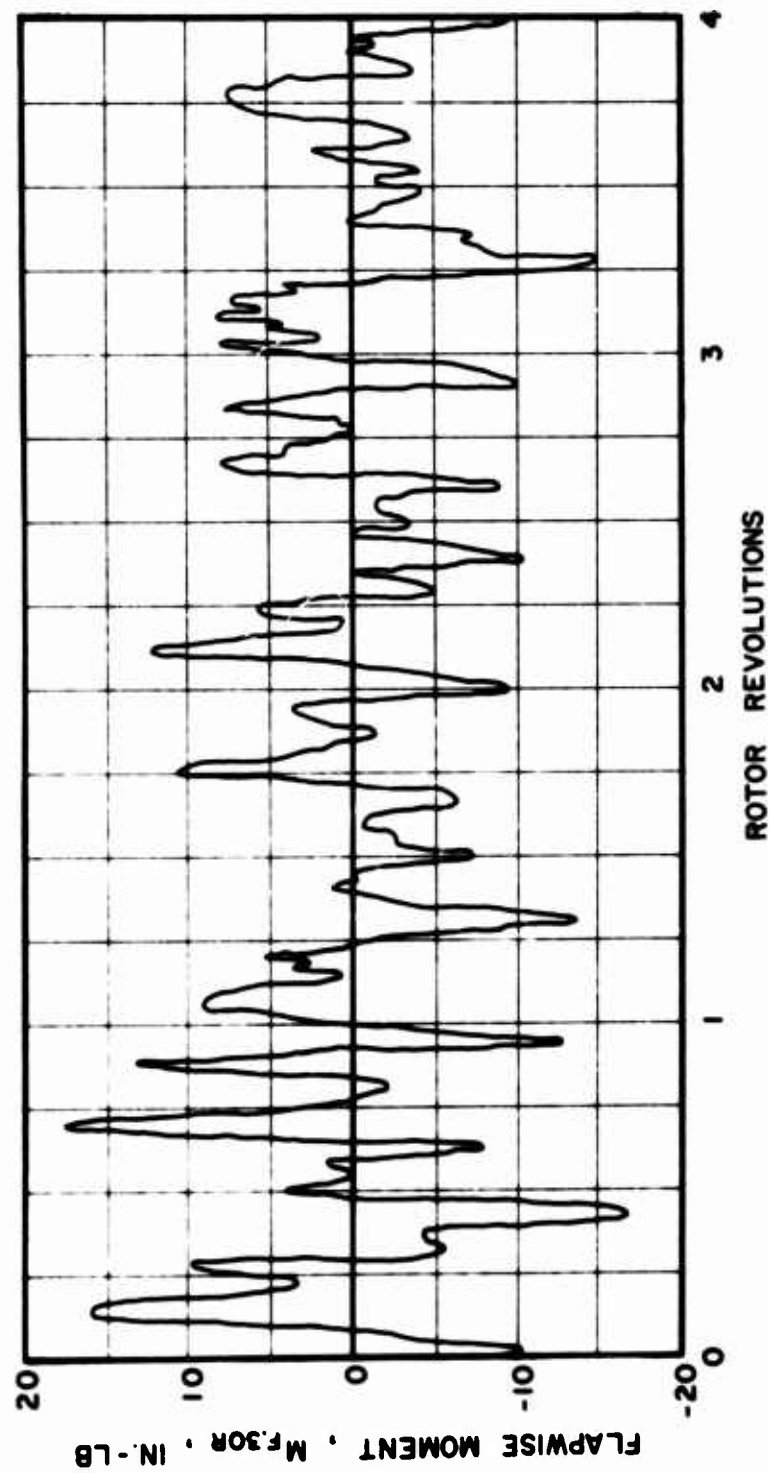


Figure 45. Concluded.



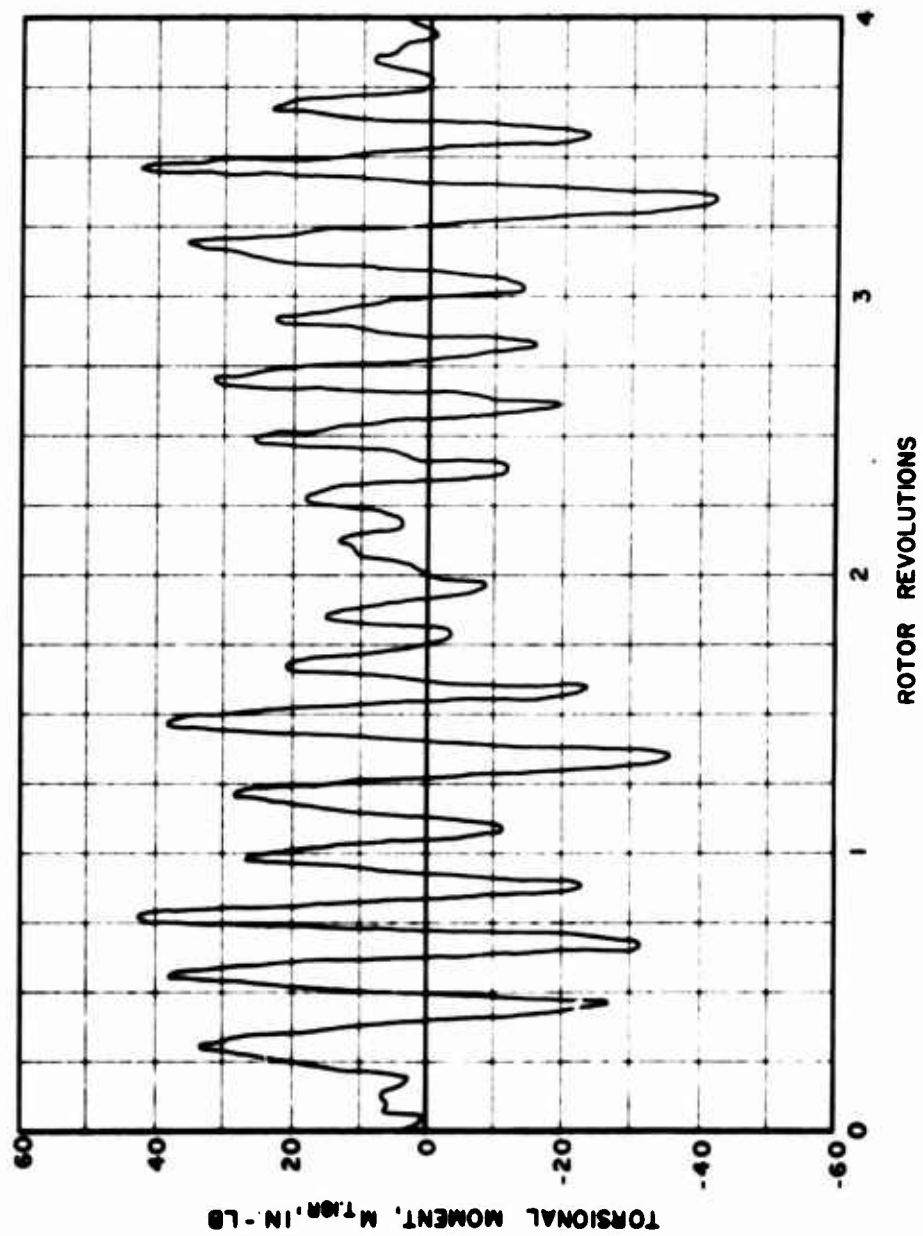
(a) $\Delta\psi = 3.0^\circ$

Figure 46. Blade Response Versus Azimuth During Recovery From Violent Instability; $Y_{CG}/c = 0.35$, $\alpha_g = 0.0^\circ$, $V_s = 260$ kn, $\Omega_g R = 500$ ft/sec, $\mu = 0.88$, $\theta_c = 4.0^\circ$, $A_{1s} = -1.3^\circ$, $B_{1s} = 4.6^\circ$.



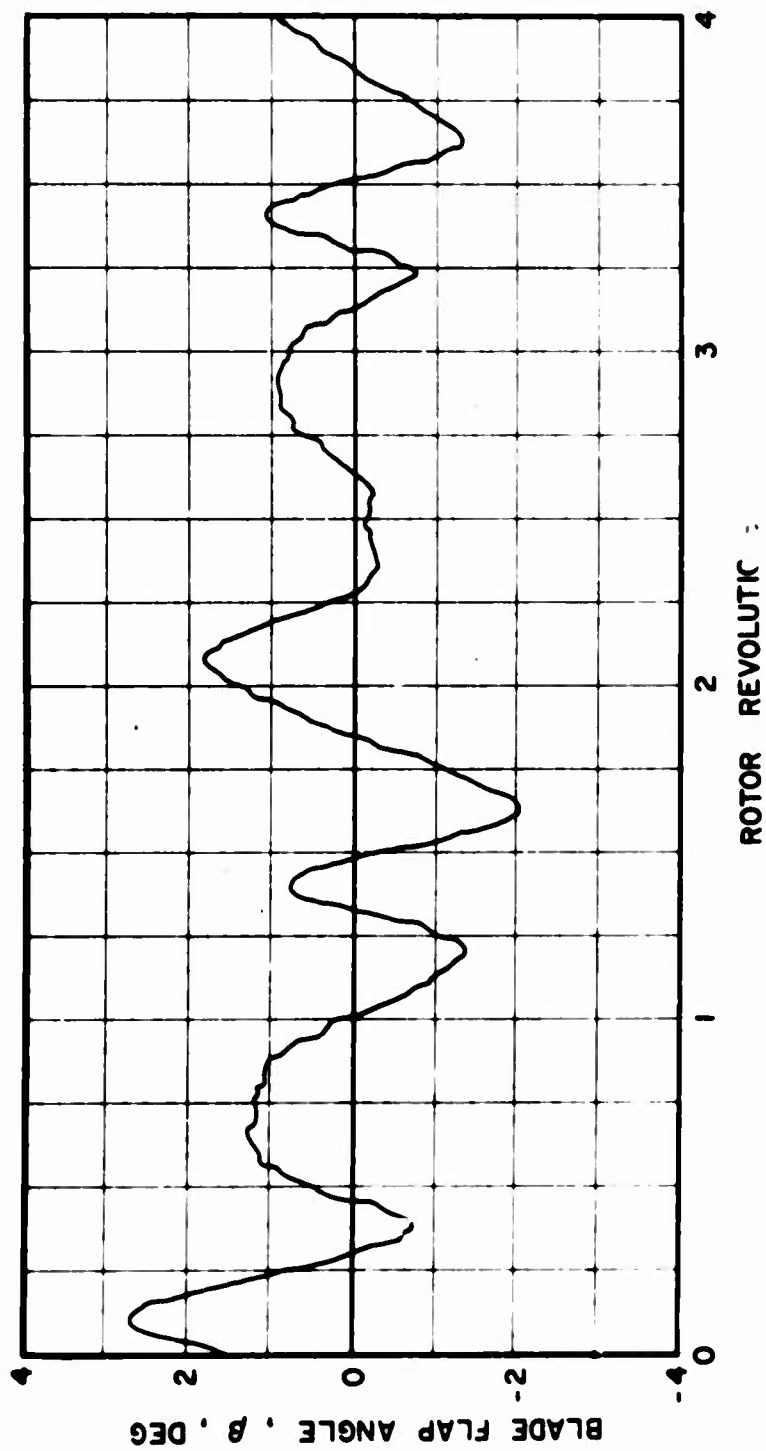
(b) $\Delta\psi = 3.0^\circ$

Figure 46. Continued.



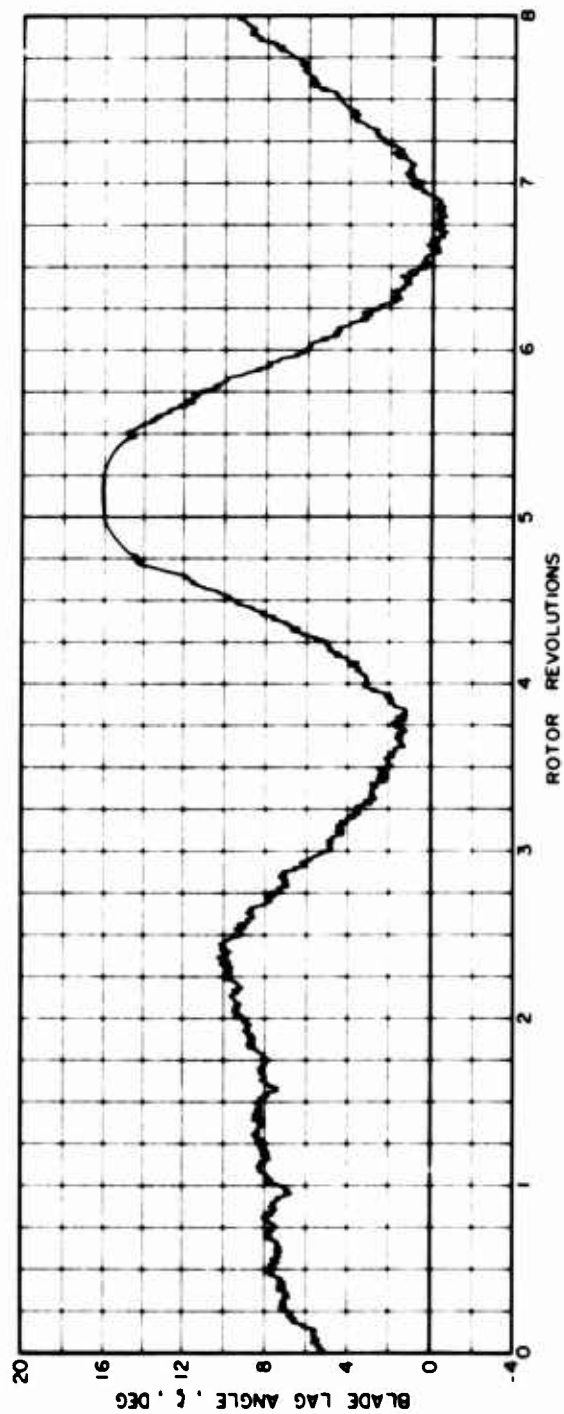
(c) $\Delta\psi = 3.0^\circ$

Figure 46. Continued.



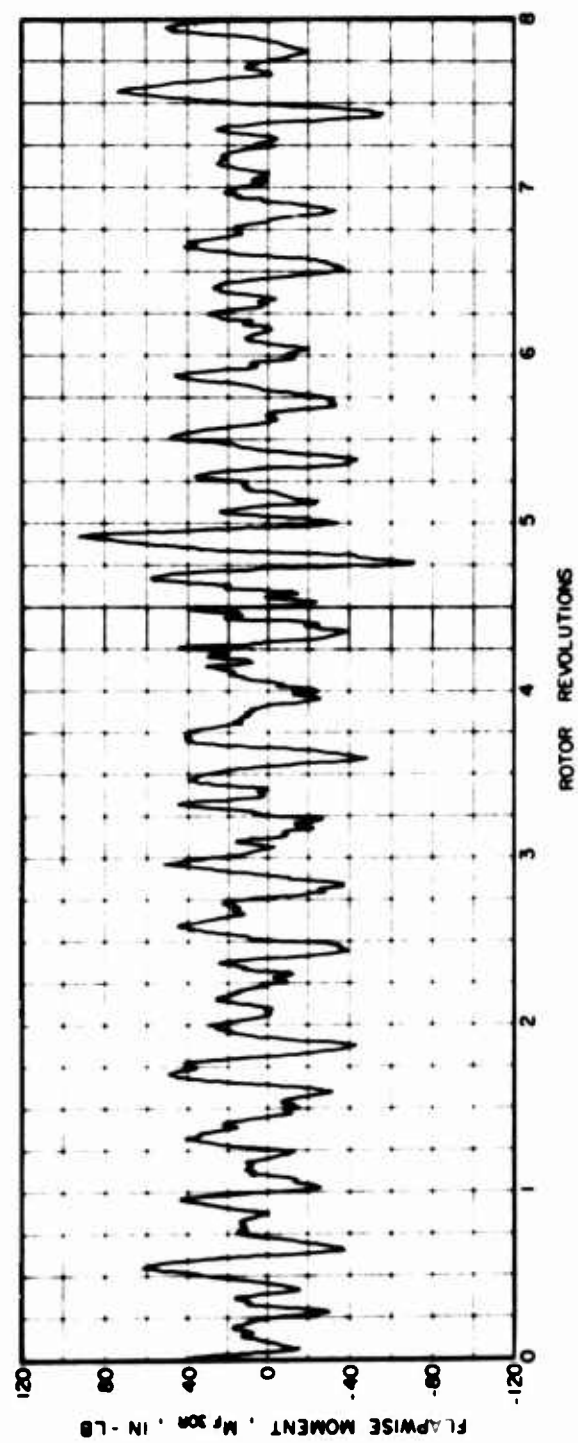
(d) $\Delta\psi = 3.0^\circ$

Figure 46. Concluded.



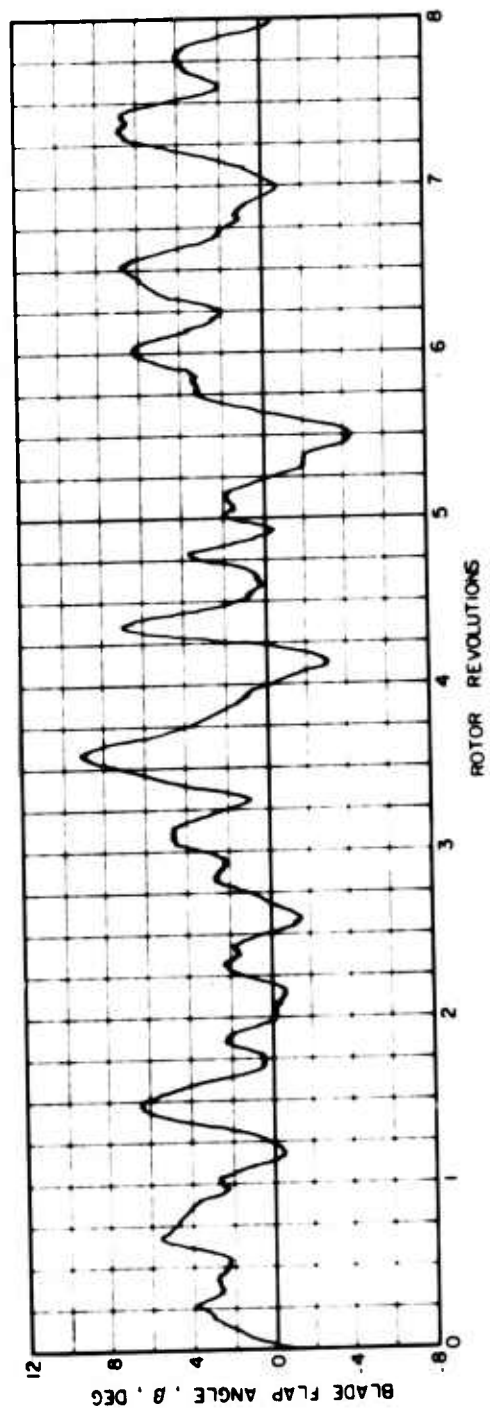
(a) $\Delta\psi = 3.0^\circ$

Figure 47. Blade Response Versus Azimuth During Violent Instability; $Y_{CG}/c = 0.35$, $\alpha_s = 0.0^\circ$, $V_s = 120$ kn, $\Omega_s R = 700$ ft/sec, $\mu = 0.29$, $\theta_c = 6.8^\circ$, $A_{ls} = -2.7^\circ$, $B_{ls} = 6.1^\circ$.



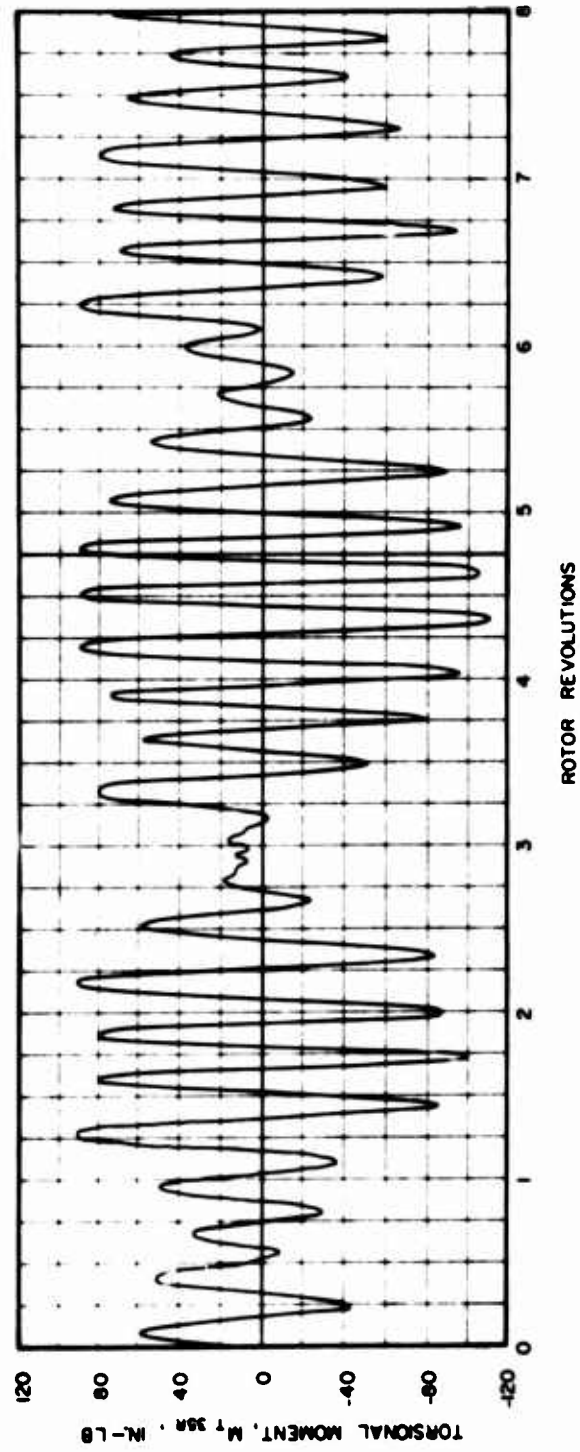
(b) $\Delta\psi = 3.0^\circ$

Figure 47. Continued.



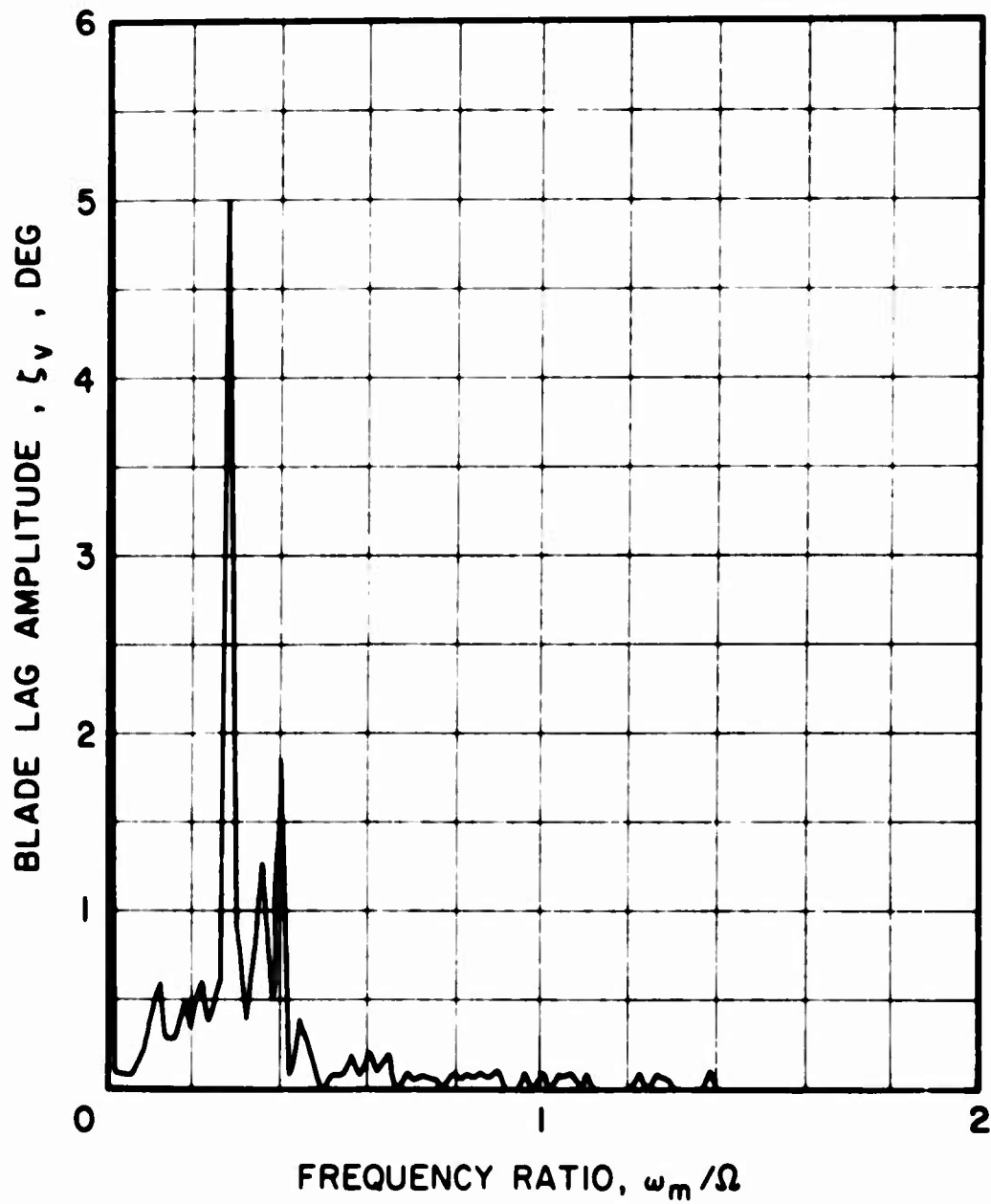
(c) $\Delta\psi = 3.0^\circ$

Figure 47. Continued.



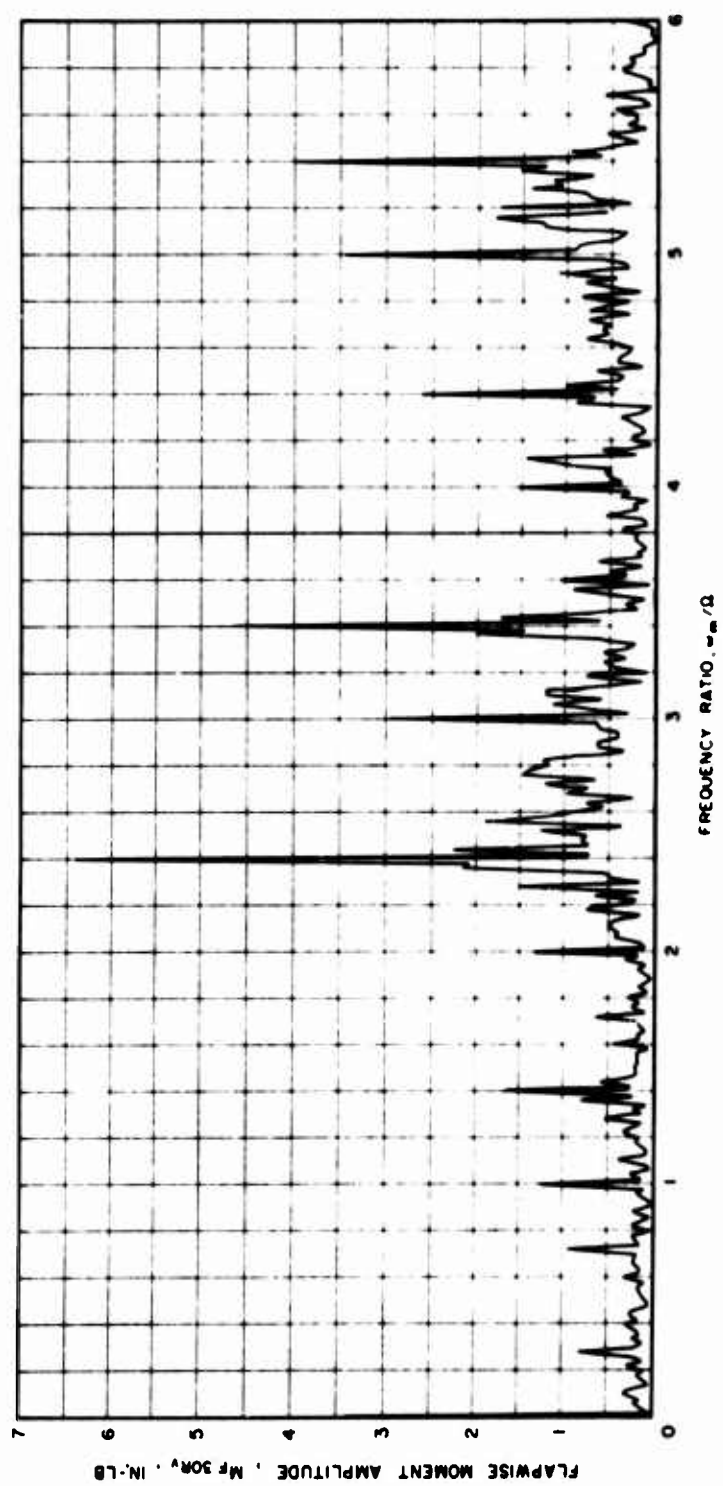
(d) $\Delta\psi = 3.0^\circ$

Figure 47. Concluded.



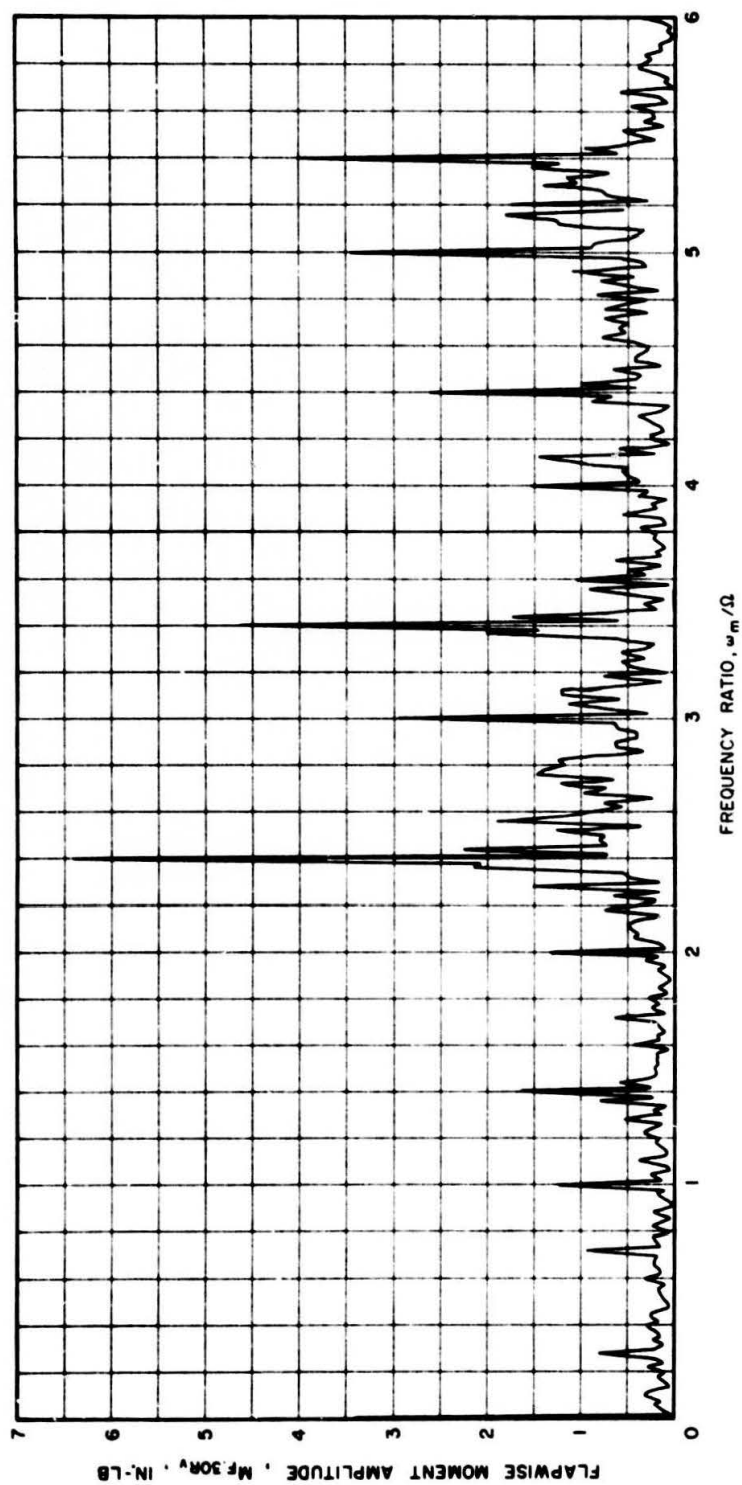
(a)

Figure 48. Blade Response Versus Frequency During Violent Instability; $Y_{CG}/c = 0.35$, $\alpha_s = 0.0^\circ$, $V_s = 120$ kn, $\Omega_s R = 700$ ft/sec, $\nu = 0.29$, $\theta_c = 6.8^\circ$, $A_{1s} = -2.7^\circ$, $B_{1s} = 6.1^\circ$.



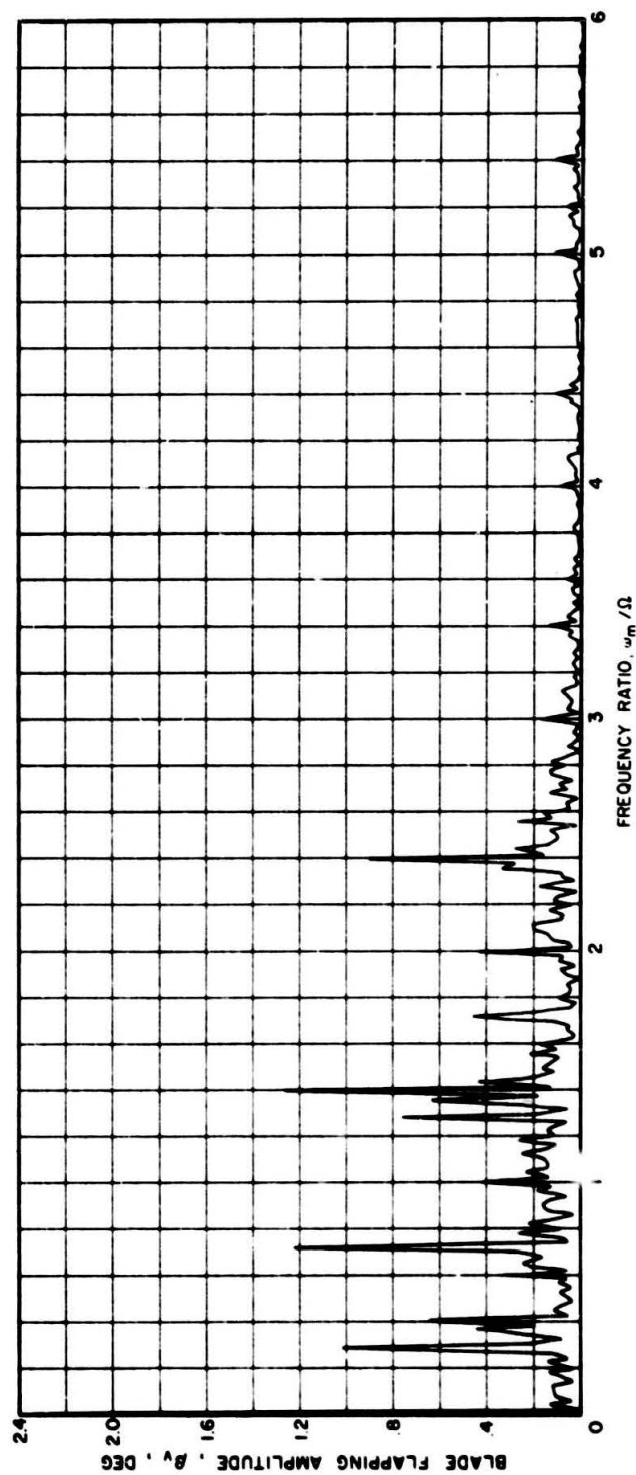
(b)

Figure 48. Continued.



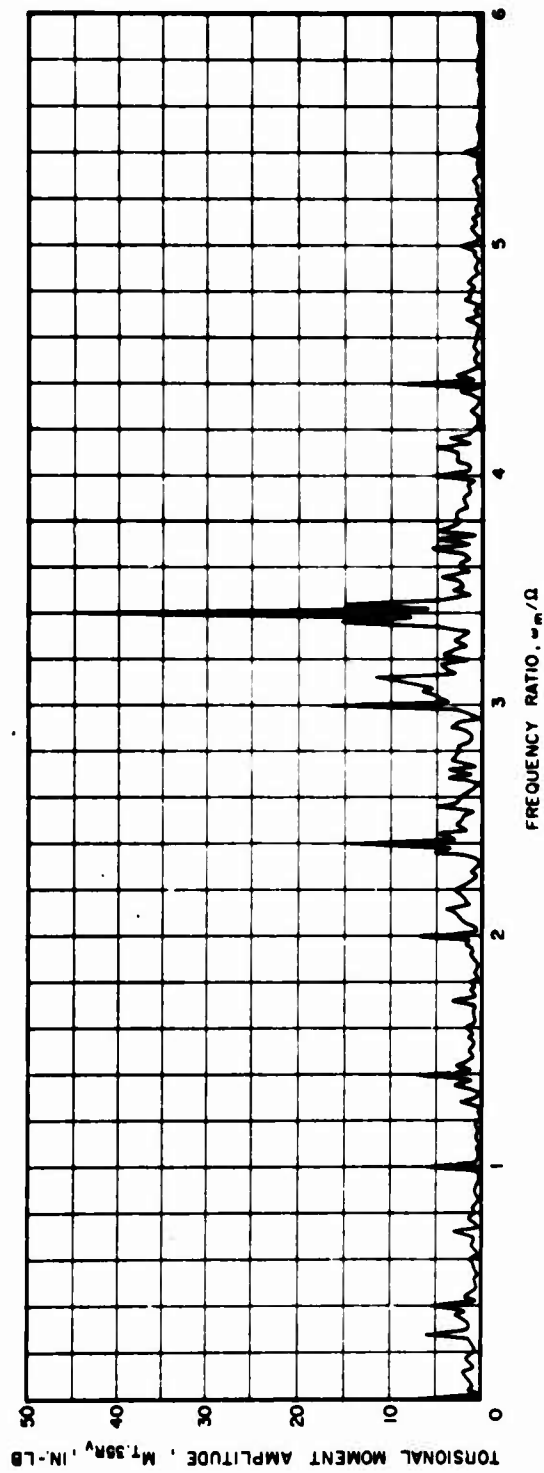
(b)

Figure 48. Continued.



(c)

Figure 48. Continued.



(d)

Figure 48. Concluded.

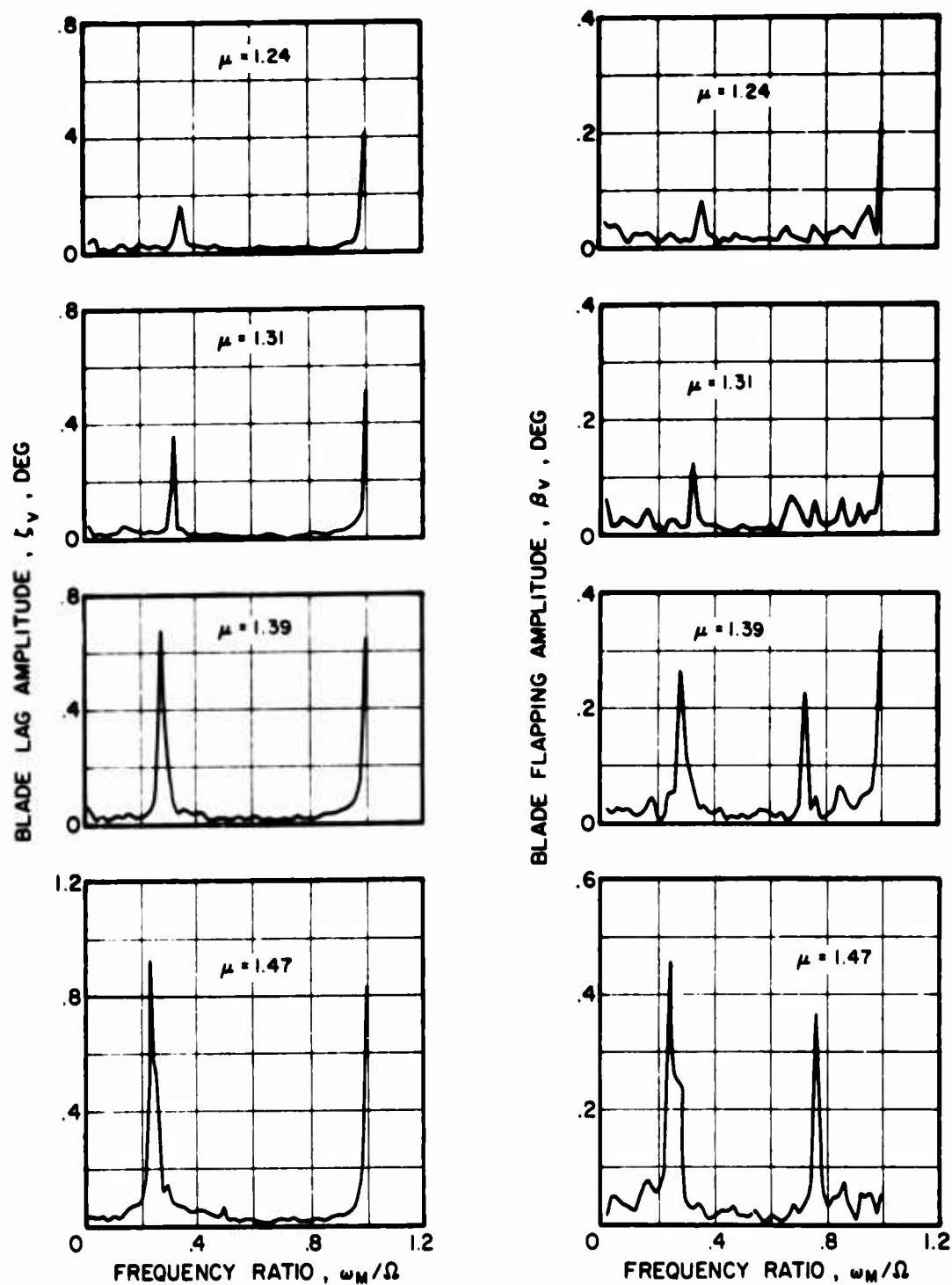


Figure 49. Blade Lag and Flap Response Versus Frequency During Retreating Blade Limits Testing; $Y_{CG}/c = 0.25$, $\alpha_s = 0.0^\circ$, $a_{1s} = b_{1s} = 0.0^\circ$, $V_s = 332$ kn, $\theta_c = 2.0^\circ$.

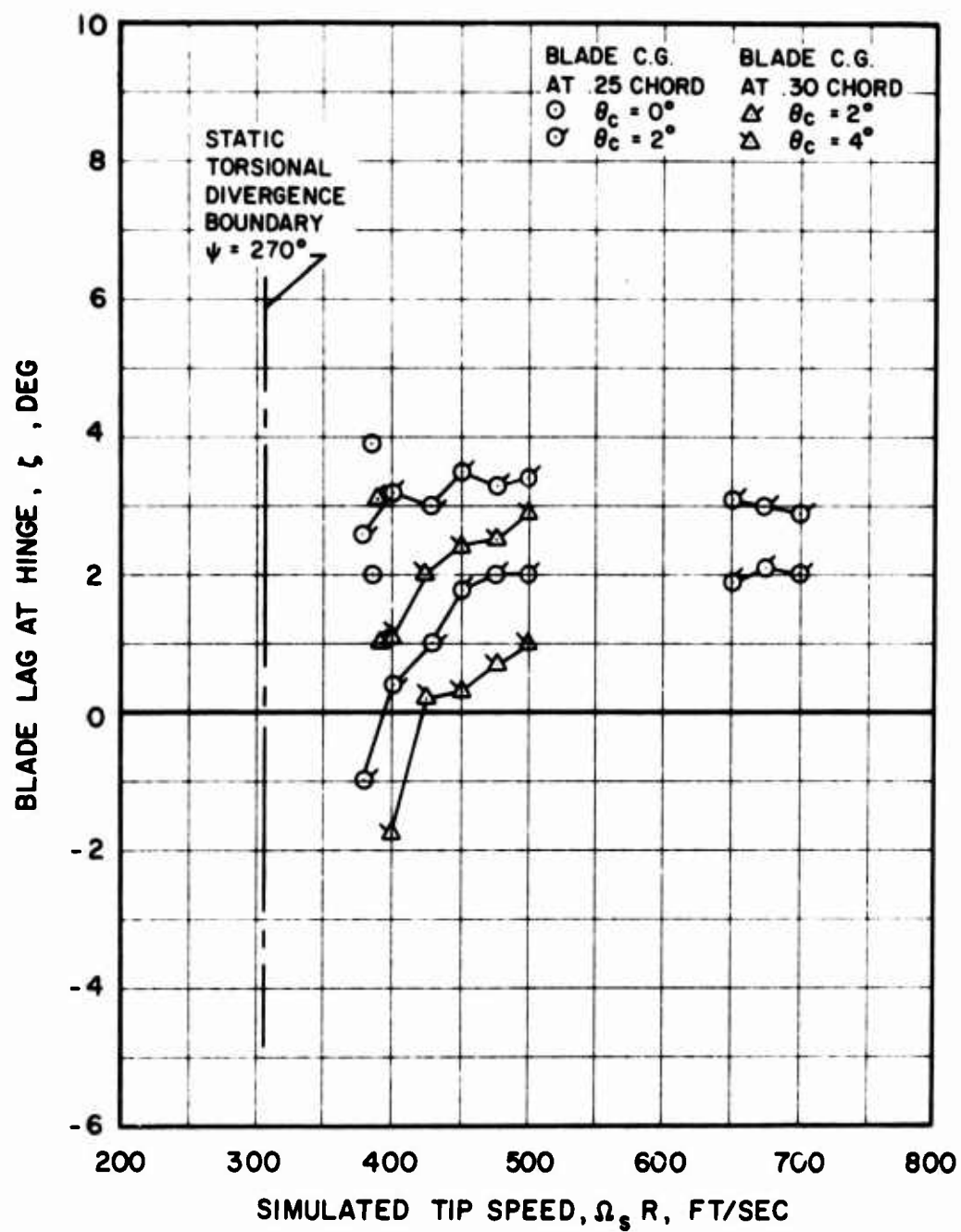


Figure 50. Range of Blade Lag Response During Retreating Blade Aeroelastic Limits Testing; $\alpha_s = 0.0^\circ$, $a_{1s} = b_{1s} = 0.0^\circ$, $V_s = 332$ kn.

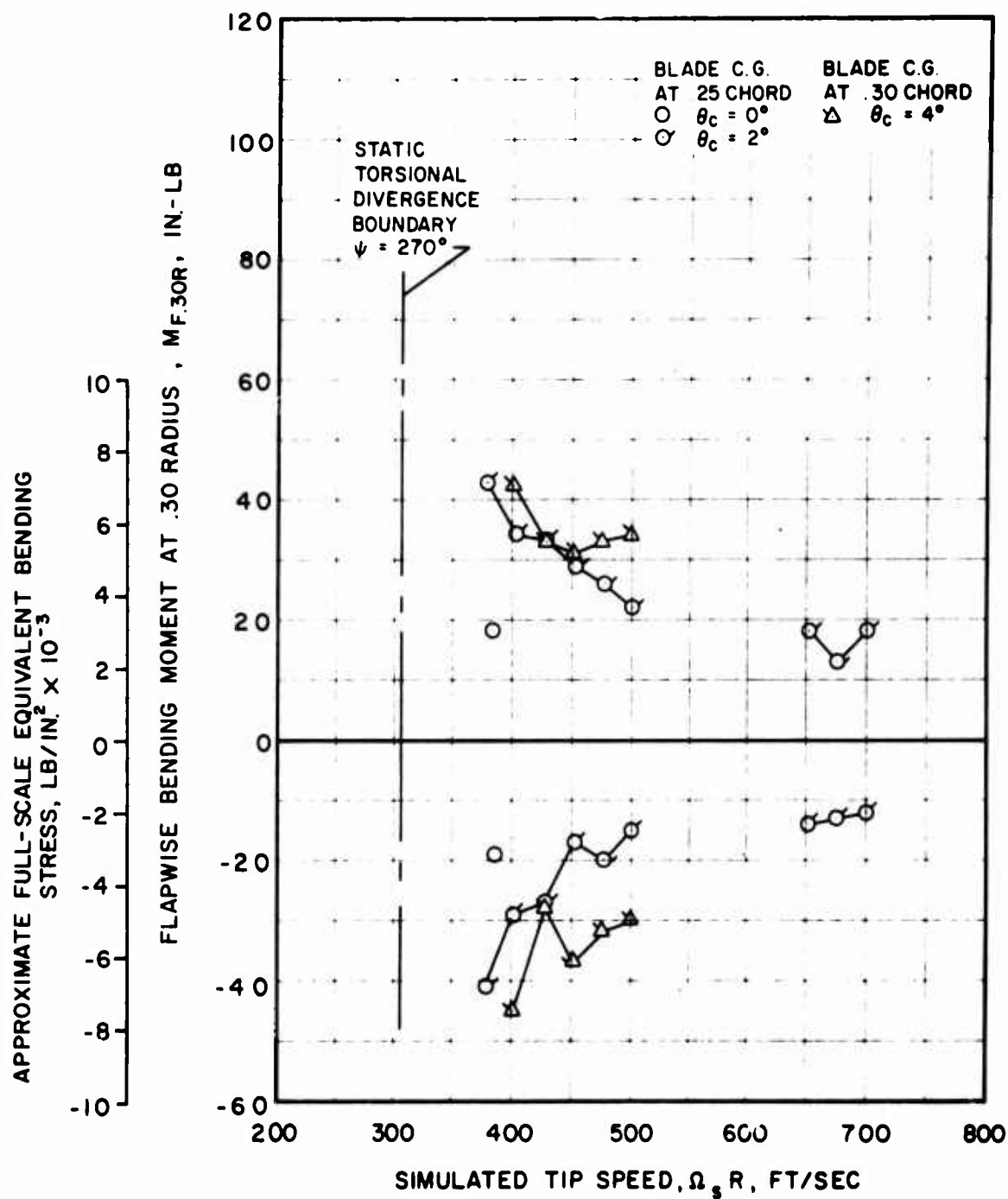


Figure 1. Range of Blade Flapwise Bending Response During Retreating Blade Aeroelastic Limits Testing; $\alpha_s = 0.0^\circ$, $a_{1s} = b_{1s} = 0.0^\circ$, $V_s = 332$ kn.

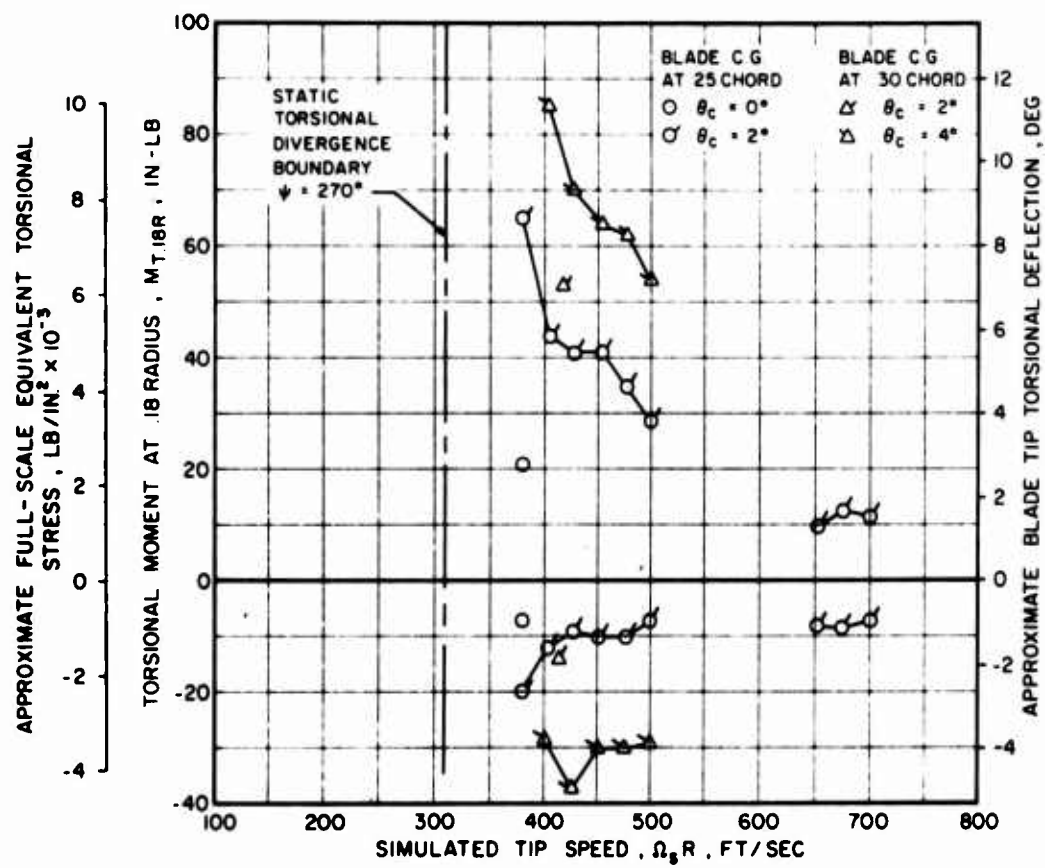


Figure 52. Range of Blade Torsional Response During Retreating Blade Aeroelastic Limits Testing; $\alpha_y = 0.0^\circ$, $a_{1s} = b_{1s} = 0.0^\circ$, $V_s = 332 \text{ kn}$.

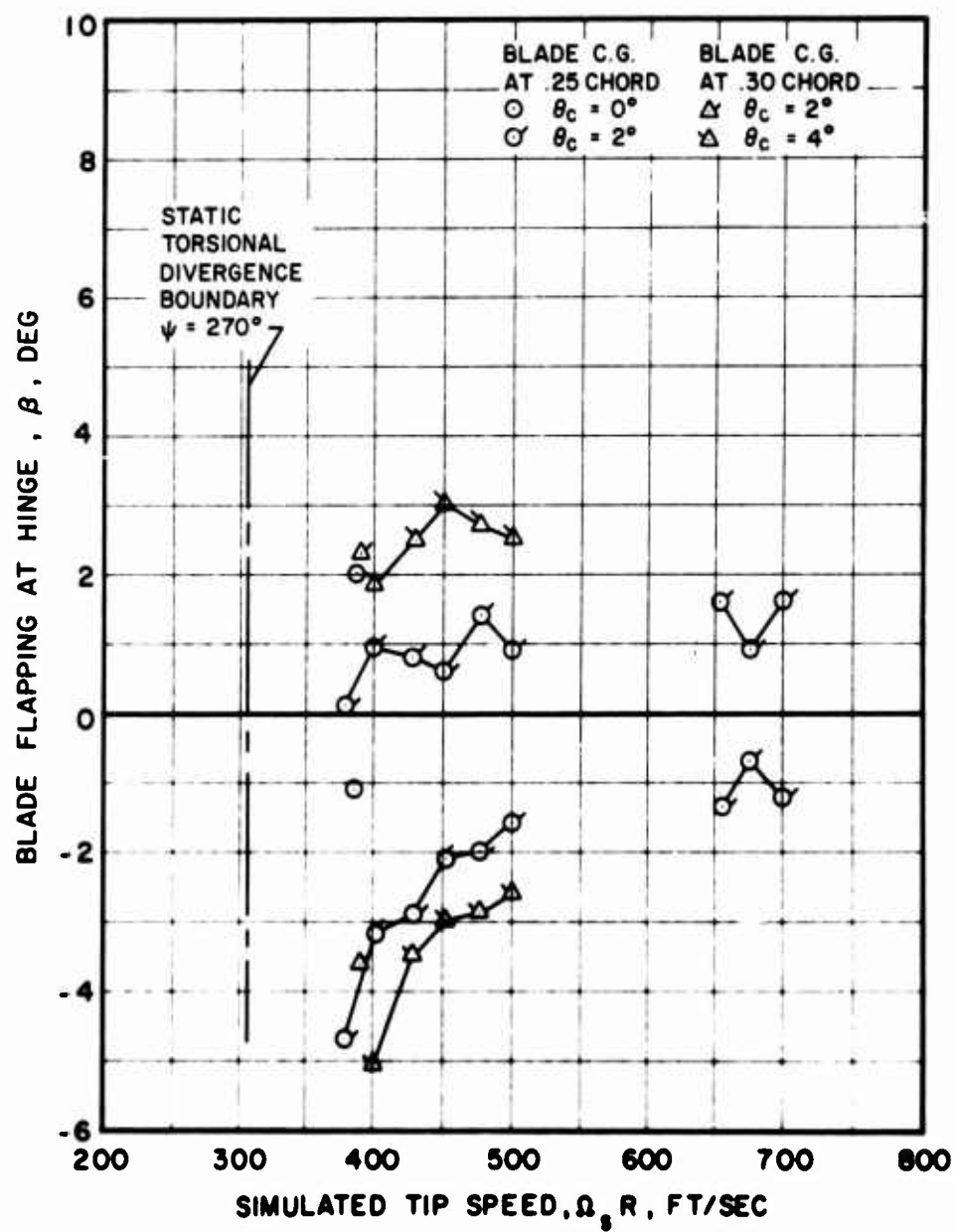


Figure 53. Range of Blade Flapping Response During Retreating Blade Aeroelastic Limits Testing; $\alpha_s = 0.0^\circ$, $a_{1s} = b_{1s} = 0.0^\circ$, $V_s = 332$ kn.

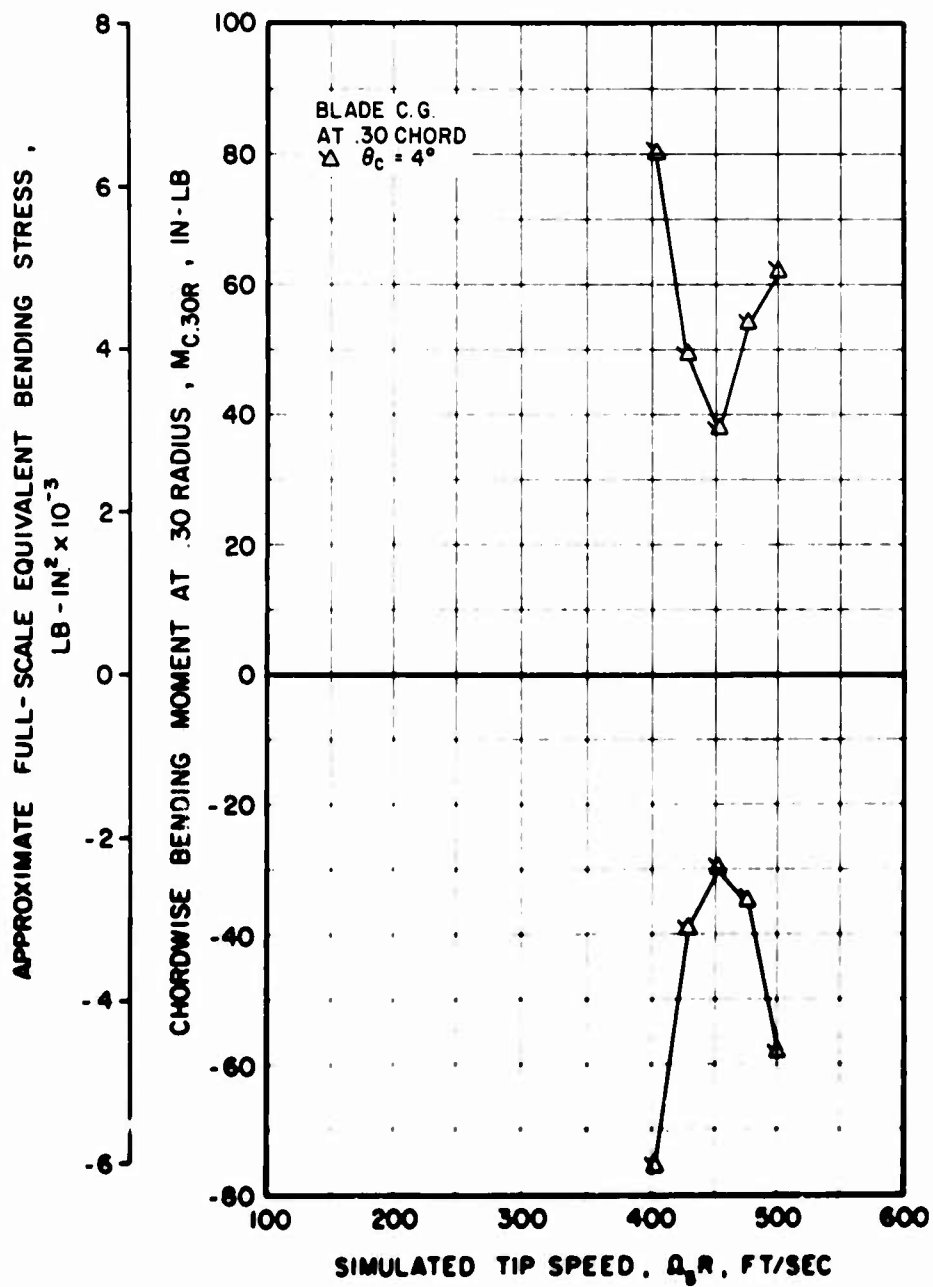


Figure 54. Range of Blade Chordwise Bending Response During Retreating Blade Aeroelastic Limits Testing.
 $\alpha_s = 0.0^\circ$, $\alpha_{1s} = \alpha_{1s} = 0.0^\circ$, $V_s = 312$ kn.

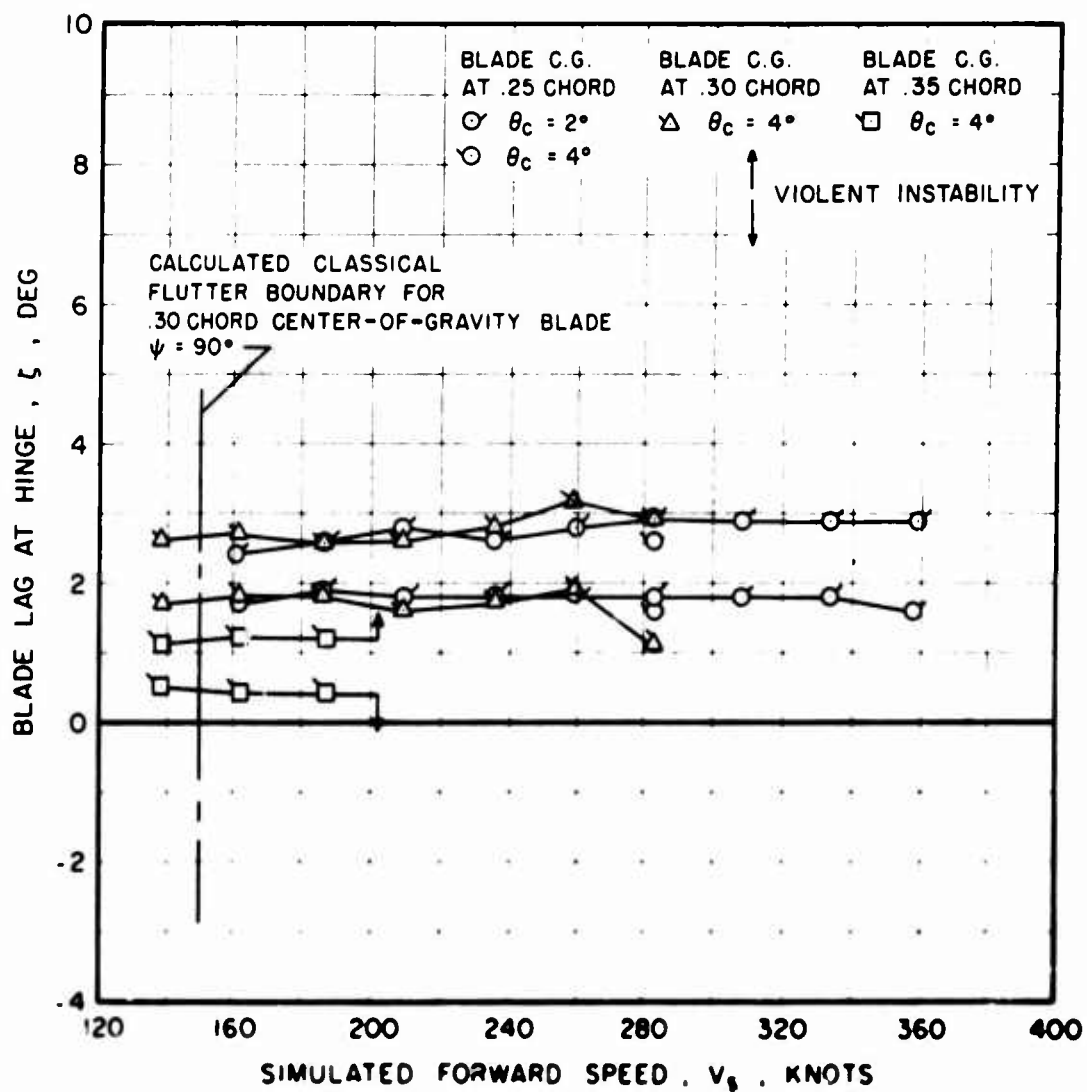


Figure 33. Range of Blade Lag Response During Advancing Blade Aeroblastic Limits Testing, $\alpha_s = 0.0^\circ$, $\alpha_{1/2} = \alpha_{3/4} = 0.0^\circ$, $\dot{\alpha}_{1/2} = 100$ ft/sec.

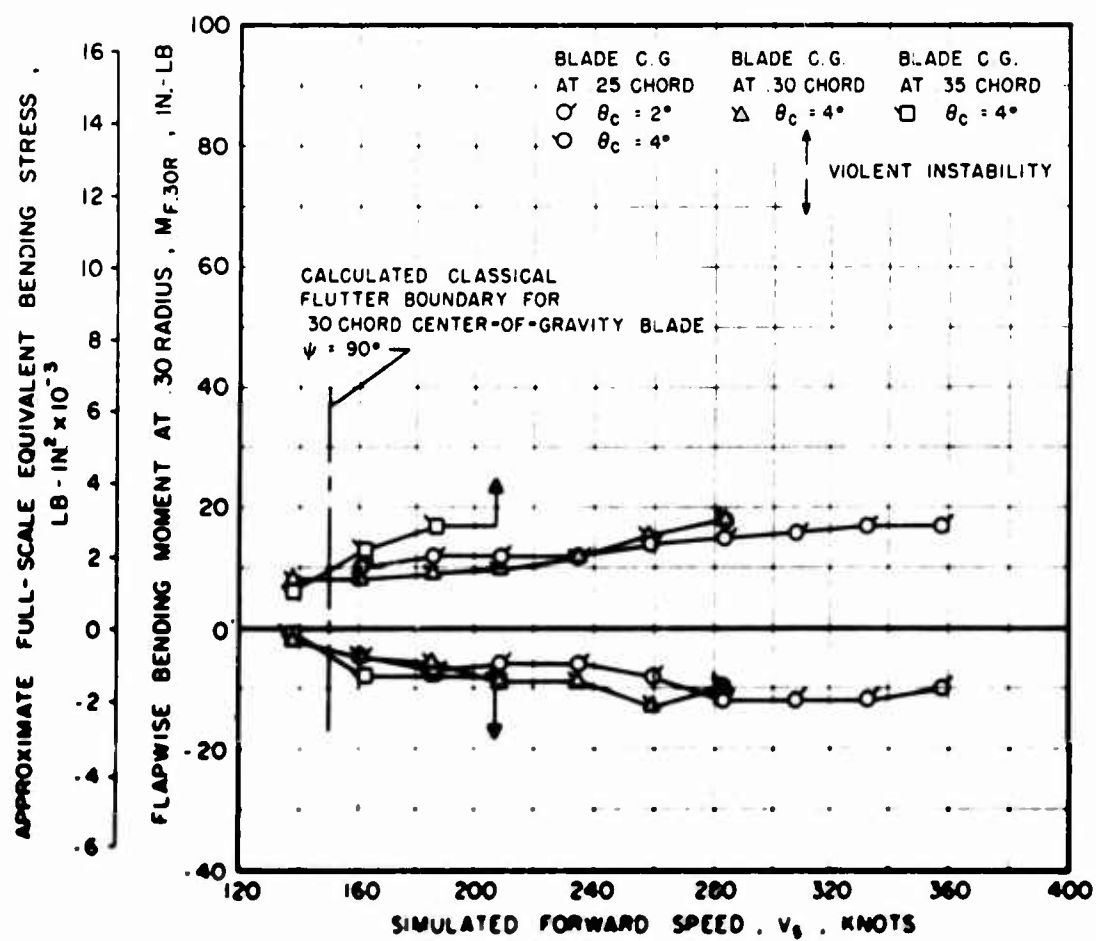


Figure 56. Range of blade flapwise bending response during advancing blade aerodynamic limits testing.
 $\alpha_0 = 0.0^\circ$, $\alpha_{1/2} = 1.5^\circ$, $\alpha_{3/4} = 0.0^\circ$, $\Delta h = 100$ ft/sec.

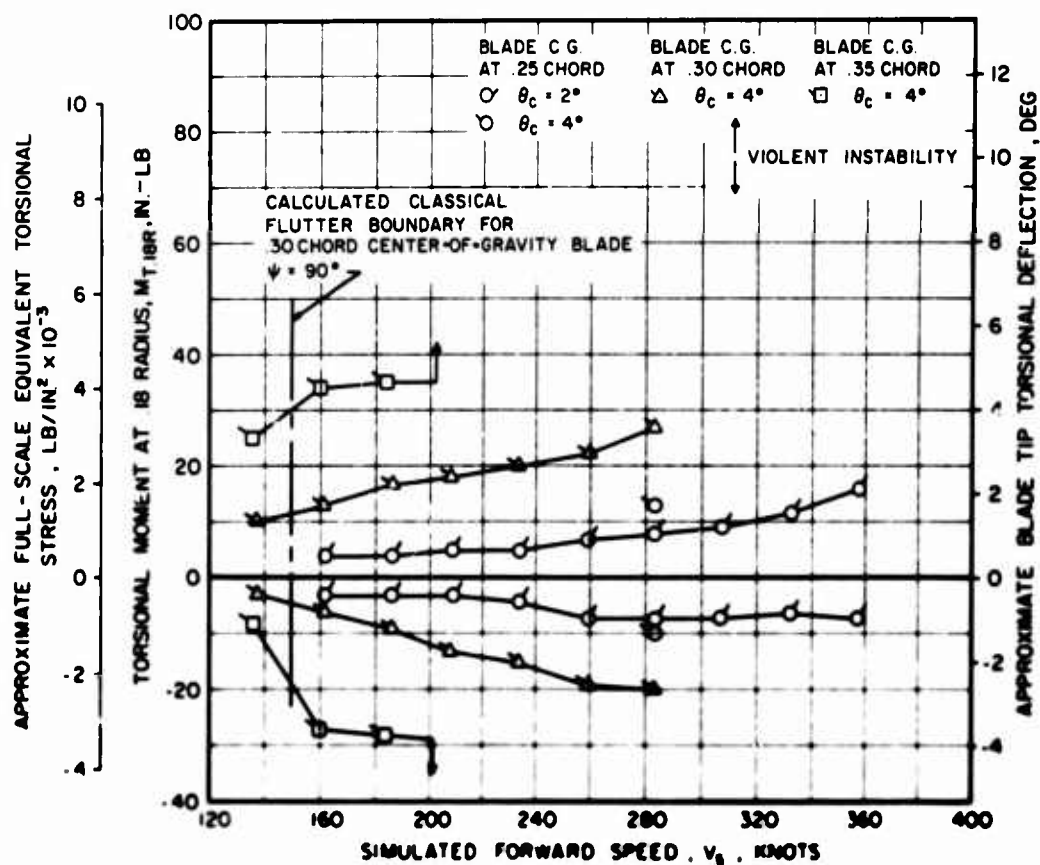


Figure 17. Range of Blade Torsional Response During Advancing Blade Aerodynamic Lifts Testing, $\alpha_s = 0.0^\circ$, $\dot{\alpha}_s = 0.0^\circ$, $\dot{\alpha}_s = 100$ ft/sec.

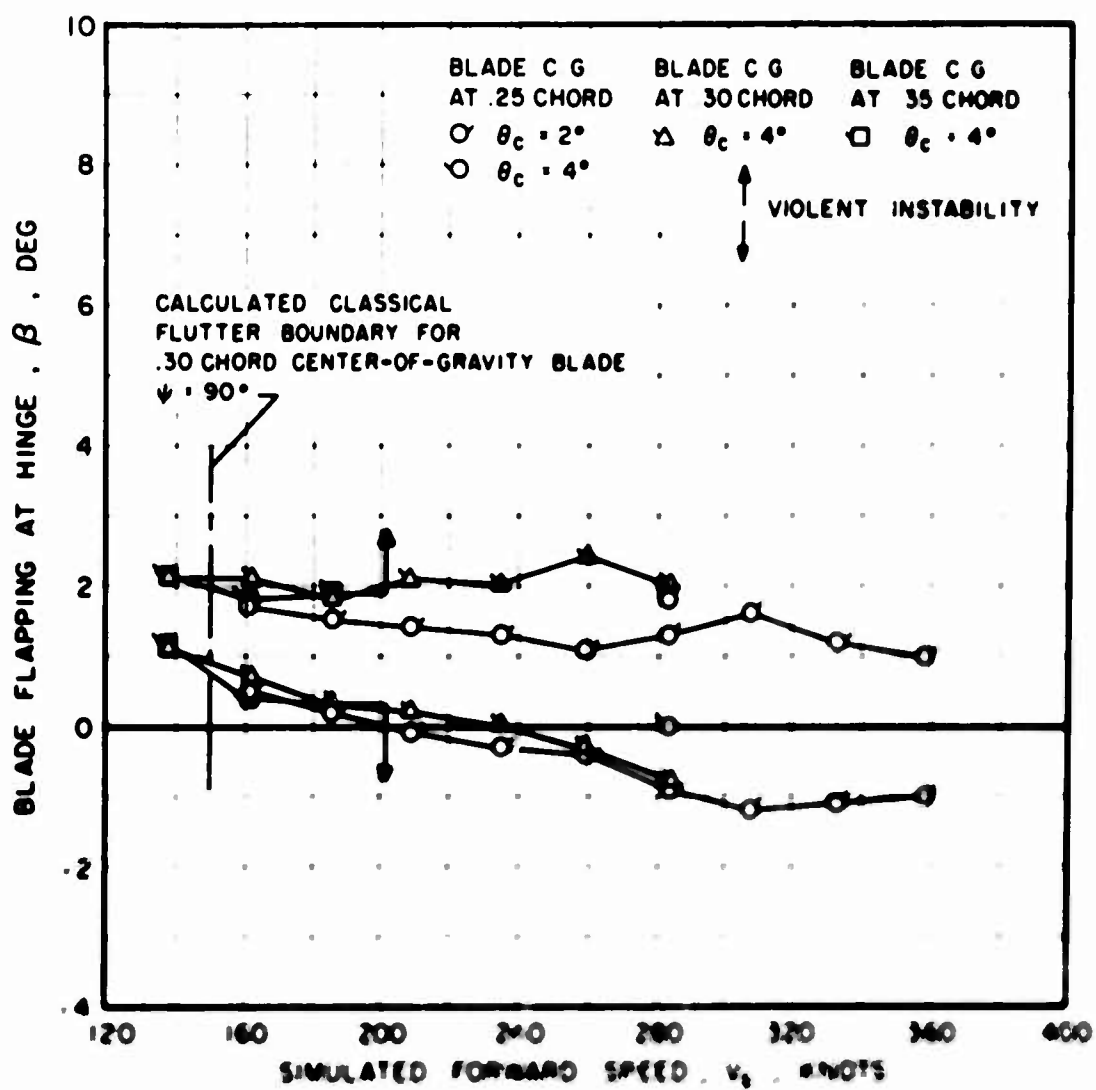


Figure 10. Range of Blade Flapping Amplitude During Approach
 Blade Section: 100% 100% 100% 100% 100%
 $\theta_c = 2^\circ$, $\theta_c = 4^\circ$, $\theta_c = 4^\circ$, $\theta_c = 4^\circ$, $\theta_c = 4^\circ$

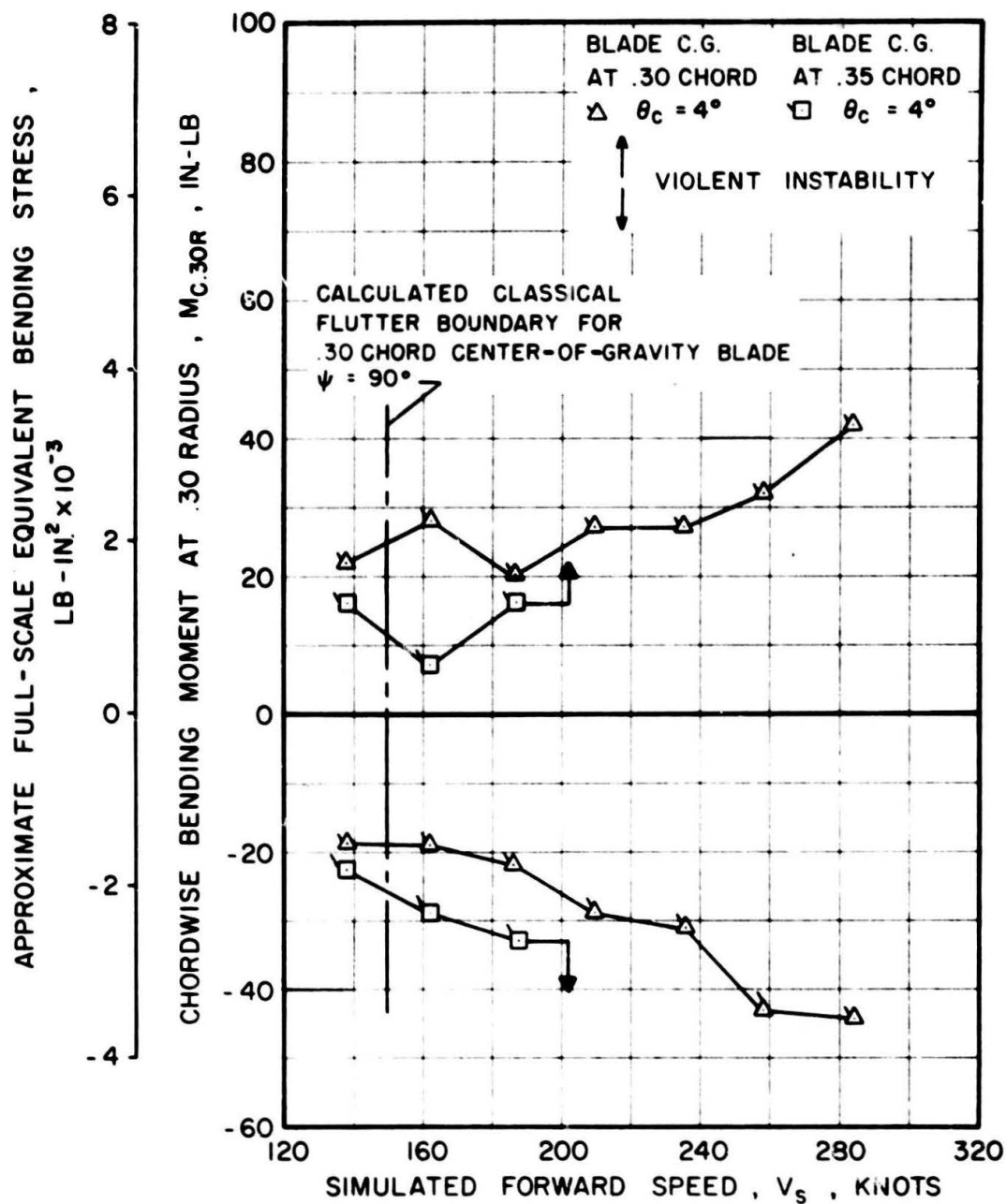


Figure 59. Range of blade chordwise bending response during Advancing Blade Aeroelastic Limits Testing; $\alpha_s = 0.0^\circ$, $a_{1s} = b_{1s} = 0.0^\circ$, $\Omega_s R = 700$ ft/sec.

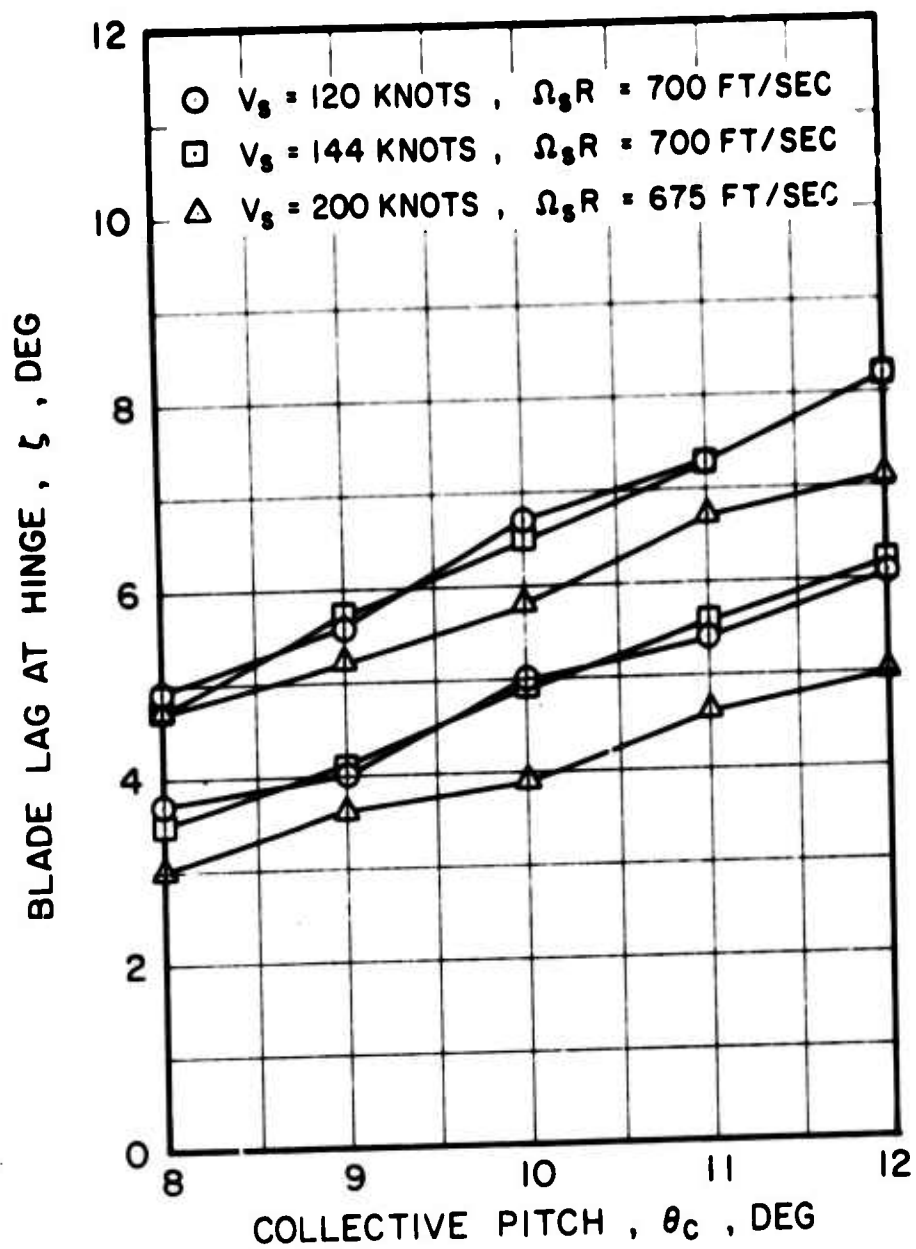


Figure 60. Range of Blade Lag Response During Stall Flutter Testing; $Y_{CG}/c = 0.25$, $\alpha_s = 0.0^\circ$, $a_{1s} = b_{1s} = 0.0^\circ$.

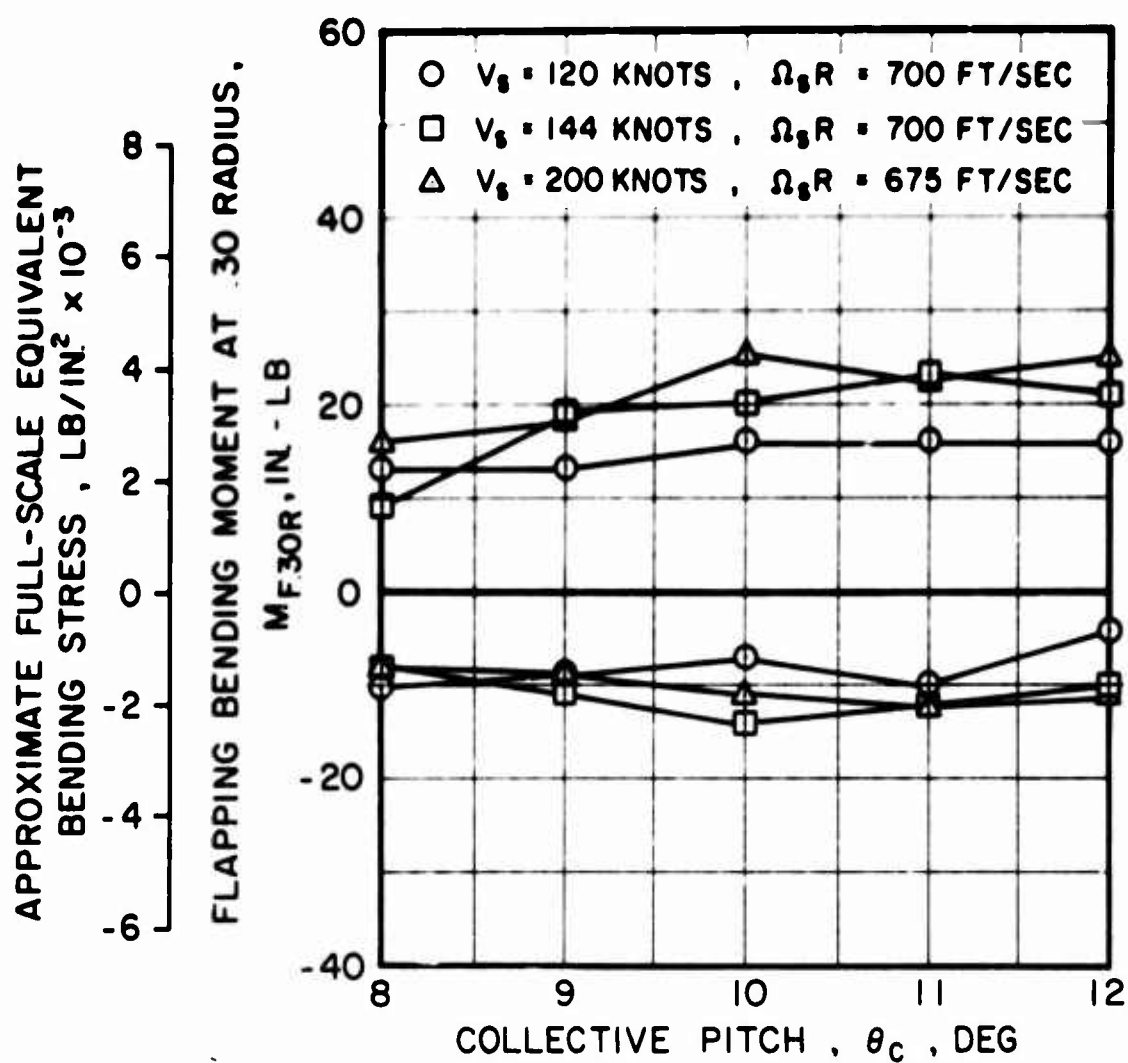


Figure 61. Range of Blade Flapwise Bending Response During Stall Flutter Testing; $Y_{CG}/c = 0.25$, $\alpha_s = 0.0^\circ$, $a_{1s} = b_{1s} = 0.0^\circ$.

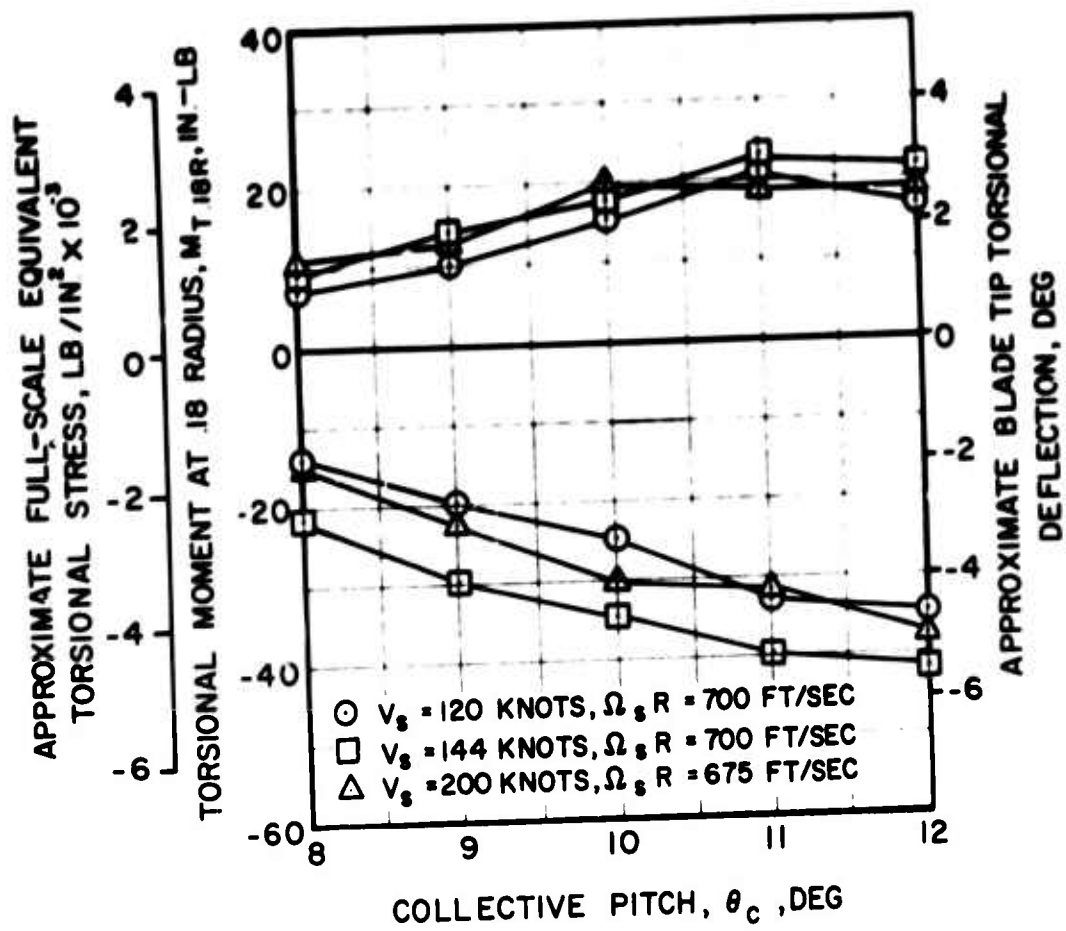


Figure 62. Range of Blade Torsional Response During Stall Flutter Testing; $Y_{CG}/c = 0.25$, $\alpha_s = 0.0^\circ$, $a_{1s} = b_{1s} = 0.0^\circ$.

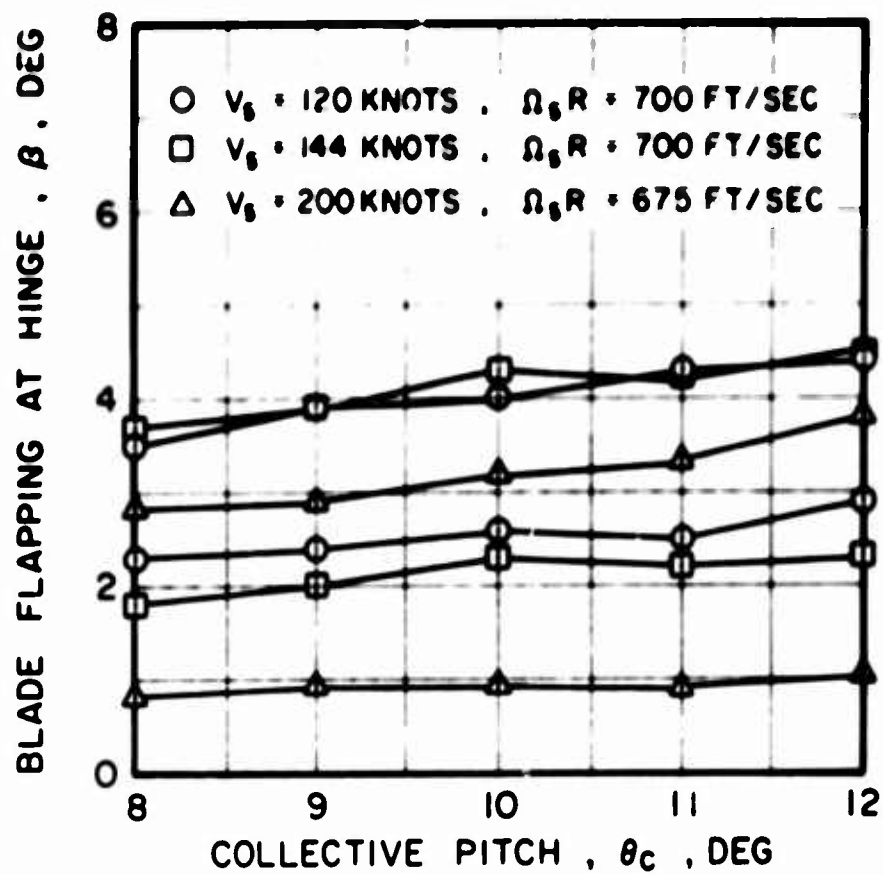


Figure 63. Range of Blade Flapping Response During Stall Flutter Testing; $Y_{CG}/c = 0.25$, $\alpha_s = 0.0^\circ$, $a_{1s} = b_{1s} = 0.0^\circ$.

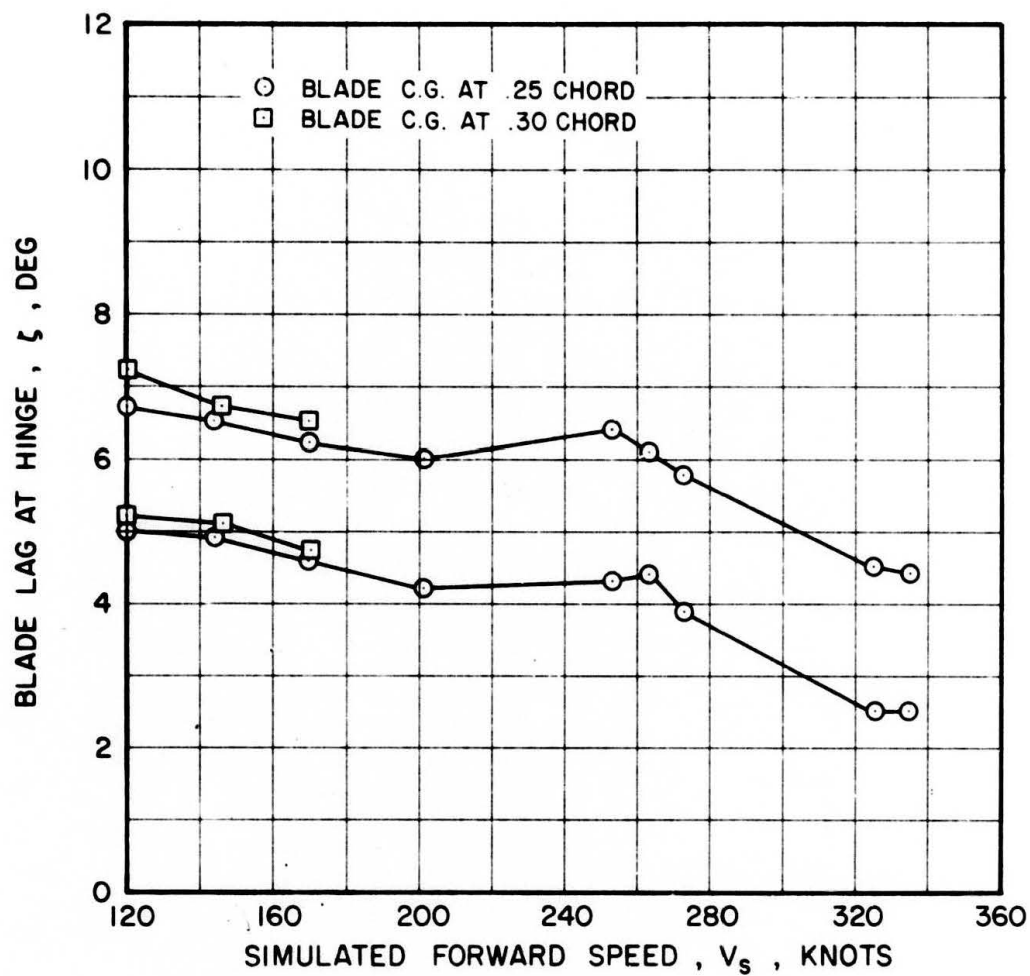


Figure 64. Range of Blade Lag Response During Combined Advancing Blade Aeroelastic Limits and Stall Flutter Testing;
 $\alpha_s = 0.0^\circ$, $a_{1s} = b_{1s} = 0.0^\circ$, $\Omega_s R = 700$ ft/sec,
 $\theta_c = 10.0^\circ$.

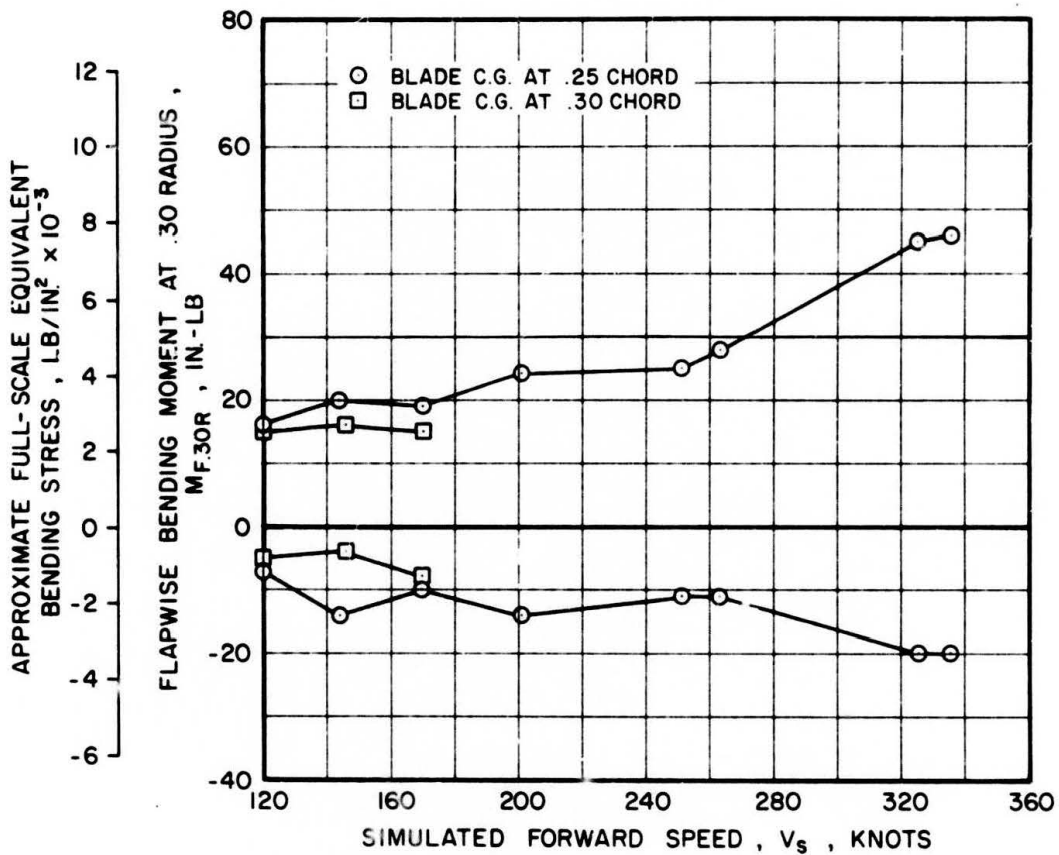


Figure 65. Range of Blade Flapwise Bending Response During Combined Advancing Blade Aeroelastic Limits and Stall Flutter Testing; $\alpha_s = 0.0^\circ$, $a_{1s} = b_{1s} = 0.0^\circ$, $\Omega_s R = 700$ ft/sec, $\theta_c = 10.0^\circ$.

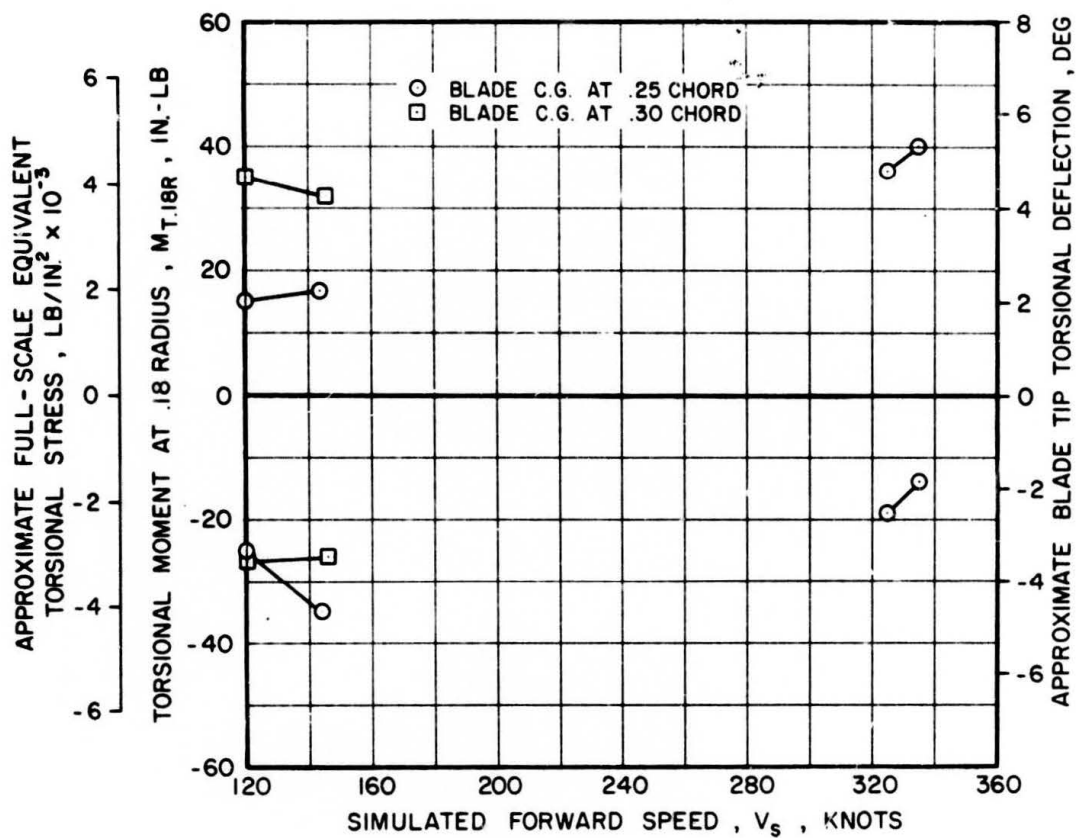


Figure 66. Range of Blade Torsional Response During Combined Advancing Blade Aeroelastic Limits and Stall Flutter Testing; $\alpha_s = 0.0^\circ$, $a_{1s} = b_{1s} = 0.0^\circ$, $\Omega_s R = 700$ ft/sec, $\theta_c = 10.0^\circ$.

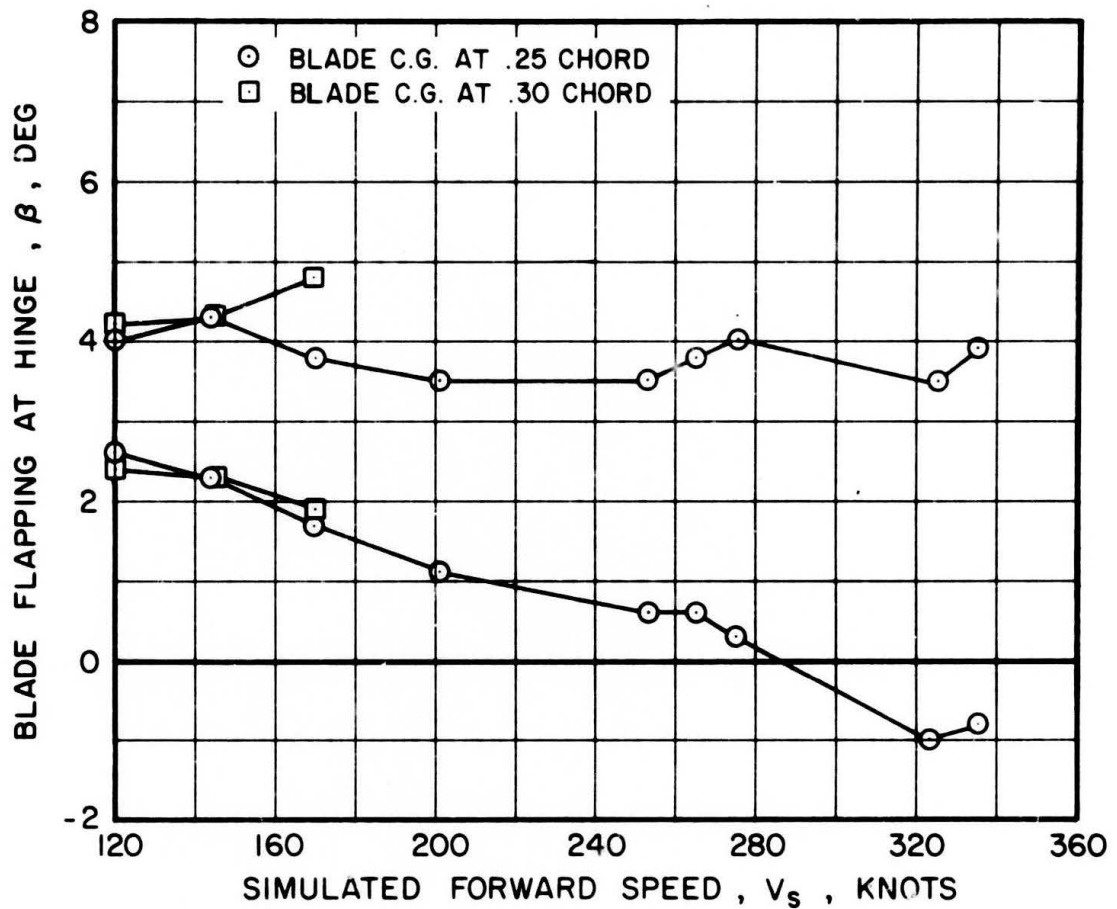


Figure 67. Range of Blade Flapping Response During Combined Advancing Blade Aeroelastic Limits and Stall Flutter Testing; $\alpha_s = 0.0^\circ$, $a_{1s} = b_{1s} = 0.0^\circ$, $\Omega_s R = 700$ ft/sec, $\theta_c = 10.0^\circ$.

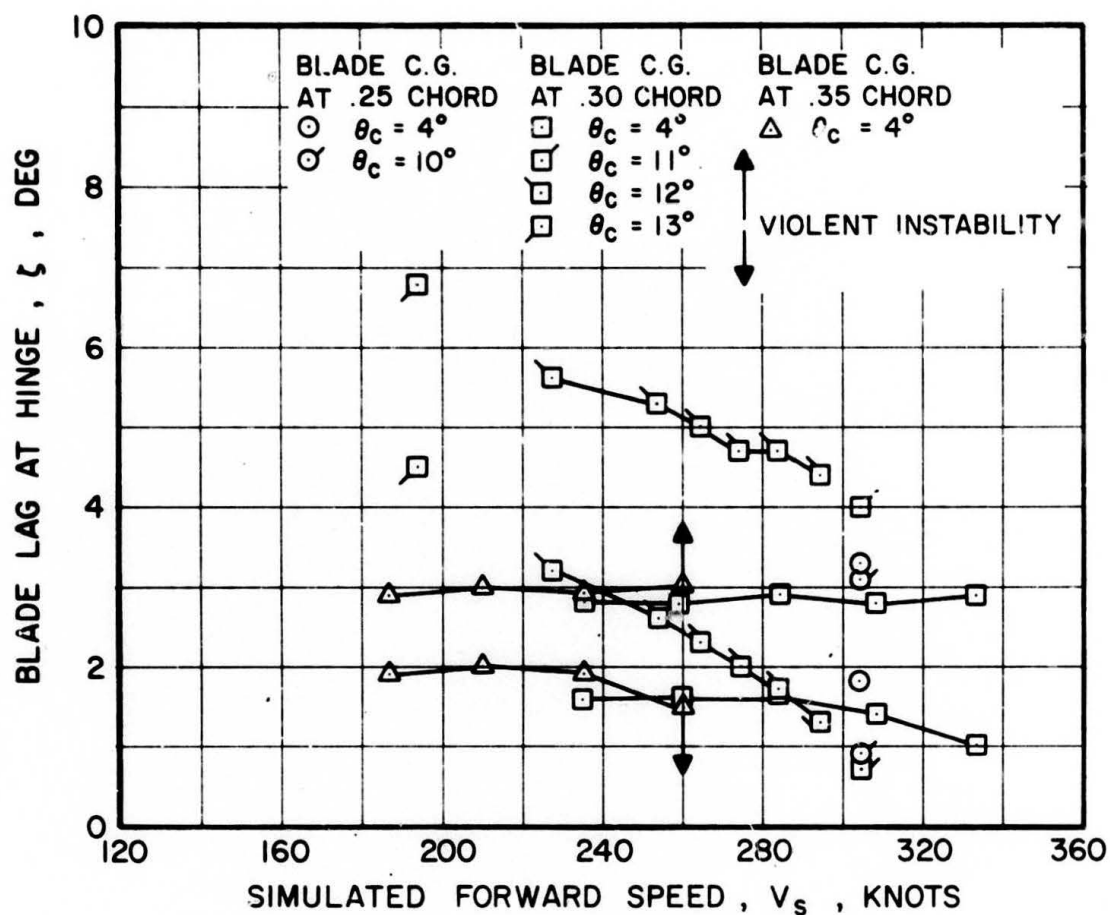


Figure 68. Range of Blade Lag Response During Advancing Blade Aeroelastic Limits Testing at Reduced Simulated Rotational Tip Speed; $\alpha_s = 0.0^\circ$, $a_{1s} = b_{1s} = 0.0^\circ$, $\Omega_s R = 500$ ft/sec.

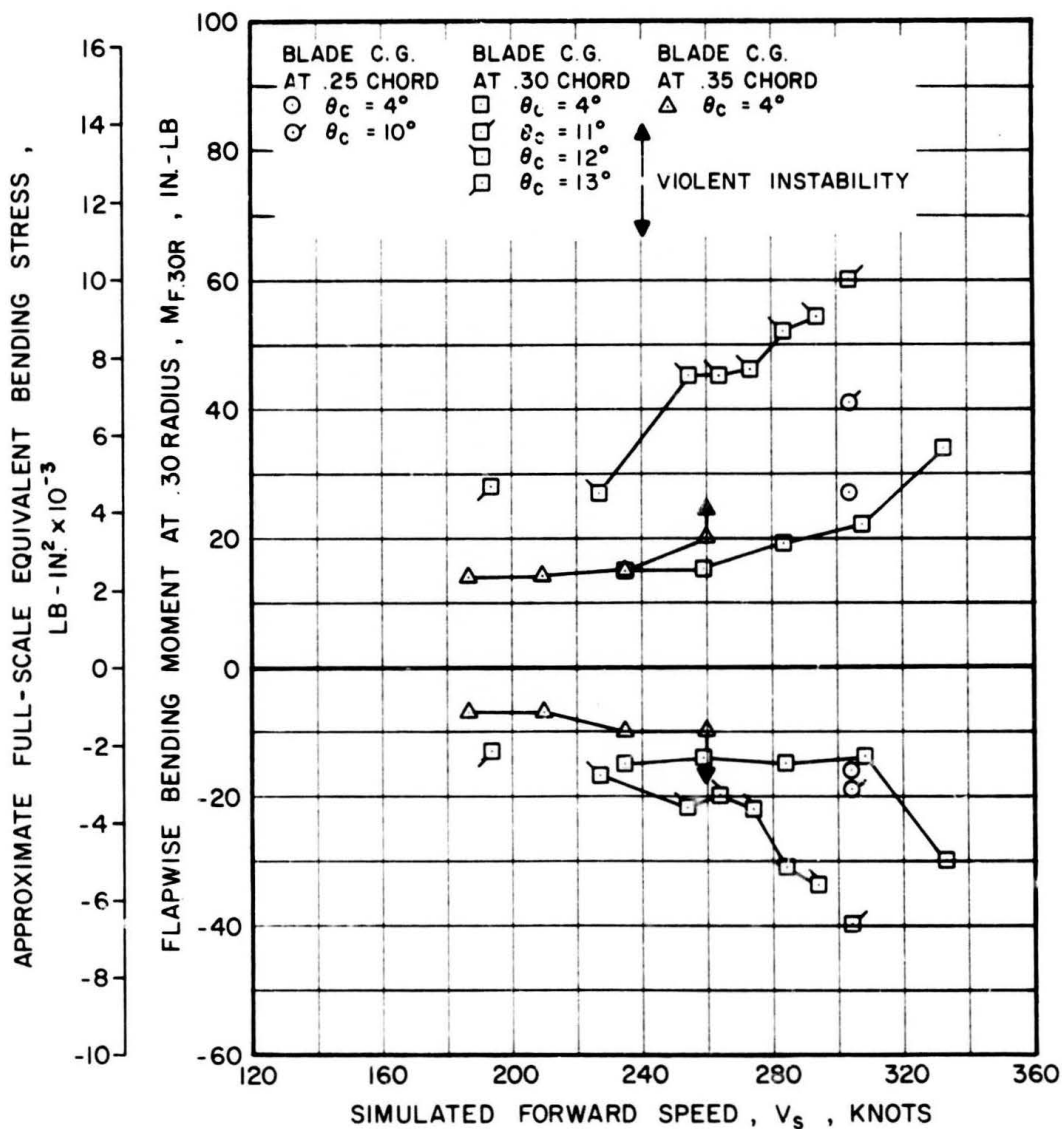


Figure 69. Range of Blade Flapwise Bending Response During Advancing Blade Aeroelastic Limits Testing at Reduced Simulated Rotational Tip Speed; $\alpha_s = 0.0^\circ$, $a_{1s} = b_{1s} = 0.0^\circ$, $\Omega_s R = 500$ ft/sec.

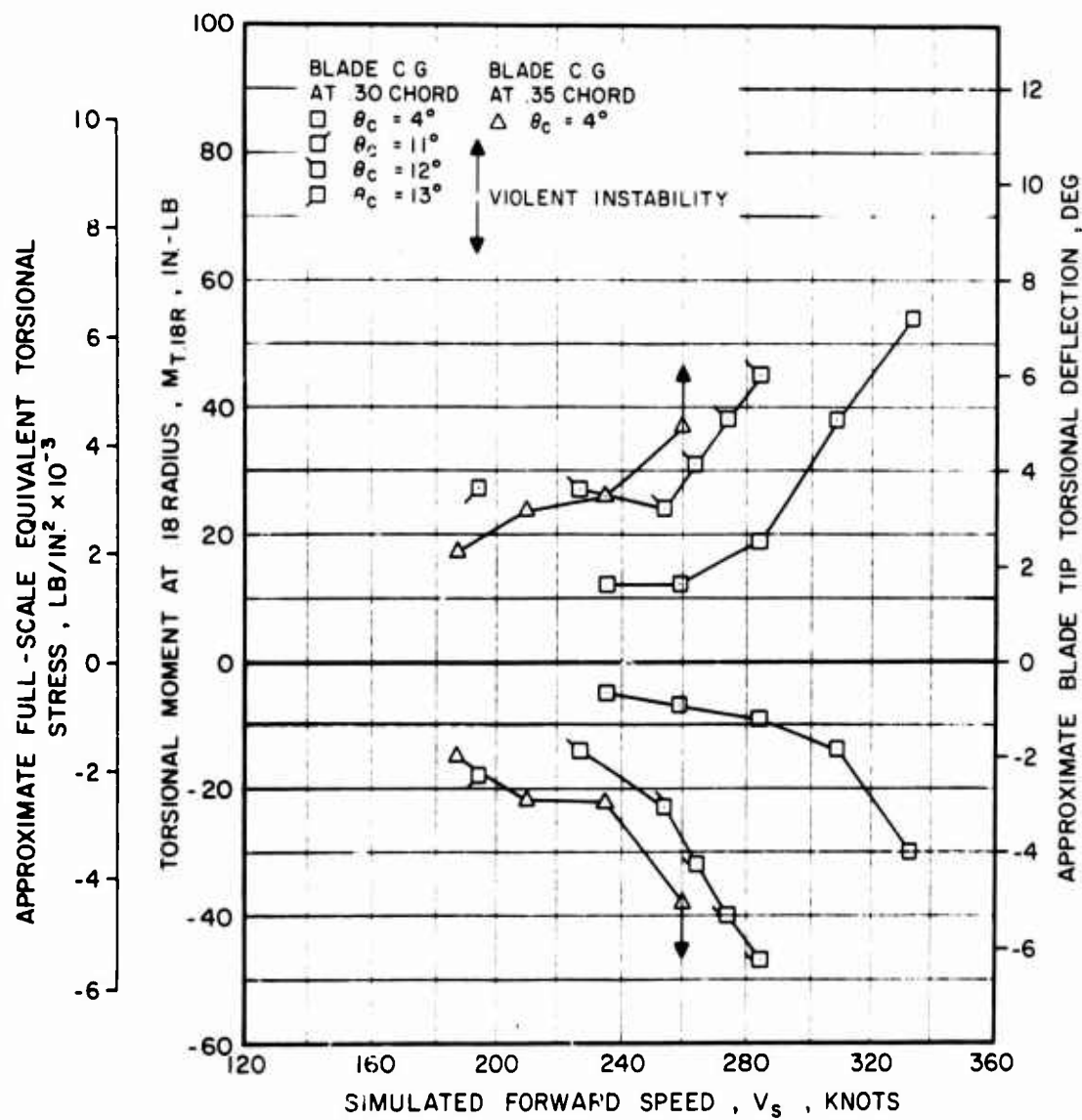


Figure 70. Range of Blade Torsional Response During Advancing Blade Aeroelastic Limits Testing at Reduced Simulated Rotational Tip Speed; $\alpha_s = 0.0^\circ$, $a_{1s} = b_{1s} = 0.0^\circ$, $\Omega_s R = 500$ ft/sec.

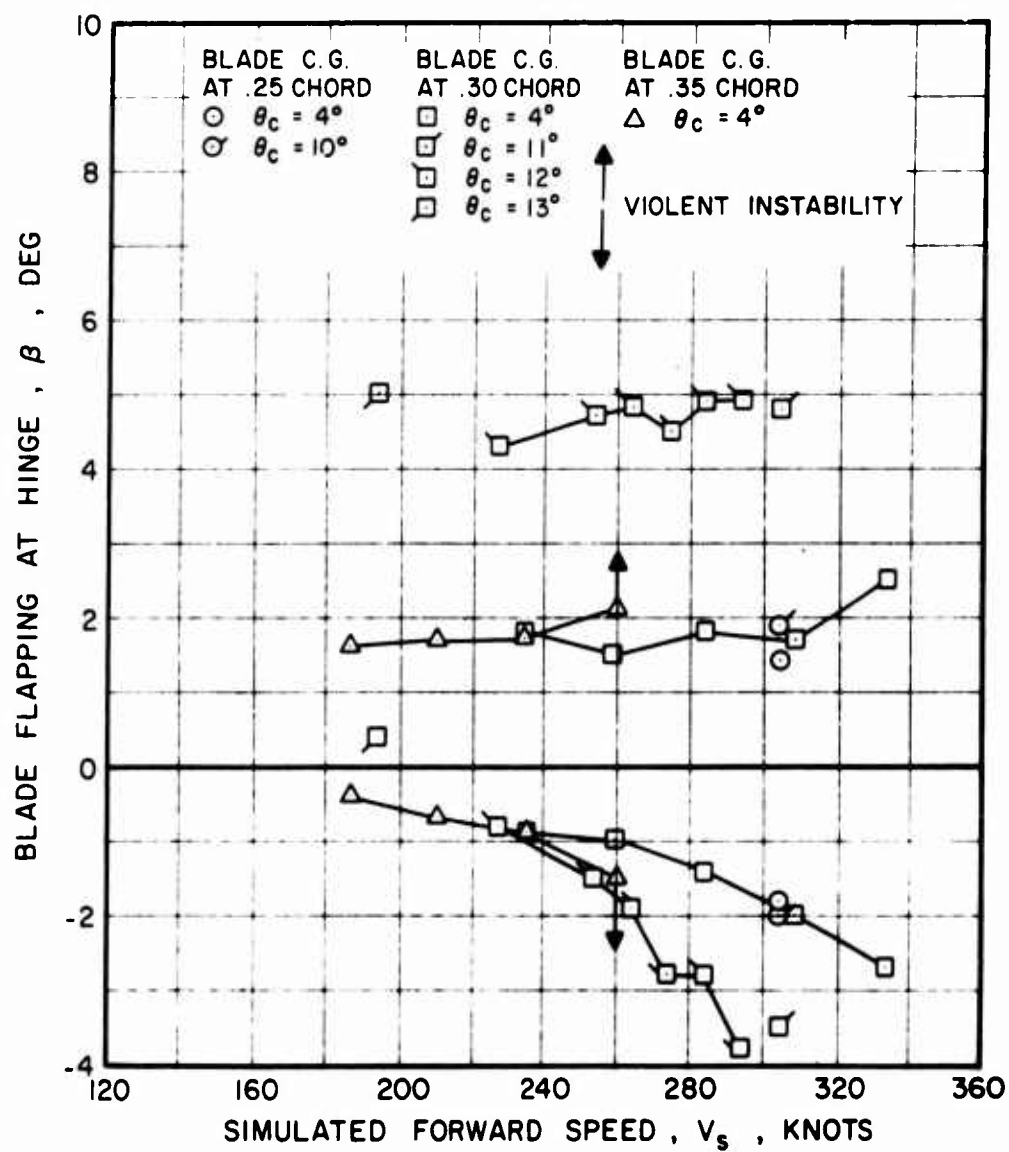


Figure 71. Range of Blade Flapping Response During Advancing Blade Aeroelastic Limits Testing at Reduced Simulated Rotational Tip Speed; $\alpha_s = 0.0^\circ$, $a_{1s} = b_{1s} = 0.0^\circ$, $\Omega_s R = 500$ ft/sec.

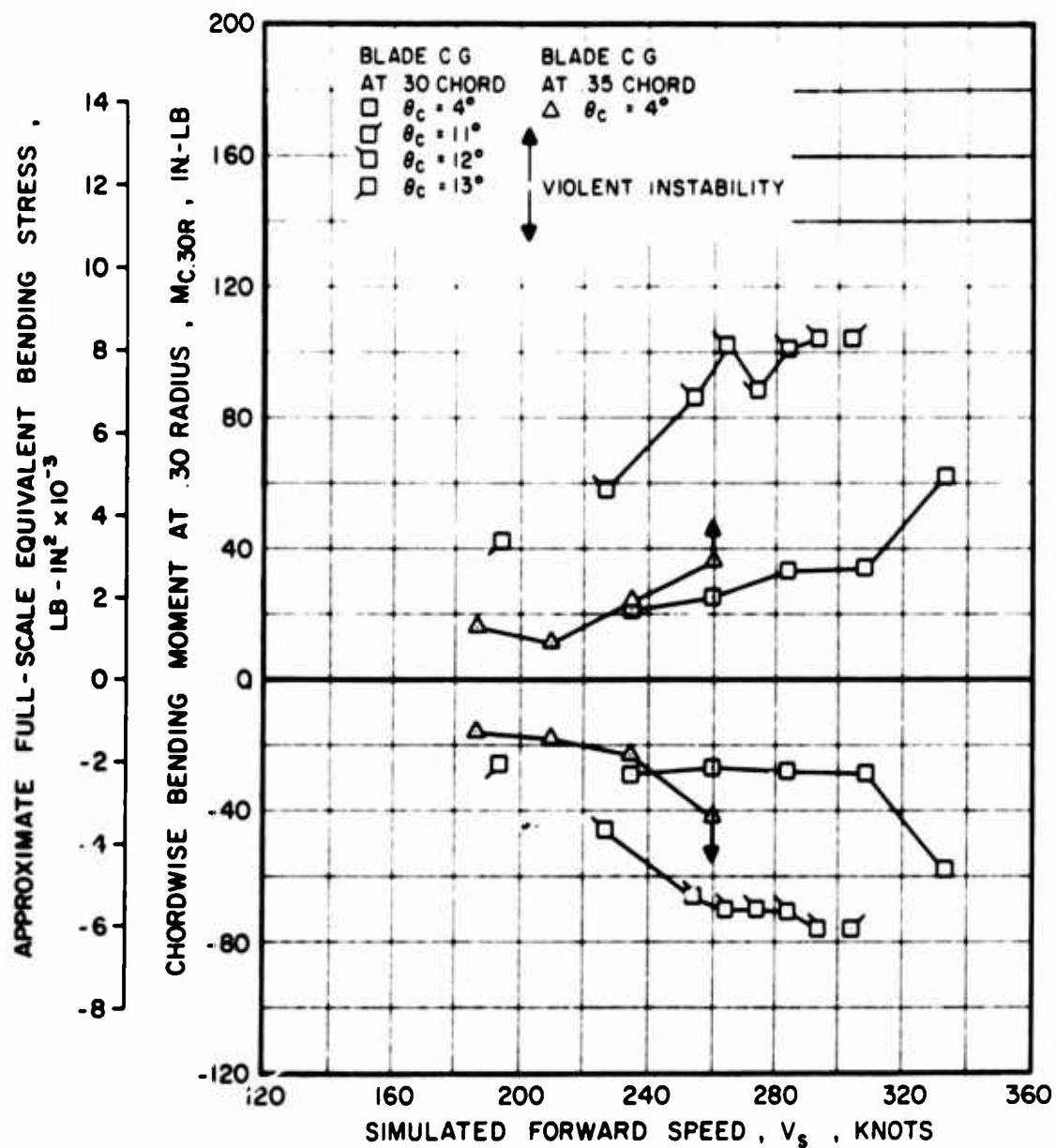


Figure 72. Range of Blade Chordwise Bending Response During Advancing Blade Aeroelastic Limits Testing at Reduced Simulated Rotational Tip Speed, $a_s = 0.0^\circ$, $a_{1s} = b_{1s} = 0.0^\circ$, $\Omega_s R = 500$ ft/sec.

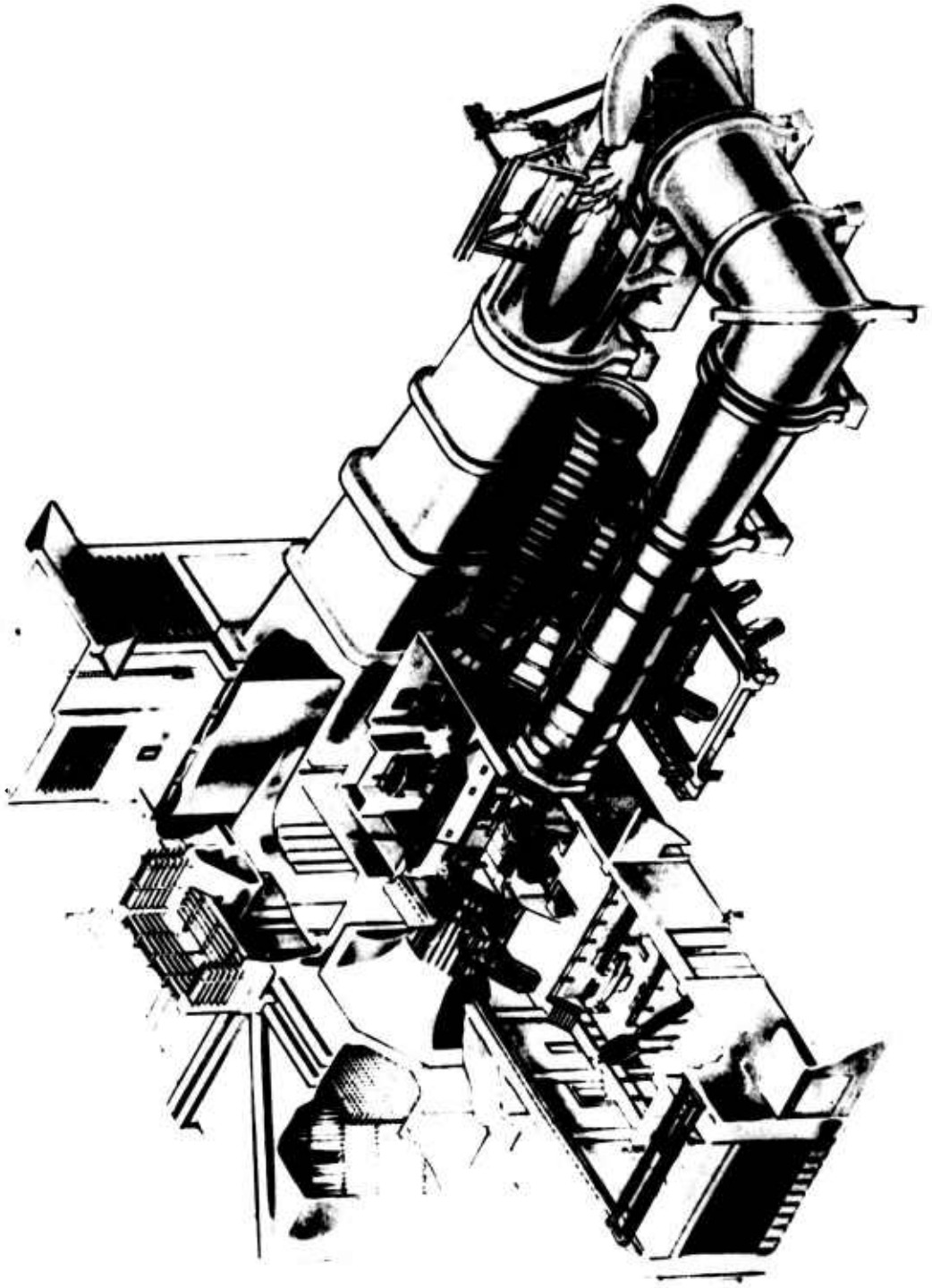


Figure 73. United Aircraft Research Laboratories 18-Foot Main Wind Tunnel.

APPENDIX I
DESCRIPTION OF FACILITIES AND EQUIPMENT

WIND TUNNEL

The 18-foot Main Wind Tunnel at the United Aircraft Research Laboratories is a closed-throat, single-return wind tunnel capable of speeds up to approximately 180 knots. A cutaway drawing of this tunnel is shown in Figure 73. The test section has an octagonal cross section. Tunnel stagnation temperature is held approximately constant by variable-opening air exchangers. Stagnation pressure is atmospheric and is constant throughout the unobstructed test section. Tunnel controls and data acquisition equipment are located in the control room adjacent to the tunnel test section. Windows permit constant observation of the model from the control room.

DATA ACQUISITION SYSTEM

The rotor balance is of the six-component, internal-strain-gage, floating-frame type. The balance is highly linear, is temperature compensated, and has small or negligible interactions between components. Interactions between balance components were determined experimentally and were included in the data reduction calculations. The rotor balance data were recorded manually from Baldwin SR-4 Precision Indicators (Type L-50).

The principal acquisition device for the dynamic data was an Ampex Model AR 200 magnetic tape recorder, which had a capacity of 14 information tracks and 2 edge tracks. The recording system was wide band F.M. A total of 11 tracks were used for dynamic data, 2 were used for rotor azimuth reference contactors, and the final track contained a data run command used in data reduction processing.

The blade strain gage instrumentation data were supplied to the tape through Sikorsky-built signal conditioning modules. Blade flap and lag angles were measured with Clifton Linear Generators. Special equipment supplied the complete flap and lag signal to the tape; it also electrically separated the first harmonic part of the flapping signal and resolved it into its longitudinal and lateral components. The first harmonic flapping components were displayed on the model control console and were recorded manually for use in the rotor performance calculations. Rotor control input data were acquired from two swash plate actuator potentiometers and the collective pitch follower potentiometer.

On-line spectral analysis was provided through the use of a tracking filter and an x-y plotter patched into the appropriate data channels.

Operation of the recording system was accomplished with a single control unit which featured selectable time duration data bursts and automatic calibration sequencing using standard resistance techniques.

DATA REDUCTION

The rotor balance readings, tunnel parameters, control console inputs, and first harmonic flapping components were transferred to punch cards and processed on a UNIVAC 1108 digital computer.

The dynamic data channels were processed by a nine-bit analogue to digital converter. The digital data were placed in the desired format on the digital tape by a Scientific Data Systems Computer, Model 910. The digital tape was processed by a UNIVAC 1108 computer to obtain the data in the desired physical units. The calibration records were converted from analog to digital form along with the actual test data to which they applied.

DATA ACCURACY AND REPEATABILITY

Rotor Performance Data

The repeatability of the rotor performance coefficient data is approximately 5 percent of the maximum reading, as demonstrated by comparison with the results of Reference 7. This figure exceeds conservative estimates of the accuracy of the rotor balance and tunnel parameter data. It is believed that the data repeatability is governed by the accuracy of the control servo, which is approximately 0.5 degree for the collective and cyclic pitch settings. The repeatability of the data can be related to physical quantities for better appreciation of its importance. The model rotor lift, for instance, repeats within approximately 10 pounds, or 5 percent of the maximum lift force obtained during the test. This is equivalent to a repeatability of 2,560 pounds for the dynamically similar condition with a 72-foot full-scale rotor.

Blade Load and Moment Data

It is estimated that the static accuracy of the blade dynamic data acquisition system is approximately 2 percent of the full-scale reading. This is equivalent to approximately 0.2 degree of flapping or lagging amplitude, or 2.0 inch-pounds of bending or twisting moment. This is similar in magnitude to the data repeatability indicated by average readings taken during the dynamic zero points for each wind tunnel run, which generally differed from zero within that tolerance. It is believed that the dynamic variations in load and moment are measured with even greater accuracy than 2 percent of full scale, since orderly variations of much smaller magnitude were noted in the data. In any event, the 2 percent full-scale accuracy represents an error in full-scale equivalent stress on the order of only 200 pounds per square inch, which is of little practical significance.

It should be noted that variations between individual time history records for different revolutions taken during actual test points include nonharmonic motions. If the rotor has significant random motion components, the concept of data repeatability has meaning only for the comparison of data intervals of appropriate time length.

APPENDIX II

TABLES OF MAXIMUM AND MINIMUM BLADE RESPONSE

TABLE XV. MAXIMUM AND MINIMUM BLADE MOTIONS AND LOADS
(BLADE CENTER OF GRAVITY AT .25 CHORD, TANGENT DELTA3 = 1.0)

RUN- PT. NO.	TYPE	BETA (DEG)		MF.30R (IN.-LB)		MF.60R (IN.-LB)		MT.35R (IN.-LB)	
		MAX.	MIN.	MAX.	MIN.	MAX.	MIN.	MAX.	MIN.
42-5	INITIAL	2.3	1.2	11.	-5.	11.	-5.	2.	-6.
42-6	TEST FINAL	6.3	-2.3	11.	-5.	12.	-7.	4.	-5.
42-7	TRANSIENT	7.0	-2.6	13.	-6.	13.	-11.	6.	-6.
42-8	INITIAL	2.2	1.1	11.	-4.	12.	-5.	2.	-5.
42-9	TEST FINAL	3.2	1.4	11.	-5.	14.	-7.	2.	-6.
42-10	TRANSIENT	2.9	1.0	11.	-4.	15.	-6.	4.	-9.
42-11	INITIAL	2.0	1.0	10.	-2.	13.	-3.	1.	-7.
42-12	TEST FINAL	3.8	-.5	12.	-3.	12.	-5.	2.	-6.
42-13	TRANSIENT	4.3	-.8	14.	-4.	13.	-5.	6.	-12.
42-14	INITIAL	2.2	.9	11.	-4.	12.	-3.	1.	-6.
42-15	TEST FINAL	4.3	-.8	13.	-4.	12.	-4.	1.	-7.
42-16	TRANSIENT	4.4	-.8	12.	-6.	12.	-4.	4.	-12.
42-17	INITIAL	2.2	1.0	10.	-4.	12.	-3.	1.	-7.
42-18	TEST FINAL	3.8	-.7	10.	-4.	12.	-2.	1.	-7.
42-19	TRANSIENT	3.9	-.8	11.	-6.	13.	-3.	2.	-9.
42-20	INITIAL	2.1	.2	11.	-4.	12.	-3.	1.	-6.
42-21	TEST FINAL	4.9	-1.5	13.	-4.	12.	-5.	1.	-7.
42-22	TRANSIENT	5.1	-1.6	13.	-4.	13.	-6.	3.	-11.
42-23	INITIAL	2.0	1.0	11.	-3.	13.	-3.	1.	-6.
42-24	TEST FINAL	5.0	-2.0	12.	-3.	13.	-4.	2.	-7.
42-25	TRANSIENT	5.7	-2.0	12.	-7.	16.	-5.	6.	-11.
42-26	INITIAL	3.4	-3.1	11.	-5.	13.	-5.	2.	-5.
42-27	TEST FINAL	9.4	-5.8	24.	-43.	42.	-22.	-	-
42-28	TRANSIENT	9.5	-5.8	25.	-44.	43.	-21.	-	-
42-29	INITIAL	6.4	-2.1	14.	-5.	16.	-7.	-	-
42-30	TEST FINAL	7.1	-2.9	12.	-5.	16.	-8.	-	-
42-31	TRANSIENT	7.3	-3.0	15.	-7.	16.	-8.	-	-
42-32	INITIAL	6.3	-2.0	12.	-4.	15.	-7.	-	-
42-33	TEST FINAL	6.9	-2.6	13.	-7.	14.	-7.	-	-
42-34	TRANSIENT	7.2	-2.9	15.	-7.	15.	-7.	-	-
42-35	INITIAL	2.2	1.6	7.	-7.	7.	-6.	-	-
42-36	TEST FINAL	4.3	1.4	11.	-7.	11.	-9.	-	-
42-37	TRANSIENT	4.7	1.1	12.	-9.	12.	-8.	-	-
42-38	INITIAL	2.9	1.7	12.	-5.	12.	-7.	-	-
42-39	TEST FINAL	6.1	-2.8	11.	-6.	14.	-6.	-	-
42-40	TRANSIENT	6.1	-3.0	17.	-9.	19.	-12.	-	-

TABLE XV - Continued

RUN- PT. NO.	TYPE	ZETA (DEG)		BETA (DEG)		MF.30R (IN.-LB)		MF.60R (IN.-LB)		MT.35R (IN.-LB)	
		MAX.	MIN.	MAX.	MIN.	MAX.	MIN.	MAX.	MIN.	MAX.	MIN.
45- 5	INITIAL	3.9	3.0	2.1	.1	14.	-8.	15.	-7.	3.	-9.
45- 7	TEST FINAL	4.3	3.3	3.5	-.1	20.	-10.	19.	-9.	5.	-11.
45- 8	TRANSIENT	4.6	3.1	3.5	-.3	18.	-9.	19.	-9.	5.	-11.
45- 9	INITIAL	3.9	2.8	2.0	.1	13.	-8.	15.	-8.	3.	-8.
45-10	TEST FINAL	3.8	2.7	3.7	-1.6	15.	-7.	18.	-9.	4.	-10.
45-11	TRANSIENT	4.0	2.7	4.1	-1.9	16.	-9.	17.	-8.	4.	-11.
45-12	INITIAL	4.0	3.1	2.0	-.1	13.	-9.	15.	-9.	4.	-9.
45-13	TEST FINAL	4.5	3.4	4.3	-1.5	18.	-9.	20.	-9.	8.	-14.
45-14	TRANSIENT	4.6	3.0	4.7	-1.5	20.	-10.	21.	-10.	8.	-16.
45-15	INITIAL	5.2	4.2	2.8	.4	20.	-10.	21.	-9.	11.	-19.
45-16	TEST FINAL	5.1	3.6	6.6	-2.9	25.	-9.	23.	-12.	11.	-24.
45-17	TRANSIENT	5.3	3.0	7.4	-3.2	25.	-11.	25.	-16.	11.	-26.
45-18	INITIAL	5.4	4.0	3.0	.4	20.	-10.	21.	-10.	9.	-19.
45-19	TEST FINAL	5.4	3.8	4.0	-1.2	22.	-11.	21.	-10.	11.	-17.
45-20	TRANSIENT	5.5	3.8	4.1	-1.1	24.	-13.	24.	-11.	11.	-20.
45-21	INITIAL	5.2	4.1	3.0	.3	19.	-10.	21.	-9.	8.	-14.
45-22	TEST FINAL	5.2	4.0	5.1	-.5	18.	-10.	20.	-9.	7.	-15.
45-23	TRANSIENT	5.4	3.9	5.3	-.8	22.	-12.	23.	-12.	13.	-20.
45-24	INITIAL	5.2	4.0	3.1	.4	23.	-12.	22.	-10.	11.	-19.
45-25	TEST FINAL	5.2	4.1	6.6	-3.3	19.	-9.	19.	-10.	5.	-12.
45-26	TRANSIENT	6.3	3.8	7.4	-4.2	22.	-14.	22.	-18.	11.	-22.
45-27	INITIAL	5.2	3.9	3.0	.4	20.	-11.	20.	-10.	11.	-19.
45-28	TEST FINAL	5.3	3.8	7.9	-3.1	22.	-11.	21.	-12.	10.	-21.
45-29	TRANSIENT	5.5	3.8	8.1	-3.4	25.	-13.	21.	-13.	11.	-22.
46- 5	INITIAL	4.8	3.5	5.9	-3.7	21.	-11.	17.	-10.	9.	-10.
46- 6	TEST FINAL	5.7	4.2	5.5	-2.3	25.	-12.	21.	-11.	11.	-14.
46- 7	TRANSIENT	5.8	3.4	5.8	-3.7	26.	-12.	22.	-12.	10.	-14.
46- 8	INITIAL	5.0	3.5	5.9	-3.6	21.	-12.	17.	-11.	9.	-11.
46- 9	TEST FINAL	4.6	3.4	4.4	-1.6	20.	-14.	19.	-11.	10.	-12.
46-10	TRANSIENT	4.8	3.3	5.7	-3.5	21.	-13.	20.	-12.	8.	-12.
46-11	INITIAL	4.9	3.6	5.8	-3.5	20.	-11.	18.	-10.	7.	-11.
46-12	TEST FINAL	5.7	4.1	4.5	-1.1	21.	-13.	21.	-12.	10.	-14.
46-13	TRANSIENT	5.6	3.4	5.7	-3.5	24.	-15.	22.	-12.	9.	-15.
46-14	INITIAL	2.7	1.9	3.3	.8	20.	-12.	17.	-16.	7.	-12.
46-15	TEST FINAL	3.8	2.3	5.9	.4	25.	-12.	25.	-21.	13.	-28.
46-16	TRANSIENT	4.0	1.4	6.1	.0	27.	-14.	26.	-18.	13.	-26.
46-17	INITIAL	3.9	3.0	1.6	-.2	16.	-9.	14.	-8.	6.	-7.
46-18	TEST FINAL	3.2	2.4	5.9	-3.5	14.	-10.	15.	-11.	5.	-9.
46-19	TRANSIENT	3.6	2.2	6.5	-3.9	16.	-11.	16.	-17.	8.	-10.
46-20	INITIAL	3.3	2.3	2.4	.4	15.	-10.	16.	-13.	5.	-8.
46-21	TEST FINAL	3.8	2.8	5.2	-4.1	17.	-10.	12.	-9.	7.	-6.
46-22	TRANSIENT	4.1	2.6	5.6	-4.8	18.	-14.	22.	-16.	8.	-10.

TABLE XV - Continued

RUN- PT. NO.	TYPE	ZETA (DEG)		BETA (DEG)		MF,30R (IN,-LB)		MF,60R (IN,-LB)		MT,35R (IN,-LB)		MC,30R (IN,-LB)	
		MAX.	MIN.	MAX.	MIN.	MAX.	MIN.	MAX.	MIN.	MAX.	MIN.	MAX.	MIN.
47- 5	INITIAL	4.7	3.7	1.6	-1.1	17.	-18.	25.	-21.	7.	-14.	19.	-31.
47- 6	TEST FINAL	3.7	2.8	6.9	-4.6	30.	-40.	41.	-31.	8.	-33.	42.	-51.
47- 7	TRANSIENT	4.6	2.6	7.4	-5.0	40.	-42.	48.	-32.	13.	-33.	44.	-56.
47- 8	INITIAL	4.7	3.7	1.3	-1.1	15.	-21.	25.	-21.	8.	-15.	23.	-34.
47- 9	TEST FINAL	5.1	3.7	5.3	-3.4	28.	-35.	40.	-32.	13.	-16.	62.	-45.
47-10	TRANSIENT	4.8	3.5	5.6	-3.4	30.	-36.	41.	-32.	14.	-17.	27.	-28.
47-11	INITIAL	4.8	3.8	1.5	-.8	13.	-18.	20.	-19.	10.	-13.	28.	-38.
47-12	TEST FINAL	4.6	3.7	3.6	-2.4	15.	-19.	26.	-21.	8.	-18.	26.	-28.
47-13	TRANSIENT	4.9	3.6	3.8	-2.8	19.	-22.	28.	-22.	8.	-20.	38.	-28.
47-14	INITIAL	4.7	3.7	1.5	-.9	18.	-19.	22.	-19.	7.	-12.	27.	-22.
47-15	TEST FINAL	4.8	3.7	2.7	-2.7	16.	-21.	22.	-20.	7.	-15.	31.	-21.
47-16	TRANSIENT	4.8	3.7	2.6	-2.8	18.	-21.	29.	-24.	9.	-14.	31.	-27.
47-17	INITIAL	4.9	3.7	4.3	-5.0	27.	-22.	22.	-27.	23.	-13.	41.	-35.
47-18	TEST FINAL	5.1	3.7	4.3	-1.3	31.	-38.	43.	-30.	14.	-21.	75.	-40.
47-19	TRANSIENT	5.2	3.5	5.0	-4.8	34.	-41.	45.	-30.	23.	-20.	68.	-39.
47-20	INITIAL	5.0	3.7	2.0	-1.7	28.	-26.	25.	-28.	22.	-12.	40.	-28.
47-21	TEST FINAL	5.0	3.8	4.1	-3.5	29.	-32.	36.	-29.	14.	-16.	68.	-47.
47-22	TRANSIENT	5.1	3.7	4.3	-3.8	29.	-35.	41.	-31.	23.	-17.	68.	-40.
47-23	INITIAL	4.7	3.7	1.8	-1.5	28.	-23.	23.	-27.	-	-	39.	-23.
47-24	TEST FINAL	5.0	3.7	4.0	-3.4	30.	-34.	39.	-30.	14.	-16.	67.	-43.
47-25	TRANSIENT	4.7	3.5	4.3	-3.3	31.	-35.	39.	-30.	25.	-14.	64.	-35.
47-26	INITIAL	4.9	3.5	1.7	-1.5	29.	-24.	25.	-25.	25.	-11.	42.	-30.
47-28	TEST FINAL	3.5	2.0	4.6	-5.6	45.	-22.	46.	-29.	49.	-9.	87.	-87.
47-29	TRANSIENT	4.6	1.8	4.8	-5.6	48.	-25.	48.	-29.	51.	-14.	70.	-77.
47-30	INITIAL	4.9	3.4	2.0	-1.4	29.	-22.	22.	-26.	23.	-12.	50.	-47.
47-31	TEST FINAL	4.8	3.5	7.1	-5.5	36.	-41.	46.	-30.	12.	-21.	87.	-40.
47-32	TRANSIENT	5.1	3.3	7.4	-5.2	31.	-40.	46.	-30.	23.	-23.	79.	-47.
47-33	INITIAL	4.8	3.6	7.1	-5.3	36.	-41.	47.	-21.	12.	-21.	80.	-48.
47-34	TEST FINAL	4.9	3.7	3.9	-3.4	28.	-31.	37.	-30.	16.	-14.	78.	-46.
47-35	TRANSIENT	5.0	3.5	7.1	-5.2	36.	-41.	46.	-30.	13.	-21.	87.	-58.
47-36	INITIAL	4.7	3.6	6.9	-5.3	33.	-40.	48.	-30.	12.	-19.	80.	-41.
47-37	TEST FINAL	4.8	3.4	1.9	-1.5	27.	-24.	22.	-27.	25.	-12.	51.	-41.
47-38	TRANSIENT	5.0	3.2	7.0	-5.4	35.	-44.	49.	-30.	26.	-21.	75.	-49.
47-39	INITIAL	5.0	3.4	4.3	-1.7	33.	-40.	45.	-30.	11.	-20.	77.	-33.
47-40	TEST FINAL	5.0	3.7	4.4	-4.9	26.	-21.	19.	-26.	26.	-11.	41.	-38.
47-41	TRANSIENT	5.2	3.4	4.6	-5.2	40.	-38.	42.	-31.	28.	-19.	78.	-63.
47-42	INITIAL	6.1	4.4	5.2	-2.2	42.	-51.	57.	-31.	35.	-20.	87.	-84.
47-43	TEST FINAL	5.1	3.7	4.5	-5.1	28.	-30.	30.	-27.	20.	-15.	68.	-27.
47-44	TRANSIENT	6.2	3.7	5.2	-5.3	47.	-47.	54.	-26.	34.	-19.	87.	-75.

TABLE XV - Concluded

RUN- PT. NO.	TYPE	ZETA (DEG)		BETA (DEG)		MF.30R (IN.-LB)		MF.60R (IN.-LB)		MT.18R (IN.-LB)		MT.35R (IN.-LB)	
		MAX.	MIN.	MAX.	MIN.	MAX.	MIN.	MAX.	MIN.	MAX.	MIN.	MAX.	MIN.
60-5	INITIAL	3.8	2.8	2.3	1.4	7.	-2.	15.	-9.	3.	-5.	2.	-5.
60-6	TEST FINAL	4.2	3.4	3.5	1.4	9.	-2.	16.	-8.	2.	-7.	2.	-7.
60-7	TRANSIENT	4.4	2.8	3.5	1.4	9.	-3.	17.	-9.	3.	-7.	3.	-6.
60-8	INITIAL	1.4	.6	2.8	1.9	6.	-4.	12.	-10.	5.	-3.	4.	-3.
60-9	TEST FINAL	2.3	1.4	5.0	2.0	9.	-2.	13.	-9.	7.	-14.	6.	-13.
60-10	TRANSIENT	2.4	.7	5.2	1.6	11.	-5.	15.	-14.	7.	-16.	6.	-15.
60-11	INITIAL	3.6	2.7	2.1	.1	14.	-6.	19.	-11.	5.	-8.	5.	-9.
60-12	TEST FINAL	4.1	3.1	3.6	.3	19.	-8.	25.	-13.	7.	-12.	6.	-12.
60-13	TRANSIENT	4.5	2.8	3.8	-.2	17.	-9.	25.	-11.	6.	-13.	5.	-12.
60-14	INITIAL	3.7	2.7	2.0	.1	13.	-6.	17.	-11.	4.	-8.	4.	-8.
60-15	TEST FINAL	4.5	3.1	4.6	-1.2	18.	-8.	25.	-13.	9.	-12.	8.	-12.
60-16	TRANSIENT	4.4	2.6	5.0	-1.3	18.	-8.	24.	-12.	9.	-13.	7.	-13.
60-17	INITIAL	3.6	2.3	6.5	-3.8	17.	-11.	21.	-13.	8.	-11.	9.	-12.
60-18	TEST FINAL	4.4	3.0	6.0	-2.8	21.	-12.	24.	-15.	10.	-14.	10.	-13.
60-19	TRANSIENT	4.5	2.4	6.4	-4.0	19.	-12.	25.	-14.	10.	-15.	9.	-13.
60-20	INITIAL	3.5	2.2	6.5	-3.8	19.	-8.	20.	-12.	10.	-10.	9.	-10.
60-21	TEST FINAL	4.4	2.8	5.0	-1.0	24.	-12.	25.	-16.	13.	-17.	12.	-19.
60-22	TRANSIENT	4.4	2.4	6.4	-3.8	23.	-11.	24.	-14.	11.	-16.	9.	-17.
60-23	INITIAL	1.3	.5	3.6	1.0	15.	-9.	19.	-18.	9.	-14.	7.	-12.
60-24	TEST FINAL	2.7	1.3	6.2	.8	19.	-9.	25.	-19.	14.	-31.	13.	-30.
60-25	TRANSIENT	2.7	.0	6.6	.2	21.	-11.	32.	-19.	14.	-29.	12.	-29.
60-26	INITIAL	3.3	2.0	1.3	-1.0	11.	-15.	22.	-21.	6.	-14.	7.	-11.
60-27	TEST FINAL	3.2	2.1	5.4	-2.9	25.	-30.	38.	-28.	14.	-16.	10.	-12.
60-28	TRANSIENT	3.3	2.0	5.4	-3.1	30.	-29.	41.	-28.	17.	-17.	12.	-14.
60-29	INITIAL	4.5	2.7	5.1	-2.1	41.	-44.	58.	-24.	43.	-24.	33.	-20.
60-30	TEST FINAL	3.5	2.3	5.0	-5.2	27.	-24.	31.	-24.	25.	-15.	20.	-13.
60-31	TRANSIENT	5.3	2.1	5.6	-5.6	48.	-40.	62.	-26.	43.	-30.	33.	-28.

TABLE XVI. MAXIMUM AND MINIMUM BLADE MOTIONS AND LOADS
(BLADE CENTER OF GRAVITY AT .25 CHORD, TANGENT DELTA3 = 0.0)

RUN- PT. NO.	TYPE	ZETA (DEG)		BETA (DEG)		MF.60R (IN.-LB)		MT.35R (IN.-LB)	
		MAX.	MIN.	MAX.	MIN.	MAX.	MIN.	MAX.	MIN.
49- 5	INITIAL	5.9	4.8	2.7	1.7	17.	- 9.	3.	- 7.
49- 6	TEST FINAL	6.2	4.5	6.8	-1.8	17.	-11.	7.	-14.
49- 7	TRANSIENT	6.1	4.6	6.9	-1.8	18.	-13.	6.	-16.
49- 8	INITIAL	5.8	4.7	2.7	1.7	17.	- 9.	2.	- 7.
49- 9	TEST FINAL	7.1	5.6	4.6	.6	23.	-10.	9.	-11.
49-10	TRANSIENT	7.3	4.8	4.6	.7	22.	-12.	10.	-16.
49-11	INITIAL	6.9	5.8	2.7	1.4	18.	- 6.	2.	- 7.
49-12	TEST FINAL	7.1	5.8	4.4	.0	20.	- 9.	2.	-10.
49-13	TRANSIENT	7.3	5.7	4.2	.2	21.	- 9.	2.	-12.
49-14	INITIAL	6.8	5.7	2.9	1.7	19.	- 7.	2.	- 7.
49-15	TEST FINAL	7.1	5.8	4.9	- .2	17.	- 7.	3.	- 7.
49-16	TRANSIENT	7.2	5.4	4.9	- .3	17.	- 8.	4.	-15.
49-17	INITIAL	7.1	5.8	2.9	1.7	18.	- 6.	1.	- 7.
49-18	TEST FINAL	7.0	5.8	4.4	.1	17.	- 6.	2.	- 9.
49-19	TRANSIENT	7.1	5.4	4.5	- .2	20.	- 7.	3.	-12.
49-20	INITIAL	6.9	5.8	2.7	1.6	17.	- 8.	2.	- 7.
49-21	TEST FINAL	7.3	5.8	6.1	-1.1	19.	- 9.	4.	-10.
49-22	TRANSIENT	7.6	5.8	5.9	- .9	18.	- 9.	5.	-14.
49-23	INITIAL	7.0	5.8	3.0	1.8	19.	- 7.	2.	- 6.
49-24	TEST FINAL	7.0	5.6	5.9	-1.2	19.	-10.	4.	-14.
49-25	TRANSIENT	7.0	5.2	5.9	-1.1	20.	-10.	4.	-13.
49-26	INITIAL	6.0	4.6	6.3	-2.6	19.	- 9.	2.	- 6.
49-27	TEST FINAL	5.2	3.4	9.0	-6.2	40.	-28.	6.	-10.
49-28	TRANSIENT	5.5	3.2	9.0	-6.2	40.	-28.	7.	-10.
49-29	INITIAL	7.7	5.7	7.1	-1.8	21.	-10.	9.	-21.
49-30	TEST FINAL	7.7	5.5	7.9	-2.7	23.	-10.	5.	-26.
49-31	TRANSIENT	8.2	5.0	8.0	-2.9	22.	-14.	10.	-24.
49-32	INITIAL	7.8	5.7	7.2	-2.0	20.	-11.	9.	-18.
49-33	TEST FINAL	7.6	5.4	7.8	-2.3	21.	-10.	12.	-20.
49-34	TRANSIENT	8.2	5.5	7.6	-2.2	20.	-11.	14.	-37.
49-35	INITIAL	2.5	1.1	3.3	2.3	15.	-16.	9.	-18.
49-36	TEST FINAL	5.7	3.1	7.0	- .1	15.	-16.	16.	-33.
49-37	TRANSIENT	5.6	1.0	7.1	- .1	17.	-21.	18.	-38.
49-38	INITIAL	5.1	3.4	3.9	2.5	18.	-18.	13.	-24.
49-39	TEST FINAL	4.8	3.4	7.1	-2.3	18.	-10.	8.	-12.
49-40	TRANSIENT	5.5	3.4	7.0	-2.1	21.	-17.	14.	-27.

TABLE XVI - Continued

RUN- FT. NO.	TYPE	ZETA (DEG)		BETA (DEG)		MF.30R (IN.-LB)		MF.60R (IN.-LB)		MT.35R (IN.-LB)	
		MAX.	MIN.	MAX.	MIN.	MAX.	MIN.	MAX.	MIN.	MAX.	MIN.
54- 5	INITIAL	5.1	3.5	5.9	-3.3	19.	-10.	19.	-13.	11.	-13.
54- 6	TEST FINAL	6.6	4.7	4.6	-.4	26.	-17.	27.	-16.	22.	-38.
54- 7	TRANSIENT	6.6	3.3	5.8	-3.1	24.	-14.	28.	-16.	21.	-37.
54- 8	INITIAL	5.0	3.6	5.8	-3.3	20.	-12.	20.	-14.	10.	-13.
54- 9	TEST FINAL	6.5	4.7	4.8	-.9	22.	-15.	26.	-17.	20.	-37.
54-11	TRANSIENT	6.4	3.0	5.7	-3.1	28.	-17.	26.	-18.	19.	-36.
54-12	INITIAL	3.3	2.2	2.8	.4	20.	-11.	17.	-16.	7.	-14.
54-13	TEST FINAL	5.8	2.8	8.6	-3.4	20.	-13.	33.	-18.	22.	-37.
54-14	TRANSIENT	5.9	1.8	8.4	-3.3	24.	-13.	34.	-20.	19.	-39.
54-15	INITIAL	3.2	2.4	.8	-.8	11.	-.9	12.	-.7	1.	-.5
54-16	TEST FINAL	3.8	2.7	4.6	-2.8	14.	-12.	16.	-10.	7.	-.7
54-17	TRANSIENT	3.9	2.4	4.6	-2.6	15.	-12.	17.	-11.	6.	-.8
54-18	INITIAL	4.6	3.3	1.8	.1	15.	-.9	17.	-.9	4.	-.7
54-19	TEST FINAL	5.9	4.2	4.9	-1.7	19.	-10.	24.	-13.	11.	-20.
54-20	TRANSIENT	6.1	3.4	4.9	-1.8	19.	-10.	24.	-11.	11.	-21.
54-21	INITIAL	5.0	4.0	2.7	1.5	11.	-.5	15.	-.7	2.	-.8
54-22	TEST FINAL	6.3	4.9	4.7	.4	14.	-10.	18.	-.8	11.	-15.
54-24	TRANSIENT	6.2	3.9	4.8	.4	16.	-.8	20.	-.9	11.	-20.
54-25	INITIAL	2.7	1.8	3.1	2.2	11.	-.6	13.	-10.	8.	-16.
54-26	TEST FINAL	5.9	3.4	6.9	-.2	12.	-13.	12.	-14.	15.	-39.
54-27	TRANSIENT	5.9	1.6	7.0	-.1	21.	-14.	22.	-18.	20.	-35.
55- 5	INITIAL	3.5	2.5	.9	-1.6	13.	-12.	17.	-15.	6.	-.4
55- 6	TEST FINAL	2.6	1.6	5.8	-4.8	23.	-23.	30.	-26.	5.	-22.
55- 7	TRANSIENT	3.5	1.7	5.7	-4.5	21.	-23.	34.	-26.	5.	-22.
55- 8	INITIAL	3.2	2.3	.6	-1.4	14.	-13.	21.	-18.	4.	-.6
55- 9	INITIAL	3.3	2.4	.7	-1.2	15.	-15.	28.	-20.	4.	-.5
55-10	TEST FINAL	2.3	1.7	6.1	-5.1	31.	-28.	38.	-26.	6.	-18.
55-11	TRANSIENT	3.0	1.3	6.6	-5.4	26.	-26.	34.	-26.	7.	-19.
55-12	INITIAL	3.2	2.1	.7	-1.5	15.	-13.	20.	-20.	3.	-.5
55-13	TEST FINAL	3.2	2.0	2.8	-3.1	12.	-11.	18.	-16.	8.	-.7
55-14	TRANSIENT	3.2	2.1	2.9	-3.6	20.	-17.	25.	-25.	9.	-.5
55-15	INITIAL	3.2	2.1	.8	-1.5	15.	-14.	24.	-23.	3.	-.7
55-16	TEST FINAL	3.2	2.3	2.1	-3.1	16.	-12.	19.	-16.	4.	-.5
55-17	TRANSIENT	3.2	1.9	2.6	-3.6	18.	-18.	23.	-19.	6.	-.8
55-18	INITIAL	3.1	1.7	4.0	-5.0	27.	-16.	25.	-18.	21.	-.8
55-19	TEST FINAL	3.4	1.7	3.2	-1.5	29.	-27.	37.	-26.	16.	-15.
55-20	TRANSIENT	3.2	1.6	4.2	-5.4	28.	-29.	35.	-25.	22.	-15.
55-21	INITIAL	3.0	1.8	.7	-1.6	26.	-18.	26.	-19.	22.	-.7
55-22	TEST FINAL	3.1	1.8	2.0	-3.8	31.	-15.	28.	-26.	28.	-.5
55-23	TRANSIENT	3.3	1.8	2.0	-3.9	28.	-15.	27.	-25.	31.	-.5
55-24	INITIAL	3.1	1.8	.8	-1.7	23.	-14.	25.	-23.	24.	-.6
55-25	TEST FINAL	2.9	1.8	2.7	-3.2	25.	-17.	26.	-21.	21.	-11.
55-26	TRANSIENT	3.0	1.6	2.8	-2.7	27.	-20.	27.	-23.	24.	-12
55-27	INITIAL	2.9	1.6	1.0	-1.4	23.	-16.	25.	-17.	20.	-.8
55-28	TEST FINAL	2.7	1.4	3.7	-5.7	34.	-19.	42.	-24.	35.	-.5
55-29	TRANSIENT	3.1	1.6	3.5	-5.7	35.	-20.	38.	-26.	36.	-.8

TABLE XVI - Continued

RUN- PT. NO.	TYPE	ZETA (DEG)		BETA (DEG)		MF.60R (IN.-LB)		MT.35R (IN.-LB)	
		MAX.	MIN.	MAX.	MIN.	MAX.	MIN.	MAX.	MIN.
52- 5	INITIAL	4.5	3.4	5.9	-3.3	19.	-13.	12.	-15.
52- 6	TEST FINAL	6.2	4.4	5.0	-4.0	26.	-14.	19.	-38.
52- 7	TRANSIENT	6.1	3.3	5.9	-3.3	28.	-16.	19.	-33.
52- 8	INITIAL	4.7	3.3	6.1	-3.4	19.	-13.	11.	-13.
52- 9	TEST FINAL	5.0	3.4	4.5	-1.2	23.	-15.	15.	-23.
52-10	TRANSIENT	4.8	3.1	5.8	-3.5	22.	-17.	16.	-26.
52-11	INITIAL	4.8	3.4	5.9	-3.1	19.	-15.	12.	-17.
52-12	TEST FINAL	6.2	4.6	5.0	-1.2	25.	-15.	21.	-37.
52-13	TRANSIENT	6.1	3.4	5.8	-3.4	26.	-17.	19.	-37.
52-14	INITIAL	3.1	1.8	2.6	.6	16.	-16.	9.	-13.
52-15	TEST FINAL	5.4	2.6	8.5	-3.2	30.	-19.	21.	-38.
52-16	TRANSIENT	5.7	1.5	8.4	-3.3	32.	-20.	21.	-40.
52-17	INITIAL	3.2	2.2	1.6	-.3	13.	-11.	4.	-5.
52-18	TEST FINAL	2.9	1.9	6.1	-3.3	16.	-13.	9.	-12.
52-19	TRANSIENT	3.2	1.7	6.1	-3.0	17.	-14.	11.	-11.
52-20	INITIAL	3.3	2.2	1.8	-.2	15.	-12.	4.	-5.
52-21	TEST FINAL	2.8	2.1	4.7	-4.7	12.	-8.	3.	-6.
52-22	TRANSIENT	3.2	2.0	4.7	-4.8	16.	-11.	6.	-6.
53- 5	INITIAL	3.6	2.4	2.0	.4	19.	-11.	4.	-6.
53- 6	TEST FINAL	4.9	3.2	5.2	-1.5	24.	-12.	14.	-20.
53- 7	TRANSIENT	5.2	2.6	5.1	-1.5	25.	-13.	11.	-17.
53- 8	INITIAL	3.6	2.3	2.2	.3	18.	-10.	4.	-7.
53- 9	TEST FINAL	3.9	2.5	4.1	-1.3	22.	-12.	6.	-10.
53-10	TRANSIENT	3.9	2.4	3.9	-1.2	23.	-13.	7.	-12.
53-11	INITIAL	3.5	2.4	2.2	.3	19.	-11.	4.	-6.
53-12	TEST FINAL	4.9	3.1	4.7	-1.1	25.	-13.	12.	-20.
53-13	TRANSIENT	4.9	2.5	4.4	-1.2	26.	-13.	11.	-18.
53-14	INITIAL	5.2	3.5	3.4	1.1	27.	-16.	18.	-27.
53-15	TEST FINAL	6.2	3.4	7.2	-2.2	31.	-17.	21.	-36.
53-16	TRANSIENT	6.0	3.3	6.8	-2.2	33.	-18.	20.	-43.
53-17	INITIAL	5.1	3.4	3.6	1.0	27.	-14.	18.	-30.
53-18	TEST FINAL	5.3	3.3	4.3	-.6	26.	-14.	19.	-29.
53-19	TRANSIENT	5.3	3.1	4.5	-.7	29.	-16.	20.	-35.
53-20	INITIAL	5.5	3.4	3.3	.8	26.	-17.	17.	-30.
53-21	TEST FINAL	5.3	3.4	5.5	-.2	28.	-15.	15.	-26.
53-22	TRANSIENT	5.6	3.4	5.3	-.1	27.	-15.	16.	-28.
53-23	INITIAL	5.8	4.1	3.1	.7	28.	-16.	18.	-30.
53-24	TEST FINAL	5.1	3.4	7.2	-3.2	23.	-16.	8.	-14.
53-25	TRANSIENT	6.1	3.5	7.1	-3.4	25.	-15.	16.	-29.
53-26	INITIAL	2.8	1.6	2.6	.5	18.	-16.	6.	-15.
53-27	TEST FINAL	2.4	1.1	5.1	-3.4	16.	-13.	2.	-6.
53-28	TRANSIENT	2.8	1.3	5.1	-3.5	20.	-14.	9.	-17.
53-29	INITIAL	5.1	3.1	3.3	.9	26.	-15.	16.	-31.
53-30	TEST FINAL	5.8	4.0	7.6	-2.4	27.	-14.	17.	-32.
53-31	TRANSIENT	6.4	3.7	7.9	-2.5	27.	-19.	19.	-34.

TABLE XVI - Concluded

RUN- PT. NO.	TYPE	ZETA (DEG)		BETA (DEG)		MF.30R (IN.-LB)		MF.60R (IN.-LB)		MT.35R (IN.-LB)	
		MAX.	MIN.	MAX.	MIN.	MAX.	MIN.	MAX.	MIN.	MAX.	MIN.
56-5	INITIAL	2.9	1.8	.6	-1.5	23.	-14.	24.	-22.	22.	-7.
56-6	TEST FINAL	3.2	1.8	6.3	-5.4	30.	-27.	41.	-26.	14.	-15.
56-7	TRANSIENT	3.1	1.6	6.1	-5.0	30.	-25.	37.	-26.	20.	-13.
56-8	INITIAL	3.3	1.8	5.8	-4.9	29.	-28.	40.	-26.	15.	-12.
56-9	TEST FINAL	3.2	1.9	3.5	-3.4	27.	-20.	30.	-22.	20.	-13.
56-10	TRANSIENT	3.5	1.8	5.9	-4.7	29.	-28.	40.	-25.	20.	-13.
56-11	INITIAL	3.0	1.8	6.2	-4.9	30.	-24.	36.	-26.	13.	-14.
56-12	TEST FINAL	3.2	1.9	.9	-1.7	23.	-15.	25.	-22.	19.	-8.
56-13	TRANSIENT	3.5	2.0	5.6	-4.8	31.	-24.	38.	-25.	23.	-11.
56-14	INITIAL	3.5	2.0	3.3	-1.5	29.	-28.	37.	-26.	15.	-13.
56-15	TEST FINAL	3.4	1.9	4.2	-4.9	27.	-16.	27.	-19.	22.	-6.
56-16	TRANSIENT	3.5	1.7	4.2	-5.1	32.	-26.	36.	-25.	23.	-15.
56-17	INITIAL	3.7	1.7	3.6	-1.2	38.	-30.	44.	-25.	37.	-22.
56-18	TEST FINAL	3.2	1.7	4.2	-5.4	39.	-23.	34.	-23.	36.	-9.
56-19	TRANSIENT	3.7	1.6	4.1	-5.6	45.	-38.	47.	-25.	39.	-16.

TABLE XVII. MAXIMUM AND MINIMUM BLADE MOTIONS AND LOADS (BLADE CENTER OF GRAVITY AT .25 CHORD, TANGENT OF LTA3 = 0.0)													
RUN- PT. NO.	TYPE	ZETA (DEG)		BETA (DEG)		MF. 30R (IN.-LB)		MF. 60R (IN.-LB)		MT. 18R (IN.-LB)		MT. 35R (IN.-LB)	
		MAX.	MIN.	MAX.	MIN.	MAX.	MIN.	MAX.	MIN.	MAX.	MIN.	MAX.	MIN.
50-5	STEADY	2.7	1.6	1.3	-1.1	15.	-13.	19.	-11.	-	-	6.	-5.
50-6	STEADY	2.9	1.8	1.9	-1.3	15.	-10.	19.	-17.	-	-	6.	-6.
50-7	STEADY	3.3	2.4	1.2	-1.9	20.	-14.	26.	-13.	-	-	13.	-7.
50-8	STEADY	3.3	2.0	1.2	-1.9	23.	-15.	25.	-16.	-	-	15.	-9.
50-9	STEADY	3.2	1.8	1.0	-2.3	25.	-14.	26.	-19.	-	-	19.	-7.
50-10	STEADY	3.5	1.6	.7	-2.0	26.	-15.	30.	-19.	-	-	22.	-4.
50-11	STEADY	2.9	1.5	.7	-2.6	30.	-19.	35.	-23.	-	-	29.	-3.
50-12	STEADY	2.8	1.3	.5	-3.4	35.	-24.	37.	-25.	-	-	38.	-3.
51-3	STEADY	5.4	3.8	3.4	2.1	18.	-8.	19.	-11.	-	-	13.	-19.
51-4	STEADY	6.2	4.5	3.6	2.1	17.	-10.	18.	-12.	-	-	17.	-30.
51-5	STEADY	7.1	5.1	3.5	2.0	19.	-8.	21.	-12.	-	-	19.	-37.
51-6	STEADY	7.9	6.0	3.7	2.4	12.	-4.	20.	-9.	-	-	15.	-34.
51-7	STEADY	4.7	3.0	2.8	.8	16.	-8.	21.	-12.	-	-	12.	-16.
51-8	STEADY	5.2	3.6	2.9	.9	18.	-9.	23.	-13.	-	-	14.	-21.
51-9	STEADY	5.8	3.9	3.2	.9	25.	-11.	25.	-15.	-	-	18.	-26.
51-10	STEADY	6.7	4.6	3.3	.9	22.	-12.	26.	-13.	-	-	18.	-32.
51-11	STEADY	7.1	5.0	3.8	1.0	25.	-11.	28.	-11.	-	-	19.	-35.
51-12	STEADY	3.3	1.8	1.4	-1.8	27.	-16.	31.	-17.	-	-	21.	-8.
51-13	STEADY	3.2	1.6	1.4	-1.9	34.	-18.	33.	-24.	-	-	27.	-8.
51-14	STEADY	3.1	1.2	2.0	-2.2	41.	-22.	41.	-29.	-	-	34.	-12.
51-15	STEADY	3.7	1.1	2.2	-1.8	38.	-23.	44.	-24.	-	-	41.	-16.
51-16	STEADY	3.1	.8	1.9	-2.0	41.	-19.	42.	-23.	-	-	43.	-15.
64-3	STEADY	2.4	1.7	1.7	.5	10.	-5.	-	-	4.	-3.	1.	-4.
64-4	STEADY	2.6	1.9	1.5	.2	12.	-7.	-	-	4.	-3.	3.	-4.
64-5	STEADY	2.8	1.8	1.4	-.1	12.	-6.	-	-	5.	-3.	3.	-4.
64-6	STEADY	2.6	1.8	1.3	-.3	12.	-6.	-	-	5.	-4.	3.	-5.
64-7	STEADY	2.8	1.8	1.1	-.4	14.	-8.	-	-	7.	-7.	4.	-6.
64-8	STEADY	2.6	1.6	1.3	-.9	15.	-12.	-	-	8.	-6.	5.	-7.
65-3	STEADY	2.9	1.8	1.2	-.5	16.	-10.	-	-	8.	-7.	-	-
65-4	STEADY	2.9	1.8	1.6	-1.2	16.	-12.	-	-	9.	-7.	-	-
65-5	STEADY	2.9	1.8	1.2	-1.1	17.	-12.	-	-	12.	-6.	-	-
65-6	STEADY	2.9	1.6	1.0	-1.0	17.	-10.	-	-	16.	-7.	-	-
67-3	STEADY	2.9	2.0	1.6	-1.2	18.	-12.	-	-	11.	-7.	-	-
67-4	STEADY	3.0	2.1	.9	-.7	13.	-13.	-	-	13.	-8.	-	-
67-5	STEADY	3.1	1.9	1.6	-1.4	18.	-14.	-	-	10.	-8.	-	-
67-6	STEADY	3.4	2.3	.7	-1.2	17.	-14.	-	-	19.	-8.	-	-
67-7	STEADY	3.4	2.0	.9	-1.6	22.	-15.	-	-	29.	-7.	-	-
67-8	STEADY	3.3	2.0	1.4	-2.0	26.	-20.	-	-	35.	-10.	-	-
67-9	STEADY	3.5	1.8	.6	-2.1	29.	-17.	-	-	41.	-10.	-	-
67-10	STEADY	3.0	1.0	.8	-2.9	33.	-27.	-	-	41.	-9.	-	-
67-11	STEADY	3.2	.4	.9	-3.2	34.	-29.	-	-	44.	-12.	-	-
67-12	STEADY	2.6	-1.0	.1	-4.7	43.	-41.	-	-	65.	-20.	-	-

TABLE XVII - Concluded											
RUN- PT. NO.	TYPE	ZETA (DEG)		BETA (DEG)		MF.30R (IN.-LB)		MF.60R (IN.-LB)		MT.18R (IN.-LB)	
		MAX.	MIN.	MAX.	MIN.	MAX.	MIN.	MAX.	MIN.	MAX.	MIN.
6A-3	STEADY	4.9	3.7	3.5	2.3	13.	-10.	17.	-11.	7.	-14.
6A-4	STEADY	5.6	4.0	3.9	2.4	13.	-9.	17.	12.	10.	-20.
6A-5	STEADY	6.7	5.0	4.0	2.6	16.	-7.	20.	-4	15.	-25.
6A-6	STEADY	7.3	5.4	4.3	2.5	16.	-10.	20.	-11.	20.	-33.
6A-7	STEADY	4.2	6.1	4.4	2.9	16.	-4.	22.	-10.	16.	-35.
6A-8	STEADY	4.7	3.5	3.7	1.8	14.	-8.	18.	-8.	9.	-22.
6A-9	STEADY	5.7	4.1	3.9	2.0	14.	-11.	19.	-12.	14.	-30.
6A-10	STEADY	6.5	4.9	4.3	2.3	20.	-4.	21.	-11.	17.	-35.
6A-11	STEADY	7.3	5.6	4.2	2.2	23.	-12.	22.	-13.	22.	-40.
6A-12	STEADY	4.2	6.2	4.5	2.3	21.	-10.	25.	-10.	21.	-42.
6A-13	STEADY	4.9	3.7	3.2	1.6	14.	-15.	17.	-11.	8.	-17.
6A-14	STEADY	5.4	4.0	3.5	1.6	17.	-5.	19.	-14.	7.	-25.
6A-15	STEADY	6.2	4.6	3.8	1.7	19.	-10.	21.	-13.	-	-
6A-16	STEADY	7.0	5.3	3.8	1.8	18.	-11.	22.	-14.	-	-
6A-17	STEADY	4.6	3.3	3.0	1.0	18.	-10.	21.	-13.	11.	-15.
6A-18	STEADY	5.3	3.8	3.5	1.0	24.	-12.	25.	-14.	16.	-21.
6A-19	STEADY	6.0	4.2	3.5	1.1	24.	-14.	27.	-15.	-	-
6A-20	STEADY	6.6	4.7	3.9	1.4	22.	-13.	27.	-10.	-	-
6A-3	STEADY	6.3	4.7	4.3	2.2	18.	-8.	19.	-11.	13.	-27.
6A-4	STEADY	8.1	6.1	4.8	2.4	25.	-10.	23.	-11.	-	-
6A-5	STEADY	6.4	4.3	3.5	.6	25.	-11.	28.	-15.	-	-
6A-6	STEADY	6.1	4.4	3.8	.6	28.	-11.	29.	-15.	-	-
6A-7	STEADY	5.8	3.9	4.0	.3	-	-	-	-	-	-
70-3	STEADY	5.2	3.4	3.3	.0	33.	-12.	-	-	14.	-15.
70-4	STEADY	3.0	1.9	1.8	.0	17.	-10.	-	-	13.	-10.
70-5	STEADY	5.5	3.9	3.9	-.3	39.	-16.	-	-	22.	-27.
70-6	STEADY	5.5	3.7	3.8	-.1	37.	-14.	-	-	18.	-21.
70-7	STEADY	5.4	3.0	4.2	-.5	43.	-17.	-	-	29.	-29.
70-8	STEADY	5.0	2.8	4.0	-.7	46.	-19.	-	-	32.	-29.
70-9	STEADY	4.5	2.5	3.5	-1.0	45.	-20.	-	-	36.	-19.
70-10	STEADY	4.4	2.5	3.9	-.8	46.	-20.	-	-	40.	-17.
71-3	STEADY	3.2	1.9	1.8	-1.5	17.	-18.	-	-	4.	-3.
71-4	STEADY	3.1	2.1	1.9	-.9	12.	-12.	-	-	3.	-3.
71-5	STEADY	3.3	2.1	.8	-1.2	11.	-11.	-	-	3.	-3.
71-6	STEADY	3.2	2.1	.7	-1.1	10.	-10.	-	-	2.	-3.
71-7	STEADY	3.1	1.8	.4	-1.1	12.	-8.	-	-	2.	-4.
71-8	STEADY	3.6	2.4	.4	-1.1	11.	-11.	-	-	1.	-4.
71-9	STEADY	3.9	2.4	.4	-1.3	10.	-11.	-	-	2.	-4.
71-10	STEADY	4.0	2.1	-.2	-2.2	15.	-17.	-	-	4.	-5.
71-11	STEADY	4.3	2.1	.3	-3.3	25.	-22.	-	-	2.	-6.
71-12	STEADY	4.4	2.0	-.6	-2.8	20.	-20.	-	-	4.	-7.
72-3	STEADY	4.2	2.0	.9	-1.5	11.	-15.	-	-	5.	-5.
72-4	STEADY	4.4	2.0	.3	-2.7	24.	-26.	-	-	7.	-6.
72-5	STEADY	4.6	2.0	.2	-2.5	24.	-23.	-	-	10.	-7.
72-6	STEADY	4.7	1.8	1.7	-3.5	26.	-25.	-	-	12.	-7.
72-7	STEADY	4.3	1.7	.1	-2.6	27.	-22.	-	-	25.	-12.
72-8	STEADY	3.6	1.4	1.5	-3.0	24.	-28.	-	-	30.	-12.
72-9	STEADY	3.9	2.0	2.0	-1.1	18.	-19.	-	-	21.	-7.

TABLE XVIII. MAXIMUM AND MINIMUM BLADE MOTIONS AND LOADS (BLADE CENTER OF GRAVITY AT .30 CHORD, TANGENT DELTA3 = 0.0)													
RUN- PT. NO.	TYPE	ZETA (DEG)		BETA (DEG)		MF.30R (IN.-LB)		MT.18R (IN.-LB)		MT.35R (IN.-LB)		MC.30R (IN.-LB)	
		MAX.	MIN.	MAX.	MIN.	MAX.	MIN.	MAX.	MIN.	MAX.	MIN.	MAX.	MIN.
74- 3	STEADY	2.6	1.7	2.1	1.1	8.	-2.	10.	-3.	9.	-2.	22.	-19.
74- 4	STEADY	2.7	1.8	2.1	.7	8.	-5.	13.	-6.	10.	-5.	28.	-19.
74- 5	STEADY	2.6	1.8	1.8	.3	9.	-6.	17.	-9.	13.	-9.	20.	-22.
74- 6	STEADY	2.6	1.6	2.1	.2	10.	-9.	18.	-13.	15.	-12.	27.	-29.
74- 7	STEADY	2.8	1.7	2.0	.0	12.	-9.	20.	-15.	16.	-14.	27.	-31.
74- 8	STEADY	3.2	1.9	2.4	-.3	15.	-13.	22.	-19.	18.	-17.	32.	-43.
74- 9	STEADY	2.9	1.1	2.0	-.8	18.	-10.	27.	-20.	19.	-17.	42.	-44.
75- 3	STEADY	2.8	1.6	1.8	-.9	15.	-15.	12.	-6.	9.	-5.	21.	-29.
75- 4	STEADY	2.8	1.6	1.5	-1.0	15.	-14.	12.	-7.	10.	-7.	25.	-27.
75- 5	STEADY	2.9	1.6	1.8	-1.4	19.	-15.	19.	-9.	11.	-9.	33.	-28.
75- 6	STEADY	2.8	1.4	1.7	-2.0	22.	-14.	37.	-14.	28.	-13.	34.	-29.
75- 7	STEADY	2.9	1.0	2.5	-2.6	34.	-30.	54.	-29.	42.	-25.	62.	-58.
75- 8	STEADY	2.5	.7	2.7	-2.9	33.	-32.	62.	-30.	49.	-26.	54.	-35.
75- 9	STEADY	2.4	.3	3.0	-3.0	26.	-37.	64.	-30.	51.	-26.	38.	-30.
75-10	STEADY	2.0	-.2	2.5	-3.5	33.	-28.	70.	-37.	57.	-32.	49.	-39.
75-11	STEADY	1.1	-1.8	1.8	-5.1	42.	-45.	85.	-28.	71.	-23.	80.	-76.
76- 3	STEADY	7.2	5.2	4.2	2.4	15.	-5.	35.	-27.	31.	-20.	33.	-13.
76- 4	STEADY	7.9	6.0	4.3	2.4	18.	-7.	36.	-25.	24.	-38.	43.	-15.
76- 5	STEADY	8.7	6.5	4.8	2.7	17.	-6.	-	-	27.	-27.	52.	-12.
76- 6	STEADY	9.8	7.5	5.0	2.7	17.	-7.	-	-	30.	-35.	59.	-11.
77- 3	STEADY	6.7	5.1	4.7	2.3	16.	-4.	32.	-26.	-	-	58.	-31.
77- 4	STEADY	7.5	6.0	4.7	2.3	15.	-5.	34.	-22.	-	-	51.	-28.
77- 5	STEADY	3.3	2.4	2.8	1.0	12.	-7.	17.	-9.	-	-	30.	-18.
77- 6	STEADY	2.4	1.3	2.1	.4	12.	-7.	19.	-14.	-	-	39.	-28.
77- 7	STEADY	2.8	1.8	2.4	.3	12.	-5.	20.	-14.	-	-	39.	-34.
77- 8	STEADY	2.4	1.3	2.0	.0	12.	-8.	20.	-18.	-	-	40.	-24.
77- 9	STEADY	2.9	1.5	2.4	.0	15.	-11.	20.	-19.	-	-	51.	-31.
77-10	STEADY	2.7	1.6	2.3	-.3	17.	-11.	24.	-21.	-	-	51.	-48.
77-11	STEADY	2.7	1.7	2.2	-.3	19.	-11.	27.	-21.	-	-	51.	-35.
77-12	STEADY	3.0	1.4	2.3	1.5	23.	-16.	9.	-18.	-	-	59.	-30.
77-13	STEADY	2.9	1.3	2.5	1.7	25.	-19.	16.	-19.	-	-	67.	-31.

TABLE XVIII - Concluded

RUN- PT. NO.	TYPE	ZETA (DEG)		BETA (DEG)		MF.30R (IN.-LB)		MT.18R (IN.-LB)		MT.35R (IN.-LB)		MC.30R (IN.-LB)	
		MAX.	MIN.	MAX.	MIN.	MAX.	MIN.	MAX.	MIN.	MAX.	MIN.	MAX.	MIN.
78- 3	STEADY	7.2	5.1	5.1	2.6	16.	-4.	33.	-27.	-	-	53.	-38.
78- 4	STEADY	8.0	6.0	5.0	2.8	14.	-4.	35.	-27.	-	-	56.	-38.
78- 5	STEADY	8.8	6.7	5.3	2.8	17.	-5.	37.	-23.	-	-	48.	-27.
78- 6	STEADY	6.5	4.7	4.8	1.9	15.	-8.	-	-	-	-	60.	-43.
79- 3	STEADY	6.8	4.5	5.0	.4	28.	-13.	27.	-18.	-	-	42.	-26.
79- 4	STEADY	5.6	3.2	4.3	-8.	27.	-17.	27.	-14.	-	-	58.	-46.
79- 5	STEADY	5.3	2.6	4.7	1.5	45.	-22.	24.	-23.	15.	-27.	86.	-66.
79- 6	STEADY	5.0	2.3	4.8	1.9	45.	-20.	31.	-32.	20.	-40.	102.	-70.
79- 7	STEADY	4.7	2.0	4.5	2.8	46.	-24.	38.	-40.	25.	-36.	88.	-70.
79- 8	STEADY	4.7	1.7	4.9	2.8	52.	-31.	45.	-47.	33.	-40.	100.	-71.
79- 9	STEADY	4.4	1.3	4.9	3.8	54.	-34.	-	-	38.	-44.	104.	-76.
79-10	STEADY	4.0	.7	4.8	3.5	60.	-40.	-	-	45.	-45.	104.	-76.
79-11	STEADY	3.5	1.0	4.0	3.5	-	-	-	-	-	-	85.	-68.
80- 3	STEADY	2.5	1.3	1.1	-1.0	14.	-23.	9.	-5.	-	-	10.	-12.
80- 4	STEADY	2.3	1.2	2.2	-2.2	19.	-24.	7.	-4.	-	-	13.	-13.
80- 5	STEADY	2.6	1.4	.8	-1.4	12.	-13.	6.	-5.	-	-	14.	-3.
80- 6	STEADY	2.6	1.4	.3	-1.5	11.	-13.	4.	-6.	-	-	20.	0.
80- 7	STEADY	2.5	1.2	.4	-2.1	12.	-13.	5.	-4.	-	-	23.	-1.
80- 8	STEADY	3.4	1.5	.1	-1.7	12.	-14.	4.	-4.	-	-	24.	4.
80- 9	STEADY	3.0	1.2	.0	-2.7	12.	-14.	7.	-4.	-	-	29.	2.
80-10	STEADY	3.3	1.2	.1	-3.8	19.	-16.	7.	-4.	-	-	33.	3.
80-11	STEADY	3.1	.7	-.1	-3.9	21.	-21.	9.	-5.	-	-	32.	2.
81- 3	STEADY	3.2	1.0	.6	-2.5	18.	-18.	14.	-3.	-	-	14.	-16.
81- 4	STEADY	2.9	.5	1.2	-4.3	23.	-19.	18.	-4.	-	-	16.	-17.
81- 5	STEADY	3.2	.4	1.2	-3.8	27.	-24.	21.	-6.	-	-	20.	-19.
81- 6	STEADY	2.8	.1	.5	-3.8	27.	-23.	32.	-8.	-	-	19.	-20.
81- 7	STEADY	2.3	-1.4	.7	-5.4	35.	-28.	53.	-8.	-	-	22.	-35.
81- 8	STEADY	2.0	-1.5	1.6	-4.7	37.	-31.	61.	-20.	-	-	22.	-48.
81- 9	STEADY	3.1	1.0	2.3	-3.6	-	-	52.	-14.	-	-	29.	-59.

TABLE XII. MAXIMUM AND MINIMUM BLADE MOTIONS AND LOADS (BLADE CENTER OF GRAVITY AT .35 CHORD, TANGENT DELTA3 = 0.0)															
BLADE PT. NO.	TYPE	ZETA (DEG)		BETA (DEG)		MF.30R (IN.-LB)		MF.60R (IN.-LB)		MT.10R (IN.-LB)		MT.35R (IN.-LB)		MC.30R (IN.-LB)	
		MAX.	MIN.	MAX.	MIN.	MAX.	MIN.	MAX.	MIN.	MAX.	MIN.	MAX.	MIN.	MAX.	MIN.
03-3	STEADY	1.1	.5	2.1	1.2	6.	-2.	5.	-9.	25.	-0.	-	-	16.	-23.
03-9	STEADY	1.2	.6	1.8	.9	13.	-0.	12.	-10.	30.	-27.	-	-	7.	-29.
03-5	STEADY	1.2	.6	1.9	.2	17.	-0.	16.	-10.	30.	-28.	-	-	16.	-33.
04-3	STEADY	2.9	1.9	1.6	.9	10.	-7.	13.	-9.	17.	-15.	20.	-10.	16.	-10.
04-9	STEADY	3.0	2.0	1.7	.7	10.	-7.	12.	-9.	20.	-22.	25.	-22.	11.	-10.
04-5	STEADY	2.9	1.9	1.7	.9	15.	-10.	11.	-10.	20.	-22.	20.	-23.	20.	-23.
04-9	STEADY	3.0	1.5	2.1	-1.5	19.	-10.	10.	-10.	37.	-30.	00.	-00.	36.	-02.
04-5	STEADY	3.1	1.9	1.7	-1.2	10.	-7.	15.	-10.	20.	-24.	30.	-25.	25.	-00.
04-9	STEADY	3.1	1.7	1.6	-1.2	15.	-0.	17.	-10.	27.	-20.	20.	-26.	30.	-35.
04-5	STEADY	3.0	1.9	2.1	-1.0	17.	-13.	19.	-20.	37.	-34.	36.	-37.	30.	-33.
04-9	STEADY	3.0	1.8	1.3	-2.2	22.	-10.	-	-	29.	-20.	26.	-36.	00.	-32.
04-10	STEADY	2.9	1.7	1.0	-1.6	10.	-20.	-	-	-	-	16.	-23.	32.	-16.
04-11	STEADY	2.9	1.6	1.3	-2.2	22.	-21.	-	-	-	-	13.	-16.	32.	-0.
04-12	STEADY	2.7	1.6	1.0	-2.6	23.	-21.	-	-	-	-	10.	-13.	32.	-4.
04-13	STEADY	2.6	.9	.3	-3.2	20.	-19.	-	-	-	-	13.	-12.	30.	-2.
04-15	STEADY	2.7	.8	.2	-3.0	20.	-20.	-	-	-	-	10.	-10.	30.	-1.
04-10	STEADY	2.9	.0	.0	-0.5	23.	-23.	11.	-9.	-	-	20.	-12.	00.	0.
05-3	STEADY	0.2	3.3	3.2	1.0	10.	-4.	-	-	-	-	20.	-1.	-1.	-37.
05-9	STEADY	0.2	3.2	2.7	1.0	12.	-3.	10.	-7.	-	-	35.	-13.	0.	-37.
05-5	STEADY	0.0	3.0	1.0	-2.2	12.	-3.	12.	-7.	10.	-10.	10.	-23.	55.	19.
05-9	STEADY	0.2	3.1	2.1	-1.1	10.	-9.	12.	-9.	20.	-20.	20.	-30.	07.	22.
05-5	STEADY	0.2	2.7	1.3	-2.3	20.	-21.	-	-	-	-	20.	-02.	00.	0.
05-9	STEADY	0.2	2.9	1.3	-2.3	21.	-21.	-	-	-	-	20.	-00.	00.	0.
06-3	STEADY	0.1	2.9	1.0	-0.9	12.	-11.	-	-	-	-	12.	-00.	13.	-10.
06-9	STEADY	0.0	2.9	.9	-1.1	12.	-11.	-	-	-	-	12.	-00.	12.	-12.
06-5	STEADY	0.2	3.0	.9	-1.3	17.	-12.	-	-	-	-	7.	-7.	12.	-17.
06-9	STEADY	0.3	3.1	.5	-1.3	13.	-12.	-	-	-	-	7.	-7.	17.	-11.
06-5	STEADY	0.3	3.0	.6	-1.3	12.	-12.	-	-	-	-	7.	-7.	10.	-11.
06-9	STEADY	0.0	3.2	-1.1	-1.0	11.	-11.	-	-	-	-	7.	-7.	10.	-11.
06-5	STEADY	0.0	3.1	-1.2	-1.9	12.	-12.	-	-	-	-	7.	-7.	21.	-11.
06-9	STEADY	0.1	3.2	-1.1	-2.2	12.	-12.	-	-	-	-	7.	-7.	27.	-19.
06-10	STEADY	0.1	3.3	-1.1	-2.0	10.	-15.	-	-	-	-	7.	-7.	22.	-13.
06-11	STEADY	0.1	3.1	-1.3	-2.0	10.	-15.	-	-	-	-	7.	-7.	22.	-13.

APPENDIX III
TABLE OF BLADE RESPONSE HARMONICS

TABLE XI. BLADE LAG MOTION HARMONICS - RUN 50 (BLADE CENTER OF GRAVITY AT .25 CHORD)								
RUN- PT. NO.	ONS OR (FPS)	VU	THEC (DEG)	BLADE LAG MOTION HARMONICS (DEG)				
				A1	A2	A3	A4	A5
50- 5 700	.731	2.0	.2	.0	.0	.2	.0	
50- 6 832	.808	2.0	.1	.0	.0	.0	.0	
50- 7 900	1.026	2.0	.2	.0	.1	-.1	.0	
50- 8 882	1.062	2.0	.0	.0	.1	.0	.1	
50- 9 857	1.119	2.0	.0	.0	.1	-.1	.0	
50-10 836	1.180	2.0	.2	.1	.1	.0	.0	
50-11 810	1.248	2.0	.0	.0	.1	.0	.0	
50-12 385	1.327	2.0	.0	.0	.1	-.1	.0	

RUN- PT. NO.	ONS OR (FPS)	VU	THEC (DEG)	BLADE LAG MOTION HARMONICS (DEG)				
				B1	B2	B3	B4	B5
50- 5 700	.731	2.0	.1	.1	.0	.1	.0	
50- 6 832	.808	2.0	.1	.1	.0	-.2	.0	
50- 7 900	1.026	2.0	-.1	.1	.1	-.1	.1	
50- 8 882	1.062	2.0	-.3	.1	.1	.0	.0	
50- 9 857	1.119	2.0	-.3	.1	.1	-.1	-.1	
50-10 836	1.180	2.0	.0	.1	.1	.1	.0	
50-11 810	1.248	2.0	-.4	.1	.1	-.1	-.1	
50-12 385	1.327	2.0	-.5	.1	.0	.0	.0	

TABLE XX - Concluded										
RUN- PT. NO.	OMS #R	THEC (DEG)	BLADE LAG MOTION HARMONICS (DEG)					R5	R4	R3
			MU	RS	R1	R2	R3			
50- 5	700	2.0	.731	2.3	.2	.1	.1	.2	.0	.0
50- 6	632	2.0	.808	2.4	.2	.1	.1	.2	.0	.0
50- 7	500	2.0	1.026	2.7	.3	.1	.1	.1	.1	.1
50- 8	482	2.0	1.062	2.7	.3	.1	.1	.1	.1	.1
50- 9	457	2.0	1.119	2.6	.3	.1	.1	.1	.1	.1
50-10	434	2.0	1.180	2.6	.4	.1	.1	.1	.1	.1
50-11	410	2.0	1.248	2.3	.4	.1	.1	.1	.1	.1
50-12	385	2.0	1.327	2.0	.5	.1	.1	.1	.1	.1

TABLE XXI. BLADE .30R FLAPWISE BENDING MOMENT HARMONICS-- RUN 50
(BLADE CENTER OF GRAVITY AT .25 CHORD)

BLADE .30R FLAPWISE BENDING MOMENT HARMONICS (IN.-LB)													
RUN- PT. NO.	OMS #R	MU (FPS)	THEC (DEG)	A1	A2	A3	A4	A5	A6	A7	A8	A9	A10
50- 5	700	.731	2.0	1.9	-1.8	-3.0	-.7	-.4	1.0	.2	.3	.4	.0
50- 6	632	.808	2.0	2.2	-1.8	-2.9	-1.0	-3.3	1.1	.6	.3	-.3	-.1
50- 7	500	1.026	2.0	3.2	-2.8	-1.3	-.5	-.6	2.5	.7	.0	-.1	.1
50- 8	482	1.062	2.0	3.3	-3.2	-1.8	-.3	-.5	.7	-.2	.0	-.2	-.2
50- 9	457	1.119	2.0	3.2	-4.2	-1.7	-1.0	-.8	-2.1	-.1	.0	-.4	-.1
50-10	434	1.180	2.0	3.0	-5.3	-3.7	-1.7	-1.0	-1.8	-1.0	-.5	-.5	-.3
50-11	410	1.248	2.0	2.6	-6.5	-3.7	-2.8	-1.3	-2.8	.2	.1	.0	-.2
50-12	385	1.327	2.0	1.9	-8.3	-2.2	-3.9	-2.3	-3.0	-.4	.3	.3	.1

BLADE .30R FLAPWISE BENDING MOMENT HARMONICS (IN.-LB)													
RUN- PT. NO.	OMS #R	MU (FPS)	THEC (DEG)	B1	B2	B3	B4	B5	B6	B7	B8	B9	B10
50- 5	700	.731	2.0	-1.9	1.9	5.4	-.4	-4.0	.0	.1	.0	-.2	.0
50- 6	632	.808	2.0	-2.6	1.7	5.9	.6	-2.2	.3	.4	.3	.0	.0
50- 7	500	1.026	2.0	-4.0	.6	9.5	.9	.4	-2.4	.4	.5	.2	.5
50- 8	482	1.062	2.0	-4.0	-.1	9.2	.8	.6	-2.1	.6	.6	.3	.1
50- 9	457	1.119	2.0	-4.0	-1.9	11.3	.3	.1	-.7	.7	.6	.0	-.2
50-10	434	1.180	2.0	-4.2	-1.9	11.6	-.1	.2	-.1	.6	.3	.1	-.2
50-11	410	1.248	2.0	-4.4	-2.7	15.6	1.5	1.2	1.7	.6	.4	.3	-.1
50-12	385	1.327	2.0	-5.2	-3.5	18.2	2.3	1.2	-.2	.6	-.1	-.2	-.2

TABLE XXI - Concluded														
BLADE .30R FLAPWISE BENDING MOMENT HARMONICS (IN.-LB)														
RUN-PT. NO.	OMS #R (FPS)	MU	THEC (DEG)	RS	R1	R2	R3	R4	R5	R6	R7	R8	R9	R10
50- 5	700	.731	2.0	.7	2.7	2.6	6.2	.8	4.0	1.0	.3	.3	.4	.0
50- 6	632	.808	2.0	1.0	3.5	2.5	6.6	1.1	4.0	1.2	.7	.5	.3	.1
50- 7	500	1.026	2.0	1.5	5.1	2.8	9.6	1.0	.7	3.4	.8	.5	.2	.5
50- 8	482	1.062	2.0	2.1	5.2	3.2	9.4	.8	.8	2.2	.7	.6	.3	.2
50- 9	457	1.119	2.0	2.5	5.1	4.3	11.5	1.1	.8	2.2	.7	.6	.4	.2
50-10	434	1.180	2.0	3.2	5.2	5.6	12.2	1.7	1.0	1.8	1.2	.6	.5	.3
50-11	410	1.248	2.0	3.4	5.1	7.1	16.1	3.2	1.7	3.3	.6	.4	.3	.2
50-12	385	1.327	2.0	3.5	5.5	9.0	18.3	4.6	2.6	3.0	.7	.3	.3	.2

TABLE XXII. BLADE .60R FLAPWISE BENDING MOMENT HARMONICS - RUN 50
(BLADE CENTER OF GRAVITY AT .25 CHORD)

BLADE .60R FLAPWISE BENDING MOMENT HARMONICS (IN.-LB)													
RUN- PT. NO.	OMS #R	MU (FPS)	THEC (DEG)	A1	A2	A3	A4	A5	A6	A7	A8	A9	A10
50- 5	700	.731	2.0	2.5	-1.6	-4.3	-2.0	-2.0	-.6	-.3	-.3	-.3	-.1
50- 6	632	.808	2.0	2.1	-2.0	-3.8	-1.3	1.6	-1.0	-.6	-.3	.2	.1
50- 7	500	1.026	2.0	2.7	-4.2	-3.0	-3.3	-1.6	-1.9	-.4	-.1	.0	-.1
50- 8	482	1.062	2.0	2.6	-5.0	-4.4	-3.9	-1.9	-1.5	-.1	-.1	.1	.1
50- 9	457	1.119	2.0	3.0	-5.4	-3.3	-4.3	-1.6	1.0	-.1	.0	.1	.1
50-10	434	1.180	2.0	3.2	-6.7	-7.0	-5.3	-1.6	.7	.0	.0	.2	.3
50-11	410	1.248	2.0	3.6	-7.5	-6.7	-6.1	-1.8	1.2	-.4	-.3	-.1	.0
50-12	385	1.327	2.0	3.7	-9.5	-5.2	-6.6	-2.1	1.0	.1	-.3	-.3	-.2

BLADE .60R FLAPWISE BENDING MOMENT HARMONICS (IN.-LB)													
RUN- PT. NO.	OMS #R	MU (FPS)	THEC (DEG)	B1	B2	B3	B4	B5	B6	B7	B8	B9	B10
50- 5	700	.731	2.0	-1.5	1.5	9.0	.5	1.6	-.4	-.3	-.2	.2	-.1
50- 6	632	.808	2.0	-1.7	1.1	8.6	-.3	1.0	-.4	-.3	-.4	-.3	-.1
50- 7	500	1.026	2.0	-.9	-.1	12.3	-.3	-.4	1.5	-.6	-.5	-.3	-.4
50- 8	482	1.062	2.0	-.7	-.9	12.0	-.4	-.3	.4	-.6	-.5	-.3	-.1
50- 9	457	1.119	2.0	-.5	-1.5	14.8	.2	-1.2	.3	-.6	-.5	-.3	-.1
50-10	434	1.180	2.0	-2.2	-2.3	15.2	.9	-1.1	.0	-.9	-.5	-.4	.0
50-11	410	1.248	2.0	-.3	-2.9	20.0	2.3	-1.2	-1.0	-.4	-.4	-.3	-.1
50-12	385	1.327	2.0	-.7	-3.2	22.0	3.0	-1.1	-1.1	-.6	-.3	-.3	-.2

TABLE XXII - Concluded														
RUN- PT. NO.	OMS #R (FPS)	MU	THEC (DEG)	BLADE .60R FLAPWISE BENDING MOMENT HARMONICS (IN.-LB)										
				RS	R1	R2	R3	R4	R5	R6	R7	R8	R9	R10
50- 5 700		.731	2.0	1.4	2.9	2.2	10.0	2.0	2.6	.7	.5	.3	.4	.2
50- 6 632		.808	2.0	1.8	2.7	2.2	9.4	1.3	1.8	1.0	.7	.5	.4	.2
50- 7 500		1.026	2.0	2.2	2.9	4.2	12.7	3.3	1.6	2.4	.7	.5	.3	.4
50- 8 482		1.062	2.0	2.6	2.7	5.1	12.8	4.0	1.9	1.5	.6	.5	.3	.2
50- 9 457		1.119	2.0	3.3	3.0	5.6	15.3	4.3	2.0	1.0	.6	.5	.3	.1
50-10 434		1.180	2.0	4.0	3.2	7.1	16.7	5.5	2.0	.7	.9	.5	.4	.3
50-11 410		1.248	2.0	4.9	3.7	8.1	21.1	6.6	2.2	1.6	.6	.5	.3	.1
50-12 385		1.327	2.0	5.4	3.8	10.0	22.6	7.2	2.3	1.5	.5	.4	.4	.3

TABLE XXIII. BLADE FLAP MOTION HARMONICS - RUN 50
(BLADE CENTER OF GRAVITY AT .25 CHORD)

BLADE FLAP MOTION HARMONICS (DEG)									
RUN- PT. NC.	OMS #R	MU (FPS)	THEC (DEG)	A1	A2	A3	A4	A5	A6
50- 5	700	.731	2.0	-.3	-.2	.2	.1	.0	.0
50- 6	632	.808	2.0	-.3	-.2	.2	.1	.2	.0
50- 7	500	1.026	2.0	-.7	-.3	.1	.1	.1	.0
50- 8	482	1.062	2.0	-.4	-.3	.1	.1	.0	.0
50- 9	457	1.119	2.0	-.4	-.3	.1	.1	.1	.1
50-10	434	1.180	2.0	.2	-.2	.2	.2	.1	.1
50-11	410	1.248	2.0	.2	-.3	.2	.3	.1	.1
50-12	385	1.327	2.0	-.1	-.4	.1	.4	.2	.1

BLADE FLAP MOTION HARMONICS (DEG)									
RUN- PT. NC.	OMS #R	MU (FPS)	THEC (DEG)	B1	B2	B3	B4	B5	B6
50- 5	700	.731	2.0	-.1	-.2	-.5	.0	.1	.0
50- 6	632	.808	2.0	-.1	-.1	-.5	.0	.1	.0
50- 7	500	1.026	2.0	-.1	-.1	-.8	.0	.0	.1
50- 8	482	1.062	2.0	-.1	.0	-.8	.0	.0	.1
50- 9	457	1.119	2.0	-.1	-.1	-.9	.0	.0	.0
50-10	434	1.180	2.0	.1	.0	-.9	.0	.0	.0
50-11	410	1.248	2.0	.0	.1	-1.1	-.1	.0	-.1
50-12	385	1.327	2.0	-.1	.1	-1.2	-.2	-.1	.0

TABLE XXIII - Concluded

TABLE XXIII - Concluded											
RUN-PT. NC.		OMS #R (FPS)	MU	THEC (DEG)	RS	R1	R2	R3	R4	R5	R6
50-	5	700	.731	2.0	.3	.3	.2	.5	.1	.1	.0
50-	6	632	.808	2.0	.1	.3	.2	.6	.1	.2	.0
50-	7	500	1.026	2.0	-.1	.7	.3	.8	.1	.1	.1
50-	8	482	1.062	2.0	-.2	.4	.3	.8	.1	.1	.1
50-	9	457	1.119	2.0	-.3	.4	.3	.9	.1	.1	.1
50-	10	434	1.180	2.0	-.7	.2	.2	.9	.2	.1	.1
50-	11	410	1.248	2.0	-.9	.2	.3	1.1	.3	.1	.1
50-	12	385	1.327	2.0	-1.3	.1	.4	1.2	.4	.2	.1

TABLE XXIV. BLADE .35R TORSIONAL MOMENT HARMONICS - RUN 50 (BLADE CENTER OF GRAVITY AT .25 CHORD)													
BLADE .35R TORSIONAL MOMENT HARMONICS (IN.-LB)													
RUN- PT. NO.	OMS OR	MU (FPS)	THEC (DEG)	A1	A2	A3	A4	A5	A6	A7	A8	A9	A10
50- 5	700	.731	2.0	1.2	-1.5	.4	2.5	1.7	-.2	.3	.1	.2	.0
50- 6	632	.808	2.0	1.1	-1.8	.3	.5	1.2	.8	.3	.3	.1	.0
50- 7	500	1.026	2.0	1.1	-2.5	-.9	1.0	1.6	.8	.1	.1	.0	.2
50- 8	482	1.062	2.0	1.2	-2.8	-1.0	1.3	1.5	.6	.2	-.1	.1	.0
50- 9	457	1.119	2.0	1.3	-3.3	-1.4	1.8	1.4	-.1	-.2	-1.2	-.2	.2
50-10	434	1.180	2.0	1.3	-4.8	-1.3	2.6	1.3	-.3	-.5	-.2	-.1	.0
50-11	410	1.248	2.0	1.3	-5.9	-1.4	3.2	1.6	-.5	-.4	-.8	-.5	.5
50-12	385	1.327	2.0	1.3	-7.2	-1.9	3.8	2.0	-.5	-1.2	-1.7	-.3	.4

BLADE .35R TORSIONAL MOMENT HARMONICS (IN.-LB)													
RUN- PT. NO.	OMS OR	MU (FPS)	THEC (DEG)	B1	B2	B3	B4	B5	B6	B7	B8	B9	B10
50- 5	700	.731	2.0	.6	1.2	.1	.2	-.4	.2	.5	.2	.2	.1
50- 6	632	.808	2.0	-.4	1.0	.8	-.4	-1.2	.6	-.2	.2	.1	.1
50- 7	500	1.026	2.0	-1.7	.3	1.4	1.5	-.5	-1.8	-1.0	-.7	.2	.2
50- 8	482	1.062	2.0	-2.4	-.1	1.8	1.8	-.9	-1.9	-1.4	-1.1	.1	.4
50- 9	457	1.119	2.0	-3.1	-.6	2.2	2.0	-.8	-1.6	-1.5	-1.1	.4	.1
50-10	434	1.180	2.0	-5.1	-1.0	3.3	2.0	-.7	-1.4	-.7	-.3	-.1	.3
50-11	410	1.248	2.0	-6.4	-1.1	3.9	2.0	-.6	-1.2	-.8	-.5	.3	.4
50-12	385	1.327	2.0	-7.8	-1.0	5.1	2.3	-1.0	-1.1	-.7	.5	1.6	.3

TABLE XXIV - Concluded														
		BLADE .35R TORSIONAL MOMENT HARMONICS (IN.-LB)												
RUN- PT. NO.	OMS #R (FPS)	MU	THEC (DEG)	R5	R1	R2	R3	R4	R5	R6	R7	R8	R9	R10
50- 5	700	.731	2.0	-1.1	1.3	2.0	.4	2.5	1.8	.3	.5	.2	.3	.1
50- 6	632	.800	2.0	-.3	1.1	2.0	.8	.6	1.7	1.0	.3	.3	.1	.1
50- 7	500	1.026	2.0	.8	2.0	2.5	1.7	1.8	1.7	2.0	1.1	.7	.2	.3
50- 8	482	1.062	2.0	1.4	2.7	2.8	2.0	2.2	1.8	1.9	1.4	1.1	.1	.4
50- 9	457	1.119	2.0	1.9	3.3	3.3	2.5	2.7	1.6	1.6	1.5	1.6	.4	.3
50-10	434	1.180	2.0	3.2	5.2	4.9	3.6	3.3	1.5	1.4	.8	.3	.2	.3
50-11	410	1.248	2.0	4.1	6.5	6.0	4.2	3.8	1.7	1.3	.9	.9	.7	.7
50-12	385	1.327	2.0	5.0	7.9	7.2	5.4	4.5	2.2	1.3	1.4	1.7	1.8	.6

TABLE XXV. BLADE LAG MOTION HARMONICS - RUN 51
(BLADE CENTER OF GRAVITY AT .25 CHORD)

RUN- PT. NO.	OMS *R (FPS)	MU	THEC (DEG)	BLADE LAG MOTION HARMONICS (DEG)				
				A1	A2	A3	A4	A5
51- 3 700	.294	9.0	9.0	-.2	.0	.0	.1	.1
51- 4 700	.294	10.0	10.0	-.3	.0	.0	.1	.0
51- 5 700	.294	11.0	11.0	-.4	.0	.0	.1	.0
51- 6 700	.294	12.0	12.0	-.4	.0	.0	.0	.0
51- 7 675	.504	8.0	8.0	-.2	.0	.1	.4	.0
51- 8 675	.504	9.0	9.0	-.2	.0	.1	.4	-.1
51- 9 675	.504	10.0	10.0	-.3	.0	.1	.4	.1
51-10 675	.504	11.0	11.0	-.3	.0	.1	.4	.0
51-11 675	.504	12.0	12.0	-.3	.0	.1	.4	.0
51-12 500	1.026	4.0	4.0	.0	.0	.1	-.1	.1
51-13 500	1.026	6.0	6.0	-.1	.0	.2	-.1	.1
51-14 500	1.026	8.0	8.0	-.1	.1	.1	-.2	.0
51-15 500	1.026	9.0	9.0	-.2	.2	.1	-.3	.0
51-16 500	1.026	10.0	10.0	-.2	.2	.2	-.2	.1

RUN- PT. NO.	OMS *R (FPS)	MU	THEC (DEG)	BLADE LAG MOTION HARMONICS (DEG)				
				B1	B2	B3	B4	B5
51- 3 700	.294	9.0	9.0	.3	.2	.1	.2	.1
51- 4 700	.294	10.0	10.0	.3	.2	.1	.2	.1
51- 5 700	.294	11.0	11.0	.4	.2	.2	.2	.1
51- 6 700	.294	12.0	12.0	.5	.2	.2	.3	.1
51- 7 675	.504	8.0	8.0	.1	.1	.1	.1	.1
51- 8 675	.504	9.0	9.0	.2	.2	.1	.0	.0
51- 9 675	.504	10.0	10.0	.2	.2	.1	-.1	.1
51-10 675	.504	11.0	11.0	.3	.2	.1	-.1	.1
51-11 675	.504	12.0	12.0	.4	.2	.1	-.1	.1
51-12 500	1.026	4.0	4.0	-.3	.1	.1	-.1	.0
51-13 500	1.026	6.0	6.0	-.3	.2	.0	-.1	.0
51-14 500	1.026	8.0	8.0	-.3	.1	-.2	-.1	-.2
51-15 500	1.026	9.0	9.0	-.3	.2	-.2	.0	-.2
51-16 500	1.026	10.0	10.0	-.4	.0	-.2	-.1	-.2

TABLE XXV - Concluded

BLADE LAG MOTION HARMONICS (DEG)										
RUN- PT. NO.	OMS *R (FPS)	MU	THEC (DEG)	RS	R1	R2	R3	R4	R5	
51- 3	700	.294	9.0	4.7	.4	.2	.1	.2	.1	
51- 4	700	.294	0.0	5.4	.4	.2	.1	.2	.1	
51- 5	700	.294	11.0	6.2	.5	.2	.2	.2	.1	
51- 6	700	.294	12.0	7.0	.6	.2	.2	.3	.1	
51- 7	675	.504	8.0	3.8	.2	.1	.1	.4	.1	
51- 8	675	.504	9.0	4.4	.3	.2	.1	.4	.1	
51- 9	675	.504	10.0	5.0	.4	.2	.2	.4	.1	
51-10	675	.504	11.0	5.6	.4	.2	.2	.4	.1	
51-11	675	.504	12.0	6.2	.5	.2	.2	.4	.1	
51-12	500	1.026	4.0	2.6	.3	.1	.1	.1	.1	
51-13	500	1.026	6.0	2.6	.3	.2	.2	.1	.0	
51-14	500	1.026	8.0	2.1	.4	.2	.2	.2	.2	
51-15	500	1.026	9.0	2.2	.4	.2	.2	.3	.2	
51-16	500	1.026	10.0	1.9	.4	.2	.3	.3	.2	

TABLE XXVI. BLADE .30R FLAPWISE BENDING MOMENT HARMONICS - RUN 51 (BLADE CENTER OF GRAVITY AT .25 CHORD)														
BLADE .30R FLAPWISE BENDING MOMENT HARMONICS (IN.-LB)														
RUN-PT. NO.	OMS #R (FPS)	MU	THEC (DEG)	A1	A2	A3	A4	A5	A6	A7	A8	A9	A10	
51- 3	700	.294	9.0	.2	-5	-2.8	-1.0	-6.0	.6	.1	-.3	-1.0	-.3	
51- 4	700	.294	10.0	.2	-4	-3.3	-1.1	-7.1	.6	.0	-.2	-.6	-.1	
51- 5	700	.294	11.0	.2	-4	-3.3	-1.1	-6.9	.3	.1	.1	-.3	.4	
51- 6	700	.294	12.0	.1	-5	-3.1	-1.2	-3.8	-.6	.0	.0	-.1	.1	
51- 7	675	.504	8.0	2.5	-1.5	-2.1	-.9	1.2	.2	.6	.0	-.2	.2	
51- 8	675	.504	9.0	2.5	-1.8	-2.0	-1.0	.1	.5	.6	.2	-.3	.1	
51- 9	675	.504	10.0	2.7	-1.8	-2.1	-1.4	-2.2	.6	.2	.2	-.6	.1	
51-10	675	.504	11.0	3.8	-2.0	-2.1	-1.6	-1.8	.9	1.1	.2	-.2	.1	
51-11	675	.504	12.0	3.7	-2.2	-2.6	-2.0	-2.9	1.1	1.3	.2	-.3	.1	
51-12	500	1.026	4.0	3.3	-5.8	-1.2	-1.2	-.9	4.2	-.1	-.2	-.2	-.1	
51-13	500	1.026	6.0	3.2	-8.8	-1.1	-.7	-2.4	7.2	.2	-.1	-.6	-.2	
51-14	500	1.026	8.0	2.7	-11.2	-1.2	-2.1	-4.4	7.8	.3	-.3	-.3	-.1	
51-15	500	1.026	9.0	4.3	-11.8	-2.7	-3.0	-3.2	6.8	-.5	-.3	-.3	-1.4	
51-16	500	1.026	10.0	3.8	-12.9	-2.4	-3.2	-5.0	8.0	-.9	-.5	-.5	-2.1	

BLADE .30R FLAPWISE BENDING MOMENT HARMONICS (IN.-LB)														
RUN-PT. NO.	OMS #R (FPS)	MU	THEC (DEG)	B1	B2	B3	B4	B5	B6	B7	B8	B9	B10	
51- 3	700	.294	9.0	-2.2	.7	1.4	-1.3	-2.0	-1.3	-.2	.9	-.6	.0	
51- 4	700	.294	10.0	-2.2	1.1	1.2	-1.3	-.6	-2.0	-.3	.7	-.5	-.2	
51- 5	700	.294	11.0	-2.2	.9	1.1	-1.5	1.4	-2.1	-.2	.7	-.5	-.2	
51- 6	700	.294	12.0	-2.2	1.0	.7	-1.9	1.5	-1.7	-.1	.3	-.5	-.1	
51- 7	675	.504	8.0	-2.3	1.7	7.5	-.4	1.7	-1.7	-.5	.4	-1.1	.0	
51- 8	675	.504	9.0	-2.4	1.7	7.8	-.7	2.4	-2.5	-.5	.6	-.6	.1	
51- 9	675	.504	10.0	-2.5	1.7	8.1	-1.0	1.2	-3.2	-.6	.5	-.6	.2	
51-10	675	.504	11.0	-2.6	1.7	8.2	-1.3	2.6	-3.5	-.5	.6	-.6	.2	
51-11	675	.504	12.0	-.4	1.7	8.3	-1.7	2.7	-3.9	-.2	.8	-.6	.1	
51-12	500	1.026	4.0	-5.8	.1	9.7	1.0	-.3	.2	.9	.3	-.3	.4	
51-13	500	1.026	6.0	-7.5	.7	10.0	2.2	-.3	-1.6	.0	.2	.9	1.4	
51-14	500	1.026	8.0	-7.8	1.0	11.2	1.1	-.4	-4.1	.7	.2	.5	1.4	
51-15	500	1.026	9.0	-8.0	-2.6	12.0	1.6	-3.1	2.9	.5	-.1	-.9	-.1	
51-16	500	1.026	10.0	-8.7	-1.4	11.1	1.4	-3.8	1.1	.5	-.1	.7	.1	

TABLE XXVI - Concluded														
RUN- PT. NO.	OMS #R	BLADE .30R FLAPWISE BENDING MOMENT HARMONICS (IN.-LB)												
		MU	THEC (DEG)	RS	R1	R2	R3	R4	R5	R6	R7	R8	R9	R10
51- 3 700		.294	9.0	4.7	2.2	.9	3.2	1.7	6.7	1.5	.2	1.0	1.2	.3
51- 4 700		.294	10.0	4.9	2.2	1.1	3.5	1.7	7.1	2.1	.3	.8	.9	.2
51- 5 700		.294	11.0	5.2	2.2	1.0	3.5	1.8	7.1	2.1	.2	.7	.4	.1
51- 6 700		.294	12.0	5.5	2.2	1.1	3.2	2.2	4.1	1.8	.1	.3	.5	.1
51- 7 675		.504	8.0	3.9	3.4	2.3	7.8	1.0	2.1	1.7	.8	.4	1.1	.2
51- 8 675		.504	9.0	4.4	3.5	2.4	8.1	1.2	2.4	2.5	.9	.6	1.1	.1
51- 9 675		.504	10.0	4.8	3.7	2.5	8.4	1.7	2.5	3.2	1.1	.6	.8	.2
51-10 675		.504	11.0	5.2	3.8	2.6	8.5	2.1	3.1	3.6	1.2	.6	.9	.2
51-11 675		.504	12.0	5.6	3.8	2.8	8.7	2.6	4.0	4.0	1.3	.8	.9	.1
51-12 500		1.026	4.0	3.9	6.7	5.8	9.8	1.6	.9	4.2	.9	.3	.3	.7
51-13 500		1.026	6.0	5.7	8.1	8.9	10.9	2.3	2.5	7.4	.6	.3	.4	1.4
51-14 500		1.026	8.0	7.3	8.2	11.2	11.2	2.4	4.4	8.8	.8	.3	.5	1.8
51-15 500		1.026	9.0	7.5	9.0	12.1	12.3	3.4	4.5	7.4	.6	.3	.5	1.4
51-16 500		1.026	10.0	8.0	9.5	13.0	11.3	3.5	6.3	8.1	1.0	.5	.9	2.1

TABLE XXVII. BLADE .60R FLAPWISE BENDING MOMENT HARMONICS - RUN 51 (BLADE CENTER OF GRAVITY AT .25 CHORD)														
RUN- PT. NO.	OMS #R	(FPS)	MU	THEC (DEG)	BLADE .60R FLAPWISE BENDING MOMENT HARMONICS (IN.-LB)									
					A1	A2	A3	A4	A5	A6	A7	A8	A9	A10
51- 3 700			.204	9.0	.1	-3.7	-4.6	.1	4.4	-.4	.2	.4	.8	.0
51- 4 700			.204	10.0	.0	-4.0	-5.5	.0	4.9	-.3	.1	.3	.6	-.1
51- 5 700			.204	11.0	.0	-4.4	-5.7	-.1	4.4	-.2	.0	-.1	.2	.0
51- 6 700			.204	12.0	-.5	-4.9	-5.4	-.2	2.3	.2	.1	.1	.1	.1
51- 7 675			.504	8.0	1.5	-3.4	-3.3	-1.3	-1.4	.0	-.5	-.1	.4	.0
51- 8 675			.504	9.0	1.4	-4.1	-3.2	-1.4	.2	-.2	-.7	-.4	.5	-.1
51- 9 675			.504	10.0	3.7	-4.4	-3.0	-1.4	.9	-.2	-.6	-.5	.2	-.2
51-10 675			.504	11.0	1.8	-4.9	-2.9	-1.2	.9	-.3	-.8	-.4	-.2	-.2
51-11 675			.504	12.0	3.9	-5.3	-3.5	-1.1	1.6	-.3	-1.0	-.5	-.2	-.2
51-12 500			1.026	4.0	3.5	-7.5	-4.3	-4.4	-1.5	-2.4	-.1	.0	.2	.2
51-13 500			1.026	6.0	4.3	-10.6	-5.6	-5.4	-.9	-4.6	.0	.1	.1	.1
51-14 500			1.026	8.0	4.4	-13.9	-7.0	-5.4	1.6	-4.6	.4	.0	.0	.2
51-15 500			1.026	9.0	3.8	-14.2	-7.4	-3.8	.0	-4.6	.4	.1	.0	.9
51-16 500			1.026	10.0	4.2	-15.9	-8.3	-4.5	1.3	-4.9	.8	.4	.2	1.6

TABLE XXVIII. BLADE .60R FLAPWISE BENDING MOMENT HARMONICS (IN.-LB)														
RUN- PT. NO.	OMS #R	(FPS)	MU	THEC (DEG)	BLADE .60R FLAPWISE BENDING MOMENT HARMONICS (IN.-LB)									
					B1	B2	B3	B4	B5	B6	B7	B8	B9	B10
51- 3 700			.204	9.0	-2.8	-1.0	3.2	-.4	1.2	.8	-.2	-1.0	.4	-.2
51- 4 700			.204	10.0	-2.9	-1.4	3.0	-.8	-.4	1.1	-.2	-.8	.3	-.1
51- 5 700			.204	11.0	-3.3	-1.9	3.2	-1.0	-1.6	1.1	-.3	-.6	.3	-.1
51- 6 700			.204	12.0	-3.6	-1.9	2.8	-.9	-1.5	.8	-.3	-.3	.5	-.2
51- 7 675			.504	8.0	-3.5	1.5	9.8	-.2	-.9	.7	.2	-.5	.8	.1
51- 8 675			.504	9.0	-3.8	1.4	10.0	.0	-1.5	1.0	.1	-.6	.8	.0
51- 9 675			.504	10.0	-4.1	1.3	10.2	.4	-1.4	1.3	.6	-.6	.6	.0
51-10 675			.504	11.0	-4.3	1.2	10.1	.8	-2.0	1.5	.5	-.7	.5	-.1
51-11 675			.504	12.0	-4.4	1.0	10.3	1.1	-2.1	1.6	.4	-.9	.7	-.2
51-12 500			1.026	4.0	-1.0	-.7	11.4	-.4	-.1	-1.8	-.8	-.3	-.3	-.5
51-13 500			1.026	6.0	-1.6	.0	12.2	-.1	.3	1.3	-.7	-.5	-.4	-1.0
51-14 500			1.026	8.0	-2.0	.1	13.3	.8	1.0	2.7	-.8	-.3	-.3	-1.4
51-15 500			1.026	9.0	-5.1	-4.9	11.7	-2.4	1.9	-1.1	-.4	.0	-.2	.1
51-16 500			1.026	10.0	-5.9	-3.6	11.3	-1.9	2.6	-.1	-.6	-.2	-.4	.0

TABLE XXVII - Concluded

TABLE XXVII - Concluded														
RUN- PT. NO.	OMS #R (FPS)	MU	THEC (DEG)	BLADE .60R FLAPWISE BENDING MOMENT HARMONICS (IN.-LB)										
				R5	R1	R2	R3	R4	R5	R6	R7	R8	R9	R10
51- 3 700		.294	9.0	2.2	2.8	4.0	5.8	.4	4.6	.9	.3	1.1	.8	.2
51- 4 700		.294	10.0	2.3	2.9	4.2	6.2	.8	4.9	1.2	.2	.8	.7	.2
51- 5 700		.294	11.0	2.6	3.3	4.7	6.6	1.0	4.7	1.1	.3	.6	.4	.1
51- 6 700		.294	12.0	2.7	3.6	5.3	6.0	.9	2.8	.8	.3	.3	.5	.2
51- 7 675		.504	8.0	2.9	4.9	3.7	10.3	1.3	1.7	.7	.5	.5	.9	.1
51- 8 675		.504	9.0	3.3	5.1	4.3	10.4	1.4	1.6	1.1	.7	.7	.9	.1
51- 9 675		.504	10.0	3.6	5.5	4.6	10.7	1.4	1.4	1.3	.9	.8	.6	.2
51-10 675		.504	11.0	3.9	5.7	5.0	10.5	1.4	2.2	1.5	.9	.8	.7	.2
51-11 675		.504	12.0	4.3	5.9	5.4	10.9	1.5	2.7	1.7	1.1	1.0	.8	.3
51-12 500		1.026	4.0	4.1	3.7	7.5	12.2	4.5	1.5	3.0	.8	.3	.3	.5
51-13 500		1.026	6.0	5.3	4.6	10.6	13.5	5.4	.9	4.8	.7	.5	.4	1.1
51-14 500		1.026	8.0	6.3	4.9	13.9	15.4	5.5	1.9	5.4	.9	.3	.4	1.4
51-15 500		1.026	9.0	6.9	6.4	15.0	13.8	4.5	1.9	4.7	.6	.1	.2	.9
51-16 500		1.026	10.0	7.6	7.2	16.4	14.0	4.9	2.9	4.9	1.0	.4	.4	1.6

TABLE XXVIII. BLADE FLAP MOTION HARMONICS -RUN 51
(BLADE CENTER OF GRAVITY AT .25 CHORD)

RUN- PT. NO.	CMS *R (FPS)	MU	THEC (DEG)	BLADE FLAP MOTION HARMONICS (DEG)					
				A1	A2	A3	A4	A5	
51- 3 700	.294		9.0	-.2	-.2	.3	.0	.1	
51- 4 700	.294		10.0	-.1	-.2	.3	.0	.2	
51- 5 700	.294		11.0	.2	-.3	.3	.0	.2	.0
51- 6 700	.294		12.0	.2	-.3	.3	.0	.1	.0
51- 7 675	.504		8.0	-.1	-.4	.1	.0	-.1	-.1
51- 8 675	.504		9.0	-.1	-.4	.1	.0	.0	.0
51- 9 675	.504		10.0	-.1	-.4	.0	.0	.1	.0
51-10 675	.504		11.0	-.1	-.5	.0	.1	.1	.0
51-11 675	.504		12.0	-.2	-.6	.1	.1	.2	.0
51-12 500	1.026		4.0	-.3	-.3	.1	.1	.1	-.1
51-13 500	1.026		6.0	-.2	-.4	.0	.2	.1	-.2
51-14 500	1.026		8.0	.7	-.5	.0	.2	.2	-.1
51-15 500	1.026		9.0	-.2	-.6	.1	.2	.2	-.2
51-16 500	1.026		10.0	.0	-.7	.1	.2	.3	-.2

RUN- PT. NO.	CMS *R (FPS)	MU	THEC (DEG)	BLADE FLAP MOTION HARMONICS (DEG)					
				B1	B2	B3	B4	B5	B6
51- 3 700	.294		9.0	.1	.0	.0	.1	.1	.0
51- 4 700	.294		10.0	.1	-.1	.0	.1	.1	.1
51- 5 700	.294		11.0	.2	-.1	.0	.1	.0	.1
51- 6 700	.294		12.0	.1	-.1	.0	.1	.0	.1
51- 7 675	.504		8.0	.0	-.1	-.6	.0	.0	.0
51- 8 675	.504		9.0	.1	-.1	-.6	.1	.0	.1
51- 9 675	.504		10.0	.0	-.1	-.6	.1	.0	.1
51-10 675	.504		11.0	.1	-.1	-.7	.1	.0	.1
51-11 675	.504		12.0	.0	-.1	-.7	.1	.0	.1
51-12 500	1.026		4.0	-.1	.0	-.8	-.1	.0	.0
51-13 500	1.026		6.0	-.1	.1	-.8	-.1	.0	.1
51-14 500	1.026		8.0	-.1	.2	-.9	-.1	.0	.2
51-15 500	1.026		9.0	-.1	.0	-1.0	.0	.1	.0
51-16 500	1.026		10.0	-.1	.1	-.9	.0	.2	.1

TABLE XXVIII - Concluded											
BLADE FLAP MOTION HARMONICS (DEG)											
RUN- PT. OMS NO. *R	MU	THEC (DEG)	RS	R1	R2	R3	R4	R5	R6		
51- 3 700	.294	9.0	2.8	.3	.2	.3	.1	.2	.0		
51- 4 700	.294	10.0	2.9	.1	.2	.3	.1	.2	.1		
51- 5 700	.294	11.0	3.1	.2	.3	.3	.1	.2	.1		
51- 6 700	.294	12.0	3.2	.2	.3	.3	.1	.1	.1		
51- 7 675	.504	8.0	1.7	.1	.4	.6	.1	.1	.1		
51- 8 675	.504	9.0	1.8	.1	.4	.6	.1	.0	.1		
51- 9 675	.504	10.0	2.0	.1	.4	.6	.1	.1	.1		
51-10 675	.504	11.0	2.2	.1	.5	.7	.1	.1	.1		
51-11 675	.504	12.0	2.4	.2	.6	.7	.1	.2	.1		
51-12 500	1.026	4.0	-.2	.3	.3	.8	.2	.1	.1		
51-13 500	1.026	6.0	-.1	.2	.4	.8	.2	.1	.2		
51-14 500	1.026	8.0	-.3	.7	.5	.9	.2	.2	.2		
51-15 500	1.026	9.0	-.1	.2	.6	1.0	.2	.2	.2		
51-16 500	1.026	10.0	-.1	.1	.7	.9	.2	.3	.2		

TABLE XXIX. BLADE .35R TORSIONAL MOMENT HARMONICS - Run 51 (BLADE CENTER OF GRAVITY AT .25 CHORD)														
BLADE .35R TORSIONAL MOMENT HARMONICS (IN.-LB)														
RUN- PT. NO.	OMS #R (FPS)	MU	THEC (DEG)	A1	A2	A3	A4	A5	A6	A7	A8	A9	A10	
51- 3	700	.204	9.9	1.3	1.3	-4	-2.6	-4.7	-3.2	-1.6	-5	-3	-2	
51- 4	700	.204	10.0	1.1	1.6	-7	-2.8	-5.0	-2.2	-5	-5	-4	-2	
51- 5	700	.204	11.0	.9	1.7	-8	-2.0	-3.3	-1.3	-1.1	-5	-1	-2	
51- 6	700	.204	12.0	.7	2.1	-1.2	-1.3	-2.2	2.1	1.8	1.2	.8	.4	
51- 7	675	.504	8.0	1.1	-3	1.5	2.7	1.4	.9	.5	-2	.2	.0	
51- 8	675	.504	9.0	1.0	-3	1.5	2.5	1.0	.8	.9	-1	.2	.0	
51- 9	675	.504	10.0	.7	-4	1.1	1.6	.1	.7	1.1	-1	.2	-1	
51-10	675	.504	11.0	.5	-5	.6	.7	-5	.5	1.0	-1	.3	-2	
51-11	675	.504	12.0	.4	-5	.0	-2	-6	.4	-1.1	-4	-3	-2	
51-12	500	1.026	4.0	1.5	-4.7	-9	1.8	2.0	.6	.3	.3	.0	.0	
51-13	500	1.026	6.0	1.3	-6.4	-2	2.8	1.1	.6	-2	-1	-3	-2	
51-14	500	1.026	8.0	.9	-7.9	.6	3.3	.0	.2	-5	-7	-2	.2	
51-15	500	1.026	9.0	2.1	-8.5	-1.1	3.2	1.4	1.9	.1	-2	-5	.1	
51-16	500	1.026	10.0	2.7	-9.7	-2.6	2.0	1.5	2.5	1.1	.1	-5	.2	

BLADE .35R TORSIONAL MOMENT HARMONICS (IN.-LB)														
RUN- PT. NO.	OMS #R (FPS)	MU	THEC (DEG)	B1	B2	B3	B4	B5	B6	B7	B8	B9	B10	
51- 3	700	.204	9.9	4.3	1.5	-7	2.0	2.8	2.8	.3	.2	-2	-2	
51- 4	700	.204	10.0	5.8	2.0	-3	3.5	5.4	5.4	2.2	.8	.3	.3	
51- 5	700	.204	11.0	7.2	2.9	.7	5.0	7.6	7.0	2.2	1.1	.6	.5	
51- 6	700	.204	12.0	8.7	3.2	1.0	5.1	7.1	5.7	1.3	.1	-1	-2	
51- 7	675	.504	8.0	3.3	3.3	.7	.0	2.9	2.7	1.7	.7	.3	.1	
51- 8	675	.504	9.0	4.1	4.0	1.1	.3	4.6	4.3	2.2	.9	.3	.1	
51- 9	675	.504	10.0	4.8	4.7	1.6	.8	5.8	6.4	2.9	1.2	.5	.2	
51-10	675	.504	11.0	5.3	5.2	2.2	1.1	7.1	7.3	2.7	1.0	.4	.2	
51-11	675	.504	12.0	6.2	5.7	2.7	1.8	7.1	8.0	2.6	.9	.2	.2	
51-12	500	1.026	4.0	-4.8	.5	3.4	2.1	-1.1	-1.6	-9	-7	.4	.3	
51-13	500	1.026	6.0	-6.9	1.4	5.2	3.0	-2.0	-2.3	-1.1	-7	.4	.4	
51-14	500	1.026	8.0	-9.0	2.0	6.5	1.5	-2.2	-2.8	-1.9	-1.0	.4	.4	
51-15	500	1.026	9.0	-9.2	1.4	7.1	3.0	-1.7	-3.7	-3.6	-1.6	-1	.1	
51-16	500	1.026	10.0	-10.5	.2	7.6	3.9	-1.0	-3.0	-2.9	-2.0	-6	-1	

TABLE XXIX - Concluded

RUN- PT. NO.	RMS SP (FPS)	MU	TIMEC (DEG)	FS	BLADE .35R TORSIONAL MOMENT HARMONICS (IN.-LB)									
					R1	R2	R3	R4	R5	R6	R7	R8	R9	R10
51- 3 700		.294	9.0	-5.0	4.5	1.9	.9	3.3	5.5	4.2	1.6	.6	.3	.3
51- 4 700		.294	10.0	-6.2	5.9	2.6	.7	4.5	7.3	6.1	2.3	.9	.5	.4
51- 5 700		.294	11.0	-7.3	7.2	3.3	1.0	5.4	8.3	7.2	2.5	1.1	.8	.5
51- 6 700		.294	12.0	-8.6	8.8	3.8	1.6	5.2	7.1	6.1	2.2	1.2	.8	.5
51- 7 675		.504	8.0	-3.9	3.5	3.4	1.7	2.7	3.2	2.8	1.8	.8	.3	.1
51- 8 675		.504	9.0	-4.7	4.2	4.0	1.9	2.5	4.7	4.4	2.4	.9	.4	.2
51- 9 675		.504	10.0	-5.6	4.8	4.7	2.0	1.8	5.8	6.5	3.1	1.2	.5	.2
51-10 675		.504	11.0	-6.4	5.4	5.3	2.2	1.3	7.1	7.3	2.9	1.0	.5	.3
51-11 675		.504	12.0	-7.4	6.2	5.7	2.7	1.9	7.2	8.0	2.8	1.0	.3	.3
51-12 500		1.026	4.0	2.1	5.0	4.7	3.5	2.8	2.3	1.7	1.0	.8	.4	.3
51-13 500		1.026	6.0	2.9	7.1	6.6	5.2	3.3	2.3	2.3	1.1	.7	.5	.4
51-14 500		1.026	8.0	3.9	9.0	8.2	6.5	3.6	2.2	2.8	2.0	1.2	.4	.5
51-15 500		1.026	9.0	4.0	9.4	8.6	7.2	4.4	2.2	4.2	3.6	1.8	.5	.2
51-16 500		1.026	10.0	4.3	10.9	9.7	8.1	4.4	1.8	3.9	3.1	2.0	.8	.2

TABLE XXX. BLADE LAG MOTION HARMONICS - RUNS 64-67 (BLADE CENTER OF GRAVITY AT .25 CHORD)											
BLADE LAG MOTION HARMONICS (DEG)											
RUN- PT. NO.	OMS #W (FPS)	MU	THEC (DEG)	A1	A2	A3	A4	A5	A6	A7	A8
64- 3 700	.390	2.0	.1	.0	.0	.0	.0	.0	.0	.0	.0
64- 4 700	.448	2.0	.1	.0	.0	.0	.0	.0	.0	.0	.0
64- 5 700	.504	2.0	.1	.1	.0	.0	.0	.0	.0	.0	.0
64- 6 700	.565	2.0	.1	.0	.0	.0	.0	.0	.0	.0	.0
64- 7 700	.623	2.0	.1	.0	.0	.0	.0	.0	.0	.0	.0
64- 8 700	.682	2.0	.2	.0	.0	.0	.0	.0	.0	.0	.0
65- 3 700	.682	2.0	.1	.0	.1	.0	.0	.0	.0	.0	.0
65- 4 700	.741	2.0	.2	.0	.1	.1	.0	.0	.0	.0	.0
65- 5 700	.801	2.0	.2	.0	.1	.1	.0	.0	.0	.0	.0
65- 6 700	.861	2.0	.2	.0	.1	.1	.0	.0	.0	.0	.0
67- 3 700	.801	2.0	.2	.0	.1	.1	.0	.0	.0	.0	.0
67- 4 674	.832	2.0	.2	.0	.1	.1	.1	.0	.0	.0	.0
67- 5 652	.862	2.0	.2	.1	.1	.3	.0	.0	.0	.0	.0
67- 6 498	1.040	2.0	.3	.0	.1	.0	.0	.0	.0	.0	.0
67- 7 498	1.126	2.0	.2	.0	.1	.0	.1	.0	.0	.0	.0
67- 8 476	1.181	2.0	.2	.0	.1	.0	.1	.0	.0	.0	.0
67- 9 452	1.243	2.0	.1	.0	.1	.0	.0	.0	.0	.0	.0
67-10 428	1.312	2.0	.1	.0	.1	.0	.0	.0	.0	.0	.1
67-11 404	1.388	2.0	-.0	.1	.1	-.1	-.1	-.1	-.1	.0	.0
67-12 380	1.474	2.0	-.1	.1	.1	-.3	-.1	-.1	-.1	-.1	.0

BLADE LAG MOTION HARMONICS (DEG)											
RUN- PT. NO.	OMS #W (FPS)	MU	THEC (DEG)	B1	B2	B3	B4	B5	B6	B7	B8
64- 3 700	.390	2.0	.0	.0	.0	.0	.0	.0	.0	.0	.0
64- 4 700	.448	2.0	.0	.0	.0	.1	.0	.0	.0	.0	.0
64- 5 700	.504	2.0	.0	.0	.0	.1	.0	.0	.0	.0	.0
64- 6 700	.565	2.0	.0	.0	.0	.1	.0	.0	.0	.0	.0
64- 7 700	.623	2.0	.0	.0	.0	.1	.0	.0	.0	.0	.0
64- 8 700	.682	2.0	.1	.1	.0	.1	.0	.0	.0	.0	.0
65- 3 700	.682	2.0	.1	.1	.0	.1	.0	.0	.0	.0	.0
65- 4 700	.741	2.0	.1	.1	.0	.2	.0	.0	.0	.0	.0
65- 5 700	.801	2.0	.1	.1	.0	.2	.0	.0	.0	.0	.0
65- 6 700	.861	2.0	.0	.1	.0	.2	.0	.0	.0	.0	.0
67- 3 700	.801	2.0	.1	.1	.0	.2	.0	.0	.0	.0	.0
67- 4 674	.832	2.0	.1	.1	.0	.1	.0	.0	.0	.0	.0
67- 5 652	.862	2.0	-.1	.0	-.0	.0	.0	.0	.0	.0	.0
67- 6 498	1.040	2.0	.3	.1	.0	.0	.0	.0	.0	.0	.0
67- 7 498	1.126	2.0	-.3	.1	.1	.0	.1	.0	.0	.0	.0
67- 8 476	1.181	2.0	-.3	.1	.1	-.1	.0	.0	.0	.0	.0
67- 9 452	1.243	2.0	-.4	.1	.1	-.1	-.1	.0	.0	.0	.0
67-10 428	1.312	2.0	-.5	.1	.1	-.1	-.1	.0	.0	.0	.0
67-11 404	1.388	2.0	-.7	.1	.0	-.1	-.0	-.1	.0	.0	.0
67-12 380	1.474	2.0	-.9	.1	.0	.0	-.1	.1	.0	.1	.1

TABLE XXX - Concluded												
BLADE LAG MOTION HARMONICS (DEG)												
RUN- PT. NO.	OMS R (FPS)	MU	THEC (DEG)	RS	R1	R2	R3	R4	R5	R6	R7	R8
64- 3 700		.390	2.0	2.1	.1	.0	.0	.0	.0	.0	.0	.0
64- 4 700		.448	2.0	2.3	.1	.0	.0	.1	.0	.0	.0	.0
64- 5 700		.504	2.0	2.3	.1	.1	.0	.1	.0	.0	.0	.0
64- 6 700		.565	2.0	2.3	.1	.0	.0	.1	.0	.0	.0	.0
64- 7 700		.623	2.0	2.3	.1	.0	.0	.1	.0	.0	.0	.0
64- 8 700		.682	2.0	2.3	.2	.1	.1	.1	.0	.0	.0	.0
65- 3 700		.682	2.0	2.4	.2	.1	.1	.1	.0	.0	.0	.0
65- 4 700		.741	2.0	2.4	.2	.1	.1	.2	.0	.0	.0	.0
65- 5 700		.801	2.0	2.4	.2	.1	.1	.2	.0	.0	.0	.0
65- 6 700		.861	2.0	2.4	.2	.1	.1	.2	.0	.0	.0	.0
67- 3 700		.801	2.0	2.4	.2	.1	.1	.2	.0	.0	.0	.0
67- 4 874		.832	2.0	2.0	.2	.1	.1	.2	.1	.0	.0	.0
67- 5 652		.862	2.0	2.4	.1	.1	.1	.3	.0	.0	.0	.0
67- 6 498		1.040	2.0	2.6	.3	.1	.1	.1	.1	.0	.0	.0
67- 7 498		1.126	2.0	2.7	.3	.1	.1	.1	.1	.0	.0	.0
67- 8 476		1.181	2.0	2.7	.4	.1	.1	.1	.1	.0	.0	.0
67- 9 452		1.243	2.0	2.5	.4	.1	.1	.1	.1	.0	.0	.0
67-10 428		1.312	2.0	2.1	.5	.1	.1	.1	.1	.1	.0	.1
67-11 404		1.388	2.0	1.9	.7	.1	.1	.1	.1	.1	.0	.0
67-12 360		1.474	2.0	.8	.9	.1	.2	.2	.1	.1	.1	.1

TABLE XXI. BLADE .30R FLAPWISE BENDING MOMENT HARMONICS (IN-CH)																			
BLADE .30R FLAPWISE BENDING MOMENT HARMONICS (IN-CH)																			
MU FT. IN.	W (LBS.)	THC (IN-CH)	A1	A2	A3	A4	A5	A6	A7	A8	A9	A10	A11	A12	A13				
65-3 700	.340	2.0	1.5	-2.5	-2.6	.5	.2	-1.1	.0	.1	.0	.0	.0	.0	.0				
65-4 700	.440	2.0	2.1	-2.4	-3.6	.3	.2	.4	.0	-1.1	.0	.0	.0	.0	.0				
65-5 700	.540	2.0	2.1	-2.5	-4.1	-1.0	-1.3	.5	.3	.1	.0	.0	.0	.0	.0				
65-6 700	.640	2.0	2.4	-2.4	-4.4	-1.3	.7	.4	.4	.3	.0	.0	.0	.0	.0				
65-7 700	.643	2.0	2.4	-2.7	-4.4	-1.3	1.1	.2	.2	.3	.0	.0	.0	.0	.0				
65-8 700	.642	2.0	2.2	-1.4	-4.9	-1.3	2.7	.3	.1	.2	.0	.0	.0	.0	.0				
65-9 700	.642	2.0	2.4	-1.4	-4.3	-1.5	1.7	.7	.0	.1	.0	.0	.0	.0	.0				
65-10 700	.741	2.0	2.4	-1.9	-3.8	-1.7	1.4	.6	.1	.1	.0	.0	.0	.0	.0				
65-11 700	.801	2.0	2.7	-2.7	-4.4	-1.9	1.8	.9	.3	.6	.0	.0	.0	.0	.0				
65-12 700	.861	2.0	2.0	-3.3	-4.9	-1.6	.5	.0	.4	.7	.0	.0	.0	.0	.0				
65-13 700	.861	2.0	2.5	-3.1	-4.9	-1.8	3.2	.4	.4	.2	.0	.0	.0	.1	.1				
65-14 700	.862	2.0	3.1	-2.7	-5.0	-1.3	2.0	.6	.2	.3	.3	.1	.0	.0	.1				
65-15 700	.862	2.0	3.2	-2.4	-4.6	-1.2	1.3	.3	.0	.2	.2	.1	.1	.1	.1				
65-16 700	.862	2.0	4.4	-3.2	-4.4	-1.4	.4	.0	.0	.2	.1	.1	.2	.2	.2				
65-17 700	1.040	2.0	4.7	-3.9	-7.1	-1.6	.0	.0	.0	.2	.0	.0	.0	.0	.0				
65-18 700	1.120	2.0	4.7	-3.9	-7.1	-1.6	.0	.0	.0	.2	.0	.0	.0	.0	.0				
65-19 700	1.121	2.0	4.3	-3.7	-5.9	-1.1	1.7	.0	.1	.2	.2	.2	.2	.2	.2				
65-20 700	1.243	2.0	4.5	-3.7	-9.1	-1.7	.3	.4	.4	.6	.2	.2	.2	.2	.2				
65-21 700	1.312	2.0	4.1	-3.8	-13.1	-1.1	.2	.7	.5	.6	.4	.4	.4	.4	.4				
65-22 700	1.366	2.0	3.7	-6.0	-11.3	-1.7	.3	.3	.8	.1	.1	.0	.0	.0	.0				
65-23 700	1.374	2.0	4.4	-4.6	-18.0	-1.1	.4	.7	.2	.7	.8	.9	.2	.2	.2				
BLADE .30R FLAPWISE BENDING MOMENT HARMONICS (IN-CH)																			
MU FT. IN.	W (LBS.)	THC (IN-CH)	B1	B2	B3	B4	B5	B6	B7	B8	B9	B10	B11	B12	B13				
65-3 700	.340	2.0	-1.2	.0	1.5	-1.5	-1.7	.5	.3	.2	.0	.0	.0	.0	.0				
65-4 700	.440	2.0	-1.1	.9	1.5	-1.5	-1.2	.4	.4	.3	.0	.0	.0	.0	.0				
65-5 700	.540	2.0	-1.3	1.3	1.5	-1.4	-1.0	-1.1	.1	.1	.0	.0	.0	.0	.0				
65-6 700	.640	2.0	-1.1	1.7	2.3	-1.3	-1.9	-1.0	.9	.4	.0	.0	.0	.0	.0				
65-7 700	.643	2.0	-1.3	1.6	2.1	-1.3	-2.1	.1	.0	.2	.0	.0	.0	.0	.0				
65-8 700	.642	2.0	-1.2	2.2	2.5	-1.6	-2.1	.5	.2	.5	.0	.0	.0	.0	.0				
65-9 700	.642	2.0	-1.2	2.1	3.2	-1.4	-3.7	.4	.1	.2	.0	.0	.0	.0	.0				
65-10 700	.741	2.0	-1.3	2.4	4.9	-1.1	-3.7	.3	.1	.2	.0	.0	.0	.0	.0				
65-11 700	.801	2.0	-1.1	1.8	4.1	-1.2	-4.6	.7	.3	.3	.0	.0	.0	.0	.0				
65-12 700	.861	2.0	-1.7	1.1	4.1	-1.7	-5.9	.6	.6	.6	.0	.0	.0	.0	.0				
65-13 700	.861	2.0	-1.3	1.7	4.2	-1.6	-3.7	.9	.3	.3	.0	.0	.0	.0	.0				
65-14 700	.862	2.0	-1.3	1.3	4.1	-1.7	-3.4	1.7	.7	.6	.0	.0	.0	.0	.0				
65-15 700	.862	2.0	-1.6	2.2	4.9	-1.3	-6.2	.9	.4	.4	.0	.0	.0	.0	.0				
65-16 700	1.040	2.0	-1.4	.6	5.4	-1.7	-1.1	.3	.6	.3	.5	.9	.3	.2	.0				
65-17 700	1.120	2.0	-2.4	-6	3.4	-1.4	-1.4	.6	.0	.0	.3	.5	.3	.2	.0				
65-18 700	1.121	2.0	-2.5	-6	6.4	-1.6	-1.5	.4	.6	.0	.3	1.0	.5	.3	.0				
65-19 700	1.243	2.0	-3.4	-1.1	5.9	-1.8	-1.1	.6	.8	.1	.1	.5	.0	.3	.0				
65-20 700	1.312	2.0	-3.7	-1.5	7.3	-1.9	.3	.4	1.0	.6	.0	.0	.2	.2	.0				
65-21 700	1.366	2.0	-3.1	-3.4	11.6	-1.0	.7	.4	.7	.6	.9	.1	.0	.2	.0				
65-22 700	1.374	2.0	-3.6	-5.3	18.2	-1.3	.2	.4	.3	.3	.3	.2	.5	.4	.0				

TABLE XXXI - Concluded

RUL- PT. NO.	OMS OR	TMEC (DEG)	SLIDE .308 FLAPWISE BENDING MOMENT HARMONICS (IN-LB)															
			MU (FPS)	R5	R4	R3	R2	R1	R6	R5	R4	R3	R2	R1	R6	R5	R4	R3
64- 3 700	.390	2.0	1.5	1.5	1.5	1.5	1.5	1.5	.7	3.3	.5	.9	.5	.3	.3	.2	.0	.0
64- 4 700	.446	2.0	1.4	1.4	1.4	1.4	1.4	1.4	1.0	3.6	.6	1.2	.6	.4	.4	.2	.0	.0
64- 5 700	.504	2.0	1.2	1.2	1.2	1.2	1.2	1.2	1.3	4.4	.7	1.7	.5	.3	.3	.2	.0	.0
64- 6 700	.565	2.0	1.0	1.0	1.0	1.0	1.0	1.0	1.9	4.3	.4	1.8	.4	.2	.2	.0	.0	.0
64- 7 700	.623	2.0	.7	.7	.7	.7	.7	.7	2.4	4.8	.4	1.8	.2	.2	.3	.0	.0	.0
64- 8 700	.682	2.0	.9	.9	.9	.9	.9	.9	2.3	5.5	.7	3.5	.6	.2	.5	.0	.0	.0
65- 3 700	.682	2.0	.5	.5	.5	.5	.5	.5	2.5	5.4	.7	3.6	.5	.2	.5	.0	.0	.0
65- 4 700	.741	2.0	.6	.6	.6	.6	.6	.6	3.0	6.2	.7	3.8	.7	.1	.5	.0	.0	.0
65- 5 700	.801	2.0	.6	.6	.6	.6	.6	.6	3.3	6.0	.9	5.1	1.2	.4	.6	.0	.0	.0
65- 6 700	.861	2.0	.9	.9	.9	.9	.9	.9	3.4	5.7	1.0	5.9	1.1	.7	.9	.0	.0	.0
67- 3 700	.801	2.0	.9	.9	.9	.9	.9	.9	3.5	6.4	.9	4.9	1.0	.4	.5	.2	.1	.1
67- 4 874	.832	2.0	1.1	1.1	1.1	1.1	1.1	1.1	3.0	5.4	.8	4.3	1.2	.7	.8	.7	.1	.1
67- 5 852	.862	2.0	1.0	1.0	1.0	1.0	1.0	1.0	3.4	6.5	1.2	4.2	1.0	.5	.6	1.1	.1	.1
67- 6 494	1.040	2.0	2.0	2.0	2.0	2.0	2.0	2.0	4.6	6.9	.7	.4	4.6	1.0	.4	.5	1.2	.1
67- 7 498	1.126	2.0	2.2	2.2	2.2	2.2	2.2	2.2	5.3	7.9	1.1	1.7	5.1	.8	.2	.3	1.3	.3
67- 8 476	1.181	2.0	2.1	2.1	2.1	2.1	2.1	2.1	5.8	8.7	1.4	2.3	8.3	.8	.4	.2	.5	.1
67- 9 452	1.283	2.0	2.0	2.0	2.0	2.0	2.0	2.0	5.7	10.9	1.9	2.5	7.2	1.1	.7	.3	.7	.2
67-10 428	1.312	2.0	3.0	3.0	3.0	3.0	3.0	3.0	6.3	15.0	3.3	2.8	6.5	1.1	.6	.4	.1	.4
67-11 404	1.348	2.0	3.0	3.0	3.0	3.0	3.0	3.0	6.3	16.4	4.8	3.4	5.8	1.1	.6	.4	.1	.4
67-12 380	1.474	2.0	4.2	4.2	4.2	4.2	4.2	4.2	6.3	25.6	7.2	4.7	6.4	3.3	.7	.9	.9	.6
																		1.3

TABLE XXXII. BLADE .18R TORSIONAL MOMENT HARMONICS
(BLADE CENTER OF GRAVITY AT .25 CHORD)

RUN- PT. NO.	QMS OR FPS	BLADE .18R TORSIONAL MOMENT HARMONICS (IN.-LB)													
		THC (DEG)	A1	A2	A3	A4	A5	A6	A7	A8	A9	A10	A11	A12	A13
64- 3 700	.390	2.0	.4	-5	.7	.1	.2	.1	.1	.1	.0	.0	.0	.0	.0
64- 4 700	.448	2.0	.4	-7	.6	.3	.2	.0	.0	.0	.0	.0	.0	.0	.0
64- 5 700	.504	2.0	.4	-1.1	.6	.4	.1	.3	.1	.1	.0	.0	.0	.0	.0
64- 6 700	.565	2.0	.5	-1.5	.5	.6	.3	.4	.1	.1	.0	.0	.0	.0	.0
64- 7 700	.623	2.0	.5	-2.0	.5	1.0	.8	.6	.1	.1	.0	.0	.0	.0	.0
64- 8 700	.682	2.0	.6	-2.4	.6	1.1	.8	.6	.1	.1	.0	.0	.0	.0	.0
65- 3 700	.642	2.0	.7	-2.6	.5	2.0	1.7	.7	.1	.1	.0	.0	.0	.0	.0
65- 4 700	.701	2.0	.8	-3.0	.9	2.9	2.1	.6	.1	.1	.0	.0	.0	.0	.0
65- 5 700	.801	2.0	1.0	-3.7	.5	2.4	2.3	.7	.1	.1	.0	.0	.0	.0	.0
65- 6 700	.861	2.0	1.7	-4.6	-1.6	1.8	1.8	.8	.2	.1	.0	.0	.0	.0	.0
67- 3 700	.801	2.0	.8	-3.7	-1	2.3	1.4	.3	-2	-1	.0	.0	.0	.0	.0
67- 4 674	.832	2.0	1.3	-3.9	-1.5	1.9	1.7	.7	-2	-1	.0	.0	.0	.0	.0
67- 5 652	.862	2.0	1.6	-3.6	-1.5	2.2	2.2	1.1	.3	.0	-1	.0	.0	.0	.0
67- 6 698	1.040	2.0	1.7	-3.9	-2.4	.8	2.1	1.8	.8	.5	-1	.0	.0	.0	.0
67- 7 698	1.126	2.0	2.1	-6.0	-3.7	.5	2.5	2.0	.6	.2	-3	.0	.0	.0	.0
67- 8 676	1.181	2.0	2.6	-6.3	-4.8	.3	3.4	2.1	.5	.6	.0	.0	.0	.0	.0
67- 9 652	1.243	2.0	2.6	-8.9	-9.1	1.7	3.4	1.5	.6	.2	.1	.1	.0	.0	.0
67-10 628	1.312	2.0	2.5	-10.5	-3.8	3.4	3.4	.4	.1	-7	.7	.5	.2	.0	.0
67-11 604	1.368	2.0	2.5	-12.0	-6.0	3.8	4.3	-1	-8	-8	-2.5	.2	-2	.0	.0
67-12 340	1.474	2.0	4.5	-15.5	-4.4	5.6	3.5	.0	-1.7	-3.4	-2.5	-1.8	-7	.0	.0

BLADE .18R TORSIONAL MOMENT HARMONICS (IN.-LB)

RUN- PT. NO.	QMS OR NO. (FPS)	THC (DEG)	BLADE .18R TORSIONAL MOMENT HARMONICS (IN.-LB)												
			B1	B2	B3	B4	B5	B6	B7	B8	B9	B10	B11	B12	B13
64- 3 700	.390	2.0	1.2	-1	-1	.3	-0	-0	.0	.1	.0	.0	.0	.0	.0
64- 4 700	.448	2.0	1.4	-1	-3	.5	-0	.3	.0	.0	.0	.0	.0	.0	.0
64- 5 700	.504	2.0	1.6	-1	-2	.5	.7	.3	.0	.0	.0	.0	.0	.0	.0
64- 6 700	.565	2.0	1.4	-1	.0	.7	.1	.1	.0	.0	.0	.0	.0	.0	.0
64- 7 700	.623	2.0	1.2	-0	.5	1.3	.4	.2	.0	.0	.0	.0	.0	.0	.0
64- 8 700	.682	2.0	1.2	.5	.7	2.1	1.4	.7	.0	.1	.0	.0	.0	.0	.0
65- 3 700	.642	2.0	.9	.5	.9	1.3	.7	.1	.0	.0	.0	.0	.0	.0	.0
65- 4 700	.701	2.0	.9	1.2	.8	1.8	.3	.2	.0	.0	.0	.0	.0	.0	.0
65- 5 700	.801	2.0	.4	.4	1.4	1.8	1.1	.2	.2	.1	.0	.0	.0	.0	.0
65- 6 700	.861	2.0	-2	.0	1.7	2.8	1.6	.7	.4	.3	.0	.0	.0	.0	.0
67- 3 700	.801	2.0	.8	.4	1.3	2.7	1.7	.7	.3	.2	.1	.1	.1	.0	.0
67- 4 674	.832	2.0	.3	-3	1.1	1.7	2.2	.8	.3	.2	.1	.1	.1	.0	.0
67- 5 652	.862	2.0	.6	.1	1.4	.6	1.2	1.2	1.1	.3	.2	.1	.1	.0	.0
67- 6 698	1.040	2.0	-2.0	-1.0	1.7	2.2	.3	.6	.7	.1	.2	.2	.1	.0	.0
67- 7 698	1.126	2.0	-5.4	-3.2	3.2	3.7	1.2	.2	.4	.2	.2	.2	.0	.0	.0
67- 8 676	1.181	2.0	-5.3	-3.1	3.1	4.9	.4	.2	-4	.4	.3	.3	.0	.0	.0
67- 9 652	1.243	2.0	-8.5	-3.5	5.0	5.6	-1	.2	-1.5	.6	.3	.3	.0	.0	.0
67-10 628	1.312	2.0	-11.1	-3.6	7.4	5.9	-1	.2	-1.6	.8	.4	.4	.0	.0	.0
67-11 604	1.368	2.0	-12.2	-3.7	7.4	6.6	-2	.3	-2.3	.8	.4	.5	.0	.0	.0
67-12 340	1.474	2.0	-15.0	-2.7	11.3	6.8	-6	.2	-3.0	.6	1.7	.1	.0	.0	.0

TABLE XXXII - Concluded

TABLE XXXII - Concluded																		
RU- PT. NO.	QMS ON (FPS)	MU	TMC (DEG)	BLADE .13R TORSIONAL MOMENT HARMONICS (IN.-LB)														
				R5	R1	R2	R3	R4	R5	R6	R7	R8	R9	R10	R11	R12	R13	
64- 3 700		.390	2.0	.2	1.3	.7	.4	.2	.1	.1	.1	.0	.0	.0	.0	.0	.0	.0
64- 4 700		.448	2.0	.4	1.5	.7	.7	.4	.1	.1	.0	.0	.0	.0	.0	.0	.0	.0
64- 5 700		.504	2.0	.6	1.6	1.1	.6	.6	.1	.4	.1	.0	.0	.0	.0	.0	.0	.0
64- 6 700		.565	2.0	.9	1.5	1.5	.5	.9	.3	.5	.1	.0	.0	.0	.0	.0	.0	.0
64- 7 700		.623	2.0	1.2	1.3	2.0	.7	1.7	.9	.5	.1	.0	.0	.0	.0	.0	.0	.0
64- 8 700		.682	2.0	1.6	1.3	2.5	.9	2.4	1.6	.6	.1	.1	.0	.0	.0	.0	.0	.0
65- 3 700		.642	2.0	1.5	1.1	2.7	1.0	2.4	1.9	.7	.1	.0	.0	.0	.0	.0	.0	.0
65- 4 700		.741	2.0	1.8	1.2	3.3	1.2	3.0	2.1	.6	.2	.1	.0	.0	.0	.0	.0	.0
65- 5 700		.801	2.0	2.4	1.1	3.7	1.5	3.1	2.5	.7	.2	.1	.0	.0	.0	.0	.0	.0
65- 6 700		.861	2.0	3.3	1.6	4.6	2.3	3.3	2.5	1.1	.5	.3	.0	.0	.0	.0	.0	.0
67- 3 700		.801	2.0	2.1	1.2	3.7	1.3	3.1	2.2	.7	.4	.2	.1	.1	.1	.2	.1	.1
67- 4 674		.852	2.0	2.3	1.3	3.9	1.9	2.6	2.8	1.1	.3	.3	.1	.1	.1	.2	.1	.1
67- 5 652		.862	2.0	1.7	1.5	3.6	2.0	2.2	2.5	1.7	1.1	.2	.2	.1	.1	.2	.2	.2
67- 6 695		1.040	2.0	.4	3.0	4.3	2.9	2.4	2.0	1.9	1.1	.5	.2	.2	.2	.0	.1	.1
67- 7 498		1.126	2.0	1.3	6.0	6.8	4.9	3.7	2.8	2.0	.7	.4	.3	.4	.2	.1	.1	.1
67- 8 476		1.141	2.0	1.0	7.1	7.0	5.7	4.9	3.4	3.4	1.6	.9	.3	.3	.3	.2	.1	.1
67- 9 652		1.243	2.0	1.1	8.9	9.1	7.1	5.9	3.4	3.2	1.7	.8	.4	.4	.1	.2	.2	.2
67-10 628		1.312	2.0	4.1	11.4	11.1	8.3	8.8	3.4	3.1	2.4	1.1	.8	.4	.7	.2	.2	.2
67-11 604		1.388	2.0	4.3	12.4	12.6	9.5	7.7	4.3	3.4	2.5	1.4	.8	.5	.2	.3	.2	.2
67-12 340		1.474	2.0	8.3	16.4	15.8	12.2	8.8	3.5	2.7	4.3	3.5	3.1	1.8	1.0	.6	.1	.1

FROM ANALYSIS OF BLADE FLAP MOTION HARMONICS
 BLADE CENTER OF GRAVITY AT 105 IN. HUB

RUN- PT. NO.	RMS OR (FPS)	MU	THEC (DEG)	BLADE FLAP MOTION HARMONICS (DEG)						
				A1	A2	A3	A4	A5	A6	A7
64- 3 700	.390	2.0	-1	-1	-0	.3	.0	.0	.0	.0
64- 4 700	.448	2.0	-1	-1	-1	.3	.0	.0	.0	.0
64- 5 700	.504	2.0	-1	-1	.4	.0	.0	.0	.0	.0
64- 6 700	.565	2.0	-2	-1	.4	.0	.0	.0	.0	.0
64- 7 700	.623	2.0	.2	-1	.5	.0	.0	.0	.0	.0
64- 8 700	.682	2.0	-2	-1	.5	.0	.0	.0	.0	.0
65- 3 700	.682	2.0	.1	-1	.4	.0	.0	.0	.0	.0
65- 4 700	.741	2.0	-4	-1	.4	.1	.0	.0	.0	.0
65- 5 700	.801	2.0	-2	.0	.5	.1	.0	.0	.0	.0
65- 6 700	.861	2.0	-2	.0	.5	.0	.0	.0	.0	.0
67- 3 700	.801	2.0	-5	.0	.5	.0	.0	.0	.0	.0
67- 4 674	.832	2.0	.4	.0	.5	.0	.0	.0	.0	.0
67- 5 652	.862	2.0	-6	.0	.4	.1	.0	.0	.0	.0
67- 6 498	1.040	2.0	.1	-1	.5	.1	.0	.0	.0	.0
67- 7 498	1.126	2.0	.3	-1	.6	.1	.1	.0	.0	.0
67- 8 476	1.181	2.0	-4	-2	.5	.2	.1	.0	.0	.0
67- 9 452	1.243	2.0	.1	-2	.7	.2	.1	.0	.0	.0
67-10 428	1.312	2.0	.1	-4	1.0	.3	.1	.1	.0	.0
67-11 404	1.368	2.0	-4	-5	.8	.4	.2	.1	.0	.0
67-12 380	1.474	2.0	.0	-7	1.2	.6	.3	.2	.0	.0

RUN- PT. NO.	RMS OR (FPS)	MU	THEC (DEG)	BLADE FLAP MOTION HARMONICS (DEG)						
				B1	B2	B3	B4	B5	B6	B7
64- 3 700	.390	2.0	-1	-1	-1	.0	.0	.0	.0	.0
64- 4 700	.448	2.0	-2	-1	.0	.0	.1	.0	.0	.0
64- 5 700	.504	2.0	-2	-1	-1	.0	.0	.0	.0	.0
64- 6 700	.565	2.0	-2	-1	-1	.0	.0	.0	.0	.0
64- 7 700	.623	2.0	-0	-2	-1	.0	.1	.0	.0	.0
64- 8 700	.682	2.0	-2	-2	-2	.1	.1	.0	.0	.0
65- 3 700	.682	2.0	-0	-2	-3	.1	.1	.0	.0	.0
65- 4 700	.741	2.0	-2	-2	-4	.0	.1	.0	.0	.0
65- 5 700	.801	2.0	-1	-2	-3	.1	.2	.0	.0	.0
65- 6 700	.861	2.0	-1	-2	-3	.1	.1	.0	.0	.0
67- 3 700	.801	2.0	-3	-2	-3	.1	.1	.0	.0	.0
67- 4 674	.832	2.0	-1	-2	-1	.1	.1	.0	.0	.0
67- 5 652	.862	2.0	-2	-2	-4	.1	.2	.0	.0	.0
67- 6 498	1.040	2.0	.0	-1	-4	.1	.1	.0	.0	.0
67- 7 498	1.126	2.0	.0	-1	-2	.1	.1	.0	.0	.0
67- 8 476	1.181	2.0	-2	-1	-5	.1	.1	.1	.0	.0
67- 9 452	1.243	2.0	.1	-2	-5	.1	.1	.2	.0	.0
67-10 428	1.312	2.0	.1	.0	-5	.1	.1	.2	.0	.0
67-11 404	1.368	2.0	-2	.0	-9	.1	.1	.1	.0	.0
67-12 380	1.474	2.0	.0	.4	-1.2	.0	.1	.1	.0	.0

TABLE XXXIII - Concluded

TABLE XXXIII - Concluded												
BLADE FLAP MOTION HARMONICS (DEG)												
RUN- PT. NO.	OMS #R (FPS)	MU	THEC (DEG)	RS	R1	R2	R3	R4	R5	R6	R7	
64- 3 700		.390	2.0	1.2	.2	.1	.3	.0	.0	.0	.0	
64- 4 700		.448	2.0	1.0	.2	.1	.3	.1	.1	.0	.0	
64- 5 700		.504	2.0	.8	.2	.1	.4	.1	.0	.0	.0	
64- 6 700		.565	2.0	.7	.2	.2	.4	.0	.0	.0	.0	
64- 7 700		.623	2.0	.5	.2	.2	.5	.1	.1	.0	.0	
64- 8 700		.682	2.0	.9	.3	.2	.5	.1	.1	.0	.0	
65- 3 700		.682	2.0	.4	.2	.2	.5	.1	.1	.0	.0	
65- 4 700		.741	2.0	.4	.4	.2	.6	.1	.1	.0	.0	
65- 5 700		.801	2.0	.3	.2	.2	.6	.1	.2	.0	.0	
65- 6 700		.861	2.0	.2	.2	.2	.6	.1	.1	.0	.0	
67- 3 700		.801	2.0	.4	.6	.2	.6	.1	.2	.0	.0	
67- 4 674		.832	2.0	.2	.4	.2	.5	.1	.1	.0	.0	
67- 5 632		.862	2.0	.4	.6	.2	.6	.1	.2	.0	.0	
67- 6 498		1.040	2.0	.0	.6	.2	.6	.1	.1	.0	.0	
67- 7 498		1.126	2.0	.3	.1	.1	.7	.2	.1	.2	.0	
67- 8 476		1.181	2.0	.2	.3	.2	.7	.2	.1	.3	.0	
67- 9 452		1.243	2.0	.6	.1	.3	.9	.3	.1	.2	.0	
67-10 428		1.312	2.0	.9	.1	.4	1.1	.3	.2	.2	.0	
67-11 404		1.388	2.0	-1.1	.5	.5	1.2	.4	.2	.2	.0	
67-12 380		1.474	2.0	-2.0	.1	.8	1.7	.6	.3	.2	.1	

TABLE XXXIV. BLADE .35R TORSIONAL MOMENT HARMONICS - RUN 64
(BLADE CENTER OF GRAVITY AT .25 CHORD)

BLADE .35R TORSIONAL MOMENT HARMONICS (IN.-LB)										
RUN- PT. NO.	OMS *R (FPS)	MU	THEC (DEG)	A1	A2	A3	A4	A5	A6	A7
64- 3 700	.390	2.0	.8	-.4	.7	.1	.1	.0	.1	.1
64- 4 700	.448	2.0	.8	-.6	.7	.4	.0	.0	.0	.0
64- 5 700	.504	2.0	.8	-.9	.8	.5	-.1	.2	.0	.0
64- 6 700	.565	2.0	.9	-1.0	.6	.7	.2	.4	.1	.1
64- 7 700	.623	2.0	.8	-1.4	.6	1.0	.6	.4	.0	.0
64- 8 700	.682	2.0	1.1	-1.8	.7	1.5	1.0	.5	-.1	.1

BLADE .35R TORSIONAL MOMENT HARMONICS (IN.-LB)										
RUN- PT. NO.	OMS *R (FPS)	MU	THEC (DEG)	B1	B2	B3	B4	B5	B6	B7
64- 3 700	.390	2.0	.8	.0	-.2	.4	-.1	-.1	.0	.0
64- 4 700	.448	2.0	.9	.0	-.5	.2	-.1	.1	.0	.0
64- 5 700	.504	2.0	1.2	.1	-.4	.5	.0	.2	.0	.0
64- 6 700	.565	2.0	1.2	.3	-.4	.7	.1	.1	.0	.0
64- 7 700	.623	2.0	1.1	.0	-.3	1.3	.3	.0	.0	.0
64- 8 700	.682	2.0	.8	.4	-.2	1.7	.9	.0	.0	.0

BLADE .35R TORSIONAL MOMENT HARMONICS (IN.-LB)											
RUN- PT. NO.	OMS *R (FPS)	MU	THEC (DEG)	R5	R1	R2	R3	R4	R5	R6	R7
64- 3 700	.390	2.0	-1.5	1.1	.4	.7	.5	.1	.1	.1	.1
64- 4 700	.448	2.0	-1.7	1.3	.6	.8	.5	.1	.1	.1	.0
64- 5 700	.504	2.0	-1.8	1.5	.9	.9	.7	.1	.3	.0	.0
64- 6 700	.565	2.0	-1.8	1.5	1.0	.7	1.0	.2	.4	.1	.1
64- 7 700	.623	2.0	-1.9	1.3	1.4	.7	1.6	.7	.4	.0	.0
64- 8 700	.682	2.0	-2.0	1.4	1.8	.7	2.3	1.3	.5	.1	.1

TABLE XXXV. BLADE LAG MOTION HARMONICS - RUN 68
(BLADE CENTER OF GRAVITY AT .25 CHORD)

RUN- PT. NO.	OMS R (FPS)	M	TIMEC (DEG)	BLADE LAG MOTION HARMONICS (DEG)				
				A1	A2	A3	A4	A5
68- 3 700	.294	8.0	-.2	.0	.1	.0	.0	.0
68- 4 700	.294	9.0	-.3	.0	.1	.1	.0	.0
68- 5 700	.294	10.0	-.4	.0	.0	.1	.0	.0
68- 6 700	.294	11.0	-.5	.0	.0	.1	.0	.0
68- 7 700	.294	12.0	-.5	.0	.0	.1	.0	.0
68- 8 700	.351	8.0	-.2	.0	.1	.0	.0	.0
68- 9 700	.351	9.0	-.3	.0	.1	.1	.0	.0
68-10 700	.351	10.0	-.4	.0	.1	.1	.0	.0
68-11 700	.351	11.0	-.5	.0	.1	.1	.0	.0
68-12 700	.351	12.0	-.5	.0	.1	.1	.0	.0
68-13 700	.410	8.0	-.2	.0	.1	.1	.0	.0
68-14 700	.410	9.0	-.3	.0	.1	.1	.0	.0
68-15 700	.410	10.0	-.3	.0	.1	.2	.0	.0
68-16 700	.410	11.0	-.4	.0	.1	.2	.0	.0
68-17 700	.486	8.0	-.2	.0	.1	.2	.0	.0
68-18 700	.486	9.0	-.3	.1	.1	.2	.0	.0
68-19 700	.486	10.0	-.3	.0	.1	.3	.0	.0
68-20 700	.486	11.0	-.4	.0	.1	.3	.0	.0

RUN- PT. NO.	OMS R (FPS)	M	TIMEC (DEG)	BLADE LAG MOTION HARMONICS (DEG)				
				B1	B2	B3	B4	B5
68- 3 700	.294	8.0	.1	.0	.0	.0	.2	.0
68- 4 700	.294	9.0	.2	.0	.0	.0	.2	.0
68- 5 700	.294	10.0	.2	.0	.0	.0	.1	.0
68- 6 700	.294	11.0	.3	.0	.1	.1	.1	.0
68- 7 700	.294	12.0	.4	.1	.1	.1	.1	.0
68- 8 700	.351	8.0	.1	.0	.0	.0	.2	.0
68- 9 700	.351	9.0	.2	.0	.0	.0	.1	.0
68-10 700	.351	10.0	.3	.0	.0	.0	.1	.0
68-11 700	.351	11.0	.3	.1	.0	.0	.0	.0
68-12 700	.351	12.0	.4	.1	.1	.1	.1	.0
68-13 700	.410	8.0	.1	.0	.0	.0	.2	.0
68-14 700	.410	9.0	.2	.1	.0	.0	.2	.0
68-15 700	.410	10.0	.2	.1	.0	.0	.2	.0
68-16 700	.410	11.0	.3	.0	.0	.0	.1	.0
68-17 700	.486	8.0	.1	.1	-.1	.1	.1	.0
68-18 700	.486	9.0	.2	.1	.0	.0	.1	.0
68-19 700	.486	10.0	.2	.1	.0	.0	.1	.0
68-20 700	.486	11.0	.3	.1	.0	.0	.0	.0

TABLE XXXV - Concluded										
RUN- PT. NC.	OMS *R (FPS)	MU	THEC (DEG)	BLADE LAG MOTION HARMONICS (DEG)						
				RS	R1	R2	R3	R4	R5	
68- 3	700	.294	8.0	4.2	.3	.0	.1	.2	.0	
68- 4	700	.294	9.0	4.9	.3	.0	.1	.2	.0	
68- 5	700	.294	10.0	5.9	.5	.0	.1	.2	.0	
68- 6	700	.294	11.0	6.6	.5	.0	.1	.1	.0	
68- 7	700	.294	12.0	7.4	.7	.1	.1	.2	.0	
68- 8	700	.351	8.0	4.1	.2	.0	.1	.2	.0	
68- 9	700	.351	9.0	5.0	.4	.0	.1	.2	.0	
68-10	700	.351	10.0	5.7	.5	.0	.1	.2	.0	
68-11	700	.351	11.0	6.6	.6	.1	.1	.1	.0	
68-12	700	.351	12.0	7.4	.6	.1	.1	.1	.0	
68-13	700	.410	8.0	4.1	.3	.0	.1	.2	.0	
68-14	700	.410	9.0	4.7	.3	.1	.1	.2	.0	
68-15	700	.410	10.0	5.4	.4	.1	.1	.2	.0	
68-16	700	.410	11.0	6.1	.5	.1	.1	.2	.0	
68-17	700	.486	8.0	4.0	.3	.1	.1	.2	.0	
68-18	700	.486	9.0	4.6	.3	.1	.1	.3	.0	
68-19	700	.486	10.0	5.2	.4	.1	.1	.3	.0	
68-20	700	.486	11.0	5.9	.5	.1	.1	.3	.0	

TABLE XXXVI. BLADE .30R FLAPWISE BENDING MOMENT HARMONICS
- RUN 68 (BLADE CENTER OF GRAVITY AT .25 CHORD)

BLADE .30R FLAPWISE BENDING MOMENT HARMONICS (IN.-LB)											
RUN- PT. NO.	OMS #R (FPS)	MU	THEC (DEG)	A1	A2	A3	A4	A5	A6	A7	A8
68- 3 700	.294	8.0	.5	-.4	-3.3	-.2	-1.6	.6	-.2	-1.0	
68- 4 700	.294	9.0	.4	-.6	-3.3	-.2	-1.7	.9	-.2	-1.1	
68- 5 700	.294	10.0	.4	-.6	-3.2	-.3	-3.8	1.3	-.2	-.9	
68- 6 700	.294	11.0	.4	-.6	-3.1	-.3	-4.9	1.3	-.1	-.5	
68- 7 700	.294	12.0	.4	-.6	-2.8	-.1	-4.1	.8	-.1	-.2	
68- 8 700	.351	8.0	1.2	-.2	-3.9	.5	1.3	1.3	.3	.1	
68- 9 700	.351	9.0	1.2	-.4	-4.0	.2	1.6	1.7	.2	.1	
68-10 700	.351	10.0	1.2	-.4	-3.8	.1	1.0	2.1	.0	-.3	
68-11 700	.351	11.0	1.2	-.4	-4.1	.1	-1.0	2.4	.0	-.1	
68-12 700	.351	12.0	1.3	-.3	-4.1	.0	-1.0	1.9	-.1	.0	
68-13 700	.410	8.0	1.7	-1.3	-5.5	-.1	.1	-.2	-.5	-1.1	
68-14 700	.410	9.0	1.6	-1.6	-5.8	-.2	-.6	.3	-.5	-1.5	
68-15 700	.410	10.0	1.6	-1.7	-5.6	-.2	-2.5	.5	-.7	-2.0	
68-16 700	.410	11.0	1.6	-1.8	-5.3	-.3	-3.2	.2	-.8	-2.2	
68-17 700	.486	8.0	2.7	-1.9	-5.1	-.3	-1.9	1.4	.4	-.9	
68-18 700	.486	9.0	2.9	-2.0	-5.5	-.5	-3.1	2.1	.6	-1.0	
68-19 700	.486	10.0	2.9	-2.2	-5.5	-.5	-4.1	2.8	.6	-1.2	
68-20 700	.486	11.0	3.0	-2.3	-5.6	-.6	-4.1	2.8	.3	-1.5	

BLADE .30R FLAPWISE BENDING MOMENT HARMONICS (IN.-LB)											
RUN- PT. NO.	OMS #R (FPS)	MU	THEC (DEG)	B1	B2	B3	B4	B5	B6	B7	B8
68- 3 700	.294	8.0	-2.0	.1	.6	-1.2	-3.3	-.9	-.5	.0	
68- 4 700	.294	9.0	-2.0	.3	.5	-1.4	-4.8	-.5	-.4	-.1	
68- 5 700	.294	10.0	-2.0	.5	.1	-1.6	-6.2	-.3	-.2	.0	
68- 6 700	.294	11.0	-1.9	.6	.2	-1.5	-4.7	-.9	-.2	-.1	
68- 7 700	.294	12.0	-1.9	.6	.0	-1.7	-1.9	-1.1	-.1	.1	
68- 8 700	.351	8.0	-1.4	.5	3.0	-.3	-3.2	.7	.1	-.6	
68- 9 700	.351	9.0	-1.5	.6	2.9	-.8	-6.6	1.2	.3	-.5	
68-10 700	.351	10.0	-1.6	.9	2.6	-1.1	-8.3	1.4	.6	-.1	
68-11 700	.351	11.0	-1.5	1.1	2.1	-1.2	-8.0	1.3	.8	.3	
68-12 700	.351	12.0	-1.4	1.2	1.9	-1.3	-8.1	1.3	.8	.5	
68-13 700	.410	8.0	-1.3	.6	1.7	-1.1	-1.1	.5	.4	.6	
68-14 700	.410	9.0	-1.4	.7	1.9	-1.3	-2.7	.3	.4	.4	
68-15 700	.410	10.0	-1.4	.9	2.1	-1.5	-3.3	-.5	.1	.1	
68-16 700	.410	11.0	-1.4	1.0	1.8	-1.9	-3.5	-1.1	-.2	-.1	
68-17 700	.486	8.0	-1.4	.8	5.1	-.5	.6	.2	.7	.3	
68-18 700	.486	9.0	-1.6	.8	5.7	-.8	-.6	.2	.9	.3	
68-19 700	.486	10.0	-1.7	.7	6.2	-1.1	-1.6	-.1	.9	.2	
68-20 700	.486	11.0	-1.7	.7	6.4	-1.6	-2.8	-.1	1.0	.2	

TABLE XXXVI - Concluded												
BLADE .30R FLAPWISE BENDING MOMENT HARMONICS (IN.-LB)												
RUI- PT. NO.	OMS #R	MU	THEC (DEG)	RS	R1	R2	R3	R4	R5	R6	R7	R8
68- 3	700	.294	8.0	4.5	2.0	.5	3.4	1.2	3.6	1.0	.5	1.0
68- 4	700	.294	9.0	4.8	2.0	.7	3.4	1.4	5.0	1.0	.4	1.2
68- 5	700	.294	10.0	5.1	2.1	.8	3.0	1.6	7.1	1.3	.3	.9
68- 6	700	.294	11.0	5.4	2.0	.9	3.2	1.5	7.1	1.7	.3	.5
68- 7	700	.294	12.0	5.6	1.9	.9	2.8	1.7	4.5	1.4	.1	.2
68- 8	700	.351	8.0	4.1	1.8	.6	4.9	.6	3.4	1.5	.3	.6
68- 9	700	.351	9.0	4.4	1.9	.7	4.9	.8	6.8	2.1	.4	.5
68-10	700	.351	10.0	4.8	2.1	1.0	4.6	1.1	8.4	2.5	.6	.3
68-11	700	.351	11.0	5.2	2.0	1.2	4.6	1.2	8.1	2.7	.8	.3
68-12	700	.351	12.0	5.5	1.9	1.3	4.5	1.3	8.1	2.2	.8	.5
68-13	700	.410	8.0	4.0	2.1	1.5	5.8	1.1	1.1	.5	.7	1.3
68-14	700	.410	9.0	4.3	2.1	1.7	6.1	1.3	2.8	.4	.6	1.6
68-15	700	.410	10.0	4.6	2.1	1.9	6.0	1.5	4.1	.7	.7	2.0
68-16	700	.410	11.0	4.8	2.2	2.0	5.6	1.9	4.7	1.1	.9	2.2
68-17	700	.486	8.0	4.2	3.1	2.0	7.2	.6	2.0	1.4	.8	1.0
68-18	700	.486	9.0	4.5	3.3	2.2	7.9	.9	3.2	2.2	1.0	1.0
68-19	700	.486	10.0	4.9	3.4	2.3	8.3	1.2	4.4	2.8	1.1	1.2
68-20	700	.486	11.0	5.2	3.5	2.4	8.5	1.7	4.9	2.8	1.1	1.5

TABLE XXXVII. BLADE .60R FLAPWISE BENDING MOMENT HARMONICS
(BLADE CENTER OF GRAVITY AT .25 CHORD)

BLADE .60R FLAPWISE BENDING MOMENT HARMONICS (IN.-LB)											
RUN- PT. NO.	OMS #R (FPS)	MU	THEC (DEG)	A1	A2	A3	A4	A5	A6	A7	A8
68- 3 700	.294	8.0	.7	-2.8	-6.3	-.3	1.4	-.4	.4	1.2	
68- 4 700	.294	9.0	.6	-3.0	-6.2	-.2	1.5	-.5	.4	1.3	
68- 5 700	.294	10.0	.3	-3.4	-5.8	.2	2.9	-.6	.5	1.0	
68- 6 700	.294	11.0	.5	-3.4	-5.9	.3	4.2	-.7	.4	.6	
68- 7 700	.294	12.0	.3	-3.9	-5.7	.1	3.2	-.4	.3	.1	
68- 8 700	.351	8.0	2.4	-1.9	-5.9	-1.2	-.6	-.8	-.2	.0	
68- 9 700	.351	9.0	2.5	-2.1	-5.8	-.9	-.5	-1.0	-.1	.1	
68-10 700	.351	10.0	2.3	-2.5	-5.3	-.7	.3	-1.1	-.1	.0	
68-11 700	.351	11.0	2.2	-3.0	-5.7	-.5	1.7	-1.2	.2	.3	
68-12 700	.351	12.0	2.1	-3.3	-6.0	-.5	1.7	-.9	.3	.2	
68-13 700	.410	8.0	1.7	-4.4	-7.9	-1.0	-.2	.4	.4	1.2	
68-14 700	.410	9.0	1.5	-5.1	-8.0	-.8	.3	.1	.3	1.6	
68-15 700	.410	10.0	1.5	-5.6	-7.6	-.8	1.6	.1	.5	2.0	
68-16 700	.410	11.0	1.9	-5.7	-6.4	-.6	1.9	.4	.6	1.7	
68-17 700	.486	8.0	3.5	-4.1	-7.1	-.5	.7	-.3	.0	.7	
68-18 700	.486	9.0	3.8	-4.3	-7.4	-.5	1.5	-.6	-.3	.7	
68-19 700	.486	10.0	3.8	-4.8	-7.3	-.7	2.3	-.8	-.3	.9	
68-20 700	.486	11.0	3.9	-4.9	-6.8	-.7	2.2	-.8	-.1	1.0	

BLADE .60R FLAPWISE BENDING MOMENT HARMONICS (IN.-LB)											
RUN- PT. NO.	OMS #R (FPS)	MU	THEC (DEG)	B1	B2	B3	B4	B5	B6	B7	B8
68- 3 700	.294	8.0	-2.4	-2.8	1.4	-.1	2.1	.6	.3	.0	
68- 4 700	.294	9.0	-2.5	-2.8	1.5	-.1	3.2	.4	.2	.0	
68- 5 700	.294	10.0	-2.7	-3.0	1.1	.0	4.1	.4	.1	-.1	
68- 6 700	.294	11.0	-3.0	-3.3	1.3	-.3	3.1	.6	.1	.1	
68- 7 700	.294	12.0	-3.6	-3.6	1.2	-.6	1.0	.5	-.2	.0	
68- 8 700	.351	8.0	-2.2	-2.3	4.3	.2	2.3	.0	-.2	.6	
68- 9 700	.351	9.0	-2.3	-2.4	4.3	.5	4.7	-.2	-.3	.5	
68-10 700	.351	10.0	-2.6	-2.6	4.1	.8	5.7	-.4	-.6	.8	
68-11 700	.351	11.0	-2.8	-2.7	3.5	.6	5.3	-.4	-.8	-.3	
68-12 700	.351	12.0	-3.0	-2.9	3.5	.5	5.3	-.5	-.9	-.6	
68-13 700	.410	8.0	-2.0	.3	2.6	-.1	.5	.0	-.4	-.7	
68-14 700	.410	9.0	-2.2	.2	2.8	-.1	1.4	.1	-.4	-.6	
68-15 700	.410	10.0	-2.4	.2	3.0	.0	1.6	.5	-.3	-.8	
68-16 700	.410	11.0	-2.5	-.7	2.3	.4	1.1	.4	-.3	-.8	
68-17 700	.486	8.0	-2.4	.8	5.9	.1	-.7	-.5	-.1	-.4	
68-18 700	.486	9.0	-2.6	-.3	6.5	.1	.0	-.6	-.3	-.5	
68-19 700	.486	10.0	-2.9	-.1	7.3	.5	.7	-.8	-.6	-.8	
68-20 700	.486	11.0	-3.0	-.8	7.1	1.3	1.1	-.8	-.5	-.3	

TABLE XXXVII - Concluded

TABLE XXXVII - Concluded												
BLADE .60R FLAPWISE BENDING MOMENT HARMONICS (IN.-LB)												
RUL- PT. NO.	QMS OR (FPS)	MU	THEC (DEG)	RS	R1	R2	R3	R4	R5	R6	R7	R8
00-3 700		.294	8.0	1.4	2.5	3.9	6.4	.3	2.6	.8	.5	1.2
00-4 700		.294	9.0	1.6	2.6	4.1	6.3	.2	3.5	.7	.5	1.3
00-5 700		.294	10.0	1.8	2.7	4.6	6.0	.1	5.0	.7	.5	1.0
00-6 700		.294	11.0	2.1	3.1	4.8	6.0	.4	4.9	.8	.4	.6
00-7 700		.294	12.0	2.4	3.6	5.3	5.8	.6	3.3	.6	.4	.1
00-8 700		.351	8.0	1.7	3.3	3.0	7.3	1.2	2.4	.8	.3	.6
00-9 700		.351	9.0	2.1	3.4	3.2	7.2	1.0	4.7	1.0	.4	.5
00-10 700		.351	10.0	2.3	3.5	3.6	6.7	1.0	5.7	1.1	.7	.4
00-11 700		.351	11.0	2.4	3.6	4.0	6.7	.8	5.6	1.2	.8	.5
00-12 700		.351	12.0	2.7	3.7	4.4	6.9	.7	5.6	1.0	.9	.7
00-13 700		.410	8.0	1.3	2.6	4.5	8.3	1.0	.5	.4	.5	1.4
00-14 700		.410	9.0	1.5	2.6	5.1	8.5	.8	1.4	.2	.5	1.7
00-15 700		.410	10.0	1.9	2.8	5.6	8.2	.8	2.2	.5	.6	2.0
00-16 700		.410	11.0	2.6	3.1	5.7	6.8	.7	2.2	.6	.7	1.8
00-17 700		.486	8.0	2.9	4.3	4.1	9.2	.5	1.0	.6	.1	.8
00-18 700		.486	9.0	3.4	4.6	4.4	9.9	.5	1.5	.7	.4	.8
00-19 700		.486	10.0	3.7	4.8	4.9	10.3	.8	2.4	.9	.5	1.0
00-20 700		.486	11.0	4.4	5.0	5.0	9.8	1.5	2.5	.9	.5	1.0

TABLE XXXVIII. BLADE .18R TORSIONAL MOMENT HARMONICS - RUN 68
(BLADE CENTER OF GRAVITY AT .25 CHORD)

RUN- PT. NO.	OMS OR (FPS)	MU	THEC (DEG)	BLADE .18R TORSIONAL MOMENT HARMONICS (IN.-LB)							
				A1	A2	A3	A4	A5	A6	A7	A8
68- 3 700	.294	8.0	1.3	.9	1.2	-.9	-2.6	-2.1	-.8	-.2	
68- 4 700	.294	9.0	1.1	1.1	.9	-1.7	-3.8	-3.4	-1.3	-.2	
68- 5 700	.294	10.0	.4	.9	-.4	-4.0	-6.8	-5.1	-2.0	-.6	
68- 6 700	.294	11.0	.0	.9	-1.4	-5.4	-8.5	-6.9	-2.3	-.7	
68- 7 700	.294	12.0	-.5	.9	-2.0	-5.5	-7.3	-4.7	-1.1	.1	
68- 8 700	.351	8.0	1.0	1.0	2.4	1.1	-.9	-2.3	-1.4	-.4	
68- 9 700	.351	9.0	.1	.6	1.7	-.3	-2.0	-3.6	-1.5	-.3	
68-10 700	.351	10.0	-.5	.2	.5	-2.3	-4.9	-6.3	-2.2	-.7	
68-11 700	.351	11.0	-.9	.3	-.2	-3.6	-7.1	-8.3	-3.1	-1.6	
68-12 700	.351	12.0	-1.1	.7	-.8	-4.8	-8.1	-8.1	-3.2	-1.8	
68-13 700	.410	8.0	.6	.1	2.7	2.5	1.1	.7	.2	.1	
68-14 700	.410	9.0	.2	.1	2.7	1.6	-.7	-.8	-.2	.2	
68-17 700	.486	8.0	.2	-2.3	.7	.7	-2.8	-2.6	-1.4	-.7	
68-18 700	.486	9.0	.4	-2.6	.1	.4	-4.5	-4.8	-2.5	-1.2	

RUN- PT. NO.	OMS OR (FPS)	MU	THEC (DEG)	BLADE .18R TORSIONAL MOMENT HARMONICS (IN.-LB)							
				B1	B2	B3	B4	B5	B6	B7	B8
68- 3 700	.294	8.0	3.2	1.4	-.6	-.9	-1.9	-.9	.1	.1	
68- 4 700	.294	9.0	4.4	1.8	-1.1	-.9	-2.3	-.9	.1	.2	
68- 5 700	.294	10.0	6.0	2.3	-1.3	-1.3	-2.6	-1.1	-.4	.0	
68- 6 700	.294	11.0	7.3	2.9	-1.1	.4	-.5	1.0	.4	.2	
68- 7 700	.294	12.0	9.3	3.7	-.4	2.1	3.6	4.2	1.8	.9	
68- 8 700	.351	8.0	3.8	2.6	-.9	-1.8	-3.3	-8.2	-.5	.1	
68- 9 700	.351	9.0	5.0	2.6	-1.5	-3.5	-6.4	-6.1	-1.6	-.6	
68-10 700	.351	10.0	6.3	3.0	-1.9	-3.6	-7.6	-4.7	-2.1	-1.1	
68-11 700	.351	11.0	8.1	3.7	-1.9	-3.9	-6.1	-3.8	-1.7	-.9	
68-12 700	.351	12.0	9.7	4.1	-2.1	-3.5	-3.8	-1.6	-1.3	.0	
68-13 700	.410	8.0	3.9	3.0	1.1	.1	-2.0	-1.6	-.8	-.3	
68-14 700	.410	9.0	5.0	3.7	.8	-.8	-3.0	-1.6	-.4	-.1	
68-17 700	.486	8.0	3.1	3.1	1.7	1.9	.4	-.1	-.1	.2	
68-18 700	.486	9.0	3.3	3.2	2.1	2.1	-.2	-.1	.0	.4	

TABLE XXXVIII - Concluded

Blade		Blade .18R Torsional Moment Harmonics (IN.-LB)										
PL. NO.	CRS. OR (RPS)	WJ	T, DEG	PS	R1	R2	R3	R4	R5	R6	R7	R8
00-1	700	.200	8.0	-2.9	3.5	1.7	1.3	1.0	2.9	2.1	.9	.2
00-4	700	.200	9.0	-3.8	4.5	2.1	1.4	1.9	4.4	3.5	1.3	.3
00-5	700	.200	10.0	-5.2	6.0	2.4	1.4	4.2	7.3	5.7	2.0	.6
00-6	700	.200	11.0	-6.2	7.6	3.1	1.8	5.4	8.5	7.0	2.4	.7
00-7	700	.200	12.0	-7.6	9.3	3.8	2.0	5.8	8.1	6.3	2.1	.9
00-8	700	.351	8.0	-3.1	3.9	2.3	2.5	2.1	3.4	3.5	1.5	.4
00-9	700	.351	9.0	-4.4	5.0	2.5	2.2	3.5	6.7	6.3	2.2	.6
00-10	700	.351	10.0	-5.7	6.5	3.0	2.0	5.1	9.1	8.8	3.1	1.3
00-11	700	.351	11.0	-6.7	8.1	3.7	2.0	5.3	9.3	9.5	3.5	1.8
00-12	700	.351	12.0	-7.8	9.7	4.2	2.3	6.0	9.5	9.0	3.5	1.8
00-13	700	.410	8.0	-3.0	3.9	3.0	3.0	2.5	2.3	1.7	.8	.3
00-14	700	.410	9.0	-3.9	5.0	3.7	2.8	1.8	3.0	1.8	.4	.2
00-17	700	.406	8.0	-2.6	3.1	3.8	1.8	2.0	2.8	2.6	1.4	.7
00-18	700	.406	9.0	-3.0	3.4	4.2	2.1	2.1	4.6	4.8	2.5	1.3

TABLE XXXIX. BLADE FLAP MOTION HARMONICS - RUN 68
(BLADE CENTER OF GRAVITY AT .25 CHORD)

RUN- PT. NO.	ONS OR (FPS)	MU	THEC (DEG)	BLADE FLAP MOTION HARMONICS (DEG)					
				A1	A2	A3	A4	A5	A6
68- 3 700	.294	8.0	.0	-.2	.3	.0	.1	.0	
68- 4 700	.294	9.0	.1	-.2	.3	.0	.1	.0	
68- 5 700	.294	10.0	.1	-.2	.3	.0	.1	.0	
68- 6 700	.294	11.0	.1	-.3	.3	.0	.2	.0	
68- 7 700	.294	12.0	.0	-.3	.3	.0	.1	.0	
68- 8 700	.351	8.0	.2	-.3	.3	.0	-.1	.0	
68- 9 700	.351	9.0	.1	-.3	.3	.0	-.1	.0	
68-10 700	.351	10.0	.0	-.3	.3	.0	.0	-.1	
68-11 700	.351	11.0	.0	-.3	.4	.0	.0	-.1	
68-12 700	.351	12.0	.2	-.3	.4	.0	.0	-.1	
68-13 700	.410	8.0	.1	-.2	.5	.0	.0	.0	
68-14 700	.410	9.0	.2	-.2	.5	.0	.0	.0	
68-15 700	.410	10.0	.1	-.3	.5	.0	.1	.0	
68-16 700	.410	11.0	.0	-.3	.5	.0	.1	.0	
68-17 700	.486	8.0	.0	-.3	.5	.0	.1	.0	
68-18 700	.486	9.0	.1	-.4	.5	.0	.1	-.1	
68-19 700	.486	10.0	.0	-.4	.5	.0	.1	-.1	
68-20 700	.486	11.0	.0	-.5	.5	.0	.1	-.1	

RUN- PT. NO.	ONS OR (FPS)	MU	THEC (DEG)	BLADE FLAP MOTION HARMONICS (DEG)					
				B1	B2	B3	B4	B5	B6
68- 3 700	.294	8.0	-.1	-.1	-.1	.0	.1	.0	
68- 4 700	.294	9.0	.0	-.2	-.1	.0	.2	.0	
68- 5 700	.294	10.0	.0	-.2	-.1	.1	.2	.0	
68- 6 700	.294	11.0	.0	-.3	-.1	.1	.2	.0	
68- 7 700	.294	12.0	.0	-.3	-.1	.1	.1	.0	
68- 8 700	.351	8.0	.1	-.2	-.2	.0	.1	.0	
68- 9 700	.351	9.0	.0	-.2	-.2	.0	.2	.0	
68-10 700	.351	10.0	.1	-.3	-.2	.1	.3	.0	
68-11 700	.351	11.0	-.2	-.3	-.2	.1	.3	.0	
68-12 700	.351	12.0	.0	-.3	-.2	.1	.3	.0	
68-13 700	.410	8.0	-.1	-.3	-.2	.0	.0	.0	
68-14 700	.410	9.0	-.0	-.3	-.2	.0	.1	.0	
68-15 700	.410	10.0	-.1	-.3	-.2	.0	.1	.0	
68-16 700	.410	11.0	-.2	-.3	-.2	.1	.1	.0	
68-17 700	.486	8.0	-.1	-.2	-.2	.0	.0	.0	
68-18 700	.486	9.0	.0	-.3	-.2	.0	.0	.0	
68-19 700	.486	10.0	-.1	-.3	-.2	.0	.1	.0	
68-20 700	.486	11.0	-.2	-.3	-.2	.1	.1	.0	

TABLE XXXIX - Concluded											
BLADE FLAP MOTION HARMONICS (DEG)											
RUN- PT. NO.	OMS OR (FPS)	MU	THEC (DEG)	RS	R1	R2	R3	R4	R5	R6	
6A- 3 700		.294	8.0	3.0	.1	.3	.3	.0	.2	.0	
6A- 4 700		.294	9.0	3.2	.1	.3	.3	.0	.2	.0	
6A- 5 700		.294	10.0	3.4	.1	.3	.3	.1	.2	.0	
6A- 6 700		.294	11.0	3.5	.1	.4	.3	.1	.3	.1	
6A- 7 700		.294	12.0	3.7	.0	.5	.3	.1	.1	.0	
6A- 8 700		.351	8.0	2.7	.2	.3	.4	.0	.1	.0	
6A- 9 700		.351	9.0	2.9	.1	.4	.4	.0	.2	.0	
6A-10 700		.351	10.0	3.1	.1	.4	.4	.1	.3	.1	
6A-11 700		.351	11.0	3.3	.2	.5	.4	.1	.3	.1	
6A-12 700		.351	12.0	3.4	.2	.6	.4	.1	.3	.1	
6A-13 700		.410	8.0	2.4	.1	.3	.5	.0	.0	.0	
6A-14 700		.410	9.0	2.6	.2	.4	.5	.0	.1	.0	
6A-15 700		.410	10.0	2.8	.1	.5	.5	.0	.1	.0	
6A-16 700		.410	11.0	3.0	.2	.5	.5	.1	.2	.0	
6A-17 700		.486	8.0	2.0	.1	.4	.6	.0	.1	.1	
6A-18 700		.486	9.0	2.2	.1	.5	.7	.0	.1	.1	
6A-19 700		.486	10.0	2.5	.1	.5	.7	.0	.2	.1	
6A-20 700		.486	11.0	2.6	.2	.6	.7	.1	.2	.1	

TABLE XL. BLADE LAG MOTION HARMONICS - RUNS 69-70
(BLADE CENTER OF GRAVITY AT .25 CHORD)

RUN- PT. NO.	OMS *R (FPS)	MU	THEC (DEG)	BLADE LAG MOTION HARMONICS (DEG)				
				A1	A2	A3	A4	A5
69- 3 700	.546	9.0	-3	.0	.1	.2	.0	
69- 4 700	.546	11.0	-4	.0	.1	.1	.0	
69- 5 700	.610	10.0	-2	.1	.1	.3	.0	
69- 6 700	.634	10.0	-2	.1	.1	.3	.0	
69- 7 700	.659	10.0	-2	.1	.1	.3	.0	
70- 3 700	.659	10.0	-2	.1	.2	.4	.0	
70- 4 700	.682	4.0	.1	.1	.1	.1	.0	
70- 5 700	.706	11.0	-3	.1	.3	.4	-.1	
70- 6 700	.682	11.0	-3	.2	.3	.5	.0	
70- 7 700	.731	11.0	-3	.2	.3	.5	.0	
70- 8 700	.756	11.0	-3	.2	.3	.5	-.1	
70- 9 700	.784	10.0	-2	.2	.3	.4	.0	
70-10 700	.808	10.0	-2	.2	.3	.5	.0	

RUN- PT. NO.	OMS *R (FPS)	MU	THEC (DEG)	BLADE LAG MOTION HARMONICS (DEG)				
				B1	B2	B3	B4	B5
69- 3 700	.546	9.0	.2	.0	.0	.0	.0	.0
69- 4 700	.546	11.0	.4	.0	.0	-.1	.0	
69- 5 700	.610	10.0	.1	.0	-.2	-.1	.0	
69- 6 700	.634	10.0	.1	.0	.2	-.2	.0	
69- 7 700	.659	10.0	.1	.0	-.2	-.2	.1	
70- 3 700	.659	10.0	.1	.1	.0	.2	.0	
70- 4 700	.682	4.0	-.1	.1	.0	.1	.0	
70- 5 700	.706	11.0	.0	.2	-.1	.2	.1	
70- 6 700	.682	11.0	.1	.2	-.1	.2	.1	
70- 7 700	.731	11.0	.0	.2	-.2	.2	.1	
70- 8 700	.756	11.0	.0	.2	-.2	.1	.1	
70- 9 700	.784	10.0	-.1	.2	-.2	.2	.1	
70-10 700	.808	10.0	-.1	.2	-.2	.2	.1	

TABLE XL - Concluded										
BLADE LAG MOTION HARMONICS (DEG)										
RUN- PT. NO.	QMS #R	MU	THEC (DEG)	RS	R1	R2	R3	R4	R5	
69- 3	700	.546	9.0	5.6	.4	.0	.1	.2	.0	
69- 4	700	.546	11.0	7.2	.6	.1	.1	.2	.0	
69- 5	700	.610	10.0	5.3	.3	.1	.2	.4	.0	
69- 6	700	.634	10.0	5.1	.3	.1	.2	.4	.0	
69- 7	700	.659	10.0	4.8	.2	.1	.2	.4	.1	
70- 3	700	.659	10.0	4.3	.2	.2	.2	.4	.1	
70- 4	700	.682	4.0	2.5	.2	.1	.1	.2	.0	
70- 5	700	.706	11.0	4.5	.3	.3	.3	.5	.1	
70- 6	700	.682	11.0	4.6	.3	.2	.3	.5	.1	
70- 7	700	.731	11.0	4.3	.3	.2	.3	.5	.1	
70- 8	700	.756	11.0	4.1	.3	.3	.4	.6	.1	
70- 9	700	.784	10.0	3.6	.2	.2	.3	.4	.1	
70-10	700	.808	10.0	3.4	.2	.2	.4	.5	.1	

TABLE XLI. BLADE .30R FLAPWISE BENDING MOMENT HARMONICS - RUNS 69-70 (BLADE CENTER OF GRAVITY AT .25 CHORD)													
RUN- PT. NO.	OMS #R (FPS)	MU	BLADE .30R FLAPWISE BENDING MOMENT HARMONICS (IN.-LB)										
			THEC (DEG)	A1	A2	A3	A4	A5	A6	A7	A8		
69- 3 700	.546	9.0	.8	-1.4	-1.4	-1.4	-1.4	-3.0	1.0	.3	.0		
69- 4 700	.546	11.0	.7	-1.9	-2.2	-1.9	-1.9	-4.5	1.3	.6	.3		
69- 5 700	.610	10.0	2.0	1.9	-3.5	1.9	-1.4	3.6	-1.8	.0	.7		
69- 6 700	.634	10.0	2.4	3.1	-3.7	3.1	-1.5	4.2	-1.7	-1.1	.9		
69- 7 700	.659	10.0	2.5	4.5	-4.5	3.2	-1.0	2.9	-1.4	-1.1	1.1		
70- 3 700	.659	10.0	4.1	5.5	-5.5	5.6	-5.4	7.4	.5	.8	-1.1		
70- 4 700	.682	4.0	2.5	3.0	-3.0	-5.3	-1.7	.6	.1	.3	.5		
70- 5 700	.706	11.0	4.1	7.9	-7.9	-6.0	-1.9	10.9	1.5	1.4	2.5		
70- 6 700	.682	11.0	4.1	6.9	-6.9	-6.5	-1.3	9.7	1.3	1.2	.9		
70- 7 700	.731	11.0	4.1	8.6	-8.6	-5.0	-2.6	10.8	2.2	1.9	3.9		
70- 8 700	.756	11.0	4.2	9.6	-9.6	-4.5	-2.6	11.7	2.3	1.8	4.4		
70- 9 700	.784	10.0	4.2	9.2	-9.2	-6.0	-2.1	12.8	1.8	1.5	3.1		
70-10 700	.808	10.0	4.6	10.1	-10.1	-4.2	-2.8	11.5	1.6	1.0	3.6		

BLADE .30R FLAPWISE BENDING MOMENT HARMONICS (IN.-LB)													
RUN- PT. NO.	OMS #R (FPS)	MU	THEC (DEG)	B1	B2	B3	B4	B5	B6	B7	B8		
69- 3 700	.546	9.0	9.0	1.2	1.2	4.9	-1.4	-2.0	-1.4	.0	.0		
69- 4 700	.546	11.0	11.0	1.5	1.5	8.7	-1.7	-2.0	-1.2	.2	.1		
69- 5 700	.610	10.0	10.0	2.9	2.9	8.7	-2.2	-1.0	-1.0	-1.0	-1.1		
69- 6 700	.634	10.0	10.0	3.3	3.3	8.4	-1.5	-3.2	-1.6	-1.7	-1.5		
69- 7 700	.659	10.0	10.0	3.8	3.8	9.7	-1.4	-5.6	-1.1	-1.3	-1.3		
70- 3 700	.659	10.0	10.0	1.8	1.8	9.3	-1.0	2.6	-1.5	-1.1	2.5		
70- 4 700	.682	4.0	4.0	1.9	1.9	4.4	-1.6	-1.6	.2	-1.1	.8		
70- 5 700	.706	11.0	11.0	.8	.8	11.8	-2.2	-3.2	-1.7	-1.3	3.5		
70- 6 700	.682	11.0	11.0	1.5	1.5	11.0	-2.0	-6.9	-1.0	.0	3.0		
70- 7 700	.731	11.0	11.0	1.2	1.2	13.2	-2.5	-7.2	-1.0	-1.7	2.2		
70- 8 700	.756	11.0	11.0	.7	.7	14.2	-2.8	-5.0	-1.9	-1.9	1.9		
70- 9 700	.784	10.0	10.0	-1.1	-1.1	12.3	-1.8	-6.2	.4	-1.5	2.2		
70-10 700	.808	10.0	10.0	-2.3	-2.3	14.5	-1.2	-6.2	-1.2	-1.1	1.2		

TABLE XLI - Concluded													
BLADE .30R FLAPWISE BENDING MOMENT HARMONICS (IN.-LB)													
RUN- PT. NO.	OMS *R (FPS)	MJ	THEC (DEG)	RS	R1	R2	R3	R4	R5	R6	R7	R8	
69- 3	700	.546	9.0	4.6	1.8	1.3	5.1	.5	3.6	1.1	.3	.1	
69- 4	700	.546	11.0	5.0	1.7	1.5	4.6	1.1	4.9	1.3	.7	.3	
69- 5	700	.610	10.0	5.4	3.8	4.6	8.9	.5	3.9	1.3	.8	.8	
69- 6	700	.634	10.0	5.2	3.8	4.9	9.0	.8	5.3	.9	.7	1.0	
69- 7	700	.659	10.0		4.2	5.9	10.2	1.1	6.3	.4	.3	1.1	
70- 3	700	.659	10.0	5.1	4.3	5.8	10.9	1.1	7.8	.7	.8	2.5	
70- 4	700	.682	4.0	1.6	2.5	3.6	6.8	.9	4.6	.2	.3	1.0	
70- 5	700	.706	11.0	5.2	4.5	7.9	13.2	2.9	11.4	1.6	1.4	3.5	
70- 6	700	.682	11.0	5.2	4.3	7.0	12.8	2.4	9.7	1.4	1.2	3.0	
70- 7	700	.731	11.0	5.2	4.6	8.7	14.1	3.5	12.8	2.4	2.0	4.5	
70- 8	700	.756	11.0	5.4	4.7	9.6	14.9	3.8	13.8	2.4	2.0	4.8	
70- 9	700	.784	10.0	5.0	4.9	9.2	13.7	2.8	13.8	1.9	1.6	3.8	
70-10	700	.808	10.0	4.9	5.2	10.2	15.1	3.1	13.1	1.6	1.5	4.0	

TABLE XLII. BLADE .60R FLAPWISE BENDING MOMENT HARMONICS - RUN 69 (BLADE CENTER OF GRAVITY AT .25 CHORD)												
BLADE .60R FLAPWISE BENDING MOMENT HARMONICS (IN.-LB)												
RUN- PT. NO.	OMS #R (FPS)	MU	THEC (DEG)	A1	A2	A3	A4	A5	A6	A7	A8	
69- 3 700	.546		9.0	1.5	-2.5	-1.3	.1	1.0	-.9	-.1	.0	
69- 4 700	.546		11.0	1.5	-3.7	-1.9	.5	3.0	-.6	-.6	-.9	
69- 5 700	.610		10.0	2.8	-5.9	.5	-1.5	-2.3	-.2	-.1	-.6	
69- 6 700	.634		10.0	2.6	-5.5	2.4	-1.2	-2.6	-.4	-.1	-.9	
BLADE .60R FLAPWISE BENDING MOMENT HARMONICS (IN.-LB)												
RUN- PT. NO.	OMS #R (FPS)	MU	THEC (DEG)	B1	B2	B3	B4	B5	B6	B7	B8	
69- 3 700	.546		9.0	-2.5	-.8	5.3	-.0	.5	.0	-.2	-.1	
69- 4 700	.546		11.0	-3.2	.1	5.8	.9	.3	-.1	-.3	-.2	
69- 5 700	.610		10.0	-3.4	4.0	11.6	.0	.3	.1	-.1	-.1	
69- 6 700	.634		10.0	-3.6	4.7	11.5	.7	1.5	.1	-.3	.2	
BLADE .60R FLAPWISE BENDING MOMENT HARMONICS (IN.-LB)												
RUN- PT. NO.	OMS #R (FPS)	MU	THEC (DEG)	R5	R1	R2	R3	R4	R5	R6	R7	R8
69- 3 700	.546		9.0	3.4	3.0	2.5	5.4	1.0	1.0	.9	.2	1.1
69- 4 700	.546		11.0	2.7	3.5	3.7	6.2	1.0	3.0	.6	.7	.1
69- 5 700	.610		10.0	4.4	4.4	7.2	11.6	1.5	2.9	.2	.1	.9
69- 6 700	.634		10.0	5.0	4.5	7.2	11.6	1.4	3.0	.9	.3	.6

TABLE XLIII. BLADE .18R TORSIONAL MOMENT HARMONICS - RUNS 69-70 (BLADE CENTER OF GRAVITY AT .25 CHORD)																								
RUN- PT. NO.	OMS OR (FPS)	MU	TMEC (DEG)	BLADE .18R TORSIONAL MOMENT HARMONICS (IN.-LB)																				
				A1	A2	A3	A4	A5	A6	A7	A8	A9	A0	A10	A11	A12	A13	A14	A15	A16	A17	A18	A19	
69- 3 700		.546	9.0	1.6	1.0	.7	-2.1	-3.3	-2.7	-.3	2	9	9	8	8	8	8	8	8	8	8	8	8	
70- 3 700		.659	10.0	2.0	-7.1	-3.6	1.3	-3.6	-2.2	-.3	-.3	2	9	9	8	8	8	8	8	8	8	8	8	
70- 4 700		.682	9.0	1.5	-3.6	.8	2.1	-.9	-.8	-.8	-.7	1	1	1	1	1	1	1	1	1	1	1	1	
70- 5 700		.706	11.0	3.5	-9.6	-3.6	.2	-3.6	-1.3	-.7	-.7	1	1	1	1	1	1	1	1	1	1	1	1	
70- 6 700		.682	11.0	2.6	-8.8	-3.3	1.2	-3.6	-3.6	-.7	-.7	1	1	1	1	1	1	1	1	1	1	1	1	
70- 7 700		.731	11.0	8.0	-10.0	-3.6	1.1	-3.6	-3.6	-1.0	-.7	1	1	1	1	1	1	1	1	1	1	1	1	
70- 8 700		.756	11.0	5.1	-9.6	-3.2	1.6	-3.7	-3.2	-1.7	-.7	1	1	1	1	1	1	1	1	1	1	1	1	
70- 9 700		.784	10.0	6.1	-10.2	-3.7	1.5	-2.3	-3.1	-1.4	-.1	1	1	1	1	1	1	1	1	1	1	1	1	
70-10 700		.808	10.0	5.5	-11.1	-3.0	3.0	-1.6	-4.0	-1.0	-.4	1	1	1	1	1	1	1	1	1	1	1	1	

BLADE .18R TORSIONAL MOMENT HARMONICS (IN.-LB)																							
RUN- PT. NO.	OMS OR (FPS)	MU	TMEC (DEG)	B1	B2	B3	B4	B5	B6	B7	B8	B9	B10	B11	B12	B13	B14	B15	B16	B17	B18	B19	
69- 3 700		.546	9.0	5.0	2.1	-2.1	-1.0	-2.2	1.0	-.3	1	1	1	1	1	1	1	1	1	1	1	1	
70- 3 700		.659	10.0	-.0	3.0	3.0	2.1	1.3	-.7	1	1	1	1	1	1	1	1	1	1	1	1	1	
70- 4 700		.682	9.0	-.0	.7	1.0	2.9	2.6	1.7	1	1	1	1	1	1	1	1	1	1	1	1	1	
70- 5 700		.706	11.0	-3.3	3.0	6.9	1.1	1.7	-.9	1	1	1	1	1	1	1	1	1	1	1	1	1	
70- 6 700		.682	11.0	-.3	3.6	6.3	1.0	1.2	1.1	1	1	1	1	1	1	1	1	1	1	1	1	1	
70- 7 700		.731	11.0	-2.0	6.3	3.0	-.6	3.2	1.4	1	1	1	1	1	1	1	1	1	1	1	1	1	
70- 8 700		.756	11.0	-2.7	5.7	6.6	-.2	2.9	1.4	1	1	1	1	1	1	1	1	1	1	1	1	1	
70- 9 700		.784	10.0	-6.0	3.3	3.6	3.0	2.3	1.3	1	1	1	1	1	1	1	1	1	1	1	1	1	
70-10 700		.808	10.0	-6.3	6.0	6.6	2.0	3.0	1.6	1	1	1	1	1	1	1	1	1	1	1	1	1	

TABLE XLIII - Concluded														
Run- PT. NO.	QMS OR (FPS)	MY	THEC (DEG)	RS	R1	R2	R3	R4	R5	R6	R7	R8	R9	R10
69- 3 700	.340	9.0	-0.5	3.2	2.0	2.2	2.0	0.3	2.9	2.9	7	1	0	0
70- 3 700	.650	10.0	1.1	2.9	7.7	0.0	2.5	3.0	2.2	2.2	3	3	3	0
70- 4 700	.602	9.0	1.0	1.5	3.9	1.9	3.6	2.0	1.0	1.0	2	2	0	0
70- 5 700	.700	11.0	1.3	0.1	10.0	7.0	1.2	3.1	0.0	0.0	1.3	7	0	0
70- 6 700	.602	11.0	0	2.7	9.0	7.0	1.0	0.0	3.4	3.4	0	0	7	0
70- 7 700	.731	11.0	2.1	0.9	10.9	0.3	1.2	2.2	0.1	0.1	1.0	0	0	0
70- 8 700	.756	11.0	3.1	0.3	11.2	0.0	1.0	3.0	0.4	0.4	1.7	1	3	7
70- 9 700	.706	10.0	5.3	9.1	10.0	0.7	3.3	3.0	3.1	3.1	2.0	0	0	0
70-10 700	.600	10.0	5.3	0.5	11.0	10.3	0.5	3.0	0.9	0.9	1.0	0	0	0

TABLE XLIV. BLADE FLAP MOTION HARMONICS - RUNS 69-70
(BLADE CENTER OF GRAVITY AT .25 CHORD)

BLADE FLAP MOTION HARMONICS (DEG)										
RUN- PT. NO.	QMS *R (FPS)	MU	THEC (DEG)	A1	A2	A3	A4	A5	A6	
69- 3 700	.546	9.0	.0	-.4	.1	.0	.1	.0		
69- 4 700	.546	11.0	-.1	-.5	.1	.0	.2	-.0		
69- 5 700	.610	10.0	.1	-.6	-.1	.0	-.1	.3		
69- 6 700	.634	10.0	.0	-.6	-.2	.0	-.1	.0		
69- 7 700	.659	10.0	-.2	-.6	-.2	.1	-.8	.2		
70- 3 700	.659	10.0	.2	-.5	.7	.0	-.3	.0		
70- 4 700	.682	4.0	.1	-.2	.6	.0	-.1	.0		
70- 5 700	.706	11.0	.3	-.6	.6	.1	-.4	.0		
70- 6 700	.682	11.0	.1	-.6	.7	.1	-.3	.0		
70- 7 700	.731	11.0	-.1	-.6	.6	.1	-.4	.0		
70- 8 700	.756	11.0	-.2	-.6	.5	.2	-.4	.0		
70- 9 700	.784	10.0	.4	-.5	.7	.1	-.4	.0		
70-10 700	.808	10.0	-.3	-.6	.5	.1	-.4	.0		

BLADE FLAP MOTION HARMONICS (DEG)										
RUN- PT. NO.	QMS *R (FPS)	MU	THEC (DEG)	B1	B2	B3	B4	B5	B6	
69- 3 700	.546	9.0	.0	-.1	-.5	.0	.1	.0		
69- 4 700	.546	11.0	-.1	-.2	-.4	.0	.1	.0		
69- 5 700	.610	10.0	.0	-.2	-.8	.1	.0	.0		
69- 6 700	.634	10.0	.0	-.1	-.8	.1	.1	.0		
69- 7 700	.659	10.0	.1	-.1	-.9	.1	.2	.0		
70- 3 700	.659	10.0	.1	-.3	-.7	.1	.1	.0		
70- 4 700	.682	4.0	.1	-.2	-.3	.1	.0	.0		
70- 5 700	.706	11.0	.2	-.3	-1.1	.1	.2	.0		
70- 6 700	.682	11.0	.0	-.3	-1.0	.1	.1	.0		
70- 7 700	.731	11.0	-.1	-.3	-1.2	.2	.2	.1		
70- 8 700	.756	11.0	-.2	-.3	-1.3	.1	.2	.0		
70- 9 700	.784	10.0	.1	-.2	-1.1	.1	.1	.0		
70-10 700	.808	10.0	.1	-.2	-1.3	.1	.2	.0		

TABLE XLIV - Concluded										
BLADE FLAP MOTION HARMONICS (DEG)										
RUN- PT. NO.	OMS #R (FPS)	MU	THEC (DEG)	RS	R1	R2	R3	R4	R5	R6
69- 3 700		.546	9.0	3.1	.0	.4	.4	.0	.1	.0
69- 4 700		.546	11.0	3.5	.1	.5	.4	.0	.2	.0
69- 5 700		.610	10.0	2.0	.2	.6	.3	.1	.1	.0
69- 6 700		.634	10.0	2.0	.0	.6	.6	.1	.2	.0
69- 7 700		.659	10.0	1.8	.2	.6	.9	.1	.2	.0
70- 3 700		.659	10.0	1.6	.2	.6	1.0	.1	.3	.0
70- 4 700		.682	4.0	.7	.1	.2	.6	.1	.1	.0
70- 5 700		.706	11.0	1.5	.3	.7	1.2	.2	.4	.0
70- 6 700		.682	11.0	1.7	.1	.7	1.2	.1	.3	.0
70- 7 700		.731	11.0	1.5	.2	.7	1.3	.2	.4	.1
70- 8 700		.756	11.0	1.4	.2	.7	1.4	.2	.5	.1
70- 9 700		.784	10.0	1.1	.4	.6	1.3	.2	.5	.0
70-10 700		.808	10.0	1.2	.3	.6	1.4	.2	.5	.1

TABLE XLV. BLADE LAG MOTION HARMONICS - RUN 71
(BLADE CENTER OF GRAVITY AT .25 CHORD)

BLADE LAG MOTION HARMONICS (DEG)									
RUN- PT. NO.	OMS *R (FPS)	MU	THEC (DEG)	A1	A2	A3	A4	A5	
71- 3	386	.795	.0	.2	.1	.0	.0	.0	
71- 4	362	.847	.0	.2	.0	.0	.0	.0	
71- 5	340	.906	.0	.2	.1	.0	.0	.0	
71- 6	316	.974	.0	.1	.1	.0	.0	.0	
71- 7	292	1.052	.0	.0	.1	.0	.0	.0	
71- 8	268	1.144	.0	.0	.1	.0	.0	.0	
71- 9	246	1.254	.0	-.1	.1	.0	.0	.0	
71-10	222	1.388	.0	-.2	.1	.0	.0	.0	
71-11	198	1.553	.0	-.4	.1	.0	.0	.0	
71-12	184	1.664	.0	-.5	.1	.1	.0	.0	

BLADE LAG MOTION HARMONICS (DEG)									
RUN- PT. NO.	OMS *R (FPS)	MU	THEC (DEG)	B1	B2	B3	B4	B5	
71- 3	386	.795	.0	-.1	.0	.0	.0	.0	
71- 4	362	.847	.0	-.1	.0	.0	.0	.0	
71- 5	340	.906	.0	-.1	.0	.0	.0	.0	
71- 6	316	.974	.0	-.3	.0	.0	.0	.0	
71- 7	292	1.052	.0	-.4	.0	.0	.0	.0	
71- 8	268	1.144	.0	-.4	.0	.0	.0	.0	
71- 9	246	1.254	.0	-.5	.0	.0	.0	.0	
71-10	222	1.388	.0	-.6	.0	.1	.0	.0	
71-11	198	1.553	.0	-.6	.1	.0	.0	.0	
71-12	184	1.664	.0	-.6	.1	.0	.0	.0	

TABLE XLV - Concluded

TABLE XLV - Concluded										
BLADE LAG MOTION HARMONICS (DEG)										
RUN- PT. NO.	OMS *R (FPS)	MU	THEC (DEG)	RS	R1	R2	R3	R4	R5	
71- 3	386	.795	.0	2.6	.3	.1	.0	.0	.0	.0
71- 4	362	.847	.0	2.6	.3	.1	.0	.0	.0	.0
71- 5	340	.906	.0	2.6	.3	.1	.0	.0	.0	.0
71- 6	316	.974	.0	2.6	.3	.1	.0	.0	.0	.0
71- 7	292	1.052	.0	2.6	.4	.1	.0	.0	.0	.0
71- 8	268	1.144	.0	2.9	.4	.1	.0	.0	.0	.0
71- 9	246	1.254	.0	3.0	.5	.1	.0	.0	.0	.0
71-10	222	1.388	.0	3.1	.6	.1	.1	.0	.0	.0
71-11	198	1.553	.0	3.2	.8	.1	.0	.0	.0	.0
71-12	184	1.664	.0	3.1	.8	.1	.1	.0	.0	.0

TABLE XLVI. BLADE .30R FLAPWISE BENDING MOMENT HARMONICS - RUN 71
(BLADE CENTER OF GRAVITY AT .25 CHORD)

BLADE .30R FLAPWISE BENDING MOMENT HARMONICS (IN-LB)												
RUN- PT. NO.	OMS #R (FPS)	THEC (DEG)	A1	A2	A3	A4	A5	A6	A7	A8	A9	A10
71- 3	386	.795	1.9	.5	4.3	.0	.0	.2	1.1	.2	-.2	-.2
71- 4	362	.847	2.1	.5	2.7	.0	-.3	-.2	1.4	.4	.1	.0
71- 5	340	.906	2.0	.4	2.6	.0	-.3	-.4	.5	.2	.1	.0
71- 6	316	.974	2.1	.8	6.2	-.1	-.3	.1	.4	-.1	.1	.1
71- 7	292	1.052	2.4	.7	5.0	.0	-.2	.3	.7	.4	-.1	-.2
71- 8	268	1.144	2.4	.9	4.9	-.1	-.5	.3	.7	1.1	-.1	-.6
71- 9	246	1.254	2.6	.9	4.2	-.3	-.1	-.1	.4	.6	1.6	-.6
71-10	222	1.388	1.6	.6	3.8	-.5	-.2	-.3	-.2	.0	.0	1.3
71-11	198	1.553	1.7	.6	5.1	-.7	-.2	-.4	-.3	.0	-.1	.1
71-12	184	1.664	1.3	.4	4.8	1.0	-.1	-.2	-.2	1.3	-.1	.0

BLADE .30R FLAPWISE BENDING MOMENT HARMONICS (IN-LB)												
RUN- PT. NO.	OMS #R (FPS)	THEC (DEG)	B1	B2	B3	B4	B5	B6	B7	B8	B9	B10
71- 3	386	.795	-.3	1.1	9.3	.7	-.3	-.6	1.7	.7	.3	.1
71- 4	362	.847	-.4	.7	8.9	.3	-.4	-.5	-.1	.3	.2	.1
71- 5	340	.906	-.5	.1	6.2	-.4	-.2	-.3	-.1	.3	.2	.1
71- 6	316	.974	-.8	.8	4.0	-.7	-.2	-.1	-.2	-.2	.0	.0
71- 7	292	1.052	-.9	.8	2.9	-.1	-.2	.0	-.1	.5	.3	.1
71- 8	268	1.144	-.9	.4	2.7	-.1	-.4	-.2	-.4	.6	1.1	.2
71- 9	246	1.254	-.1	.6	3.4	-.1	-.6	-.3	-.6	-.1	.9	.6
71-10	222	1.388	-.1	.9	3.8	2.5	.4	-.1	-.4	-.1	-.3	-.7
71-11	198	1.553	-.6	1.1	1.9	8.0	1.5	-.3	-.3	-.1	-.2	-.4
71-12	184	1.664	-.8	1.8	2.0	8.9	1.8	.0	-.3	.0	.0	-.3

TABLE XLVI - Concluded														
BLADE .30R FLAPWISE BENDING MOMENT HARMONICS (IN-LB)														
RUN- PT. NO.	QMS #R (FPS)	MU	THEC (DEG)	RS	R1	R2	R3	R4	R5	R6	R7	R8	R9	R10
71- 3 386		.795	.0	.0	1.9	1.2	10.2	.7	.3	.7	2.1	.7	.4	.2
71- 4 362		.847	.0	.0	2.1	.9	9.2	.3	.4	.5	1.6	.4	.2	.1
71- 5 340		.906	.0	-.3	2.0	.4	6.7	.4	.4	.5	1.4	.4	.2	.1
71- 6 316		.974	.0	-.8	2.2	1.1	7.4	.8	.4	.1	.5	.2	.1	.1
71- 7 292		1.052	.0	-.7	2.6	1.0	5.7	1.2	.3	.3	.7	.9	.3	.2
71- 8 268		1.144	.0	-.4	2.5	.9	5.6	2.0	.7	.3	.8	1.2	1.8	.7
71- 9 246		1.254	.0	-.4	2.7	1.0	5.4	4.0	1.3	.3	.7	.6	1.9	.9
71-10 222		1.368	.0	-.6	2.0	.6	5.4	6.0	2.0	.3	.4	.1	.3	1.5
71-11 198		1.553	.0	-.7	1.9	1.3	5.5	10.7	2.8	.5	.6	.1	.3	.4
71-12 184		1.664	.0	-.4	1.5	1.9	5.5	10.0	2.1	.2	.3	.1	.1	.3

TABLE XLVII. BLADE .18R TORSIONAL MOMENT HARMONICS - RUN 71 (BLADE CENTER OF GRAVITY AT .25 CHORD)													
BLADE .18R TORSIONAL MOMENT HARMONICS (IN.-LB)													
RUL- PT. NO.	OMS #R	MU (FPS)	THEC (DEG)	A1	A2	A3	A4	A5	A6	A7	A8	A9	A10
71- 3	386	.795	.0	.2	-.4	-.4	.2	.3	.1	.1	.1	.2	.3
71- 4	362	.847	.0	-.1	-.5	-.4	.2	.3	.1	.1	.2	.3	.3
71- 5	340	.906	.0	.0	-.6	-.5	.2	.3	.0	.1	.1	.2	.0
71- 6	316	.974	.0	.0	-.4	-.4	.2	.2	.0	.1	.1	.4	.6
71- 7	292	1.052	.0	.0	-.4	-.3	.3	.3	.0	.1	.2	.1	.1
71- 8	268	1.144	.0	.1	-.4	-.2	.4	.3	.0	.1	.0	.0	.1
71- 9	246	1.254	.0	.1	-.4	-.2	.6	.4	.1	.1	.1	.1	.1
71-10	222	1.388	.0	-.2	-.8	.2	.8	.3	.7	.1	.9	.2	.2
71-11	198	1.553	.0	-.4	-.8	.5	.7	.4	.1	.1	.0	.1	.1
71-12	184	1.664	.0	-.7	-1.3	.9	.8	.3	.2	.0	.1	.2	.1

BLADE .18R TORSIONAL MOMENT HARMONICS (IN.-LB)													
RUL- PT. NO.	OMS #R	MU (FPS)	THEC (DEG)	B1	B2	B3	B4	B5	B6	B7	B8	B9	B10
71- 3	386	.795	.0	1.1	.0	-.4	-.2	-.1	-.3	-.1	-.1	.1	.3
71- 4	362	.847	.0	.9	-.2	-.4	-.1	-.1	-.3	-.2	-.1	.0	.0
71- 5	340	.906	.0	.7	-.1	-.2	.0	-.2	-.3	-.1	-.1	-.2	-.4
71- 6	316	.974	.0	1.0	.0	-.1	-.1	-.2	-.3	-.1	-.2	-.1	-.1
71- 7	292	1.052	.0	.8	.0	.2	.0	-.2	-.2	-.1	-.1	-.1	.0
71- 8	268	1.144	.0	.8	-.1	.3	.0	-.3	.0	.0	.0	.1	.0
71- 9	246	1.254	.0	.7	.0	.3	.0	-.1	-.1	.1	.0	.2	.0
71-10	222	1.388	.0	.0	.1	.5	-.4	-.2	.0	.0	.0	.0	.0
71-11	198	1.553	.0	.3	.8	.6	-.7	-.3	.0	.0	.0	.0	.0
71-12	184	1.664	.0	-.4	1.0	1.0	-.7	-.5	-.2	-.1	.1	.0	.0

TABLE XLVII - Concluded														
RUN- PT. NO.	OMS #R (FPS)	MU	TMEC (DEG)	RS	BLADE .18R TORSIONAL MOMENT HARMONICS (IN.-LB)									
					R1	R2	R3	R4	R5	R6	R7	R8	R9	R10
71- 3	386	.795	.0	.2	1.1	.4	.5	.3	.3	.3	.1	.2	.3	.4
71- 4	362	.847	.0	.0	.9	.5	.5	.2	.3	.3	.2	.2	.3	.3
71- 5	340	.906	.0	-.1	.7	.6	.5	.2	.4	.3	.1	.2	.3	.4
71- 6	316	.974	.0	-.5	1.0	.4	.4	.2	.3	.3	.1	.2	.1	.1
71- 7	292	1.052	.0	-.6	.8	.4	.4	.3	.4	.2	.1	.2	.1	.1
71- 8	268	1.144	.0	-.7	.8	.4	.3	.4	.4	.1	.1	.1	.1	.1
71- 9	246	1.254	.0	-.8	.7	.4	.4	.6	.4	.1	.2	.1	.3	.1
71-10	222	1.398	.0	-.6	.2	.8	.5	.9	.4	.8	.1	.1	.2	.2
71-11	198	1.553	.0	-.9	.5	1.1	.8	1.0	.5	.1	.1	.0	.1	.1
71-12	184	1.664	.0	-.8	.8	1.6	1.3	1.0	.6	.2	.1	.1	.2	.1

TABLE XLVIII. BLADE FLAP MOTION HARMONICS - RUN 71 (BLADE CENTER OF GRAVITY AT .25 CHORD)												
BLADE FLAP MOTION HARMONICS (DEG)												
RUI.- PT. NO.	OMS *R (FPS)	MU	THEC (DEG)	A1	A2	A3	A4	A5	A6			
71- 3	386	.795	.0	-.7	.0	-.2	.0	.0	.0			
71- 4	362	.847	.0	.0	.1	-.1	.0	.0	.0			
71- 5	340	.906	.0	.6	.0	-.1	.0	.0	.0			
71- 6	316	.974	.0	-.6	.0	-.3	.1	.0	.0			
71- 7	292	1.052	.0	-.3	-.1	-.2	.1	.0	.0			
71- 8	268	1.144	.0	-.1	-.1	-.2	.2	.1	.0			
71- 9	246	1.254	.0	-.2	-.1	-.2	.3	.1	.0			
71-10	222	1.388	.0	.3	.0	-.1	.4	.1	.0			
71-11	198	1.553	.0	-.2	.0	-.2	.5	.2	.0			
71-12	164	1.664	.0	.2	.0	-.1	.1	.1	.0			

BLADE FLAP MOTION HARMONICS (DEG)												
RUI.- PT. NO.	OMS *R (FPS)	MU	THEC (DEG)	B1	B2	B3	B4	B5	B6			
71- 3	386	.795	.0	.0	-.2	-.7	.0	.0	.0			
71- 4	362	.847	.0	.0	-.2	-.6	.0	.0	.0			
71- 5	340	.906	.0	.2	-.2	-.4	.1	.0	.0			
71- 6	316	.974	.0	-.1	-.2	-.4	.1	.0	.0			
71- 7	292	1.052	.0	.0	-.2	-.3	.1	.0	.0			
71- 8	268	1.144	.0	.0	-.2	-.2	.1	.0	.0			
71- 9	246	1.254	.0	-.1	-.2	-.2	.1	.1	.0			
71-10	222	1.388	.0	.1	-.1	-.2	-.1	.0	.0			
71-11	198	1.553	.0	-.1	-.1	-.1	-.6	-.1	.0			
71-12	164	1.664	.0	.3	-.1	-.1	-.6	-.1	.0			

TABLE XLVIII - Concluded												
BLADE FLAP MOTION HARMONICS (DEG)												
RUN- PT. NO.	OMS #R (FPS)	MU	THEC (DEG)	RS	R1	R2	R3	R4	R5	R6		
71- 3	386	.795	.0	.1	.7	.2	.7	.0	.0	.0		
71- 4	362	.847	.0	-.1	.1	.2	.7	.0	.0	.0		
71- 5	340	.906	.0	-.3	.6	.2	.5	.1	.0	.0		
71- 6	316	.974	.0	-.2	.6	.2	.5	.1	.0	.0		
71- 7	292	1.052	.0	-.3	.3	.2	.3	.1	.0	.0		
71- 8	268	1.144	.0	-.4	.1	.2	.3	.2	.1	.0		
71- 9	246	1.254	.0	-.5	.2	.2	.3	.3	.1	.0		
71-10	222	1.388	.0	-1.1	.3	.1	.3	.5	.1	.0		
71-11	198	1.553	.0	-1.4	.2	.1	.2	.7	.2	.0		
71-12	184	1.664	.0	-2.0	.4	.1	.1	.6	.1	.0		

TABLE XLIX. BLADE LAG MOTION HARMONICS - RUN 72 (BLADE CENTER OF GRAVITY AT .25 CHORD)											
RUN- PT. NO.			BLADE LAG MOTION HARMONICS (DEG)								
OMS #R	MU	THEC (DEG)	A1	A2	A3	A4	A5				
(FPS)											
72- 3 236	1.488	.0	-.2	.1	.0	.0	.0				
72- 4 202	1.739	.0	-.4	.1	.0	.0	.0				
72- 5 214	1.842	.0	-.4	.1	.0	.0	.0				
72- 6 228	1.914	.0	-.4	.1	.0	.0	.0				
72- 7 252	1.891	.0	-.3	.0	.0	.0	.0				
72- 8 296	1.753	.0	-.2	.1	.0	.0	.0				
72- 9 386	1.452	.0	.3	.1	.0	.0	.0				

RUN- PT. NO.			BLADE LAG MOTION HARMONICS (DEG)								
OMS #R	MU	THEC (DEG)	B1	B2	B3	B4	B5				
(FPS)											
72- 3 236	1.488	.0	-.6	.1	.0	.0	.0				
72- 4 202	1.739	.0	-.8	.1	.0	.0	.0				
72- 5 214	1.842	.0	-.9	.1	.0	.0	.0				
72- 6 228	1.914	.0	-1.0	.1	.0	.0	.0				
72- 7 252	1.891	.0	-1.0	.1	.0	.0	.0				
72- 8 296	1.753	.0	-.9	.1	.0	.0	.0				
72- 9 386	1.452	.0	-.5	.0	.0	.0	.0				

TABLE XLIX - Concluded										
		BLADE LAG MOTION: HARMONICS (DEG)								
RUN- PT. NO.	OMS or (FPS)	MU	THEC (DEG)	RS	R1	R2	R3	R4	RS	
72- 3	236	1.488	.0	3.1	.9	.1	.0	.0	.0	
72- 4	202	1.739	.0	3.1	.9	.1	.1	.0	.0	
72- 5	214	1.842	.0	3.1	1.0	.1	.1	.0	.0	
72- 6	228	1.914	.0	3.3	1.1	.1	.0	.0	.0	
72- 7	252	1.891	.0	2.9	1.0	.1	.0	.0	.0	
72- 8	296	1.753	.0	2.5	.9	.1	.0	.0	.0	
72- 9	306	1.452	.0	3.0	.6	.1	.0	.0	.0	

TABLE L. BLADE .30R FLAPWISE BENDING MOMENT HARMONICS - RUN 72 (BLADE CENTER OF GRAVITY AT .25 CHORD)																
BLADE .30R FLAPWISE BENDING MOMENT HARMONICS (IN.-LB)																
RUN- PT. NO.	OMS OR (FPS)	MU	TMEC (DEG)	A1	A2	A3	A4	A5	A6	A7	A8	A9	A10	A11	A12	A13
72- 3	236	1.988	.0	2.0	-.6	5.9	-5.6	-1.8	.0	.2	.2	1.0	-.9	-.9	-.2	.1
72- 4	202	1.739	.0	1.6	.0	6.9	-6.2	-2.5	.0	-.1	.2	.0	.5	2.6	.3	-.9
72- 5	214	1.842	.0	2.0	-.7	6.3	-8.0	-3.1	.1	-.1	.2	.3	1.6	-.4	-.9	-.3
72- 6	228	1.914	.0	2.8	-1.4	6.7	-9.3	-3.5	.1	.9	.9	.9	2.1	-.1	-.4	-.3
72- 7	252	1.891	.0	1.6	-3.7	7.9	-5.3	-2.6	-1.0	.5	.5	2.0	.6	-.4	-.6	-.4
72- 8	296	1.753	.0	2.0	-1.8	7.4	-4.5	-2.3	-1.3	.6	.2	.5	.5	-.1	-.2	-.1
72- 9	386	1.452	.0	3.5	-2.0	-2.7	-1.8	-.7	-2.8	1.3	.1	-.2	.0	.2	.0	-.3
BLADE .30R FLAPWISE BENDING MOMENT HARMONICS (IN.-LB)																
RUN- PT. NO.	OMS OR (FPS)	MU	TMEC (DEG)	B1	B2	B3	B4	B5	B6	B7	B8	B9	B10	B11	B12	B13
72- 3	236	1.488	.0	-1.1	.0	3.3	-1.4	-.7	-.2	-.5	.0	.4	.5	-.1	-.2	-.1
72- 4	202	1.739	.0	-.6	1.8	4.2	8.5	.6	-.3	-.6	-.2	-.2	-.2	1.0	.8	.1
72- 5	214	1.842	.0	-1.1	1.6	6.0	7.2	.3	-.5	-1.0	-.5	-.7	-.6	1.9	.3	-.2
72- 6	228	1.914	.0	-1.0	1.2	7.5	1.7	-.8	-.2	-1.0	-.3	-.8	.5	1.1	.6	.1
72- 7	252	1.891	.0	-.2	-.3	14.0	3.2	.3	.5	-1.2	-.4	-.9	1.0	.0	.1	-.1
72- 8	296	1.753	.0	-1.5	-4.6	18.1	1.1	-.2	1.3	-.9	-.2	.5	.5	.4	.1	.1
72- 9	386	1.452	.0	-.1	-3.2	14.8	-.3	-.4	-2.0	2.2	.7	.0	.0	.1	.6	-.1

TABLE L - Concluded																			
RUN- PT. NO.		OMS #R (FPS)	MU	TWEC (DEG)	RS	R1	R2	R3	R4	R5	R6	R7	R8	R9	R10	R11	R12	R13	
72-	3	236	1.488	.0	-1.0	2.3	.6	6.3	5.7	1.9	.2	.5	.2	1.1	1.0	.5	.3	.1	
72-	4	202	1.734	.0	-1.1	1.8	1.8	7.7	10.5	2.6	.3	.6	.3	.2	.5	2.8	.8	.4	
72-	5	214	1.842	.0	-1.4	2.3	1.8	8.7	10.8	3.1	.5	1.0	.6	.8	1.7	1.9	.9	.4	
72-	6	228	1.914	.0	-1.8	3.0	1.8	10.1	9.4	3.6	.2	1.1	.5	1.2	2.1	1.1	.7	.3	
72-	7	252	1.891	.0	-.3	1.6	3.7	15.9	6.1	2.6	1.1	1.2	.6	2.1	1.1	1.0	.6	.4	
72-	8	296	1.753	.0	-.6	2.5	4.9	19.6	4.6	2.3	1.8	1.1	1.2	.6	.7	.4	.2	.1	
72-	9	386	1.452	.0	-1.3	3.5	3.8	15.0	1.9	.8	3.5	2.6	.7	.2	.0	.3	.6	.3	

TABLE LI. BLADE .18R TORSIONAL MOMENT HARMONICS - RUN 72 (BLADE CENTER OF GRAVITY AT .25 CHORD)																								
BLADE .18R TORSIONAL MOMENT HARMONICS (IN.-LB)																								
RUN- PT. NO.	OMS #R	MU (FPS)	THEC (DEG)	A1	A2	A3	A4	A5	A6	A7	A8	A9	A10	A11	A12	A13								
72- 3	236	1.488	.0	-.1	-1.2	-.2	1.2	.5	.1	.1	.0	.2	.1	.0	.1	.0								
72- 4	202	1.739	.0	-.9	-1.7	1.1	1.3	.3	.1	.1	.1	.2	.1	.3	.1	.1								
72- 5	214	1.842	.0	-.7	-2.2	.8	2.0	.8	.1	.0	.1	.4	.2	.2	.1	.0								
72- 6	228	1.914	.0	-.4	-2.4	.2	2.7	1.4	-.4	-.3	.1	.5	.3	.2	-.1	-.1								
72- 7	252	1.891	.0	-1.5	-5.4	.8	4.7	2.4	.1	-1.0	-.2	1.0	.4	.5	.4	-.7								
72- 8	296	1.753	.0	.9	-6.1	-2.1	4.8	3.5	.8	-1.5	-1.0	1.3	.6	1.0	.7	-.3								
72- 9	386	1.452	.0	2.1	-2.8	-3.4	1.2	2.7	1.5	.7	-.8	-1.3	-.6	-.5	-.4	-.1								
BLADE .18R TORSIONAL MOMENT HARMONICS (IN.-LB)																								
RUN- PT. NO.	OMS #R	MU (FPS)	THEC (DEG)	B1	B2	B3	B4	B5	B6	B7	B8	B9	B10	B11	B12	B13								
72- 3	236	1.488	.0	.2	.1	1.0	-.1	-.3	-.1	.0	.1	-.2	.1	.2	.1	.2								
72- 4	202	1.739	.0	-.4	1.4	1.4	-.9	-.5	.0	.0	.1	-.1	.0	.1	.0	.1								
72- 5	214	1.842	.0	-.5	1.0	2.1	-.5	-.7	-.1	.1	.3	.0	.1	.1	.1	.1								
72- 6	228	1.914	.0	.3	.7	2.9	.9	-.7	-.3	.3	.4	.2	.1	.2	-.1	.1								
72- 7	252	1.891	.0	-2.7	1.5	5.1	.4	-1.3	-1.5	-.2	1.0	.1	.1	.6	-.4	.1								
72- 8	296	1.753	.0	-3.1	-1.0	5.4	3.0	-1.3	-2.3	-1.1	1.2	.5	.0	.7	.4	-.4								
72- 9	386	1.452	.0	1.2	-3.1	.7	3.4	.9	-1.2	-1.3	-.8	.8	.0	-.2	.2	.1								

TABLE LI - Concluded

RUR- P1. NG.		QMS #R (FPS)	MU	THEC (DEG)	PS	R1	R2	R3	R4	R5	R6	R7	R8	R9	R10	R11	R12	R13
72-	3	236	1.488	.0	.5	.2	1.2	1.0	1.2	.6	.1	.1	.1	.3	.2	.2	.2	.2
72-	4	202	1.739	.0	.5	1.0	2.2	1.8	1.6	.6	.1	.1	.1	.2	.1	.3	.1	.1
72-	5	214	1.842	.0	.6	.9	2.4	2.2	2.1	1.0	.1	.1	.3	.4	.2	.2	.1	.2
72-	6	228	1.914	.0	.5	.5	2.5	2.9	2.8	1.5	.5	.4	.4	.5	.3	.3	.2	.5
72-	7	252	1.891	.0	2.2	3.1	5.6	5.1	4.7	2.7	1.5	1.0	1.0	1.0	.4	.6	.5	.7
72-	8	296	1.753	.0	3.0	3.2	6.1	5.8	5.6	3.7	2.5	1.9	1.6	1.4	.6	1.2	.9	.7
72-	9	386	1.452	.0	2.7	2.4	4.2	3.5	3.6	2.9	1.9	1.4	1.1	1.3	.7	.5	.4	.2

TABLE LII. BLADE FLAP MOTION HARMONICS - RUN 72
(BLADE CENTER OF GRAVITY AT .25 CHORD)

BLADE FLAP MOTION HARMONICS (DEG)										
RUN- PT. NO.	OMS *R (FPS)	MU	THEC (DEG)	A1	A2	A3	A4	A5	A6	
72- 3	236	1.488	.0	-.1	.0	-.2	.5	.1	.0	
72- 4	202	1.739	.0	.0	.1	-.2	.5	.2	.0	
72- 5	214	1.842	.0	-.1	.0	-.3	.7	.2	.0	
72- 6	228	1.914	.0	-.1	-.1	-.3	.7	.3	.0	
72- 7	252	1.891	.0	.0	.1	-.2	.4	.2	.0	
72- 8	296	1.753	.0	-.4	-.3	-.2	.4	.2	.0	
72- 9	386	1.452	.0	-.3	-.1	.6	.2	.1	.0	

BLADE FLAP MOTION HARMONICS (DEG)										
RUN- PT. NO.	OMS *R (FPS)	MU	THEC (DEG)	B1	B2	B3	B4	B5	B6	
72- 3	236	1.488	.0	-.1	-.2	-.3	.1	.1	.0	
72- 4	202	1.739	.0	.3	.0	-.2	-.5	-.1	.0	
72- 5	214	1.842	.0	-.4	.0	-.3	-.3	-.2	.1	
72- 6	228	1.914	.0	-.8	-.1	-.5	-.2	.0	.1	
72- 7	252	1.891	.0	.1	.2	-.8	-.2	.0	.0	
72- 8	296	1.753	.0	-.4	.1	-1.2	.0	.0	.0	
72- 9	386	1.452	.0	.0	-.1	-1.0	.1	.1	.1	

TABLE LII - Concluded											
BLADE FLAP MOTION HARMONICS (DEG)											
RUN- PT. NO.	QMS #R	MU	THEC (DEG)	RS	R1	R2	R3	R4	R5	R6	
72- 3	236	1.488	.0	-.3	.2	.2	.3	.5	.1	.0	
72- 4	202	1.739	.0	-1.3	.3	.1	.3	.7	.2	.1	
72- 5	214	1.842	.0	-1.0	.4	.1	.4	.8	.2	.1	
72- 6	228	1.914	.0	-.5	1.0	.2	.6	.7	.3	.1	
72- 7	252	1.891	.0	-1.4	.1	.2	.9	.5	.2	.0	
72- 8	296	1.753	.0	-.7	.6	.3	1.3	.4	.2	.1	
72- 9	386	1.452	.0	.3	.3	.2	1.2	.2	.1	.1	

TABLE LIII. BLADE LAG MOTION HARMONICS - RUN 74 (BLADE CENTER OF GRAVITY AT .30 CHORD)										
BLADE LAG MOTION HARMONICS (DEG)										
RUN- PT. NO.	OMS #R	(FPS)	MU	THEC (DEG)	A1	A2	A3	A4	A5	
74- 3	700		.333	4.0	-.1	.0	.0	.0	.0	
74- 4	700		.390	4.0	-.1	.0	.0	.0	.0	
74- 5	700		.448	4.0	-.1	.0	.0	.0	.0	
74- 6	700		.504	4.0	-.1	.0	.1	.1	.0	
74- 7	700		.565	4.0	.1	.0	.1	.1	.0	
74- 8	700		.623	4.0	.1	.0	.1	.1	.0	
74- 9	700		.682	4.0	.1	.0	.1	.2	.0	
BLADE LAG MOTION HARMONICS (DEG)										
RUN- PT. NO.	OMS #R	(FPS)	MU	THEC (DEG)	B1	B2	B3	B4	B5	
74- 3	700		.333	4.0	.0	.1	.1	.1	.0	
74- 4	700		.390	4.0	-.1	.1	.1	.1	.0	
74- 5	700		.448	4.0	-.1	.1	.1	.1	.0	
74- 6	700		.504	4.0	-.1	.1	.1	.2	.0	
74- 7	700		.565	4.0	.1	.1	.1	.2	.0	
74- 8	700		.623	4.0	.1	.1	.1	.2	.0	
74- 9	700		.682	4.0	-.1	.1	.0	.2	.0	

TABLE LIII - Concluded										
RUN- PT. NO.		OMS R	THEC (DEG)		BLADE LAG MOTION HARMONICS (DEG)					
		(FPS)	MU		RS	R1	R2	R3	R4	R5
74-	3	700	.333	4.0	2.2	.1	.1	.1	.1	.0
74-	4	700	.390	4.0	2.3	.1	.1	.1	.1	.0
74-	5	700	.448	4.0	2.2	.1	.1	.1	.1	.0
74-	6	700	.504	4.0	2.2	.1	.1	.1	.2	.0
74-	7	700	.565	4.0	2.2	.1	.1	.1	.2	.0
74-	8	700	.623	4.0	2.7	.1	.1	.1	.2	.0
74-	9	700	.682	4.0	2.1	.2	.1	.1	.2	.0

TABLE LIV. BLADE .30R FLAPWISE BENDING MOMENT HARMONICS - RUN 74
(BLADE CENTER OF GRAVITY AT .30 CHORD)

BLADE .30R FLAPWISE BENDING MOMENT HARMONICS (IN.-LB)													
RUN- PT. NO.	OMS #R (FPS)	MU	THEC (DEG)	A1	A2	A3	A4	A5	A6	A7	A8	A9	A10
74- 3 700		.333	4.0	.8	.2	-2.6	.2	.3	.4	.2	.0	.4	.1
74- 4 700		.390	4.0	.6	-.4	-3.6	.5	-.2	-.2	-.2	-.2	-.3	-.1
74- 5 700		.448	4.0	1.4	-.7	-3.5	.3	.3	.6	.1	-.3	-.4	-.1
74- 6 700		.504	4.0	1.1	-1.2	-4.0	.2	.1	.8	.2	-.7	.7	.0
74- 7 700		.565	4.0	1.4	-1.8	-4.0	.3	.9	.7	.7	-.7	.7	.0
74- 8 700		.623	4.0	1.7	-2.5	-4.4	.1	4.6	.2	1.1	-.2	.1	.1
74- 9 700		.682	4.0	1.4	-3.5	-4.8	-.9	6.5	-.7	.5	1.2	.4	.1

BLADE .30R FLAPWISE BENDING MOMENT HARMONICS (IN.-LB)													
RUN- PT. NO.	OMS #R (FPS)	MU	THEC (DEG)	B1	B2	B3	B4	B5	B6	B7	B8	B9	B10
74- 3 700		.333	4.0	.4	.0	1.1	-.7	.0	.1	.1	-.2	.0	-.1
74- 4 700		.390	4.0	.9	.3	.3	-.7	1.7	.2	.3	.3	.3	.0
74- 5 700		.448	4.0	.9	.4	1.3	-1.6	.8	.4	.5	.2	.1	.1
74- 6 700		.504	4.0	1.4	.8	2.0	-1.4	3.3	-.1	.7	.3	.0	.1
74- 7 700		.565	4.0	1.6	1.0	1.8	-1.4	4.3	-.3	.7	.8	-.6	-.1
74- 8 700		.623	4.0	2.0	1.4	1.9	-1.8	4.1	-.6	-.1	1.6	-.9	-.1
74- 9 700		.682	4.0	2.5	1.8	2.8	-1.9	.2	-.2	-.8	1.3	-.6	-.1

TABLE LIV - Concluded														
BLADE .30R FLAPWISE BENDING MOMENT HARMONICS (IN.-LB)														
RUN- PT. NO.	OMS #R (FPS)	MU	THEC (DEG)	R5	R1	R2	R3	R4	R5	R6	R7	R8	R9	R10
74- 3 700		.333	4.0	2.3	.9	.2	2.8	.7	.3	.4	.2	.2	.5	.1
74- 4 700		.390	4.0	1.3	1.1	.5	3.6	.8	1.7	.3	.4	.4	.4	.1
74- 5 700		.448	4.0	.9	1.6	.8	3.7	1.6	.9	.8	.5	.4	.4	.1
74- 6 700		.504	4.0	.9	1.8	1.4	4.5	1.4	3.4	.8	.7	.7	.7	.1
74- 7 700		.565	4.0	.9	2.1	2.0	4.4	1.4	4.4	.8	1.0	1.1	1.0	.1
74- 8 700		.623	4.0	1.7	2.6	2.8	4.9	1.8	6.2	.7	1.1	1.6	.9	.1
74- 9 700		.682	4.0	1.8	2.9	4.0	5.6	2.0	6.5	.7	1.0	1.8	.7	.2

TABLE LV. BLADE .18R TORSIONAL MOMENT HARMONICS - RUN 74 (BLADE CENTER OF GRAVITY AT .30 CHORD)														
BLADE .18R TORSIONAL MOMENT HARMONICS (IN.-LB)														
RUN-PT. NO.	GMS *R (FPS)	MU	THEC (DEG)	A1	A2	A3	A4	A5	A6	A7	A8	A9	A10	
74- 3	700	.333	4.0	.7	1.0	-1.1	3.7	.4	.2	.2	.0	-.1	-.1	
74- 4	700	.390	4.0	.9	.2	-2.7	4.7	.2	.0	.1	.1	.1	.0	
74- 5	700	.448	4.0	1.0	.1	-3.5	6.7	.7	.2	.0	.0	.0	.0	
74- 6	700	.504	4.0	1.3	-.5	-5.4	8.7	.6	.2	.1	-.1	.1	.1	
74- 7	700	.565	4.0	1.3	-1.0	-6.1	9.6	.8	.3	.0	-.1	-.1	.1	
74- 8	700	.623	4.0	1.5	-.7	-7.8	11.2	1.3	.2	.4	.2	-.1	.1	
74- 9	700	.682	4.0	1.6	-1.2	-8.8	13.2	1.8	.5	.2	.0	-.1	-.1	

BLADE .18R TORSIONAL MOMENT HARMONICS (IN.-LB)														
RUN-PT. NO.	GMS *R (FPS)	MU	THEC (DEG)	B1	B2	B3	B4	B5	B6	B7	B8	B9	B10	
74- 3	700	.333	4.0	1.8	1.7	.0	.2	.1	.1	.3	.0	.0	.1	
74- 4	700	.390	4.0	2.0	2.6	-.7	.8	-.5	.3	.1	.1	.1	.0	
74- 5	700	.448	4.0	2.1	2.4	-2.2	.3	-.6	.2	.2	.1	.1	.1	
74- 6	700	.504	4.0	2.0	3.1	-1.9	1.0	-1.3	.4	.4	.2	.0	.1	
74- 7	700	.565	4.0	1.7	3.7	-3.2	1.8	-1.9	.3	.5	.1	.0	.1	
74- 8	700	.623	4.0	1.4	4.2	-1.6	2.2	-2.0	.2	.4	.2	.1	.1	
74- 9	700	.682	4.0	.8	4.7	-.1	2.5	-1.8	.0	.6	.3	.1	-.1	

TABLE LV - Concluded														
BLADE .10R TORSIONAL MOMENT HARMONICS (IN.-LB)														
RUN- PT. NO.	QMS OR (FPS)	TMEC (DEG)	MU	RS	R1	R2	R3	R4	R5	R6	R7	R8	R9	R10
74- 3 700	.333	4.0		3.7	1.9	2.0	1.1	3.7	.5	.3	.2	.1	.1	.1
74- 4 700	.340	4.0		3.6	2.2	2.6	2.0	6.7	.6	.3	.2	.1	.1	.1
74- 5 700	.448	4.0		3.6	2.3	2.4	4.1	6.7	.9	.3	.2	.1	.1	.2
74- 6 700	.504	4.0		3.4	2.4	3.2	5.0	8.0	1.4	.5	.4	.2	.1	.1
74- 7 700	.545	4.0		3.3	2.2	3.8	6.9	9.8	2.0	.5	.5	.1	.1	.1
74- 8 700	.623	4.0		3.2	2.0	4.4	7.9	11.4	2.4	.6	.4	.2	.2	.2
74- 9 700	.662	4.0		3.7	1.8	4.9	8.8	13.5	2.6	.5	.6	.3	.2	.1

TABLE LVI. BLADE FLAP MOTION HARMONICS - RUN 74
(BLADE CENTER OF GRAVITY AT .30 CHORD)

BLADE FLAP MOTION HARMONICS (DEG)										
RUN- PT. NO.	OMS #R (FPS)	MU	THEC (DEG)	A1	A2	A3	A4	A5	A6	
74- 3 700		.333	4.0	.1	-.1	.3	.0	.0	.0	
74- 4 700		.390	4.0	.1	-.1	.4	.0	.0	.0	
74- 5 700		.448	4.0	.1	-.1	.4	.0	.0	.0	
74- 6 700		.504	4.0	-.1	-.1	.5	.0	.0	.0	
74- 7 700		.565	4.0	.0	-.1	.5	.0	.0	.0	
74- 8 700		.623	4.0	-.1	-.1	.6	.0	-.2	.0	
74- 9 700		.682	4.0	.0	-.1	.6	.0	-.2	.0	
BLADE FLAP MOTION HARMONICS (DEG)										
RUN- PT. NO.	OMS #R (FPS)	MU	THEC (DEG)	B1	B2	B3	B4	B5	B6	
74- 3 700		.333	4.0	.1	.0	.0	.0	.0	.0	
74- 4 700		.390	4.0	.1	-.2	.1	.1	-.1	.0	
74- 5 700		.448	4.0	.1	-.2	.0	.1	.0	.0	
74- 6 700		.504	4.0	.0	-.3	-.1	.1	-.1	.0	
74- 7 700		.565	4.0	.1	-.4	.0	.1	-.1	.0	
74- 8 700		.623	4.0	-.1	-.4	-.1	.1	-.1	.0	
74- 9 700		.682	4.0	-.1	-.4	-.2	.2	.0	.0	

TABLE LVI - Concluded											
BLADE FLAP MOTION HARMONICS (DEG)											
RUN- PT. NO.	OMS #R (FPS)	MU	THEC (DEG)	RS	R1	R2	R3	R4	R5	R6	
74- 3	700	.333	4.0	1.6	.1	.1	.3	.0	.0	.0	
74- 4	700	.390	4.0	1.5	.1	.2	.4	.1	.1	.0	
74- 5	700	.448	4.0	1.2	.2	.2	.4	.1	.0	.0	
74- 6	700	.504	4.0	1.0	.1	.3	.5	.1	.1	.0	
74- 7	700	.565	4.0	.8	.1	.4	.5	.1	.1	.0	
74- 8	700	.623	4.0	.9	.1	.4	.6	.2	.2	.0	
74- 9	700	.682	4.0	.5	.1	.4	.6	.2	.2	.0	

TABLE LVII. BLADE .30R CHORDWISE BENDING MOMENT HARMONICS - RUN 74 (BLADE CENTER OF GRAVITY AT .30 CHORD)													
BLADE .30R CHORDWISE BENDING MOMENT HARMONICS (IN.-LB)													
RUN- PT. NO.	OMS OR	MU (FPS)	THEC (DEG)	A1	A2	A3	A4	A5	A6	A7	A8	A9	A10
74- 3 700		.333	4.0	-2.1	.9	-.3	.4	.8	.1	.1	.0	-.3	-.4
74- 4 700		.390	4.0	-2.1	1.1	-.4	-.7	.9	.1	.1	.1	-.1	-.3
74- 5 700		.448	4.0	-2.4	1.2	-.1	-8.9	.6	-.2	.3	.2	.0	.4
74- 6 700		.504	4.0	-2.3	1.5	-.3	-13.2	.5	-.3	.3	.3	-.2	.3
74- 7 700		.565	4.0	-2.2	1.8	-.6	-15.9	.5	-.3	.2	.3	-.2	-.1
74- 8 700		.623	4.0	-1.9	2.6	-.7	-17.9	.4	-.1	.1	.2	.5	.2
74- 9 700		.682	4.0	-2.5	3.4	-.7	-30.4	-.5	.3	.0	-.6	-.4	.3

BLADE .30R CHORDWISE BENDING MOMENT HARMONICS (IN.-LB)													
RUN- PT. NO.	OMS OR	MU (FPS)	THEC (DEG)	B1	B2	B3	B4	B5	B6	B7	B8	B9	B10
74- 3 700		.333	4.0	-.2	.7	-1.3	-10.1	-.1	-.2	-.2	.1	.1	.9
74- 4 700		.390	4.0	-.1	.9	-1.1	-11.3	.4	.0	-.1	-.1	-.3	.8
74- 5 700		.448	4.0	-1.4	.9	-.8	-8.4	.2	.0	-.1	-.1	-.4	.4
74- 6 700		.504	4.0	-2.1	1.0	-.7	-13.6	-.1	-.1	-.3	-.2	-.5	.4
74- 7 700		.565	4.0	-2.8	1.2	-.3	-12.5	.1	-.1	-.4	-.4	-.1	.6
74- 8 700		.623	4.0	-3.5	1.3	-.1	-16.6	.0	.4	-.2	-.5	.3	1.0
74- 9 700		.682	4.0	-4.7	.1	.5	-.2	-.4	.1	-.4	-.1	-.8	-.7

TABLE LVII - Concluded														
BLADE .30R CHORDWISE BENDING MOMENT HARMONICS (IN.-LB)														
RUN- PT. NO.	OMS #R (FPS)	MU	THEC (DEG)	RS	R1	R2	R3	R4	R5	R6	R7	R8	R9	R10
74- 3	700	.333	4.0	1.6	2.1	1.2	1.3	10.1	.8	.2	.2	.1	.3	1.0
74- 4	700	.390	4.0	1.8	2.3	1.4	1.2	11.4	1.0	.1	.2	.2	.3	.8
74- 5	700	.448	4.0	.2	2.8	1.5	.8	12.3	.6	.2	.3	.4	.4	.5
74- 6	700	.504	4.0	.6	3.1	1.8	.7	18.9	.5	.3	.4	.5	.2	.6
74- 7	700	.565	4.0	.5	3.6	2.2	.7	20.3	.4	.4	.2	.5	.6	1.0
74- 8	700	.623	4.0	-.3	4.0	2.9	.7	24.4	.4	.4	.4	.6	.9	.8
74- 9	700	.682	4.0	-1.4	5.3	3.4	.9	30.4	.6	.4	.4	.6	.9	.8

TABLE LVIII. BLADE .35R TORSIONAL MOMENT HARMONICS - RUN 74 (BLADE CENTER OF GRAVITY AT .30 CHORD)													
BLADE .35R TORSIONAL MOMENT HARMONICS (IN.-LB)													
RUN- PT. NO.	OMS #R (FPS)	MU	THEC (DEG)	A1	A2	A3	A4	A5	A6	A7	A8	A9	A10
74- 3 700		.333	4.0	.9	.8	-.8	3.0	.4	.2	.1	.1	.0	.0
74- 4 700		.390	4.0	1.1	.2	-2.1	4.0	-.1	.1	.1	.1	.0	.0
74- 5 700		.448	4.0	.9	.0	-2.9	5.9	.6	.2	.0	.0	.0	.0
74- 6 700		.504	4.0	1.3	-.2	-4.0	7.7	.5	.1	.0	-.1	.0	.0
74- 7 700		.565	4.0	1.4	-.5	-5.2	8.5	.6	.1	-.1	-.1	.1	.0
74- 8 700		.623	4.0	1.5	-1.0	-5.7	9.1	1.4	.1	-.2	-.1	.0	.0
74- 9 700		.682	4.0	1.8	-.2	-6.9	11.1	.4	.6	.2	.2	-.1	.2
BLADE .35R TORSIONAL MOMENT HARMONICS (IN.-LB)													
RUN- PT. NO.	OMS #R (FPS)	MU	THEC (DEG)	B1	B2	B3	B4	B5	B6	B7	B8	B9	B10
74- 3 700		.333	4.0	1.5	1.6	-.1	.7	.1	.3	.1	.0	.0	.0
74- 4 700		.390	4.0	1.8	2.3	-.7	.0	-.5	.3	.1	.1	.0	.1
74- 5 700		.448	4.0	2.1	2.2	-2.0	.0	-.4	.2	.0	.1	.1	.1
74- 6 700		.504	4.0	2.3	2.9	-2.7	1.0	-1.1	.3	.2	.0	.1	.1
74- 7 700		.565	4.0	2.2	3.4	-2.3	-.3	-1.6	.3	.4	.1	.0	.1
74- 8 700		.623	4.0	1.9	3.7	-2.9	3.2	-1.3	.6	.4	.1	-.1	.1
74- 9 700		.682	4.0	1.3	4.1	1.3	-3.0	-2.2	.1	.4	.4	.1	.1

TABLE LVIII - Concluded															
RUN- PT. NO.		OMS *R (FPS)	MU	THC (DEG)	RS	R1	R2	R3	R4	R5	R6	R7	R8	R9	R10
74-	3	700	.333	4.0	3.0	1.7	1.7	.8	3.1	.4	.3	.1	.1	.0	.1
74-	4	700	.390	4.0	2.6	2.1	2.3	2.3	4.0	.5	.3	.1	.1	.1	.1
74-	5	700	.448	4.0	2.3	2.3	2.2	3.5	5.9	.7	.3	.1	.1	.1	.1
74-	6	700	.504	4.0	2.1	2.6	2.9	4.8	7.8	1.2	.3	.1	.1	.1	.1
74-	7	700	.565	4.0	1.9	2.6	3.5	5.7	8.5	1.7	.3	.4	.1	.1	.1
74-	8	700	.623	4.0	2.0	2.5	3.8	6.4	9.7	1.9	.6	.4	.2	.1	.1
74-	9	700	.682	4.0	2.1	2.3	4.2	7.0	11.5	2.2	.6	.5	.4	.2	.2

TABLE LIX. BLADE LAG MOTION HARMONICS - RUN 75-76
(BLADE CENTER OF GRAVITY AT .30 CHORD)

RUN-PT. NO.			BLADE LAG MOTION HARMONICS (DEG)						
QMS R (FPS)			MU	THEC (DEG)	A1	A2	A3	A4	A5
75-	3	500	.793	4.0	.2	.0	.1	-.1	.1
75-	4	500	.876	4.0	.2	.0	.1	-.1	.1
75-	5	500	.958	4.0	.0	.0	.1	-.1	.1
75-	6	500	1.040	4.0	.0	.0	.1	-.1	.2
75-	7	500	1.126	4.0	.0	.0	.1	-.1	.3
75-	8	475	1.181	4.0	.0	.0	.1	.0	.0
75-	9	452	1.243	4.0	.0	.1	.1	.0	-.1
75-	10	427	1.312	4.0	-.1	.1	.1	.1	-.1
75-	11	404	1.388	4.0	-.2	.1	.2	-.1	.0
76-	3	700	.294	10.0	-.5	.0	.0	.1	.0
76-	4	700	.294	11.0	-.5	.0	.0	.0	.0
76-	5	700	.294	12.0	-.4	.1	.1	.1	.1
76-	6	700	.294	13.0	-.6	.1	.0	.0	.0

RUN-PT. NO.			BLADE LAG MOTION HARMONICS (DEG)						
QMS R (FPS)			MU	THEC (DEG)	B1	B2	B3	B4	B5
75-	3	500	.793	4.0	.0	.1	.0	-.1	.0
75-	4	500	.876	4.0	-.1	.1	.1	.0	.0
75-	5	500	.958	4.0	-.3	.1	.0	-.1	-.1
75-	6	500	1.040	4.0	-.3	.1	.0	-.1	.0
75-	7	500	1.126	4.0	-.4	.1	.0	-.1	-.1
75-	8	475	1.181	4.0	-.5	.1	.0	.0	-.2
75-	9	452	1.243	4.0	-.5	.1	.0	-.1	-.1
75-	10	427	1.312	4.0	-.7	.1	.1	-.1	.0
75-	11	404	1.388	4.0	-.8	.1	.0	-.1	-.1
76-	3	700	.294	10.0	.3	.1	.1	.0	.0
76-	4	700	.294	11.0	.4	.1	.1	.0	.0
76-	5	700	.294	12.0	.6	.1	.1	.1	.1
76-	6	700	.294	13.0	.5	.1	.1	.1	.0

TABLE LIX - Concluded

TABLE LIX - Concluded									
BLADE LAG MOTION HARMONICS (DEG)									
RUN-PT. NO.	GMS #R (FPS)	MU	THEC (DEG)	RS	R1	R2	R3	R4	R5
75- 3 500		.793	4.0	2.3	.2	.1	.1	.1	.1
75- 4 500		.876	4.0	2.2	.2	.1	.1	.1	.1
75- 5 500		.958	4.0	2.2	.3	.1	.1	.1	.1
75- 6 500		1.040	4.0	2.1	.3	.1	.1	.1	.2
75- 7 500		1.126	4.0	2.0	.4	.1	.1	.1	.3
75- 8 475		1.181	4.0	1.8	.5	.1	.1	.1	.2
75- 9 452		1.243	4.0	1.6	.5	.1	.1	.1	.1
75-10 427		1.312	4.0	1.3	.7	.1	.1	.1	.1
75-11 404		1.388	4.0	.1	.8	.1	.2	.2	.1
76- 3 700		.294	10.0	6.2	.6	.1	.1	.1	.0
76- 4 700		.294	11.0	7.0	.6	.1	.1	.1	.0
76- 5 700		.294	12.0	7.8	.7	.2	.2	.1	.1
76- 6 700		.294	13.0	8.7	.8	.1	.1	.1	.0

TABLE LX. BLADE .30R FLAPWISE BENDING MOMENT HARMONICS - RUNS 75-76 (BLADE CENTER OF GRAVITY AT .30 CHORD)																
BLADE .30R FLAPWISE BENDING MOMENT HARMONICS (IN.-LB)																
RUN- PT. NO.	OMS PR (FPS)	MU	THEC (DEG)	A1	A2	A3	A4	A5	A6	A7	A8	A9	A10	A11	A12	A13
75- 3 500	.793	4.0		1.4	-2.9	-4.1	-1.6	.8	.8	-3	.1	-.4	-.2	-.2	.0	.0
75- 4 500	.876	4.0		1.8	-3.1	-4.6	-1.6	.5	1.2	-.1	.4	-.4	-.7	.5	.0	.1
75- 5 500	.958	4.0		2.2	-3.8	-4.6	-1.6	1.0	-1.8	-.4	.5	-.1	-1.5	.6	.0	.0
75- 6 500	1.040	4.0		2.5	-4.8	-3.6	-2.8	1.6	-3.0	-.8	.5	1.1	-1.4	.7	.0	-.1
75- 7 500	1.126	4.0		3.4	-5.7	3.2	-4.4	2.4	-9.8	-2.1	.0	1.1	-.2	.1	.1	.1
75- 8 505	1.181	4.0		3.6	-6.2	1.4	-5.5	1.9	-4.6	-1.9	-.2	.7	.4	-1.7	.4	.1
75- 9 852	1.243	4.0		3.3	-5.3	-2.4	-6.7	-.1	6.6	-1.0	-.4	.3	.2	-2.7	.1	.0
75-10 827	1.312	4.0		3.7	-6.6	-6.2	-7.5	-5.1	8.8	-2.7	-1.0	-.1	.1	-.1	-.3	-.3
75-11 804	1.388	4.0		3.2	-8.5	-15.9	-8.2	-7.2	-.1	-3.9	-.8	-.6	-.3	-.7	-.3	-.2
76- 3 700	.294	10.0		.0	-.5	-1.3	.9	3.7	.1	-.4	-.7	.3	.2	.0	.0	.0
76- 4 700	.294	11.0		.0	-.5	-1.2	.9	4.2	.2	-.1	-.1	.5	.2	.0	.0	.0
76- 5 700	.294	12.0		.0	-.7	-1.7	.1	4.2	.4	.2	.4	.6	.4	.0	.0	.0
76- 6 700	.294	13.0		-.1	-.5	-1.2	.8	5.0	.6	.4	.5	1.1	.3	.0	.0	.0

BLADE .30R FLAPWISE BENDING MOMENT HARMONICS (IN.-LB)																
RUN- PT. NO.	OMS PR (FPS)	MU	THEC (DEG)	B1	B2	B3	B4	B5	B6	B7	B8	B9	B10	B11	B12	B13
75- 3 500	.793	4.0		.7	.2	8.1	-.8	-2.0	3.9	.4	.5	.1	.3	.0	-.1	.1
75- 4 500	.876	4.0		.9	-1.3	8.4	-.4	-1.8	3.3	.4	.5	.6	.4	.2	-.1	.1
75- 5 500	.958	4.0		1.2	-1.7	8.4	-.4	-1.7	4.4	-.4	.5	.8	.2	.0	-.1	.1
75- 6 500	1.040	4.0		.8	-3.0	8.9	-1.0	-3.0	4.7	-.7	.5	.6	1.5	.1	-.1	.1
75- 7 500	1.126	4.0		-.3	-4.0	13.0	.4	-5.3	6.3	.0	.8	-.5	3.2	.1	-.1	.1
75- 8 505	1.181	4.0		-1.6	-4.2	11.1	-.3	-5.7	12.6	-.4	.9	.3	1.8	.2	-.1	.1
75- 9 852	1.243	4.0		-3.7	-4.2	10.7	-1.3	-6.5	9.3	-.4	.9	.3	1.8	.2	-.1	.1
75-10 827	1.312	4.0		-3.5	-3.3	6.7	.7	-6.0	-4.6	.3	.1	.1	1.0	.9	-.9	-.3
75-11 804	1.388	4.0		-3.6	-4.2	8.1	1.1	-2.4	-7.2	2.1	.7	.0	-.2	.0	.7	-.5
76- 3 700	.294	10.0		-.8	-.3	-.9	-2.1	.6	.0	.1	.4	.3	-.3	.0	.0	.0
76- 4 700	.294	11.0		-.7	-.2	-1.5	-2.4	.9	.3	.1	.4	-.5	.0	.0	.0	.0
76- 5 700	.294	12.0		-.7	.0	-1.7	-2.6	-3.0	.6	.2	.1	-.4	-.2	.0	.0	.0
76- 6 700	.294	13.0		-.5	-.1	-2.2	-2.4	-2.5	.9	.2	.2	-.1	-.0	.0	.0	.0

TABLE LX - Concluded																			
RUN- PT. NO.	QMS OR (FPS)	BLADE .30R FLAPWISE BENDING MOMENT HARMONICS (IN.-LB)																	
		MU	TMEC (DEG)	R5	R1	R2	R3	R4	R5	R6	R7	R8	R9	R10	R11	R12	R13		
75- 3 500		.793	4.0	1.6	1.6	2.9	9.1	1.8	2.1	4.0	.5	.5	.5	.4	.2	.1	.1		
75- 4 500		.876	4.0	2.0	2.0	3.4	9.6	1.7	1.9	3.5	.4	.6	.7	.8	.5	.1	.1		
75- 5 500		.958	4.0	2.3	2.5	4.2	9.6	1.7	1.9	4.8	.6	.5	.8	1.5	.6	.1	.1		
75- 6 500		1.040	4.0	2.4	2.6	5.6	9.7	3.0	3.4	5.6	1.1	.7	1.1	3.1	.7	.1	.1		
75- 7 500		1.126	4.0	2.2	3.4	6.9	13.4	4.4	5.8	11.7	2.1	.8	1.2	3.2	1.7	.4	.1		
75- 8 475		1.181	4.0	2.0	4.0	7.5	11.1	5.5	6.0	13.4	2.0	.9	.8	1.8	3.7	.7	.1		
75- 9 452		1.243	4.0	1.6	4.9	6.8	10.9	6.8	6.5	11.4	1.1	.8	.4	1.0	2.7	.5	.2		
75-10 427		1.312	4.0	2.0	5.1	7.3	9.1	7.5	7.9	9.9	2.8	1.0	.2	.3	.9	1.5	.4		
75-11 884		1.388	4.0	3.0	4.8	9.5	17.9	8.3	7.6	7.2	4.4	1.1	.6	.4	.7	.8	.5		
76- 3 700		.294	10.0	4.5	.6	1.6	2.3	3.7	.1	.4	.8	1.4	.3	.3	.0	.0	.0		
76- 4 700		.294	11.0	4.8	.7	.5	1.9	2.5	4.3	.4	.2	.4	.7	.2	.0	.0	.0		
76- 5 700		.294	12.0	5.0	.7	.7	2.4	2.6	5.1	.7	.3	.4	.7	.4	.0	.0	.0		
76- 6 700		.294	13.0	5.3	.5	.5	2.6	2.5	5.6	1.0	.5	.6	1.1	.3	.0	.0	.0		

TABLE LXI. BLADE .18R TORSIONAL MOMENT HARMONICS - RUNS 75-76 (BLADE CENTER OF GRAVITY AT .30 CHORD)																								
BLADE .18R TORSIONAL MOMENT HARMONICS (IN.-LB)																								
RUN- PT. NO.	OMS OR (FPS)	MU	THEC (DEG)	A1	A2	A3	A4	A5	A6	A7	A8	A9	A10	A11	A12	A13								
75- 3 500	.793	4.0	4.0	.8	-1.7	-3.2	.6	1.5	1.4	.8	.2	.0	-.1	.0	.0	.0								
75- 4 500	.876	4.0	4.0	1.4	-1.4	-4.2	.6	2.4	1.9	.9	.3	.0	-.1	-.2	.0	.0								
75- 5 500	.958	4.0	4.0	2.3	-2.3	-5.5	.5	3.4	2.3	1.0	.4	-.1	-.1	-.3	-.1	-.1								
75- 6 500	1.040	4.0	4.0	3.1	-3.8	-7.3	-3.4	7.1	3.4	1.7	.8	-.1	.0	-.3	-.1	-.1								
75- 7 500	1.126	4.0	4.0	4.3	-3.4	-7.9	-8.8	13.8	5.1	1.0	.4	.3	.1	.0	-.1	.0								
75- 8 475	1.181	4.0	4.0	4.4	-6.0	-8.0	-6.6	13.4	7.1	3.6	-.1	-.3	.2	-.3	-.2	-.1								
75- 9 452	1.243	4.0	4.0	4.5	-7.8	-9.0	-7.4	9.0	10.0	3.0	-.5	-.3	.1	.0	-.3	-.1								
75-10 427	1.312	4.0	4.0	3.8	-10.0	-2.7	-6.4	.2	9.8	-.6	-.1	.2	.0	.5	.6	.0								
75-11 404	1.388	4.0	4.0	3.6	-13.2	-4.0	-.8	-2.3	3.8	.0	.9	.6	.8	.3	.3	.2								
76- 3 700	.294	10.0	10.0	-.9	-1.0	-6.7	1.4	2.6	1.6	.7	.3	.1	.1	.0	.0	.0								
76- 4 700	.294	11.0	11.0	-1.3	-.9	-8.4	-1.3	.8	.1	-.1	-.1	-.2	.1	.0	.0	.0								
BLADE .18R TORSIONAL MOMENT HARMONICS (IN.-LB)																								
RUN- PT. NO.	OMS OR (FPS)	MU	THEC (DEG)	B1	B2	B3	B4	B5	B6	B7	B8	B9	B10	B11	B12	B13								
75- 3 500	.793	4.0	4.0	.3	.9	2.2	-1.2	-.6	.1	.5	.4	.2	.2	.0	.0	.0								
75- 4 500	.876	4.0	4.0	-.5	.7	3.0	-1.3	.2	1.3	.5	.5	.3	.3	.0	.0	.0								
75- 5 500	.958	4.0	4.0	-2.2	-.7	3.6	-.4	1.7	1.7	.7	.8	.3	.3	.0	.0	.1								
75- 6 500	1.040	4.0	4.0	-4.9	-1.7	6.0	.6	2.3	3.5	-.5	-.3	.0	.4	.2	.0	.0								
75- 7 500	1.126	4.0	4.0	-6.7	-3.4	12.0	3.2	.3	3.7	1.6	-.6	-.1	.6	.3	.1	.2								
75- 8 475	1.181	4.0	4.0	-9.3	-4.8	12.9	1.4	-.3	3.2	.2	-1.6	-.4	.4	.6	.2	.0								
75- 9 452	1.243	4.0	4.0	-10.8	-5.1	12.5	1.4	-8.5	.7	-.6	.0	.2	.4	.7	.4	.1								
75-10 427	1.312	4.0	4.0	-13.2	-4.9	14.7	9.6	-10.3	-7.3	-.8	.4	.8	.4	.3	.7	.4								
75-11 404	1.388	4.0	4.0	-15.9	-4.8	14.2	12.1	-5.8	-11.4	-3.8	-.9	.3	.7	.0	-.8	-.1								
76- 3 700	.294	10.0	10.0	6.5	5.5	-4.3	-11.0	-5.3	-2.5	-.9	-.4	-.1	.1	.0	.0	.0								
76- 4 700	.294	11.0	11.0	7.8	6.6	-3.5	-10.0	-5.5	-3.0	-1.2	-.4	.1	.3	.0	.0	.0								

TABLE LXI - Concluded

RUN- PT. NO.	OMS #R (FPS)	THC (DEG)	BLADE .18R TORSIONAL MOMENT HARMONICS (IN.-LB)														
			MU	R5	R1	R2	R3	R4	R5	R6	R7	R8	R9	R10	R11	R12	R13
75- 3 500		4.0	.793	2.0	.9	1.2	3.9	1.4	1.6	1.4	.9	.5	.2	.2	.0	.0	.0
75- 4 500		4.0	.876	2.7	1.5	1.6	5.2	1.4	2.4	1.6	1.0	.6	.3	.3	.2	.1	.1
75- 5 500		4.0	.958	3.6	3.1	2.4	6.6	.7	3.8	2.8	1.2	.9	.3	.3	.3	.1	.1
75- 6 500		4.0	1.040	5.2	5.8	4.2	9.4	3.4	7.5	4.9	1.7	1.5	.1	2.1	.7	.1	.2
75- 7 500		4.0	1.126	6.4	7.9	4.8	14.4	8.9	13.8	6.3	1.9	1.5	.3	.6	.3	.2	.1
75- 8 475		4.0	1.181	14.1	10.3	7.6	15.2	7.4	13.8	7.7	3.7	1.6	.5	.5	.7	.5	.2
75- 9 452		4.0	1.243	14.7	11.7	9.3	15.4	7.5	12.4	10.0	3.4	.5	.4	.4	.7	.9	.6
75-10 427		4.0	1.312	15.4	13.8	11.1	15.0	11.5	10.3	12.3	1.9	.4	.8	.4	.6	.9	.3
75-11 404		4.0	1.388	16.7	16.3	14.1	14.7	12.1	6.3	12.0	3.8	1.3	.6	1.0	.3	.9	.3
76- 3 700		10.0	.294	1.5	6.6	5.5	8.0	11.1	5.9	3.0	1.1	.5	.1	.1	.0	.0	.0
76- 4 700		11.0	.294	.7	8.0	6.6	9.1	10.1	5.6	3.0	1.2	.5	.2	.4	.0	.0	.0

TABLE LXII. BLADE FLAP MOTION HARMONICS - RUNS 75-76
(BLADE CENTER OF GRAVITY AT .30 CHORD)

RUN- PT. NO.	OMS #R (FPS)	MU	THEC (DEG)	BLADE FLAP MOTION HARMONICS (DEG)					
				A1	A2	A3	A4	A5	A6
75- 3 500	.793	4.0	.4	-.2	.5	.1	.0	.0	.0
75- 4 500	.876	4.0	.3	-.2	.6	.1	.0	.0	.0
75- 5 500	.958	4.0	.3	-.2	.6	.1	.0	.1	.1
75- 6 500	1.040	4.0	.4	-.3	.4	.2	-.1	.1	.1
75- 7 500	1.126	4.0	-.3	-.6	.0	.5	-.1	.3	.3
75- 8 475	1.181	4.0	.0	-.6	.1	.6	.0	.1	.1
75- 9 452	1.243	4.0	-.1	-.8	.2	.7	.1	-.3	-.3
75-10 427	1.312	4.0	.2	-.8	.3	.8	.4	-.4	-.4
75-11 404	1.388	4.0	.1	-.9	.9	.7	.5	.0	.0
76- 3 700	.294	10.0	-.1	-.1	.2	-.1	-.1	.0	.0
76- 4 700	.294	11.0	.2	-.1	.2	.0	-.1	.0	.0
76- 5 700	.294	12.0	.1	-.3	.2	.0	-.1	.0	.0
76- 6 700	.294	13.0	.0	-.2	.2	.0	-.2	.0	.0

RUN- PT. NO.	OMS #R (FPS)	MU	THEC (DEG)	BLADE FLAP MOTION HARMONICS (DEG)					
				B1	B2	B3	B4	B5	B6
75- 3 500	.793	4.0	.0	-.2	-.7	.1	.1	.1	-.1
75- 4 500	.876	4.0	.0	-.1	-.7	.1	.1	.1	-.1
75- 5 500	.958	4.0	.1	-.1	-.7	.1	.1	.1	-.1
75- 6 500	1.040	4.0	.1	.1	-.8	.2	.2	.2	-.1
75- 7 500	1.126	4.0	-.1	.2	-1.4	.1	.3	-.2	-.2
75- 8 475	1.181	4.0	.0	.2	-1.1	.1	.4	-.4	-.4
75- 9 452	1.243	4.0	.0	.1	-1.1	.1	.4	-.3	-.3
75-10 427	1.312	4.0	.1	.3	-.8	-.2	.4	.2	.2
75-11 404	1.388	4.0	.2	.3	-.9	-.2	.3	.3	.3
76- 3 700	.294	10.0	.0	-.4	.2	.1	.0	.0	.0
76- 4 700	.294	11.0	.2	-.5	.2	.2	.0	.0	.0
76- 5 700	.294	12.0	.1	-.5	.2	.1	.1	.0	.0
76- 6 700	.294	13.0	.2	-.6	.2	.1	.1	.0	.0

TABLE LXII - Concluded

BLADE FLAP MOTION HARMONICS (DEG)											
RUN- PT. NO.	QMS PR	MU	TREC (DEG)	RS	R1	R2	R3	R4	R5	R6	
75- 3 500		.793	4.0	.3	.4	.3	.9	.1	.1	.1	
75- 4 500		.876	4.0	.2	.3	.3	.9	.2	.1	.1	
75- 5 500		.958	4.0	.1	.3	.3	.9	.2	.1	.2	
75- 6 500		1.040	4.0	-.1	.4	.3	.9	.3	.2	.2	
75- 7 500		1.126	4.0	-.2	.3	.6	1.4	.5	.3	.4	
75- 8 475		1.181	4.0	-.5	.1	.6	1.2	.6	.4	.4	
75- 9 452		1.243	4.0	-.7	.1	.8	1.2	.7	.4	.4	
75-10 427		1.312	4.0	-1.1	.2	.9	.8	.8	.6	.4	
75-11 404		1.388	4.0	-1.5	.2	1.0	1.3	.7	.6	.3	
76- 3 700		.294	10.0	3.2	.1	.4	.3	.2	.1	.0	
76- 4 700		.294	11.0	3.4	.3	.5	.3	.2	.2	.0	
76- 5 700		.294	12.0	3.5	.2	.6	.3	.1	.2	.0	
76- 6 700		.294	13.0	3.7	.2	.6	.3	.1	.2	.0	

TABLE LXIII. BLADE .30R CHORDWISE BENDING MOMENT HARMONICS - RUNS 75-76 (BLADE CENTER OF GRAVITY AT .30 CHORD)														
BLADE .30R CHORDWISE BENDING MOMENT HARMONICS (IN.-LB)														
RUN- PT. OMS NO. #R	MU (FPS)	THEC (DEG)	A1	A2	A3	A4	A5	A6	A7	A8	A9	A10	A11	A12 A13
75- 3 500	.793	4.0	-0.6	2.3	.2	1.9	-6.1	-5	-2	-1	.0	.1	.0	.4
75- 4 500	.876	4.0	-1.1	2.2	-6	1.5	-8.8	-9	-2	.7	.0	.3	-1	.4
75- 5 500	.958	4.0	-1.6	2.4	-6	2.1	-11.3	-7	-5	.2	-1	.6	-4	.4
75- 6 500	1.040	4.0	-1.7	2.3	-1.4	.4	-20.9	-9	-1.1	.5	.0	.5	-1.0	.4
75- 7 500	1.126	4.0	-2.8	3.5	-2.7	.5	-31.7	.0	-2.0	.2	-1	2.0	-1.7	.4
75- 8 475	1.181	4.0	-2.0	2.9	-4.0	-9	-1.7	-3.2	-1.0	-3	-1	.8	-1.8	-1.6
75- 9 452	1.243	4.0	-3.9	2.6	-1.2	-1.9	7.2	-5.4	.1	-1	.2	-5	2.4	-2
75-10 427	1.312	4.0	-6.4	2.3	.3	-1.9	5.5	.0	-1.6	-7	.6	.9	-2	-7
75-11 404	1.388	4.0	-10.0	4.4	2.2	-6.3	7.6	22.6	4.3	.1	-1.2	1.2	-6	.2
76- 3 700	.294	10.0	-2.8	.9	2.5	-2.0	-1.9	-1	.1	-2	.0	.4	.0	.0
76- 4 700	.294	11.0	-3.2	-5	3.0	1.6	-1.2	.5	.4	-4	-1	.2	.0	.0
76- 5 700	.294	12.0	-2.5	-1.8	2.2	1.3	-0.8	.2	.4	-6	-1.0	-2	.0	.0

BLADE .30R CHORDWISE BENDING MOMENT HARMONICS (IN.-LB)														
RUN- PT. OMS NO. #R	MU (FPS)	THEC (DEG)	B1	B2	B3	B4	B5	B6	B7	B8	B9	B10	B11	B12 B13
75- 3 500	.793	4.0	-4.0	.5	-1.7	4.5	6.8	-2	-4	-2	.3	-1	.1	.4
75- 4 500	.876	4.0	-5.0	.9	-2.3	5.0	7.7	-1	-3	-3	-2	.0	.1	-5
75- 5 500	.958	4.0	-6.3	1.0	-2.9	5.4	10.9	.6	-1	-3	-4	-1	.2	.0
75- 6 500	1.040	4.0	-7.8	1.8	-3.8	6.9	11.5	-8	1.4	-7	-5	.8	.0	.0
75- 7 500	1.126	4.0	-10.6	1.4	-7.3	8.8	22.6	-1.0	3.9	-7	-7	-1.9	.9	-8
75- 8 475	1.181	4.0	-10.4	1.0	-4.3	7.7	28.1	-3	4.4	.5	-5	-1.4	3.0	.8
75- 9 452	1.243	4.0	-11.4	.6	-2.1	9.4	9.9	-5.4	.1	-9	-1.1	-5	.4	-5
75-10 427	1.312	4.0	-13.3	1.1	-1.6	10.6	5.7	17.8	5.2	-7	-1.9	.1	-1.2	-3
75-11 404	1.388	4.0	-14.9	2.3	-1.5	21.8	9.8	16.1	15.6	4.4	-4.2	-2.6	.3	1.8
76- 3 700	.294	10.0	8.6	.1	-1.4	6.0	.6	.1	.3	-5	-2	1.0	.0	.0
76- 4 700	.294	11.0	10.8	-1	-2.8	1.0	2.3	-2	.1	-4	-6	-6	.0	.0
76- 5 700	.294	12.0	14.3	-0.9	-4.7	-2.8	2.4	-7	.2	-2	-6	-1.0	.0	.0

TABLE LXIV. BLADE .35R TORSIONAL MOMENT HARMONICS - RUNS 75-76
(BLADE CENTER OF GRAVITY AT .30 CHORD)

BLADE .35R TORSIONAL MOMENT HARMONICS (IN.-LB)													
RUN- PT. NO.	QMS #R	MU	THEC (DEG)	A1	A2	A3	A4	A5	A6	A7	A8	A9	A10
75- 3 900	.793	4.0	.6	-1	-2.3	.1	1.2	1.2	.8	.4	.0	.0	.0
75- 4 500	.876	4.0	.9	-6	-3.3	.1	2.0	1.3	.6	.4	.1	.1	-.1
75- 5 500	.958	4.0	1.5	-1.2	-3.8	.0	3.0	2.2	1.1	.7	.1	.0	.0
75- 6 500	1.040	4.0	2.2	-2.1	-3.6	-3.0	6.2	3.1	1.4	.5	-.1	.0	.0
75- 7 500	1.126	4.0	3.3	-9	-7.1	-7.7	11.6	3.3	1.7	1.0	-.1	.1	.1
75- 8 475	1.181	4.0	3.4	-3.3	-6.9	-6.2	12.0	5.7	3.2	.2	-.2	.1	.1
75- 9 452	1.243	4.0	3.2	-5.4	-6.1	-5.8	6.8	9.1	1.3	-.5	.0	.1	.1
75-10 427	1.312	4.0	3.0	-7.2	-1.9	-5.8	.1	9.0	-1.2	-.3	.4	.2	.2
75-11 404	1.388	4.0	2.9	-10.2	-2.6	1.3	-2.7	2.2	-1.5	-.3	.7	1.0	.0
76- 3 700	.294	10.0	-.4	-.9	-6.1	.6	2.0	1.0	.4	.0	.0	.3	.5
76- 4 700	.294	11.0	-2.8	-.2	-7.6	-3.4	-1.1	-.5	-.2	.1	.3	.1	.4
76- 5 700	.294	12.0	-2.1	.7	-9.5	-4.8	.8	-.1	-.3	-.2	.1	.1	.1
76- 6 700	.294	13.0	-2.5	.8	-12.4	-5.1	-1.9	-1.1	-.7	.3	.3	.7	.7

BLADE .35R TORSIONAL MOMENT HARMONICS (IN.-LB)													
RUN- PT. NO.	QMS #R	MU	THEC (DEG)	B1	B2	B3	B4	B5	B6	B7	B8	B9	B10
75- 3 900	.793	4.0	.4	1.0	1.6	-1.1	-.8	.0	.1	.3	.1	.3	.1
75- 4 500	.876	4.0	.1	.8	2.0	-1.2	.0	.6	.2	.3	.3	.3	.3
75- 5 500	.958	4.0	-1.1	.2	2.9	-.5	.8	1.3	.0	.4	.4	.4	.4
75- 6 500	1.040	4.0	-3.1	-1.1	6.1	.3	1.6	3.1	-.6	.1	.1	.4	.4
75- 7 500	1.126	4.0	-4.5	-2.8	8.7	-.6	2.5	4.3	.3	-.3	.3	.4	.4
75- 8 475	1.181	4.0	-6.6	-3.7	9.7	1.6	-1.4	4.1	-.7	-.3	.2	.3	.3
75- 9 452	1.243	4.0	-8.1	-3.4	10.6	3.4	-8.4	-.7	-2.5	.6	.6	.3	.3
75-10 427	1.312	4.0	-9.9	-3.6	11.9	8.2	-9.1	-6.8	-1.5	-.9	.1	.3	.3
75-11 404	1.388	4.0	-12.4	-3.3	11.5	10.3	-4.6	-10.5	-2.9	-.8	.1	.3	.3
76- 3 700	.294	10.0	5.9	4.8	-3.6	-9.7	-4.6	-2.3	-.8	-.4	-.2	.0	.0
76- 4 700	.294	11.0	8.4	6.7	-3.1	-10.5	-6.0	-3.9	-1.8	-.5	-.2	.1	.1
76- 5 700	.294	12.0	9.2	6.9	-1.5	-6.8	-4.5	-3.2	-1.2	.3	.1	.1	.1
76- 6 700	.294	13.0	11.1	7.7	-1.7	-6.8	-4.3	-2.8	-.8	.5	-.2	.5	.5

TABLE LXIV - Concluded

TABLE LXIV - Concluded														
BLADE .35R TORSIONAL MOMENT HARMONICS (IN.-LB)														
RUN- PT. NO.	OMS #R (FPS)	MU	THEC (DEG)	RS	R1	R2	R3	R4	R5	R6	R7	R8	R9	R10
75- 3 500		.793	4.0	.9	.8	1.0	2.9	1.1	1.5	1.2	.8	.5	.3	.1
75- 4 500		.876	4.0	1.4	.9	1.0	3.8	1.2	2.0	1.4	.9	.6	.3	.2
75- 5 500		.958	4.0	2.1	1.9	1.2	4.8	.5	3.2	2.6	1.1	.8	.4	.3
75- 6 500		1.040	4.0	3.3	1.9	2.4	7.0	3.0	6.4	4.4	1.6	.8	.2	.4
75- 7 500		1.126	4.0	4.5	5.6	2.9	11.3	7.7	11.9	5.5	1.7	1.6	.3	.4
75- 8 475		1.181	4.0	5.2	7.4	4.9	11.9	6.4	12.1	7.0	3.2	1.5	.4	.3
75- 9 452		1.243	4.0	5.7	8.7	6.3	12.3	6.7	10.8	9.2	3.2	.5	.3	.4
75-10 427		1.312	4.0	6.4	10.3	8.0	12.0	10.0	9.1	11.2	1.9	.5	.7	.4
75-11 404		1.388	4.0	7.4	12.8	10.6	11.8	10.4	5.3	10.8	3.3	.9	.7	1.0
76- 3 700		.294	10.0	1.4	5.9	4.9	7.1	9.7	5.0	2.5	.9	.4	.2	.0
76- 4 700		.294	11.0	-7.2	8.8	6.7	8.2	11.0	6.1	3.9	1.8	.5	.4	.5
76- 5 700		.294	12.0	-4.5	9.4	6.9	9.6	8.3	4.5	3.2	1.2	.3	.2	.4
76- 6 700		.294	13.0	-6.7	11.4	7.7	12.6	8.6	4.8	3.0	1.1	.6	.3	.9

TABLE LXV. BLADE LAG MOTION HARMONICS - RUNS 77-78
(BLADE CENTER OF GRAVITY AT .30 CHORD)

RUN- PT. NO.	OMS WR (FPS)	MU	THEC (DEG)	BLADE LAG MOTION HARMONICS (DEG)				
				A1	A2	A3	A4	A5
77- 3 700	.351	10.0	-0.4	.0	.1	.2	.0	.0
77- 4 700	.351	11.0	-0.5	.0	.0	.1	.0	.0
77- 5 700	.410	6.0	-0.2	.0	.1	.1	.0	.0
77- 6 700	.486	4.0	-0.1	.0	.1	.1	.0	.0
77- 7 700	.486	5.0	-0.1	.0	.1	.1	.0	.0
77- 8 700	.546	4.0	.0	.0	.1	.1	.0	.0
77- 9 700	.546	5.0	-0.1	.0	.1	.2	.0	.0
77-10 700	.610	5.0	-0.1	.0	.1	.1	.0	.0
77-11 700	.634	5.0	.0	.0	.1	.2	.0	.0
77-12 500	.926	5.0	-0.1	.1	.1	-0.1	.2	.0
77-13 500	.958	5.0	-0.1	.1	.1	-0.1	.2	.0
78- 3 700	.351	10.0	-0.4	.1	.1	.3	.0	.0
78- 4 700	.351	11.0	-0.5	.1	.1	.2	.0	.0
78- 5 700	.351	12.0	-0.5	.1	.1	.2	.0	.0
78- 6 700	.410	10.0	-0.3	.1	.1	.3	.0	.0

RUN- PT. NO.	OMS WR (FPS)	MU	THEC (DEG)	BLADE LAG MOTION HARMONICS (DEG)				
				B1	B2	B3	B4	B5
77- 3 700	.351	10.0	.3	.1	.1	.0	.0	.0
77- 4 700	.351	11.0	.3	.1	.1	.0	.0	.0
77- 5 700	.410	6.0	.0	.0	.0	.1	.0	.0
77- 6 700	.486	4.0	-0.1	.0	.0	.1	.0	.0
77- 7 700	.486	5.0	-0.1	.0	.0	.2	.0	.0
77- 8 700	.546	4.0	-0.1	.0	.0	.1	.0	.0
77- 9 700	.546	5.0	-0.1	.0	.0	.2	.0	.0
77-10 700	.610	5.0	-0.1	.0	.0	.2	.0	.0
77-11 700	.634	5.0	-0.1	.0	.0	.2	.0	.0
77-12 500	.926	5.0	-0.2	.1	.0	-0.1	.0	.0
77-13 500	.958	5.0	-0.3	.1	.0	-0.1	.0	.0
78- 3 700	.351	10.0	.3	.1	.1	.0	.0	.0
78- 4 700	.351	11.0	.4	.0	.1	-0.1	.0	.0
78- 5 700	.351	12.0	.4	.1	.1	-0.1	.0	.0
78- 6 700	.410	10.0	.3	.1	.1	.1	.2	.0

TABLE LXV - Concluded										
BLADE LAG MOTION HARMONICS (DEG)										
RUN- PT. NO.	OMS SR (FPS)	MU	THEC (DEG)	RS	R1	R2	R3	R4	R5	
77- 3 700		.351	10.0	6.0	.5	.1	.1	.2	.0	
77- 4 700		.351	11.0	6.7	.6	.1	.1	.2	.0	
77- 5 700		.410	6.0	2.8	.2	.0	.1	.2	.0	
77- 6 700		.406	4.0	2.0	.1	.0	.1	.2	.0	
77- 7 700		.406	5.0	2.3	.1	.1	.1	.2	.0	
77- 8 700		.546	4.0	2.0	.1	.0	.1	.2	.0	
77- 9 700		.546	5.0	2.2	.1	.1	.1	.2	.0	
77-10 700		.610	5.0	2.2	.1	.0	.1	.2	.0	
77-11 700		.634	5.0	2.1	.1	.0	.1	.2	.0	
77-12 500		.926	5.0	2.2	.2	.1	.1	.1	.2	
77-13 500		.958	5.0	2.2	.3	.1	.1	.1	.2	
78- 3 700		.351	10.0	6.2	.5	.1	.1	.3	.0	
78- 4 700		.351	11.0	7.0	.6	.1	.1	.2	.0	
78- 5 700		.351	12.0	7.9	.7	.1	.1	.2	.0	
78- 6 700		.410	10.0	5.7	.4	.2	.2	.3	.0	

TABLE LXVI. BLADE .30R FLAPWISE BENDING MOMENT HARMONICS - RUNS 77-78 (BLADE CENTER OF GRAVITY AT .30 CHORD)														
BLADE .30R FLAPWISE BENDING MOMENT HARMONICS (IN.-LB)														
RUN- PT. NO.	OMS OR (FPS)	MU	THEC (DEG)	A1	A2	A3	A4	A5	A6	A7	A8	A9	A10	
77- 3 700	.351	10.0	.4	.4	-.4	-3.1	1.5	1.8	-.2	-.6	-.9	.3	.0	
77- 4 700	.351	11.0	.4	.4	-.4	-3.0	1.4	2.3	-.3	-.7	-1.0	-.1	.0	
77- 5 700	.410	6.0	.6	.6	-.7	-4.7	.5	-3.2	.1	-.4	-.8	-.1	-.1	
77- 6 700	.486	4.0	1.3	1.3	-.9	-4.1	.1	-.9	.7	.0	-.7	.7	-.1	
77- 7 700	.486	5.0	1.2	1.2	-1.2	-4.4	.3	-1.0	.8	.1	-.7	.6	.0	
77- 8 700	.546	4.0	1.4	1.4	-1.8	-4.3	.0	.0	1.1	.7	-.6	.6	.0	
77- 9 700	.546	5.0	1.0	1.0	-2.1	-4.8	.3	.0	1.2	.7	-.7	1.0	.0	
77-10 700	.610	5.0	1.7	1.7	-2.9	-4.5	.5	.4	.5	1.1	-.4	.6	-.1	
77-11 700	.634	5.0	1.6	1.6	-3.3	-4.7	.5	5.4	.0	1.1	-.7	.5	.0	
77-12 500	.926	5.0	2.2	2.2	-4.5	-1.6	-2.2	1.4	-1.3	-.4	.7	-.4	-1.3	
77-13 500	.958	5.0	2.4	2.4	-4.9	-1.1	-2.4	1.2	-1.4	-.6	.5	.1	-1.7	
78- 3 700	.351	10.0	.6	.6	-.1	-2.0	1.1	2.9	1.3	-.4	-1.0	.1	.0	
78- 4 700	.351	11.0	.6	.6	-.2	-2.5	1.0	2.9	.0	-.3	-.8	-.2	.0	
78- 5 700	.351	12.0	.4	.4	-.4	-2.6	.9	3.3	-.5	-.7	-.6	-.3	.0	
78- 6 700	.410	10.0	.5	.5	-1.4	-4.7	.5	-1.9	.4	-.3	-1.6	-.6	-.4	

BLADE .30R FLAPWISE BENDING MOMENT HARMONICS (IN.-LB)														
RUN- PT. NO.	OMS OR (FPS)	MU	THEC (DEG)	B1	B2	B3	B4	B5	B6	B7	B8	B9	B10	
77- 3 700	.351	10.0	.5	.5	.4	1.4	-.9	2.8	.1	.1	-.5	.0	-.1	
77- 4 700	.351	11.0	.6	.6	.6	1.2	-1.2	2.6	.3	.6	-.2	-.3	-.1	
77- 5 700	.410	6.0	1.1	1.1	.2	-.2	-1.1	.6	.2	.2	-.1	-.2	-.2	
77- 6 700	.486	4.0	1.3	1.3	.5	1.8	-1.5	.3	.2	.7	.1	.1	.0	
77- 7 700	.486	5.0	1.4	1.4	.4	2.1	-1.6	3.4	.2	.9	-.1	.2	.0	
77- 8 700	.546	4.0	1.5	1.5	.9	1.8	-1.7	3.5	-.1	.8	.6	-.3	.0	
77- 9 700	.546	5.0	2.0	2.0	.8	2.3	-1.8	4.7	-.3	.4	.8	-.3	.0	
77-10 700	.610	5.0	1.9	1.9	.8	1.8	-1.9	6.0	-.6	.3	1.6	-.6	.0	
77-11 700	.634	5.0	2.1	2.1	.9	1.7	-2.0	5.7	-.5	.0	1.4	-.9	.0	
77-12 500	.926	5.0	.7	.7	-1.1	12.6	.1	-2.3	5.5	-.4	.2	.9	.1	
77-13 500	.958	5.0	.6	.6	-1.4	12.6	.2	-2.6	6.0	.5	.4	.9	.3	
78- 3 700	.351	10.0	.5	.5	.4	2.6	-1.3	1.4	.1	.5	-.4	-.2	.0	
78- 4 700	.351	11.0	.5	.5	.6	1.7	-1.4	1.7	.3	.8	.6	-.2	.0	
78- 5 700	.351	12.0	.6	.6	.7	1.0	-1.5	1.8	1.0	1.0	.6	-.1	.0	
78- 6 700	.410	10.0	1.0	1.0	.6	2.0	-2.1	3.3	-.3	.5	.9	-.3	-.2	

TABLE LXVI - Concluded														
BLADE .30R FLAPWISE BENDING MOMENT HARMONICS (IN.-LB)														
RUN- PT. NO.	OMS OR (FPS)	MU	THEC (DEG)	RS	R1	R2	R3	R4	RS	R6	R7	R8	R9	R10
77- 3 700		.351	10.0	4.5	.7	.5	3.4	1.7	3.3	.2	.6	1.1	.3	.1
77- 4 700		.351	11.0	4.9	.9	.7	3.2	1.8	3.5	.4	1.0	1.0	.3	.1
77- 5 700		.410	6.0	3.3	1.3	.7	4.7	1.2	3.2	.2	.5	.8	.2	.2
77- 6 700		.486	4.0	2.7	1.8	1.1	4.5	1.5	3.0	.7	.7	.7	.8	.1
77- 7 700		.486	5.0	3.0	1.8	1.3	4.9	1.6	3.5	.8	.7	.7	.7	.1
77- 8 700		.546	4.0	2.5	2.0	2.1	4.6	1.7	3.5	1.1	1.1	.9	.7	.0
77- 9 700		.546	5.0	3.0	2.3	2.2	5.3	1.9	4.7	1.2	1.1	1.0	1.1	.0
77-10 700		.610	5.0	3.2	2.6	3.0	4.8	2.0	7.3	.5	1.2	1.6	1.2	.1
77-11 700		.634	5.0	3.2	2.7	3.4	5.0	2.1	7.9	.6	1.2	1.6	.8	.1
77-12 500		.926	5.0	1.8	2.3	4.6	12.7	2.2	2.7	5.6	.4	.7	1.0	1.3
77-13 500		.958	5.0	1.5	2.5	5.1	12.7	2.5	2.8	6.2	.7	.6	.9	1.7
78- 3 700		.351	10.0	4.7	.8	.4	3.3	1.7	3.2	.2	.6	1.1	.5	.1
78- 4 700		.351	11.0	4.9	.8	.6	3.0	1.7	3.3	.3	.8	1.0	.3	.0
78- 5 700		.351	12.0	5.1	.7	.8	2.7	1.7	3.6	1.1	1.2	.8	.4	.0
78- 6 700		.410	10.0	4.5	1.1	1.5	5.1	2.1	3.8	.6	.6	1.8	.8	.4

TABLE LXVII. BLADE .18R TORSIONAL MOMENT HARMONICS - RUNS 77-78 (BLADE CENTER OF GRAVITY AT .30 CHORD)														
RUN- PT. NO.	GMS OR (PPS)	MU	TMEC (DEC)	BLADE .18R TORSIONAL MOMENT HARMONICS (IN.-LB)										
				A1	A2	A3	A4	A5	A6	A7	A8	A9	A10	
77- 3 700	.351	10.0		-5	.2	-4.9	10.1	3.0	2.3	1.1	.7	.5	.4	
77- 4 700	.351	11.0		-5	.0	-0.1	6.7	2.7	2.0	1.5	.9	.5	.2	
77- 5 700	.410	6.0		1.0	1.3	-1.9	6.5	.9	.0	.1	.2	.2	.3	
77- 6 700	.406	4.0		1.4	.0	-4.7	7.0	.7	.1	-.1	-.2	.1	.0	
77- 7 700	.406	5.0		1.6	.7	-5.2	8.3	.4	.5	.0	-.1	.1	.0	
77- 8 700	.546	4.0		1.4	-.5	-6.2	8.5	1.2	.2	.1	-.1	-.1	.0	
77- 9 700	.546	5.0		1.6	.0	-7.2	9.5	1.3	.7	.3	-.1	-.3	.1	
77-10 700	.610	5.0		.5	-1.2	-8.6	10.8	1.0	.5	-.2	.1	-.2	.1	
77-11 700	.634	5.0		1.9	-1.5	-9.5	11.1	1.0	.7	-.2	.9	-.4	.0	
77-12 500	.926	5.0		.7	-1.0	-3.4	.4	3.6	1.7	.8	1.0	.6	.6	
78- 3 700	.351	10.0		.0	3.1	-4.4	8.5	2.9	.9	1.3	1.1	.6	.4	
78- 4 700	.351	11.0		.3	2.7	-6.0	7.0	2.6	.9	1.3	1.1	.6	.4	
78- 5 700	.351	12.0		-.1	2.0	-10.3	1.9	1.7	1.4	1.1	.6	.0	-.1	

BLADE .18R TORSIONAL MOMENT HARMONICS (IN.-LB)														
RUN- PT. NO.	GMS OR (PPS)	MU	TMEC (DEC)	BLADE .18R TORSIONAL MOMENT HARMONICS (IN.-LB)										
				B1	B2	B3	B4	B5	B6	B7	B8	B9	B10	
77- 3 700	.351	10.0		9.1	7.7	-3.0	-0.5	-4.0	-.9	.5	.7	.3	.2	
77- 4 700	.351	11.0		7.7	7.9	-5.0	-10.2	-6.0	-2.3	-.6	-.1	-.2	-.2	
77- 5 700	.410	6.0		3.0	4.5	-.4	3.7	-5.9	.0	.3	.2	.3	.1	
77- 6 700	.406	4.0		1.0	2.9	-2.3	1.9	-1.0	.4	.3	.2	.1	.1	
77- 7 700	.406	5.0		1.9	3.7	-1.9	2.0	-.3	.4	.3	.2	.0	.1	
77- 8 700	.546	4.0		1.6	4.0	-3.2	2.1	-.3	.5	.5	.2	.1	.0	
77- 9 700	.546	5.0		2.2	6.2	-2.7	4.6	-1.2	.7	.7	-.2	-.3	.0	
77-10 700	.610	5.0		1.0	5.0	-1.8	4.7	-2.4	.2	.4	.5	.1	.1	
77-11 700	.634	5.0		1.0	5.0	-1.0	11.4	-3.0	.3	.0	.1	.1	.0	
77-12 500	.906	5.0		-.7	2.0	6.0	-11.4	-3.2	-2.7	-.1	.3	.1	.0	
78- 3 700	.351	10.0		9.2	7.2	-3.5	-12.2	-6.4	-2.4	-.5	-.2	-.3	-.2	
78- 4 700	.351	11.0		8.4	6.1	-3.0	-12.2	-8.4	-2.5	-1.0	-.8	-.9	-.1	
78- 5 700	.351	12.0		10.0	4.0	-3.0				-1.0	-.8	-.9	-.1	

TABLE LXVII - Concluded														
BLADE .10R TORSIONAL MOMENT HARMONICS (IN.-LB)														
RUN- PT. NO.	ONS OR (FPS)	MU	THC (DEG)	R5	R1	R2	R3	R4	R5	R6	R7	R8	R9	R10
77- 3 700	.351	10.0	.7	7.2	7.7	7.9	7.2	13.0	8.5	2.4	1.2	.9	.6	.4
77- 4 700	.351	11.0	.3	7.7	7.9	7.9	9.5	12.2	8.6	3.0	1.6	.9	.5	.3
77- 5 700	.410	6.0	3.3	3.2	4.7	4.7	2.9	7.5	1.2	.8	.3	.3	.3	.2
77- 6 700	.406	4.0	3.0	2.4	2.9	2.9	5.3	7.0	1.2	.4	.3	.2	.1	.1
77- 7 700	.406	5.0	3.2	2.6	3.7	3.7	5.4	6.3	1.2	.4	.3	.2	.1	.1
77- 8 700	.546	4.0	2.9	2.3	3.9	3.9	7.0	6.7	1.3	.6	.4	.2	.1	.1
77- 9 700	.546	5.0	3.1	2.4	4.6	4.6	7.7	9.7	1.4	.5	.5	.2	.1	.1
77-10 700	.610	5.0	2.0	2.2	6.3	6.3	8.6	11.5	1.8	1.0	.8	.2	.1	.1
77-11 700	.624	5.0	3.4	2.2	5.2	5.2	9.6	12.1	3.0	.5	.4	.3	.2	.2
77-12 500	.926	5.0	-2.9	1.0	2.2	2.2	6.9	1.5	3.7	1.7	1.1	1.0	.4	.0
78- 3 700	.351	10.0	1.5	7.2	7.9	7.9	5.7	14.2	8.9	2.6	1.3	1.0	.8	.6
78- 4 700	.351	11.0	1.1	8.4	8.5	8.5	7.7	14.2	6.1	2.9	1.4	1.1	.7	.5
78- 5 700	.351	12.0	-1.3	10.0	9.3	9.3	10.7	12.3	8.7	2.9	1.5	.9	.4	.1

TABLE LXVIII. BLADE FLAP MOTION HARMONICS - RUNS 77-78
(BLADE CENTER OF GRAVITY AT .30 CHORD)

RUN- PT. NO.	ONS OR (FPS)	MU	THEC (DEG)	BLADE FLAP MOTION HARMONICS (DEG)					
				A1	A2	A3	A4	A5	A6
77- 3 700	.351	10.0	.1	-.3	.4	-.1	-.1	.0	
77- 4 700	.351	11.0	.2	-.3	.4	-.1	-.1	.0	
77- 5 700	.410	6.0	.1	-.2	.4	.0	.1	.0	
77- 6 700	.406	4.0	.1	-.1	.5	-.1	.1	.0	
77- 7 700	.406	5.0	.1	-.2	.5	-.1	.1	.0	
77- 8 700	.546	4.0	.0	-.1	.5	-.1	.0	.0	
77- 9 700	.546	5.0	.0	-.2	.6	-.1	.0	.0	
77-10 700	.610	5.0	.2	-.1	.6	-.1	-.1	.0	
77-11 700	.634	5.0	.2	-.1	.6	-.1	-.2	.0	
77-12 800	.926	5.0	-.4	-.4	.3	.2	.0	-.1	
77-13 800	.958	5.0	-.3	-.4	.3	.2	.0	.1	
78- 3 700	.351	10.0	.1	-.5	.4	-.1	-.1	.0	
78- 4 700	.351	11.0	.3	-.5	.4	-.1	-.1	.0	
78- 5 700	.351	12.0	.3	-.5	.4	.0	-.1	.0	
78- 6 700	.410	10.0	.2	-.5	.6	-.1	.1	.0	

RUN- PT. NO.	ONS OR (FPS)	MU	THEC (DEG)	BLADE FLAP MOTION HARMONICS (DEG)					
				B1	B2	B3	B4	B5	B6
77- 3 700	.351	10.0	.1	-.5	.1	.1	-.1	.0	
77- 4 700	.351	11.0	.3	-.6	.1	.1	-.1	.0	
77- 5 700	.410	6.0	.0	-.3	.1	.0	.0	.0	
77- 6 700	.406	4.0	.1	-.3	.0	.1	-.1	.0	
77- 7 700	.406	5.0	.2	-.3	-.1	.1	-.1	.0	
77- 8 700	.546	4.0	.1	-.4	.0	.1	-.1	.0	
77- 9 700	.546	5.0	.1	-.4	-.1	.1	-.2	.0	
77-10 700	.610	5.0	.1	-.5	-.1	.2	-.2	.0	
77-11 700	.634	5.0	.1	-.5	-.1	.2	-.2	.0	
77-12 800	.926	5.0	-.1	-.1	-1.1	.1	.1	.1	
77-13 800	.958	5.0	-.1	-.1	-1.2	.1	.2	-.2	
78- 3 700	.351	10.0	.1	-.4	-.1	.2	.0	.0	
78- 4 700	.351	11.0	.2	-.6	.0	.2	.0	.0	
78- 5 700	.351	12.0	.3	-.7	.0	.2	.0	.0	
78- 6 700	.410	10.0	.1	-.6	-.1	.2	.0	.0	

TABLE LXVIII - Concluded

BLADE FLAP MOTION HARMONICS (DEG)										
RUN- PT. NO.	OMS SR (FPS)	MU	THEC (DEG)	RS	R1	R2	R3	R4	R5	R6
77- 3 700		.351	10.0	3.1	.2	.6	.4	.2	.1	.0
77- 4 700		.351	11.0	3.2	.3	.7	.4	.2	.1	.0
77- 5 700		.410	6.0	1.9	.1	.3	.5	.1	.1	.0
77- 6 700		.406	4.0	1.1	.2	.3	.5	.1	.1	.0
77- 7 700		.406	5.0	1.4	.2	.4	.5	.1	.1	.0
77- 8 700		.546	4.0	.9	.1	.4	.5	.1	.1	.0
77- 9 700		.546	5.0	1.1	.1	.4	.6	.1	.2	.0
77-10 700		.610	5.0	.8	.3	.5	.6	.2	.3	.0
77-11 700		.634	5.0	.8	.2	.5	.6	.2	.3	.0
77-12 800		.926	5.0	.6	.4	.4	1.2	.2	.1	.2
77-13 800		.958	5.0	.3	.4	.4	1.2	.2	.1	.2
78- 3 700		.351	10.0	3.5	.2	.6	.4	.2	.1	.0
78- 4 700		.351	11.0	3.6	.4	.7	.4	.2	.1	.0
78- 5 700		.351	12.0	3.8	.4	.8	.4	.2	.1	.0
78- 6 700		.410	10.0	3.2	.2	.7	.6	.2	.1	.0

TABLE LXIX. BLADE .30R CHORDWISE BENDING MOMENT HARMONICS - RUNS 77-78
(BLADE CENTER OF GRAVITY AT .30 CHORD)

BLADE .30R CHORDWISE BENDING MOMENT HARMONICS (IN.-LB)													
RUN- PT. NO.	OMS #R (FPS)	MU	(DEG)	A1	A2	A3	A4	A5	A6	A7	A8	A9	A10
77- 3 700	.351	10.0	-7.0	2.9	.7	-26.9	-1.7	-1.2	-.5	.2	1.6	1.6	1.2
77- 4 700	.351	1.0	-7.5	2.8	1.6	-17.8	-2.0	-1.2	-.4	.0	1.6	1.6	.3
77- 5 700	.410	6.0	-4.3	1.9	-1.5	-19.8	.3	-.5	-.5	-.4	.4	.4	.6
77- 6 700	.486	4.0	-2.6	2.0	-.5	-13.8	.7	-.8	.0	.1	-.3	-.3	-.3
77- 7 700	.486	5.0	-3.6	2.2	-1.1	-19.2	1.1	-.6	.2	.1	-.6	-.5	.0
77- 8 700	.546	4.0	-2.0	2.4	-1.1	-17.2	.5	-.8	-.1	.0	-.5	-.5	.5
77- 9 700	.546	5.0	-2.7	2.7	-1.5	-22.2	.6	-.8	.0	.3	-.7	-.7	.7
77-10 700	.610	5.0	-2.0	2.9	2.0	-20.0	-.2	.0	-.0	.3	.0	.0	-.6
77-11 700	.634	5.0	-1.9	3.3	-2.3	-23.8	-.6	-.5	-.2	-.3	.4	.4	.8
77-12 800	.926	5.0	.1	4.0	-1.2	3.1	-19.0	1.2	-.7	.4	.0	.0	.6
77-13 800	.958	5.0	-1.0	4.4	-1.3	3.7	-20.2	1.5	-.8	.3	.1	.7	.1
78- 3 700	.351	10.0	-2.5	2.2	-.3	-18.4	-1.6	-.9	-.3	-.3	1.3	1.3	.1
78- 4 700	.351	11.0	-2.2	2.2	.3	-10.3	-1.2	-.6	-.8	-.9	.3	.3	-.3
78- 5 700	.351	12.0	-1.7	2.0	.8	-1.9	-1.0	-.3	.0	-.8	.2	.2	-.3
78- 6 700	.410	10.0	-3.1	-.9	-2.5	-31.6	2.0	-.3	.2	.9	1.1	1.1	2.5

BLADE .30R CHORDWISE BENDING MOMENT HARMONICS (IN.-LB)													
RUN- PT. NO.	OMS #R (FPS)	MU	THEC (DEG)	B1	B2	B3	B4	B5	B6	B7	B8	B9	B10
77- 3 700	.351	10.0	6.6	1.1	-4.5	9.3	-1.4	-.5	-.9	-1.3	-.1	-.1	-.2
77- 4 700	.351	11.0	6.8	.2	-5.3	11.2	-.5	-.3	-.4	-1.3	-.6	-.6	.3
77- 5 700	.410	6.0	-1.9	-.2	-2.1	1.3	-1.9	-.2	-.2	-.2	.1	-.1	-.8
77- 6 700	.486	4.0	-4.4	.9	-1.3	-15.2	.1	-.5	-.6	-.3	-.8	-.8	.5
77- 7 700	.486	5.0	-2.9	.8	-1.3	-16.4	-.6	-.2	-.4	-.4	-.8	-.7	.7
77- 8 700	.546	4.0	-4.8	.8	-1.1	-14.1	.0	-.2	-.6	-.4	-.6	-.6	.8
77- 9 700	.546	5.0	-5.1	.7	-1.7	-18.5	-.3	-.1	-.6	-.6	-.7	1.0	1.0
77-10 700	.610	5.0	-5.5	.7	-1.2	-22.0	-.7	.8	-.4	-1.0	.7	1.2	1.2
77-11 700	.634	5.0	-5.6	.7	-1.3	-21.6	-.6	.2	-.4	-1.1	.3	1.0	1.0
77-12 800	.926	5.0	-7.7	.3	-5.9	10.8	13.4	.7	.1	-.4	-.8	-.8	-.3
77-13 800	.958	5.0	-9.2	.3	-5.3	11.3	17.4	.2	.6	-.5	-.8	-.5	.5
78- 3 700	.351	10.0	8.8	2.1	-3.3	20.9	-.2	.0	-.2	-1.3	-.9	-.9	.5
78- 4 700	.351	11.0	10.6	1.8	-4.1	20.7	.2	.4	-.2	-.8	-1.8	-.5	.8
78- 5 700	.351	12.0	12.6	1.2	-5.4	15.8	.5	.3	-.5	-.5	-1.2	1.8	.3
78- 6 700	.410	10.0	7.4	2.2	-3.9	2.1	-.5	.0	-.9	-.8	1.8	1.8	.3

TABLE LXIX - Concluded

TABLE LXIX - Concluded														
BLADE .30R CHORDWISE BENDING MOMENT HARMONICS (IN.-LB)														
RUN- PT. NO.	OMS #R (FPS)	MU	THEC (DEG)	RS	R1	R2	R3	R4	R5	R6	R7	R8	R9	R1
77- 3 700		.351	10.0	13.1	9.7	3.1	4.5	28.5	2.2	1.3	1.0	1.3	1.6	1.3
77- 4 700		.351	11.0	14.1	11.6	2.8	5.5	21.0	2.1	1.2	.6	1.3	1.7	.4
77- 5 700		.410	6.0	8.1	4.7	1.9	2.6	19.8	1.9	.5	.7	.5	.4	1.9
77- 6 700		.486	4.0	7.4	5.1	2.2	1.4	20.6	.8	.9	.6	.4	.8	.6
77- 7 700		.486	5.0	7.6	4.6	2.3	1.7	25.3	1.2	.6	.5	.4	1.0	.9
77- 8 700		.546	4.0	7.5	5.3	2.6	1.6	22.3	.5	.9	.6	.4	.8	1.0
77- 9 700		.546	5.0	7.9	5.7	2.7	2.2	28.9	.7	.8	.6	.6	1.0	1.2
77-10 700		.610	5.0	7.8	5.8	3.0	2.3	29.8	.8	.8	.4	1.0	.7	1.4
77-11 700		.634	5.0	7.4	5.9	3.4	2.6	32.2	.8	.6	.5	1.1	.3	1.3
77-12 500		.926	5.0	18.4	7.7	4.0	5.3	11.2	23.2	1.4	.7	.6	.5	.6
77-13 500		.958	5.0	18.3	9.3	4.4	6.1	11.9	26.7	1.5	1.0	.8	.8	1.0
78- 3 700		.351	10.0	10.4	9.1	3.1	3.6	27.9	1.6	.9	.4	1.3	1.6	.5
78- 4 700		.351	11.0	12.3	10.8	2.9	4.2	23.1	1.3	.7	.2	1.2	1.5	.6
78- 5 700		.351	12.0	13.9	12.7	2.4	5.4	15.9	1.1	.4	.1	1.0	1.3	.9
78- 6 700		.410	10.0	10.4	8.0	2.3	4.7	31.7	2.0	.3	.9	1.1	2.1	2.5

TABLE LXX. BLADE LAG MOTION HARMONICS - RUN 79
(BLADE CENTER OF GRAVITY AT .30 CHORD)

RUN- PT. NO.	OMS *R (FPS)	MU	THEC (DEG)	BLADE LAG MOTION HARMONICS (DEG)				
				A1	A2	A3	A4	A5
79- 3	500	.657	13.0	-.5	.1	.3	-.2	.0
79- 4	500	.766	12.0	-.4	.1	.2	-.2	.2
79- 5	500	.857	12.0	-.4	.1	.1	-.3	.1
79- 6	500	.890	12.0	-.4	.1	.2	-.3	.1
79- 7	500	.926	12.0	-.4	.1	.2	-.3	.1
79- 8	500	.958	12.0	-.4	.1	.2	-.3	.2
79- 9	500	.991	12.0	-.4	.1	.2	-.3	.1
79-10	500	1.026	11.0	-.3	.2	.1	-.3	.2
79-11	500	1.062	8.0	-.2	.1	.2	-.1	.2

RUN- PT. NO.	OMS *R (FPS)	MU	THEC (DEG)	BLADE LAG MOTION HARMONICS (DEG)				
				B1	B2	B3	B4	B5
79- 3	500	.657	13.0	.2	.2	.0	-.1	.0
79- 4	500	.766	12.0	.0	.2	-.2	-.2	-.1
79- 5	500	.857	12.0	-.1	.2	-.3	-.1	-.3
79- 6	500	.890	12.0	-.2	.2	-.3	-.1	-.3
79- 7	500	.926	12.0	-.3	.2	-.4	-.1	-.3
79- 8	500	.958	12.0	-.3	.3	-.4	-.1	-.3
79- 9	500	.991	12.0	-.4	.3	-.4	-.1	-.4
79-10	500	1.026	11.0	-.5	.2	-.4	-.1	-.4
79-11	500	1.062	8.0	-.5	.2	-.2	-.1	-.3

TABLE LXX - Concluded										
RUN- PT. NO.	OMS #R (FPS)	MU	THEC (DEG)	BLADE LAG MOTION HARMONICS (DEG)					R5	R5
				RS	R1	R2	R3	R4		
79- 3	500	.657	13.0	5.7	.5	.2	.3	.2	.0	.0
79- 4	500	.766	12.0	4.2	.4	.2	.3	.3	.2	.2
79- 5	500	.857	12.0	3.8	.4	.2	.4	.3	.3	.3
79- 6	500	.890	12.0	3.6	.4	.3	.4	.3	.3	.3
79- 7	500	.926	12.0	3.7	.5	.3	.4	.3	.4	.4
79- 8	500	.958	12.0	3.1	.5	.3	.4	.3	.4	.4
79- 9	500	.991	12.0	2.8	.6	.3	.4	.3	.4	.4
79-10	500	1.026	11.0	2.3	.6	.3	.4	.3	.4	.4
79-11	500	1.062	8.0	2.2	.5	.2	.3	.2	.4	.4

TABLE LXXI. BLADE .30R FLAPWISE BENDING MOMENT HARMONICS - RUN 79 (BLADE CENTER OF GRAVITY AT .30 CHORD)															
BLADE .30R FLAPWISE BENDING MOMENT HARMONICS (IN.-LB)															
RUN- PT. NO.	QMS OR (FPS)	MU	THEC (DEG)	A1	A2	A3	A4	A5	A6	A7	A8	A9	A10	A11	A12 A13
79- 3 500	.657	13.0	1.8	-5.0	-3.7	-1.6	2.4	-0.8	1.0	.0	-0.4	.6	-0.6	-0.1	-0.1
79- 4 500	.766	12.0	1.9	-7.2	.9	-3.6	-1.0	3.2	.5	1.2	.0	-0.2	.2	.1	.1
79- 5 500	.857	12.0	2.7	-8.9	1.7	-4.2	.8	3.7	-0.1	1.0	.1	1.6	1.4	-0.1	-0.1
79- 6 500	.890	12.0	3.1	-9.4	4.3	-4.3	.3	4.7	-0.1	1.3	.1	-2.4	1.8	.1	-0.1
79- 7 500	.926	12.0	3.5	-11.1	6.6	-4.6	-0.1	3.8	-0.5	.6	1.1	-2.7	1.4	.1	-0.2
79- 8 500	.958	12.0	3.7	-12.0	7.9	-4.9	-1.1	2.4	-0.8	.4	1.5	-1.6	.9	.2	-0.1
79- 9 500	.991	12.0	4.1	-12.7	9.6	-6.3	.1	.1	-1.3	.5	1.7	-1.6	.9	.3	.0
79-10 500	1.026	11.0	4.1	-13.3	8.8	-5.4	-2.4	-1.4	-1.9	-0.3	1.4	1.1	-0.5	.1	.1

BLADE .30R FLAPWISE BENDING MOMENT HARMONICS (IN.-LB)															
RUN- PT. NO.	QMS OR (FPS)	MU	THEC (DEG)	B1	B2	B3	B4	B5	B6	B7	B8	B9	B10	B11	B12 B13
79- 3 500	.657	13.0	.6	.3	1.0	12.4	-1.1	-1.3	-1.1	1.0	1.0	.4	.3	.2	.0
79- 4 500	.766	12.0	-0.3	1.0	16.4	1.1	1.5	-2.3	2.6	-0.2	-0.3	1.2	-0.7	.5	-0.1
79- 5 500	.857	12.0	-1.3	-2.2	18.4	1.6	2.4	-6.8	8.1	.3	.5	1.5	.0	-0.4	.0
79- 6 500	.890	12.0	-1.0	-2.2	18.4	2.5	2.5	-8.0	9.9	-0.1	-0.9	1.0	2.6	-1.7	.0
79- 7 500	.926	12.0	-2.2	-3.2	17.8	2.2	2.2	-9.4	10.9	-0.3	-1.1	.5	4.3	-2.2	-0.1
79- 8 500	.958	12.0	-2.3	-3.2	17.5	4.0	4.0	-10.8	9.1	-0.1	-1.3	.5	4.9	-2.1	-0.1
79- 9 500	.991	12.0	-3.7	-0.1	16.9	4.0	4.0	-11.5	10.9	.0	-1.2	-0.7	4.9	-2.6	-0.2
79-10 500	1.026	11.0													

TABLE LXXI - Concluded																			
RUN- PT. QMS NO. OR		BLADE .30R FLAPWISE BENDING MOMENT HARMONICS (IN.-LB)																	
(FPS)		MU	THEC (DEG)	RS	R1	R2	R3	R4	R5	R6	R7	R8	R9	R10	R11	R12	R13		
79- 3	500	.657	13.0	5.1	1.9	5.0	12.9	1.9	2.8	1.3	1.4	1.0	.6	.7	.6	.1	.1		
79- 4	500	.766	12.0	5.2	1.9	7.3	16.1	3.6	4.4	4.1	1.0	1.2	.6	.7	.5	.1	.2		
79- 5	500	.857	12.0	5.5	2.8	8.9	18.5	4.4	5.4	8.3	.2	1.1	1.2	1.6	1.4	.1	.1		
79- 6	500	.890	12.0	5.2	3.4	9.7	18.9	4.6	6.8	9.4	.3	1.3	1.5	2.4	1.8	.1	.1		
79- 7	500	.926	12.0	5.6	3.7	11.3	18.8	5.2	8.0	10.6	.5	1.1	1.5	3.7	2.2	.3	.2		
79- 8	500	.958	12.0	5.5	4.3	12.3	19.5	5.5	9.4	11.1	.9	1.2	1.6	4.7	2.4	.4	.1		
79- 9	500	.991	12.0	5.5	4.7	13.1	20.0	6.7	10.8	9.1	1.3	1.3	1.8	5.2	2.3	.5	.1		
79-10	500	1.026	11.0	5.4	5.5	13.3	19.0	6.7	11.8	11.0	1.9	1.3	1.6	5.0	2.6	.6	.2		

TABLE LXXII. BLADE .18R TORSIONAL MOMENT HARMONICS - RUN 79 (BLADE CENTER OF GRAVITY AT .30 CHORD)																										
BLADE .18R TORSIONAL MOMENT HARMONICS (IN.-LB)																										
RUN- PT. NO.	OMS OR (FPS)	THEC (DEG)	MJ	A1	A2	A3	A4	A5	A6	A7	A8	A9	A10	A11	A12	A13										
79- 3 500	.657	13.0		.7	.4	-5.5	-4.5	-2.7	-2.7	-4	-2	.1	.2	.2	.1	-.1										
79- 4 500	.766	12.0		2.2	.0	-2.7	-3.5	.1	-1.5	-.8	-.1	-.3	-.3	.0	.0	.1										
79- 5 500	.857	12.0		2.5	-.7	-4.4	-4.6	4.1	-.5	.3	.5	.3	.2	-.1	.1	.1										
79- 6 500	.890	12.0		2.8	-1.2	-5.4	-7.5	5.7	.0	.1	.0	.4	.4	-.3	.1	.2										
79- 7 500	.926	12.0		2.9	-2.1	-4.0	-8.9	7.5	.3	.5	-.7	.4	.8	-.2	.2	.2										
BLADE .18R TORSIONAL MOMENT HARMONICS (IN.-LB)																										
RUN- PT. NO.	OMS OR (FPS)	THEC (DEG)	MJ	B1	B2	B3	B4	B5	B6	B7	B8	B9	B10	B11	B12	B13										
79- 3 500	.657	13.0		-.3	3.8	7.6	-1.6	.6	-4.7	-2.0	-.7	.0	-.9	-.5	-.4	-.4										
79- 4 500	.766	12.0		-.4	2.6	11.3	2.2	1.4	-3.3	-.6	-.6	.6	-.1	-.1	-.1	.0										
79- 5 500	.857	12.0		-6.1	2.5	13.3	1.0	-.1	-1.5	-.8	-1.6	.2	.3	-.2	-.2	-.1										
79- 6 500	.890	12.0		-7.4	2.6	15.2	1.3	-1.6	-1.2	-1.2	-2.5	-.3	.4	-.1	-.2	-.2										
79- 7 500	.926	12.0		-9.6	2.3	17.3	.5	-3.6	1.2	-.6	-2.3	-.8	.2	.1	-.2	-.4										
BLADE .18R TORSIONAL MOMENT HARMONICS (IN.-LB)																										
RUN- PT. NO.	OMS OR (FPS)	THEC (DEG)	MJ	R5	R1	R2	R3	R4	R5	R6	R7	R8	R9	R10	R11	R12	R13									
79- 3 800	.657	13.0		.9	.7	3.8	9.4	4.5	2.8	5.4	2.1	.7	.6	.9	.6	.4	.4									
79- 4 800	.766	12.0		2.4	4.2	2.6	11.6	4.1	1.4	3.6	1.0	.6	.4	.3	.1	.1	.1									
79- 5 500	.857	12.0		3.6	6.6	2.6	14.0	4.7	4.1	1.6	.9	1.6	.3	.4	.2	.2	.2									
79- 6 500	.890	12.0		4.3	7.9	2.8	16.1	7.6	5.9	1.2	1.2	2.5	.5	.5	.3	.2	.3									
79- 7 500	.926	12.0		5.3	10.0	3.1	17.8	8.9	8.3	1.2	.8	2.5	.9	.8	.3	.2	.5									

TABLE LXXIII. BLADE FLAP MOTION HARMONICS - RUN 79 (BLADE CENTER OF GRAVITY AT .30 CHORD)										
BLADE FLAP MOTION HARMONICS (DEG)										
RUN- PT. NO.	OMS #R (FPS)	MU	THEC (DEG)	A1	A2	A3	A4	A5	A6	
79- 3 500		.657	13.0	-.8	-1.0	.5	.2	.0	.0	
79- 4 500		.766	12.0	.2	-1.0	.0	.3	.1	-.1	
79- 5 500		.857	12.0	-.2	-1.0	.0	.4	.1	.0	
79- 6 500		.890	12.0	-.5	-1.1	-.3	.4	.0	-.1	
79- 7 500		.926	12.0	.3	-1.0	-.6	.5	.1	.0	
79- 8 500		.958	12.0	-.2	-1.1	-.7	.6	.1	-.1	
79- 9 500		.991	12.0	.2	-1.2	-.6	.7	.1	.0	
79-10 500		1.026	11.0	.0	-.9	-.9	.7	.4	.0	
79-11 500		1.062	8.0	-.1	-.8	-.9	.7	.2	.0	

BLADE FLAP MOTION HARMONICS (DEG)										
RUN- PT. NO.	OMS #R (FPS)	MU	THEC (DEG)	B1	B2	B3	B4	B5	B6	
79- 3 500		.657	13.0	-.1	-.2	-1.2	.2	.1	.1	
79- 4 500		.766	12.0	.0	.1	-1.6	.0	.2	.2	
79- 5 500		.857	12.0	-.3	.2	-1.9	.0	.3	-.3	
79- 6 500		.890	12.0	-.3	.2	-2.0	.0	.4	-.3	
79- 7 500		.926	12.0	.0	.4	-2.0	.0	.5	-.4	
79- 8 500		.958	12.0	-.2	.3	-2.0	-.1	.6	-.4	
79- 9 500		.991	12.0	-.2	.4	-2.1	-.1	.6	-.3	
79-10 500		1.026	11.0	-.3	.7	-2.0	-.1	.6	-.4	
79-11 500		1.062	8.0	-.2	.5	-1.8	-.3	.6	-.3	

TABLE LXXIII - Concluded										
BLADE FLAP MOTION HARMONICS (DEG)										
RUN- PT. NO.	QMS OR (FPS)	MU	THEC (DEG)	RS	R1	R2	R3	R4	R5	R6
79- 3 500		.657	13.0	2.4	.2	.9	1.3	.2	.1	.1
79- 4 500		.766	12.0	1.6	.2	1.0	1.6	.3	.2	.1
79- 5 500		.857	12.0	1.3	.4	1.0	1.9	.4	.3	.3
79- 6 500		.890	12.0	1.2	.6	1.1	2.0	.4	.4	.3
79- 7 500		.926	12.0	.9	.3	1.1	2.0	.5	.5	.4
79- 8 500		.958	12.0	.9	.3	1.2	2.2	.6	.6	.4
79- 9 500		.991	12.0	.7	.3	1.2	2.3	.7	.7	.3
79-10 500		1.026	11.0	.5	.3	1.2	2.2	.7	.7	.4
79-11 500		1.062	8.0	.2	.2	1.0	1.9	.7	.6	.3

TABLE LXXIV. BLADE .30R CHORDWISE BENDING MOMENT HARMONICS - RUN 79																								
(BLADE CENTER OF GRAVITY AT .30 CHORD)																								
BLADE .30R CHORDWISE BENDING MOMENT HARMONICS (IN.-LB)																								
BLADE	CT.	CHORD	Y	Y ²	Y ³	Y ⁴	Y ⁵	Y ⁶	Y ⁷	Y ⁸	Y ⁹	Y ¹⁰	Y ¹¹	Y ¹²	Y ¹³	Y ¹⁴	Y ¹⁵	Y ¹⁶	Y ¹⁷	Y ¹⁸	Y ¹⁹	Y ²⁰	Y ²¹	Y ²²
PT.	CHORD	Y	Y ²	Y ³	Y ⁴	Y ⁵	Y ⁶	Y ⁷	Y ⁸	Y ⁹	Y ¹⁰	Y ¹¹	Y ¹²	Y ¹³	Y ¹⁴	Y ¹⁵	Y ¹⁶	Y ¹⁷	Y ¹⁸	Y ¹⁹	Y ²⁰	Y ²¹	Y ²²	Y ²³
NO.	CHORD	Y	Y ²	Y ³	Y ⁴	Y ⁵	Y ⁶	Y ⁷	Y ⁸	Y ⁹	Y ¹⁰	Y ¹¹	Y ¹²	Y ¹³	Y ¹⁴	Y ¹⁵	Y ¹⁶	Y ¹⁷	Y ¹⁸	Y ¹⁹	Y ²⁰	Y ²¹	Y ²²	Y ²³
1	100	1.000	1.000	1.000	1.000	1.000	1.000	1.000	1.000	1.000	1.000	1.000	1.000	1.000	1.000	1.000	1.000	1.000	1.000	1.000	1.000	1.000	1.000	1.000
2	100	1.000	1.000	1.000	1.000	1.000	1.000	1.000	1.000	1.000	1.000	1.000	1.000	1.000	1.000	1.000	1.000	1.000	1.000	1.000	1.000	1.000	1.000	1.000
3	100	1.000	1.000	1.000	1.000	1.000	1.000	1.000	1.000	1.000	1.000	1.000	1.000	1.000	1.000	1.000	1.000	1.000	1.000	1.000	1.000	1.000	1.000	1.000
4	100	1.000	1.000	1.000	1.000	1.000	1.000	1.000	1.000	1.000	1.000	1.000	1.000	1.000	1.000	1.000	1.000	1.000	1.000	1.000	1.000	1.000	1.000	1.000
5	100	1.000	1.000	1.000	1.000	1.000	1.000	1.000	1.000	1.000	1.000	1.000	1.000	1.000	1.000	1.000	1.000	1.000	1.000	1.000	1.000	1.000	1.000	1.000
6	100	1.000	1.000	1.000	1.000	1.000	1.000	1.000	1.000	1.000	1.000	1.000	1.000	1.000	1.000	1.000	1.000	1.000	1.000	1.000	1.000	1.000	1.000	1.000
7	100	1.000	1.000	1.000	1.000	1.000	1.000	1.000	1.000	1.000	1.000	1.000	1.000	1.000	1.000	1.000	1.000	1.000	1.000	1.000	1.000	1.000	1.000	1.000
8	100	1.000	1.000	1.000	1.000	1.000	1.000	1.000	1.000	1.000	1.000	1.000	1.000	1.000	1.000	1.000	1.000	1.000	1.000	1.000	1.000	1.000	1.000	1.000
9	100	1.000	1.000	1.000	1.000	1.000	1.000	1.000	1.000	1.000	1.000	1.000	1.000	1.000	1.000	1.000	1.000	1.000	1.000	1.000	1.000	1.000	1.000	1.000
10	100	1.000	1.000	1.000	1.000	1.000	1.000	1.000	1.000	1.000	1.000	1.000	1.000	1.000	1.000	1.000	1.000	1.000	1.000	1.000	1.000	1.000	1.000	1.000
11	100	1.000	1.000	1.000	1.000	1.000	1.000	1.000	1.000	1.000	1.000	1.000	1.000	1.000	1.000	1.000	1.000	1.000	1.000	1.000	1.000	1.000	1.000	1.000

TABLE LXXIV - Concluded

TABLE LXXIV - Concluded																
		BLADE .308 CALIBRE WOLF BULLET HARMONICS (IN.-LB)														
Order	Wt. (lb.)	Wt. (lb.)	R1	R2	R3	R4	R5	R6	R7	R8	R9	R10	R11	R12	R13	
1	100	12.0	7.3	7.0	6.8	13.0	9.5	9.1	2.3	.5	1.1	.5	.2	.6	.5	
2	100	12.0	6.9	6.7	6.6	20.2	24.3	5.2	3.4	1.0	1.2	.3	.4	.9	.5	
3	100	12.0	6.7	6.5	6.4	22.9	37.2	.6	6.5	1.2	1.4	1.4	1.3	1.4	2.7	
4	100	12.0	6.5	6.3	6.2	24.1	43.7	9.7	6.5	1.2	1.5	3.1	1.7	1.4	3.5	
5	100	12.0	6.3	6.1	6.0	25.3	48.1	4.3	6.5	1.2	1.5	3.1	2.0	1.9	3.4	
6	100	12.0	6.1	5.9	5.8	26.5	53.5	2.1	7.0	1.2	1.4	4.5	2.1	2.4	2.8	
7	100	12.0	5.9	5.7	5.6	27.7	58.9	1.9	6.3	1.2	1.1	5.0	2.6	2.1	1.5	
8	100	12.0	5.7	5.5	5.4	28.9	64.3	1.1	6.2	1.2	1.2	6.4	3.4	3.2	1.7	
9	100	12.0	5.5	5.3	5.2	30.1	69.7	1.1	6.2	.3	.5	5.2	3.4	3.2	1.7	

TABLE LXXV. BLADE .35R TORSIONAL MOMENT HARMONICS - RUN 79 (BLADE CENTER OF GRAVITY AT .30 CHORD)																									
BLADE .35R TORSIONAL MOMENT HARMONICS (IN.-LB)																									
RUN- PT. NO.	QMS PR (FPS)	MU	THEC (DEG)	A1	A2	A3	A4	A5	A6	A7	A8	A9	A10	A11	A12	A13									
79- 5 500	.857	12.0	1.5	.2	-1.1	-3.6	1.6	.2	-.2	.1	1.1	.1	-.1	-.9	.3										
79- 6 500	.890	12.0	1.9	.7	-3.7	-8.0	5.4	.5	.2	-.5	.6	.3	-.3	-.6	.4										
79- 7 500	.926	12.0	1.2	-.8	-2.2	-9.1	5.8	-.2	3.9	-1.3	.2	.2	.2	-.4	.6										
79- 8 500	.958	12.0	1.7	-.6	-3.5	-8.2	8.0	.6	.8	-1.2	.3	.3	.4	-.7	.4										
79- 9 500	.991	12.0	2.2	-1.3	-4.0	-10.5	8.6	1.8	1.1	-1.0	.0	.0	.3	-.3	.4										
79-10 500	1.026	11.0	2.5	-2.0	-3.2	-9.8	9.1	3.2	1.1	-1.1	.7	.5	.4	-.1	.2										
BLADE .35R TORSIONAL MOMENT HARMONICS (IN.-LB)																									
RUN- PT. NO.	QMS PR (FPS)	MU	THEC (DEG)	B1	B2	B3	B4	B5	B6	B7	B8	B9	B10	B11	B12	B13									
79- 5 500	.857	12.0	-2.7	2.2	11.4	2.3	-1.7	-.6	-.3	-1.5	.3	.1	.1	.1	.3	-.4									
79- 6 500	.890	12.0	-5.0	2.8	14.6	1.9	-3.4	-.5	.4	-4.3	.1	.1	.1	-.1	-.5										
79- 7 500	.926	12.0	-5.4	1.8	14.6	1.6	-4.7	.8	-.7	-2.6	.0	.5	.5	-.5	-.3	-.9									
79- 8 500	.958	12.0	-6.7	1.6	15.5	1.9	-6.1	1.0	-.8	-3.0	-.1	.2	.2	-.4	-.5	-.8									
79- 9 500	.991	12.0	-7.8	.8	16.8	.6	-8.8	1.9	-.2	-2.8	-.3	-.1	-.1	-.6	-.3	-.3									
79-10 500	1.026	11.0	-8.6	.8	17.4	3.1	-10.8	.6	-.3	-2.1	-.1	-.1	-.4	-.4	-.2	.0									
BLADE .35R TORSIONAL MOMENT HARMONICS (IN.-LB)																									
RUN- PT. NO.	QMS PR (FPS)	MU	THEC (DEG)	R5	R1	R2	R3	R4	R5	R6	R7	R8	R9	R10	R11	R12	R13								
79- 5 500	.857	12.0	-4.1	3.1	2.2	11.4	4.3	2.4	.6	.3	.3	1.5	1.1	.1	.2	.9	.5								
79- 6 500	.890	12.0	-3.0	5.3	2.9	15.0	8.3	6.4	.8	.4	.4	4.3	.6	.4	.3	1.3	.7								
79- 7 500	.926	12.0	1.7	5.5	2.0	14.7	8.2	7.4	.9	.8	.8	2.9	.2	.5	.6	.5	1.0								
79- 8 500	.958	12.0	3.5	6.9	1.7	15.9	9.4	10.1	1.2	.8	.8	3.2	.3	.3	.4	.7	.6								
79- 9 500	.991	12.0	5.6	8.1	1.5	17.2	10.5	12.3	2.6	1.2	1.2	3.0	.3	.5	.7	.4	.5								
79-10 500	1.026	11.0	7.1	9.0	2.1	17.6	10.3	14.1	3.2	1.1	1.1	2.4	.7	.6	.6	.3	.3								

TABLE LXXVI. BLADE LAG MOTION HARMONICS - RUN 80
(BLADE CENTER OF GRAVITY AT .30 CHORD)

BLADE LAG MOTION HARMONICS (DEG)										
RUN- PT. NO.	OMS #R	MU (FPS)	THEC (DEG)	A1	A2	A3	A4	A5		
80- 3	367	.795	2.0	.3	.1	.0	.0	.0		
80- 4	363	.847	2.0	.2	.1	.0	.0	.0		
80- 5	339	.906	2.0	.2	.0	.0	.0	.0		
80- 6	316	.974	2.0	.2	.0	.0	.0	.0		
80- 7	292	1.052	2.0	.0	.0	.0	.0	.0		
80- 8	269	1.144	2.0	-.1	.0	.0	.0	.0		
80- 9	245	1.254	2.0	-.1	.0	.0	.0	.0		
80-10	221	1.388	2.0	-.2	.0	.0	.0	.0		
80-11	211	1.456	2.0	-.3	.1	.0	.0	.0		
BLADE LAG MOTION HARMONICS (DEG)										
RUN- PT. NO.	OMS #R	MU (FPS)	THEC (DEG)	B1	B2	B3	B4	B5		
80- 3	367	.795	2.0	.0	.1	.0	.0	.0		
80- 4	363	.847	2.0	-.1	.1	.0	.0	.0		
80- 5	339	.906	2.0	.2	.1	.0	.0	.0		
80- 6	316	.974	2.0	-.3	.1	.0	.0	.0		
80- 7	292	1.052	2.0	-.4	.1	.0	.0	.0		
80- 8	269	1.144	2.0	-.5	.1	.1	.1	.0		
80- 9	245	1.254	2.0	-.6	.1	.1	.0	.1		
80-10	221	1.388	2.0	-.7	.1	.1	.0	.0		
80-11	211	1.456	2.0	-.7	.1	.1	.1	.1		

TABLE LXXVI - Concluded										
RUN- PT. NO.	OMS GR (FPS)	MU	THEC (DEG)	BLADE LAG MOTION HARMONICS (DEG)					R5	R4
				RS	R1	R2	R3	R4		
80- 3	387	.795	2.0	1.8	.3	.1	.1	.0	.0	.0
80- 4	363	.847	2.0	1.7	.3	.1	.0	.0	.0	.0
80- 5	339	.906	2.0	2.0	.3	.1	.1	.0	.0	.0
80- 6	316	.974	2.0	1.9	.3	.1	.0	.0	.0	.0
80- 7	292	1.052	2.0	1.9	.4	.1	.0	.0	.0	.0
80- 8	269	1.144	2.0	2.4	.5	.1	.1	.1	.0	.0
80- 9	245	1.234	2.0	2.1	.6	.1	.1	.0	.1	.0
80-10	221	1.388	2.0	2.2	.7	.1	.1	.0	.0	.0
80-11	211	1.456	2.0	2.0	.8	.1	.1	.1	.0	.0

TABLE LIXVII. BLADE .30R FLAPWISE BENDING MOMENT HARMONICS - RUN 80 (BLADE CENTER OF GRAVITY AT .30 CHORD)														
BLADE .30R FLAPWISE BENDING MOMENT HARMONICS (IN.-LB)														
BLADE PT. NO.	CMG OR (PPS)	TIME (SEC)	A1	A2	A3	A4	A5	A6	A7	A8	A9	A10		
00-3	207	.795	1.6	-.5	0.7	-.8	-.2	.4	2.0	.3	-.7	-.3		
00-6	203	.607	1.7	-1.2	12.1	-.3	-.6	-.3	1.5	.2	.4	-.5		
00-9	209	.006	1.7	-1.6	6.2	-.3	-.5	.2	.4	.5	.0	-.1		
00-6	206	.076	1.6	-1.6	6.7	-.9	-.6	.3	.5	.5	.3	-.2		
00-7	208	1.002	1.9	-1.9	5.4	-1.0	-.6	.1	.8	.7	.6	-.2		
00-8	200	1.100	1.8	-1.9	5.3	-2.8	-.7	.2	.8	.7	.7	-.2		
00-9	200	1.200	1.6	-2.3	9.7	-.9	-1.1	.1	.5	.4	.7	-.2		
00-10	201	1.300	1.8	-2.7	5.0	-9.6	-2.7	-.2	.0	.2	-.2	2.2		
00-11	211	1.400	.8	-3.0	5.0	-5.9	-2.9	-.4	-.1	.1	-.6	.3		
BLADE .30R FLAPWISE BENDING MOMENT HARMONICS (IN.-LB)														
BLADE PT. NO.	CMG OR (PPS)	TIME (SEC)	B1	B2	B3	B4	B5	B6	B7	B8	B9	B10		
00-3	207	.795	.2	-1.2	0.0	.0	-.8	-2.3	.7	.9	.9	.1		
00-6	203	.607	-.1	-.3	0.0	1.0	-.9	-.6	.7	.7	.3	.2		
00-9	209	.006	.7	-.2	0.0	1.0	-.5	-.6	.0	.5	.6	.3		
00-6	206	.076	-.1	-.1	0.0	-.9	-.3	.0	.4	-.4	.0	.9		
00-7	208	1.002	.8	-.4	2.0	-1.3	-.8	-.6	-.2	.3	.8	.9		
00-8	200	1.100	.3	.9	2.0	5.8	-.8	-.6	-.3	.1	-.3	.9		
00-9	200	1.200	-.1	.7	2.0	5.8	-.8	-.6	-.3	-.1	-.6	-.9		
00-10	201	1.300	-.2	-.3	2.0	10.6	1.2	-.3	-.2	.0	-.3	-1.0		
00-11	211	1.400												

TABLE LXXVII - Concluded															
BLADE .30R FLAPWISE BENDING MOMENT HARMONICS (IN.-LB)															
RUN- PT. NO.	OMS PR (PPS)	MU	THEC (DEG)	RS	R1	R2	R3	R4	R5	R6	R7	R8	R9	R10	
80- 3	387	.795	2.0	-.7	1.6	1.3	13.1	.9	.0	2.4	2.1	.7	1.1	.3	
80- 4	363	.847	2.0	-.4	1.6	1.2	14.7	1.6	1.3	.9	1.6	.7	1.0	.5	
80- 5	334	.906	2.0	.0	1.7	1.5	8.3	.4	.7	.4	.4	.7	.5	.3	
80- 6	316	.974	2.0	.8	1.9	1.4	7.9	1.0	.3	.3	.6	.5	.5	.2	
80- 7	292	1.032	2.0	1.1	1.9	1.9	6.7	1.9	.8	.4	.9	.6	.7	.5	
80- 8	269	1.144	2.0	.0	1.9	1.9	6.0	3.1	1.1	.4	.6	.4	1.0	1.0	
80- 9	245	1.254	2.0	.9	1.4	2.5	5.4	5.0	1.4	.4	.4	.2	.6	2.4	
80-10	221	1.368	2.0	.5	1.0	2.7	5.2	10.9	2.8	.4	.2	.1	.5	1.4	
80-11	211	1.456	2.0	.9	.8	3.0	5.9	12.0	2.7	.5	.2	.1	.5		

TABLE LXXVIII. BLADE .18R TORSIONAL MOMENT HARMONICS - RUN 80 (BLADE CENTER OF GRAVITY AT .30 CHORD)														
BLADE .18R TORSIONAL MOMENT HARMONICS (IN.-LB)														
RUN- PT. NO.	OMS #R (FPS)	MU	THEC (DEG)	A1	A2	A3	A4	A5	A6	A7	A8	A9	A10	
80- 3	387	.795	2.0	.2	-.8	-1.2	-.2	.3	-.1	.3	.8	.3	.1	
80- 4	363	.847	2.0	.2	-.4	-.9	-.4	.2	-.2	.2	.9	.6	.3	
80- 5	339	.906	2.0	.0	-.9	-1.1	-.2	.2	-.1	.2	.6	.4	.2	
80- 6	316	.974	2.0	.1	-1.0	-.9	-.1	.1	.0	-.1	.1	.3	.0	
80- 7	292	1.052	2.0	.0	-1.3	-.8	.2	.1	.0	.1	-.1	.1	.3	
80- 8	269	1.144	2.0	.2	-1.2	-.8	.3	-.1	.0	.1	.1	.0	.2	
80- 9	245	1.254	2.0	-.1	-1.7	-.4	.6	.0	-.1	.2	.0	.1	.0	
80-10	221	1.388	2.0	.1	-1.6	.0	.6	.0	-.1	.2	.0	.1	.0	
80-11	211	1.456	2.0	-.7	-2.3	.3	.4	.0	.0	.1	.0	.1	.0	
BLADE .18R TORSIONAL MOMENT HARMONICS (IN.-LB)														
RUN- PT. NO.	OMS #R (FPS)	MU	THEC (DEG)	B1	B2	B3	B4	B5	B6	B7	B8	B9	B10	
80- 3	387	.795	2.0	.7	.5	.6	-.8	-.7	-1.9	-.9	-.1	.2	.3	
80- 4	363	.847	2.0	.6	.4	.9	-.6	-.9	-.9	-.7	-.4	.3	.1	
80- 5	339	.906	2.0	.2	.1	.9	-.5	-.7	-.7	-.3	-.6	.1	.0	
80- 6	316	.974	2.0	.0	.1	1.0	-.3	-.7	-.6	-.2	-.3	-.2	.0	
80- 7	292	1.052	2.0	-.6	-.1	1.2	-.3	-.7	-.4	-.2	-.3	.0	-.1	
80- 8	269	1.144	2.0	-.5	-.1	1.3	-.3	-.7	-.3	-.2	-.2	.0	-.2	
80- 9	245	1.254	2.0	-1.3	-.1	1.5	-.5	-.6	-.3	-.1	-.1	-.1	-.1	
80-10	221	1.388	2.0	-1.1	.2	1.6	-.6	-.6	-.2	-.1	-.1	-.1	-.1	
80-11	211	1.456	2.0	-2.0	.5	1.7	-1.1	-.6	-.2	-.3	-.1	-.1	.0	

TABLE LXXVIII - Concluded

TABLE LXXVIII - Concluded														
BLADE .10R TORSIONAL MOMENT HARMONICS (IN.-LB)														
RUN- PT. NO.	QMS PR (FPS)	MU	THEC (DEG)	RS	R1	R2	R3	R4	R5	R6	R7	R8	R9	R10
80- 3	387	.795	2.0	1.1	.7	.9	1.3	.9	.8	1.0	1.0	.8	.9	.3
80- 4	363	.847	2.0	1.3	.6	.7	1.5	.8	.9	.9	.7	1.0	.6	.3
80- 5	339	.906	2.0	.6	.2	1.0	1.4	.5	.8	.7	.5	.8	.6	.3
80- 6	316	.974	2.0	.1	.1	1.0	1.4	.4	.7	.6	.3	.6	.4	.3
80- 7	292	1.052	2.0	-.2	.6	1.3	1.5	.4	.7	.4	.2	.3	.2	.2
80- 8	269	1.144	2.0	-.6	.5	1.2	1.5	.4	.7	.3	.2	.2	.2	.1
80- 9	245	1.254	2.0	-.6	1.3	1.7	1.6	.7	.6	.3	.2	.2	.1	.0
80-10	221	1.388	2.0	-1.0	1.1	1.6	1.6	.9	.8	.2	.2	.1	.2	.0
80-11	211	1.456	2.0	-.8	2.2	2.3	1.7	1.2	.8	.2	.3	.1	.2	.0

TABLE LXXIX. BLADE FLAP MOTION HARMONICS - RUN 80 (BLADE CENTER OF GRAVITY AT .30 CHORD)													
BLADE FLAP MOTION HARMONICS (DEG)													
RUN- PT. NO.	OMS PR (FPS)	MU	THEC (DEG)	A1	A2	A3	A4	A5	A6				
80- 3	387	.795	2.0	.1	-.1	-.5	.0	.0	.0				
80- 4	363	.847	2.0	-1.1	-.1	-.8	.1	.0	.0				
80- 5	339	.906	2.0	.4	.0	-.4	.1	.0	.0				
80- 6	316	.974	2.0	.2	-.1	-.5	.2	.1	.0				
80- 7	292	1.052	2.0	.9	.0	-.3	.2	.1	.0				
80- 8	269	1.144	2.0	.2	-.1	-.2	.3	.1	.0				
80- 9	245	1.254	2.0	.6	-.1	-.3	.5	.1	.0				
80-10	221	1.386	2.0	-.4	-.2	-.3	.9	.2	.0				
80-11	211	1.456	2.0	.4	-.2	-.3	.6	.2	.1				

BLADE FLAP MOTION HARMONICS (DEG)													
RUN- PT. NO.	OMS PR (FPS)	MU	THEC (DEG)	B1	B2	B3	B4	B5	B6				
80- 3	387	.795	2.0	-.2	-.1	-.8	.0	.0	.0				
80- 4	363	.847	2.0	.1	-.1	-.7	.0	.0	.0				
80- 5	339	.906	2.0	.0	-.1	-.5	.1	.0	.0				
80- 6	316	.974	2.0	.1	-.1	-.4	.1	.0	.0				
80- 7	292	1.052	2.0	.1	-.1	-.4	.1	.0	.0				
80- 8	269	1.144	2.0	-.1	-.1	-.4	.2	.1	.0				
80- 9	245	1.254	2.0	.2	.0	-.3	.0	.0	.0				
80-10	221	1.386	2.0	-.3	-.2	-.3	-.4	.0	.0				
80-11	211	1.456	2.0	.1	.0	-.3	-.4	-.1	.1				

TABLE LIXIX - Concluded										
BLADE FLAP MOTION HARMONICS (DEG)										
RUN- PT. NO.	ONS OR (PPS)	MU	THEC (DEG)	R5	R1	R2	R3	R4	R5	R6
80- 3 367		.796	2.0	.0	.2	.1	.1	.1	.1	.1
80- 4 363		.847	2.0	.1	1.1	.2	1.1	.1	.1	.1
80- 5 359		.906	2.0	-.3	.4	.1	.6	.1	.1	.1
80- 6 316		.974	2.0	-.4	.3	.1	.5	.2	.1	.1
80- 7 292		1.052	2.0	-.6	.9	.1	.4	.3	.1	.1
80- 8 269		1.144	2.0	-.8	.2	.2	.4	.5	.1	.1
80- 9 245		1.254	2.0	-1.4	.6	.1	.4	1.0	.2	.1
80-10 221		1.366	2.0	-1.5	.5	.3	.4	1.0	.2	.1
80-11 211		1.456	2.0	-2.3	.4	.2	.4			

TABLE LXXX. BLADE .30R CHORDWISE BENDING MOMENT HARMONICS - RUN 80 (BLADE CENTER OF GRAVITY AT .30 CHORD)													
BLADE .30R CHORDWISE BENDING MOMENT HARMONICS (IN.-LB)													
RUN- PT. NO.	OMS #R (FPS)	MU	(DEG)	A1	A2	A3	A4	A5	A6	A7	A8	A9	A10
80- 3 387		.795	2.0	-1.1	1.1	-5	2.0	1.0	2.1	-2	-.3	-.2	-.2
80- 4 363		.847	2.0	-1.7	1.1	-2.1	2.2	.7	-1.2	.0	-.4	-.2	.0
80- 5 339		.906	2.0	-1.3	.9	-1.4	1.1	.1	.2	.4	-.2	-.1	.0
80- 6 316		.974	2.0	-1.8	.7	-1.1	1.1	.2	.1	-.6	-.3	-.1	.0
80- 7 292		1.052	2.0	-2.4	.8	-.6	1.0	.2	-.1	-.3	-.2	-.1	-.1
80- 8 269		1.144	2.0	-3.2	.3	-.6	.9	.7	.1	-.1	-.2	-.2	.0
80- 9 245		1.254	2.0	-4.9	1.0	-.9	1.3	.0	.3	.1	.1	-.4	-.1
80-10 221		1.388	2.0	-7.0	.8	-2.2	2.6	-.4	.0	.3	-.1	-.4	-.5
80-11 811		1.456	2.0	-7.4	1.2	-2.5	2.3	.0	-.2	.1	.0	-.2	-.1

BLADE .30R CHORDWISE BENDING MOMENT HARMONICS (IN.-LB)													
RUN- PT. NO.	OMS #R (FPS)	MU	THEC (DEG)	B1	B2	B3	B4	B5	B6	B7	B8	B9	B10
80- 3 387		.795	2.0	-3.7	-.2	-1.6	.7	.3	-1.1	.4	.2	.1	.0
80- 4 363		.847	2.0	-3.8	-.7	-1.2	.3	.0	.4	.5	.1	.0	-.1
80- 5 339		.906	2.0	-3.9	.1	-.2	.2	-.5	.2	.5	.3	.1	-.2
80- 6 316		.974	2.0	-4.6	.5	.0	.5	.3	.1	.6	.4	.1	.0
80- 7 292		1.052	2.0	-4.9	.3	-.2	.9	.2	.2	.5	.1	-.1	.0
80- 8 269		1.144	2.0	-5.2	.7	-.2	.8	-.3	.3	.4	.4	.3	.0
80- 9 245		1.254	2.0	-5.5	.7	-1.1	.8	-.3	-.1	.2	.1	.0	.4
80-10 821		1.388	2.0	-5.0	.6	-.4	-.6	.0	.3	.1	.1	.1	.4
80-11 811		1.456	2.0	-4.2	.2	.1	-1.6	.4	.2	-.1	.2	.5	.4

TABLE LXXX - Concluded

BLADE .36R CHOROVISE BODING WOODRUFF MECHANICS (BL.-LB)															
RUN- PT. NO.	QMS NR (FPS)	MU	THEC (DEG)	RS	R1	R2	R3	R4	R5	R6	R7	R8	R9	R10	R11
80- 3	367	.795	2.0	-2	3.9	1.1	1.7	2.2	1.0	2.0	.3	.0	.2	.2	.2
80- 4	363	.847	2.0	2.9	4.2	1.3	2.0	2.2	.7	1.2	.3	.0	.2	.2	.2
80- 5	339	.906	2.0	6.0	4.1	.9	1.0	1.2	.5	.2	.0	.3	.1	.1	.1
80- 6	316	.974	2.0	8.7	4.9	.9	1.1	1.2	.0	.2	.0	.3	.1	.1	.1
80- 7	292	1.052	2.0	10.9	5.0	.9	.7	1.0	.3	.2	.0	.3	.1	.1	.1
80- 8	269	1.144	2.0	12.2	6.1	.8	.6	1.2	.7	.3	.0	.3	.1	.1	.1
80- 9	245	1.254	2.0	15.1	7.0	1.3	1.3	1.3	.3	.3	.2	.2	.0	.0	.0
80-10	221	1.508	2.0	16.5	8.6	1.1	2.3	2.0	.0	.3	.3	.1	.0	.0	.0
80-11	211	1.456	2.0	16.8	8.0	1.2	2.5	2.0	.0	.2	.1	.2	.0	.0	.0

TABLE LXXXI. BLADE LAG MOTION HARMONICS - RUN 81 (BLADE CENTER OF GRAVITY AT .30 CHORD)										
BLADE LAG MOTION HARMONICS (DEG)										
RUN- PT. NO.	OMS #R	MU (FPS)	THEC (DEG)	A1	A2	A3	A4	A5		
81- 3	236	1.488	2.0	-.2	.0	.0	.0	.0		.0
81- 4	218	1.611	2.0	-.5	.1	.0	.0	.0		.0
81- 5	232	1.692	2.0	-.4	.1	.0	.0	.1		.0
81- 6	260	1.678	2.0	-.3	.1	.0	.0	.0		.0
81- 7	288	1.656	2.0	-.2	.0	.1	.0	.0		.0
81- 8	314	1.605	2.0	-.1	.1	.1	.1	.0		.0
81- 9	392	1.431	2.0	.0	.0	.1	.0	.0		.0
BLADE LAG MOTION HARMONICS (DEG)										
RUN- PT. NO.	OMS #R	MU (FPS)	THEC (DEG)	B1	B2	B3	B4	B5		
81- 3	236	1.488	2.0	-.7	.1	.1	.0	.0		.0
81- 4	218	1.611	2.0	-.7	.0	.1	.0	.0		.0
81- 5	232	1.692	2.0	-1.0	.1	.0	.0	.0		.0
81- 6	260	1.678	2.0	-1.0	.1	.0	.0	.0		.0
81- 7	288	1.656	2.0	-1.0	.0	.0	.0	.0		.0
81- 8	314	1.605	2.0	-.9	.1	.0	.0	.0		.0
81- 9	392	1.431	2.0	-.6	.1	.0	.0	.0		.0

TABLE LXXXI - Concluded

		BLADE LAG MOTION HARMONICS (DEG)									
RUN- PT. NO.	OMS #R (FPS)	MU	THEC (DEG)	RS	R1	R2	R3	R4	R5		
81- 3	236	1.488	2.0	2.1	.8	.1	.1	.0	.0		
81- 4	218	1.611	2.0	1.6	.9	.1	.1	.1	.0		
81- 5	232	1.692	2.0	1.8	1.1	.1	.1	.0	.1		
81- 6	260	1.678	2.0	1.5	1.0	.1	.1	.0	.0		
81- 7	288	1.656	2.0	-.1	1.0	.1	.1	.0	.0		
81- 8	314	1.605	2.0	.7	1.0	.1	.1	.1	.0		
81- 9	392	1.431	2.0	1.6	.6	.1	.1	.1	.0		

TABLE LXXXII. BLADE .30R FLAPWISE BENDING MOMENT HARMONICS - RUN 81
(BLADE CENTER OF GRAVITY AT .30 CHORD)

BLADE .30R FLAPWISE BENDING MOMENT HARMONICS (IN.-LB)																				
RUN- PT. NO.	OMS #R (FPS)	THEC (DEG)	MU	A1	A2	A3	A4	A5	A6	A7	A8	A9	A10	A11	A12	A13				
81- 3 236	1.488	2.0		1.5	-4.2	5.6	-7.4	-2.4	-2.4	.1	-1	-5	1.8	-2	-2	-2				
81- 4 218	1.611	2.0		.1	-4.2	8.0	-6.1	-2.5	-1	.1	-1	-6	.2	.5	-3	-1				
81- 5 232	1.692	2.0		.6	-6.0	7.4	-9.3	-3.5	-1	.4	.4	-3	2.7	.4	-3	-1				
81- 6 260	1.673	2.0		.7	-7.5	9.9	-7.1	-3.2	.5	.7	.8	1.7	.3	-2	-1	-1				
81- 7 288	1.656	2.0		-1.1	-8.4	13.0	-5.0	-3.0	-6	.9	.1	.2	.4	.1	-2	.0				
81- 8 314	1.605	2.0		.8	-9.3	4.2	-5.3	-3.6	-2.3	3.0	-1.0	.2	.6	.4	-2	-1				

BLADE .30R FLAPWISE BENDING MOMENT HARMONICS (IN.-LB)																				
RUN- PT. NO.	OMS #R (FPS)	THEC (DEG)	MU	B1	B2	B3	B4	B5	B6	B7	B8	B9	B10	B11	B12	B13				
81- 3 236	1.488	2.0		-1	-1	4.5	2.5	-1	-3	-2	.1	-8	1.0	.8	.2	.2				
81- 4 218	1.611	2.0		-6	-1.0	3.6	9.1	.5	-3	-3	.3	-2	-1.7	.7	.2	-1				
81- 5 232	1.692	2.0		-7	-1.3	5.6	5.6	.3	-4	-8	-3	-5	.7	1.1	.3	.2				
81- 6 260	1.678	2.0		-2	-2.6	6.9	2.4	-6	.1	-1.1	.0	.0	.6	.6	-1	.0				
81- 7 288	1.656	2.0		-7	-4.9	16.0	4.8	.4	1.3	-8	.7	-3	.1	.3	.1	-1				
81- 8 314	1.605	2.0		-9	-6.5	21.9	5.1	1.1	1.1	-3.4	-6	-1.3	.8	.0	-2	-2				

BLADE .30R FLAPWISE BENDING MOMENT HARMONICS (IN.-LB)																				
RUN- PT. NO.	OMS #R (FPS)	THEC (DEG)	MU	R5	R1	R2	R3	R4	R5	R6	R7	R8	R9	R10	R11	R12	R13			
81- 3 236	1.488	2.0		.7	1.5	4.2	7.2	7.9	2.4	.4	.2	.1	1.0	2.0	.8	.2	.2			
81- 4 218	1.611	2.0		1.6	.8	4.3	8.7	10.9	2.5	.3	.4	.3	.6	1.7	.9	.4	.2			
81- 5 232	1.692	2.0		1.6	.9	6.1	9.3	10.8	3.5	.4	.9	.5	.7	2.8	1.1	.7	.2			
81- 6 260	1.678	2.0		2.6	.7	8.0	12.1	7.5	3.2	.5	1.3	.6	1.7	.7	.7	.1	.1			
81- 7 288	1.656	2.0		4.7	1.3	9.7	20.6	7.0	3.0	1.4	1.2	.7	.3	.4	.4	.2	.1			
81- 8 314	1.605	2.0		3.7	1.1	11.3	22.3	7.3	3.8	2.5	4.5	1.2	1.3	.8	.4	.2	.3			

TABLE LXXXIII. BLADE .18R TORSIONAL MOMENT HARMONICS - RUN 81 (BLADE CENTER OF GRAVITY AT .30 CHORD)																
BLADE .18R TORSIONAL MOMENT HARMONICS (IN.-LB)																
RUN- PT. NO.	OMS #R (FPS)	MJ	THEC (DEG)	A1	A2	A3	A4	A5	A6	A7	A8	A9	A10	A11	A12	A13
01- 3 236	1.488		2.0	-1.5	-2.8	-1.1	1.3	.2	.0	.1	.1	.3	.0	.3	.5	-.1
01- 4 218	1.611		2.0	-1.4	-3.6	.8	1.6	.1	.1	.0	.1	.1	.0	.2	.4	.2
01- 5 232	1.692		2.0	-1.1	-4.0	.4	2.5	.3	-.4	-.1	.0	.3	.1	.5	.6	.0
01- 6 260	1.678		2.0	-1.0	-5.9	-.6	3.5	1.0	-.7	-.6	.4	1.1	-.3	-.7	.1	-.3
01- 7 288	1.656		2.0	-1.8	-9.6	-.4	5.5	2.2	-.8	-2.1	-.4	3.8	1.9	.5	.2	.1
01- 8 314	1.685		2.0	-1.0	-10.9	-2.1	6.7	3.2	-2.3	-2.9	-1.5	-.5	.6	-.3	.1	.0
01- 9 392	1.431		2.0	5.0	-7.5	-5.1	2.3	3.2	.8	2.0	.9	-.1	.2	-.1	-.1	.1

BLADE .18R TORSIONAL MOMENT HARMONICS (IN.-LB)																
RUN- PT. NO.	OMS #R (FPS)	MJ	THEC (DEG)	B1	B2	B3	B4	B5	B6	B7	B8	B9	B10	B11	B12	B13
01- 3 236	1.488		2.0	-2.8	.9	2.6	-.3	-.8	-.2	-.2	-.1	-.2	-.1	.3	.5	.0
01- 4 218	1.611		2.0	-4.3	1.9	5.0	-.9	-.8	-.3	-.3	.0	-.3	-.1	-.1	-.4	.2
01- 5 232	1.692		2.0	-3.9	1.8	4.4	-.1	-1.8	-.6	-.2	-.1	-.2	-.1	.0	-.1	.3
01- 6 260	1.678		2.0	-5.9	2.7	6.2	.9	-1.8	-1.3	-.2	.2	-.2	-.5	.7	.7	.2
01- 7 288	1.656		2.0	-10.4	2.7	9.0	1.3	-2.2	-2.1	-.7	1.2	-.1	-.3	.9	.5	.1
01- 8 314	1.685		2.0	-11.4	1.6	11.8	3.6	-3.1	-3.6	-2.5	2.6	3.3	1.8	.9	.2	.1
01- 9 392	1.431		2.0	-5.2	-3.2	9.5	7.5	-1.7	-6.1	-5.1	-1.0	-.3	.0	.2	.1	-.1

TABLE LXXXIII - Concluded																	
BLADE .10R TORSIONAL MOMENT HARMONICS (IN.-LB)																	
BLR- PT. NO.	ONS or (FPS)	MU	THEC (DEG)	R5	R1	R2	R3	R4	R5	R6	R7	R8	R9	R10	R11	R12	R13
01- 3 236	1.400	2.0	2.0	2.5	2.0	2.9	2.6	1.3	.0	2.5	.5	1	.3	.1	.9	7	1
01- 4 218	1.411	2.0	2.0	2.8	4.5	4.1	3.1	1.0	.8	.5	.5	.1	.4	.1	.2	.6	.3
01- 5 232	1.492	2.0	2.0	3.9	6.1	6.0	4.5	2.6	1.4	.7	.2	.5	.4	.1	.5	.4	.3
01- 6 260	1.678	2.0	2.0	6.3	6.0	6.1	6.3	3.4	2.1	1.5	.7	.5	1.1	.6	.9	.7	.3
01- 7 288	1.686	2.0	2.0	6.3	10.5	10.0	9.0	8.7	3.1	2.2	2.2	1.2	3.0	1.9	.8	.8	.2
01- 8 310	1.695	2.0	2.0	7.7	11.4	11.1	12.0	7.6	4.3	4.3	3.9	3.0	3.3	1.9	1.0	.5	.2
01- 9 392	1.931	2.0	2.0	7.6	7.2	8.2	10.0	7.0	3.6	6.1	5.5	1.3	.3	.2	.2	.1	.1

TABLE LXXXIV. BLADE FLAP MOTION HARMONICS - RUN 81 (BLADE CENTER OF GRAVITY AT .30 CHORD)										
BLADE FLAP MOTION HARMONICS (DEG)										
RUN- PT. NO.	OMS *R (FPS)	MU	THEC (DEG)	A1	A2	A3	A4	A5	A6	A7
81- 3	236	1.488	2.0	.1	-.3	-.3	.7	.2	.0	.0
81- 4	218	1.611	2.0	1.1	-.3	-.5	.6	.2	.0	.0
81- 5	232	1.692	2.0	-.7	-.5	-.5	.9	.3	.0	.0
81- 6	260	1.678	2.0	-.5	-.4	-.6	.6	.3	.0	-.1
81- 7	288	1.656	2.0	.5	-.3	-.6	.4	.2	.0	.0
81- 8	314	1.605	2.0	-.4	-.6	-.3	.6	.3	.1	-.1
81- 9	392	1.431	2.0	-.9	-.6	.1	.5	.3	.2	.1
BLADE FLAP MOTION HARMONICS (DEG)										
RUN- PT. NO.	OMS *R (FPS)	MU	THEC (DEG)	B1	B2	B3	B4	B5	B6	B7
81- 3	236	1.488	2.0	.3	.0	-.5	-.2	.0	.0	.0
81- 4	218	1.611	2.0	1.2	.2	-.4	-.8	-.1	.0	.0
81- 5	232	1.692	2.0	.2	.1	-.6	-.5	-.1	.1	.0
81- 6	260	1.678	2.0	-.2	.2	-.8	-.4	.0	.0	.0
81- 7	288	1.656	2.0	.3	.7	-1.5	-.5	-.1	.0	.0
81- 8	314	1.605	2.0	-.1	.5	-1.8	-.3	-.1	.0	.1
81- 9	392	1.431	2.0	-.2	.0	-1.6	-.1	.1	.2	-.2

TABLE LXXXIV - Concluded												
BLADE FLAP MOTION HARMONICS (DEG)												
RUN- PT. NO.	OMS #R	(FPS)	MU	TIMEC (DEG)	RS	R1	R2	R3	R4	R5	R6	
81- 3	236		1.488	2.0	-1.3	.3	.3	.6	.7	.2	.1	
81- 4	218		1.611	2.0	-2.5	1.6	.4	.6	1.0	.2	.1	
81- 5	232		1.692	2.0	-1.8	.7	.5	.8	1.0	.3	.1	
81- 6	260		1.678	2.0	-1.9	.5	.5	1.0	.7	.3	.1	
81- 7	288		1.656	2.0	-2.7	.6	.8	1.6	.7	.3	.1	
81- 8	314		1.605	2.0	-1.9	.4	.8	1.8	.7	.3	.1	
81- 9	392		1.431	2.0	-.1	.9	.6	1.6	.5	.4	.3	

TABLE LXXXV. BLADE .30R CHORDWISE BENDING MOMENT HARMONICS - RUN 81 (BLADE CENTER OF GRAVITY AT .30 CHORD)														
BLADE .30R CHORDWISE BENDING MOMENT HARMONICS (IN.-LB)														
RUN- PT. NO.	QMS OR	MU (FPS)	THC (DEG)	A1	A2	A3	A4	A5	A6	A7	A8	A9	A10	A11
01- 3 236	1.000	2.0	-7.0	1.3	-2.4	1.9	-1.1	-1.1	-1.1	-1.1	.1	.5	.1	-.5
01- 4 210	1.011	2.0	-8.9	.9	-3.2	1.9	.3	-1.1	-1.1	-.3	.2	.1	.0	.4
01- 5 232	1.092	2.0	-10.8	1.6	-3.0	2.6	.5	-.4	-.4	-.1	-.3	-.3	1.0	-.8
01- 6 240	1.078	2.0	-10.9	2.1	-3.3	1.8	.7	-.9	-.9	-.6	-1.2	-.5	-.1	.2
01- 7 200	1.056	2.0	-12.3	3.6	-4.5	3.5	.7	-2.1	-2.1	-3.6	-6.1	-3.8	-1.1	.2
01- 8 314	1.085	2.0	-11.4	3.9	-.7	4.0	5.1	-.4	-.4	-7.7	.2	-.5	-2.1	-.6
01- 9 392	1.031	2.0	-6.3	3.1	1.0	6.2	4.1	17.1	17.1	4.0	1.1	-.4	-1.0	-.9

BLADE .30R CHORDWISE BENDING MOMENT HARMONICS (IN.-LB)														
RUN- PT. NO.	QMS OR	MU (FPS)	THC (DEG)	B1	B2	B3	B4	B5	B6	B7	B8	B9	B10	B11
01- 3 236	1.000	2.0	-6.0	-.4	-1.6	-.9	-.9	.0	-.3	.1	.4	.2	-.4	-.3
01- 4 210	1.011	2.0	-3.6	-.5	-.3	-2.0	-1.0	-.1	-.1	-.3	.0	.4	.5	.6
01- 5 232	1.092	2.0	-6.7	-.4	-2.3	-1.0	-.3	-.2	.4	-.3	.5	-.6	.1	-.5
01- 6 240	1.078	2.0	-8.9	.3	-1.9	-.2	-.6	-.2	-.6	-.1	.1	-.7	.9	-.6
01- 7 200	1.056	2.0	-9.1	1.1	-5.1	-.4	-.4	.3	-2.4	.0	.5	1.6	1.2	-.5
01- 8 314	1.085	2.0	-12.3	1.2	-5.7	.8	-.7	-.7	-6.0	-8.2	-5.1	-2.2	.4	.7
01- 9 392	1.031	2.0	-13.4	.8	-3.2	6.5	5.7	5.7	2.1	3.2	1.2	-.6	-1.6	-.6

TABLE LXXXV - Concluded

RUN- PT. NO.	OHS SR (FPS)	MU	THEC (DEG)	BLADE .30R CHORDWISE BENDING MOMENT HARMONICS (IN.-LB)																
				R5	R1	R2	R3	R4	R5	R6	R7	R8	R9	R10	R11					
81- 3	236	1.488	2.0	-1.0	9.8	1.3	2.9	2.8	.1	.4	.1	.4	.5	.4	.5					
81- 4	218	1.611	2.0	-.1	9.6	1.0	3.3	2.5	.4	.2	.3	.2	.4	.5	.7					
81- 5	232	1.692	2.0	-.7	12.7	1.7	3.8	2.8	.6	.6	.3	.6	.7	1.0	.9					
81- 6	260	1.678	2.0	-2.8	16.1	2.1	3.8	1.9	.8	1.1	.6	1.2	.8	.9	.6					
81- 7	288	1.656	2.0	-5.6	15.3	3.6	6.8	3.8	.7	3.2	3.6	6.1	4.1	1.6	.5					
81- 8	314	1.605	2.0	-8.0	16.7	4.1	5.7	4.9	5.2	6.0	11.3	5.1	2.2	2.1	.9					
81- 9	332	1.431	2.0	-11.2	14.8	3.2	3.3	9.0	7.0	17.3	5.1	1.6	.7	1.9	1.0					

TABLE LXXXVI. BLADE LAG MOTION HARMONICS - RUNS 83-84
(BLADE CENTER OF GRAVITY AT .35 CHORD)

RUN- PT. NO.	OMS R (FPS)	MU	THEC (DEG)	BLADE LAG MOTION HARMONICS (DEG)				
				A1	A2	A3	A4	A5
83- 3 700	.333	4.0	4.0	-.1	.0	.0	.0	.0
83- 4 700	.390	4.0	4.0	.0	.0	.0	.0	.0
83- 5 700	.450	4.0	4.0	.0	.0	.0	.0	.0
84- 3 500	.632	4.0	4.0	.1	.0	.0	.0	.0
84- 4 500	.708	4.0	4.0	.2	.0	.0	.0	.0
84- 5 500	.793	4.0	4.0	.2	.0	.0	.0	.0
84- 6 500	.876	4.0	4.0	.2	.0	.0	.0	.0
84- 7 475	.832	4.0	4.0	.2	.0	.0	.0	-.1
84- 8 451	.876	4.0	4.0	.2	.0	.0	.0	.1
84- 9 428	.924	4.0	4.0	.0	.0	.1	-.1	.0
84-10 381	1.038	4.0	4.0	.0	.1	.0	.0	-.1
84-11 357	1.107	4.0	4.0	.0	.1	.0	.0	.0
84-12 334	1.185	4.0	4.0	.0	.1	.1	.0	.0
84-13 310	1.275	4.0	4.0	-.1	.1	.0	.0	.0
84-14 287	1.380	4.0	4.0	-.2	.1	.0	.0	.0
84-15 263	1.504	4.0	4.0	-.3	.1	.0	.0	.0
84-16 239	1.652	4.0	4.0	-.6	.1	.0	.0	.0

RUN- PT. NO.	OMS R (FPS)	MU	THEC (DEG)	BLADE LAG MOTION HARMONICS (DEG)				
				B1	B2	B3	B4	B5
83- 3 700	.333	4.0	4.0	-.1	.0	.0	.0	.0
83- 4 700	.390	4.0	4.0	-.1	.0	.0	.0	.0
83- 5 700	.450	4.0	4.0	-.1	.0	.0	.0	.0
84- 3 500	.632	4.0	4.0	.1	.1	.1	.0	.0
84- 4 500	.708	4.0	4.0	.1	.1	.1	.0	.0
84- 5 500	.793	4.0	4.0	.0	.1	.1	.0	.0
84- 6 500	.876	4.0	4.0	-.1	.1	.1	.0	.0
84- 7 475	.832	4.0	4.0	.0	.1	.1	.0	.1
84- 8 451	.876	4.0	4.0	-.1	.1	.1	.0	.1
84- 9 428	.924	4.0	4.0	-.3	.1	.0	.0	-.1
84-10 381	1.038	4.0	4.0	-.3	.1	-.1	.0	.0
84-11 357	1.107	4.0	4.0	-.3	.1	-.1	.0	.0
84-12 334	1.185	4.0	4.0	-.4	.1	.0	.0	.0
84-13 310	1.275	4.0	4.0	-.5	.1	.0	.0	.0
84-14 287	1.380	4.0	4.0	-.6	.1	.0	.0	.0
84-15 263	1.504	4.0	4.0	-.8	.1	.0	.0	.0
84-16 239	1.652	4.0	4.0	-.9	.0	.0	.0	.0

TABLE LXXXVI - Concluded										
RUN- PT. NO.		OMS *R (FPS)	MU	THEC (DEG)	RS	R1	R2	R3	R4	R5
83-	3	700	.333	4.0	.8	.1	.0	.0	.0	.0
83-	4	700	.390	4.0	.7	.1	.0	.0	.0	.0
83-	5	700	.450	4.0	.8	.1	.0	.0	.0	.0
84-	3	500	.632	4.0	.8	.2	.1	.1	.0	.0
84-	4	500	.708	4.0	1.0	.2	.1	.1	.0	.0
84-	5	500	.793	4.0	1.0	.2	.1	.1	.0	.0
84-	6	500	.876	4.0	1.0	.3	.1	.1	.0	.0
84-	7	475	.832	4.0	1.0	.2	.1	.1	.1	.1
84-	8	451	.876	4.0	.9	.3	.1	.1	.0	.2
84-	9	428	.924	4.0	1.0	.3	.1	.1	.1	.1
84-	10	381	1.038	4.0	.9	.3	.1	.1	.1	.1
84-	11	357	1.107	4.0	.9	.3	.1	.1	.0	.0
84-	12	334	1.185	4.0	.9	.4	.1	.1	.0	.0
84-	13	310	1.275	4.0	.6	.5	.1	.0	.0	.0
84-	14	287	1.380	4.0	.2	.6	.1	.0	.0	.0
84-	15	263	1.504	4.0	.4	.8	.1	.0	.0	.0
84-	16	239	1.652	4.0	-.2	1.1	.1	.0	.0	.0

TABLE LXXXVII. BLADE .30R FLAPWISE BENDING MOMENT HARMONICS - RUNS 83-84 (BLADE CENTER OF GRAVITY AT .35 CHORD)																
BLADE .30R FLAPWISE BENDING MOMENT HARMONICS (IN.-LB)																
RUN- PT. NO.	OMS OR (FPS)	MU	THEC (DEG)	A1	A2	A3	A4	A5	A6	A7	A8	A9	A10	A11	A12	A13
83- 3 700	.333	4.0	.7	1.7	-1	.1	.6	-3.7	.0	.1	-3	-2	.4	.1	.0	.0
83- 4 700	.390	4.0	1.4	1.4	-5	.4	1.5	-3.7	.0	.1	-3	-2	.3	-.1	.0	.0
83- 5 700	.450	4.0	1.8	1.5	-5	1.0	1.5	-3.7	.0	.1	-3	-2	.3	.0	.0	.0
84- 3 500	.632	4.0	1.5	-1.6	-1.6	-2.5	-5	1.6	-1.0	.3	.3	.3	.0	1.6	-1	.1
84- 4 500	.708	4.0	1.4	-2.6	-2.6	-3.5	-8	1.6	-.1	.4	.1	.1	.2	2.4	-3	.2
84- 5 500	.793	4.0	2.0	-2.6	-2.6	-2.9	-4	.8	.9	.4	.1	.1	.7	2.4	-3	.2
84- 6 500	.876	4.0	2.8	-2.7	-2.7	-3.6	.1	.3	1.1	.3	.3	.5	.2	.9	-1	.1
84- 7 475	.631	4.0	1.9	-2.9	-2.9	-4.0	.0	.7	2.5	.3	.3	.7	.2	.3	-1	.1
84- 8 451	.876	4.0	1.9	-3.8	-3.8	-5.0	.0	1.1	-1.3	.2	.2	.7	.2	.3	-.4	.0
84- 9 428	.924	4.0	1.9	-4.1	-4.1	-5.9	.2	1.2	-.4	-1.2	.4	.2	.2	-.4	1.2	.0
84-10 381	1.034	4.0	2.7	-5.1	-5.1	7.0	-1.6	.5	1.3	-3.1	-5	.9	.3	-.3	-7	-2
84-11 357	1.107	4.0	2.5	-3.9	-3.9	8.9	-2.2	-.9	2.2	-5.6	-.6	.2	.2	-.2	-.4	.5
84-12 334	1.185	4.0	3.2	-3.9	-3.9	4.5	-2.5	-.9	1.1	1.5	-5	.5	.2	-.1	-2	.0
84-13 310	1.275	4.0	2.6	-5.2	-5.2	7.1	-3.4	-1.6	.3	2.1	-8	.1	.1	-.1	-.1	.1
84-14 287	1.340	4.0	4.9	-6.9	-6.9	4.9	-4.2	-2.1	.2	1.1	-7	.6	.3	-.1	-.2	.1
84-15 263	1.504	4.0	1.4	-8.3	-8.3	7.7	-5.2	-2.8	-.1	.6	.1	.7	.8	-.7	.1	.1
84-16 239	1.652	4.0	-.1	-9.6	-9.6	9.8	-7.0	-3.0	.0	-.3	-.4	-1.2	.7	.4	.1	.1

BLADE .30R FLAPWISE BENDING MOMENT HARMONICS (IN.-LB)																
RUN- PT. NO.	OMS OR (FPS)	MU	THEC (DEG)	B1	B2	B3	B4	B5	B6	B7	B8	B9	B10	B11	B12	B13
83- 3 700	.333	4.0	.3	.9	.6	.9	-.9	-1.2	.2	.0	-.3	-.1	.0	.0	.0	.0
83- 4 700	.390	4.0	.2	2.1	2.2	2.1	-1.2	-2.1	.4	.5	-.2	-.1	.0	.0	.0	.0
83- 5 700	.450	4.0	-.1	4.0	2.1	2.3	-1.5	-2.9	.1	.5	-.4	.0	.0	.0	.0	.0
84- 3 500	.632	4.0	1.2	1.7	1.7	1.1	-.5	-1.0	-2.0	-.6	.2	.0	-.6	.2	.0	.0
84- 4 500	.708	4.0	1.3	2.0	2.0	1.1	-.9	-1.0	-1.3	-.3	.3	-.2	-.2	.1	-.1	.1
84- 5 500	.793	4.0	.8	2.7	2.7	.0	-.7	-.4	.3	.2	.6	.0	-1.4	-.1	-.2	-.1
84- 6 500	.876	4.0	.3	3.3	3.3	-1.0	-1.0	-.6	1.3	.3	.5	.3	-2.7	-.1	-.2	.0
84- 7 475	.832	4.0	1.2	2.1	2.1	1.6	-.3	-.6	-.3	.3	.5	.5	1.2	-.1	-.2	.2
84- 8 451	.876	4.0	1.1	1.1	1.1	2.5	.0	-.4	-.5	-.5	.1	.5	-.6	.7	-.1	.1
84- 9 428	.924	4.0	1.0	.0	.0	8.0	-.1	-.7	2.8	-.4	-.4	.4	-.2	.1	-.2	.2
84-10 381	1.034	4.0	-.1	-.7	10.7	.3	.3	-1.3	3.9	-.1	-1.2	-.1	.7	.3	-.4	.4
84-11 357	1.107	4.0	-2.6	-.9	9.1	.7	1.7	-1.7	1.1	2.6	-.5	-.4	.3	.5	-.4	.1
84-12 334	1.185	4.0	-2.2	-2.1	11.6	.5	1.0	-.9	.4	.3	.0	-.4	.3	.0	.0	.3
84-13 310	1.275	4.0	-2.7	-2.7	10.8	.5	.5	-.5	.4	.6	.3	.2	.3	.0	.0	.1
84-14 287	1.340	4.0	-3.3	-2.5	11.2	1.6	1.6	-.5	.5	-.1	.3	-.2	.3	.3	.0	.1
84-15 263	1.504	4.0	-4.0	-.9	8.8	4.3	4.3	.9	.4	-.7	.7	-1.4	.3	.3	.0	.0
84-16 239	1.652	4.0	-5.2	1.2	7.6	7.1	7.1	1.5	.5	-.5	-.3	-3.1	-.6	.2	.1	.1

TABLE LXXXVII - Concluded

TABLE LXXXVII - Concluded																
RUN- PT. NO.	OMS #R (FPS)	NU	THEC (DEG)	BLADE .30R FLAPWISE BENDING MOMENT HARMONICS (IN.-LB)												
				PS	R1	R2	R3	R4	R5	R6	R7	R8	R9	R10	R11	R12
83- 3 700		.333	4.0	2.5	.8	.0	.9	1.1	1.2	.2	.1	.4	.4	.1	.0	.0
83- 4 700		.390	4.0	2.3	1.4	2.3	2.1	2.1	4.3	.4	.6	.2	.3	.1	.0	.0
83- 5 700		.450	4.0	2.1	1.8	2.1	4.1	2.1	5.5	.0	.5	.4	.2	.1	.3	.0
84- 3 500		.632	4.0	1.2	1.9	2.3	3.4	.7	2.1	2.7	.7	.4	.6	1.7	.2	.1
84- 4 500		.708	4.0	2.0	1.9	3.3	3.6	1.2	1.9	1.3	.5	.4	.3	2.4	.3	.2
84- 5 500		.793	4.0	1.7	2.2	3.8	2.9	.8	.9	1.0	.4	.6	.7	2.0	.1	.2
84- 6 500		.876	4.0	1.5	2.8	4.3	3.7	1.0	.4	1.7	.4	.6	.5	2.9	.3	.3
84- 7 475		.832	4.0	1.6	2.2	3.6	4.3	.4	.9	2.5	.4	.7	.4	1.2	.0	.1
84- 8 451		.876	4.0	2.9	2.6	3.9	5.6	.3	1.1	1.4	.5	.7	.5	.7	.0	.2
84- 9 428		.924	4.0	2.4	2.7	4.1	8.6	.2	1.4	2.8	1.2	.6	.4	.4	1.2	.6
84-10 381		1.038	4.0	2.6	2.7	5.1	12.8	1.6	1.4	4.1	3.1	1.3	.4	.7	.7	.3
84-11 357		1.107	4.0	.5	3.6	4.0	12.7	2.3	2.0	2.4	6.2	.0	.0	.3	.4	.3
84-12 334		1.185	4.0	1.1	3.8	4.4	12.5	2.7	1.3	1.2	9.4	.3	.1	.3	.2	.1
84-13 310		1.275	4.0	2.0	3.8	5.9	12.9	3.4	1.7	.6	2.3	.8	.7	.3	.1	.2
84-14 287		1.380	4.0	1.6	3.8	7.3	12.3	4.5	2.2	.5	1.1	.7	.4	.0	.3	.1
84-15 263		1.504	4.0	1.7	4.2	8.3	11.7	6.7	3.0	.4	.9	.7	1.4	.0	.0	.1
84-16 239		1.652	4.0	1.6	5.2	9.6	12.4	10.0	3.4	.5	.4	.5	3.3	.9	.0	.1

TABLE LXXXVIII. BLADE .60R FLAPWISE BENDING MOMENT HARMONICS - RUNS 83-84 (BLADE CENTER OF GRAVITY AT .35 CHORD)													
RUN- PT. NO.	OMS #R (FPS)	MU	THEC (DEG)	BLADE .60R FLAPWISE BENDING MOMENT HARMONICS (IN.-LB)									
				A1	A2	A3	A4	A5	A6	A7	A8	A9	A10
83- 3 700	333	4.0	2.3	5	1.5	1.1	1.1	1.1	1.1	1.1	1.1	1.1	1.1
83- 4 700	390	4.0	2.3	5	1.5	1.1	1.1	1.1	1.1	1.1	1.1	1.1	1.1
83- 5 700	450	4.0	2.3	5	1.5	1.1	1.1	1.1	1.1	1.1	1.1	1.1	1.1
84- 3 500	632	4.0	2.4	5	1.5	1.1	1.1	1.1	1.1	1.1	1.1	1.1	1.1
84- 4 500	708	4.0	2.6	5	1.5	1.1	1.1	1.1	1.1	1.1	1.1	1.1	1.1
84- 5 500	793	4.0	2.1	5	1.5	1.1	1.1	1.1	1.1	1.1	1.1	1.1	1.1
84- 6 500	876	4.0	1.9	5	1.5	1.1	1.1	1.1	1.1	1.1	1.1	1.1	1.1
84- 7 475	832	4.0	1.8	5	1.5	1.1	1.1	1.1	1.1	1.1	1.1	1.1	1.1
84- 8 451	876	4.0	1.6	5	1.5	1.1	1.1	1.1	1.1	1.1	1.1	1.1	1.1
84- 9 428	924	4.0	1.5	5	1.5	1.1	1.1	1.1	1.1	1.1	1.1	1.1	1.1
84-10 381	1.038	4.0	2.6	5	1.5	1.1	1.1	1.1	1.1	1.1	1.1	1.1	1.1
84-11 357	1.107	4.0	2.8	5	1.5	1.1	1.1	1.1	1.1	1.1	1.1	1.1	1.1
84-12 334	1.185	4.0	2.5	5	1.5	1.1	1.1	1.1	1.1	1.1	1.1	1.1	1.1
84-13 310	1.275	4.0	2.6	5	1.5	1.1	1.1	1.1	1.1	1.1	1.1	1.1	1.1
84-14 287	1.380	4.0	2.3	5	1.5	1.1	1.1	1.1	1.1	1.1	1.1	1.1	1.1
84-15 263	1.504	4.0	2.4	5	1.5	1.1	1.1	1.1	1.1	1.1	1.1	1.1	1.1
84-16 239	1.652	4.0	1.7	5	1.5	1.1	1.1	1.1	1.1	1.1	1.1	1.1	1.1

RUN- PT. NO.	OMS #R (FPS)	MU	THEC (DEG)	BLADE .60R FLAPWISE BENDING MOMENT HARMONICS (IN.-LB)									
				B1	B2	B3	B4	B5	B6	B7	B8	B9	B10
83- 3 700	333	4.0	1.0	1.1	1.1	1.1	1.1	1.1	1.1	1.1	1.1	1.1	1.1
83- 4 700	390	4.0	1.5	1.1	1.1	1.1	1.1	1.1	1.1	1.1	1.1	1.1	1.1
83- 5 700	450	4.0	2.1	1.1	1.1	1.1	1.1	1.1	1.1	1.1	1.1	1.1	1.1
84- 3 500	632	4.0	2	1.1	1.1	1.1	1.1	1.1	1.1	1.1	1.1	1.1	1.1
84- 4 500	708	4.0	5	1.1	1.1	1.1	1.1	1.1	1.1	1.1	1.1	1.1	1.1
84- 5 500	793	4.0	1.0	1.1	1.1	1.1	1.1	1.1	1.1	1.1	1.1	1.1	1.1
84- 6 500	876	4.0	1.9	1.1	1.1	1.1	1.1	1.1	1.1	1.1	1.1	1.1	1.1
84- 7 475	832	4.0	1.1	1.1	1.1	1.1	1.1	1.1	1.1	1.1	1.1	1.1	1.1
84- 8 451	876	4.0	7	1.1	1.1	1.1	1.1	1.1	1.1	1.1	1.1	1.1	1.1
84- 9 428	924	4.0	1.5	1.1	1.1	1.1	1.1	1.1	1.1	1.1	1.1	1.1	1.1
84-10 381	1.038	4.0	3.0	1.1	1.1	1.1	1.1	1.1	1.1	1.1	1.1	1.1	1.1
84-11 357	1.107	4.0	1.4	1.1	1.1	1.1	1.1	1.1	1.1	1.1	1.1	1.1	1.1
84-12 334	1.185	4.0	2	1.1	1.1	1.1	1.1	1.1	1.1	1.1	1.1	1.1	1.1
84-13 310	1.275	4.0	5	1.1	1.1	1.1	1.1	1.1	1.1	1.1	1.1	1.1	1.1
84-14 287	1.380	4.0	1	1.1	1.1	1.1	1.1	1.1	1.1	1.1	1.1	1.1	1.1
84-15 263	1.504	4.0	1.9	1.1	1.1	1.1	1.1	1.1	1.1	1.1	1.1	1.1	1.1
84-16 239	1.652	4.0	2.6	1.1	1.1	1.1	1.1	1.1	1.1	1.1	1.1	1.1	1.1

TABLE LXXXVIII - Concluded

TABLE LXXXVIII - Concluded														
BLADE .60R FLAPWISE BENDING MOMENT HARMONICS (IN.-LB)														
RUN- PT. NO.	OMS #R (FPS)	MU	THEC (DEG)	R5	R1	R2	R3	R4	R5	R6	R7	R8	R9	R10
83- 3 700		.333	4.0	1.5	2.5	1.2	2.5	1.1	.7	.2	.1	.5	.5	.2
83- 4 700		.390	4.0	-.2	2.7	3.9	6.6	.4	2.6	.4	.6	.4	.2	.1
83- 5 700		.450	4.0	.3	3.8	3.1	9.5	1.0	3.2	.8	.8	.5	.2	.1
84- 3 500		.632	4.0	1.6	2.4	1.7	5.1	1.3	1.4	1.8	.3	.1	.0	1.5
84- 4 500		.708	4.0	1.0	2.7	2.0	5.1	1.8	1.5	1.0	.4	.2	.2	2.4
84- 5 500		.793	4.0	.4	2.3	1.9	3.9	2.3	1.4	1.4	.7	.6	.7	2.7
84- 6 500		.876	4.0	.4	2.1	2.0	5.3	3.5	1.3	1.8	.7	.6	.5	2.8
84- 7 475		.832	4.0	.2	1.8	2.0	7.5	2.0	1.4	2.9	.9	.6	.4	1.1
84- 8 451		.876	4.0	1.0	1.8	3.1	10.2	2.4	1.2	.8	.5	.6	.4	.5
84- 9 428		.924	4.0	.8	2.1	4.4	13.9	2.4	1.9	.4	.5	.8	.6	.4
84-10 381		1.038	4.0	2.4	4.0	8.1	16.1	2.5	3.4	4.1	1.9	1.4	.9	.8
84-11 357		1.107	4.0	1.1	3.2	6.4	14.6	2.1	2.6	2.9	4.6	1.1	.2	.8
84-12 334		1.185	4.0	1.6	2.5	6.7	14.9	3.3	1.7	1.0	3.4	.3	.4	.7
84-13 310		1.275	4.0	1.5	2.7	7.1	15.0	4.6	2.0	.9	1.5	.4	.1	.4
84-14 287		1.380	4.0	2.4	2.3	8.8	13.4	6.2	2.2	1.4	.7	.3	.5	.3
84-15 263		1.504	4.0	2.5	2.6	9.7	11.8	8.6	2.7	2.0	.3	.5	1.6	.8
84-16 239		1.652	4.0	2.3	3.1	11.0	11.7	11.6	3.7	2.7	.9	1.1	2.6	1.1

TABLE LXXXIX. BLADE .18R TORSIONAL MOMENT HARMONICS - RUNS 83-84 (BLADE CENTER OF GRAVITY AT .35 CHORD)																								
BLADE .18R TORSIONAL MOMENT HARMONICS (IN.-LB)																								
RUN- PT. NO.	OMS #R (FPS)	MU	THEC (DEG)	A1	A2	A3	A4	A5	A6	A7	A8	A9	A10	A11	A12	A13								
83- 3 700		.333	4.0	.9	1.1	-7.3	-3	.4	.0	.0	.0	-.1	-.6	.0	.0	.0								
83- 4 700		.390	4.0	1.1	-4.4	-4.8	-6.5	-.6	.4	-.4	-.1	.1	.3	.0	.0	.0								
83- 5 700		.450	4.0	1.0	-4.4	-6.7	-4.9	-.1	.7	-.5	-.2	.1	.2	.0	.0	.0								
84- 3 500		.632	4.0	.7	1.3	-6.5	3.4	-2.2	.7	.4	.1	.1	.2	-.1	-.1	-.2								
84- 4 500		.708	4.0	.5	.4	-8.6	7.7	-4.1	.5	.3	-.1	.1	.3	.0	-.1	-.1								
84- 5 500		.793	4.0	.6	-.7	-8.6	12.1	-4.0	.6	.6	-.2	.0	.4	.0	.1	.0								
84- 6 500		.876	4.0	1.1	-2.5	-8.9	14.4	-8.6	.8	.6	.1	.1	.2	.1	.1	.1								
84- 7 475		.832	4.0	.6	-.1	-9.1	6.6	-8.6	2.7	.8	.1	-.1	-.1	.1	.0	.1								
84- 8 451		.876	4.0	1.1	-.2	-8.0	4.4	-2.9	4.5	.9	.6	-.2	-.0	.1	.0	-.1								
84- 9 428		.924	4.0	1.1	.2	-8.2	3.1	7.6	5.2	1.3	.6	.0	-.0	.0	.1	.0								
84-10 381		1.038	4.0	1.7	-1.9	-3.4	-2.2	9.4	-1.4	1.6	.5	.6	-.0	.1	-.3	-.1								

BLADE .18R TORSIONAL MOMENT HARMONICS (IN.-LB)																								
RUN- PT. NO.	OMS #R (FPS)	MU	THEC (DEG)	B1	B2	B3	B4	B5	B6	B7	B8	B9	B10	B11	B12	B13								
83- 3 700		.333	4.0	2.0	6.1	-4.3	3.9	.7	.4	.2	.1	.0	.2	.0	.0	.0								
83- 4 700		.390	4.0	2.6	7.4	-18.3	2.6	.5	.4	-.1	-.1	.1	-.1	.0	.0	.0								
83- 5 700		.450	4.0	2.6	6.8	-19.9	6.6	.5	.2	.3	-.1	.3	.4	.0	.0	.0								
84- 3 500		.632	4.0	.9	2.9	2.0	-6.1	1.2	.3	.1	.2	.0	-.1	.0	.0	-.1								
84- 4 500		.708	4.0	.6	4.1	.3	-6.2	-.9	1.0	.4	.3	.0	-.1	.1	.1	.0								
84- 5 500		.793	4.0	.4	4.7	-.4	-5.1	-3.5	1.6	.5	.3	.2	-.3	.1	.1	.0								
84- 6 500		.876	4.0	-1.1	4.6	-.4	-4.6	-5.3	1.9	.5	.4	.3	-.3	.0	.0	.0								
84- 7 475		.832	4.0	.4	4.1	1.8	-7.9	4.2	2.4	.4	.7	.1	.1	.0	.0	.0								
84- 8 451		.876	4.0	.0	3.1	2.8	-6.5	9.7	2.7	.1	.7	.3	.1	-.2	.0	.0								
84- 9 428		.924	4.0	-.5	1.9	4.4	-7.5	10.1	-6.7	-.3	.5	.5	.1	-.2	.0	.0								
84-10 381		1.038	4.0	-1.8	-.2	7.2	-4.6	-3.8	7.2	-1.1	-.4	.2	.4	.0	-.1	-.1								

TABLE LXXXIX - Concluded																			
RUN- PT. NO.		BLADE .18R TORSIONAL MOMENT HARMONICS (IN.-LB)																	
	OMS #R (FPS)	MU	THEC (DEG)	RS	P1	R2	R3	R4	R5	R6	R7	R8	M9	R10	R11	R12	R13		
83-	3 700	.333	0.0	8.2	2.2	6.2	8.5	4.0	.8	.9	.2	.1	.1	.7	.0	.0	.0		
83-	4 700	.390	0.0	5.6	2.8	8.6	18.9	7.0	.8	.5	.4	.1	.1	.3	.0	.0	.0		
83-	5 700	.450	0.0	5.2	2.8	8.1	21.0	6.3	.5	.7	.5	.3	.4	.4	.0	.0	.0		
84-	3 500	.632	0.0	1.7	1.1	3.2	6.8	7.0	2.5	.7	.5	.3	.1	.2	.1	.1	.3		
84-	4 500	.708	0.0	1.9	.8	4.1	8.6	9.9	4.2	1.1	.6	.3	.1	.3	.0	.1	.3		
84-	5 500	.793	0.0	2.0	.7	4.7	8.6	13.1	5.4	1.7	.7	.4	.2	.4	.1	.2	.1		
84-	6 500	.876	0.0	1.9	1.6	5.3	8.9	15.1	7.0	2.1	.8	.4	.3	.4	.1	.1	.2		
84-	7 475	.832	0.0	1.9	.7	4.1	9.3	10.3	9.6	3.6	.9	.7	.1	.2	.1	.0	.1		
84-	8 451	.876	0.0	2.5	1.1	3.1	8.4	7.9	10.1	4.5	.9	.9	.3	.1	.2	.1	.1		
84-	9 428	.924	0.0	5.0	1.2	1.9	9.4	6.1	12.7	6.4	1.3	.6	.5	.1	.2	.1	.1		
84-10	361	1.036	0.0	3.6	2.5	1.9	7.9	5.1	10.2	7.3	2.0	.7	.6	.4	.1	.3	.1		

TABLE XC. BLADE FLAP MOTION HARMONICS - RUNS 83-84
(BLADE CENTER OF GRAVITY AT .35 CHORD)

RUN- PT. NO.	ONS *R (FPS)	MU	THEC (DEG)	BLADE FLAP MOTION HARMONICS (DEG)						
				A1	A2	A3	A4	A5	A6	A7
83- 3 700	.333	4.0	.0	.0	-.2	.1	.0	.0	.0	.0
83- 4 700	.390	4.0	.1	.1	.2	.1	-.1	.1	.0	.0
83- 5 700	.450	4.0	-.1	.1	.1	.1	-.1	.1	.0	.0
84- 3 500	.632	4.0	.0	-.3	.4	.0	.0	.0	.0	.0
84- 4 500	.708	4.0	-.1	-.2	.5	.0	.0	.0	.0	.0
84- 5 500	.793	4.0	-.1	-.2	.5	.0	.0	.0	.0	.0
84- 6 500	.876	4.0	.0	-.2	.5	.0	.0	.0	.0	.0
84- 7 475	.832	4.0	-.2	-.3	.6	.0	.0	.0	.0	.0
84- 8 451	.876	4.0	.2	-.2	.6	.0	.0	-.1	.0	.0
84- 9 428	.924	4.0	.0	-.2	.5	.0	.0	-.1	-.1	.0
84-10 381	1.038	4.0	.6	-.1	-.3	.2	.0	.0	.0	.0
84-11 357	1.107	4.0	-.4	-.3	-.3	.3	.1	.1	-.1	.1
84-12 334	1.185	4.0	.5	-.3	-.2	.3	.1	.1	.0	.0
84-13 310	1.275	4.0	.4	-.3	-.2	.3	.1	.1	.0	-.1
84-14 287	1.380	4.0	.4	-.3	-.3	.4	.1	.1	.0	.0
84-15 263	1.504	4.0	-.2	-.5	-.6	.5	.2	.2	.0	.0
84-16 239	1.652	4.0	-.4	-.7	-.6	.4	.2	.2	.0	.0

RUN- PT. NO.	ONS *R (FPS)	MU	THEC (DEG)	BLADE FLAP MOTION HARMONICS (DEG)						
				B1	B2	B3	B4	B5	B6	B7
83- 3 700	.333	4.0	.1	-.2	.0	.0	.0	.0	.0	.0
83- 4 700	.390	4.0	.2	-.5	.1	.0	.1	.1	.0	.0
83- 5 700	.450	4.0	.1	-.4	-.1	.1	.1	.1	.0	.0
84- 3 500	.632	4.0	.1	-.3	-.2	.1	.1	.0	.0	.0
84- 4 500	.708	4.0	.1	-.4	-.1	.1	.1	.0	.0	.0
84- 5 500	.793	4.0	.0	-.6	.1	.1	.1	.0	.0	.0
84- 6 500	.876	4.0	.1	-.6	.1	.2	.2	.0	.0	.0
84- 7 475	.832	4.0	.0	-.5	-.1	.1	.1	.0	.0	.0
84- 8 451	.876	4.0	-.1	-.4	-.3	.1	.1	.0	.0	.0
84- 9 428	.924	4.0	-.1	-.3	-.7	.2	.2	.0	.0	.0
84-10 381	1.038	4.0	.2	.0	-.9	.1	.1	.1	-.1	.0
84-11 357	1.107	4.0	.0	-.1	-1.0	.0	.1	.1	-.1	-.1
84-12 334	1.185	4.0	.1	.0	-.9	-.1	.1	.1	.0	-.1
84-13 310	1.275	4.0	.0	.1	-.9	-.1	.1	.0	.0	-.1
84-14 287	1.380	4.0	.0	.0	-.8	-.1	.1	.0	.0	.0
84-15 263	1.504	4.0	-.1	.2	-.7	-.3	-.1	.1	.0	.0
84-16 239	1.652	4.0	-.4	.3	-.7	-.7	-.1	.1	.0	.0

TABLE XC - Concluded												
RUN- PT. NO.			BLADE FLAP MOTION HARMONICS (DEG)									
OMS *R (FPS)	MU	THEC (DEG)	RS	R1	R2	R3	R4	R5	R6	R7		
83- 3 700	.333	4.0	1.6	.1	.3	.1	.0	.0	.0	.0		
83- 4 700	.390	4.0	1.1	.2	.5	.1	.1	.1	.0	.0		
83- 5 700	.450	4.0	1.1	.2	.5	.1	.1	.2	.0	.0		
84- 3 500	.632	4.0	.5	.1	.4	.4	.1	.1	.0	.0		
84- 4 500	.708	4.0	.4	.1	.5	.5	.1	.0	.0	.0		
84- 5 500	.793	4.0	.3	.1	.6	.5	.1	.0	.0	.0		
84- 6 500	.876	4.0	.1	.1	.6	.6	.2	.0	.0	.0		
84- 7 475	.832	4.0	.3	.2	.6	.6	.1	.0	.0	.0		
84- 8 451	.876	4.0	.1	.3	.4	.7	.1	.1	.0	.0		
84- 9 428	.924	4.0	.0	.1	.4	.9	.2	.1	.1	.0		
84-10 381	1.038	4.0	-.5	.6	.1	.9	.3	.1	.2	.0		
84-11 357	1.107	4.0	-.2	.4	.4	1.0	.3	.2	.1	.1		
84-12 334	1.185	4.0	-.7	.5	.3	1.0	.3	.1	.0	.1		
84-13 310	1.275	4.0	-1.0	.4	.3	1.0	.3	.1	.0	.1		
84-14 287	1.380	4.0	-1.6	.4	.3	.9	.4	.1	.0	.0		
84-15 263	1.504	4.0	-1.9	.2	.5	.9	.6	.2	.0	.0		
84-16 239	1.652	4.0	-2.4	.6	.8	.9	.8	.2	.0	.0		

TABLE XCI. BLADE .30R CHORDWISE BENDING MOMENT HARMONICS - RUNS 83-84
(BLADE CENTER OF GRAVITY AT .35 CHORD)

BLADE .30R CHORDWISE BENDING MOMENT HARMONICS (IN.-LB)																
RUN-PT. NO.	OMS #R (FPS)	MU	(DEG)	A1	A2	A3	A4	A5	A6	A7	A8	A9	A10	A11	A12	A13
83- 3 700	.333	4.0	1.8	-1.5	2.3	1.4	-9	-2	-1	-1	.2	.9	1.4	.0	.0	.0
83- 4 700	.390	4.0	.5	-2	.3	2.1	.5	1.0	1.7	-1.3	.7	-2.0	-1.4	.0	.0	.0
83- 5 700	.450	4.0	1.0	-1.7	.6	7.4	-2	-2	.8	.2	1.4	.3	.0	.0	.7	.6
84- 3 500	.632	4.0	1.2	-1.7	2.4	-3.3	-3.3	-2.8	.8	-1	.2	.1	.0	.0	.9	-1.1
84- 4 500	.708	4.0	1.1	-1.7	3.1	-4.1	-4.1	-3.4	.8	-1	.2	.4	.0	.0	1.8	-1.5
84- 5 500	.793	4.0	.7	-1.6	3.9	-6.3	-6.3	-2.5	.3	-6	.1	.4	.0	.0	.4	.7
84- 6 500	.876	4.0	.6	-1.7	3.3	-7.9	-7.9	-5.3	1.3	-7	.0	.6	-6	.0	1.8	.7
84- 7 475	.832	4.0	1.1	-1.7	2.9	-4.4	-4.4	-13.9	1.3	-1	.1	.0	.0	.0	.4	.4
84- 8 451	.876	4.0	2.1	-1.4	1.7	.0	.0	27.2	2.6	.5	-1	-2	.3	.0	.4	1.1
84- 9 428	.924	4.0	3.7	-2.4	2.3	-2.5	-2.5	-1.1	1.6	1.9	-1	.6	.3	.0	.4	.4
84-10 361	1.036	4.0	2.4	-1.2	2.0	-3.9	-3.9	-0.5	4.0	-9	3.1	-1.1	-2	.0	.4	.4
84-11 357	1.107	4.0	2.1	-1.5	-1.4	-1.4	-1.4	-4.3	3.1	-6	2.0	-1.7	.4	.0	.4	.4
84-12 334	1.185	4.0	2.6	-1.3	-1.4	-1.0	-1.0	-2.3	-1.0	-1.1	1.2	.6	.1	.0	.1	.0
84-13 310	1.275	4.0	1.7	-1.1	-1.1	-1.1	-1.1	-2.2	.3	-4	1.8	.7	.1	.1	.0	.1
84-14 287	1.380	4.0	4.1	-6	-6	-2.4	-2.4	-3	-1	-5	-2	.6	.4	.2	.0	.1
84-15 263	1.504	4.0	8.7	-9	-9	2.0	2.0	.0	1.1	-2	-3	1.8	.4	.1	.2	.1
84-16 239	1.652	4.0	14.0	-5	-5	3.7	-1.3	-6	1.0	1.3	.0	.1	.6	.4	.1	.0

BLADE .30R CHORDWISE BENDING MOMENT HARMONICS (IN.-LB)																
RUN-PT. NO.	OMS #R (FPS)	MU	(DEG)	B1	B2	B3	B4	B5	B6	B7	B8	B9	B10	B11	B12	B13
83- 3 700	.333	4.0	.5	-1.2	-1.0	2.2	3.7	.6	.3	.3	-2	-6	.2	.0	.0	.0
83- 4 700	.390	4.0	1.6	-1.6	-1.6	4.5	.6	-1	-1.4	-4	-1.1	-2	.3	.0	.0	.0
83- 5 700	.450	4.0	1.9	-1.6	-1.6	5.3	2.3	.7	-1.4	-3	-1.4	.3	.1	.0	.0	.0
84- 3 500	.632	4.0	2.6	-1.2	-1.2	-1.7	-1.0	-6	.4	.6	.0	.0	.2	.0	.1	.0
84- 4 500	.708	4.0	3.9	-1.3	-1.3	-1.9	-9	-1.1	.1	.7	.1	.0	.3	.0	.6	.2
84- 5 500	.793	4.0	5.5	-1.6	-1.6	-6	-1.9	-4.5	.6	.4	.4	.1	.0	.0	.4	.6
84- 6 500	.876	4.0	7.7	-1.8	-1.8	-2.4	-2.4	-6.4	.4	1.2	.7	.1	.0	.0	.9	1.2
84- 7 475	.832	4.0	6.0	-1.5	-1.5	-1.5	-1.2	6.4	-4	1.2	.4	.4	.0	.0	1.6	1.6
84- 8 451	.876	4.0	6.6	-1.8	-1.8	-1.2	-2.2	4.0	4.0	.0	1.6	.4	.2	.4	.3	.7
84- 9 428	.924	4.0	7.2	-1.1	-1.1	-1.4	-2.7	-12.0	-5.2	-3	2.1	-1	.0	.0	.0	.6
84-10 361	1.036	4.0	7.7	1.5	1.5	-2.2	1.0	-1.5	19.6	-9	.7	.6	.6	.5	.2	.3
84-11 357	1.107	4.0	7.7	.8	.8	-2.0	-2.0	2.3	-8.2	-2.7	.1	1.0	.2	.3	.3	.4
84-12 334	1.185	4.0	4.4	.6	.6	-1.6	-2.9	.3	.6	.4	.1	.6	.1	.3	.1	.0
84-13 310	1.275	4.0	9.9	1.0	1.0	-3	-2.4	.8	.7	-1.2	.8	.6	.2	.3	.2	.1
84-14 287	1.380	4.0	11.1	1.3	.8	.9	-3	.5	.6	.3	-2.7	.5	.6	.1	.4	.2
84-15 263	1.504	4.0	11.8	1.6	.9	.9	.1	1.0	.6	.8	.4	.6	.3	.4	.4	.3
84-16 239	1.652	4.0	11.1	3.0	3.0	-1.8	-3	-7	-3	1.1	.8	-3.2	-1.1	.3	.8	.5

TABLE XCI - Concluded

RUN- PT. NO.	OHS R (FPS)	BLADE .30P CHORUMISE RELOADING MOMENT HARMONICS (IN.-LB)																			
		THEC (DEG)	PS	R1	R2	R3	R4	R5	R6	R7	R8	R9	R10	R11	R12	R13					
83- 3 700	.333	4.0	-4.4	1.6	2.0	3.2	3.9	1.0	.4	.3	.3	1.1	1.8	.0	.0	.0					
83- 4 700	.340	4.0	-7.9	1.6	1.7	4.5	2.1	.5	1.7	.8	1.3	.4	.3	.0	.0	.0					
83- 5 700	.450	4.0	-10.2	2.2	1.7	5.3	7.7	.7	2.5	1.3	2.0	2.0	1.4	.0	.0	.0					
84- 3 500	.632	4.0	-1.5	2.9	2.0	3.0	3.4	2.0	.9	.6	.1	.2	.2	.4	.7	.6					
84- 4 500	.708	4.0	-3.0	4.1	2.2	3.6	4.2	3.6	.8	.7	.2	.1	.3	.4	1.2	1.1					
84- 5 500	.793	4.0	-9.0	5.6	2.4	4.0	6.6	5.1	1.4	.8	.4	.5	.4	.3	1.8	1.6					
84- 6 500	.876	4.0	-6.5	7.8	2.4	4.1	8.3	7.7	1.0	.8	.4	.7	.6	.5	2.0	1.4					
84- 7 475	.832	4.0	-7.9	6.2	2.3	3.3	4.5	15.3	1.3	1.2	.7	.4	.5	.4	1.0	1.7					
84- 8 451	.876	4.0	-4.3	6.9	2.3	2.1	2.2	27.5	2.6	1.6	.9	.3	.4	.3	.3	1.3					
84- 9 428	.924	4.0	.0	8.1	2.4	2.7	3.7	12.1	5.4	2.5	2.6	1.0	.1	.2	.4	.7					
84-10 381	1.038	4.0	6.8	8.1	1.9	2.9	4.0	8.5	20.1	1.2	3.1	1.4	.8	.7	1.0	.6					
84-11 357	1.107	4.0	10.4	6.0	1.7	3.1	2.4	4.9	8.2	2.8	2.1	1.2	.6	.5	.4	.4					
84-12 334	1.185	4.0	12.3	8.8	1.4	2.1	3.1	2.4	1.2	1.1	1.2	.9	.1	.3	.1	.1					
84-13 310	1.275	4.0	14.0	10.0	1.5	.7	3.1	2.3	.8	1.3	2.0	.4	.4	.3	.1	.1					
84-14 287	1.380	4.0	16.7	11.8	1.5	.9	2.4	.6	.6	.6	2.7	.4	.7	.2	.2	.2					
84-15 263	1.504	4.0	18.9	14.7	1.8	2.2	1.7	1.0	1.3	.8	.5	1.9	.9	.4	.4	.3					
84-16 239	1.652	4.0	24.9	17.9	3.0	4.1	1.3	.9	1.0	1.7	.8	3.2	1.2	.5	.8	.5					

TABLE XCII. BLADE .35R TORSIONAL MOMENT HARMONICS - RUN 84
(BLADE CENTER OF GRAVITY AT .35 CHORD)

BLADE .35R TORSIONAL MOMENT HARMONICS (III.-LB)																
RUN- PT. NO.	OMS #R	MU (FPS)	THEC (DEG)	A1	A2	A3	A4	A5	A6	A7	A8	A9	A10	A11	A12	A13
84- 3 500	.632	4.0	.8	-6.6	3.0	-2.8	1.1	1.1	1.1	.3	.0	.1	-.1	.1	.1	.1
84- 4 500	.708	4.0	.1	-8.6	6.6	-4.8	1.1	1.1	1.1	.3	-.2	.1	.0	.0	.2	.1
84- 5 500	.793	4.0	.6	-1.1	11.5	-5.4	1.1	1.1	1.1	.4	.2	.3	.0	.0	.2	.0
84- 6 500	.876	4.0	.8	-1.4	14.0	-6.8	1.5	1.5	1.5	.7	.2	.3	.0	.1	.1	.0
84- 7 475	.832	4.0	.6	-9.0	6.3	-9.3	3.1	3.1	3.1	.8	-.1	.1	-.2	.0	.0	-.1
84- 8 451	.876	4.0	.8	-7.9	3.0	1.8	5.4	5.4	5.4	.8	.3	-.2	.0	.0	-.1	.0
84- 9 428	.924	4.0	1.3	-8.3	1.0	11.5	2.0	2.0	2.0	1.5	.7	.3	.0	.0	.1	.0
84-10 381	1.038	4.0	.7	-5.1	1.1	10.3	-1.4	4.9	4.9	2.0	.4	.5	.1	.1	.2	.1
84-11 357	1.107	4.0	.5	-2.2	-4.9	2.0	2.0	2.0	2.0	-.5	-.2	.4	.3	.1	.0	.0
84-12 334	1.185	4.0	.6	-2.4	-1.8	.7	2.5	2.5	2.5	-.3	-.6	.1	.1	.2	.0	.1
84-13 310	1.275	4.0	.3	-1.6	-1.2	-.4	.6	.6	.6	.9	.6	.0	.2	.3	.0	.0
84-14 287	1.360	4.0	-.1	-3.3	-.6	-.7	-.2	-.2	-.2	.4	.0	.1	.6	.3	.0	.0
84-15 263	1.504	4.0	-.9	-3.8	1.0	1.2	1.2	-.3	-.5	.2	.6	1.4	1.2	.3	.1	-.2
84-16 239	1.652	4.0	.1	-4.8	2.2	2.2	2.2	-.3	-.5	-.4	.4	1.4	.4	.2	.4	.1

BLADE .35R TORSIONAL MOMENT HARMONICS (IN.-LB)																
RUN- PT. NO.	OMS #R	MU (FPS)	THEC (DEG)	B1	B2	B3	B4	B5	B6	B7	B8	B9	B10	B11	B12	B13
84- 3 500	.632	4.0	1.4	1.2	3.4	1.2	-6.5	1.4	1.0	.4	.3	-.1	.0	.1	-.1	.1
84- 4 500	.708	4.0	1.2	.9	4.3	-.9	-8.3	.4	1.3	.5	.3	.0	-.1	.1	-.1	.1
84- 5 500	.793	4.0	1.0	.1	4.7	-2.6	-7.6	-2.8	1.6	.6	.3	.2	.0	.2	.1	.0
84- 6 500	.876	4.0	.1	5.1	5.1	.2	-8.0	-4.4	1.7	.6	.2	.2	.2	.1	.2	.0
84- 7 475	.832	4.0	-.6	.6	4.4	1.6	-8.9	5.7	2.4	.5	.7	.0	.1	.1	-.1	.1
84- 8 451	.876	4.0	.4	.7	3.4	.7	-7.9	11.1	-1.2	.6	.9	.3	.2	.1	.0	.0
84- 9 428	.924	4.0	.2	2.3	2.4	2.3	-9.0	7.3	-9.6	-.3	.5	.4	.1	.1	.2	.1
84-10 381	1.038	4.0	-1.7	5.1	.3	5.1	-5.5	-3.9	6.0	-1.4	-.4	.2	.2	.2	.1	.0
84-11 357	1.107	4.0	-1.4	6.6	-.1	6.6	-.9	-7.4	-.1	-3.5	-.2	.0	.0	.2	.1	.0
84-12 334	1.185	4.0	-3.0	5.0	-.9	5.0	-.3	-3.8	-.6	.2	.2	-.1	.2	.1	.1	.0
84-13 310	1.275	4.0	-3.8	5.2	-.9	5.2	.3	-2.9	-2.0	-.2	-.3	.1	.3	-.2	.1	.1
84-14 287	1.360	4.0	-5.1	5.4	-.8	5.4	.7	-2.2	-1.7	-.5	-.8	.6	.2	-.2	.2	.1
84-15 263	1.504	4.0	-5.6	5.6	-.4	5.6	1.5	-1.8	-1.4	-.7	-.2	.5	.0	.1	.2	-.1
84-16 239	1.652	4.0	-6.7	5.8	.2	5.8	1.0	-1.8	-.7	-.6	-.8	-.9	-1.5	.2	.2	.1

TABLE XCII - Concluded

TABLE XCII - Concluded																
RUN- PT. NO.	QMS OR (EPS)	MU	THC (DEG)	BLADE .35R TORSIONAL MOMENT HARMONICS (IN.-LB)												
				R5	R1	R2	R3	R4	R5	R6	R7	R8	R9	R10	R11	R12
84- 3 500		.632	9.0	2.1	1.6	3.5	6.7	7.5	3.1	1.5	.5	.3	.1	.1	.1	.2
84- 4 500		.708	9.0	2.1	1.5	4.3	8.6	10.6	4.6	1.7	.6	.5	.2	.1	.1	.2
84- 5 500		.793	9.0	2.3	1.2	4.8	8.9	13.9	6.1	2.0	.8	.3	.3	.1	.2	.1
84- 6 500		.876	9.0	2.2	.8	5.3	9.2	16.1	8.1	2.3	.9	.3	.4	.2	.2	.0
84- 7 475		.832	9.0	2.2	.9	4.4	9.1	10.9	10.9	3.9	1.0	.7	.1	.3	.1	.1
84- 8 451		.876	9.0	1.5	.8	3.5	7.9	8.4	11.1	5.5	1.0	1.0	.3	.2	.1	.1
84- 9 428		.929	9.0	.8	.9	2.7	8.6	9.1	13.6	9.8	1.5	.9	.5	.1	.1	.2
84-10 381		1.036	9.0	-.8	1.8	.5	7.2	5.8	11.0	8.1	2.5	.6	.5	.2	.1	.2
84-11 357		1.107	9.0	-1.1	1.5	.2	7.0	4.9	7.7	4.9	3.5	.3	.4	.3	.2	.0
84-12 334		1.185	9.0	-1.0	3.0	1.8	5.6	1.9	3.9	2.6	1.3	.6	.1	.2	.1	.1
84-13 310		1.275	9.0	-1.6	3.8	2.5	5.4	1.3	2.9	2.1	.4	.9	.1	.4	.3	.1
84-14 287		1.380	9.0	-1.3	5.1	3.3	5.4	1.0	2.3	1.7	.6	.8	.7	.7	.2	.1
84-15 263		1.504	9.0	-1.5	5.7	4.8	5.7	1.2	1.8	1.5	.7	.6	1.5	1.2	.3	.2
84-16 239		1.652	9.0	-1.4	6.7	4.8	6.2	2.4	1.8	.9	.8	.9	1.6	1.5	.3	.5

TABLE XCIII. BLADE LAG MOTION HARMONICS - RUNS 85-86
(BLADE CENTER OF GRAVITY AT .35 CHORD)

RUN- PT. NO.	OMS R (FPS)	MU	THEC (DEG)	BLADE LAG MOTION HARMONICS (DEG)				
				A1	A2	A3	A4	A5
85- 3 700	.294	5.0	.0	.0	.0	.0	.0	.0
85- 4 700	.351	5.0	.0	.0	.0	.0	.0	.0
85- 5 500	.657	5.0	.2	.0	.0	.0	.0	.0
85- 6 500	.766	5.0	.2	.0	.0	.0	.0	.0
85- 7 400	1.067	2.0	.2	.0	.1	-.1	.0	.0
85- 8 400	1.108	2.0	.4	.0	.1	.0	.0	.0
86- 3 387	.795	2.0	.3	.1	.1	.0	.0	.0
86- 4 363	.847	2.0	.3	.0	.0	.0	.0	.0
86- 5 339	.906	2.0	.3	.1	.0	.0	.0	.0
86- 6 316	.974	2.0	.3	.0	.0	.0	.0	.0
86- 7 292	1.052	2.0	.0	.1	.0	.0	.0	.0
86- 8 269	1.144	2.0	.0	.1	.0	.0	.0	.0
86- 9 245	1.254	2.0	-.1	.1	.0	.0	.0	.0
86-10 221	1.388	2.0	-.3	.1	.0	.0	.0	.0
86-11 211	1.456	2.0	-.4	.0	.0	.0	.0	.0

RUN- PT. NO.	OMS R (FPS)	MU	THEC (DEG)	BLADE LAG MOTION HARMONICS (DEG)				
				B1	B2	B3	B4	B5
85- 3 700	.294	5.0	.2	.1	.1	.1	.1	.1
85- 4 700	.351	5.0	.1	.1	.1	.1	.1	.1
85- 5 500	.657	5.0	.2	.1	.1	.1	.0	.0
85- 6 500	.766	5.0	.2	.1	.1	.1	.1	.0
85- 7 400	1.067	2.0	-.3	.1	.0	.0	.0	-.1
85- 8 400	1.108	2.0	-.2	.2	.1	.0	.0	-.1
86- 3 387	.795	2.0	.0	.1	.1	.1	.0	.0
86- 4 363	.847	2.0	.0	.1	.1	.1	.0	.0
86- 5 339	.906	2.0	.0	.1	.1	.1	.0	.0
86- 6 316	.974	2.0	-.2	.1	.1	.1	.0	.0
86- 7 292	1.052	2.0	-.4	.1	.0	.0	.0	.0
86- 8 269	1.144	2.0	-.5	.1	.0	.1	.1	.0
86- 9 245	1.254	2.0	-.6	.1	.1	.1	.1	.0
86-10 221	1.388	2.0	-.7	.1	.1	.1	.1	.0
86-11 211	1.456	2.0	-.7	.1	.1	.1	.0	.0

TABLE XCIII - Concluded										
RUN- PT. NO.		OMS #R (FPS)	MU	THEC (DEG)	RS	R1	R2	R3	R4	R5
85-	3	700	.294	5.0	1.1	.2	.1	.1	.1	.1
85-	4	700	.351	5.0	.8	.1	.1	.1	.1	.1
85-	5	500	.657	5.0	.7	.2	.1	.1	.1	.0
85-	6	500	.766	5.0	.8	.3	.1	.1	.1	.0
85-	7	400	1.067	2.0	.5	.4	.1	.1	.1	.1
85-	8	400	1.108	2.0	.7	.4	.2	.1	.1	.1
86-	3	387	.795	2.0	.5	.3	.1	.1	.0	.0
86-	4	363	.847	2.0	.5	.3	.1	.1	.0	.0
86-	5	339	.906	2.0	.7	.3	.1	.1	.0	.0
86-	6	316	.974	2.0	.6	.4	.1	.0	.0	.0
86-	7	292	1.052	2.0	.6	.4	.1	.1	.0	.0
86-	8	269	1.144	2.0	1.0	.5	.1	.1	.1	.0
86-	9	245	1.254	2.0	1.0	.6	.1	.1	.1	.1
86-10	221		1.388	2.0	1.1	.7	.1	.1	.1	.1
86-11	211		1.456	2.0	1.1	.8	.1	.1	.1	.0

TABLE XCIV. BLADE .30R FLAPWISE BENDING MOMENT HARMONICS - RUNS 65-86
(BLADE CENTER OF GRAVITY AT .35 CHORD)

RUN- PT. NO.	ONS #R (FPS)	THEC (DEG)	BLADE .30R FLAPWISE BENDING MOMENT HARMONICS (IN.-LB)												
			A1	A2	A3	A4	A5	A6	A7	A8	A9	A10	A11	A12	A13
85- 3 700	.294	5.0	-5	.5	-1.7	-4.8	-4.8	-5	.2	.4	-2	.0	-1	-1	.0
85- 4 700	.351	5.0	.4	.5	.5	1.6	-3.0	.4	.0	.1	.1	.1	.1	.0	-.1
85- 5 500	.657	5.0	1.6	-2.4	-3.3	-.5	2.6	-1.0	.6	.1	-2	.8	.1	.0	.0
85- 6 500	.766	5.0	2.0	-3.1	-3.3	-1.2	.9	.7	.2	.5	-2	.4	-1	-2	.1
85- 7 400	1.067	2.0	2.7	-8.8	1.2	-1.5	.1	-.4	-3.1	.1	.9	-1	-.9	.1	-.4
85- 8 400	1.108	2.0	2.7	-4.5	1.7	-.5	.7	-.9	-4.4	-.4	.4	-2	-.5	.4	-.4
86- 3 387	.795	2.0	1.7	-1.3	3.2	-4.8	.5	-.2	.5	.5	.1	-1	-.2	.2	.2
86- 4 363	.847	2.0	1.8	-1.0	4.5	-.2	.2	.4	-1.0	.2	.1	.0	-1	-1	-.2
86- 5 339	.906	2.0	1.9	-1.1	5.8	.1	.3	.4	.1	-.3	-.1	-2	-.1	-1	-.4
85- 6 316	.974	2.0	2.1	-1.1	5.2	-.1	-.2	.4	.8	-.2	.0	-.3	.0	.1	.2
86- 7 292	1.052	2.0	2.0	-1.0	6.4	-.9	-.4	.4	.8	-1.4	-.1	-2	-.1	-1	-.1
86- 8 269	1.144	2.0	1.8	-1.7	4.9	-1.7	-.5	.3	.6	.6	-.1	-.2	-.1	-1	-.1
86- 9 245	1.254	2.0	1.8	-1.6	5.3	-3.3	-1.2	.1	.3	.3	1.7	-.1	-.2	.0	.0
86-10 221	1.388	2.0	1.4	-1.9	4.8	-5.0	-1.5	.1	.1	.0	.6	-.9	.0	.1	.1
86-11 211	1.456	2.0	1.3	-2.1	5.3	-6.4	-1.9	.0	.1	-.2	-.6	.0	.2	-1	.1

BLADE .30R FLAPWISE BENDING MOMENT HARMONICS (IN.-LB)

RUN- PT. NO.	ONS #R (FPS)	THEC (DEG)	BLADE .30R FLAPWISE BENDING MOMENT HARMONICS (IN.-LB)												
			B1	B2	B3	B4	B5	B6	B7	B8	B9	B10	B11	B12	B13
85- 3 700	.294	5.0	-.2	.3	.4	-.5	2.6	.2	.3	1.3	.0	.0	.1	.1	.1
85- 4 700	.351	5.0	.5	1.3	2.2	-.0	-.6	.0	.0	-.7	.1	.1	.0	.0	.1
85- 5 500	.657	5.0	1.3	1.4	1.4	-.7	.0	-2.9	-.3	.5	.0	1.1	.1	.0	.0
85- 6 500	.766	5.0	.9	3.1	.6	-.8	-1.5	-.5	-.3	.0	.4	-2.5	.0	-.2	-.1
85- 7 400	1.067	2.0	.9	-2.9	13.5	.2	-1.0	2.1	.3	-1.4	.2	.4	-.5	1.0	.0
85- 8 400	1.108	2.0	2.5	-1.7	13.0	.2	-.2	1.8	1.0	-1.3	.0	.3	-.6	.9	.1
86- 3 387	.795	2.0	.3	.7	.8	.2	-.5	1.1	-1.3	-.2	.9	.2	-.6	.2	.1
86- 4 363	.847	2.0	-.1	.7	.6	.5	-.5	.5	-.6	.0	.2	.2	.1	.1	-.3
86- 5 339	.906	2.0	.0	.7	5.1	.5	-.3	.4	1.8	.0	.2	.2	.0	.1	.3
86- 6 316	.974	2.0	.0	.3	5.5	-.4	-.3	.3	.9	-.1	.2	.1	.1	.1	.1
86- 7 292	1.052	2.0	-.4	.9	5.5	-.6	-.1	.4	.6	1.4	.1	.0	-.1	.0	.0
86- 8 269	1.144	2.0	-.4	.3	2.6	-.6	-.2	.1	.2	.6	.4	.2	.1	.0	.0
86- 9 245	1.254	2.0	-.7	.2	2.1	-.2	-.2	.0	-.2	-.1	.6	.3	.0	-.1	.0
86-10 221	1.388	2.0	-.4	1.2	.9	.9	.1	-.1	-.2	-.1	-.7	-1.1	-.2	-.1	-.1
86-11 211	1.456	2.0	-.6	.7	1.2	3.4	.4	-.1	.0	.1	-.3	-1.1	-.1	-.1	-.1

TABLE XCIV - Concluded

TABLE XCIV - Concluded																	
RUN- PT. NO.		OMS #R (FPS)	THEC (DEG)	PS	R1	R2	R3	R4	R5	R6	R7	R8	R9	R10	R11	R12	R13
85-	3	700	.294	5.0	3.2	.5	.6	1.7	.6	2.7	.5	.3	1.3	.2	.0	.1	.1
85-	4	700	.351	5.0	3.1	.7	1.4	2.3	1.6	3.1	.4	.0	.7	.2	.1	.1	.1
85-	5	500	.657	5.0	2.9	2.1	2.8	3.6	.9	2.6	1.1	.7	.5	.2	1.3	.1	.2
85-	6	500	.766	5.0	2.9	2.2	4.3	3.3	1.4	1.8	1.0	.4	.5	.5	2.6	.1	.2
85-	7	400	1.067	2.0	2.2	2.8	8.9	13.5	1.5	1.0	2.1	3.1	1.4	.9	.8	1.0	.4
85-	8	400	1.108	2.0	2.4	3.6	4.8	13.0	.6	.8	2.0	4.5	1.4	.4	.3	.8	.4
86-	3	387	.795	2.0	.3	1.8	1.5	8.9	.5	.7	1.2	1.4	.6	.3	.2	.2	.2
86-	4	363	.847	2.0	.2	1.8	1.2	7.8	.5	.5	.7	1.2	.2	.3	.2	.1	.3
86-	5	339	.906	2.0	.2	1.9	1.3	7.7	.4	.4	.5	1.8	.3	.3	.2	.2	.5
86-	6	316	.974	2.0	.3	2.1	1.2	7.6	.4	.4	.5	1.2	.2	.2	.1	.1	.2
86-	7	292	1.052	2.0	.3	2.0	1.3	7.2	1.0	.5	.5	1.0	2.0	.2	.2	.1	.1
86-	8	269	1.144	2.0	.2	1.9	1.7	5.6	1.8	.6	.3	.7	.9	.4	.3	.1	.1
86-	9	245	1.254	2.0	.3	1.9	1.7	5.7	3.3	1.2	.1	.4	.3	1.8	.3	.2	.1
86-	10	221	1.388	2.0	.4	1.4	2.2	4.9	5.1	1.5	.1	.2	.1	.9	1.4	.2	.1
86-	11	211	1.456	2.0	.3	1.5	2.2	5.4	7.2	1.9	.1	.1	.2	.7	1.8	.2	.1

TABLE XCV. BLADE .60R FLAPWISE BENDING MOMENT HARMONICS - RUNS 85-86
(BLADE CENTER OF GRAVITY AT .35 CHORD)

BLADE .60R FLAPWISE BENDING MOMENT HARMONICS (IN.-LB)												
RUN- PT. NO.	OMS *R (FPS)	THEC (DEG)	A1	A2	A3	A4	A5	A6	A7	A8	A9	A10
85- 3 700	.294	5.0	-1.5	-2.7	-2.2	-6.6	.3	.3	-2.2	-7.7	.1	.0
85- 4 700	.351	5.0	2.8	.8	3.5	-1.0	2.0	-3.3	-1.1	-1.1	-1.1	.0
85- 5 500	.657	5.0	2.8	-1.1	-5.0	-1.7	-1.8	.3	-1.1	.0	.1	-1.7
85- 6 500	.766	5.0	2.5	-5	-3.4	-1.5	.9	-1.0	-5	-1.3	.4	-6
85- 7 400	1.067	2.0	2.8	-8.8	.6	-3.1	-3.1	3.0	1.8	-1.3	-3.3	-4
86- 3 387	.765	2.0	1.3	-2.5	5.1	-4	-9	.5	-3	-2	.0	.2
86- 4 363	.847	2.0	1.4	-1.8	6.7	-1	-7	-5	.6	-1	.0	.0
86- 5 339	.906	2.0	1.7	-1.7	8.0	.0	-4	-5	-2	.1	.1	-1
86- 6 316	.974	2.0	1.9	-1.6	6.9	-1.0	-6	-5	-3	.0	-1	-1
86- 7 292	1.052	2.0	1.9	-1.5	8.0	-2.2	-7	-6	-9	1.1	.1	.1
86- 8 269	1.144	2.0	1.5	-2.1	5.9	-3.1	-7	-4	-6	-5	.0	.1
86- 9 245	1.254	2.0	1.8	-1.9	6.2	-4.9	-1.4	-5	-4	-3	-1.4	.2
86-10 221	1.388	2.0	1.3	-2.3	5.1	-6.7	-1.7	-4	.0	.1	.6	-9
86-11 211	1.456	2.0	1.2	-2.6	5.4	-8.0	-2.1	-7	.1	.1	.3	.5

BLADE .60R FLAPWISE BENDING MOMENT HARMONICS (IN.-LB)												
RUN- PT. NO.	OMS *R (FPS)	THEC (DEG)	B1	B2	B3	B4	B5	B6	B7	B8	B9	B10
85- 3 700	.294	5.0	-1.3	-1.7	2.2	-4	-1.6	-1	-4	-1.5	-1	-1
85- 4 700	.351	5.0	-1.8	.4	2.6	-3	.8	.2	-2	.7	.0	.1
85- 5 500	.657	5.0	.7	1.8	2.3	-6	.5	1.9	-2	-2	.0	-9
85- 6 500	.766	5.0	-6	1.9	.9	1.6	1.4	.2	-1	-3	-3	2.3
85- 7 400	1.067	2.0	3.1	-3.9	14.3	.1	2.1	-5	.2	1.3	-5	-1.2
86- 3 387	.765	2.0	1.0	.0	11.5	.5	.3	-1.3	.9	.4	.1	.0
86- 4 363	.847	2.0	1.1	-5	8.8	.6	.6	-2	.6	.0	-2	-2
86- 5 339	.906	2.0	1.1	-4	6.7	-5	.6	-2	1.4	.1	-1	.1
86- 6 316	.974	2.0	.9	-3	7.1	-7	.5	-2	-5	.1	-1	.0
86- 7 292	1.052	2.0	.7	.5	4.3	-9	.6	.2	-1	-1.2	-1	.1
86- 8 269	1.144	2.0	1.1	-3	3.1	-7	.3	-3	.1	-6	-4	-1
86- 9 245	1.254	2.0	.9	-3	2.7	.0	.2	-4	.1	.1	-1.0	-3
86-10 221	1.388	2.0	.4	.8	1.3	1.0	.2	-9	-2	.1	.3	.6
86-11 211	1.456	2.0	.5	.1	1.4	4.1	.9	-9	-4	-1	.3	1.4

TABLE XCV - Concluded														
RUN- PT. NO.	OMS #R (FFS)	MU	THEC (DEG)	BLADE .60R FLAPWISE BENDING MOMENT HARMONICS (IN.-LB) .										
				RS	R1	R2	R3	R4	R5	R6	R7	R8	R9	R10
85- 3	700	.294	5.0	3.1	2.0	1.7	3.1	.7	1.6	.3	.4	1.6	.1	.1
35- 4	700	.351	5.0	2.5	3.3	.9	5.8	1.0	2.1	.4	.3	.8	.1	.1
85- 5	500	.657	5.0	1.6	2.9	2.1	5.5	1.8	1.9	1.9	.2	.2	.1	1.2
85- 6	500	.766	5.0	1.5	2.6	2.0	3.6	2.2	1.7	1.0	.5	.3	.5	2.4
85- 7	400	1.067	2.0	.7	4.2	9.6	14.3	3.1	3.7	3.1	1.8	1.9	.6	1.2
86- 3	387	.795	2.0	.4	2.1	2.5	12.6	.6	.9	1.4	.9	.4	.1	.2
86- 4	363	.847	2.0	.3	1.8	1.9	11.0	.6	.9	.5	.9	.1	.2	.2
86- 5	339	.906	2.0	.7	2.0	1.7	10.5	.5	.7	.5	1.4	.2	.2	.1
86- 6	316	.974	2.0	.8	2.1	1.6	9.9	1.2	.8	.5	1.0	.2	.1	.1
86- 7	292	1.052	2.0	1.0	2.0	1.6	9.1	2.4	1.0	.7	.9	1.6	.1	.1
86- 8	269	1.144	2.0	1.0	1.9	2.1	6.7	3.3	.8	.4	.6	.8	.4	.2
86- 9	245	1.254	2.0	1.4	2.0	1.9	6.8	4.9	1.5	.6	.4	.3	1.7	.3
86-10	221	1.388	2.0	1.3	1.4	2.4	5.3	6.8	1.7	1.0	.3	.2	.7	1.1
86-11	211	1.456	2.0	1.5	1.3	2.6	5.6	9.0	2.3	1.2	.4	.1	.4	1.4

TABLE XCVI. BLADE FLAP MOTION HARMONICS - RUNS 85-86
(BLADE CENTER OF GRAVITY AT .35 CHORD)

BLADE FLAP MOTION HARMONICS (DEG)									
RUN- PT. NO.	ONS R (FPS)	MU	THEC (DEG)	A1	A2	A3	A4	A5	A6
85- 3 700	.294	5.0	.1	-.3	.2	.0	.0	.0	.0
85- 4 700	.351	5.0	.1	-.2	.1	-.1	.1	.0	.0
85- 5 500	.657	5.0	.1	-.3	.5	.0	-.1	.0	.0
85- 6 500	.766	5.0	.2	-.4	.6	.1	.0	.0	.0
85- 7 400	1.067	2.0	.5	-.2	.2	.3	.0	.0	.0
85- 8 400	1.108	2.0	-.3	-.1	.4	.1	-.1	.1	.0
86- 3 387	.795	2.0	.2	.0	-.1	.1	.0	.0	.0
86- 4 363	.847	2.0	.2	.0	-.2	.1	.0	.0	.0
86- 5 339	.906	2.0	.1	-.1	-.3	.1	.0	.0	.0
86- 6 316	.974	2.0	.1	-.1	-.3	.1	.0	.0	.0
86- 7 292	1.052	2.0	-.2	-.1	-.4	.2	.1	.0	.0
86- 8 269	1.144	2.0	.0	-.0	-.3	.2	.1	.0	.0
86- 9 245	1.254	2.0	.1	-.1	-.2	.3	.1	.0	.0
86-10 221	1.388	2.0	-.2	-.1	-.2	.4	.1	.0	.0
86-11 211	1.476	2.0	-.2	-.1	-.3	.5	.1	.0	.0

BLADE FLAP MOTION HARMONICS (DEG)									
RUN- PT. NO.	ONS R (FPS)	MU	THEC (DEG)	B1	B2	B3	B4	B5	B6
85- 3 700	.294	5.0	.2	-.1	.1	.0	-.1	.0	.0
85- 4 700	.351	5.0	.3	-.4	-.1	.0	.1	.0	.0
85- 5 500	.657	5.0	.1	-.5	-.1	.1	.0	.0	.1
85- 6 500	.766	5.0	-.1	-.7	-.1	.2	.0	.0	.0
85- 7 400	1.067	2.0	.1	.0	-1.3	.2	.1	-.1	.0
85- 8 400	1.108	2.0	-.2	-.3	-1.2	.2	.0	-.1	.0
86- 3 387	.795	2.0	.0	-.2	-.7	.1	.0	.0	.0
86- 4 363	.847	2.0	.0	-.2	-.6	.0	.1	.0	.0
86- 5 339	.906	2.0	.2	.2	-.5	.1	.0	.0	.0
86- 6 316	.974	2.0	.1	-.1	-.5	.1	.0	.0	.0
86- 7 292	1.052	2.0	.1	-.1	-.3	.1	.0	.0	.0
86- 8 269	1.144	2.0	-.1	-.2	-.3	.1	.0	.0	.0
86- 9 245	1.254	2.0	.0	-.1	-.3	-.1	.0	.0	.0
86-10 221	1.388	2.0	-.1	-.1	-.2	-.2	.0	.0	.0
86-11 211	1.476	2.0	.0	-.1	-.2	-.2	.0	.0	.0

TABLE XCVI - Concluded

BLADE FLAP MOTION HARMONICS (DEG)												
RUN- PT. NO.	OMS #R	MU	THEC (DEG)	RS	R1	R2	R3	R4	R5	R6		
85- 3	700	.294	5.0	2.4	.2	.3	.2	.1	.1	.0		
85- 4	700	.351	5.0	1.9	.3	.4	.1	.1	.1	.0		
85- 5	500	.657	5.0	.6	.1	.6	.5	.1	.1	.1		
85- 6	500	.766	5.0	.3	.2	.4	.6	.2	.0	.0		
85- 7	400	1.067	2.0	-.5	.5	.2	1.3	.3	.1	.1		
85- 8	400	1.108	2.0	-.3	.3	.3	1.2	.2	.1	.1		
86- 3	387	.795	2.0	.0	.2	.2	.7	.1	.1	.0		
86- 4	363	.847	2.0	-.1	.2	.2	.6	.1	.1	.0		
86- 5	339	.906	2.0	-.2	.2	.2	.6	.1	.1	.0		
86- 6	316	.974	2.0	-.3	.2	.2	.5	.1	.0	.0		
86- 7	292	1.052	2.0	-.5	.2	.2	.5	.2	.1	.0		
86- 8	269	1.144	2.0	-.7	.1	.2	.4	.2	.1	.0		
86- 9	245	1.254	2.0	-1.0	.1	.2	.4	.3	.1	.0		
86-10	221	1.388	2.0	-1.3	.2	.1	.3	.5	.1	.0		
86-11	211	1.456	2.0	-1.6	.2	.1	.3	.6	.1	.0		

TABLE XC VII. BLADE .30R CHORDWISE BENDING MOMENT HARMONICS - RUNS 85-86 (BLADE CENTER OF GRAVITY AT .35 CHORD)																
BLADE .30P CHORDWISE BENDING MOMENT HARMONICS (IN.-LB)																
RUN- PT. OMS NO. #R	MJ	(DEG)	A1	A2	A3	A4	A5	A6	A7	A8	A9	A10	A11	A12	A13	
85- 3 700	.294	5.0	.9	-1.1	3.4	2.5	.4	.2	-.3	-.6	.6	-1.8	.2	-.8	.0	
85- 4 700	.351	5.0	1.6	-.7	2.1	5.1	-.4	.3	.0	.1	1.1	.7	.8	-.1	.1	
85- 5 500	.657	5.0	-.8	-1.6	3.8	-2.7	-2.9	.8	-.4	.0	.0	-.1	-.3	.8	-.8	
85- 6 500	.766	5.0	-.8	-1.7	4.4	-5.2	-5.5	1.2	-.2	.1	.3	-.2	-.2	1.4	-.4	
85- 7 400	1.067	2.0	.2	-2.6	3.5	-4.4	-9.2	-17.6	.5	1.3	.5	-.5	.4	-.1	.2	
85- 8 400	1.108	2.0	-.9	-1.9	.4	-3.0	-2.2	-11.8	3.9	-.6	2.1	.3	.0	-.1	.0	
86- 3 387	.795	2.0	.5	-.9	-.1	-1.2	-2.7	-1.8	.8	.6	.0	.1	-.1	-.1	.0	
86- 4 363	.847	2.0	.6	-.8	-.5	-1.0	-1.7	-.2	-.7	.6	.2	.2	.0	.0	-.1	
86- 5 339	.906	2.0	.7	-.5	-.6	-.9	-.7	-1.3	-.2	.4	.3	.2	.0	.0	-.1	
86- 6 316	.974	2.0	.8	-.4	-.9	-.7	.2	-.7	.6	.5	.1	.0	.0	-.1	-.1	
86- 7 292	1.052	2.0	1.7	-.5	-1.2	-.9	-.2	.0	.3	1.1	.3	.1	.1	.0	.1	
86- 8 269	1.144	2.0	2.8	-.3	-1.3	-.5	-.6	-.1	-.2	-.5	.4	.2	.2	-.1	-.2	
86- 9 245	1.254	2.0	4.7	-.7	-.9	-.4	.1	-.1	-.4	-.6	.2	.3	.1	-.1	.0	
86-10 221	1.388	2.0	5.6	-.3	-.2	-.3	.6	.0	-.2	-.1	.0	.2	.4	.1	.0	
86-11 211	1.456	2.0	5.4	-.3	.5	-.4	.6	-.2	-.3	.2	.4	-.1	.3	.0	.1	

BLADE .30P CHORDWISE BENDING MOMENT HARMONICS (III -L3)																
RUN- PT. OMS NO. #R	MJ	THEC (DEG)	B1	B2	B3	B4	B5	B6	B7	B8	B9	B10	B11	B12	B13	
85- 3 700	.294	5.0	-.4	-1.6	2.5	6.1	.3	-.7	-.7	.5	.3	.4	.5	.1	-.2	
85- 4 700	.351	5.0	-.2	-1.5	2.7	2.7	.4	-.3	.4	-.4	-.2	1.0	-.3	-.7	-.3	
85- 5 500	.657	5.0	3.9	-1.5	-.1	-3.2	-1.6	-.9	.7	.3	.2	.3	-.4	.7	-.1	
85- 6 500	.766	5.0	5.6	-1.4	-1.5	.9	-.3	.4	.6	.4	.2	.4	.4	-1.7	1.2	
85- 7 400	1.067	2.0	9.2	2.3	.0	-6.3	-9.5	-1.2	-3.9	4.0	-1.6	.0	.5	.6	.3	
85- 8 400	1.108	2.0	9.5	.6	-2.8	-3.2	-8.8	-8.4	-1.2	4.0	-.1	.3	.5	.3	.4	
86- 3 387	.795	2.0	4.4	.3	-1.1	-.7	-.1	.7	-.3	.4	-.1	.1	.1	-.1	-.1	
86- 4 363	.847	2.0	4.1	.1	-1.3	-.8	.3	-2.4	-.4	.0	.2	.1	.0	.1	.2	
86- 5 339	.906	2.0	4.3	.3	-1.1	-.3	.5	-.2	-1.0	-.3	.0	-.1	.0	.0	.0	
86- 6 316	.974	2.0	5.1	.1	-1.0	-.6	-.6	-.1	-.4	.1	.2	.1	.1	.0	.0	
86- 7 292	1.052	2.0	5.6	.2	-.6	-.5	-.1	.2	-.8	-.9	.0	.1	.1	.0	.0	
86- 8 269	1.144	2.0	6.5	-.2	-.1	-.2	.6	-.2	-.7	.0	.3	.1	.2	.1	.0	
86- 9 245	1.254	2.0	6.8	.0	.6	-.1	.7	.1	.0	.0	-.3	.2	.2	.1	.0	
86-10 221	1.388	2.0	7.9	.3	1.4	-.3	.5	.2	.0	.1	-.1	-.4	-.2	.2	.2	
86-11 211	1.456	2.0	7.7	.4	1.4	-.6	.5	.1	.0	-.1	.2	-.5	-.6	.2	.1	

TABLE XCVII - Concluded

TABLE XCVII - Concluded																	
RUN- PT. NO.	OHS OR (FPS)	ML	THEC (DEG)	BLADE JOINT CHOICEWISE BENDING MOMENT HARMONICS (IN.-LB)													
				PS	R1	R2	R3	R4	R5	P6	R7	R8	R9	R10	R11	R12	R13
85-3 700		.294	5.0	-18.0	1.2	1.9	4.2	6.6	.5	.7	.8	.8	.7	2.0	.5	.8	.2
85-4 700		.351	5.0	-13.0	1.6	1.7	3.6	5.7	.6	.4	.4	.4	1.1	1.2	.6	.7	.3
85-5 500		.657	5.0	35.4	4.0	2.2	3.6	4.2	3.3	1.2	.8	.3	.2	.3	.5	1.0	.8
85-6 500		.766	5.0	30.8	5.7	2.2	4.6	5.3	5.5	1.3	.6	.4	.4	.4	.4	2.2	1.3
85-7 400		1.067	2.0	62.5	3.2	3.4	3.5	7.7	13.2	17.7	4.0	4.6	1.7	.5	.6	.6	.5
85-8 400		1.108	2.0	65.0	3.6	1.9	2.9	4.4	9.1	14.4	4.0	4.1	2.1	.4	.5	.4	.4
86-3 387		.795	2.0	.0	4.4	1.0	1.1	1.4	2.7	1.9	.8	.7	.1	.1	.1	.1	.1
86-4 363		.847	2.0	.6	4.2	.8	1.4	1.3	1.7	2.4	.8	.6	.3	.2	.0	.1	.2
86-5 339		.906	2.0	1.5	4.4	.6	1.2	1.0	.8	1.3	1.0	.5	.7	.2	.1	.0	.1
86-6 316		.974	2.0	2.3	5.1	.4	1.4	.9	.7	.7	.8	.6	.7	.2	.1	.1	.1
86-7 292		1.052	2.0	3.1	5.9	.5	1.3	1.0	.2	.2	.7	1.5	.3	.2	.1	.1	.1
86-8 269		1.144	2.0	3.8	7.1	.5	1.2	.5	.8	.3	.7	.9	.4	.2	.1	.1	.1
86-9 245		1.254	2.0	4.6	8.3	.7	1.2	.4	.7	.1	.4	.6	.4	.4	.2	.1	.2
86-10 221		1.388	2.0	5.6	9.7	.4	1.4	.4	.8	.2	.2	.2	.1	.4	.4	.2	.2
86-11 211		1.456	2.0	6.0	10.0	.5	1.5	.7	.6	.2	.3	.2	.4	.5	.7	.2	.2

TABLE XCVIII. BLADE .35R TORSIONAL MOMENT HARMONICS - RUNS 85-86
(BLADE CENTER OF GRAVITY AT .35 CHORD)

BLADE .35R TORSIONAL MOMENT HARMONICS (IN.-LB)																
RUN- PT. NO.	OMS #R (FPS)	MU (DEG)	THEC (DEG)	A1	A2	A3	A4	A5	A6	A7	A8	A9	A10	A11	A12	A13
85- 3 700	.294		5.0	1.1	5.1	-6.5	1.2	.6	.2	.0	.1	.1	.0	.2	-.1	-.1
85- 4 700	.351		5.0	1.8	5.5	-8.5	-1.6	.7	.3	.1	.1	.0	.2	-.1	.2	.0
85- 5 500	.657		5.0	.9	1.8	-8.5	6.0	-3.2	.7	-.1	-.2	.0	.0	-.1	.2	.0
85- 6 500	.766		5.0	1.1	1.6	-11.8	8.3	-7.5	1.3	.8	-.3	.0	-.1	.1	.0	.1
85- 7 400	1.067		2.0	1.4	-.2	-7.2	-.8	12.7	-11.0	.0	-.8	.5	-.1	.1	-.1	.1
85- 8 400	1.108		2.0	-.9	-.4	-8.6	1.1	11.0	-5.3	.5	-.7	-.2	-.1	.0	.1	.1
86- 3 387	.795		2.0	.1	-.3	-2.6	-.8	3.2	-1.0	1.2	.4	.1	.0	.0	.0	.0
86- 4 363	.847		2.0	.1	-.4	-1.8	-1.6	1.0	1.6	1.1	.5	.3	.1	.1	.0	-.1
86- 5 339	.906		2.0	.1	-.4	-1.6	-1.4	.0	1.1	1.3	.7	.4	.2	.1	.1	.1
86- 6 316	.974		2.0	.1	-.6	-1.5	-.9	.4	.1	.2	.9	.3	.2	.1	.0	.0
86- 7 292	1.052		2.0	.1	-.4	-1.2	-.6	.0	.4	.2	.4	.2	.5	.1	.1	.0
86- 8 269	1.144		2.0	.1	-.6	-1.1	-.6	-.2	.2	.2	.3	.4	.5	.1	.1	.0
86- 9 245	1.254		2.0	.1	-.9	-.8	-.2	-.1	.6	.1	.3	.4	.5	.1	.1	.0
86-10 221	1.388		2.0	-.1	-1.0	-.3	-.1	-.2	.0	.1	-.2	.1	.5	.1	.1	.0
86-11 211	1.456		2.0	.0	-1.5	-.5	.1	.0	.1	.1	-.1	.1	.2	.2	.1	.1

BLADE .35R TORSIONAL MOMENT HARMONICS (IN.-LB)																
RUN- PT. NO.	OMS #R	MU (FPS)	THEC (DEG)	B1	B2	B3	B4	B5	B6	B7	B8	B9	B10	B11	B12	B13
85- 3 700	.294		5.0	2.4	4.3	.5	2.9	.5	.3	.1	.0	.2	.3	.8	.2	.1
85- 4 700	.351		5.0	3.5	7.7	-10.8	5.8	1.0	.4	.2	.1	.1	-.1	-.2	.1	.1
85- 5 500	.657		5.0	1.3	4.1	-.3	-5.2	-.6	1.4	.6	.0	.1	-.1	.0	.1	.1
85- 6 500	.766		5.0	.5	5.9	3.0	-13.1	1.0	1.7	.2	.4	.1	.0	.1	-.2	.0
85- 7 400	1.067		2.0	-3.2	.2	8.2	-6.9	2.2	-7.0	.5	-.3	.2	.2	.2	.0	-.1
85- 8 400	1.108		2.0	5.6	10.8	3.5	-8.1	4.3	-12.9	-.9	.3	.3	.2	.1	.1	.0
86- 3 387	.795		2.0	1.0	.7	1.4	-3.5	-1.1	1.0	.1	.3	.2	.2	.1	.0	.0
86- 4 363	.847		2.0	.9	.5	1.4	-2.1	-2.5	-.5	-.5	.3	.2	.1	.1	.1	.0
86- 5 339	.906		2.0	.7	.5	.9	-1.2	-2.0	-1.0	-.4	.0	.1	.3	.1	.1	.0
86- 6 316	.974		2.0	.6	.5	.7	-.9	-1.5	-.8	-.4	.0	.1	.1	.1	.1	.0
86- 7 292	1.052		2.0	.5	.5	.9	-.7	-1.2	-.7	-.2	-.4	.0	.1	.0	.0	.0
86- 8 269	1.144		2.0	.2	.4	1.0	-.3	-1.0	-.7	-.3	-.4	.2	.2	.0	.0	.0
86- 9 245	1.254		2.0	-.2	.1	1.0	-.4	-.8	-.4	-.3	-.4	.2	.2	.0	.0	.0
86-10 221	1.388		2.0	-.4	.3	1.2	-.3	-.7	-.4	-.2	-.3	-.4	-.4	-.1	.2	.1
86-11 211	1.456		2.0	-.7	.3	1.0	-.5	-.7	-.2	-.1	-.2	-.4	-.4	-.1	.3	.1

TABLE XCVIII - Concluded

TABLE XCVIII - Concluded																	
RUN- PT. NO.	OMS or (FPS)	MU	TMEC (DEG)	BLADE .35R TORSIONAL MOMENT HARMONICS (IN.-LB)													
				R5	R1	R2	R3	R4	R5	R6	R7	R8	R9	R10	R11	R12	R13
85- 3 700		.294	5.0	14.2	2.6	6.7	6.6	3.2	.8	.4	.1		.2	.3	.8	.2	.1
85- 4 700		.351	5.0	11.6	3.9	7.7	13.7	6.1	1.2	.5	.2		.1	.2	.2	.1	.1
85- 5 500		.657	5.0	1.8	1.6	4.5	8.5	9.5	3.3	1.5	.6		.1	.1	.1	.2	.1
85- 6 500		.766	5.0	-3.2	1.2	6.1	12.1	15.5	7.5	2.1	.8		.1	.1	.2	.2	.1
85- 7 400		1.067	2.0	-5.1	3.4	.3	10.9	6.9	12.9	13.1	.5		.5	.2	.2	.1	.1
85- 8 400		1.108	2.0	-6.6	1.1	1.1	9.3	8.2	11.8	14.0	1.0		.7	.2	.2	.1	.1
86- 3 387		.795	2.0	5.3	1.0	.8	3.0	3.6	3.4	1.4	1.2		.5	.2	.1	.1	.0
86- 4 363		.847	2.0	2.9	.9	.8	2.3	2.6	2.7	1.7	1.2		.6	.2	.1	.0	.1
86- 5 339		.906	2.0	-.1	.7	.7	1.8	1.8	2.0	1.5	.9		.5	.3	.1	.1	.1
86- 6 316		.974	2.0	-1.2	.6	.7	1.6	1.3	1.5	1.1	.4		.7	.2	.2	.1	.1
86- 7 292		1.052	2.0	-.9	.5	.6	1.5	1.0	1.2	.8	.2		1.0	.3	.1	.0	.0
86- 8 269		1.144	2.0	-1.2	.2	.7	1.4	.7	1.0	.7	.3		.6	.2	.1	.0	.0
86- 9 245		1.254	2.0	-1.4	.2	.9	1.3	.4	.8	.4	.3		.5	.5	.2	.1	.1
86-10 221		1.388	2.0	-1.6	.4	1.1	1.2	.3	.7	.4	.2		.3	.4	.1	.2	.1
86-11 211		1.456	2.0	-1.6	.7	1.3	1.1	.5	.7	.3	.2		.2	.4	.3	.3	.1

UNCLASSIFIED
Security Classification

DOCUMENT CONTROL DATA - R & D		
(Security classification of title, body of abstract and indexing annotation must be entered when the overall report is classified)		
1. ORIGINATING ACTIVITY (Corporate author) United Aircraft Corporation Sikorsky Aircraft Division Stratford, Connecticut		2a. REPORT SECURITY CLASSIFICATION Unclassified
		2b. GROUP
3. REPORT TITLE ROTOR AEROELASTIC INSTABILITY AND TRANSIENT CHARACTERISTICS		
4. DESCRIPTIVE NOTES (Type of report and inclusive dates) Final Report		
5. AUTHOR(S) (First name, middle initial, last name) Charles F. Niebanck Lawrence J. Bain		
6. REPORT DATE February 1970	7a. TOTAL NO. OF PAGES 450	7b. NO. OF REFS 18
8a. CONTRACT OR GRANT NO. DA 44-177-AMC-203(T)	8a. ORIGINATOR'S REPORT NUMBER(S) USAAVLABS Technical Report 69-88	
A. PROJECT NO. 1F162204A13903		
C.	8b. OTHER REPORT NO(S) (Any other numbers that may be assigned this report)	
D.	SER-50597	
10. DISTRIBUTION STATEMENT This document is subject to special export controls, and each transmittal to foreign governments or foreign nationals may be made only with prior approval of US Army Aviation Materiel Laboratories, Fort Eustis, Virginia 23604.		
11. SUPPLEMENTARY NOTES	12. SPONSORING MILITARY ACTIVITY U. S. Army Aviation Materiel Laboratories Fort Eustis, Virginia	
13. ABSTRACT A dynamically scaled model rotor, 9 feet in diameter, was tested in the 18-foot United Aircraft Research Laboratories Wind Tunnel. The purposes of the test included the determination of rotor transient response to sudden control inputs, the investigation of blade aeroelastic limits, and the generation of detailed dynamic data for the evaluation and improvement of theoretical calculations. The rotor was of a conventional articulated type.		

DD FORM 1473 REPLACES DD FORM 1473, 1 JAN 64, WHICH IS OBSOLETE FOR ARMY USE.

UNCLASSIFIED
Security Classification

UNCLASSIFIED
Security Classification

14. KEY WORDS	LINK A		LINK B		LINK C	
	ROLE	WT	ROLE	WT	ROLE	WT
Dynamically Scaled Model Rotor Wind Tunnel Test Rotor Transient Response Rotor Instability Rotor Blade Flutter						

UNCLASSIFIED
Security Classification